

Copyright  
by  
Gwendolyn Ann Marriner  
2009

**The Dissertation Committee for Gwendolyn Ann Marriner Certifies that this is  
the approved version of the following dissertation:**

**Synthesis and Evaluation of Small Molecule DNA-Interactive  
Compounds: Total Synthesis of ( $\pm$ )-NNN-5'-Acetate, Synthesis of  
Skipped Benzimidazolium Aza-Enediynes, and Synthesis of a Series  
of C2-Aryl UK-1 Analogs**

**Committee:**

---

Sean M. Kerwin Supervisor

---

Philip D. Magnus

---

Brent L. Iverson

---

Jennifer S. Brodbelt

---

Christian P. Whitman

**Synthesis and Evaluation of Small Molecule DNA-Interactive  
Compounds: Total Synthesis of ( $\pm$ )-NNN-5'-Acetate, Synthesis of  
Skipped Benzimidazolium Aza-Enediyne, and Synthesis of a Series  
of C2-Aryl UK-1 Analogs**

**by**

**Gwendolyn Ann Marriner, B. S.**

**Dissertation**

Presented to the Faculty of the Graduate School of

The University of Texas at Austin

in Partial Fulfillment

of the Requirements

for the Degree of

**Doctor of Philosophy**

**The University of Texas at Austin**

**August, 2009**

## **Dedication**

To dad, who still has all the answers

To Adam, I couldn't have done this without you



## **Acknowledgements**

There are so many people to thank. First, thanks to Prof. Kerwin, who has served as a mentor and an example of how a scientist should think. Second, I'd like to thank my labmates. From the Krische lab, I am especially grateful to Dr. Long-Cheng Wang, Ryan Huddleston, Dr. Hye-Young Jang, and Dr. Susan Garner. From the Kerwin lab, thanks are due to all my labmates, but especially Dr. Bodin Tuesuwan, who was kind enough to teach me how to handle radiolabeled DNA and perform analysis of DNA covalent modification, and Jeannie Li, who performed cytotoxicity assays. Also, Jess White-Phillip from Liu lab has been an invaluable resource for molecular biology techniques. Thank you to both Sarah Pierce and Suncerae Smith from the Brodbelt group, who performed ESI-MS analysis of a number of samples. Dr. Brian Bocknack has been kind enough to continue allowing me to teach with him. He has been an excellent model for teaching, and I appreciate the opportunity to have learned from him. Thanks are also due to Dr. Ruth Shear for the chance to teach in the FRI program. It was a nice change of pace and a chance to broaden my horizons. I would be remiss if I didn't thank the staff at UT. I appreciate all the hard work that goes into making UT run smoothly. Steve Sorey, Dr. Ben Shoulders, and Jim Wallin at the NMR facility as well as Dr. Karin Keller, Aaron Rogers, and Damon Belveal with the LC-MS facility have all been wonderful for analytical assistance (especially on short notice). Penny Kile has spent many hours making sure I was appointed and helping with mountains of paper work. Finally, thank you to Dr. Adam Berro for all your help, both technical and non-technical, for the past six years.

**Synthesis and Evaluation of Small Molecule DNA-Interactive  
Compounds: Total Synthesis of ( $\pm$ )-NNN-5'-Acetate, Synthesis of  
Skipped Benzimidazolium Aza-Enediynes, and Synthesis of a Series of  
C2-Aryl UK-1 Analogs**

Publication No. \_\_\_\_\_

Gwendolyn Ann Marriner, Ph.D.

The University of Texas at Austin, 2009

Supervisor: Sean M. Kerwin

Small-molecule DNA interactive compounds are critical as both carcinogens and therapeutic agents. In this research, a synthetic precursor to a known carcinogen, ( $\pm$ )-N'-nitrosornicotine-5'-acetate was synthesized, and its interactions with DNA were evaluated by polyacrylamide gel electrophoresis and electrospray-ionization mass spectrometry. A library of skipped benzimidazolium aza-enediynes which selectively target unmethylated cytosines in presence of unmethylated cytosines were synthesized, and their biological properties were evaluated in a nicking assay and cytotoxicity study. Finally, a series of structural analogs to an antineoplastic agent, UK-1, were synthesized *via* a biaryl coupling at C2 on the benzoxazole.

## Table of Contents

List of Tables .....	xi
List of Figures .....	xiii
List of Schemes.....	xix
1. Introduction.....	1
1.1. Structure of DNA.....	2
1.2. DNA Sequencing .....	4
1.3. Small Molecule-DNA Interactions .....	6
1.3.1. DNA Alkylation.....	8
1.3.2. Analysis of DNA Alkylation .....	10
1.3.3. DNA Footprinting.....	15
1.3.4. Assays for DNA cleavage.....	21
1.3.5. Analysis of Non-Covalent DNA-Small Molecule Interactions.....	23
1.4. Examples of Small Molecule DNA-Interactive Compounds .....	29
1.4.1. Alkylating Agents .....	30
1.4.2. Crosslinkers .....	34
1.4.3. Oxidizers ( <i>via</i> H-atom Abstraction) .....	37
1.4.4. Intercalators .....	43
1.4.5. Minor Groove Binders .....	49
1.5. Conclusions.....	53
1.6. References.....	54
2. Synthesis of ( $\pm$ )-N'-Nitrosonornicotine-5'-Acetate .....	65
2.1. Background.....	65
2.1.1. Tobacco Carcinogens.....	65
2.2. NNN-5'-OAc Synthesis Background.....	72
2.2.2. Previous isomyosmine syntheses.....	74
2.2.3. Sulfinimine Chemistry .....	75

2.3.	Synthesis of NNN-5'-OAc .....	85
2.4.	Interaction of NNN-5'-OAc with DNA in presence of Pig Liver Esterase 93	
2.4.1.	Simple enzymatic hydrolysis in absence of nucleosides .....	93
2.4.2.	Incubations of NNN-5'-OAc and PLE with single nucleosides	94
2.4.3.	Incubations of NNN-5'-OAc and PLE with short oligomer ...	98
2.5.	Conclusions.....	107
2.5.1.	Chemical DNA Synthesis .....	113
2.5.2.	Preparation of Duplex DNA for ESI-MS .....	114
2.5.3.	DNA synthesis by PCR .....	114
2.5.4.	DNA-Drug Incubations for ESI-MS.....	115
2.5.5.	DNA-Drug Incubations with Radiolabelled DNA .....	116
2.5.6.	Mobility Shift Assays .....	117
2.6.	References.....	119
3.	Structure-Activity Relationships of a Series of Propargylic Alkynylbenzimidazolium Salts on Cytosine and 5-Methylcytosine .....	125
3.1.	Background.....	125
3.1.1.	Aza-Enediynes .....	125
3.1.2.	Diradical-generating cyclizations .....	126
3.1.3.	Biological Activity of Azaenediynes.....	134
3.1.4.	DNA Methylation .....	141
3.2.	Proposed Research: Selective targeting of unmethylated cytosines in presence of methylated cytosines .....	145
3.2.1.	Kinetics .....	145
3.2.2.	DNA Sequence Selection .....	146
3.2.3.	Small Molecule-DNA Interactions .....	150
3.3.	Synthesis <sup>68,69</sup> .....	157
3.4.	Biological Evaluation of AZB library .....	160
3.5.	Conclusions.....	164
3.6.	Future Directions .....	164
3.7.	Experimental Section .....	165

3.7.1. Chemistry.....	165
3.7.2. Biology .....	176
3.8. References.....	180
4. UK-1 Analog Synthesis .....	186
4.1. Background.....	186
4.1.1. Benzoxazole Natural Products.....	186
4.1.2. Mode of Action.....	189
4.1.3. Previous Total Synthesis of UK-1 and Biaryl Analogs .....	190
4.1.4. Mono-Benzoxazole or -Benzimidazole UK-1 Analogs.....	193
4.1.5. C4 Benzoxazole Polar Analogs .....	196
4.1.6. Methods of 2-Arylbenzoxazole Synthesis .....	198
4.2. Proposed Research.....	204
4.2.1. Proposed C2 Analog Series .....	205
4.3. Synthesis .....	206
4.3.1. Copper (I) Catalyzed Ring Closing .....	206
4.3.2. Thiobenzoxazole-Derived Coupling Partner .....	210
4.3.3. Attempted Extension of Thiobenzoxazole Route to Synthesis of UK-1 .....	215
4.4. Conclusions.....	216
4.5. Future Work.....	216
4.6. Experimental Section.....	217
Appendices .....	228
Appendix I .....	228
Scanned <sup>1</sup> H and <sup>13</sup> C NMR spectra .....	228
X-ray Crystallography data.....	242
References.....	262
Appendix II.....	263
Scanned <sup>1</sup> H and <sup>13</sup> C NMR spectra .....	263
Appendix III.....	277
Scanned <sup>1</sup> H and <sup>13</sup> C NMR spectra .....	277

References.....301

Vita 325

## List of Tables

Table 2.1. Attempts to effect photorearrangement of <b>MIS090</b> .....	86
Table 2.2. Optimization of temperature for nitroso-acylation.....	89
Table 2.3. Summary of ions containing proposed mass of NNN adduct .....	101
Table 3.1. Computational estimates for energies of Bergman cyclization <sup>3</sup> .....	129
Table 3.2. EC <sub>25</sub> for pyridinium skipped aza-enediyne <sup>27</sup> .....	135
Table 3.3. Nicking ability of benzothiazolium salts at 100 μM <sup>24</sup> .....	138
Table 3.4. Nicking ability of benzimidazolium salts .....	138
Table 3.5. Quantitation of DNA cleavage with various alkylating agents. ....	152
Table 3.6. Quantitation of cleavage with <b>AZB004</b> .....	154
Table 3.7. Quantitation of DNA cleavage with <b>CRW054</b> .....	155
Table 3.8. Nicking assay to determine extent of DNA cleavage.....	163
Table 3.9. Cytotoxicity data on electronically varied benzimidazolium library .	163
Table 4.1. Activity of Caboxamycin against various bacteria and yeasts .....	187
Table 4.2. Cytotoxicity vs. antibacterial activity of minimum pharmacophore ..	194
Table 4.3. Cytotoxicity studies on analogs varying the heteroaromatic ring <sup>12</sup> ....	196
Table 4.4. Cytotoxicity data for C4 UK-1 minimum pharmacophore analogs. <sup>13</sup>	197
Table 4.5. Metal binding of C4 polar analogs .....	197
Table 4.6. Amide formation optimization .....	206
Table 4.7. Optimization of Cu(I)-catalyzed ring-closing .....	208
Table 4.8. Optimization of Liebeskind coupling for R = H.....	213
Table 4.9. Optimization of Liebeskind coupling for R = Me <sup>a</sup> .....	214
Table A.1. Crystal data and structure refinement for 1. ....	246
Table A.2. Atomic coords., equiv. isotropic displacement parameters for 1. ....	247

Table A.3. Bond lengths [ $\text{\AA}$ ] and angles [ $^\circ$ ] for <b>MIS087</b> .....	250
Table A.4. Anisotropic displacement parameters ( $\text{\AA}^2 \times 10^3$ ) for <b>MIS087</b> .....	255
Table A.5. Hydrogen coordinates and isotropic displacement parameters for 1.257	
Table A.6. Torsion angles [ $^\circ$ ] for 1 .....	259
Table A.7. Hydrogen bonds for <b>MIS087</b> [ $\text{\AA}$ and $^\circ$ ] .....	261



## List of Figures

Figure 1.1. DNA damage leading to cell death. ....	1
Figure 1.2. DNA's function in biological systems <sup>1</sup> .....	2
Figure 1.3. Structure of Nucleotides .....	2
Figure 1.4. Diagram of B-form DNA. ....	3
Figure 1.5. Watson-Crick Base Pairs.....	4
Figure 1.6. DNA binding motifs .....	8
Figure 1.7. Electrophoretic mobility shift assay .....	10
Figure 1.8. DNA crosslinking assay .....	12
Figure 1.9. Analysis of DNA Modification <i>via</i> Piperidine/Heat Treatment.....	14
Figure 1.10. <sup>32</sup> P -Postlabeling to identify covalent modification.....	15
Figure 1.11. Iron (II)-EDTA (l) and Iron (II)-MPE-EDTA (r).....	16
Figure 1.12. DNA footprinting .....	17
Figure 1.13. Polymerase chain reaction amplifies a DNA sequence.....	19
Figure 1.14. DNA Polymerase Interruption Assay.....	19
Figure 1.15. ss-QPCR .....	21
Figure 1.16. DNA nicking assay.....	22
Figure 1.17. "Break-Light" Assay .....	23
Figure 1.18. Cartoon of a triple quadrupole mass spectrometer.....	24
Figure 1.19. Competition Dialysis.....	25
Figure 1.20. Cartoon depicting DNA alkylation .....	30
Figure 1.21. CC-1065 (l) and Duocarmycin A (r) .....	31
Figure 1.22. Nitrosoureas .....	33
Figure 1.23. Polyaromatic hydrocarbon diol epoxides.....	34

Figure 1.24. Cartoon depicting interstrand DNA crosslinking .....	34
Figure 1.25. Nitrogen mustards .....	35
Figure 1.26. Proposed mechanism for reaction of nitrogen mustards with DNA. <sup>93</sup>	36
Figure 1.27. Proposed activation and DNA adduct formation. ....	36
Figure 1.28. Cisplatin .....	36
Figure 1.29. Cartoon of oxidative damage of DNA .....	37
Figure 1.30. Calicheamicin $\gamma_1$ (l) and Esperamycin A <sub>1</sub> (r) .....	38
Figure 1.31. Reactive diradicals from enediynes <sup>114</sup> .....	40
Figure 1.32. Bleomycin A2 .....	42
Figure 1.33. Cartoon depicting DNA intercalation .....	44
Figure 1.34. Mitoxantrone .....	44
Figure 1.35. Ethidium Bromide .....	45
Figure 1.36. Daunorubicin, doxorubicin, and iremycin.....	46
Figure 1.37. Echinomycin.....	47
Figure 1.38. Triostin A (l) and TANDEM (r).....	48
Figure 1.39. Cartoon of minor groove binding on DNA .....	49
Figure 1.40. Netropsin (L) and Distamycin (R) .....	50
Figure 1.41. Hoechst 33258 dye .....	51
Figure 1.42. Berenil (l), Pentamidine (center), and DAPI (r).....	52
Figure 1.43. Chromomycin A <sub>3</sub> (l) and Mithramycin (r) <sup>145</sup> .....	53
Figure 2.1. Structures of NNK (l) and NNK (r) .....	67
Figure 2.2. NNAL and NNK DNA adducts of pyrimidine bases .....	70
Figure 2.3. X-ray structure of <b>MIS087</b> showing the atom labeling scheme.....	87
Figure 2.4. Possible isomers and conformers of NNN-5'-OAc.....	90
Figure 2.5. LC-MS analysis of NNN-5'-OAc.....	91

Figure 2.6. LC chromatogram of NNN-5'-OAc .....	92
Figure 2.7. ESI-MS of guanosine with NNN-5'-OAc in presence of PLE.....	96
Figure 2.8. ESI-MS of adenosine with NNN-5'-OAc in the presence of PLE .....	96
Figure 2.9. ESI-MS of cytidine with NNN-5'-OAc in the presence of PLE. ....	97
Figure 2.10. ESI-MS of NNN-5'-OAc with thymidine in presence of PLE.....	97
Figure 2.11. Adducts of NNN-5'-OAc with G, A, and T by Hecht <i>et al.</i> <sup>66</sup> .....	98
Figure 2.12. ESI-MS on 11-mer shows multiple adduction. ....	99
Figure 2.13. CAD experiment on parent ion (*) from Figure 2.12. ....	99
Figure 2.14. Sequence information about the "upper" strand in the 11-mer duplex	100
Figure 2.15. CAD and IRMPD spectra of DNA singly adducted with NNN.....	102
Figure 2.16. EMSA on NNN-5'-OAc in presence of 11-mer and PLE.....	103
Figure 2.17. PAGE analysis of 227 bp DNA with acrolein or NNN-5'-OAc .....	104
Figure 2.18. EMSA using various post-incubation techniques. ....	106
Figure 3.1. Calculated energy for aza-Bergman and retro-aza-Bergman <sup>a</sup> .....	129
Figure 3.2. Pyridinium skipped aza-enediyne library <sup>27</sup> .....	135
Figure 3.3. Propargyl alkynyl benzothiazolium salts and control compounds .....	137
Figure 3.4. Benzimidazole compounds used in nicking assay .....	138
Figure 3.5. G-C base pair with unmodified cytosine (left) and 5-methylcytosine	142
Figure 3.6. DNA methylation following replication <sup>41</sup> .....	142
Figure 3.7. Non-denaturing PAGE analysis of annealing of 12-mer. ....	148
Figure 3.8. Annealing of 22-mer. ....	149
Figure 3.9. Benzyl bromide and styrene oxide .....	151
Figure 3.10. Acrolein, styrene oxide, and benzyl bromide with 22-mer .....	152
Figure 3.11. Structures of CRW054 and AZB004 .....	153
Figure 3.12. AZB004 with 22-mer DNA in 50 mM sodium phosphate, pH 6. ....	154

Figure 3.13. <b>CRW054</b> incubated with 22-mer at pH 8. ....	155
Figure 3.14. <b>AZB017</b> .....	156
Figure 3.15. Incubations of <b>AZB017</b> at pH 6 or pH 8.....	156
Figure 3.16. Benzimidazolium library .....	160
Figure 3.17. Nicking assay using skipped benzimidazolium triflates. ....	161
Figure 3.18. Nicking assay using skipped benzimidazolium triflates .....	162
Figure 4.1. Benzoxazole-containing natural products. ....	186
Figure 4.2. UK-1-metal ion complex .....	189
Figure 4.3. UK-1, Demethyl UK-1, and minimum pharmacophore.....	190
Figure 4.4. Synthesis of analogs of UK-1 lacking C4-methyl ester <sup>12</sup> .....	192
Figure 4.5. Synthesis by Smith <i>et al.</i> of UK-1 analogs lacking 2'-hydroxyl group <sup>12</sup> 192	
Figure 4.6. Model of Lewis basic sites on topoII inhibitors.....	193
Figure 4.7. <i>Bis</i> (benzimidazole) UK1 analog reported by Kerwin <i>et al.</i> <sup>9</sup> .....	193
Figure 4.8. Structures assayed to find a minimum pharmacophore .....	194
Figure 4.9. Benzimidazole and benzothiazole analogs of UK-1 .....	195
Figure 4.10. Positions to vary for SAR study .....	196
Figure 4.11. Proposed C2 analogs .....	205
Figure A.1. <b>MIS086</b> <sup>1</sup> H NMR .....	228
Figure A.2. <b>MIS086</b> <sup>13</sup> C NMR .....	229
Figure A.3. <b>MIS087</b> <sup>1</sup> H NMR .....	230
Figure A.4. <b>MIS087</b> <sup>13</sup> C NMR .....	231
Figure A.5. Isomyosmine <sup>1</sup> H NMR .....	232
Figure A.6. <sup>13</sup> C NMR of isomyosmine .....	233
Figure A.7. <sup>1</sup> H NMR of NNN-5'-OAc.....	234
Figure A.8. <sup>13</sup> C NMR of NNN-5'-OAc.....	235

Figure A.9. $^1\text{H}$ NMR of <b>MIS089</b> .....	236
Figure A.10. $^{13}\text{C}$ NMR of <b>MIS089</b> .....	237
Figure A.11. $^1\text{H}$ NMR of <b>MIS096</b> .....	238
Figure A.12. $^{13}\text{C}$ NMR of <b>MIS096</b> .....	239
Figure A.13. $^1\text{H}$ NMR of <b>MIS097</b> .....	240
Figure A.14. $^{13}\text{C}$ NMR of <b>MIS097</b> .....	241
Figure A.15. View of molecule 1 of <b>MIS087</b> showing the atom labeling scheme..	243
Figure A.16. View of molecule 2 of <b>MIS087</b> showing the atom labeling scheme..	244
Figure A.17. View of the fit by least-squares of selected atoms of molecule 1 ..	245
Figure A.18. Unit cell packing figure for <b>MIS087</b> .....	246
Figure A2.1. $^1\text{H}$ NMR of <b>AZB344</b> .....	263
Figure A2.2. $^{13}\text{C}$ NMR of <b>AZB344</b> .....	264
Figure A2.3. $^1\text{H}$ NMR of <b>AZB345</b> .....	265
Figure A2.4. $^{13}\text{C}$ NMR of <b>AZB345</b> .....	266
Figure A2.5. $^1\text{H}$ NMR of <b>AZB347</b> .....	267
Figure A2.6. $^1\text{H}$ NMR of <b>AZB348</b> .....	268
Figure A2.7. $^1\text{H}$ NMR of <b>AZB349</b> .....	269
Figure A2.8. $^1\text{H}$ NMR of <b>AZB379</b> .....	270
Figure A2.9. $^{13}\text{C}$ NMR of <b>AZB379</b> .....	271
Figure A2.10. $^1\text{H}$ NMR of <b>AZB380</b> .....	272
Figure A2.11. $^{13}\text{C}$ NMR of <b>AZB380</b> .....	273
Figure A2.12. $^1\text{H}$ NMR of <b>AZB381</b> .....	274
Figure A2.13. $^{13}\text{C}$ NMR of <b>AZB381</b> .....	275
Figure A2.14. $^1\text{H}$ NMR of <b>AZB384</b> .....	276
Figure A3.1. $^1\text{H}$ NMR of <b>TOP053</b> .....	277

Figure A3.2. $^{13}\text{C}$ NMR of <b>TOP053</b> .....	278
Figure A3.3. $^1\text{H}$ NMR of <b>TOP054</b> .....	279
Figure A3.4. $^{13}\text{C}$ NMR of <b>TOP054</b> .....	280
Figure A3.5. $^1\text{H}$ NMR of <b>TOP061</b> .....	281
Figure A3.6. $^{13}\text{C}$ NMR of <b>TOP061</b> .....	282
Figure A3.7. $^1\text{H}$ NMR of <b>TOP062</b> .....	283
Figure A3.8. $^{13}\text{C}$ NMR of <b>TOP062</b> .....	284
Figure A3.9. $^1\text{H}$ NMR of <b>TOP063</b> .....	285
Figure A3.10. $^{13}\text{C}$ NMR of <b>TOP063</b> .....	286
Figure A3.11. $^1\text{H}$ NMR of <b>TOP064</b> .....	287
Figure A3.12. $^{13}\text{C}$ NMR of <b>TOP064</b> .....	288
Figure A3.13. $^1\text{H}$ NMR of <b>TOP066</b> .....	289
Figure A3.14. $^{13}\text{C}$ NMR of <b>TOP066</b> .....	290
Figure A3.15. $^1\text{H}$ NMR of <b>TOP067</b> .....	291
Figure A3.16. $^{13}\text{C}$ NMR of <b>TOP067</b> .....	292
Figure A3.17. $^1\text{H}$ NMR of <b>TOP068</b> .....	293
Figure A3.18. $^{13}\text{C}$ NMR of <b>TOP068</b> .....	294
Figure A3.19. $^1\text{H}$ NMR of <b>TOP069</b> .....	295
Figure A3.20. $^{13}\text{C}$ NMR of <b>TOP069</b> .....	296
Figure A3.21. $^1\text{H}$ NMR of <b>TOP070</b> .....	297
Figure A3.22. $^{13}\text{C}$ NMR of <b>TOP070</b> .....	298
Figure A3.23. $^1\text{H}$ NMR of <b>TOP075</b> .....	299
Figure A3.24. $^{13}\text{C}$ NMR of <b>TOP075</b> .....	300

## List of Schemes

Scheme 1.1. Proposed mechanism for Maxam-Gilbert sequencing on purines <sup>13</sup> ....	6
Scheme 1.2. Maxam-Gilbert Sequencing on C .....	6
Scheme 1.3. Alkylation of guanosine by electrophile .....	9
Scheme 1.4. Covalent modification of adenosine .....	10
Equation 1.1. Determining binding of small molecules to DNA .....	27
Scheme 1.5. Proposed mechanism for cyclopropyl-based alkylating agents .....	32
Scheme 1.6. Triggering of esperamicin <sup>103,105</sup> .....	39
Scheme 1.7. Different H-abstraction motifs on the ribose backbone of DNA <sup>114</sup> ..	41
Scheme 1.8. Proposed mechanism of BLM-Fe(II)-induced DNA cleavage .....	43
Scheme 2.1. Possible DNA replication outcomes .....	66
Scheme 2.2. DNA modification at guanosine by benzo[ $\alpha$ ]pyrene diol epoxide <sup>11</sup> ..	66
Scheme 2.3. Conversion of nicotine to NNN-5'-OH .....	67
Scheme 2.4. Metabolic activation of NNK .....	68
Scheme 2.5. NNAL DNA adduct formation .....	69
Scheme 2.6. NNN DNA adducts on guanosine .....	71
Scheme 2.7. Using PLE to mimic biological oxidation of NNN .....	72
Scheme 2.8. Proposed mechanism of enzymatic deprotection of NNN-5'-OAc ...	72
Scheme 2.9. Previously reported route to NNN-5'-OAc .....	73
Scheme 2.10. Retrosynthetic analysis of NNN-5'-OH .....	73
Scheme 2.11. Previous synthesis of isomyosmine .....	74
Scheme 2.12. Thermal rearrangement of cyclopropylimine to give isomyosmine <sup>27</sup>	74
Scheme 2.13. Sulfonamide cyclization to generate pyrroline .....	75
Scheme 2.14. Route to racemic <i>tert</i> -butylsulfonamide <sup>33</sup> .....	76

Scheme 2.15. <i>Organic Syntheses</i> preparation for ( <i>R</i> )- <i>tert</i> -butyl sulfinamide <sup>34</sup> .....	76
Scheme 2.16. Asymmetric synthesis of <i>tert</i> -butyl sulfinamide <sup>33</sup> .....	77
Scheme 2.17. Nucleophilic Addition to Sulfinimines. <sup>35</sup> .....	77
Scheme 2.18. Open and closed transition states for addition to chiral sulfinimine.	78
Scheme 2.19. Addition of $\alpha$ -phosphonate <sup>43</sup> and phosphites <sup>43,44</sup> to sulfinimines.....	79
Scheme 2.20. Asymmetric Rh(I)-catalyzed addition to <i>t-butyl</i> sulfinimine. <sup>45</sup> .....	79
Scheme 2.21. Sulfinimine three-component coupling with allene and aryl iodide <sup>46</sup>	80
Scheme 2.22. Enolate addition to sulfinimines. ....	80
Scheme 2.23. Aziridinations using sulfinimines <sup>50-52</sup> .....	81
Scheme 2.24. Sulfinimines in 1,4-conjugate addition-electrophilic trapping <sup>53</sup> .....	82
Scheme 2.25. <i>N</i> -sulfinyliminoacetates under reductive conditions. <sup>54</sup> .....	82
Scheme 2.26. Reductive asymmetric coupling of sulfinimines with aldehydes. <sup>55</sup>	83
Scheme 2.27. Formation of $\alpha$ -fluoroamines using chiral sulfinamines. <sup>55</sup> .....	83
Scheme 2.28. Use of TMS-alkanes as pro-nucleophiles to alkylate sulfinimines.	84
Scheme 2.29. Vinylation using rhodium catalyst. ....	85
Scheme 2.30. Attempts to perform photocyclization to generate isomyosmine. ..	86
Scheme 2.31. Grignard addition to sulfinimine .....	86
Scheme 2.32. Deprotection of <b>MIS087</b> to generate isomyosmine .....	88
Scheme 2.33. Optimization of temperature for nitroso-acylation of isomyosmine	89
Scheme 2.34. Deprotection of <b>MIS087</b> followed by nitroso-acylation.....	89
Scheme 2.35. Total synthesis of NNN-5'-OAc. ....	93
Scheme 2.36. Independent synthesis of hydrolyzed NNN-5'-OAc .....	94
Scheme 2.37. Proposed mechanism for hydrolysis of NNN-5'-OAc .....	94
Scheme 2.38. Adduction of 2-deoxyguanosine by NNN-5'-OAc. <sup>21</sup> .....	95
Scheme 2.39. Reversibility of NNN-5'-OAc adduct formation with guanosine .	105



Scheme 3.1. Possible mechanisms for DNA modification by aza-enediyne.....	126
Scheme 3.2. Bergman and aza-Bergman cyclization .....	127
Scheme 3.3. Aza-Bergman followed by retro-aza-Bergman <sup>6</sup> .....	128
Scheme 3.4. Unsuccessful attempts to trap proposed intermediate .....	128
Scheme 3.5. Position of protonation of aza-enediyne .....	131
Scheme 3.6. Attempt to mimic a protonated aza-Bergman cyclization. ....	131
Scheme 3.7. Proposed pathway for thermolysis of dialkynylimidazoles. <sup>12</sup> .....	132
Scheme 3.8. Myers-Saito cyclization .....	133
Scheme 3.9. Schmittel cyclization .....	133
Scheme 3.10. Aza-Schmittel and Aza-Myers-Saito .....	134
Scheme 3.11. Trapping products of an aza-Myers-Saito cyclization <sup>18</sup> .....	134
Scheme 3.12. Possible modes of DNA modification .....	137
Scheme 3.13. Possible outcomes of benzimidazolium with various nucleophiles	140
Scheme 3.14. Modification of guanosine N7 .....	151
Equation 3.1. Normalization of % cleavage .....	151
Scheme 3.15. Proposed <b>AZB017</b> analog synthesis .....	157
Scheme 3.16. Synthesis of benzimidazoles .....	158
Scheme 3.17. Initial methylation strategy .....	159
Scheme 3.18. Synthesis of methylated benzimidazolium salts .....	159
Scheme 3.19. Cyclization of <b>AZB380</b> .....	160
Equation 3.2. Determination of % Nicking .....	161
Equation 3.3. Normalization of % Nicking .....	161
Scheme 4.1. Proposed Biosynthesis of UK-1 <sup>2</sup> .....	189
Scheme 4.2. Total Synthesis of UK-1 <sup>11</sup> .....	191
Scheme 4.3. Route to benzoxazole UK-1 analog <b>TOP027</b> .....	194

Scheme 4.4. C4 analogs of minimum pharmacophore <sup>13</sup> .....	197
Scheme 4.5. General scheme for benzoxazole from <i>o</i> -aminophenol. ....	199
Scheme 4.6. Combination of acid chloride with <i>o</i> -aminophenol. ....	199
Scheme 4.7. Synthesis from trifluoromethyl ketone and <i>o</i> -aminophenol. ....	199
Scheme 4.8. 2-Aryl benzoxazole using <i>o</i> -aminophenol and aryl aldehyde.....	200
Scheme 4.9. Synthesis of 2-aryl benzoxazoles using a benzylic alcohol .....	200
Scheme 4.10. Triphenylphosphine-carbon tetrachloride mediated coupling .....	201
Scheme 4.11. Using copper (I) to combine 1,2-dihalobenzene and amide .....	201
Scheme 4.12. O-Arylation to close benzoxazole ring .....	202
Scheme 4.13. Pd-catalyzed CO insertion to form benzoxazole ring .....	202
Scheme 4.14. Coupling at C2 of unsubstituted benzoxazole. <sup>44</sup> .....	203
Scheme 4.15. Modified Suzuki coupling at C2 of benzoxazole. <sup>46</sup> .....	204
Scheme 4.16. Retrosynthetic analysis of minimum pharmacophore analogs. ....	206
Scheme 4.17. Amide from benzyloxysalicylic acid and 2,6-dibromoaniline.....	206
Scheme 4.18. Optimization of Cu(I)-catalyzed benzoxazole ring closing. ....	208
Scheme 4.19. CO insertion onto 4-bromobenzoxazole .....	209
Scheme 4.20. Amide formation with varied acid chlorides.....	209
Scheme 4.21. Revised retrosynthetic analysis .....	210
Scheme 4.22. Synthesis of 3-methoxy-2-nitrobenzoic acid. ....	211
Scheme 4.23. Synthesis of the HCl salt of 3-hydroxy anthranilic acid methyl ester.	211
Scheme 4.24. Formation of thiobenzoxazole via aqueous, basic carbon disulfide <sup>49</sup>	211
Scheme 4.25. Phosgene addition to 3-hydroxyanthranilic acid methyl ester .....	212
Scheme 4.26. Synthesis of coupling partner.....	212
Scheme 4.27. Optimization of Coupling Reaction .....	213
Scheme 4.28. Couplings to assemble library of C2-aryl benzoxazoles.....	215

Scheme 4.29. Proposed route to UK-1. ....215

## 1. Introduction

Small molecules that interact with DNA are important as potential pharmaceuticals and carcinogens. Understanding these DNA-small molecule interactions is critical to drug design, because DNA is responsible for all cellular functions. Small molecules that interact strongly with DNA can cause damage to the cell or organism.<sup>1</sup> Covalent or non-covalent DNA modification can cause errors in transcription and subsequent translation of DNA to proteins (Figure 1.1).<sup>2</sup> Damage that prevents proper replication and cell division can lead to cell death, and damage that affects genetic function can have deleterious effects, such as cancer. Luckily, agents that damage DNA can also have positive effects, such as antineoplastic or antibacterial compounds, which also cause cell death, but for therapeutic purposes. In this dissertation, both carcinogenic and cytotoxic DNA-interactive agents will be examined.

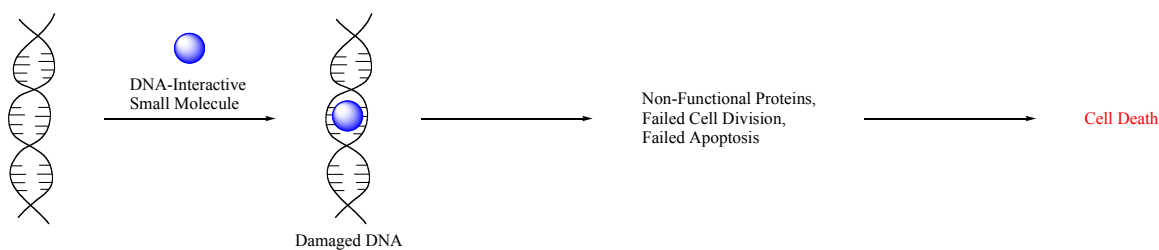


Figure 1.1. DNA damage leading to cell death.

In this introductory chapter, a brief overview of methods to quantify and determine the nature of DNA-small molecule interactions will be discussed. Following an introduction to the structure of B-form DNA and methods to determine the sequence of unmodified DNA, methods used to analyze small molecule covalent adducts of DNA will be described. Then, an overview of some common methods of analyzing non-covalent

DNA-small molecule interactions will be provided. Finally, some examples of DNA-interactive small molecules will illustrate common structural motifs that direct DNA binding mode and sequence selectivity.

### 1.1. STRUCTURE OF DNA

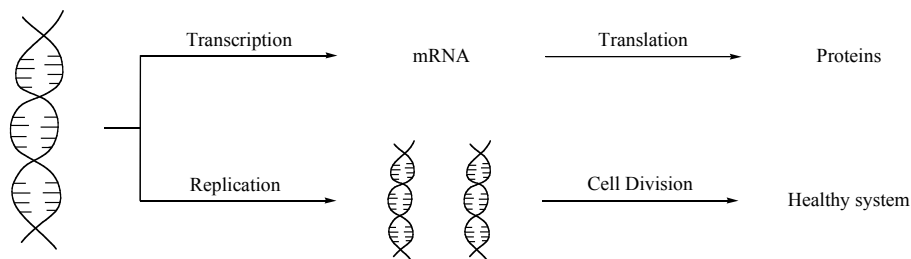


Figure 1.2. DNA's function in biological systems<sup>1</sup>

Deoxyribonucleic acid (DNA) is the simple and robust genetic code for all living things. Through variation of four nucleotide bases, DNA encodes all the genetic information for entire organisms. A basic principle of molecular biology is the transcription of DNA to messenger RNA (mRNA), which then is translated into proteins (Figure 1.2).<sup>1</sup> It is a polymeric structure consisting of a sugar-phosphate backbone with either a purine or pyrimidine ring system attached at the 1'-position on the ribose. Numbering of atoms on the nucleotides is shown in Figure 1.3. Nucleotides are linked together in a polymer from the 5' to 3' position on the ribose unit to form single strands of DNA.

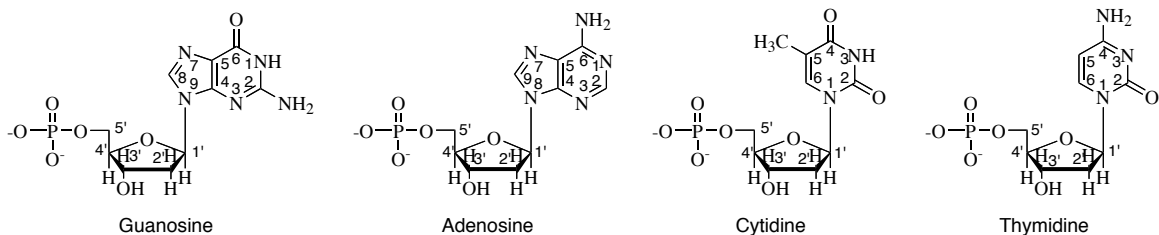


Figure 1.3. Structure of Nucleotides

This single-stranded polymer assembles into a tertiary structure, commonly a duplex form in an antiparallel double-helix where the bases  $\pi$  stack internally and the phosphate backbones form a hydrophilic exterior (Figure 1.4). For the purposes of this discussion, only the most common tertiary structure, B-form DNA,<sup>3</sup> will be discussed. The formation of a double-helix is driven by hydrogen-bonding interactions between purine and pyrimidine base pairs (with guanosine paired to cytidine and adenosine to thymidine) and hydrophobic interactions when the bases  $\pi$  stack. The free energy of an A-T base pair has been computationally estimated to be -4.3 kcal/mol, and a G-C base pair is estimated to be -5.8 kcal/mol.<sup>4</sup> The distance from C1' to C1' in a G-C base pair is 10.67 Å, and an A-U pair is 10.48 Å.<sup>5</sup> The purine C1'-N9 base-sugar bonds or pyrimidine C1'-N1 base-sugar bonds are on the minor groove of the helix, and the C6/N7 (purine) or C4 (pyrimidine) atoms and their substituents are on the major groove (Figure 1.5).<sup>5</sup> In B-DNA, the right-handed helix contains ten base pairs per complete turn, with the base pairs nearly perpendicular to and stacking over the helical axis.<sup>5</sup> The helical axis in B-form DNA is not linear; it is distorted by approximately 19°.<sup>5</sup>

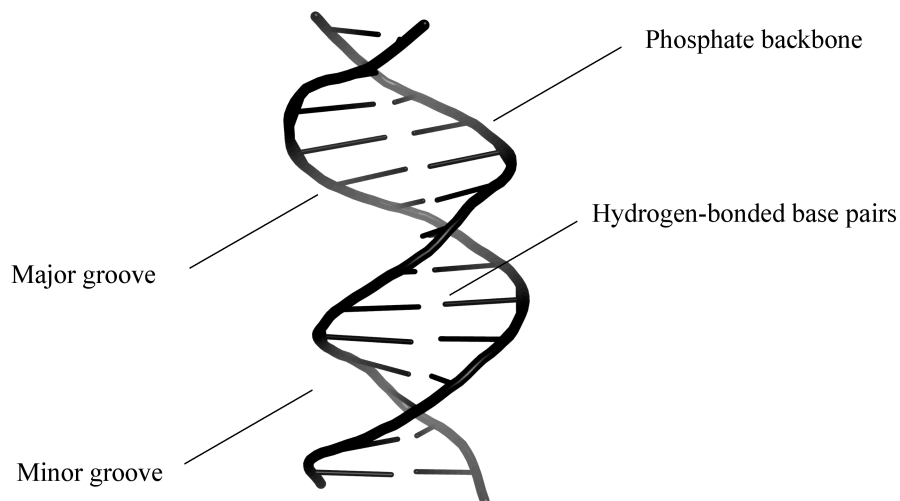


Figure 1.4. Diagram of B-form DNA.

The major groove of B-DNA is 11.6 Å wide and 8.5 Å deep. The minor groove is, on average, 6.0 Å wide (ranging from 2.6-8.9 Å as determined for a series of decamers by X-ray crystallography<sup>6</sup>) and 8.2 Å deep.<sup>5</sup> AT-rich DNA tends to have a wider major groove (and thus a more narrow minor groove) than GC-rich DNA.<sup>5,6</sup> The repulsion between the anionic backbone phosphates is the structural feature that limits minimum width of the helical grooves.<sup>6</sup> Normal distance along the helical axis between the parallel  $\pi$  stacked bases is 3.4 Å.<sup>5</sup>

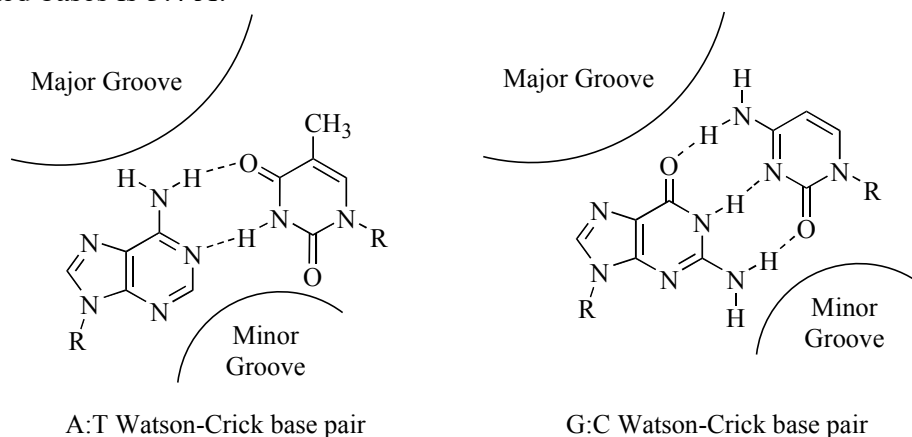


Figure 1.5. Watson-Crick Base Pairs

## 1.2. DNA SEQUENCING

Techniques to sequence DNA were initially developed nearly 15 years after the structure of DNA was elucidated. Since the development of sequencing, the number of reported DNA sequences has doubled every 16 months, increasing logarithmically by nine orders of magnitude between 1965 and 2005.<sup>7</sup>

The original method for chemically sequencing DNA was described by Maxam and Gilbert.<sup>7,8</sup> This method has been supplanted by more efficient and high-throughput methods,<sup>7,9</sup> but it is still widely used for sequencing short DNA fragments and in studies

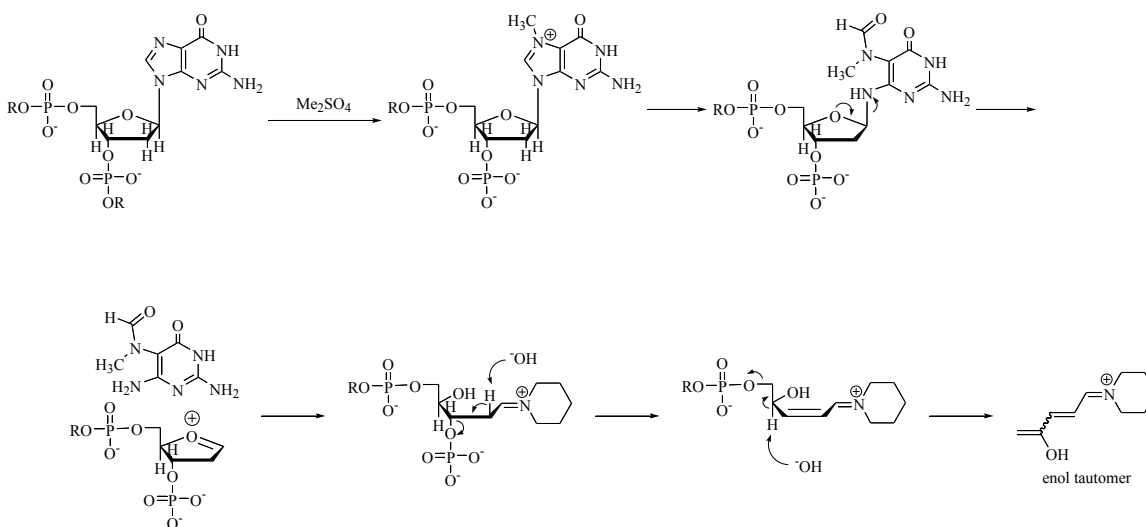
of small-molecule DNA interactions. The Maxam-Gilbert sequencing technique relies upon chemical reactions that selectively modify either for purines (G+A) or pyrimidines (T+C), and reactions selective for G or C,<sup>8</sup> followed by treatment with piperidine at elevated temperatures to cause DNA strand cleavage at the modified positions.

The original series of chemical reactions involved selective reactions with either purines or pyrimidines.<sup>8</sup> Guanosine residues are modified at the N7 position (located in the major groove), and adenosines are modified at N3 and N7 by dimethyl sulfate (Scheme 1.1).<sup>10</sup> Alkylated adenosines and guanosine residues both undergo depurination in the presence of either acid or piperidine and heating.<sup>8,11</sup> Thymidine and cytidine are both modified by incubation with hydrazine, but performing the same incubation in the presence of sodium chloride attenuates reactivity of the hydrazine with thymidines, allowing selective sequencing of cytosines.<sup>8,10</sup> The hydrazine opens the pyrimidine ring, converting it to a good leaving group (Scheme 1.2).<sup>10</sup>

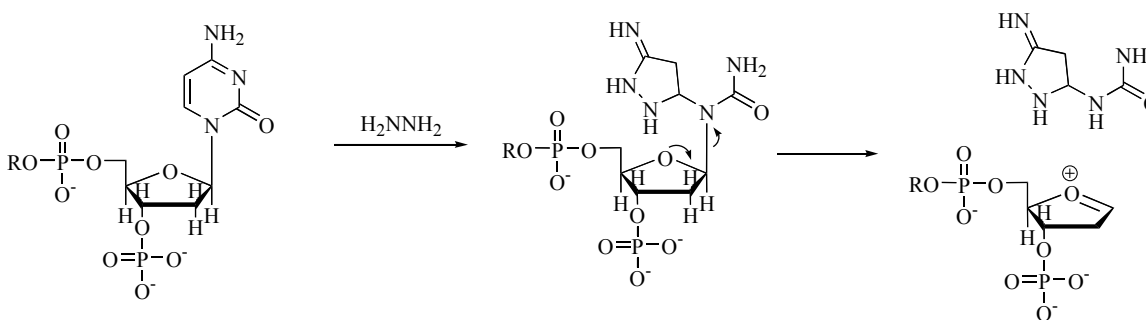
After the base-selective reactions, the DNA is purified via ethanol precipitation (to remove both excess reagents and short fragments of DNA cleaved by frank strand cleavage during the selective reactions). The purified DNA is then subjected to piperidine-heat treatment, which causes quantitative cleavage of the DNA at its backbone.<sup>12,13</sup> Upon heating the modified base leaves, assisted by electron donation from the oxygen in the furanose ring (Scheme 1.1). Piperidine attacks the resultant cyclic oxonium ion to generate the acyclic iminium ion, which then undergoes two elimination reactions (losing both phosphates) to give cleavage of the phosphate DNA backbone. The first elimination is likely a  $\beta$ -elimination, but the loss of the proton at C4' of the deoxyribose has not been shown experimentally, and the products of this proposed elimination have not been characterized.<sup>14</sup> The resulting DNA fragments are separated by polyacrylamide gel electrophoresis (PAGE).<sup>8</sup> Visualization of these fragments on the gel



often is accomplished by autoradiography, which requires that the original DNA be labeled, typically with  $^{32}\text{P}$ , at either the 5'- or 3'-end.<sup>8</sup>



Scheme 1.1. Proposed mechanism for Maxam-Gilbert sequencing on purines<sup>13</sup>



Scheme 1.2. Maxam-Gilbert Sequencing on C

### 1.3. SMALL MOLECULE-DNA INTERACTIONS

Agents with the ability to disrupt DNA replication or transcription are potentially useful as antineoplastic agents. In this section, methods of analyzing small molecule-DNA interactions will be discussed. Either covalent or non-covalent interactions can significantly alter DNA replication. When a DNA-small molecule interaction is analyzed,

two pieces of information are key to understanding the downstream effects: where the DNA-drug interaction occurs (sequence specificity and binding mode), and how strongly the two molecules interact (covalent modification, tight non-covalent binding, or weak noncovalent interaction). There are several types of both covalent and noncovalent interactions. Figure 1.6 illustrates the types of interactions that will be described in this introductory chapter. Alkylating agents with one reactive electrophilic site can modify nucleotide bases (alkylation), and alkylating agents with two reactive electrophilic sites can covalently link the two strands (crosslinking). Some small molecules modify DNA via oxidative damage, i.e. removal of a hydrogen atom from the ribose backbone. Intercalating agents, which typically contain a planar extended conjugated  $\pi$  system, noncovalently bind in between the  $\pi$ -stacked nucleotide bases. Minor groove binders, which are usually rigid, bent molecules, bind along the minor groove of DNA.

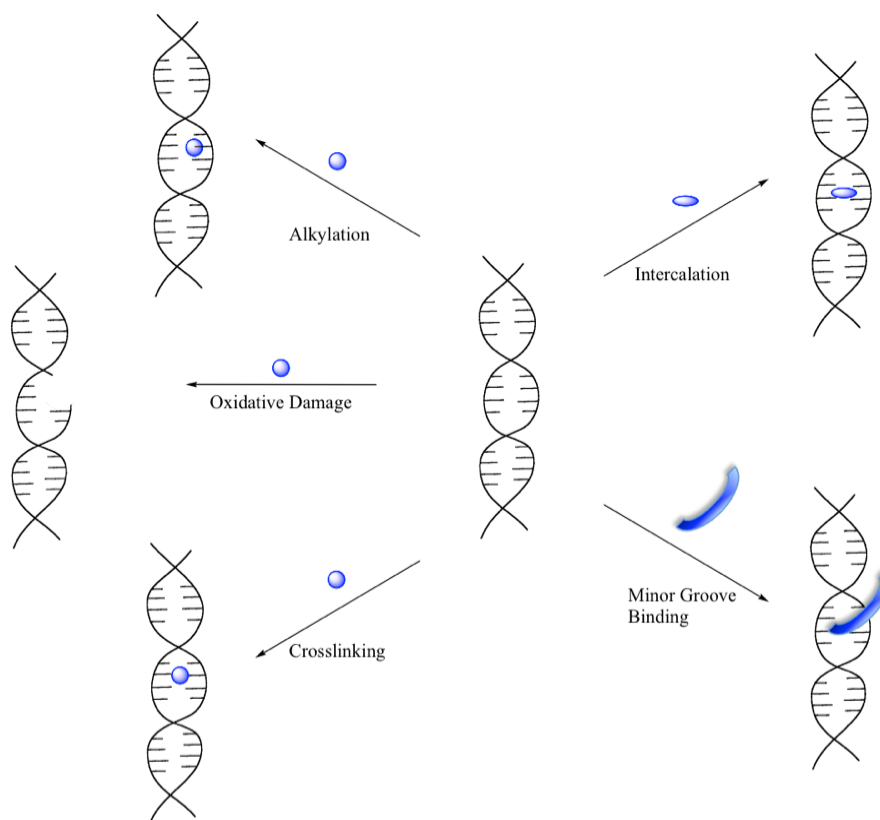
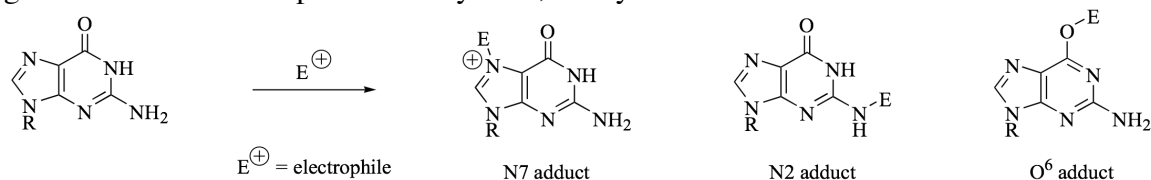


Figure 1.6. DNA binding motifs

### 1.3.1. DNA Alkylation

DNA alkylation is a common mode of covalent modification. Alkylation can either lead to cytotoxicity (cell death), or mutagenicity.<sup>15</sup> In the case of antineoplastic agents, cell death is therapeutic (rather than harmful). Examples of alkylating agents that react with a bimolecular rate as a neutral compound ( $S_N2$ ) include alkyl halides, alkyl sulfonates, and epoxides.<sup>15</sup> Alkylating agents that react by an  $S_N1$  type mechanism typically generate cationic intermediates as the electrophile that covalently modifies DNA.<sup>16</sup> Guanine contains three commonly modified nucleophilic sites, N2, N7, and O<sup>6</sup> (Scheme 1.3). Cytidine contains two nucleophilic sites that can react with these

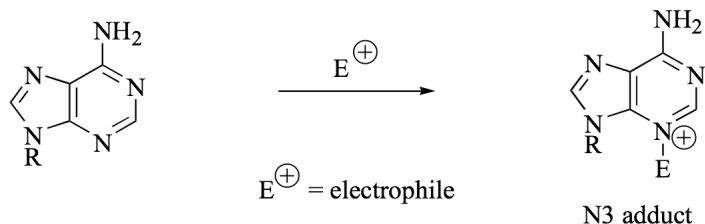
electrophiles, the exocyclic amine (N3) and carbonyl (O<sup>1</sup>). Simple alkylating agents (mustard gases, chloroethyl-nitrosourea,<sup>17</sup> and dimethylsulfonates<sup>18</sup> – discussed in detail in a later section of this chapter) commonly modify guanosines.<sup>16</sup> More complex alkylating reagents (i.e. CC-1065 or tallimustine, discussed in Section 1.4.1.1.) typically alkylate on N3 of adenosine (Scheme 1.4), which is located in the minor groove of duplex DNA.<sup>19</sup> Alkylation at N3 of adenine is especially harmful because it creates a nucleoside that is incapable of forming a hydrogen-bonded base pair.<sup>1</sup> This causes DNA replication to stall, which leads to cell death.<sup>1</sup> Alkylations of guanine proceeding via an S<sub>N</sub>1-type mechanism show increased modification of N7 and O<sup>6</sup>; S<sub>N</sub>2-type alkylations occur at N7, which is located in the major groove of the double helix.<sup>15</sup> The biological consequences of O-alkylation of guanine are typically severe, as this modification can result in more mutations than any other alkylation of DNA because of mis-pairing at the alkylated position during replication.<sup>15</sup> Alkylation at O<sup>6</sup> changes the tautomeric form of guanine so that it base pairs with thymine, not cytosine.<sup>1</sup>



Scheme 1.3. Alkylation of guanosine by electrophile

Duplex DNA is less easily modified by alkylating agents than single-stranded DNA because Watson-Crick pairing increases steric bulk at nucleophilic sites and decreases nucleophilicity because of the hydrogen bonding.<sup>15</sup> Although alkylations were once thought to have base selectivity but no sequence selectivity (for example, the G reaction in Maxam-Gilbert sequencing), it has been shown that even simple alkylating reagents such as diazomethane or acetoxymethylmethylnitrosamine have a sequence selectivity that depends on the 5' neighboring base (G leads to more frequent

modification) and slightly on the 3' neighboring base (GG>GA>GC>GT).<sup>15</sup> This data, in concert with theoretical calculations,<sup>16</sup> shows that sequence selectivity can be attributed to electrostatic interactions between charged alkylating agents and the nucleophilic guanosine.<sup>15</sup>



Scheme 1.4. Covalent modification of adenosine

### 1.3.2. Analysis of DNA Alkylation

#### 1.3.2.1. Electrophoretic mobility shift assays

Possibly the simplest assay to probe for covalent modification of DNA is an electrophoretic mobility shift assay (EMSA, Figure 1.7). In this method, a short radiolabeled DNA oligomer is incubated with the potential alkylating agent, and the mixture is analyzed by gel electrophoresis.<sup>20</sup> In the case of DNA modified by alkylating agents, this method can show singly and multiply adducted DNA, provided that the modification changes the electrophoretic mobility of the oligomer.<sup>21</sup>

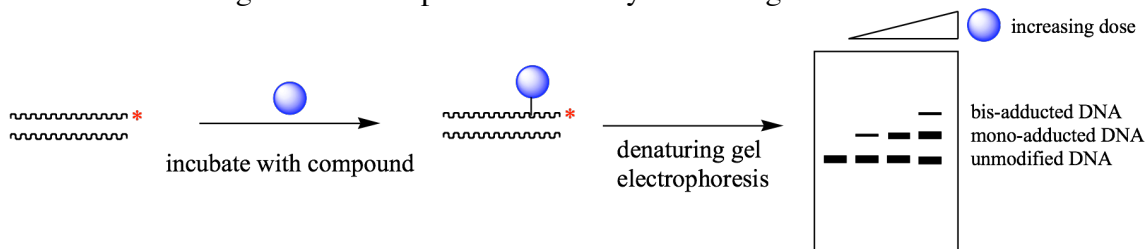


Figure 1.7. Electrophoretic mobility shift assay

A similar mobility shift assay can be used to measure effective concentrations of the small molecule, as well as to explore sequence selectivity of crosslinkers (Figure 1.8).<sup>21</sup> Crosslinkers are agents that chemically link two molecules, in this case two DNA strands, by a covalent bond. Although other methods are known to evaluate potentially crosslinked DNA<sup>22</sup> a simple method for analyzing crosslinks is denaturing gel electrophoresis.<sup>22</sup> Self-complementary double-stranded DNA is typically used because having identical upper and lower strands simplifies oligomer design; however, only one oligomer in the duplex must be labeled for quantification.<sup>21,22</sup> Incorporating unnatural bases and determining whether they inhibit crosslinking can provide information regarding structure of the crosslinked site on the bases.<sup>21</sup> The DNA is prepared by radiolabeling and annealing as described in Figure 1.9. Increasing concentrations of the compound of interest are incubated with the ds-DNA (Figure 1.8) then the DNA is denatured using either alkali (sodium hydroxide, pH 12-12.5) or heating followed by rapid cooling.<sup>22</sup> The denatured DNA can then be analyzed using either gel electrophoresis (agarose or denaturing polyacrylamide gel) or chromatography (ion-exchange, size-exclusion, or affinity).<sup>22</sup> The crosslinked DNA will not denature to single-stranded DNA because the two strands are covalently linked, so lower mobility bands will be observed. Sequence information about the crosslinks can be obtained by subjecting the DNA to exonuclease III digestion.<sup>21</sup> This digestion causes exolytic degradation from the unlabeled 3'-end of the DNA (stopping 1-3 bases before the adduct), which provides information about the site of the crosslink based on the mobility of the covalently bound duplex.<sup>21</sup>

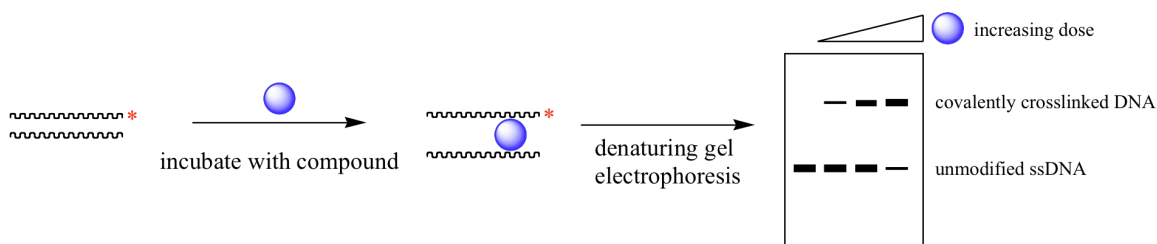


Figure 1.8. DNA crosslinking assay

### 1.3.2.2. Chemical cleavage of covalent adducts

While the gel-shift assays described above are useful for revealing the presence of covalent DNA modification, they do not provide information about which DNA residues are involved in these covalent adducts. Fortunately, in many cases this information can be obtained by simply treating the modified DNA with piperidine at elevated temperature. As in Maxam-Gilbert sequencing (Scheme 1.1), this causes DNA strand breaks at the position of the modified DNA base, allowing visualization of the positions of adduction (Figure 1.9) by polyacrylamide gel electrophoresis (PAGE). Piperidine-heat treatment can be used to map N7 guanine or adenosine adducts.<sup>12,23</sup> The cationic alkylated base is cleaved (depurination), leaving an abasic site, which is labile to hydrolysis of the backbone.<sup>24</sup> Depurination of methylated adenosines (N3 or N7) and guanosines (N7) can occur at room temperature under neutral pH, but the rate is very slow (half-life of 2.8 h-155 h).<sup>17,25</sup> Although N1 of cytosine is subject to alkylation, piperidine/heat treatment does not generate an abasic site and subsequent strand break.<sup>24</sup>

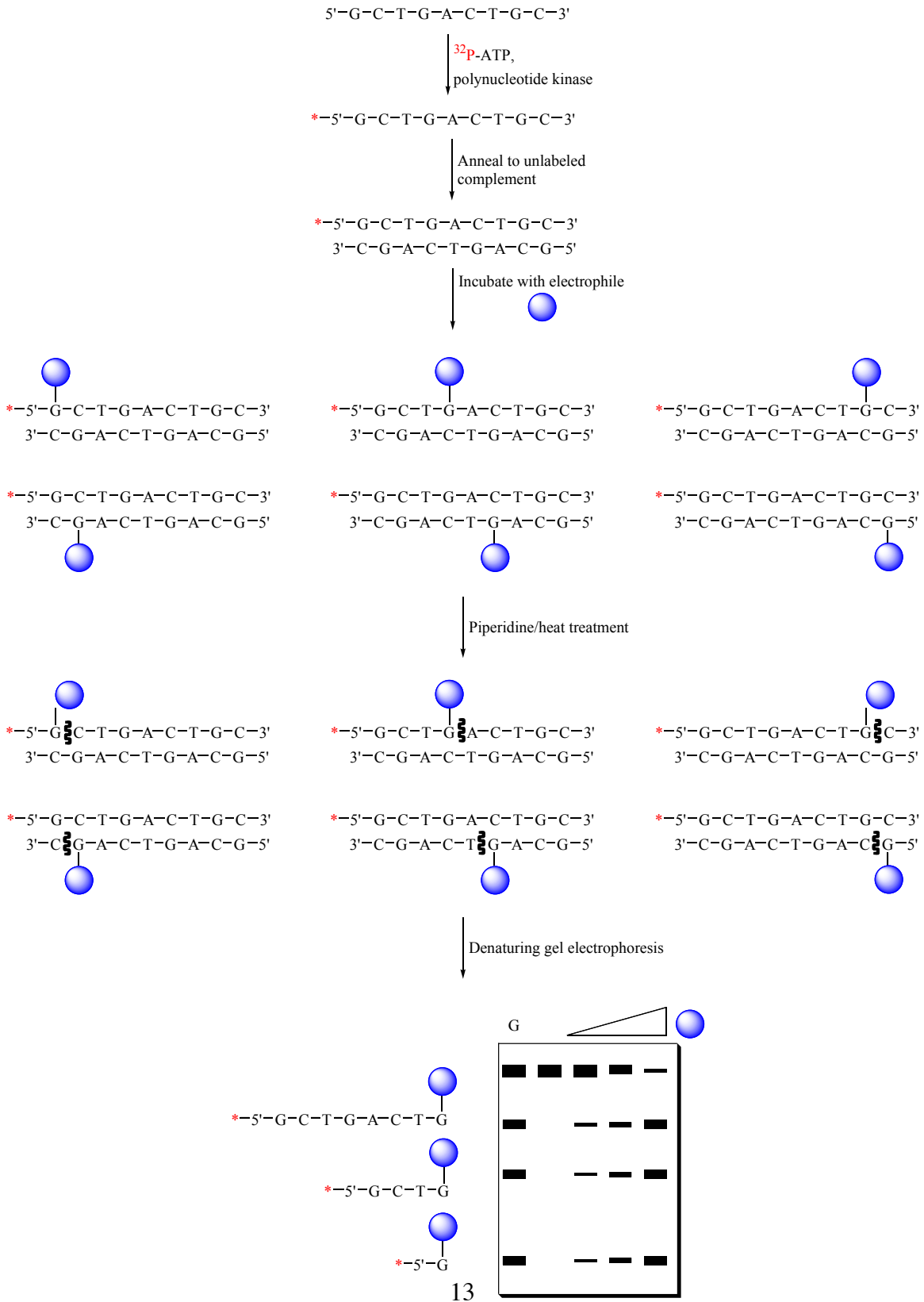




Figure 1.9. Analysis of Covalent DNA Modification *via* Piperidine/Heat Treatment

### 1.3.2.3. <sup>32</sup>P-Postlabeling

First reported in 1981 by Randerath,<sup>26</sup> <sup>32</sup>P-postlabeling (Figure 1.10) rapidly became the most widely used and sensitive method for detecting DNA adducts in biological samples. In <sup>32</sup>P-postlabeling the sample of DNA incubated with the small molecule is subjected to digestion with nucleases (typically micrococcal endonuclease and spleen exonuclease) to afford a mixture of unmodified and modified nucleotide 3'-phosphates *via* cleavage of the glycosidic linkages.<sup>26-28</sup> This mixture of modified and unmodified nucleotide monophosphates then can be analyzed in one of two ways. One way to analyze samples is to quantitate adduction by using a large excess of <sup>32</sup>P-labeled adenosine triphosphate ([ $\gamma$ -<sup>32</sup>P]-ATP) in the presence of polynucleotide kinase to radiolabel the nucleotides.<sup>26,27</sup> This mixture can then be analyzed by two-dimensional thin layer chromatography (2D-TLC) on cellulose paper to quantify adducts.<sup>29</sup> Because a large excess of [ $\gamma$ -<sup>32</sup>P]-ATP is used to drive the reaction to completion, all the bases are assumed to be labeled with equal efficiency, regardless of covalent modification, and the method is considered quantitative.<sup>29</sup> Alternatively, to intensify detection of the covalent adducts relative to the background signal of the unmodified bases, P<sub>1</sub> nuclease can be used to selectively dephosphorylate the unmodified nucleotides to their deoxyribosides preferentially to the modified nucleotides.<sup>30,31</sup> Because the unmodified bases do not have the required monophosphate or free hydroxyl group, only the modified adducts are enzymatically labeled at the 5' position.<sup>31</sup> This effectively amplifies the signal from modified bases, allowing greater sensitivity. These labeled nucleotides are then separated by 2D chromatography using cellulose paper. The P<sub>1</sub> nuclease digestion leads to a 300-

1000-fold increase in radioactivity at the modified bases.<sup>31</sup> This technique works well, particularly for DNA adducts where the modified nucleotides are easily separated from unmodified nucleotides, e.g., in the case of polycyclic aromatic hydrocarbon adducts.<sup>30</sup> Another advantage is sensitivity. <sup>32</sup>P-postlabeling can detect 0.5-5 adducts in 10<sup>8</sup> DNA bases employing samples as small as 10 μg of DNA.<sup>31</sup> Also, because radiolabeling occurs post-exposure, it can be very practical for analyzing biological samples without requiring radiolabeled alkylating agents or oligomer. A disadvantage of this approach is that it does not provide information about the structure of the adduct, unless suitable authentic samples are available. Because of this limitation, particularly for DNA adducts which are difficult to resolve by TLC (because of lability or polarity), mass spectrometric methods (discussed in section 1.3.5.1) are beginning to supplant <sup>32</sup>P-postlabeling as the method of choice for adduct detection and identification.

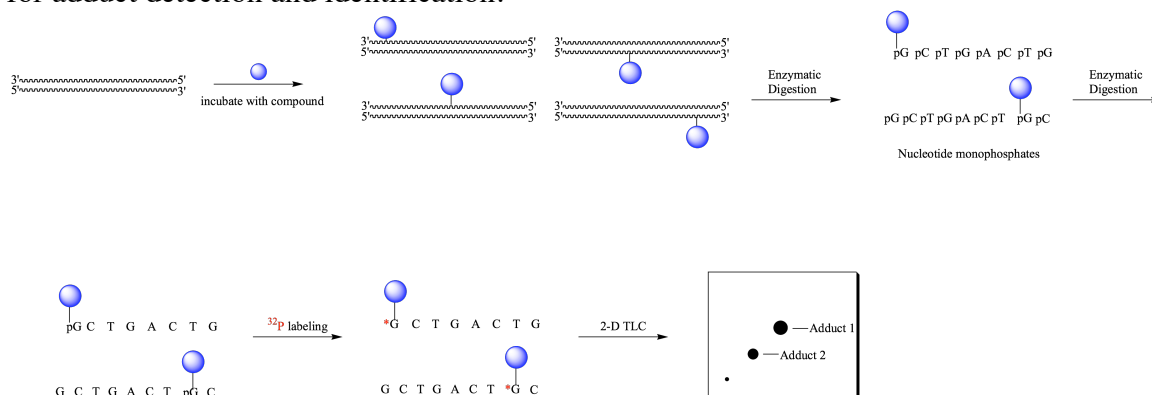


Figure 1.10. <sup>32</sup>P -Postlabeling to identify covalent modification

### 1.3.3. DNA Footprinting

#### 1.3.3.1. Enzymatic and Chemical Footprinting

Since its development in 1978, DNA footprinting (Figure 1.12) has been used to analyze sequence selectivity of both covalent and non-covalent interactions.<sup>32</sup> For the purposes of this discussion, only techniques that analyze small-molecule-DNA

interactions will be reviewed. To analyze small-molecule-DNA interactions, a small (100-200bp) radiolabeled DNA oligomer of known sequence is combined with the DNA-interactive compound (Figure 1.12).<sup>32</sup> The DNA is then exposed to some agent that will cleave the DNA backbone at each base, except where the DNA-interactive compound is bound. Cleavage agents can be either chemical or enzymatic.<sup>32</sup> Common enzymes used include DNase I, DNase II, micrococcal nuclease,<sup>33</sup> and exonuclease III.<sup>32,34,35</sup> DNase I footprinting is extremely common<sup>36</sup> and requires mild, physiologically relevant conditions, but it has the disadvantage that the enzymatic DNA cleavage exhibits a slight sequence selectivity.<sup>32,37</sup> Also, enzymatic footprinting typically leaves a footprint that extends several bases beyond the actual modification.<sup>38-40</sup> Chemical footprinting reactions have the advantage that the cleavage is typically less sequence selective and generates a smaller footprint. Chemical cleavage agents include copper/phenanthroline,<sup>41,42</sup> Fe (II) methidium propyl-ethylene diamine tetraacetic acid (Fe(II)-MPE-EDTA, ),<sup>43</sup> and uranyl photocleavage.<sup>42,44-46</sup> The chemical cleavage agents operate by causing oxidative damage to the ribose units in the backbone of the DNA.

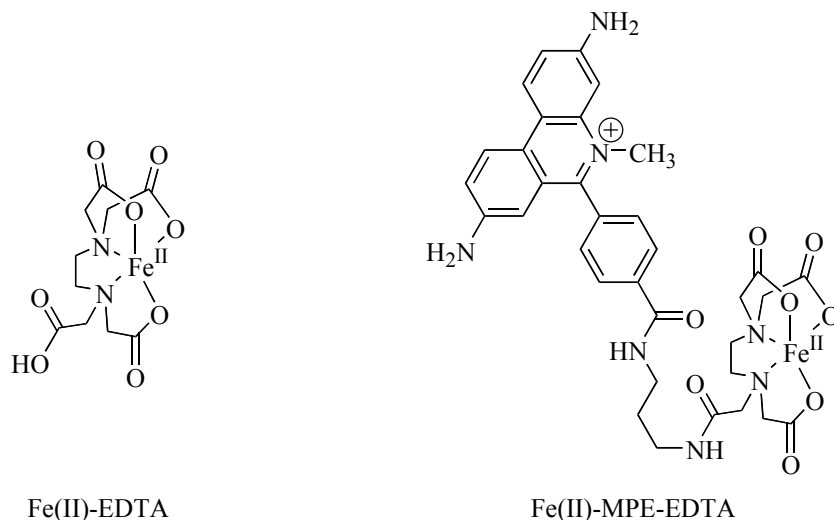


Figure 1.11. Iron (II)-EDTA (l) and Iron (II)-MPE-EDTA (r)

If the bound compound prevents a DNA cleavage event from occurring, a characteristic “footprint” appears when the DNA fragments are separated by gel electrophoresis and visualized using autoradiography (Figure 1.12). The footprint consists of an area where cleavage does not occur, which is observed as an absence of bands on the gel. Because only one end of one complementary strand of the DNA is labeled, only the labeled fragments will appear.<sup>32</sup> These observed fragments can be compared to sequencing lanes to determine the sequence selectivity of the DNA-interactive agent.<sup>32</sup> It is key to obtaining accurate results to ensure that each band is due to a single cleavage event (i.e. the DNA is cut only one time by the agent used).<sup>32</sup> This is termed “single-hit kinetics.”<sup>37</sup> In a typical experiment, to obtain a distinct footprint (under single-hit kinetics), the majority (60-90%) of the DNA is not cleaved.<sup>32</sup> Also, footprinting can be used to estimate binding constants for certain areas of the DNA sequence, if it is assumed that no cooperativity or interaction between binding sites occurs.<sup>47</sup>

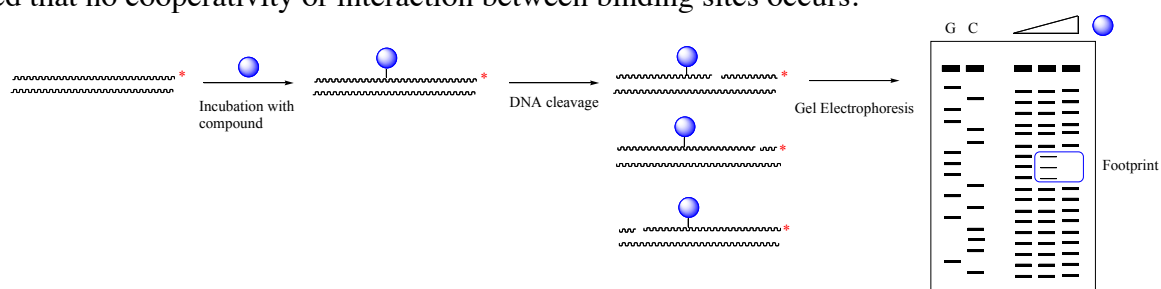


Figure 1.12. DNA footprinting

### 1.3.3.2. PCR-Based Footprinting

A variety of DNA polymerase inhibition assays adapt the typical PCR process to map DNA adduct positions. They give information about the position of adduction, but unlike footprinting, they do not provide information about the size of the binding region. Typical polymerase chain reaction (PCR), first described in 1985,<sup>48</sup> allows exponential

amplification of a DNA sequence (Figure 1.13). This process has been adapted to identify sequence selectivity of adduct formation. In routine PCR, duplex DNA containing the sequence of interest is denatured by heating in presence of a large excess of primers (12-20 base) single-stranded fragments of DNA complementary to either the 3' end of the lower strand or the 5' end of the upper strand of interest), a mix of deoxynucleotide triphosphates, and a polymerase enzyme. Because a large excess of primer is used, the primers anneal at the start of the desired sequence of each long strand when the PCR reaction mixture is cooled to temperatures 5 °C below the melting temperature of the primer-DNA duplex. The reaction mixture is heated to the optimal temperature for the polymerase to perform DNA chain elongation. The polymerase synthesizes the DNA beginning at the primer until it reaches the end of the sequence. The cycle is repeated, i.e. the DNA is denatured with heat, then the primers anneal, and the DNA is incubated to synthesize duplex DNA. In each successive PCR cycle, the desired sequence is amplified, and the initial sequence used (which may contain a longer sequence than desired) represents a smaller and smaller proportion of the reaction mixture. After many cycles (30 is typical), the desired sequence has been amplified and is highly homogeneous.

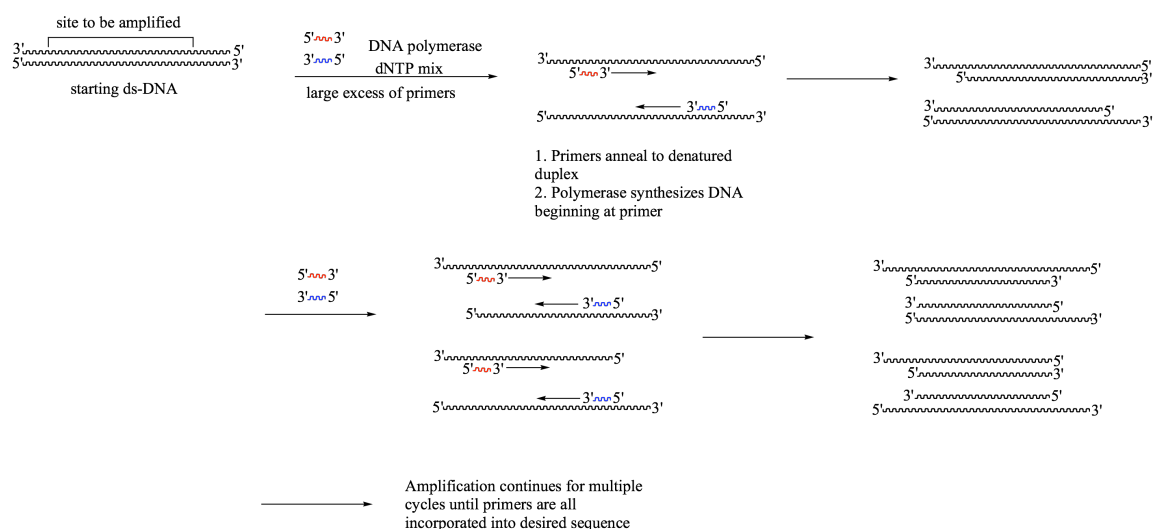


Figure 1.13. Polymerase chain reaction amplifies a DNA sequence

A variety of DNA polymerase inhibition assays adapt the typical PCR process to map DNA adduct positions (Figure 1.14).<sup>49</sup> They provide information about the position of adduction, but unlike footprinting, they do not provide information about the size of the binding region because the synthesis stops at the adduct, and the other (3') primer is unlabeled.

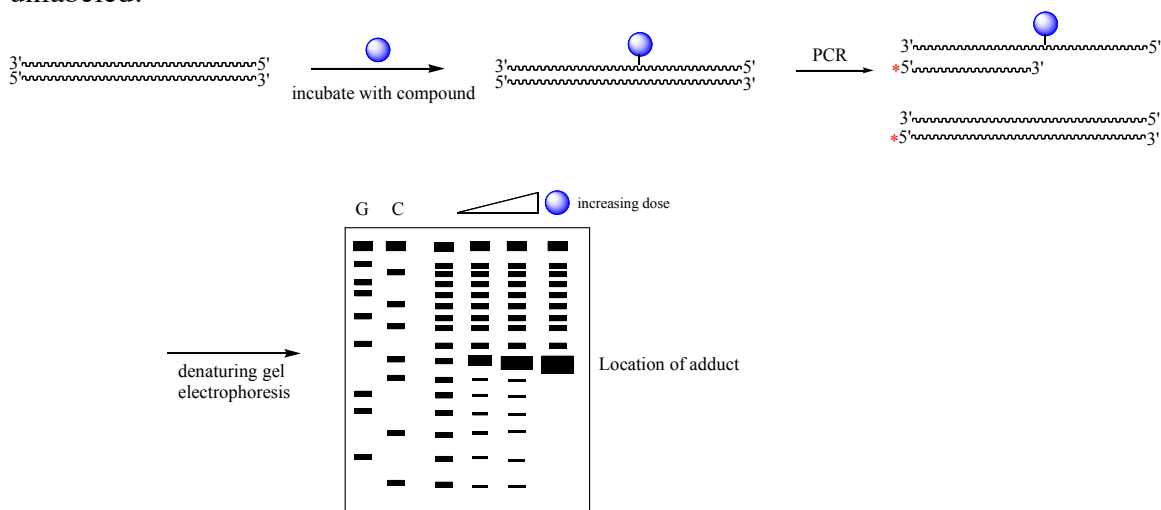


Figure 1.14. DNA Polymerase Interruption Assay

Commonly used PCR-based footprinting techniques include quantitative PCR (QPCR), strand-specific PCR (ss-QPCR), and single-strand ligation PCR (ssligPCR).<sup>50</sup> QPCR uses PCR techniques to analyze damage to both strands of DNA in the duplex.<sup>51,52</sup> The duplex is incubated with the drug of interest, then PCR is performed. The covalent modification prevents the strand from being properly amplified, so the PCR terminates prematurely,<sup>52</sup> which leads to failed amplification on covalently modified strands.<sup>52</sup> These PCR products can be compared to PCR using unmodified DNA as its template to quantitate the extent of the damage.<sup>52</sup> Ss-QPCR (Figure 1.15) measures lesions on either the transcribed or non-transcribed strand.<sup>51</sup> Isolated DNA (from cells subjected to incubation with the drug of interest) is subjected to a single round of PCR, using a biotinylated primer (primer 1) complementary to the transcribed strand to yield a series of biotinylated sequences of varying lengths due to modification of the original DNA by the drug.<sup>51</sup> This biotinylated DNA is bound to streptavidin-coated paramagnetic beads, using a strongly basic solution to wash away excess DNA.<sup>51</sup> After neutralization, this DNA is used as a template for subsequent PCR cycles.<sup>51</sup> The downstream primer (primer 2) for this PCR is complementary to the transcribed strand and binds a sequence inside the sequence bound by the first primer.<sup>51</sup> The third primer is complementary to the nontranscribed strand and its binding site determines the size of the resulting amplified region.<sup>51</sup> If the PCR is stopped during the exponential phase, the amount of product formed is proportional to the amount of unmodified template in the original genomic DNA.<sup>51</sup> Sslig-PCR also begins with a single round of PCR using a 5'-biotinylated primer.<sup>52</sup> Linear amplification generates ss-DNA of varying length for which the 5'-end is biotinylated and the 3'-end is limited by the position of the DNA modification.<sup>52</sup> These products are isolated on streptavidin-coated magnetic beads.<sup>52</sup> In order to amplify these sequences (because all the 3' ends are different), a 5'-phosphorylated single-stranded

oligonucleotide is ligated to their 3'-OH ends using T4 RNA ligase.<sup>52</sup> This ligated DNA can then undergo exponential amplification using a primer complementary to the ligated sequence.<sup>52</sup> Adduct positions are determined using a sequencing gel.<sup>52</sup>

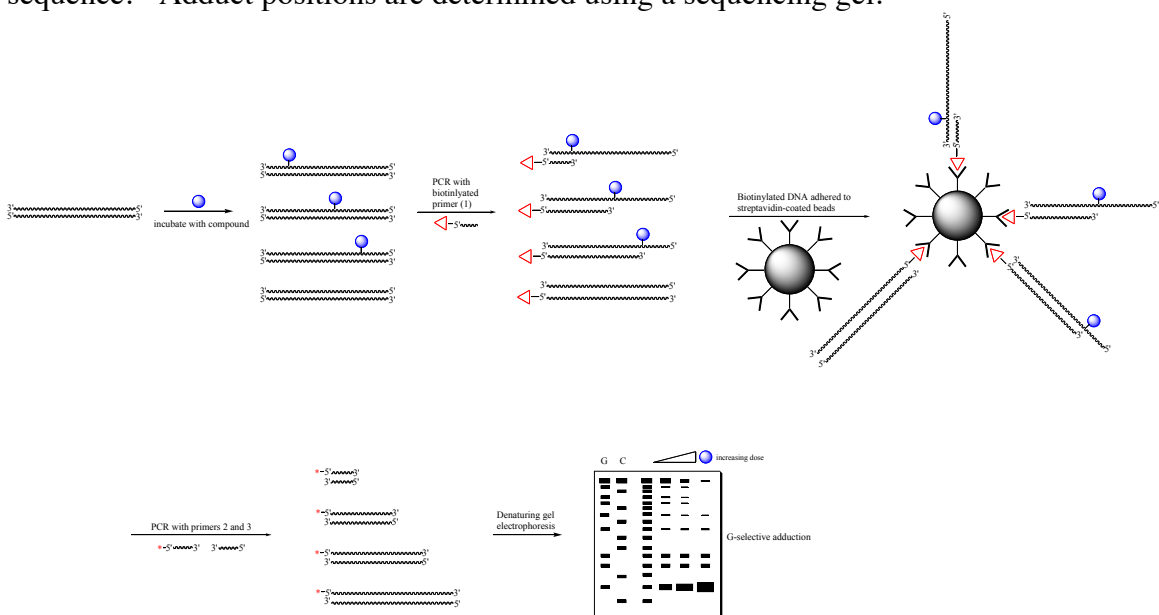


Figure 1.15. ss-QPCR

### 1.3.4. Assays for DNA cleavage

#### 1.3.4.1. Nicking Assay on Supercoiled DNA

Supercoiled DNA can be used to determine the extent to which a small molecule creates single-stranded breaks.<sup>53</sup> Supercoiled DNA is incubated with the compound of interest. If the compound causes DNA nicking, the supercoiled DNA relaxes to the circular form. If both strands are cleaved, or multiple proximal sites are nicked, the DNA can linearize. The three possible DNA structures (supercoiled, nicked (relaxed), or linear) can be separated by gel electrophoresis.<sup>54,55</sup> Visualization of the DNA can be achieved either by incorporating a radiolabel into the supercoiled DNA (by using a radiolabeled



nucleotide and cellular machinery), or by ethidium bromide staining.<sup>53</sup> Nicking assays of supercoiled DNA are extremely sensitive, as they can detect as little as a single break in a plasmid (e.g. 1 break per 3,000 bp).<sup>56</sup> 100 ng is sufficient DNA for a single experiment. The limit of detection is reported to be 4% nicking DNA in a sample for radiolabeled samples.<sup>53</sup>

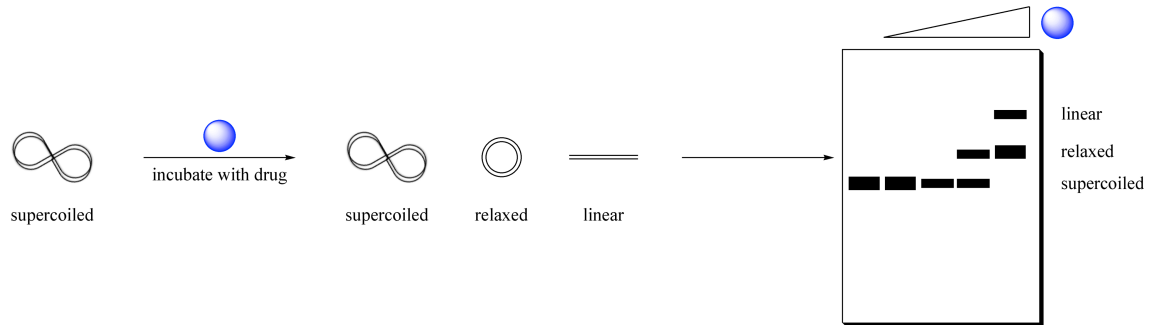


Figure 1.16. DNA nicking assay

#### 1.3.4.2. FRET-Based Assays

Another type of assay is the “break light” assay (so named because a break in the DNA causes a light). In the “break-light” system, a stem-and-loop DNA structure is designed which has the appropriate cleavage sequence as part of its stem.<sup>57</sup> A fluorescent resonance energy transfer (FRET) pair is used as the signal for cleavage. At the 5' end of the DNA is a fluorescent tag, and at the 3' end is a quencher (Figure 1.17).<sup>57</sup> The assay is designed for continuous monitoring of cleavage by fluorimetry.<sup>57</sup> As cleavage occurs, the quencher and the fluorescent tag are separated, which removes the FRET quenching of the fluorescent signal (Figure 1.17).<sup>58</sup> The extent of cleavage is then proportional to the fluorescence signal.<sup>57</sup> “Break-lights” work for both enzyme restriction sites and small-molecule cleavage agents. In the seminal publication by Biggins *et al.*, the sequence used contained the recognition sequence 5'-TCCT-3' for calicheamicin and used fluorescein (FAM) as the fluorophore and 4-(4'-dimethylaminophenylazo)benzoic acid (DABCYL)

as the quencher.<sup>57</sup> The FRET is 99.9% complete between this pair because of large spectral overlap.<sup>57</sup> Because this assay is continuous, kinetic parameters of cleavage can be calculated.

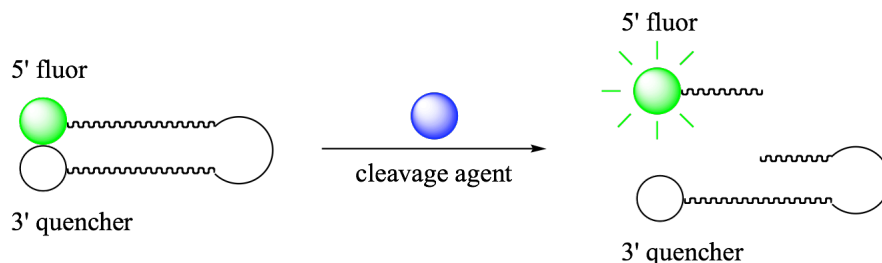


Figure 1.17. "Break-Light" Assay

### 1.3.5. Analysis of Non-Covalent DNA-Small Molecule Interactions

#### 1.3.5.1. Mass Spectrometry

Electrospray ionization mass spectrometry (ESI-MS) is rapidly becoming the preferred method for analyzing covalent and non-covalent small-molecule-DNA interactions.<sup>59</sup> Because this method uses a relatively gentle method of ionization, ESI-MS works well for analyzing large biomolecules without creating high levels of fragmentation, which allows this method to provide structural and sequence information.<sup>60</sup> Interestingly, DNA containing alkylated nucleotides shows simplified fragmentation patterns compared to the unmodified DNA because alkylation of guanine weakens the glycosidic bond, which causes ready loss of the alkylated base and enhanced cleavage of the 3' C-O bond.<sup>60</sup> The cleavage pattern can then be used to analyze the position of modification, providing information about sequence selectivity of the alkylating agent. One difficulty in effectively mapping DNA sequence selectivity is the sequence of the ds-DNA being examined. Unlike proteins, DNA contains subunits with highly similar molecular weight, making it difficult to differentiate between the upper or

lower strands of the duplex.<sup>60</sup> This is typically addressed by designing non-self-complementary sequences.<sup>60</sup> ESI-MS typically uses oligomers similar in length to X-ray crystallography or NMR; however, methods exist for analyzing longer sequences.<sup>61,62</sup> As in <sup>32</sup>P-postlabeling, amplification of the signal from modified samples is key to good detection. Mass spectrometry can be coupled with a variety of separation techniques, including liquid chromatography,<sup>63</sup> capillary electrophoresis, and capillary electrochromatography.<sup>64</sup> Recent advances in ESI-MS analysis of DNA include the use of selective ion monitoring (SIM) and selective reaction monitoring (SRM).<sup>59</sup> In selective ion monitoring, the quadrupole array is tuned to retain the predicted mass. For SRM, the first trap Q1, is tuned to trap the predicted mass, which then travels to q2, the collision chamber (Figure 1.18). In this chamber, the selected ions undergo collisions and pass through to Q3, a second mass analyzer. This mass analyzer is then used to look for the predicted product ion.<sup>59</sup> SIM has been shown to detect DNA on picomole scale, whereas SRM is able to detect adducts on femtomole scale.<sup>59,63</sup> Quantitation of DNA adducts by mass spectrometry is possible but requires an authentic sample of the adduct being analyzed, in order to calculate ionization potentials.<sup>59</sup> Qualitative information about relative binding affinities, however, can be obtained. A key advantage to the use of mass spectrometry to analyze DNA adduction is that it gives information about the structure of the adducts, which is valuable when the structure is unknown.<sup>63</sup> Also, it is easier to analyze multiple modes of adduction by ESI-MS than by traditional methods.<sup>2</sup>



Figure 1.18. Cartoon of a triple quadrupole mass spectrometer.

Q1 is a mass analyzer, q2 is a collision cell filled with inert gas, and Q3 is a second mass analyzer.

### 1.3.5.2. Competition Dialysis

Competition dialysis (Figure 1.19) is a method used to assess DNA binding selectivity of small molecules. Multiple small dialysis tubes containing different sequences or structures of DNA (in equal volumes at identical concentrations) are stirred in a solution of the small molecule of interest (dialysate).<sup>65</sup> After the system reaches equilibrium (usually in less than 24 h), the concentration of drug in each tube is compared to the concentration of the analyte in the large chamber using either fluorescence or absorbance. The dialysis tubes containing the highest concentration of the compound of interest represent the structures with the highest binding affinities.

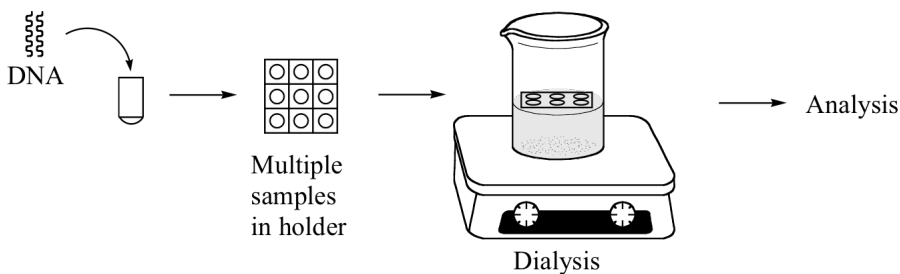


Figure 1.19. Competition Dialysis

### 1.3.5.3. Melting Curves

Thermal melting curves are a method of obtaining general information about drug-DNA interactions.<sup>66</sup> “Melting” refers to denaturation of DNA from its secondary structure to its single-stranded form. Multiple factors create the underlying physical basis for DNA stabilization by a small molecule, including the ligand binding constant, binding enthalpy, and site size.<sup>65</sup> When DNA melts, AT rich sequences denature first (because

they have only two hydrogen-bonding interactions per base pair), causing partial unwinding, then GC rich regions (which have three hydrogen bonds between the base pairs, leading to stronger association) dissociate.<sup>66</sup> Changes in melting temperature,  $T_m$ , can be measured using a number of techniques, including UV absorbance, NMR, circular dichroism, viscosity, electrophoresis, or calorimetry. UV absorbance is most commonly used because it is sensitive (so only small amounts of material are required) and operationally simple.<sup>66</sup>  $T_m$  values give only general binding information, not specific, and data acquisition requires elevated temperatures in buffers that are optically transparent. Melting curves are typically obtained at 260 nm.<sup>66</sup> As the duplex melts, the absorbance increases (hyperchromicity) approaching the absorbance of single monomers because base-stacking is lessened.<sup>66</sup> The inflection point on a plot of absorbance vs. temperature is the  $T_m$ .

Drugs that bind (and stabilize) duplex DNA cause an increase in  $T_m$ .<sup>66</sup> Also, a drug that binds tightly to the DNA can cause a broadened transition or even a biphasic transition (in a situation where the DNA polymer is more heterogeneous and the drug can bind multiple sites).<sup>66</sup> Classical intercalators raise the  $T_m$  significantly and act similarly with regard to AT-rich vs. GC rich DNA sequences. Major and minor groove binders typically raise the  $T_m$  of the duplex. They have very low binding to ss-DNA because it exists as a random coil, without a structured groove with a specific electrostatic environment.

#### ***1.3.5.4. Spectroscopic Titrations<sup>67</sup>***

Non-covalent complexation between DNA and small molecules can be monitored spectroscopically using several methods. Frequently, the fluorescence or electronic absorption spectrum of a small molecule will be altered by binding to DNA.<sup>68</sup> For

example, ethidium bromide displays enhanced fluorescence upon DNA binding<sup>69</sup> whereas some aminoacridines and anthracyclines (see section 1.4.4.2) show fluorescence quenching.<sup>68</sup> In UV-Visible spectroscopy, the absorption spectrum of the drug changes to a longer wavelength (bathochromic shift) and the extinction coefficient ( $\epsilon_{\max}$ ) at the maximum absorbance ( $\lambda_{\max}$ ) decreases (hypochromic effect).<sup>68</sup> Although titrations have the advantage of being operationally simple, they do not distinguish binding modes (i.e. intercalation vs. minor groove binding).<sup>68</sup> Quantification of DNA binding requires a linear relationship between absorption or fluorescence and concentration and an unchanging extinction coefficient or normalized fluorescence intensity over a wide range of concentrations. A nonlinear relationship implies polymerization, aggregation, or precipitation of the compound of interest.<sup>68</sup> Equilibrium binding titrations are commonly used to analyze DNA-drug binding interactions. Aliquots of DNA solution are added serially to a drug solution of fixed concentration. Optical changes are measured and analyzed according to the concentration ratios of free drug and DNA-drug complex.<sup>68</sup>

$$A = A_f + A_b = \epsilon_f \cdot C_f + \epsilon_b \cdot C_b$$

Equation 1.1. Determining binding of small molecules to DNA

A represents Absorbance, C represents concentration, and  $\epsilon$  is extinction coefficient. The subscripts f and b refer to free and bound small molecule.

A complementary method varies the concentration of the drug while holding the DNA concentration constant. Using a wide range of concentrations is important, because the shape of the isotherm can vary as drug concentration increases.<sup>68</sup> Continuous variation plots (or Job plots) of binding titrations provide the DNA:drug binding stoichiometry.<sup>70</sup> A series of measurements are taken at independently varying DNA and drug concentrations,

and the signal (fluorescence or absorbance) is plotted against the mole fraction of drug to DNA.<sup>70</sup> The inflection point of the plot gives the binding stoichiometry.<sup>70</sup>

#### **1.3.5.5. Displacement Assays**

An indirect method of determining binding constants uses ethidium bromide displacement from DNA (a discussion of ethidium bromide as a DNA-interactive compound follows in Section 1.4.4.1).<sup>68</sup> Increasing concentrations of the compound of interest are added to a DNA-ethidium bromide complex while monitoring changes in fluorescence. The DNA-ethidium complex is highly fluorescent, whereas free ethidium bromide is only weakly fluorescent.<sup>68</sup> This method works not only for intercalators but also for minor groove binders using an appropriate drug-DNA complex. Fluorescent compounds or compounds which do not bind strongly enough to displace ethidium bromide ( $K_a < 10^4 \text{ M}^{-1}$ ) do not work in this type of determination. The concentration at which 50% of the ethidium bromide is displaced ( $C_{50}$ ) is inversely proportional to the  $K_a$  for the DNA-drug association.

#### **1.3.5.6. NMR Binding Studies**

Both 1D and 2D NMR have been invaluable in characterizing solution-state DNA-small molecule interactions.<sup>71</sup> Because of the complexity of the data obtained, it is easier to use self-complementary, short (6-12 bp) DNA oligomers and highly site-specific compounds.<sup>72</sup> NMR is one of the least sensitive solution-state methods used for DNA characterization, with 2 mM in 600  $\mu\text{L}$  solvent of the drug-DNA complex preferred for 2D experiments.<sup>72</sup> Exchangeable protons are of special interest, as DNA-drug interactions frequently involve hydrogen bonding.<sup>72</sup> Small-molecule binding can induce characteristic spectral changes. For example, intercalators commonly cause a 1 ppm upfield shift in the imino protons near the drug-binding site, and minor groove binders shift protons H1' and

H4' on the deoxyribose units.<sup>72</sup> 2D NMR studies have similar features<sup>72</sup> but will not be discussed here.

#### ***1.3.5.7. X-ray Crystallography***

X-ray crystallography provides information about DNA-small molecule interactions in a solid state. Successful crystallization of samples is nontrivial,<sup>73</sup> but X-ray crystallography provides detailed information about the relative positions of the bases compared to NMR, because the structures are rigid.<sup>74</sup> Because of distortions due to crystal packing forces, the information obtained does not necessarily represent the solution-state or *in vivo* structure.<sup>6</sup> For most X-ray methods, the absolute stereochemistry of the crystal cannot be determined, so models rely on a mathematical set of assumptions. Although multiple sets of refinement algorithms exist, at a nominal resolution of 2.0 Å or better, the refinement used does not affect the proposed structure.<sup>6</sup> Different DNA-drug complexes have been characterized by this methods, leading to improved design of analogs or explanations of biological activities.<sup>74</sup>

### **1.4. EXAMPLES OF SMALL MOLECULE DNA-INTERACTIVE COMPOUNDS**

This section will give examples of types of DNA modification and compounds associated with that modification pattern.



### 1.4.1. Alkylating Agents



Figure 1.20. Cartoon depicting DNA alkylation

Alkylating agents contain electrophilic moieties that can covalently modify nucleophilic sites on the nucleoside bases (Figure 1.20). Damage of this type can often be repaired by cellular repair machinery (such as base excision repair), depending on the size of the lesion.<sup>75</sup> Alkylation most commonly occurs at the purine bases but can also occur at pyrimidines.

#### *1.4.1.1. Cyclopropane-Containing Alkylating Agents*

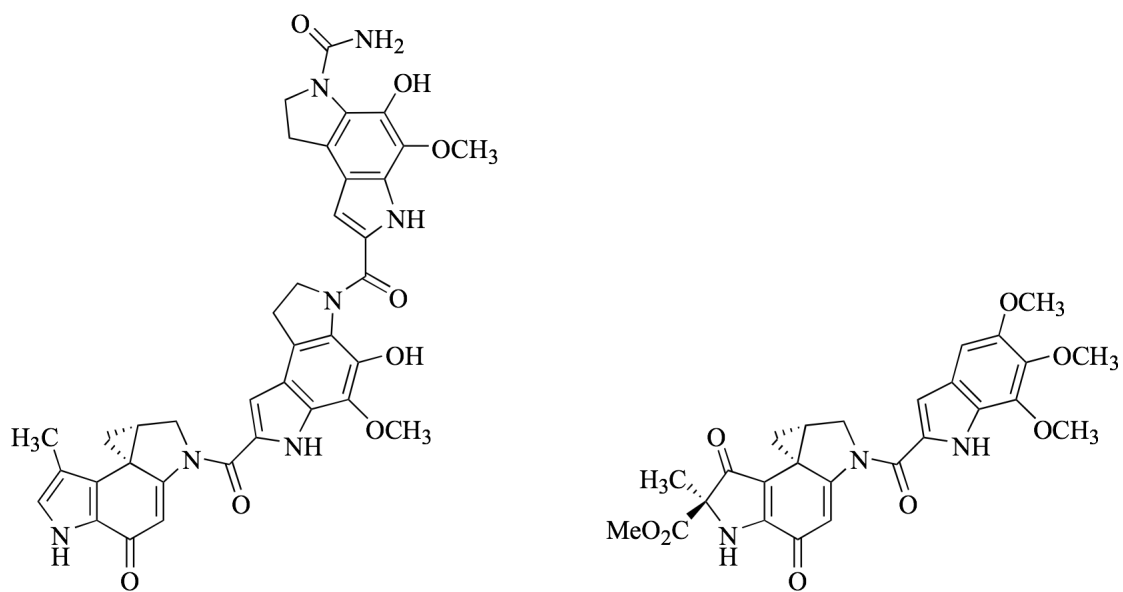
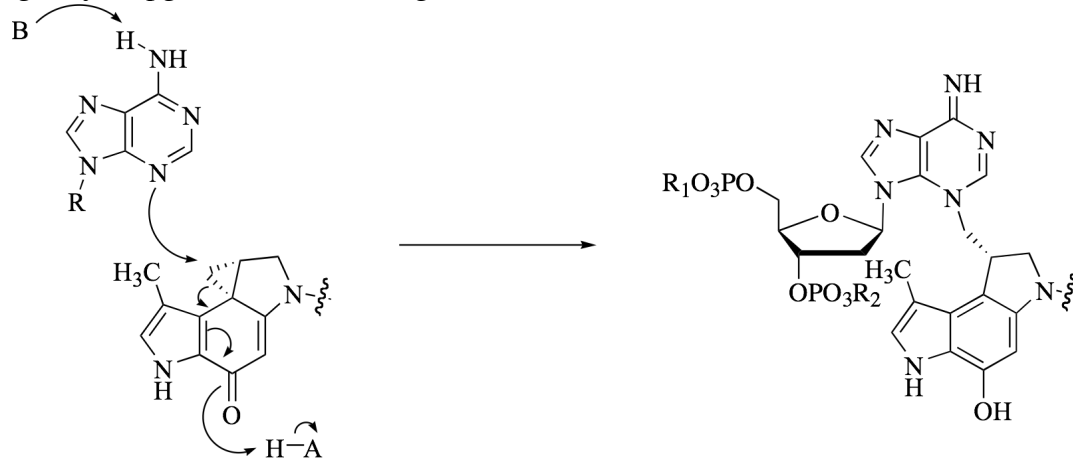


Figure 1.21. CC-1065 (l) and Duocarmycin A (r)

CC-1065 and Duocarmycin A (Figure 1.21) are known to alkylate N3 of adenine.<sup>76</sup> CC-1065 binds double-stranded DNA at the sequence 5'-TTA-3', and forms a covalent adduct at the adenosine.<sup>77</sup> The structure of the covalent DNA adduct was determined by X-ray crystallography and NMR spectroscopy using a single base.<sup>76</sup> The proposed mechanism of adduction for both compounds begins with a noncovalent association with DNA as minor groove binders followed by covalent modification by the nucleophilic N3 site at adenine (Scheme 1.5).<sup>78,79</sup> The tetracyclic unit containing the cyclopropyl moiety is largely responsible for the sequence specificity and the ability of CC-1065 to bend duplex DNA.<sup>80</sup> CC-1065 shows protection in hydroxyl radical footprinting at sequences of 5'-AAAAA-3' and 5'-PuNTTA-3' (Pu = purine). Alkylation occurs almost exclusively at the 3'-A of the sequence.<sup>80</sup> These consensus sequences are bent by an angle of 17-22°.<sup>80</sup> Covalent modification by CC-1065 does not change the angle of DNA bending, but it changes the center of the angle from the central A (A<sub>3</sub>) to

the A one base nearer the 3' end ( $A_4$ ).<sup>80</sup> Hurley *et al.* propose that in order to achieve the geometry required for alkylation, the duplex DNA must be flexible, as shown by its ability to bend, and once the desired geometry is achieved, alkylation at adenine holds the DNA at the angle of bending.<sup>81</sup> CC-1065 is an extremely potent antineoplastic agent, requiring only 40 pg/mL to show 90% growth inhibition on mouse leukemia cells.<sup>82</sup>



Scheme 1.5. Proposed mechanism for DNA modification by cyclopropyl-based alkylating agents

#### 1.4.1.2. Nitrosoureas

Nitrosoureas have been used as antineoplastic agents.<sup>83</sup> The mechanism by which they damage DNA is unclear, although most proposals agree that a diazonium ion is the intermediate responsible for alkylation.<sup>83,84</sup> N-alkylnitrosoureas methylate DNA at several positions.<sup>85</sup> As expected, N-methylnitrosourea preferentially alkylates the N7 position of guanine, but it also alkylates N7 of and N3 of adenine in a ratio of 1:0.03:0.15 (N7MeGua:N7Ade:N3Ade).<sup>86</sup> Adduct formation can be mapped using piperidine-heat treatment.<sup>86</sup> Effective concentrations of NMU in incubations with DNA to see distinctive cleavage *via* PAGE analysis of radiolabeled DNA are in the  $\mu\text{M}$  range.<sup>86</sup> NMU appears to modify guanines without preference for flanking sequences. CNU's (Figure 1.22) are

bisfunctionalized, but the vast majority of adduct formation is monoalkylation, not crosslinking.<sup>83</sup> BCNU modifies O<sup>6</sup> of guanine.<sup>87,88</sup> Streptozocin is an antibiotic nitrosourea formed by a *streptomyces* strain, which acts as a potent alkylating agent by modifying N7 of guanine, O<sup>6</sup> of guanine, and N3 and N7 of adenine.<sup>89</sup> A single dose to rat kidney cells at 2.5 mg/kg was enough to cause detectable DNA damage.<sup>89</sup>

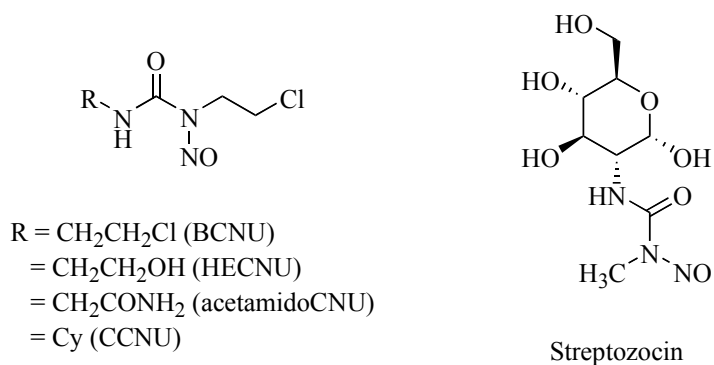


Figure 1.22. Nitrosoureas

#### 1.4.1.3. Polyaromatic hydrocarbon diol epoxides

Commonly occurring polyaromatic hydrocarbons are metabolically activated to form a mixture of diastereomeric diol epoxides (Figure 1.23).<sup>90</sup> Adducts arise from attack by the exocyclic amine of either guanine (N2) or adenine (N6) at the benzylic position of the epoxide to form a covalent adduct.<sup>90</sup> Adduction can occur with either retention or inversion at the carbon stereocenter. Ratios of the stereochemical outcome for both DNA and single nucleosides have been determined for benzo[*g*]chrysene diol epoxide.<sup>91</sup> In all cases, *trans* ring-opening is favored, but ratios vary from 51:2 in the case of deoxyadenosine in DNA to 37.5:15 in the case of deoxyguanosine as a nucleoside.<sup>91</sup> Benzochrysene epoxide at 10 ng/μg DNA shows a mutation rate of approximately 300-

fold more than background.<sup>91</sup> Out of 106 mutations, 2 were large deletions, and 104 were point mutations. 99 of the point mutations were single base mutations over the entire sequence, and 5 had two sites where bases were exchanged.<sup>91</sup> The mutations observed were AT→TA, 41%, GC→CG, 12% (53% transversions, see section 2.1.1 for a discussion), GC→AT, 5%, AT→GC, 3% (8% transitions).<sup>91</sup>

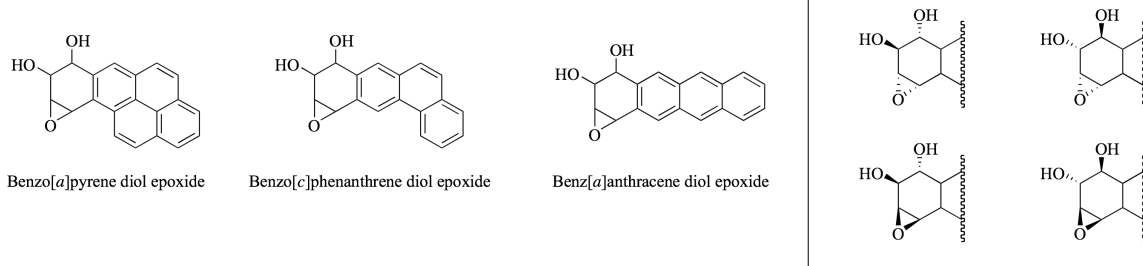


Figure 1.23. Polyaromatic hydrocarbon diol epoxides.

#### 1.4.2. Crosslinkers

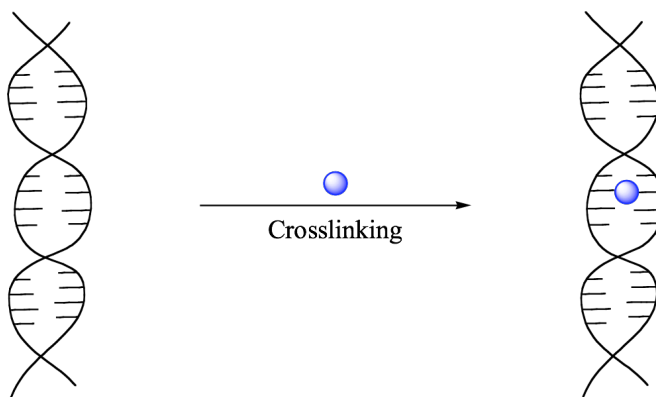


Figure 1.24. Cartoon depicting interstrand DNA crosslinking

Crosslinkers are bifunctional alkylating agents. They can create either inter- or intrastrand links. Crosslinks are thought to have more severely damaging effects than simple alkylating agents, because they effectively cause two lesions, which foils most repair mechanisms.<sup>92</sup> Interstrand crosslinks covalently join bases (or ribose units) on two

complementary strands and prevent DNA denaturation. Interstrand crosslinks occur between bases (or ribose units) along the same strand.

#### 1.4.2.1. Nitrogen Mustards

Nitrogen mustards are some of the oldest chemotherapeutics.<sup>93</sup> They contain bifunctional alkylating agents, containing two primary alkyl chloride moieties.<sup>93</sup> Mechlorethamine, registered by Merck as Mustargen for treatment of multiple tumor types, modifies DNA through both monoalkylation and crosslinking, but monoalkylation at N7 of guanine comprises 93-95% of DNA modification.<sup>93</sup> The remainder of the modifications are G-G interstrand crosslinks.<sup>93</sup> Intrastrand crosslinks can occur, but only in very limited sequence-specific cases. Mechlorethamine has been shown to crosslink DNA at 5'-GNC sites.<sup>22,94</sup>

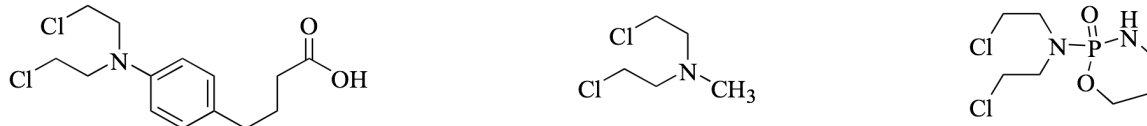


Figure 1.25. Nitrogen mustards chlorambucil (l), mechlorethamine (center), and cyclophosphamide (r)

The proposed mechanism of DNA modification is displacement of a chloride by the amine to form an aziridinium ring, which then undergoes nucleophilic attack by the nucleoside base (Figure 1.26).<sup>95,96</sup> The free amine then forms a second aziridinium ring with the other electrophilic arm.<sup>93,95</sup> This ring can then be opened by either water to form a mono-alkylated adduct or a second nucleoside base to form a cross-link.<sup>93</sup> Chlorambucil is less base-selective, with 75% of adducts formed at guanosine and 25% at adenosine. Chlorambucil has a higher affinity for the minor groove of DNA than mechlorethamine.

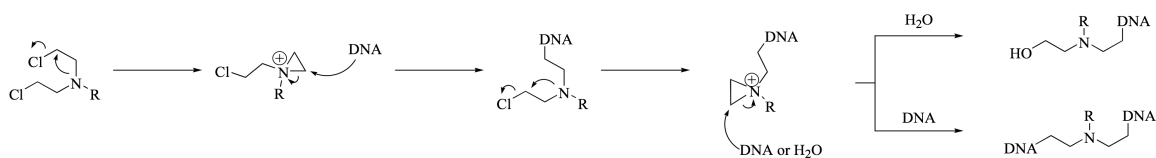


Figure 1.26. Proposed mechanism for reaction of nitrogen mustards with DNA.<sup>93</sup>

Phosphamides modify N7 of guanine,<sup>87</sup> but can also alkylate the phosphodiester backbone,<sup>97</sup> which comprises 67% of DNA adducts formed.<sup>93</sup> Cyclophosphamide, registered by Bristol-Myers Squibb as Cytosan, for use against leukemia, requires metabolic activation to alkylate DNA. A cytochrome P<sub>450</sub> adds a hydroxyl group to the amide nitrogen.<sup>93</sup> The cyclic product then spontaneously opens to generate acrolein and a phosphoramidate mustard, which is the active alkylating agent.<sup>93</sup> The activity of the independently synthesized phosphoramidate mustard with DNA has been confirmed in cells studies<sup>98</sup> and by mass spectrometric analysis.<sup>99</sup>

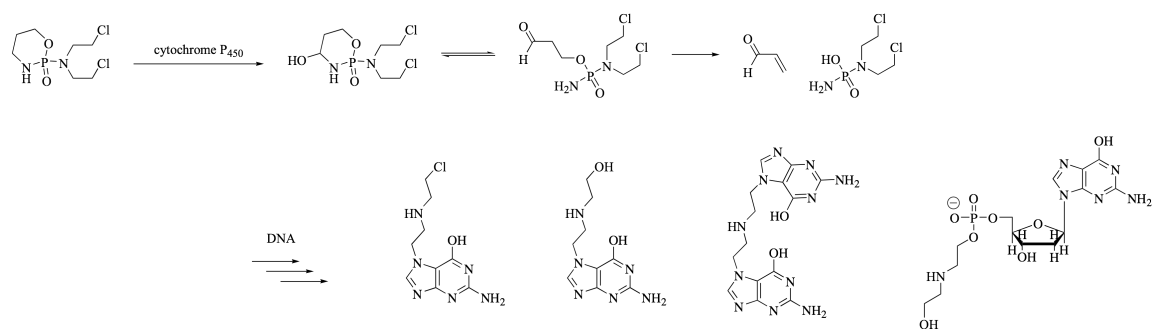


Figure 1.27. Proposed activation of cyclophosphamide and subsequent DNA adduct formation.

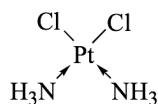


Figure 1.28. Cisplatin

Cisplatin (trade name Platinol, from Bristol-Myers Squibb, Figure 1.28) is an antineoplastic agent indicated for treatment of testicular, ovarian, and bladder cancer<sup>100</sup> that works as a DNA crosslinking agent. The mode of action is thought to be disruption of replication through formation of 1,2-intrastrand crosslinks of neighboring purines, which cause bending and partial unwinding of the duplex and widening of the minor groove, which can cause secondary effects enhancing the cytotoxicity.<sup>51,52,101</sup> Cisplatin modifies DNA at guanine N7 as well as adenine N1 and N7.<sup>87</sup> Although these lesions account for approximately 80% of the DNA modification caused by cisplatin, evidence also suggests that 1,2 GG interstrand links, although less common, might cause similar effects to the intrastrand crosslinks.<sup>102</sup>

#### 1.4.3. Oxidizers (via H-atom Abstraction)

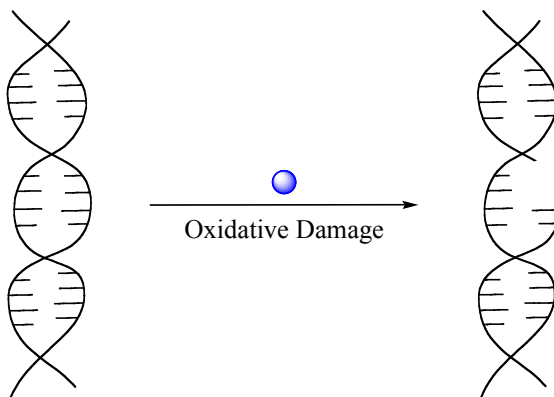


Figure 1.29. Cartoon of oxidative damage of DNA

##### 1.4.3.1. Eneidyne

Eneidyne are a well-known class of compounds that covalently modify DNA. Esperamicin and calicheamicin (Figure 1.30) can induce both double-stranded and single-stranded DNA strand breaks.



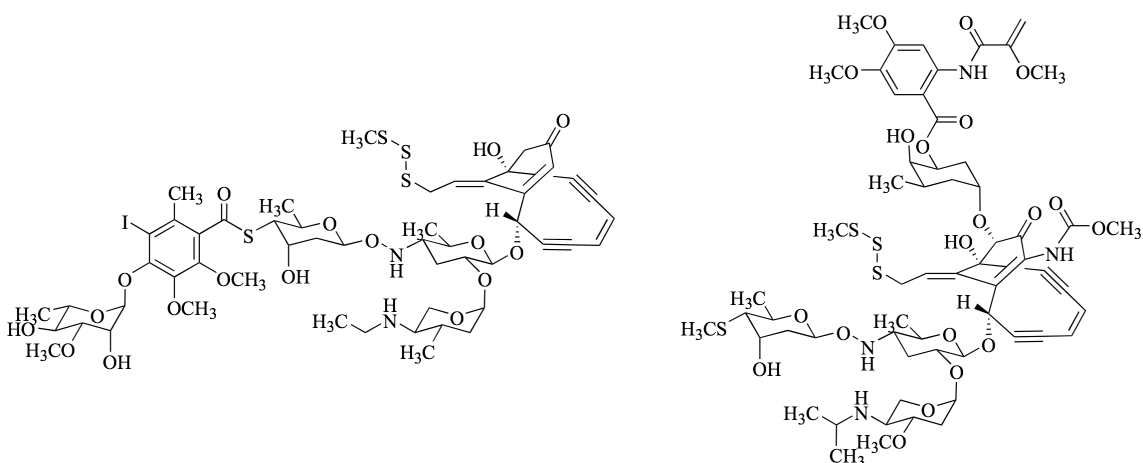
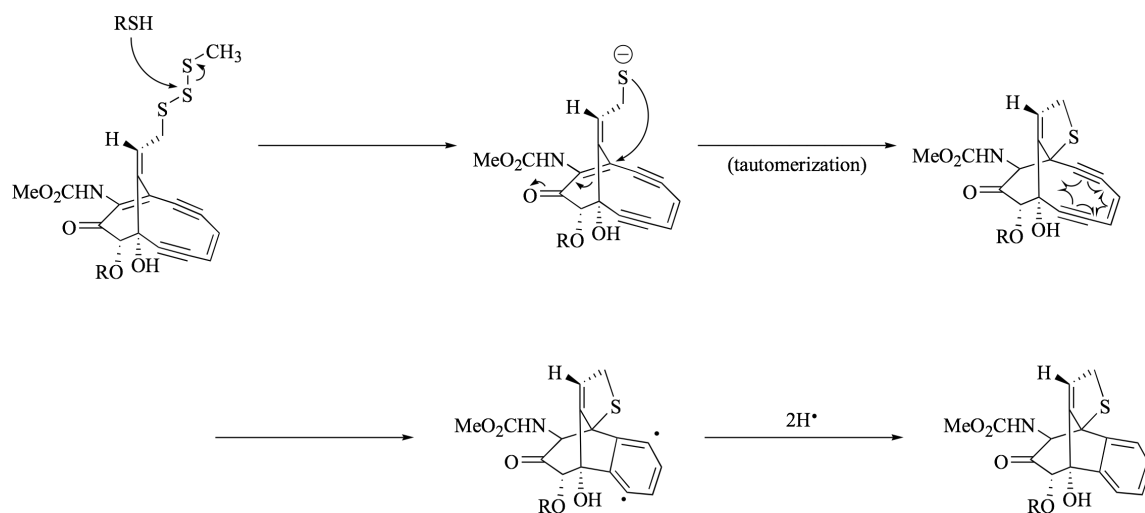


Figure 1.30. Calicheamicin  $\gamma_1$  (l) and Esperamycin A<sub>1</sub> (r)

The mechanism of DNA damage by enediynes has been well-studied<sup>103,104</sup> and is thought to proceed through reduction of the trisulfide (Scheme 1.6). The anionic sulfur can then perform conjugate addition to the  $\alpha,\beta$ -unsaturated carbonyl to form a five-membered ring, which has been characterized by NMR.<sup>105</sup> Subsequent tautomerization reforms the carbonyl, and the ene-diyne moiety then relieves ring strain by undergoing a Bergman cyclization<sup>106</sup> to form the *p*-benzyne diradical. The activation energy,  $\Delta G^\ddagger$ , of the Bergman cyclization of activated calicheamicin has been determined to be 20.1 kcal/mol,<sup>105</sup> significantly lower than the 28.8 kcal/mol barrier for Bergman cyclization of (*Z*)-hex-3-ene-1,4-diyne.<sup>107</sup> Thus, this triggering reaction serves two purposes: it reduces the distance between C2 and C7 prior to the cyclization, which accounts for approximately one quarter of the reduction in activation energy, and it also reduces the strain at the bridgehead carbons by saturating the bridgehead alkene, which reduces the activation barrier to cyclization.<sup>108</sup> This diradical then abstracts hydrogen atoms from the DNA.<sup>109</sup> Depending on the structure of the enediyne and the DNA sequence of the cleavage site, DNA hydrogen atom abstraction occurs at C1', C4' or C5' of the deoxyribose unit (Scheme 1.7).



Scheme 1.6. Triggering of esperamicin<sup>103,105</sup>

A deuterium-exchange reaction with using deuterio-buffer and proteo-DNA showed that H-atom incorporation onto the cyclized enediyne comes exclusively from the DNA,<sup>103,109</sup> although a subsequent experiment using a different oligomer sequence failed to observe such high selectivity (80% incorporation).<sup>110</sup> The majority of DNA damage caused by esperamicin consists of single-stranded DNA breaks, as determined by a nicking assay.<sup>103</sup> Hydroxyl radical footprinting on calicheamicin shows protection at pyrimidine-rich sites (i.e. TTTT, TTGT, CCCA, etc.) over seven bases, and footprints were consistent with positions of cleavage,<sup>111</sup> which has been corroborated by NMR analysis.<sup>112</sup> Esperamicin cleaves DNA selectively at repeated pyrimidines (CTC, TTC, or TTT) and shows a base selectivity (T>C>A>G) different than calicheamicin (i.e. C>>T>A=G).<sup>113</sup>

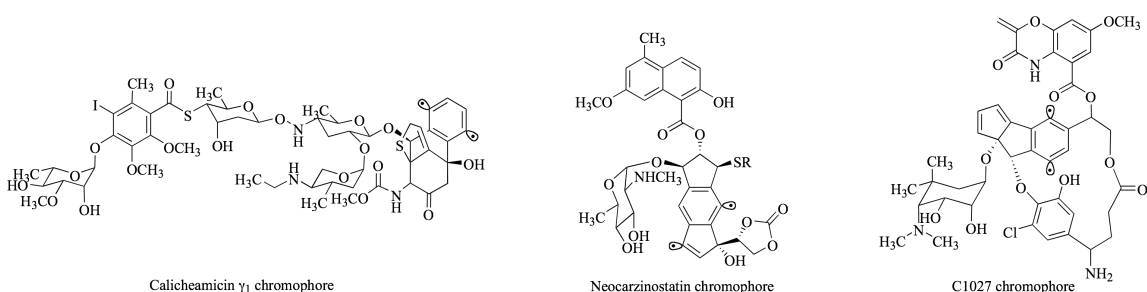
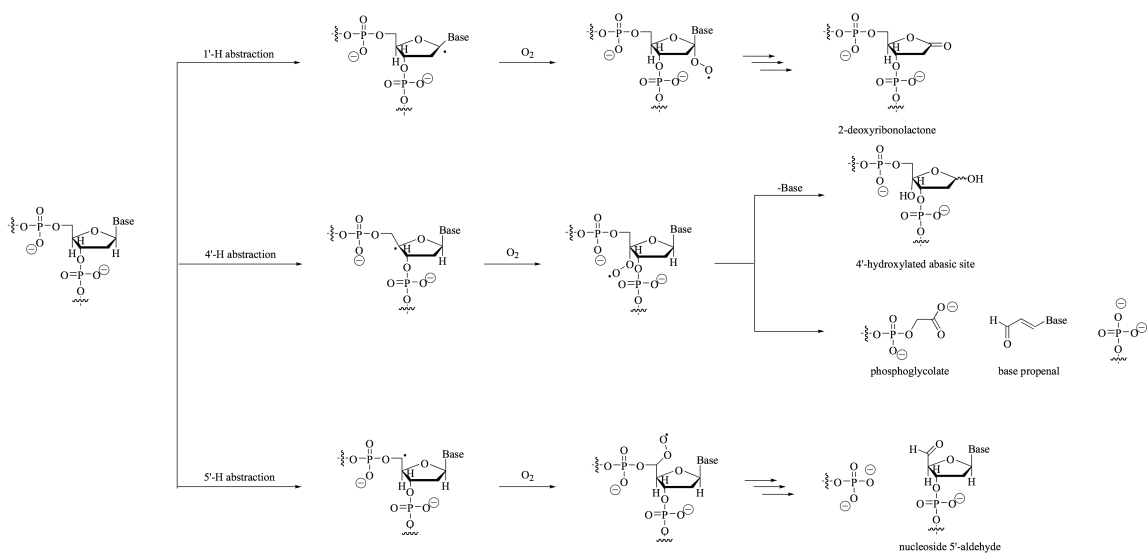


Figure 1.31. Reactive diradicals from enediynes<sup>114</sup>

Neocarzinostatin (NCS) is a potent antitumor natural product that consists of a protein and a DNA-cleaving chromophore. Although the NCS chromophore lacks the 3-ene-1,5-diyne core common to the ten-membered enediynes such as calicheamicin and esperamicin, thiol addition generates a reactive enyne cumulene system that cyclizes to afford a reactive diradical intermediate (Figure 1.31). Like calicheamicin and esperamicin, NCS chromophore cleaves DNA by hydrogen atom abstraction. However, under anaerobic conditions, neocarzinostatin does not exhibit DNA cleavage; rather, it forms covalent adducts with DNA.<sup>115,116</sup> The mechanism of formation and structure of these adducts are not well-characterized, but they appear to involve hydrogen atom abstraction by NCS chromophore at the DNA 5' position followed by addition of the resulting DNA-centered radical onto the reduced NCS chromophore.<sup>115,116</sup> Calicheamicin  $\gamma_1$  also mainly produces DNA monoadducts under anaerobic conditions (Figure 1.31).<sup>114</sup>



Scheme 1.7. Different H-abstraction motifs on the ribose backbone of DNA<sup>114</sup>

C1027, a metabolite isolated from *Streptomyces globisporus* C1027 strain, under aerobic conditions, shows C4' hydrogen atom abstraction at A<sub>1</sub> of the duplex 5'-GTTA<sub>1</sub>T-3'/3'-CA<sub>3</sub>A<sub>2</sub>TA-5', as evidenced by gel electrophoresis showing a phosphoglycolate fragment (running slightly faster than the Maxam-Gilbert 3'-phosphates).<sup>114</sup> Under aerobic conditions, C5' hydrogen atom abstraction at A<sub>3</sub> leads to a strand break containing a 3'-phosphate, as well as C1' hydrogen atom abstraction at A<sub>2</sub>, which forms the ribonolactone (Scheme 1.7).<sup>114</sup> When the DNA is incubated under anaerobic conditions, the chromophore associated with C1027 remains associated with the DNA even after extensive extraction and precipitation.<sup>114</sup> Additionally, under anaerobic conditions, low mobility bands were observed, suggesting that these compounds were also causing crosslinking. An additional experiment using oligonucleotides of differing length confirmed that the lower mobility bands were crosslinked DNA.<sup>114</sup> Replacing the H at C1' on the ribose unit of A<sub>2</sub> with deuterium severely limits damage ( $k_H/k_D = 7.8$ ) and shifts damage to A<sub>3</sub>.<sup>114</sup> In this deuterated system, the crosslinking  $k_H/k_D$  is 1.8,

significantly lower than for H-atom abstraction, suggesting the crosslinking occurs mostly between A<sub>1</sub> and A<sub>3</sub>.<sup>114</sup> Fe(II)-EDTA/H<sub>2</sub>O<sub>2</sub> footprinting showed that crosslinks are formed between A<sub>1</sub> and A<sub>2</sub> or A<sub>3</sub>.<sup>114</sup>

#### 1.4.3.2. Metal-Dependent Cleavage Agents

One example of a DNA-interactive agent that displays metal-dependent oxidative DNA damage is bleomycin.

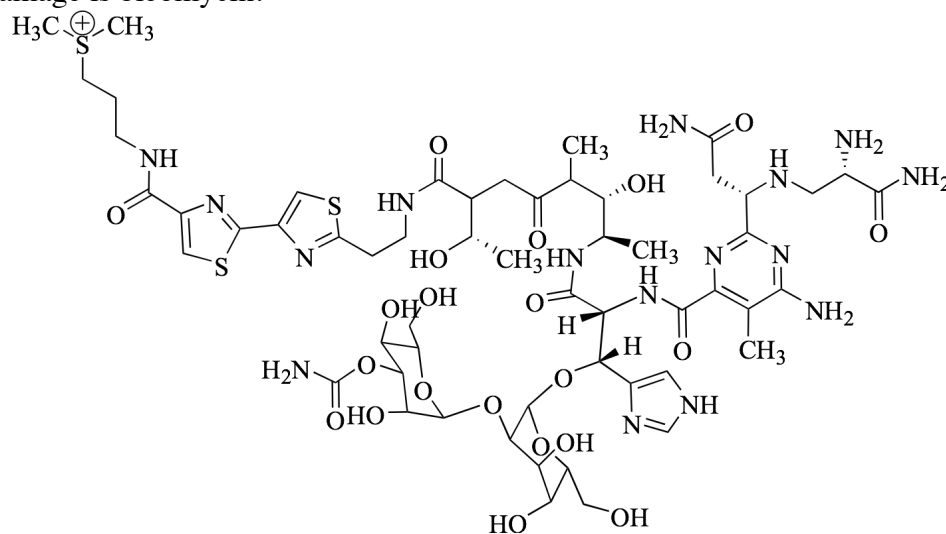
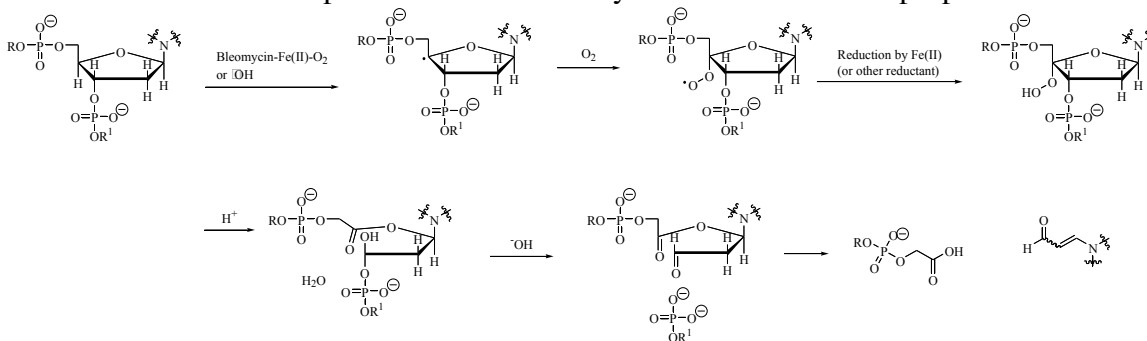


Figure 1.32 Bleomycin A2

Bleomycin (BLM, Figure 1.32) is an antineoplastic agent which causes single- and double-stranded DNA strand breaks in presence of several transition metals, including Ni(III),<sup>117</sup> Cu(I) or Fe(II).<sup>118</sup> BLM is registered by Bristol-Myers Squibb (trade name Blenoxane) as effective against squamous cell lymphomas and testicular cancer.<sup>100</sup> Bleomycin cleavage on DNA is selective for GC and GT sequences, but the extent and selectivity of the cleavage depends on the chelated metal.<sup>118</sup> Sequence selectivity of the BLM-Ni(III) complex was analyzed by incubating short (100-200 bp) oligomers with the BLM-Ni(III) complex (generated by using BLM:Ni 1.0:1.2 in presence of an oxidizing agent, oxone or Ir(IV)) followed by piperidine-heat treatment and denaturing gel

electrophoresis.<sup>117</sup> Additionally, addition of both Cu(I) and Fe(II) causes amplified cleavage, greater than what would be predicted by using each separately.<sup>118</sup> Mechanistic studies suggest that DNA cleavage proceeds via H-atom abstraction at C4' (Scheme 1.8).<sup>119</sup> The subsequent radical then traps molecular oxygen to form a peroxy radical.<sup>119</sup> This radical is further reduced to the peroxide, possibly by the Fe(II) present (although the identity of the reductant has not been determined).<sup>119</sup> The peroxide then rearranges to cleave the C3'-C4' bond in the ribose unit, leaving a phosphate hemiacetal, which forms the open-chain aldehyde under basic conditions.<sup>119</sup> Following loss of the phosphate, the hemi-aminal at C1' collapses to lose the carboxylic acid and the base-propenal.<sup>119</sup>



Scheme 1.8. Proposed mechanism of BLM-Fe(II)-induced DNA cleavage

#### 1.4.4. Intercalators

Although no intercalating compounds will be described later in this dissertation, any overview of DNA-small molecule interactions would be remiss in not covering this common binding mode. Intercalators bind DNA *via*  $\pi$  stacking between nucleoside bases (Figure 1.33). They extend the distance between the  $\pi$  stacked bases from 3.4 Å to 6.8 Å.<sup>5</sup> This causes lengthening and unwinding of the DNA duplex. Crystal structures of intercalated duplex-DNA show little change in the backbone conformation of DNA regardless of the structure of the intercalated compound.<sup>120</sup>

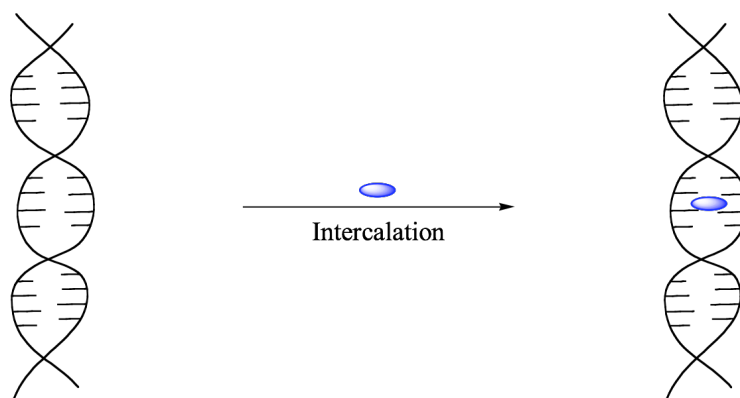


Figure 1.33. Cartoon depicting DNA intercalation

#### 1.4.4.1. Synthetic Dyes

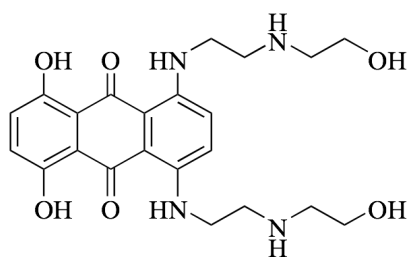


Figure 1.34. Mitoxantrone

Mitoxantrone (Figure 1.34) is an anthracenedione registered by Lederle as Novantrone for activity against acute leukemia.<sup>100</sup> Mitoxantrone shows cytotoxicity against multiple types of cancer (*in vitro* against human lung adenocarcinoma, small cell lung carcinoma, melanoma, biliary tree cancer, and adenocarcinoma, with good activity against breast cancer,<sup>121</sup> ovarian cancer, non-Hodgkin's lymphoma, head and neck cancer, squamous cell lung cancer, soft tissue carcinoma, gastric cancer, and hepatoma. Mitoxantrone is extremely potent, showing effects in doses as small as 1 ng/mL *in vitro*.<sup>122</sup> It arrests the cell cycle at the transition from G2 phase (the phase which follows DNA synthesis, when cells are tetraploid) to M phase, when mitosis occurs.<sup>123</sup> Studies

show a synergistic effect with doxorubicin (see section 1.4.4.2), as well as other chemotherapeutic agents.<sup>123</sup> Mitoxantrone induces the same type of DNA damage as doxorubicin, suggesting that its mechanism of action might be similar, acting by both intercalation and inducing strand breaks.<sup>123</sup>

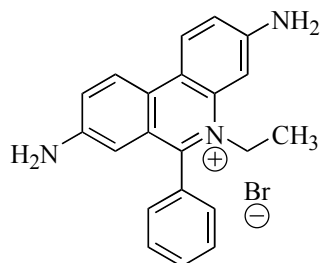


Figure 1.35. Ethidium Bromide

Ethidium bromide (Figure 1.35) is an intercalator selective for AT-rich DNA sequences.<sup>69</sup> It causes unwinding of DNA from a 36° base turn angle for unmodified B-DNA to 18°, shown in the crystal structure of ethidium bromide with 5-iodouridylyl (3'-5') adenosine and 5-iodouridylyl (3'-5') guanosine reported in 1977.<sup>124,125</sup> The heavy atom incorporation was for use in X-ray crystallography. Ethidium bromide shows enhanced fluorescence upon DNA binding, making it a useful stain for imaging gel work and as a probe for displacement assays. Ethidium bromide shows strongest binding with double-stranded DNA, showing about 54% less enhancement in fluorescence when bound to denatured calf thymus DNA and 58% decrease in fluorescence enhancement when binding to supercoiled DNA.<sup>126</sup>

#### 1.4.4.2. Anthracyclines



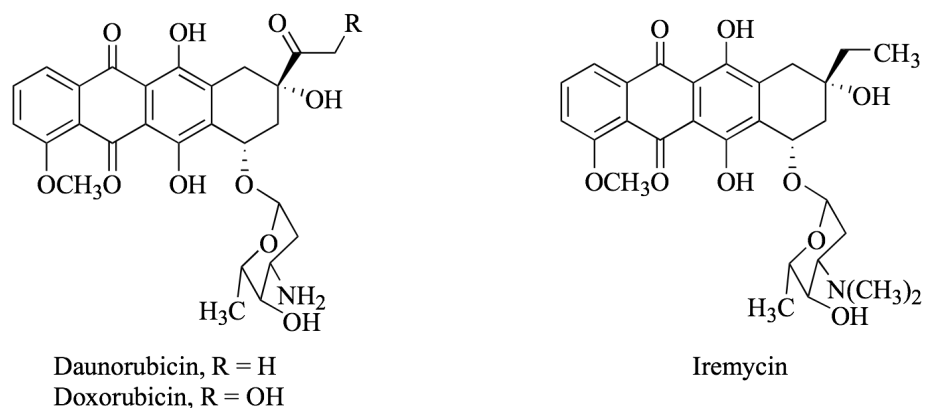


Figure 1.36. Daunorubicin, doxorubicin, and iremycin.

Daunorubicin (Figure 1.36) is used to treat leukemia and is registered by Wyeth-Ayerst as Cerubidine, and doxorubicin (trade name adriamycin) is indicated for multiple tumor types by Adria and Others.<sup>100</sup> The anthracycline antibiotics are known to intercalate DNA and inhibit Topoisomerase II.<sup>127</sup> The flat, conjugated  $\pi$ -system intercalates between nucleosides, and the sugar moiety extends into the major groove.<sup>127</sup> Binding of doxorubicin to DNA was determined to be  $1.0 \times 10^6 \text{ M}^{-1} \text{ bp}^{-1}$  by fluorescence titration and  $29 \pm 2 \times 10^5 \text{ M}^{-1}$  using equilibrium dialysis.<sup>128</sup> Daunomycin binds DNA at  $6.9 \pm 2 \times 10^5 \text{ M}^{-1}$  as determined by equilibrium dialysis.<sup>128</sup> Both binding constants for daunomycin and doxorubicin show a concentration-dependence on monovalent cations, which may be attributed to a change in distance between the phosphates upon intercalation.<sup>128</sup> This shift causes a change in electrostatic interactions, with the small molecule intercalators having an overall favorable electrostatic effect.<sup>128</sup> Daunomycin displays a DNA unwinding angle of  $15.4 \pm 1.5^\circ$  and iremycin unwinds DNA at an angle of  $15.0 \pm 1.5^\circ$ .<sup>129</sup> Circular dichroism has been used to determine the degree of DNA lengthening caused by intercalation of daunorubicin and iremycin. Daunomycin lengthens DNA by  $0.31 \pm 0.02 \text{ nm}$  per molecule intercalated.<sup>129</sup> Iremycin lengthens DNA by  $0.40 \pm 0.02 \text{ nm}$  per molecule intercalated.<sup>129</sup> The  $\text{IC}_{50}$  value for inhibition of DNA

synthesis for iremycin is 29  $\mu\text{M}$ , and daunomycin is 23  $\mu\text{M}$ , as determined using radiolabeled monophosphate deoxyribosides.<sup>130</sup> Inhibition constants were proportional to DNA binding affinity.<sup>130</sup> In footprinting experiments, doxorubicin, daunomycin, and iremycin, protect the DNA from DNase I digestion and show site selectivity for intercalation between CG and CA intervals.<sup>131</sup> DNase I footprinting was used to determine the binding site of daunomycin at 5'-A(T)GC or 5'-A(T)CG.<sup>47</sup> Daunomycin and doxorubicin show increased protection compared to iremycin.<sup>131</sup>

#### 1.4.4.3. Quinoxaline Antibiotics

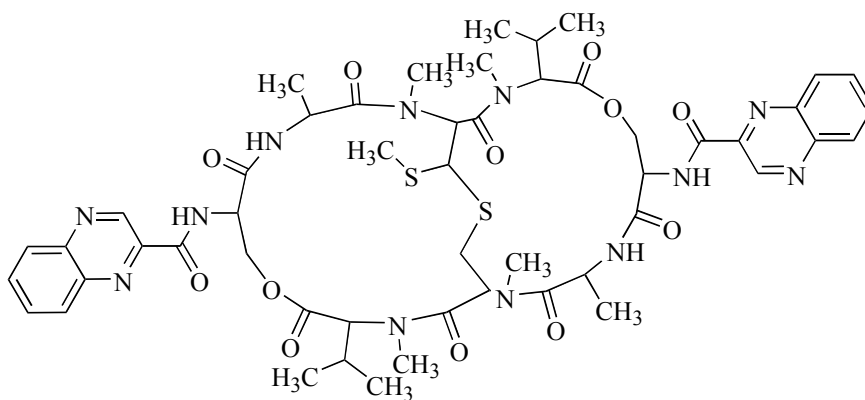


Figure 1.37. Echinomycin

Echinomycin (Figure 1.37) is a member of the quinoxaline antitumor antibiotics (effective against Gram-negative bacteria), a family of octapeptide macrocycles with sulfur-containing cross-bridges.<sup>132,133</sup> The quinoxaline moieties are thought to intercalate DNA and sandwich two DNA bases, but DNase footprinting does not indicate whether the preferred two base sequence is ApT or TpA.<sup>132</sup> Echinomycin is a member of the quinomycin family of this class of compounds, which contain a thioacetal cross-bridge. Echinomycin is thought to interact with DNA by intercalation of the two heteroaromatic rings with the bases. Unlike most intercalators, echinomycin exhibits a sequence

selectivity for GC-rich DNA.<sup>133</sup> DNase I footprinting using a 160-base oligomer (from *E. coli* containing the *tyr T* promoter region) shows protection at sites that have a CpG step in common, but the footprints comprise six bases with no clear consensus sequence.<sup>133</sup> CpG steps, then, are a prerequisite but not the minimum requirement for binding.<sup>133</sup> NMR modeling suggests that the intercalators sandwich four bases, which include a CpG interval. DNase I cleavage is significantly enhanced at AT-rich bases adjacent to the protected site.<sup>133</sup> The intercalation may slightly unwind the DNA (or cause bulges), allowing the nuclease to more easily recognize and cleave the DNA.<sup>133</sup>

Triostin A and TANDEM (Figure 1.38) are also examples of quinoxaline antitumor antibiotics belonging to the triostin family, which is defined by the disulfide bridge across the octapeptide. Triostin A, like echinomycin, binds GC-rich DNA, but has a slightly lower sequence selectivity. TANDEM is a des-*N*-tetramethyl synthetic analog of triostin A that shows the opposite sequence selectivity (5000-fold binding preference to poly(dA-dT) compared to poly(dG-dC)).<sup>132</sup> DNase I footprinting shows binding similar to echinomycin (six bases, two CpG steps) but with less pronounced footprints.<sup>132</sup> TANDEM, however, shows footprints centered around ATAT and ATAA sequences. Its protection of DNA from cleavage is nearly 20-fold lower than either triostin A or echinomycin, and it appears to be slightly more specific in its binding, since not all AT-rich tracts are protected from DNase I cleavage.<sup>132</sup>

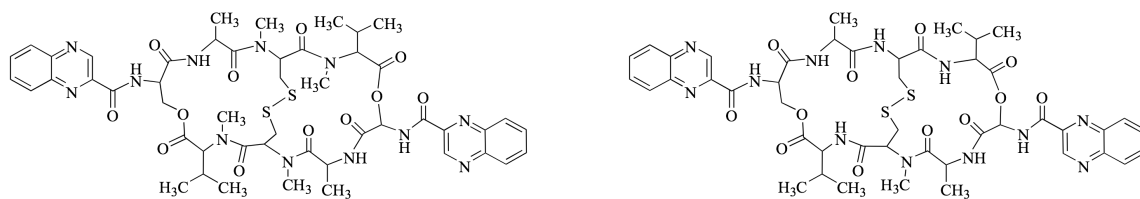


Figure 1.38. Triostin A (l) and TANDEM (r)

### 1.4.5. Minor Groove Binders

Compounds that bind to the hydrophobic minor groove of DNA (Figure 1.39) have historically been used as models for DNA binding but have recently gained prominence as potential anticancer agents. There are several proposed mechanisms by which minor groove binding compounds can serve as antineoplastic agents. The ligand-DNA interaction can distort the DNA structure, interfering with transcription or replication. These distortions can interfere with topoisomerases (which cleave and re-attach parts of the phosphate backbone of DNA), helicases (which unwind DNA), and polymerases (involved in transcription of DNA).<sup>134</sup> Other effects can be classified as being global (selective binding to long AT repeat sequences critical to chromosome metabolism) or specific (lesions might interrupt a specific nuclear process such as transcription of a gene).<sup>134</sup>



Figure 1.39. Cartoon of minor groove binding on DNA

#### 1.4.5.1. Polypyrrroles

Polypyrrroles are a class of minor groove binders that selectively bind AT-rich sequences, which are more electron-rich than GC rich sequences.<sup>134</sup> Hairpin polyamides

generally bind specific sequences of bases. Their binding typically interferes with DNA binding of endogenous compounds (i.e. binding of transcription factors). Distamycin (Figure 1.40), a classical example of a minor groove binder, inhibits helicases associated with Werner and Bloom syndrome as well as topoisomerase I and II and inhibits RNA polymerase I and II.<sup>134</sup> Distamycin inhibits RNA polymerase II by causing longer pauses at the enzyme's natural pause sites, which inhibits transcription.<sup>134</sup> Tight binding of distamycin directly to RNA polymerase I blocks chain elongation.<sup>134</sup> Netropsin (Figure 1.40), which binds DNA with a 1:1 stoichiometry inhibits the same helicase family as well as topoisomerases I and II.<sup>134</sup>

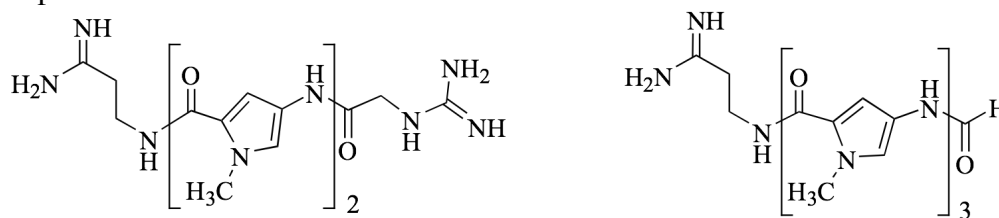


Figure 1.40. Netropsin (L) and Distamycin (R)

Netropsin shows two footprints on a restriction enzyme digest (*Hae*III/*Hind*III) of plasmid pBR322 consisting of 142 base pairs.<sup>135</sup> Both sites contain more than 70% A+T residues, but one footprint is 7 base pairs in length, and the other includes 14 base pairs. Distamycin-DNA interactions have been extensively studied. Hydroxyl radical footprinting has been used to analyze the interactions of distamycin with 5S ribosomal RNA genes of *Xenopus*.<sup>136</sup> Hydroxyl radical footprinting shows protection of three to four base pairs by distamycin at AT rich regions, with a minimum of two base pairs required for recognition.<sup>136</sup> Distamycin has been subjected to DNase I footprinting, but results using this technique are less specific than others because DNase I has a lower affinity for AT-rich sequences, to which distamycin binds preferentially.<sup>40</sup> The footprint does, however, show enhanced cleavage at AT bases adjacent to the poorly defined footprint.<sup>40</sup>

The footprints are offset on the complementary strand by two to three bases, indicating that distamycin interacts with approximately five bases on the two strands at each binding site.<sup>136</sup>

#### 1.4.5.2. *Bis(benzimidazoles)*

Bis(benzimidazoles) are fluorescent dyes that induce DNA strand breaks.<sup>134</sup> Hoechst 33258 (Figure 1.41) inhibits topoisomerase and helicases and also elevates endoreplication and polyploidy in Chinese hamster ovary (CHO) cells.<sup>134</sup> Additionally, this dye causes decondensation of heterochromatin and aneuploidy in mouse L cells.<sup>134</sup> Bis(benzimidazoles) have been conjugated to nitrogen mustards, which allows for alkylation.<sup>134</sup> Short linkers lead to alkylation at N3 of adenine; longer linkers allow alkylation at N7 of guanine.<sup>134</sup> These compounds are highly cytotoxic but display low rates of mutagenesis in bacterial assays.<sup>134</sup> The combination of a groove-binding moiety with alkylating moiety allows these conjugates to bind DNA with greater affinity than the alkylating agents themselves, which correlates to the increased cytotoxicity observed with these conjugates. This increased cytotoxicity might also be related to topoisomerase inhibition by the groove binding, rather than increase alkylation.<sup>134</sup>

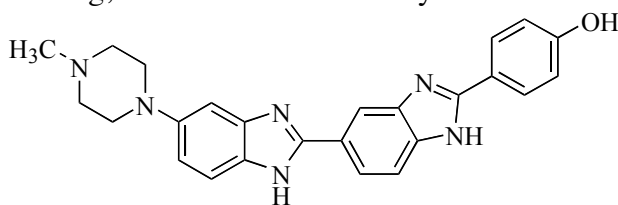


Figure 1.41. Hoechst 33258 dye

Bisquaternary ammonium heterocycles (Figure 1.42), which are structurally similar to polyamides, bind to AT tracts containing at least 4 base pairs, causing distortion of DNA structure and inhibiting DNA and RNA polymerases.<sup>134</sup>

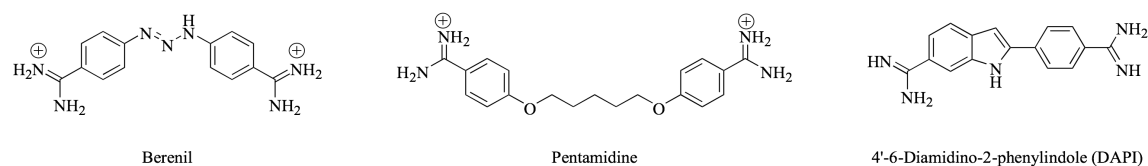


Figure 1.42. Berenil (l), Pentamidine (center), and DAPI (r)

### 1.4.5.3. Aureolic Acids

The aureolic acids include the microbial secondary metabolites mithramycin<sup>137</sup> and chromomycin<sup>138</sup> (Figure 1.43), which are antitumor antibiotics. These natural products inhibit gene expression and appear to exert their biological activity by metal dependent DNA binding in the minor groove. The saccharide moieties on both mithramycin and chromomycin are important for sequence selectivity. NMR studies suggest a 2:1 aureolic acid to metal ion binding stoichiometry, and demonstrate that mithramycin selectively binds DNA at GpC steps.<sup>139,140</sup> Mithramycin has traditionally been thought to act as a 2:1 complex of mithramycin to  $Mg^{2+}$ , although recent studies suggest that other metal-complexes might also be biologically active.<sup>141,142</sup> Two  $Mg^{2+}$  complexes have been characterized in solution, with different association constants. The 2:1 drug:metal complex has a  $K_a$  of  $1.6 \times 10^3$ , and the 1:1 complex has a  $K_a$  of  $1.8 \times 10^4$ . Lower concentrations of drug and metal favor formation of a 1:1 complex (25  $\mu M$   $Mg^{2+}$  : 50  $\mu M$  mithramycin); higher concentrations favor 2:1 (100  $\mu M$   $Mg^{2+}$  : 200  $\mu M$  mithramycin). Both complexes have been shown to be minor groove binders. Fluorescence titrations showed that both complexes bind calf thymus DNA with very similar binding constants ( $2.8 \pm 0.3 \times 10^5$  for 1:1 and  $1.15 \pm 0.1 \times 10^5$ ) and ratios of drug:nucleoside (0.15 for 1:1 and 0.19 for 2:1).<sup>107</sup> Although the 2:1 complex appears to be slightly larger than the minor groove, NMR data for both mithramycin and

chromomycin, as well as displacement assays, suggest that the minor groove becomes slightly distorted to accommodate the ligand.<sup>107,143</sup> Chromomycin shows a binding selectivity for GC-rich DNA, preferring GpC to CpG intervals (determined by NMR titrations).<sup>144</sup> Fe(II)-MPE footprinting for chromomycin A<sub>3</sub> shows the strongest protecting effect at 5'-GGG-3' and 5'-CGA-3'.<sup>138</sup>

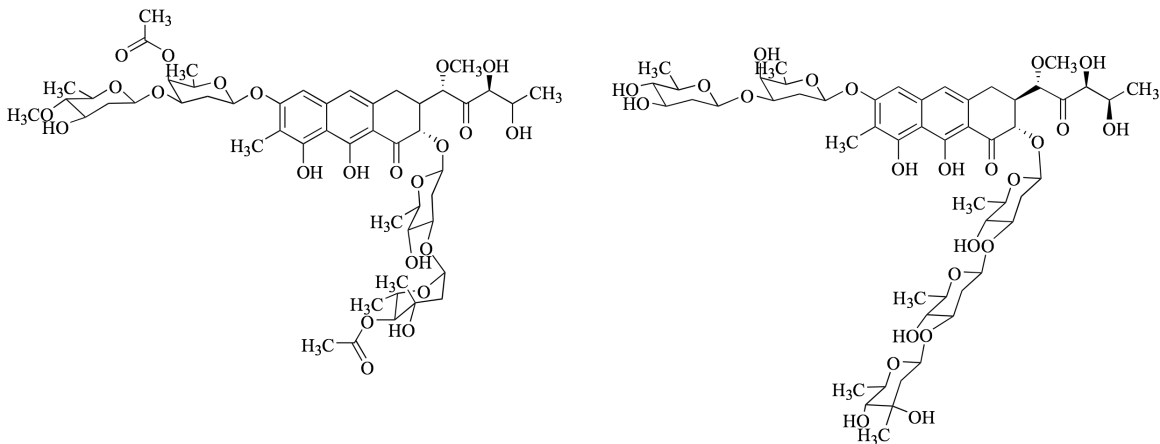


Figure 1.43. Chromomycin A<sub>3</sub>(l) and Mithramycin (r)<sup>145</sup>

## 1.5. CONCLUSIONS

This is only a brief overview of small-molecule DNA interactions. Covalent and non-covalent modification of DNA is an active field of research because of its effects on cell growth or death. Newer, more rapid and sensitive methods of analysis are under development. Additionally, although many of the drugs shown here are used therapeutically or are under development, much more can be done in this area to improve drug-like properties (i.e. selectivity, toxicity, etc.). Understanding both therapeutic and harmful small molecule-DNA interactions is key to understanding and treating many diseases.



## 1.6. REFERENCES

- (1) Weaver, R. F. *Molecular Biology*; The McGraw-Hill Companies: St. Louis, 2005.
- (2) Sturla, S. J. *Current Opinion in Molecular Biology* **2007**, *11*, 293-299.
- (3) Dickerson, R. E.; Drew, H.; Conner, B. N.; Wing, R. M.; Fratini, A. V.; Kopka, M. L. *Science* **1982**, *216*, 475-485.
- (4) Stofer, E.; Chipot, C.; Lavery, R. *J. Am. Chem. Soc.* **1999**, *121*, 9503.
- (5) Neidle, S. *Nucleic Acid Structure and Recognition*; Oxford University Press: New York, 2002.
- (6) Heinemann, U.; Alings, C.; Hahn, M. *Biophys. Chem.* **1994**, *50*, 157-167.
- (7) Hutchison, C. A. *Nucleic Acids Res.* **2007**, *35*, 6227-6237.
- (8) Maxam, A. M.; Gilbert, W. *Proc. Natl. Acad. Sci. U.S.A.* **1977**, *74*, 560-564.
- (9) Franca, L. T. C.; Carrilho, E.; Kist, T. B. L. *Q. Rev. Biophys.* **2002**, *35*, 169-200.
- (10) Cashmore, A. R.; Petersen, G. B. *Biochim. Biophys. Acta* **1969**, *174*, 591-603.
- (11) Lhomme, J.; Constant, J.-F.; Demeunyk, M. *Biopolymers* **1999**, *52*, 65-83.
- (12) Mattes, W. B.; Hartley, J. A.; Kohn, K. W. *Biochim. Biophys. Acta* **1986**, *868*, 71-76.
- (13) Warpehoski, M. A.; Hurley, L. H. *Chem. Res. Toxicol.* **1988**, *1*, 315-333.
- (14) Stuart, G. R.; Chambers, R. W. *Nucleic Acids Res.* **1987**, *15*, 7451-7562.
- (15) Gold, B.; Marky, L. M.; Stone, M. P.; Williams, L. D. *Chem. Res. Toxicol.* **2006**, *19*, 1402-1414.
- (16) Ford, G. P.; Scribner, J. D. *Chem. Res. Toxicol.* **1990**, *3*, 219-230.

- (17) Lawley, P. D.; Orr, D. J. *Chem.-Biol. Interact.* **1970**, *2*, 61-164.
- (18) Tong, W. P.; Ludlum, D. B. *Biochim. Biophys. Acta* **1980**, *608*, 174-181.
- (19) Broggini, M.; Coley, H. M.; Mongelli, N.; Pesenti, E.; Wyatt, M. D.; Hartley, J. A.; D'Incalci, M. *Nucleic Acids Res.* **1995**, *23*, 81-87.
- (20) Cutts, S. M.; Masta, A.; Panousis, C.; Parsons, P. G.; Sturm, R. A.; Phillips, D. R. In *Drug-DNA Interaction Protocols*; Fox, K. R., Ed.; Humana Press: Totowa, New Jersey, 1997; Vol. 90, p 1-22.
- (21) Cutts, S. M.; Panousis, C.; Masta, A.; Phillips, D. R. In *Drug-DNA Interaction Protocols*; Fox, K. R., Ed.; Humana Press: Totowa, New Jersey, 1997; Vol. 90, p 1-22.
- (22) Hartley, J. A.; Souhami, R. L.; Berardini, M. D. *J. Chromatogr.* **1993**, *618*, 277-288.
- (23) Skibo, E. B.; Xing, C.; Groy, T. *Bioorg. Med. Chem. Lett.* **2001**, *9*, 244502459.
- (24) Lawley, P. D.; Brookes, P. *Biochem. J.* **1963**, *89*, 127-138.
- (25) Greer, S.; Zamenhof, S. *J. Mol. Biol.* **1962**, *4*, 123-141.
- (26) Randerath, K.; Reddy, M. V.; Gupta, R. C. G. *Proc. Natl. Acad. Sci. U. S. A.* **1981**, *78*, 6126-6129.
- (27) Randerath, E.; Agrawal, H. P.; Weaver, J. A.; Bordelon, C. B.; Randerath, K. *Carcinogenesis* **1985**, *6*, 1117-1126.
- (28) Randerath, K.; Randerath, E.; Agrawal, H. P.; Gupta, R. C.; Schurdak, M. E.; Reddy, M. V. *Environ. Health Perspect.* **1985**, *62*, 57-65.
- (29) Reddy, M. V.; Gupta, R. C.; Randerath, K. *Anal. Biochem.* **1981**, *117*, 271-279.

- (30) Reddy, M. V.; Randerath, K. *Environ. Health Perspect.* **1987**, *76*, 41-47.
- (31) Reddy, M. V.; Randerath, K. *Carcinogenesis* **1986**, *7*, 1543-1551.
- (32) Fox, K. R. In *Methods in Molecular Biology*; Walker, J. M., Ed.; Humana Press: Totowa, 1997; Vol. 90, p 278.
- (33) Terron, A.; Fiol, J. J.; Garcia-Raso, A.; Barcelo-Oliver, M.; Moreno, V. *Coord. Chem. Rev.* **2007**, *251*, 1973-1986.
- (34) Price, P. A. *J. Biol. Chem.* **1975**, *250*, 1981-1986.
- (35) Hurley, L. H.; Reck, T.; Thurston, D. E.; Langley, D. R.; Holden, K. G.; Hertzberg, R. P.; Hoover, J. R. E.; Gallagher, G.; Faucette, L. F.; Mong, S.-M.; Johnson, R., K. *Chem. Res. Toxicol.* **1988**, *1*.
- (36) Fox, K. R.; Waring, M. J. *Biochemistry* **1986**, *25*, 4349-3456.
- (37) Galas, D. J.; Schmitz, A. *Nucleic Acids Res.* **1978**, *5*, 3157-3170.
- (38) Lane, M. J.; Dabrowiak, J. C.; Vournakis, J. N. *Proc. Natl. Acad. Sci. U.S.A.* **1983**, *80*, 3260-3264.
- (39) Scamrov, A. V.; Beabealashvilli, R. S. *FEBS Lett.* **1983**, *164*, 97-101.
- (40) Fox, K. R.; Waring, M. J. *Nucleic Acids Res.* **1984**, *12*, 9271-9285.
- (41) Spassky, A.; Sigman, D. S. *Biochemistry* **1985**, *24*, 8050-8056.
- (42) Sigman, D. S. *Biochemistry* **1990**, *29*, 9097-9105.
- (43) Hertzberg, R. P.; Dervan, P. B. *Biochemistry* **1984**, *23*, 3934-3945.
- (44) Nielsen, P. E.; Hiort, C.; Sonnichsen, S. H.; Buchardt, O.; Dahl, O.; Norden, B. J. *Am. Chem. Soc.* **1992**, *114*, 4967-4975.
- (45) Nielsen, P. E.; Jeppesen, C.; Buchardt, O. *FEBS Lett.* **1988**, *235*, 122-124.

- (46) Mollegaard, N. E.; Nielsen, P. E. In *Drug-DNA Interaction Protocols*; Fox, K. R., Ed.; Humana Press: Totowa, New Jersey, 1997; Vol. 90, p 1-22.
- (47) Chaires, J. B.; Herrera, J. E.; Waring, M. J. *Biochemistry* **1990**, *29*, 6145-6153.
- (48) Saiki, R. K.; Scharf, S.; Faloona, F.; Mullis, K. B.; Horn, G. T.; Erlich, H. A.; Arnheim, N. *Science* **1985**, *230*, 1350-1354.
- (49) Pfeifer, G. P.; Denissenko, M. F.; Tang, M.-s. *Toxicol. Lett.* **1998**, *102-103*, 447-451.
- (50) Dooley, T. P.; Weiland, K. L. In *Drug-DNA Interaction Protocols*; Fox, K. R., Ed.; Humana Press: Totowa, New Jersey, 1997; Vol. 90, p 1-22.
- (51) Bingham, J. P.; Hartley, J. A.; Souhami, R. L.; Grimaldi, K. A. *Nucleic Acids Res.* **1996**, *24*, 987-989.
- (52) Grimaldi, K. A.; Bingham, J. P.; Souhami, R. L.; Hartley, J. A. *Anal. Biochem.* **1994**, *222*, 236-242.
- (53) Seawell, P. C.; Ganesan, A. K. In *DNA Repair*; Dekker: New York, 1981, p 425-430.
- (54) Sousa, F.; Tomaz, C. T.; Prazeres, D. M. F.; Queiroz, J. A. *Anal. Biochem.* **2005**, *343*, 183-185.
- (55) Akerman, B. *Biophys. J.* **1998**, *74*, 3140-3151.
- (56) Newkome, G. R.; Kawato, T.; Kohli, D. K.; Puckett, W. E.; Olivier, B. D.; Chiari, G.; Fronczek, F. R.; Deutsch *J. Am. Chem. Soc.* **1981**, *103*, 3423-3429.
- (57) Biggins, J. B.; Prudent, J. R.; Marshall, D. J.; Ruppen, M.; Thorson, J. S. *Proc. Natl. Acad. Sci. U.S.A.* **2000**, *97*, 13537-13542.

- (58) Miller, J. N. *Analyst* **2005**, *130*, 265-270.
- (59) Singh, R.; Farmer, P. B. *Carcinogenesis* **2006**, *27*, 178-196.
- (60) Beck, J. L.; Colgrave, M. L.; Ralph, S. F.; Sheil, M. M. *Mass Spectrom. Rev.* **2001**, *20*, 61-87.
- (61) Bellis, G. D.; Salani, G.; Battaglia, C.; Pietta, P.; Rosti, E.; Mauri, P. *Rapid Commun. Mass Spectrom.* **2000**, *14*, 243-249.
- (62) Murray, K. R. *J. Mass Spectrom.* **1996**, *31*, 1203-1215.
- (63) Cadet, J.; Douki, T.; Frelon, S.; Sauviago, S.; Pouget, J.-P.; Ravanat, J.-L. *Free Radical Biol. Med.* **2002**, *33*, 441-449.
- (64) Ding, J.; Vouros, P. *J. Chromatogr. A* **2000**, *887*, 103-113.
- (65) Ren, J.; Chaires, J. B. *Biochemistry* **1999**, *38*, 16067-16075.
- (66) Wilson, W. D.; Tanious, F. A.; Fernandez-Saiz, M.; Rigl, C. T. In *Methods in Molecular Biology*; Walker, J. M., Ed.; Humana Press: Totowa, 1997; Vol. 90, p 278.
- (67) Dougherty, G.; Pilbrow, J. R. *Int. J. Biochem.* **1984**, *16*, 1179-1192.
- (68) Jenkins, T. C. In *Methods in Molecular Biology*; Walker, J. M., Ed.; Humana Press: Totowa, 1997; Vol. 90, p 278.
- (69) Morgan, A. R.; Lee, J. S.; Pulleyblank, D. E.; Murray, N. L.; Evans, D. H. *Nucleic Acids Res.* **1979**, *7*, 547-569.
- (70) Likussar, W.; Boltz, D. F. *Anal. Chem.* **1971**, *43*, 1265-1272.
- (71) Russu, I. M. *Trends Biotechnol.* **1991**, *9*, 96-104.

- (72) Keniry, M. A.; Shafer, R. H. In *Methods Enzymol.*; Academic Press: New York, 1995; Vol. 261, p 575-604.
- (73) Peek, M. E.; Williams, L. D. In *Methods Enzymol.*; Academic Press: New York, 2001; Vol. 340, p 282-290.
- (74) Joshua-Tor, L.; Sussman, J. L. *Curr. Opin. Struct. Bio.* **1993**, *3*, 323-335.
- (75) Lawley, P. D.; Orr, D. J. *Chem.-Biol. Interact.* **1970**, *2*, 154-157.
- (76) Hurley, L. H.; Reynolds, V. L.; Swenson, D. H.; Petzold, G. L.; Scahill, T. A. *Science* **1984**, *226*, 843-844.
- (77) Needham-VanDevanter, D. R.; Hurley, L. H.; Reynolds, V. L.; Thierault, N. Y.; Krueger, W. C.; Wierenga, W. *Nucleic Acids Res.* **1984**, *12*, 6159-6168.
- (78) Reynolds, V. L.; Molineux, I. J.; Kaplan, D. J.; Swenson, D. H.; Hurley, L. R. *Biochemistry* **1985**, *24*, 6228-6237.
- (79) Tang, M.-s.; Lee, C.-S.; Doisy, R.; Ross, L.; Needham-VanDevanter, D. R.; Hurley, L. H. *Biochemistry* **1988**, *27*, 893-901.
- (80) Sun, D.; Lin, C. H.; Hurley, L. H. *Biochemistry* **1993**, *32*, 4487-4495.
- (81) Lin, C. H.; Sun, D.; Hurley, L. H. *Chem. Res. Toxicol.* **1991**, *4*, 21-26.
- (82) Hanka, L. J.; Dietz, S. A.; Gerpheide, S. A.; Kuentzel, S. L.; Martin, D. G. *J. Antibiot.* **1978**, *XXXI*, 1211-1217.
- (83) Eisenbrand, G.; Muller, N.; Denker, E.; Sterzel, W. *Journal of Cancer Research and Clinical Oncology* **1986**, *112*, 196-204.
- (84) Wurdeman, R. L.; Church, K. M.; Gold, B. *J. Am. Chem. Soc.* **1989**, *111*, 6408-6412.

- (85) Singer, B. *J. Natl. Cancer Inst.* **1979**, *62*, 1329-1339.
- (86) Kelly, J. D.; Shah, D.; Chen, F.-X.; Wurdeman, R.; Gold, B. *Chem. Res. Toxicol.* **1998**, *11*, 1481-1486.
- (87) Hemminki, K.; Ludlum, D. B. *J. Natl. Cancer Inst.* **1984**, *73*, 1021-1028.
- (88) Gorbacheva, L. B.; Dederer, L. Y. *Pharm. Chem. J.* **2009**, *43*, 73-76.
- (89) Bolzan, A. D.; Bianchi, M. S. *Mutat. Res.* **2002**, *512*, 121-134.
- (90) Cheh, A. M.; Yagi, H.; Jerina, D. M. *Chem. Res. Toxicol.* **1990**, *3*, 545-550.
- (91) Szeliga, J.; Lee, H.; Harvey, R. G.; Page, J. E.; Ross, H. L.; Routledge, M. N.; Hilton, B. D.; Dipple, A. *Chem. Res. Toxicol.* **1994**, *7*, 420-427.
- (92) Ponti, M.; Souhami, R. L.; Fox, B. W.; Hartley, J. A. *Br. J. Cancer* **1991**, *63*, 743-747.
- (93) Povirk, L.; Shuker, D. E. *Mutat. Res.* **1994**, *318*, 205-226.
- (94) Millard, J. T.; Raucher, S.; Hopkins, P. B. *J. Am. Chem. Soc.*, *112*, 2459-2460.
- (95) Kohn, K. W.; Hartlet, J. A.; Mattes, W. B. *Nucleic Acids Res.* **1987**, *14*, 10531-10549.
- (96) Price, C. C.; Gaucher, G. M.; Koneru, P.; Shibakawa, R.; Sowa, J. R.; Yamaguchi, M. *Biochim. Biophys. Acta* **1968**, *166*, 327-359.
- (97) Maccrubin, A. E.; Caballes, L.; Riordan, J. M.; Huang, D. H.; Gurtoo, H. L. *Cancer Res.* **1991**, *51*, 886-892.
- (98) Colvin, M.; Hilton, J. *Cancer Treatment Reports* **1981**, *65*, 89-95.
- (99) Cushnir, J. R.; Naylor, S.; Lamb, J. H.; Farmer, P. B.; Brown, N. A.; Mirkes, P. E. *Rapid Commun. Mass Spectrom.* **1990**, *4*, 410-414.

- (100) Schacter, L. P.; Anderson, C.; Canetta, R. M.; Kelley, S.; Nicaise, C.; Onetto, N.; Rozenzweig, M.; Smaldone, L.; Winograd, B. *Seminars in Oncology* **1992**, *19*, 613-621.
- (101) Baruah, H.; Barry, C. G.; Bierback, U. *Curr. Top. Med. Chem.* **2004**, *4*, 1537-1549.
- (102) Hopkins, P. B.; Millard, J. T.; Woo, J.; Weidner, M. F.; Kirchner, J. J.; Sigurdsson, S. T.; Raucher, S. *Tetrahedron* **1991**, *47*, 2475-2489.
- (103) Epstein, J. L.; Zhang, X.; Doss, G. A.; Liesch, J. M.; Krishnan, B.; Stubbe, J.; Kozarich, J. W. *J. Am. Chem. Soc.* **1997**, *119*, 6731-6738.
- (104) Nicolaou, K. C.; Smith, A. L. *Acc. Chem. Res.* **1992**, *25*, 497-503.
- (105) Voss, J. J. D.; Hangeland, J. J.; Townsend, C. A. *J. Am. Chem. Soc.* **1990**, *112*, 4554-4556.
- (106) Jones, R. R.; Bergman, R. G. *J. Am. Chem. Soc.* **1972**, *94*, 660-661.
- (107) Aich, P.; Dasgupta, D. *Biochemistry* **1995**, *34*, 1376-1385.
- (108) Lindh, R.; Ryde, U.; Schutz, M. *Theor. Chem. Acc.* **1997**, *97*, 203-210.
- (109) Zein, N.; McGahren, W. J.; Morton, G. O.; Ashcroft, J.; Ellestad, J. *J. Am. Chem. Soc.* **1989**, *111*, 6888-6890.
- (110) Voss, J. J. D.; Townsend, C. A.; Ding, W.-D.; Orton, G. O.; Ellestad, G. A.; Zein, N.; Tabor, A. B.; Schreiber, S. L. *J. Am. Chem. Soc.* **1990**, *112*, 9699-9670.
- (111) Mah, S. C.; Townsend, C. A.; Tullius, T. D. *Biochemistry* **1994**, *33*, 614-621.
- (112) Kalben, A.; Pal, S.; Andreotti, A. H.; Walker, S.; Gange, D.; Biswas, K.; Kahne, D. *J. Am. Chem. Soc.* **2000**, *122*, 8403-8412.



- (113) Sugiura, Y.; Uesawa, Y.; Takahashi, Y.; Kuwahara, J.; Golik, J.; Doyle, T. W. *Proc. Natl. Acad. Sci. U. S. A.* **1989**, *86*, 7672-7676.
- (114) Xu, Y.-j.; Xi, Z.; Zhen, Y.-s.; Goldberg, I. H. *Biochemistry* **1997**, *36*, 14975-14984.
- (115) Kappen, L. S.; Goldberg, I. H. *Biochemistry* **1993**, *32*, 13138-13145.
- (116) Povirk, L. F.; Goldberg, I. H. *Nucleic Acids Res.* **1982**, *10*, 6255-6264.
- (117) Guan, L. L.; Kuwahara, J.; Sugiura, Y. *Biochemistry* **1993**, *1993*, 6141-6145.
- (118) Ehrenfield, G. M.; Shipley, J. B.; Heimbrook, D. C.; Sugiyama, H.; Long, E. E.; van Bloom, J. J.; van der Marel, G. A.; Oppenheimer, N. J.; Hecht, S. M. *Biochemistry* **1987**, *36*, 931-942.
- (119) Giloni, L.; Takeshita, M.; Johnson, F.; Iden, C.; Grollman, A. P. *The Journal of Biological Chemistry* **1981**, *256*, 8608-8615.
- (120) Collier, D. A.; Neidle, S.; Brown, J. R. *Biochem. Pharmacol.* **1984**, *33*, 2877-2880.
- (121) Corbleet, M. A.; Stuart-Harris, R. C.; Smith, I. E.; Coleman, R. E.; Rubens, R. D.; McDonald, M.; Mouridsen, H. T.; Ranier, H.; van Oosterom, A. T.; Smyth, J. F. *European Journal of Cancer and Clinical Oncology* **1984**, *20*, 1141-1146.
- (122) Dackiewicz, P.; Skladanowski, A.; Konopa, J. *Chem.-Biol. Interact.* **1995**, *98*, 153-166.
- (123) Faulds, D.; Balfour, J. A.; Chrisp, P.; Langtry, H. D. *Drugs* **1991**, *41*, 400-449.
- (124) Tsai, C.-C.; Jain, S.; Sobell, H. M. *J. Mol. Biol.* **1977**, *114*, 301-315.
- (125) Jain, S. C.; Tsai, C.-C.; Sobell, H. M. *J. Mol. Biol.* **1977**, *114*, 317-331.
- (126) LePecq, J.-B.; Paoletti, C. *J. Mol. Biol.* **1967**, *27*, 87-106.

- (127)Moro, S.; Beretta, G. L.; Dal Ben, D.; Nitiss, J.; Palumbo, M.; Capranico, G.  
*Biochemistry* **2004**, *43*, 7503-7513.
- (128)Chaires, J. B.; Priebe, W.; Graves, D. E.; Burke, T. G. *J. Am. Chem. Soc.* **1993**,  
*115*, 5360-5364.
- (129)Fritzche, H.; Triebel, H.; Chaires, J. B.; Dattagupta, N.; Crothers, D. M.  
*Biochemistry* **1982**, *21*, 3940-3946.
- (130)Fritzsche, H.; Wahnert, U.; Chaires, J. B.; Dattagupta, N.; Schlessinger, F. B.;  
Crothers, D. M. *Biochemistry* **1987**, *26*, 1996-2000.
- (131)Jolles, B.; Laigle, A.; Priebe, W.; Garnier-Suillerot, A. *Chem.-Biol. Interact.* **1996**,  
*100*, 165-176.
- (132)Low, C. M. L.; Olsen, R. K.; Waring, M. J. *FEBS Lett.* **1984**, *176*, 414-420.
- (133)Low, C. M. L.; Drew, H. R.; Waring, M. J. *Nucleic Acids Res.* **1984**, *12*, 4865-  
4879.
- (134)Nelson, S. M.; Ferguson, L. R.; Denny, W. A. *Mutat. Res.* **2007**, *623*, 24-40.
- (135)Dyke, M. W. V.; Hertzberg, R. P.; Dervan, P. B. *Proc. Natl. Acad. Sci. U. S. A.*  
**1982**, *79*, 5470-5474.
- (136)Churchill, M. E. A.; Hayes, J. J.; Tullius, T. D. *Biochemistry* **1990**, *29*, 6043-6050.
- (137)Grundy, W. E.; Goldstein, A. W.; Rickher, C. J.; Hanes, M. E.; Warren, H. B., Jr.;  
Sylvester, J. C. *Antibiotic Chemotherapeutics* **1953**, *3*, 1215-1217.
- (138)Dyke, M. W. V.; Dervan, P. B. *Biochemistry* **1983**, *22*, 2373-2377.
- (139)Cons, B. M. G.; Fox, K. R. *FEBS Lett.* **1990**, *264*, 100-104.
- (140)Fox, K. R.; Howarth, N. R. *Nucleic Acids Res.* **1985**, *13*, 8695-8714.

- (141) Hou, M.-H.; Wang, A. H.-J. *Nucleic Acids Res.* **2005**, *33*, 1352-1361.
- (142) Devi, P. G.; Pal, S.; Banerjee, R.; Dasgupta, D. *J. Inorg. Biochem.* **2007**, *101*, 127-137.
- (143) Liu, C.; Chen, F.-M. *Biochemistry* **1994**, *33*, 1419-1424.
- (144) Banville, D. L.; Keniery, M. A.; Shafer, R. H. *Biochemistry* **1990**, *29*, 9294-9302.
- (145) Wohlert, S. E.; Kunzel, E.; Machinek, R.; Mendez, C.; Salas, J. A.; Rohr, J. *J. Nat. Prod.* **1999**, *62*, 119-121.

## 2. Synthesis of ( $\pm$ )-N'-Nitrosonornicotine-5'-Acetate

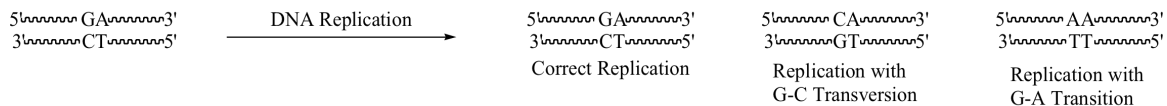
### 2.1. BACKGROUND

This chapter will describe the biological damage caused by nicotine ingestion, and previous work characterizing DNA adducts from nicotine metabolites. A review of sulfinimine chemistry follows, then the ( $\pm$ )-N'-nitrosonornicotine-5'-acetate (NNN-OAc) synthesis is described. Finally, biological studies on DNA interactions with NNN-5'-OAc are reported.

#### 2.1.1. Tobacco Carcinogens

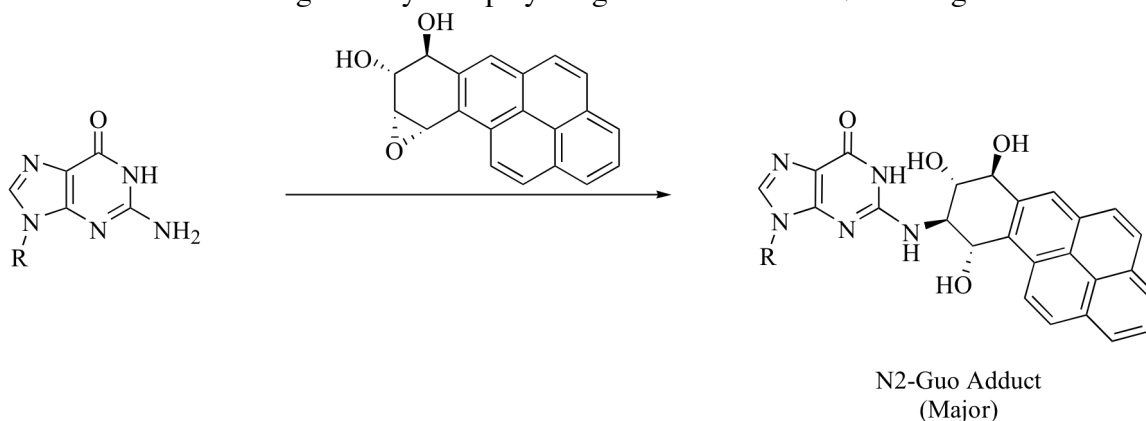
Cigarette smoking causes not only 87% of lung cancer deaths (the leading cause of cancer death for both men and women) but also 30% of all cancer deaths, including cancer of the larynx, oral cavity, pharynx, esophagus, stomach, renal body, liver, colon, and bladder.<sup>1,2</sup> Furthermore, smoking has been linked to kidney, pancreatic, cervical, and stomach cancers, as well as acute myeloid leukemia.<sup>3,4</sup> Nicotine, a constituent of cigarette smoke, also has been shown to induce angiogenesis and arteriogenesis, both of which are associated with not only cancer but also heart disease, macular degeneration, and diabetic retinopathy.<sup>5</sup> Although the causal relationship between cigarette smoking and cancer has been known since 1957,<sup>6</sup> relatively little is known about the mechanism by which carcinogens found in cigarette smoke cause DNA damage. A key component of the pathway appears to be nicotine carcinogen-associated damage of tumor suppressor gene p53. A damaged p53 gene is found in at least half of all cancers,<sup>7</sup> and an increased number of G→T transversions is found in about 60% of smokers who develop lung cancer.<sup>8,9</sup> Transversions are unusual mutations because they substitute a purine for a pyrimidine or a pyrimidine for a purine,<sup>10</sup> in contrast with more common transitions, in

which a purine (i.e. G) is exchanged for another purine (A) or one pyrimidine is substituted for the other.<sup>10</sup>



Scheme 2.1. Possible DNA replication outcomes

Although most work concerning DNA damage caused by smoking has focused on the role of polyaromatic hydrocarbons (i.e. benzopyrenes) on p53 mutations (Scheme 2.2), nicotine-based carcinogens may also play a significant role in DNA damage.



Scheme 2.2. DNA modification at guanosine by benzo[α]pyrene diol epoxide<sup>11</sup>

Additionally, polyaromatic hydrocarbons are ubiquitous,<sup>12</sup> whereas nicotine derivatives are specific to tobacco products and might leave a more unambiguous “fingerprint” as to the source of DNA damage. Two carcinogenic nicotine-derived components of cigarette smoke are 4-(methylnitrosamino)-1-(3-pyridyl)-1-butanone (NNK) and N'-nitrosonornicotine (NNN) (Figure 2.1).<sup>13</sup>

In tobacco plants, nornicotine is derived from N-demethylation of nicotine by nicotine N-demethylase (Scheme 2.3), which is a cytochrome P<sub>450</sub> enzyme.<sup>14</sup> Following

tobacco harvesting, depending on curing conditions, as much as 90% of the nicotine may be converted to nornicotine.<sup>15</sup> During curing and storage of the tobacco from plants, nornicotine is then converted to the established carcinogen N-nitrosornnicotine in a microbe-mediated nitrosation.<sup>14-17</sup>

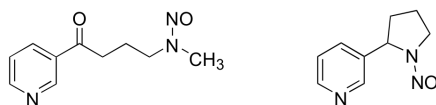
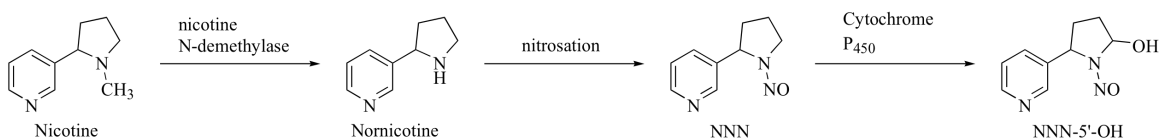


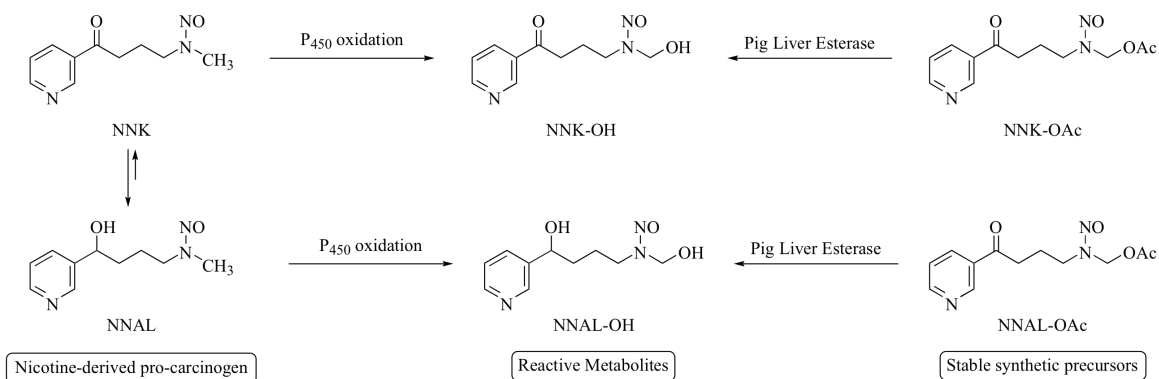
Figure 2.1. Structures of NNK (l) and NNK (r)



Scheme 2.3. Conversion of nicotine to NNN-5'-OH

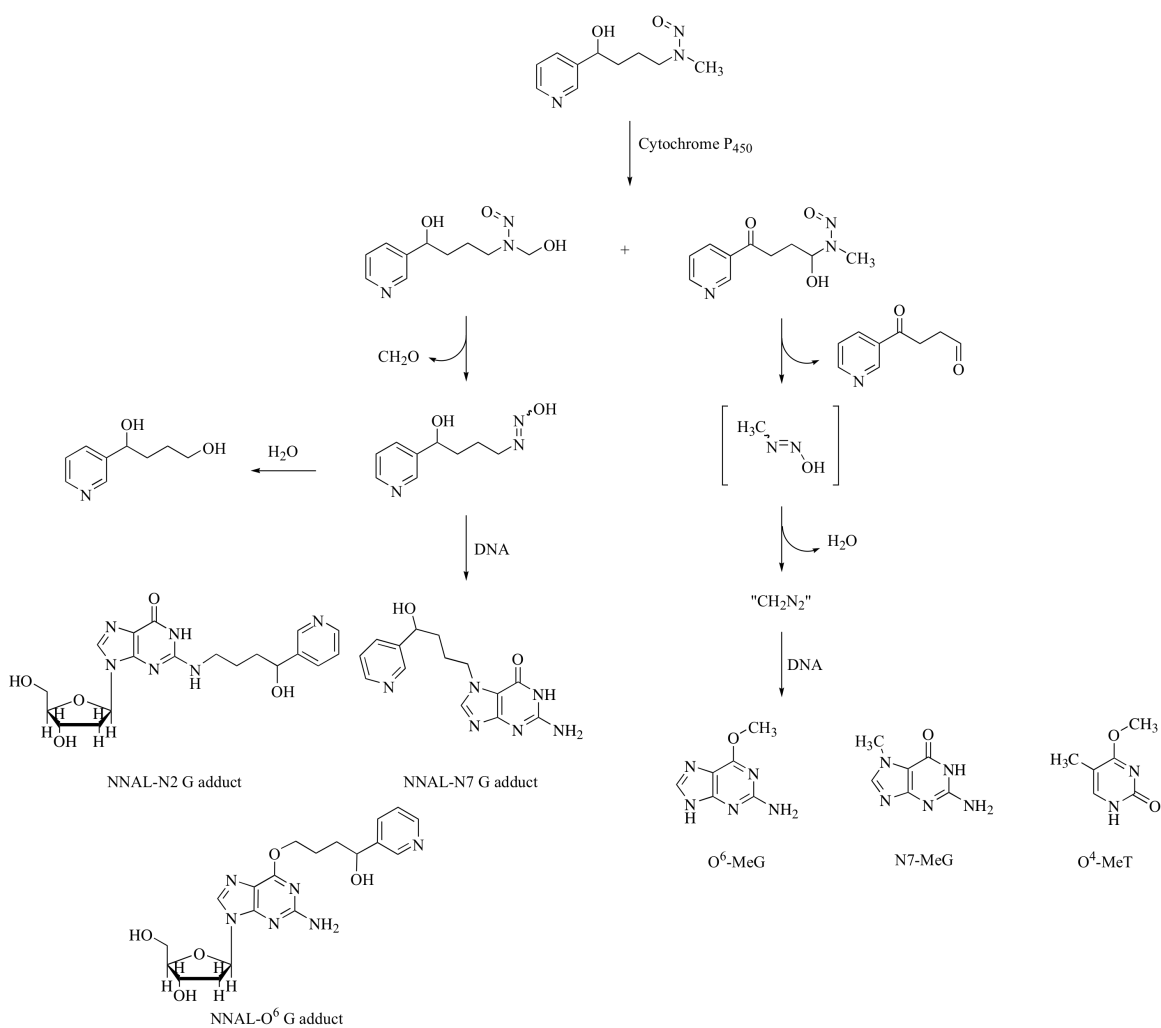
Upon ingestion, tobacco smoke carcinogens are oxidized by cytochrome P<sub>450</sub> enzymes,<sup>18</sup> (Scheme 2.4) which hydroxylate alpha to the N'-nitrosoamine. In general, cytochrome P<sub>450</sub> oxidation increases water solubility and rate of excretion of metabolites. These metabolites also sometimes form reactive intermediates containing electrophilic moieties that can covalently modify DNA.<sup>13</sup> Prior to hydroxylation  $\alpha$  to the N'-nitrosoamine, NNK can be reduced to its metabolite, 4-(methylnitrosamino)-1-(3-pyridyl)-1-butanol (NNAL), which is the predominant species *in vivo*.<sup>19</sup> Both NNAL-OH and NNK-OH have been shown to covalently modify DNA.<sup>19</sup> These oxidized nicotine derivatives are unstable and cannot be synthesized or stored easily, which makes studying their *in vitro* interactions with DNA difficult. A solution to this problem is to synthesize

the more stable acetate-protected alcohol and to deprotect it *in situ* using pig liver esterase (PLE) (Scheme 2.4).



Scheme 2.4. Metabolic activation of NNK; synthetic precursors for reactive metabolites

Adducts of NNAL with DNA have been characterized by Hecht and coworkers, who incubated NNAL-OAc with calf thymus DNA or deoxyguanosine and compared the products to independently synthesized standards using high performance liquid chromatography (HPLC), UV-Vis, and selective ion monitoring (SIM) mass spectrometry.<sup>20</sup>



Scheme 2.5. NNAL DNA adduct formation

Additionally, O<sup>2</sup> adducts of the pyrimidine bases have been identified and characterized (Figure 2.2).<sup>20</sup> Incubation of single deoxyribonucleosides with the stable NNK-OAc and NNAL-OAc precursors yielded adducts in quantities large enough for characterization by standard techniques (NMR, UV-Vis, MS). Incubation of each carcinogen precursor with calf-thymus DNA and pig liver esterase followed by either



thermal or enzymatic hydrolysis, was compared using selective ion monitoring LC-MS to the single-base samples.<sup>20</sup>

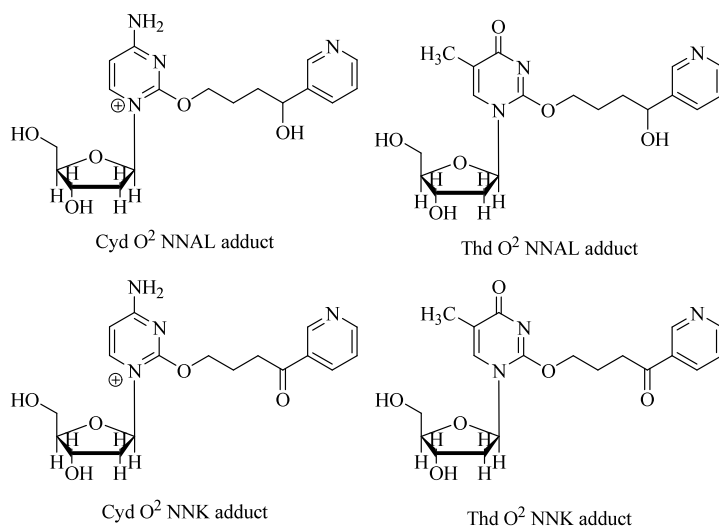
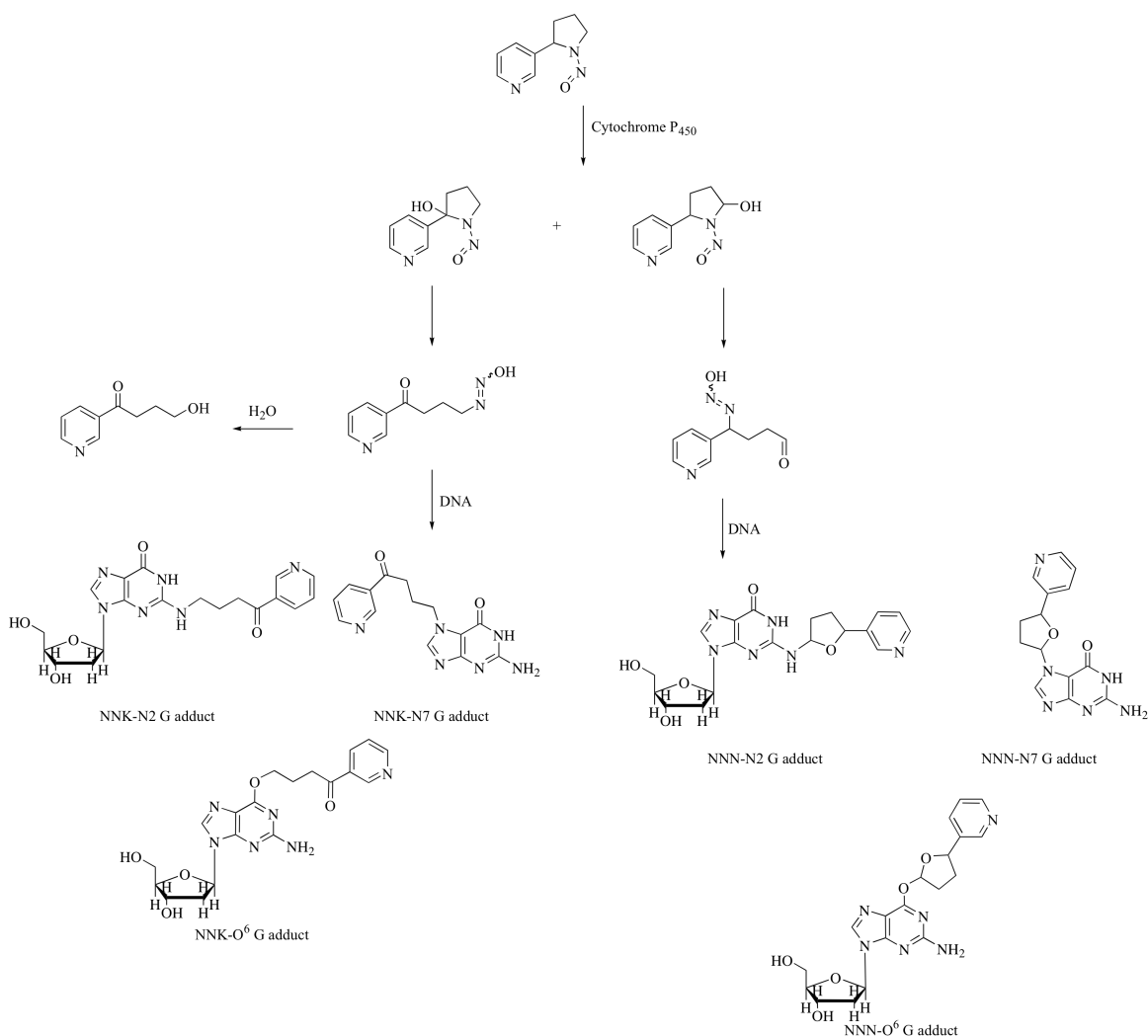


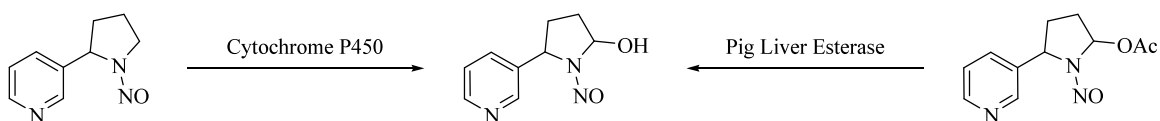
Figure 2.2. NNAL and NNK DNA adducts of pyrimidine bases



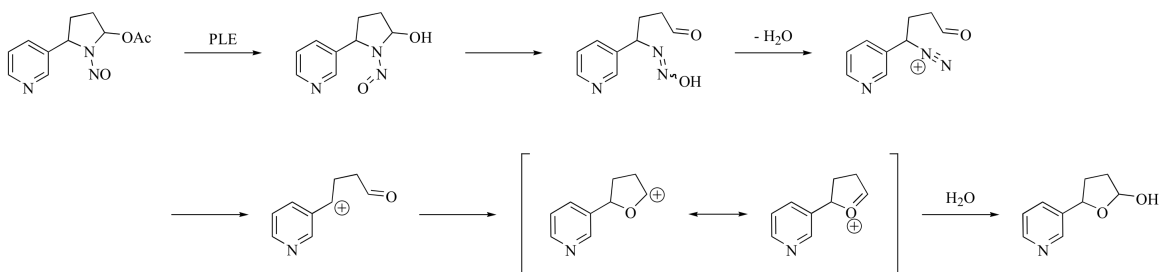
Scheme 2.6. NNN DNA adducts on guanosine

During early stages of the work discussed here, characterization of adducts of NNN-5'-OH with guanosine had been reported (Scheme 2.6),<sup>21</sup> but no other studies had been published regarding sequence selectivity or reactions of NNN-5'-OH with other nucleotide bases. Although NNN had been synthesized both racemically<sup>22</sup> and asymmetrically (through use of chiral auxiliaries),<sup>23</sup> a facile route to NNN-5'-OAc (and NNN-5'-OH) has remained unavailable. To access the 5'-hydroxylated NNN formed by

cytochrome P<sub>450</sub> *in vivo*,<sup>13</sup> NNN-5'-OAc can be deprotected using pig liver esterase (Scheme 2.7); so, it is an attractive synthetic precursor for examining DNA damage. The proposed mechanism of activation of NNN-5'-OAc as an electrophile is shown in Scheme 2.8. The acetate is deprotected to leave the free hydroxyl group, which can ring-open to the acyclic aldehyde. Loss of water generates an alkyldiazonium species which then loses nitrogen gas and is attacked by either a nucleoside base or water to trap the cation.



Scheme 2.7. Using PLE to mimic biological oxidation of NNN

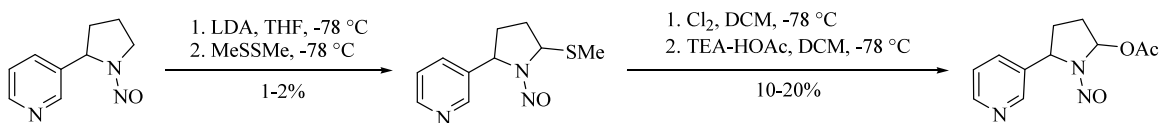


Scheme 2.8. Proposed mechanism of enzymatic deprotection of NNN-5'-OAc

## 2.2. NNN-5'-OAc SYNTHESIS BACKGROUND

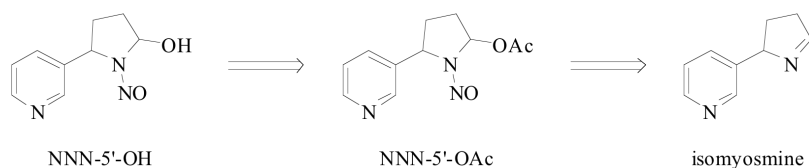
The only reported synthesis of NNN-5'-OAc is inefficient (Scheme 2.9), using a minor product from deprotonation and electrophilic trapping at the 5' position of NNN.<sup>24</sup> Additionally, this synthesis is racemic, whereas in tobacco products, (*S*)-NNN is the predominant enantiomer (50% enantiomeric excess).<sup>25</sup> The synthesis relies on electrophilic trapping of an anion generated  $\alpha$  to the cyclic nitrosamine. Using dimethyl

disulfide. Substitution at the 2' position (the thermodynamic product) predominates, but the minor 5' product was isolated and carried forward. Chlorine activates the thioether to undergo nucleophilic substitution with the acetate under buffered conditions. The final product is isolated in yields ranging from 0.01-0.04%.<sup>24</sup>



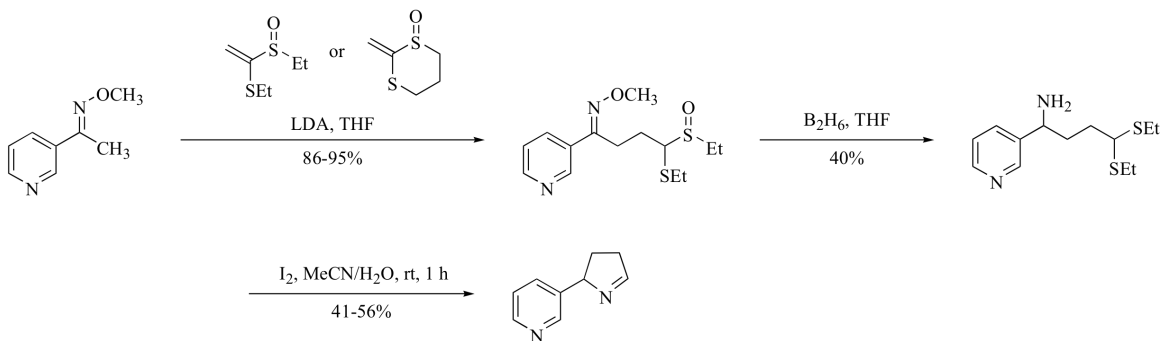
Scheme 2.9. Previously reported route to NNN-5'-OAc

Retrosynthetic analysis (Scheme 2.10) suggests that isomyosmine (3-(3,4-dihydro-2H-pyrrol-2-yl)-pyridine) could provide the desired NNN-5'-OAc product. Isomyosmine poses an interesting synthetic challenge because the carbon-nitrogen  $\pi$  bond is not conjugated with the pyridine ring, suggesting that it might prove a difficult target because of possible isomerization and hydrolysis of the aliphatic imine.



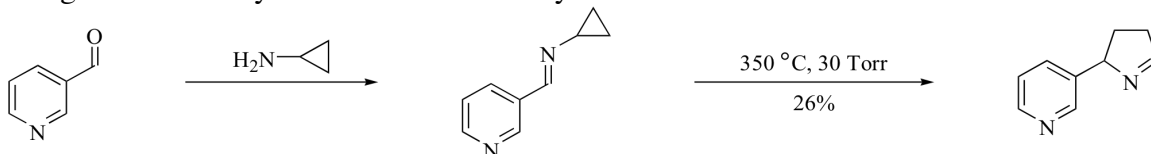
Scheme 2.10. Retrosynthetic analysis of NNN-5'-OH

### 2.2.2. Previous isomyosmine syntheses



Scheme 2.11. Previous synthesis of isomyosmine using condensation to form pyrroline ring<sup>26</sup>

Two syntheses of isomyosmine have been reported.<sup>26,27</sup> In earlier reports regarding isomyosmine, the structural assignment was incorrect, assigning the double bond of the pyrroline ring as being conjugated with the pyridine ring (C4'-C5') rather than out of conjugation (N1'-C2').<sup>28</sup> One previous route approaches isomyosmine through an intramolecular imine formation between an aldehyde and a primary amine (Scheme 2.11). Deprotonation of the methyl oxime of 3-acetylpyridine yields a nucleophile suitable for 1,4 addition to the  $\alpha,\beta$ -unsaturated sulfoxide to provide the carbon skeleton for the pyrroline ring in good yield. Reduction of the methoxime using diborane provides the primary amine as well as the diethylthioacetal, which closes to form the pyrroline upon oxidative deprotection of the thioacetal using iodine in aqueous acetonitrile. The overall yield ranges from 14-23%. The authors comment on the instability of isomyosmine, which they isolated by preparative "thick-layer" chromatography on silica using ammonium hydroxide in the eluent system.<sup>26</sup>



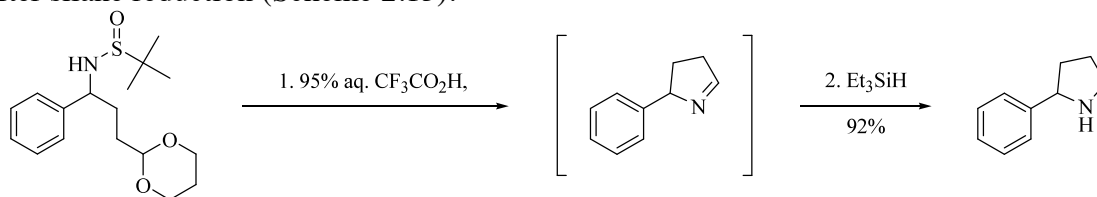
Scheme 2.12. Thermal rearrangement of cyclopropylimine to give isomyosmine<sup>27</sup>

The second reported synthesis by Campos and coworkers proceeds via flash vacuum thermolysis of an N-cyclopropylimine, affording isomyosmine in 26% yield (Scheme 2.12).<sup>27</sup> Campos *et al.* do not report the yield for the imine formation. Similar rearrangements using photochemistry have been previously reported, but no heteroaromatic substrates were used.<sup>29-31</sup>

### 2.2.3. Sulfinimine Chemistry

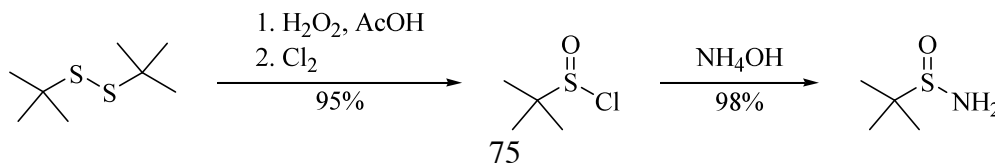
#### 2.2.3.1. Synthesis of Sulfinimines

Recently, Ellman *et al.* reported a novel cyclization to form 2-substituted pyrrolines from  $\alpha$ -chiral amines using with *tert*-butyl sulfinamides as a chiral auxiliary.<sup>32</sup> They propose the deconjugated cyclic imine as an intermediate but isolate the product after silane reduction (Scheme 2.13).

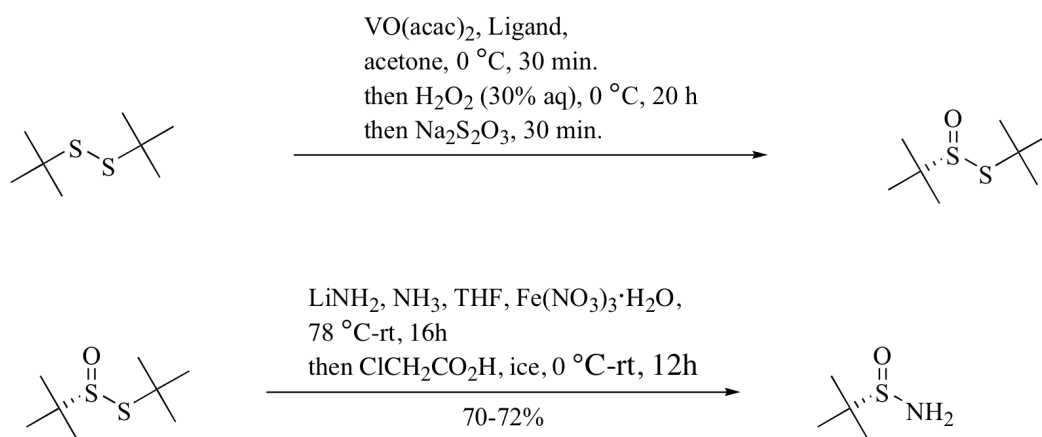
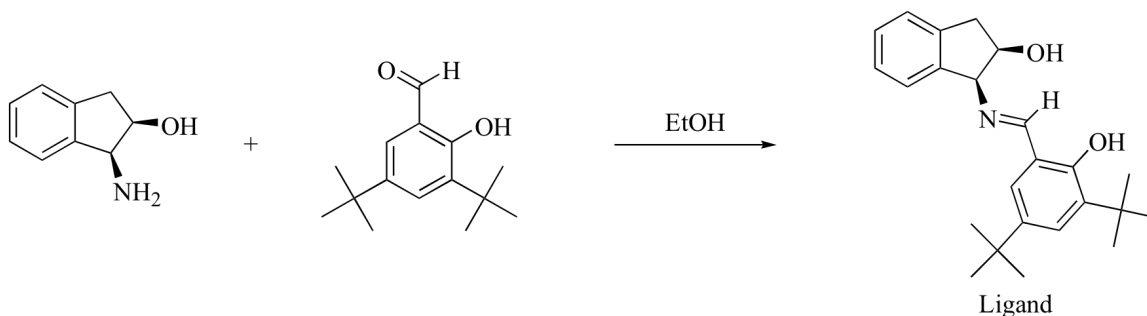


Scheme 2.13. Sulfinamide cyclization to generate pyrroline

The chiral *tert*-butylsulfinamide is commercially available in both racemic and enantiomerically enriched form, and either enantiomer can be easily synthesized from di-*tert*-butyl disulfide. Racemic synthesis commences with hydrogen peroxide oxidation of one of the sulfides is followed by sulfinyl chloride formation (Scheme 2.14). The sulfinamide is generated by treatment of this sulfinyl chloride with concentrated ammonium hydroxide.

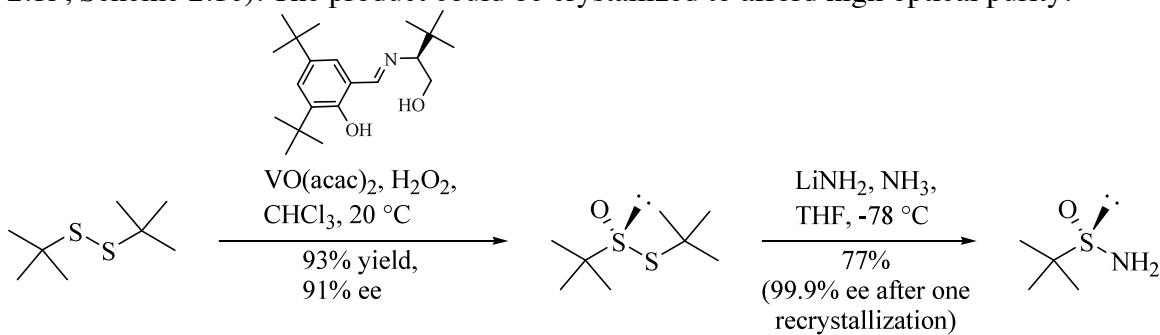


Scheme 2.14. Route to racemic *tert*-butylsulfonamide<sup>33</sup>



Scheme 2.15. *Organic Syntheses* preparation for (*R*)-*tert*-butyl sulfonamide<sup>34</sup>

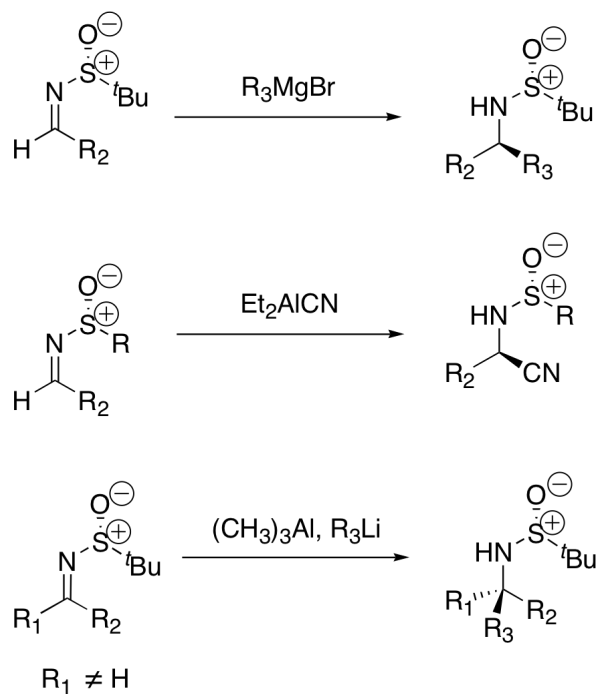
The asymmetric synthesis of *tert*-butyl sulfonamide uses a vanadium catalyst with a *tert*-leucine-derived (Scheme 2.16) or indane-derived (Scheme 2.15) ligand in the oxidation step, followed by displacement of the sulfide using lithium amide (Scheme 2.15, Scheme 2.16). The product could be crystallized to afford high optical purity.



Scheme 2.16. Asymmetric synthesis of *tert*-butyl sulfinamide<sup>33</sup>

Condensation of the *tert*-butanesulfinamide with aldehydes to sulfinimines proceeds more slowly than imine formation between amines and aldehydes; however, the rates can be improved with addition of MgSO<sub>4</sub> and pyridinium *p*-toluenesulfonate.<sup>35,36</sup> Although conditions which can racemize the chiral center at sulfur are known,<sup>37</sup> nucleophilic addition to sulfinimines does not cause racemization as judged by HPLC.<sup>35</sup> In fact, sulfinamide formation from amides using *tert*-butylsulfinyl chloride can be used to determine stereoselectivity of amine formations.<sup>37</sup> The chiral *tert*-butylsulfinamide may also be recovered and recycled following deprotection of the amine.<sup>38</sup>

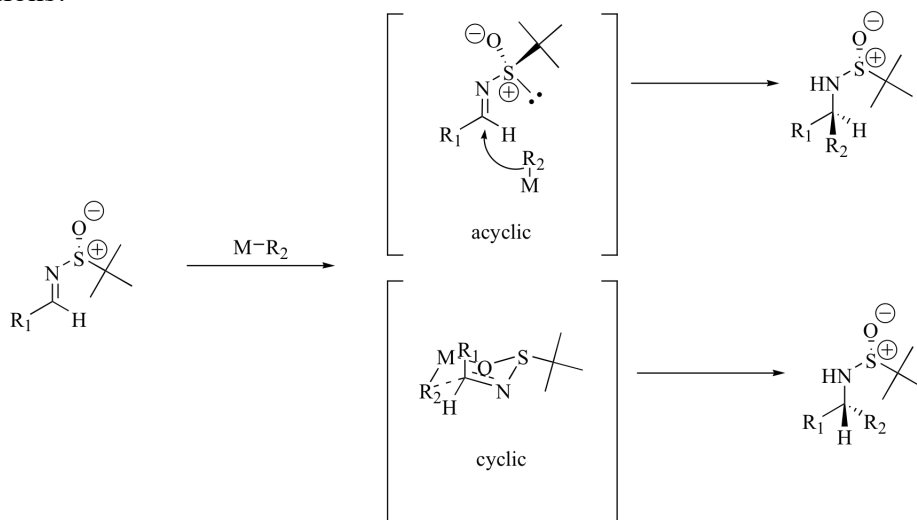
2.2.3.2. Use of Sulfinamides as Chiral Auxiliaries



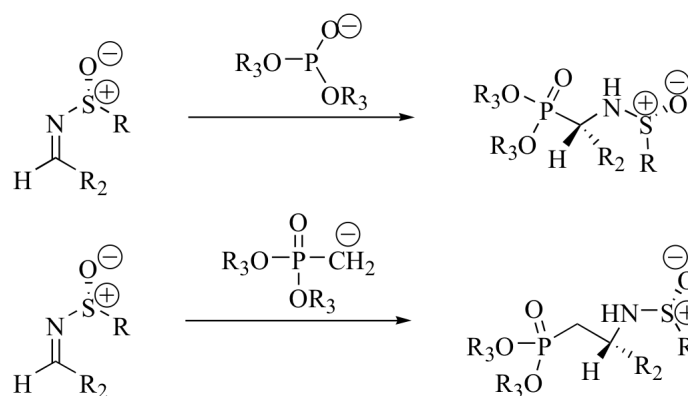
Scheme 2.17. Nucleophilic Addition to Sulfinimines.<sup>35</sup>



These sulfinimines have been shown to be versatile building blocks for a variety of transformations. They undergo nucleophilic addition by Grignard reagents to yield protected  $\alpha$ -branched amines (Scheme 2.17).<sup>35,39,40</sup> Stereoselectivity depends most on the group attached to the sulfur of the sulfinimine. *p*-Toluenesulfonyl (tosyl) sulfinimines typically provide moderate diastereoselectivities, typically ~4:1, and moderate yields.<sup>39</sup> Other, more sterically demanding chiral auxiliaries improve diastereoselectivities.<sup>40</sup> With *p*-tosylsulfinimines, diastereoselectivities were modest to poor until chiral auxiliaries (i.e. menthyloxy, bornyloxy) were appended to the metal, which improved ratios to a minimum of ~9:1.<sup>41</sup> Trialkylaluminum reagents also mediate 1,2-additions of organolithium reagents to sulfinimines, showing good yields and good to excellent diastereoselectivities.<sup>42</sup> Metal-hydrides can perform similar 1,2-addition chemistry, with varying degrees of diastereoselectivity.<sup>41</sup> Both open (acyclic) and closed (cyclic) transition states (Scheme 2.18) have been proposed to explain the diastereoselectivity of the additions.

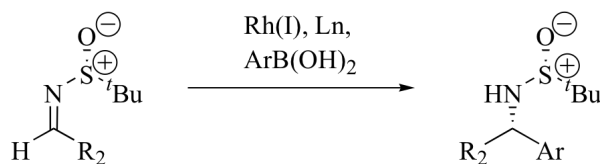


Scheme 2.18. Open and closed transition states for nucleophilic addition to chiral sulfinimine.



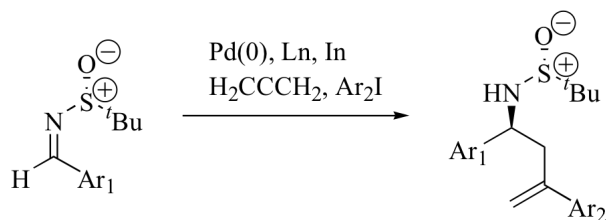
Scheme 2.19. Addition of  $\alpha$ -phosphonate anions<sup>43</sup> and phosphites<sup>43,44</sup> to chiral sulfinimines.

Phosphonates can be deprotonated with strong base and added to sulfinimines to generate precursors to  $\beta$ -aminophosphonic acids (Scheme 2.19).<sup>43</sup> Diastereoselectivities range from  $\sim 5:1$  to  $\sim 10:1$ , and yields are moderate.<sup>43</sup> Phosphite anions can also attack sulfinimines to form precursors to  $\alpha$ -aminophosphonic acids in good yields and diastereoselectivities.<sup>43,44</sup>



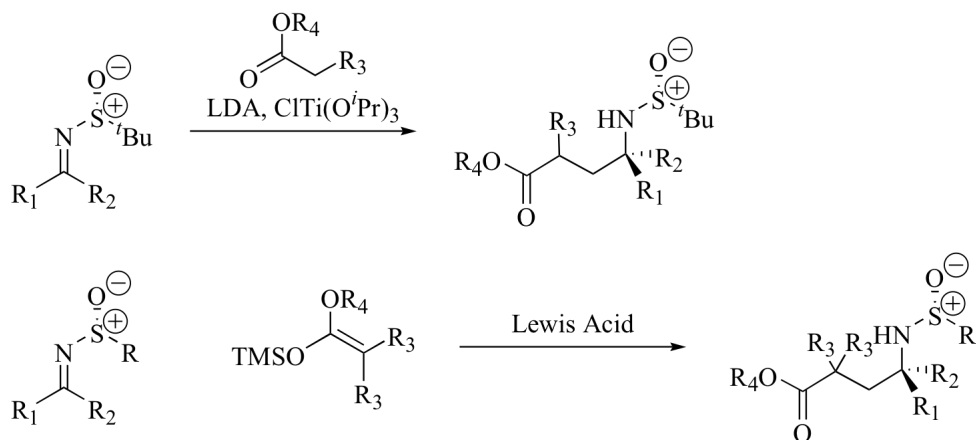
Scheme 2.20. Asymmetric Rh(I)-catalyzed addition to *t*-butyl sulfinimine.<sup>45</sup>

An alternative to Grignard additions to add aromatic substituents at the imine carbon employs rhodium-catalyzed arylboronic acid (Scheme 2.20).<sup>45</sup> This transformation is more functional-group tolerant than using a strongly nucleophilic organometallic reagent. The transformation proceeds in 70-96% yield, with good diastereomeric ratios. Highly electron-poor or -rich boronic acids (*p*-CF<sub>3</sub>Ph, *p*-OMePh) show diminished yields.<sup>45</sup>



Scheme 2.21. Sulfinimine three-component coupling with allene and aryl iodide<sup>46</sup>

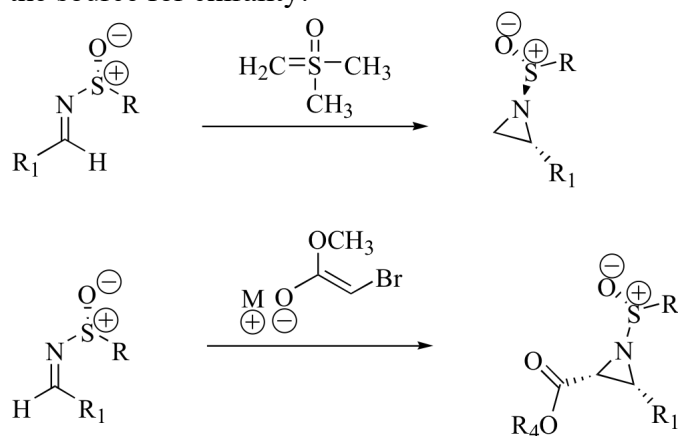
Sulfinimines participate in a palladium-catalyzed 3-component coupling using an allene and an aryl iodide to generate a 2-aryl palladium  $\pi$ -allyl species, which then undergoes an indium-mediated nucleophilic addition to the sulfinimine in a closed, six-membered transition state, to generate the allylated sulfinimide (Scheme 2.21)<sup>46</sup> These transformations yield products in moderate yields (46-56%) as a single diastereomer as determined by <sup>1</sup>H and <sup>13</sup>C NMR.<sup>46</sup> Only electron-poor aryl groups on the sulfinimine (Ar<sub>1</sub> in Scheme 2.21) were reported.



Scheme 2.22. Enolate addition to sulfinimines.

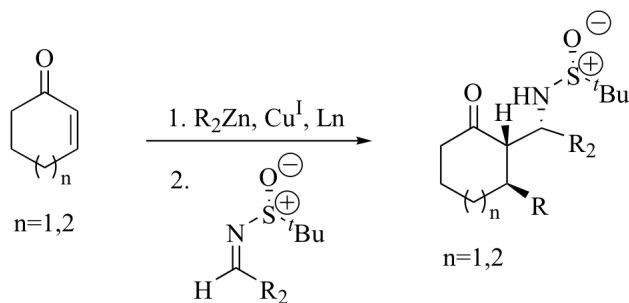
Sulfinimines can also undergo attack by metal enolates<sup>47,48</sup> or Lewis-activated trimethylsilyl enol ethers (Scheme 2.22).<sup>49</sup> The use of Lewis acids to activate the silyl ketene acetal proceeds in moderate to good yield, with diastereomeric ratios typically

near 9:1.<sup>49</sup> The authors propose that the addition proceeds *via* an open transition state. The scope of the reaction remains largely unexplored. Early reports of the addition of ester enolates to *p*-tosyl sulfinimines exhibited modest diastereoselectivities, until HMPA was added to the reaction, leading to excellent diastereoselectivity with a reverse in selectivity. This switch was attributed to a change from a closed six-membered transition state to an open transition state.<sup>48</sup> The addition of metal enolates to the sulfinimines tolerates both aldimines and methyl ketimines with good yields and good to excellent diastereoselectivities with *tert*-butanesulfinimines as electrophilic partners.<sup>47</sup> Ellman *et al.* used this template to synthesize hexameric peptides containing  $\beta$ -amino acids using *tert*-butane sulfinamide as the source for chirality.<sup>47</sup>



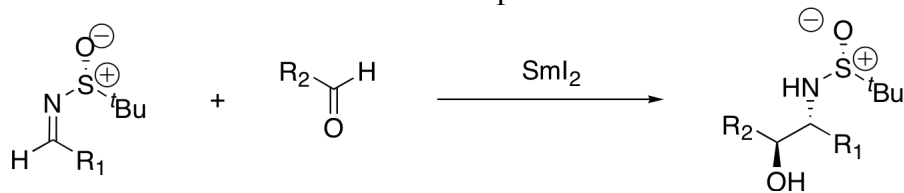
Scheme 2.23. Aziridinations using sulfinimines<sup>50-52</sup>

Sulfinimines can be used for asymmetric aziridine formation, either via an aza-Darzen condensation<sup>50,52</sup> or sulfur ylides (Scheme 2.23).<sup>51</sup> The aza-Darzen condensations proceed in good yield with diastereoselectivities typically greater than 9:1, thought to be caused by a closed, cyclic transition state.<sup>50,52</sup> The aziridine formations using sulfur ylides proceed in generally good yields, but diastereoselectivities depend largely on the identity of the R group on the sulfur, with *tert*-butyl groups providing the best selectivities.<sup>51</sup>



Scheme 2.24. Sulfinimines as electrophilic trap in 1,4-conjugate addition-electrophilic trapping<sup>53</sup>

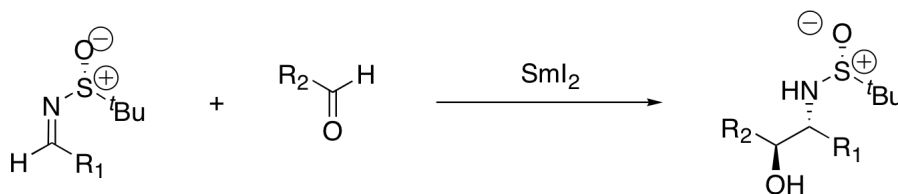
In addition to serving as electrophilic traps for enolates generated by  $\alpha$ -deprotonation of a carbonyl compound, sulfinimines also serve as electrophilic partners in 1,4-conjugate addition-electrophilic trapping reactions on  $\alpha,\beta$ -unsaturated carbonyl compounds (Scheme 2.24).<sup>53</sup> The dialkyl zinc adds to the  $\beta$  position to generate a metallo-enolate, which then attacks the sulfinimine. The authors propose an open transition state, but do not discount a closed six-membered cyclic transition state. Yields are moderate to good for dimethyl, dibutyl, and diethyl zinc, as well as a range of aromatic and aliphatic substituents for  $R_2$ .<sup>53</sup> A single diastereomer was observed by  $^1\text{H}$  NMR in the crude reaction mixtures under the optimized conditions.<sup>53</sup>



Scheme 2.25. *N*-sulfinyliminoacetates undergo C-C bond formation under reductive conditions.<sup>54</sup>

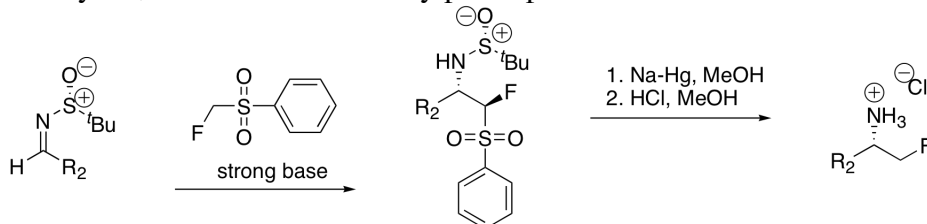
*Tert*-butylsulfonamide may also be used to form *N*-sulfinyliminoacetates, which can undergo vinylation under reductive conditions to generate precursors to unnatural  $\alpha$ -amino acids (Scheme 2.25). These reactions proceed in good to excellent yields with

excellent diastereoselectivity (>95:5 in all reported cases).<sup>54</sup> Krische *et al.* suggest that the mode of stereoinduction comes from a coordination of rhodium by the nitrogen lone pair, which directs delivery of the vinylrhodium species to the less hindered  $\pi$  face of the imine.<sup>54</sup>



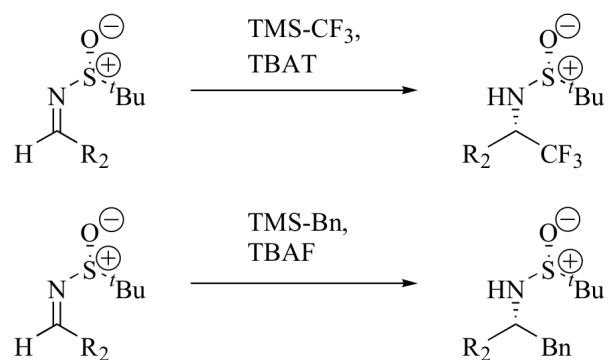
Scheme 2.26. Reductive asymmetric coupling of sulfinimines with aldehydes.<sup>55</sup>

Another reductive asymmetric coupling using the *tert*-butylsulfinimine as a chiral auxiliary is an aza-pinacol coupling using samarium diiodide (Scheme 2.26).<sup>55</sup> Typical yields for a range of substrates ranged from 70-90%, with drs after chromatographic purification ranging from 10:1 to >25:1.<sup>55</sup> Although the coupling appears general for a range of aldehydes, ketones do not readily participate.<sup>55</sup>



Scheme 2.27. Formation of  $\alpha$ -fluoroamines using chiral sulfinamines.<sup>55</sup>

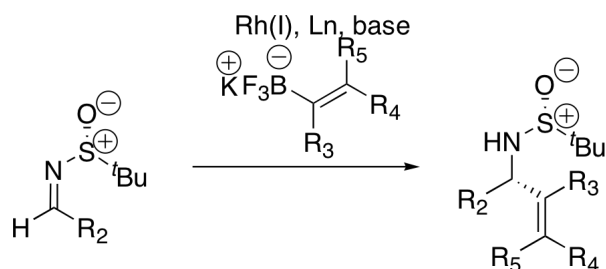
Sulfinimines undergo nucleophilic attack by sulfone-stabilized carbon nucleophiles to generate precursors to  $\alpha$ -fluoroamines (Scheme 2.27).<sup>56</sup> The  $\pi$ -facial selectivity is reported as 99:1 in most examples, where  $R_2$  can be either aromatic or aliphatic with varying electronic properties.<sup>56</sup> Yields on the nucleophilic addition are also excellent and do not appear to be very sensitive to either sterics or electronics at  $R_2$ . Overall yields for the ammonium salts range from 70-80%.<sup>56</sup>



Scheme 2.28. Use of TMS-alkanes as pro-nucleophiles to alkylate sulfinimines

In addition to forming mono- $\alpha$ -fluorinated chiral amines, sulfinimines have been used to form  $\alpha$ -trifluoromethyl amines (Scheme 2.28).<sup>57</sup> Olah *et al.* report the use of tetrabutylammonium difluorotriphenylsilicate (TBAT) in presence of (trifluoromethyl)trimethylsilane (Ruppert's reagent).<sup>57</sup> The fluoride forms an “ate” complex with silicon to activate the trifluoromethyl group as a nucleophile which adds to the electrophilic carbon of the sulfinimine. Yields were good to excellent, with electron-poor aromatic R<sub>2</sub> groups having the best yields.<sup>57</sup> Diastereoselectivities were excellent (>95:5) in all reported cases.<sup>57</sup> The diastereoselectivity was rationalized by invoking an open transition state.<sup>57</sup> In a similar system, benzyltrimethylsilane is used in conjunction with tetrabutylammonium fluoride to benzylate the sulfinimine.<sup>58</sup> Yields and diastereoselectivities in these benzylations were moderate.<sup>58</sup>

Most recently, chiral sulfinimines have been shown to undergo vinylation reactions (Scheme 2.29).<sup>59</sup> Using a variety of potassium trifluoroborate salts similar to those first reported by Vedejs<sup>60,61</sup> and popularized for transition metal-catalyzed couplings by Molander,<sup>62</sup> Ellman *et al.* were able to perform vinylation with good to excellent yields on both aliphatic and aromatic sulfinimines. The diastereoselectivity in all reported cases was >95:5.<sup>59</sup>



Scheme 2.29. Vinylation using rhodium catalyst and potassium trifluoroborate salt.

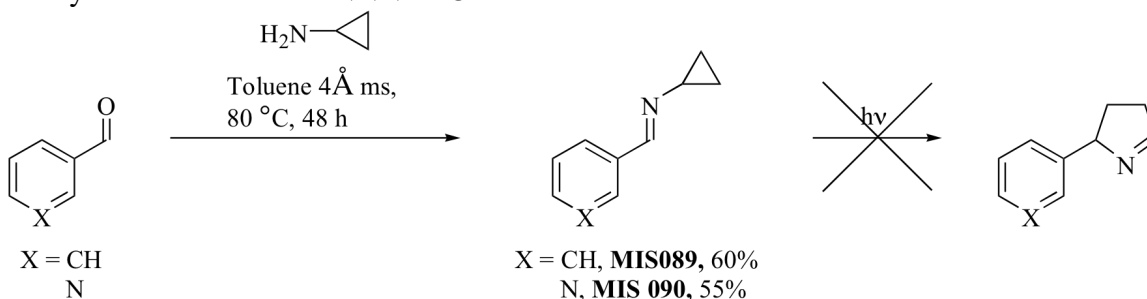
Sulfinimine chemistry can generate structurally diverse  $\alpha$ -chiral amines with a variety of nucleophiles. Yields and diastereoselectivities are typically good, so we were interested in applying this chemistry to the synthesis of NNN-5'-OAc, as it affords the possibility of an enantioselective variant.

### 2.3. SYNTHESIS OF NNN-5'-OAc

The original planned route to NNN-5'-OAc was to synthesize isomyosmine using a photochemical rearrangement of the cyclopropylimine, as reported by Sampedro *et al.*<sup>27</sup> Condensation of cyclopropylamine to pyridine-3-carboxaldehyde yielded **MIS090** in 55% yield (Scheme 2.30). This imine was stable to silica gel chromatography. Although imine formation proceeded smoothly, the photorearrangement was unsuccessful in our hands (Table 2.1). Because the rearrangement has not been reported using heteroaromatic groups,<sup>31</sup> **MIS089**, derived from benzaldehyde, was synthesized. This attempt at photorearrangement was also unsuccessful under the reported conditions.<sup>29</sup> It is possible that the Hg lamp and photoreactor were sufficiently different as to prevent excitation.<sup>63</sup> Given our inability to reproduce the reported photochemical isomerization, no conclusion concerning the viability of this route to isomyosmine can be made. However, because this



route required very dilute conditions, it was less attractive for gram-scale synthesis of isomyosmine *en route* to NNN-5'-OAc.

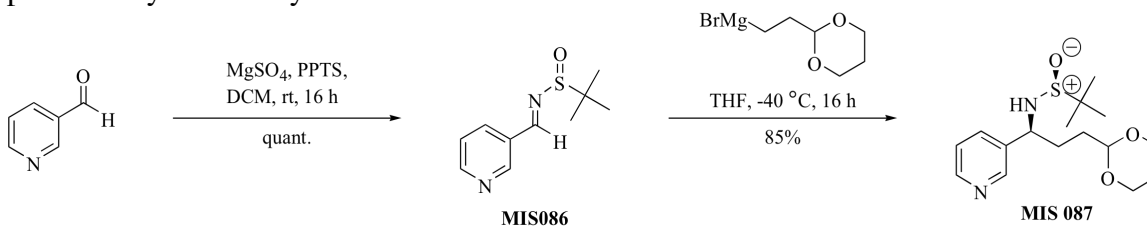


Scheme 2.30. Attempts to perform photocyclization to generate isomyosmine.

Table 2.1. Attempts to effect photorearrangement of **MIS090**

Entry	Solvent	Sensitizer (mol%)	Outcome
1	Hexanes		No conversion
2	Hexanes	Rose Bengal	Sensitizer insoluble; no conversion
3	Hexanes	Benzophenone	No conversion
4	MeCN		No conversion
5	MeCN	Rose Bengal	No conversion

At this point, we turned our attention to using sulfinimine chemistry to generate isomyosmine. This route would require one more step but afforded the advantage of a possible asymmetric synthesis of NNN-5'-OAc.



Scheme 2.31. Grignard addition to sulfinimine

Generating the racemic sulfinamide **MIS086** was straightforward (Scheme 2.31).<sup>64</sup> Using catalytic pyridinium *p*-toluenesulfonate and magnesium sulfate as a dehydrating agent, imine formation from pyridine-3-carboxaldehyde proceeded in quantitative yield at room temperature overnight, or until judged complete by TLC. Grignard addition at low temperature overnight to the sulfinimine gave the desired sulfinamide **MIS087** in good yield. The product was isolated after column chromatography as a single diastereomer as determined by <sup>1</sup>H and <sup>13</sup>C NMR. X-ray crystallography on a single crystal showed either (*R,R*) or (*S,S*) stereochemical configuration (Figure 2.3).

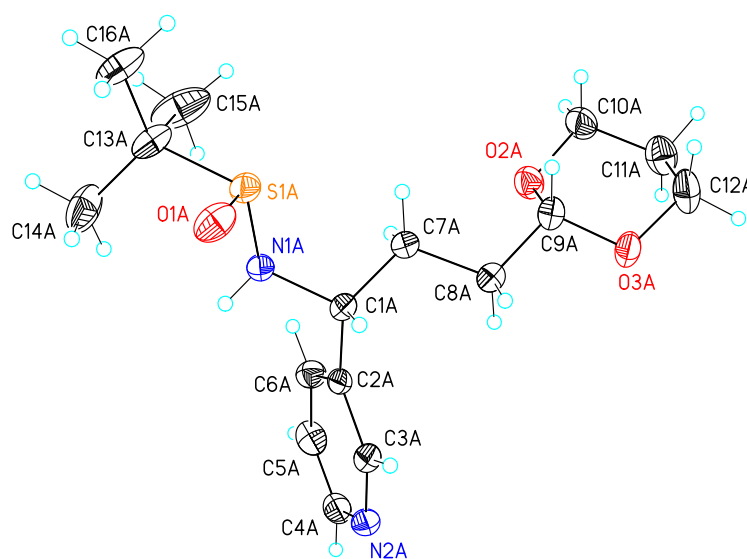
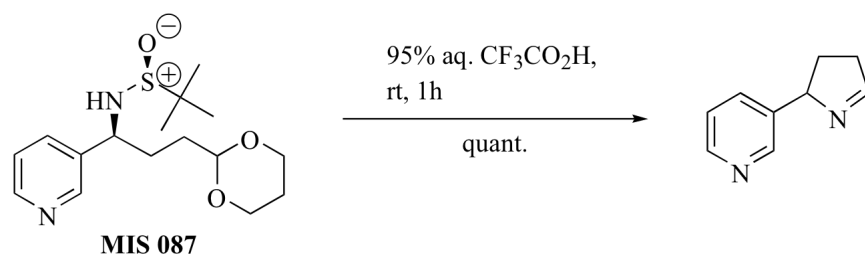


Figure 2.3. X-ray structure of **MIS087** showing the atom labeling scheme.

Displacement ellipsoids are scaled to the 50% probability level.

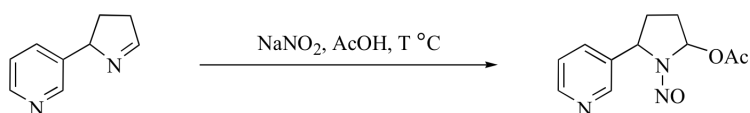


Scheme 2.32. Deprotection of **MIS087** to generate isomyosmine

Deprotection of **MIS087** using trifluoroacetic acid yielded isomyosmine in quantitative yield. The isomyosmine was not stable to silica gel chromatography unless the silica was neutralized by washing the column with 0.5% triethylamine in the column eluent. A preferred method for purification used Fluorasil as the solid support for chromatography, which gave better separation than neutralized silica. Basic alumina also did not cause decomposition but did not provide good separation. Upon obtaining characterization data for the isomyosmine, we noticed a discrepancy between our <sup>13</sup>C NMR data and the previously reported spectral data. <sup>1</sup>H NMR data was identical in the prepared compound to both previous reports.<sup>26,27</sup> The only previous <sup>13</sup>C NMR characterization by Campos *et al.* reported the following <sup>13</sup>C NMR (75 MHz, CDCl<sub>3</sub>): δ 168.2, 154.8, 149.6, 148.2, 136.4, 130.1, 73.5, 37.5, 30.1.<sup>27</sup> Our <sup>13</sup>C NMR data was similar, but not identical: (75 MHz, CDCl<sub>3</sub>) δ 168.3, 148.2, 139.3, 133.9, 123.4, 73.5, 61.5, 37.5, 30.1. Our compound lacked peaks at 154.8, 149.6, 136.4, and 130.1 but had peaks at 139.3, 133.9, 123.4, and 61.5. The pyrroline contains 9 carbons; so first we acquired <sup>13</sup>C NMR in different solvents, as the peak at 148.2 was twice the height of other peaks. The peak resolved in both *d*<sub>6</sub>-benzene (148.8 and 148.5) and *d*<sub>2</sub>-DCM (148.6 and 148.4). Along our synthetic route, the aromatic carbons of each intermediate had similar chemical shifts. In an e-mail communication to clarify the ambiguity, Soldevilla suggests

that because limited quantities were prepared in the vacuum thermolysis, the data presented here is likely the correct  $^{13}\text{C}$  NMR spectrum.<sup>65</sup>

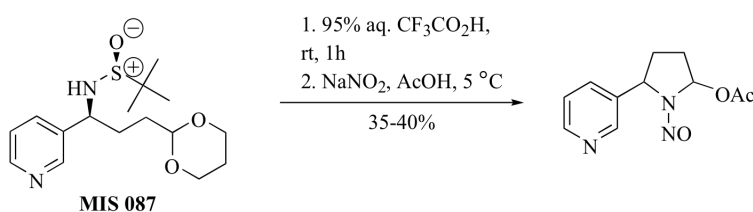
The nitro-acylation of isomyosmine gave the desired product in somewhat low yields, which were dependent on the reaction temperature. The maximum yields were obtained between 5 °C and 15 °C (Table 2.2).



Scheme 2.33. Optimization of temperature for nitroso-acylation of isomyosmine

Table 2.2. Optimization of temperature for nitroso-acylation.

Temp (°C)	Yield (%)
0	23
5	40
10	33
15	36
20	28



Scheme 2.34. Deprotection of **MIS087** followed by nitroso-acylation.

To our pleasure, the isomyosmine could be subjected without purification to nitroso-acylation to generate the NNN-5'-OAc in four steps in a 30% overall yield

(Scheme 2.34). Purification of isomyosmine did not improve the combined yield of the two steps. The  $^1\text{H}$  NMR was consistent with the literature data, but it showed a mixture of what we believe to be rotamers and diastereomers (Figure 2.4).

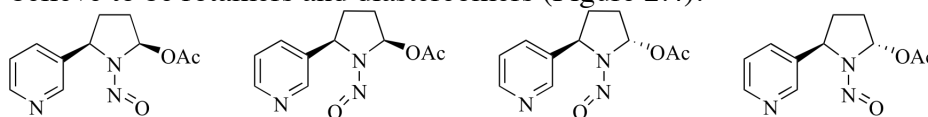


Figure 2.4. Possible isomers and conformers of NNN-5'-OAc.

In order to confirm that the isolated NNN-5'-OAc was in fact a mixture of isomers, we first tried to use VT-NMR to cause the proposed rotamers to converge. Unfortunately, NNN-5'-OAc is not thermally stable, decomposing at room temperature over extended periods. A sample in *deuterio*-chloroform was heated to 50 °C, but no convergence was observed. In a second attempt to establish that the mixture was isomeric, liquid chromatography-mass spectrometry (LC-MS) was obtained. The mass spectrum shows that the major component, which comprises 93% of the sample as determined by UV-Vis detection on the LC, has  $m/z$  of 236, which corresponds to the mass of NNN-5'-OAc (Figure 2.6). Neither this reverse-phase column nor  $\text{C}_8$  or  $\text{SiO}_2$  HPLC columns showed resolution into multiple peaks. Although the proposed diastereomers and rotamers could not be resolved, the sample showed a single peak with uniform  $m/z$  at all timepoints examined.

msf /2009 12:34:24 PM ct02119557\_120756

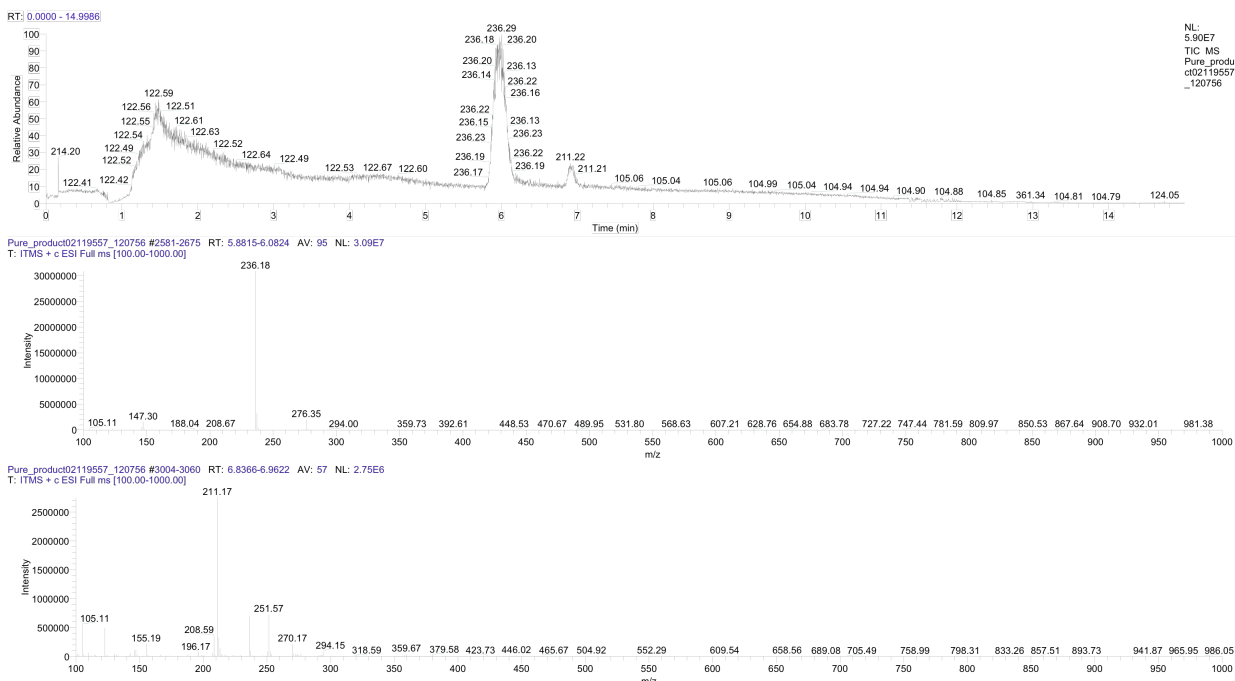


Figure 2.5. LC-MS analysis of NNN-5'-OAc.

Top: Total ion current; middle: MS on major component (93%;  $m/z$  236); bottom: MS on minor component (7%,  $m/z$  211).

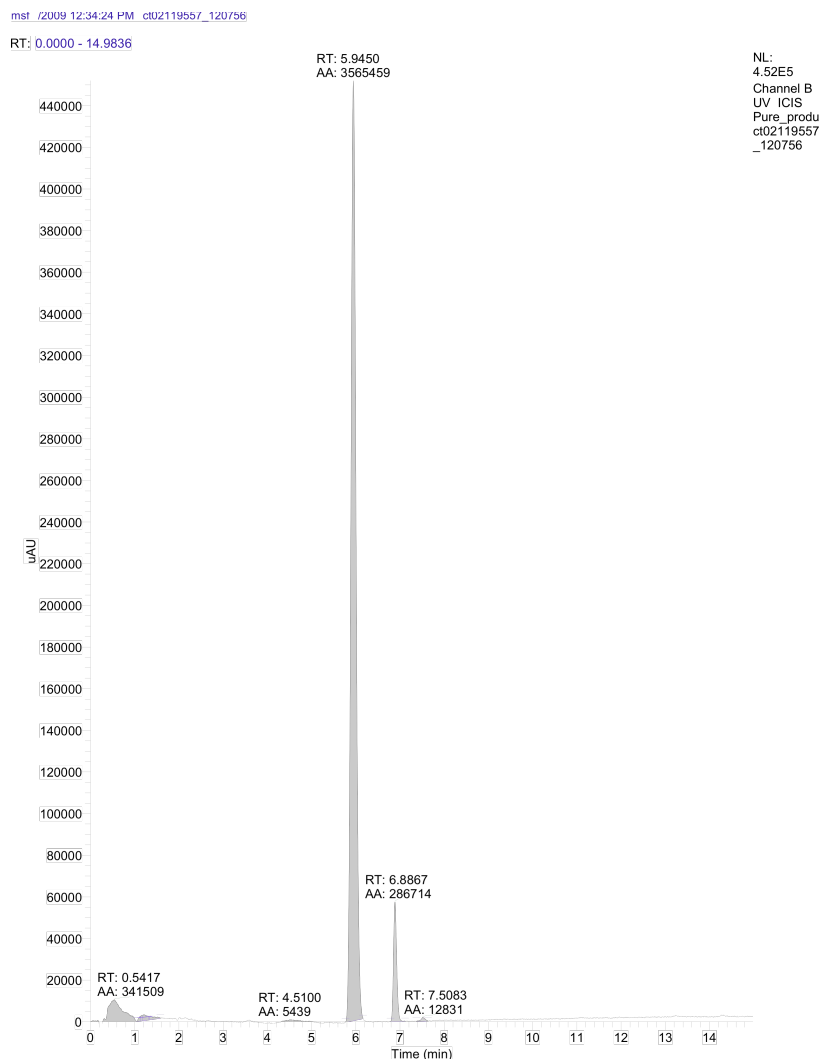
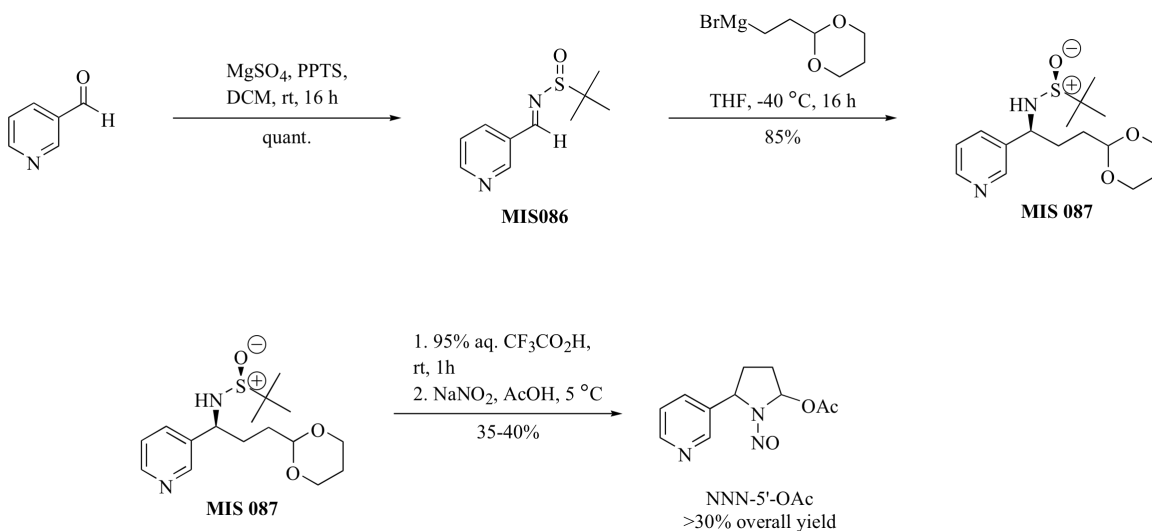


Figure 2.6. LC chromatogram of NNN-5'-OAc using 254 nm UV detection showing ratio of 93:7 NNN-OAc isomers to minor component.

Overall, this synthesis of ( $\pm$ )-NNN-5'-OAc proceeded in good yield and was amenable to medium scale synthesis. No significant loss in yield was noted upon increasing the scale of the first three steps to >1 g. For the final step increasing the scale to 600 mg led to a decreased yield of 17%, but this is likely because of the increased exothermicity of the  $\text{NaNO}_2$  addition. Portionwise addition of the sodium nitrite would

likely lead to more consistent internal temperature and increased yields. The route is four steps, with three chromatographic purifications, and proceeds in >30% overall yield.



Scheme 2.35. Total synthesis of NNN-5'-OAc.

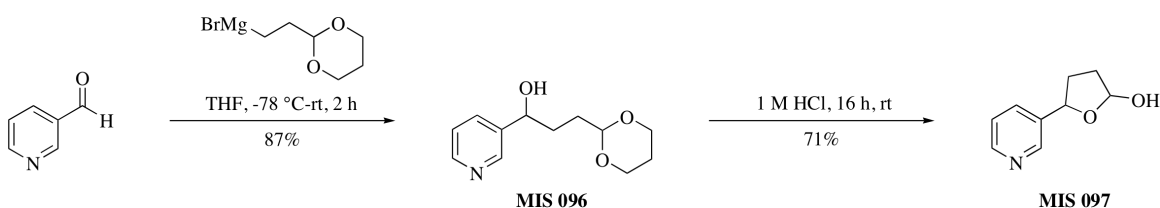
## 2.4. INTERACTION OF NNN-5'-OAc WITH DNA IN PRESENCE OF PIG LIVER ESTERASE

### 2.4.1. Simple enzymatic hydrolysis in absence of nucleosides

With ready access to multigram quantities of NNN-5'-OAc, preliminary studies on its interactions with DNA and single nucleosides were performed. First, NNN-5'-OAc was subjected to hydrolysis in neutral (pH 7) sodium phosphate with pig liver esterase in the absence of DNA or nucleosides, which provided conversion to a new compound, observable by TLC as a new spot. We theorized that this compound resulted from trapping the tetrahydrofuranyl cation with water to deliver a 2-hydroxytetrahydrofuran. During the hydrolysis, gas evolution was observed, supporting the idea that N<sub>2</sub> was evolved.

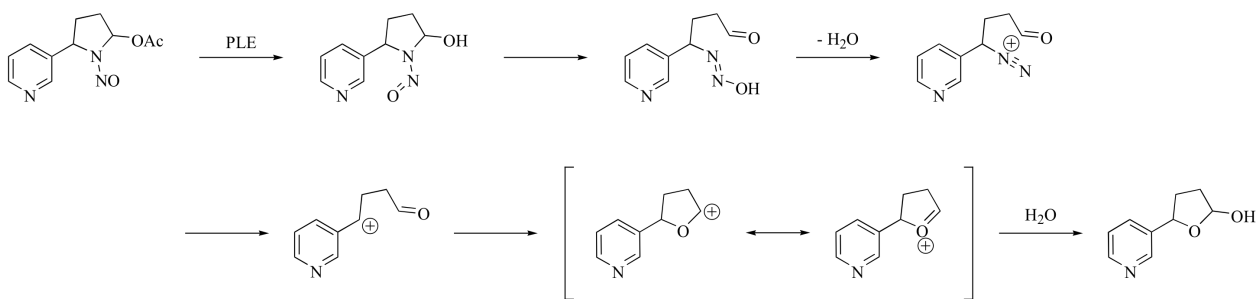


Unambiguous characterization of the proposed hydrolysis product was difficult due to its high water solubility and poor stability to chromatography; so, the proposed intermediate was independently synthesized. Grignard addition to 3-pyridine carboxaldehyde generates the alcohol, which can be deprotected in aqueous acid to generate the cyclic hemiacetal (Scheme 2.36). Interestingly, **MIS096** and **MIS 097** have the same  $R_f$ , so the reaction appears not to work as judged by TLC analysis.



Scheme 2.36. Independent synthesis of hydrolyzed NNN-5'-OAc

The synthetic product was identical to the product of NNN-5'-OAc hydrolysis by  $^1\text{H}$  NMR, TLC, and LRMS.

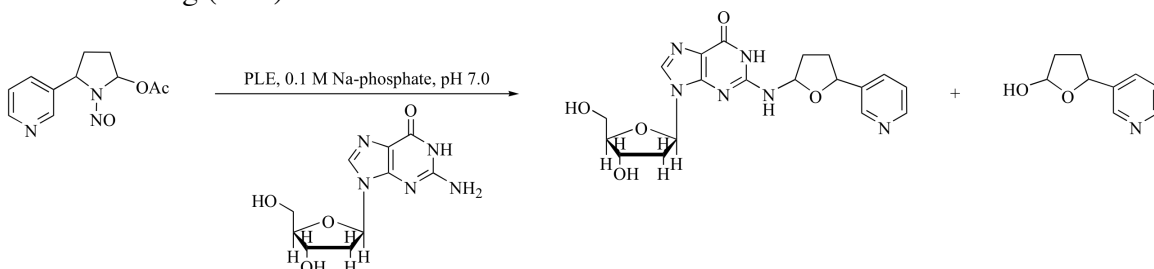


Scheme 2.37. Proposed mechanism for hydrolysis of NNN-5'-OAc in presence of PLE.

#### 2.4.2. Incubations of NNN-5'-OAc and PLE with single nucleosides

Adducts of deoxyguanosine and NNN-5'-OAc formed *via* incubation of the NNN-5'-OAc with 2-deoxyguanosine or calf thymus DNA in presence of PLE have been reported by Hecht *et al.*<sup>21</sup> Following incubation with the NNN-5'-OAc and PLE, calf

thymus DNA was then digested either thermally or enzymatically, and the products were compared to independently synthesized authentic samples using LC-MS with selective ion monitoring (SIM).



Scheme 2.38. Adduction of 2-deoxyguanosine by NNN-5'-OAc.<sup>21</sup>

We performed similar incubations of NNN-5'-OAc with single bases (guanosine, adenosine, thymidine, cytidine) in neutral sodium phosphate in presence of pig liver esterase, which were analyzed by electrospray impact mass spectrometry (ESI-MS) by Ms. Suncerae Smith in the Brodbelt group at the University of Texas at Austin.<sup>1</sup> Mass spectrometric analysis of the incubation of guanosine with NNN-5'-OAc in the presence of pig liver esterase shows significant adduct formation (Figure 2.7). Preliminary ESI-MS shows  $m/z$  commensurate with the previously reported guanosine adduct.<sup>66</sup>

<sup>1</sup> All ESI-MS spectra were provided by Ms. Suncerae Smith, Brodbelt Research Group, UT-Austin

2007-06-14j #1-20 RT: 0.00-0.34 AV: 20 NL: 1.59E5  
T: -p ms [50.00-1000.00]

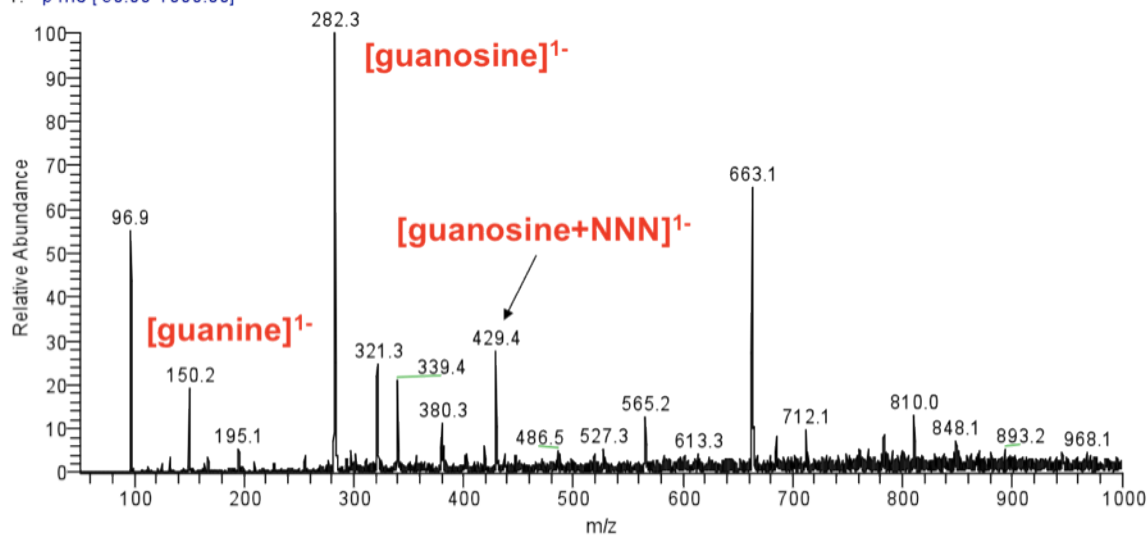


Figure 2.7. ESI-MS of incubation of guanosine with NNN-5'-OAc in presence of PLE.

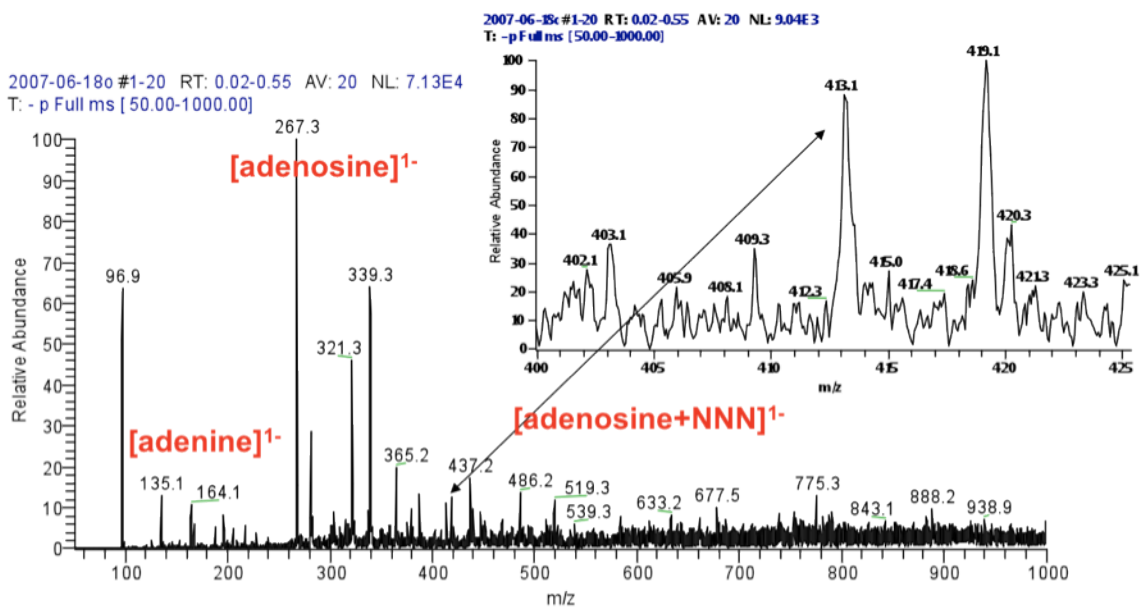


Figure 2.8. ESI-MS of incubation of adenosine with NNN-5'-OAc in the presence of PLE

2007-06-18i #1-20 RT: 0.02-0.55 AV: 20 NL: 7.37E4  
T: - p Full ms [ 50.00-1000.00]

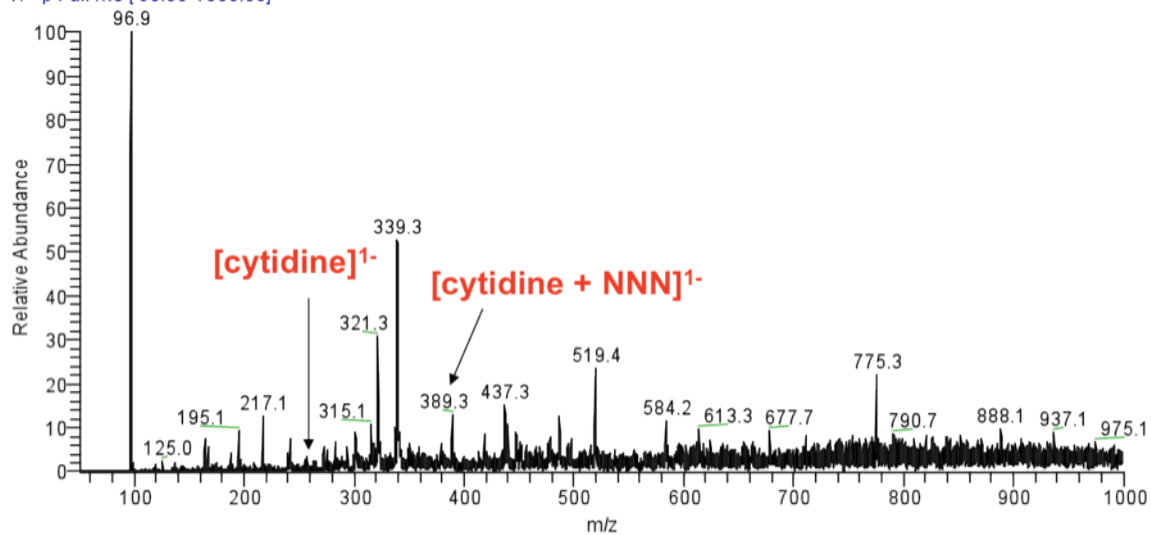


Figure 2.9. ESI-MS of incubation of cytidine with NNN-5'-OAc in the presence of PLE.

2007-06-18h #1-20 RT: 0.04-1.21 AV: 20 NL: 1.60E5  
T: - p Full ms [ 50.00-1000.00]

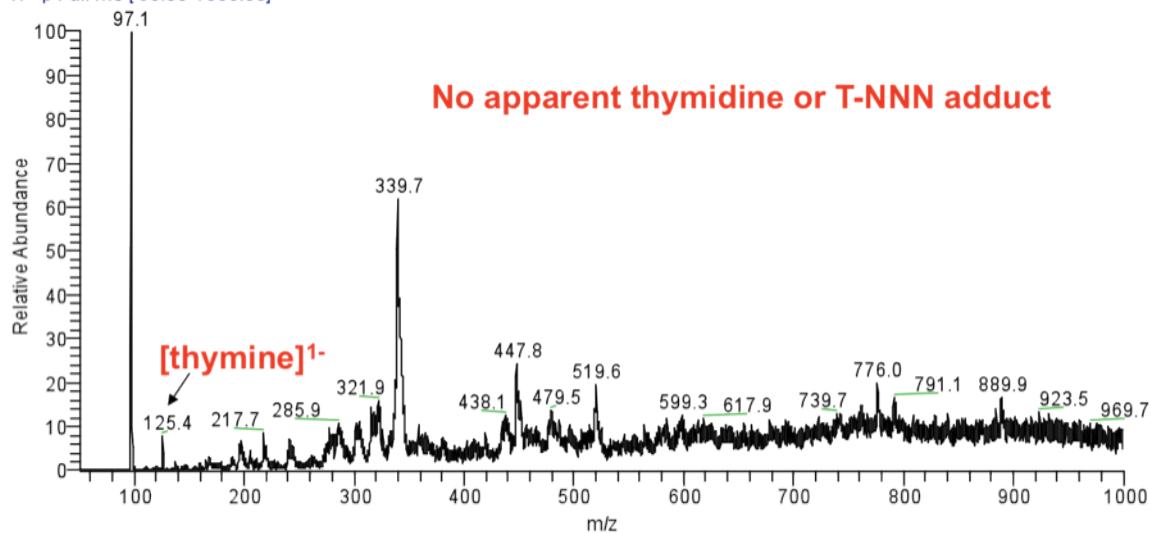


Figure 2.10. ESI-MS of incubation of NNN-5'-OAc with thymidine in presence of PLE

Incubation of NNN-5'-OAc with adenosine affords a product whose ESI-MS displays a peak having the mass of the proposed NNN-adduct, albeit at a low intensity with respect to the peak corresponding to unmodified adenosine (Figure 2.8).<sup>67</sup> Mass spectrometric analysis of the incubation of cytidine with NNN-5'-OAc also shows a peak that might represent a covalent modification (Figure 2.9).<sup>67</sup> ESI-MS analysis of incubation of thymidine in presence of NNN-5'-OAc and pig liver esterase did not show any peaks corresponding to proposed adducts (Figure 2.10). In summary, the ESI-MS suggests formation of covalent DNA adducts not only at guanosines but also at adenosines and cytidines. Subsequent to this work, Hecht *et al.* published further investigations on the interaction of NNN-5'-OAc with single bases.<sup>66</sup> They reported adducts with guanosine, adenosine, and thymidine, and characterized them by comparison with independently synthesized authentic samples (Figure 2.11).

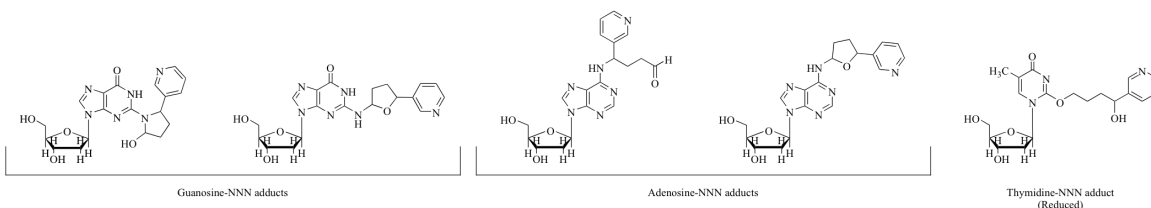


Figure 2.11. Adducts of NNN-5'-OAc with G, A, and T characterized by Hecht *et al.*<sup>66</sup>

### 2.4.3. Incubations of NNN-5'-OAc and PLE with short oligomer

To study sequence selectivity of the DNA adduct formation NNN-5'-OAc, the compound was incubated with short synthetic deoxyribonucleotides (5'-CCGCGTCCGCG-3' duplex with complement, 11 base pairs).<sup>67</sup> Incubations were performed in 0.1 M sodium phosphate at pH 7, using 10  $\mu$ M DNA duplex (110  $\mu$ M base pair) with 11 mM NNN-5'-OAc (100 equivalents per base pair).<sup>67</sup> The reaction mixture was analyzed by ESI-MS, which showed ion peaks corresponding to predicted  $m/z$  of

mono, bis, and tris-adducted DNA (Figure 2.12). Collision-activated dissociation on an ion corresponding to adducted DNA showed that loss of associated NNN occurred more readily than loss of a nucleoside or cleavage of the phosphate backbone.

2007-04-26a #1-50 RT: 0.02-3.91 AV: 50 NL: 1.42E5  
T: - p ms [50.00-2000.00]

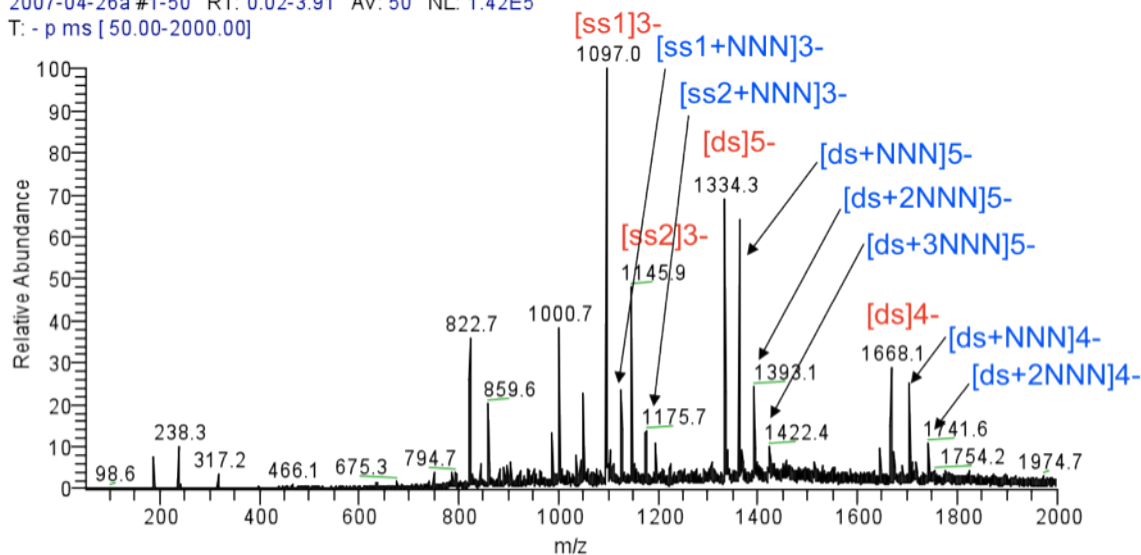


Figure 2.12. ESI-MS on an incubation of 11-mer (10  $\mu$ M duplex) with NNN-5'-OAc (11 mM) in presence of pig liver esterase shows multiple adduction.

2007-04-26k #1-16 RT: 0.12-4.22 AV: 16 NL: 8.58E4  
T: - p Full ms2 1366.00@16.00 [375.00-2000.00]

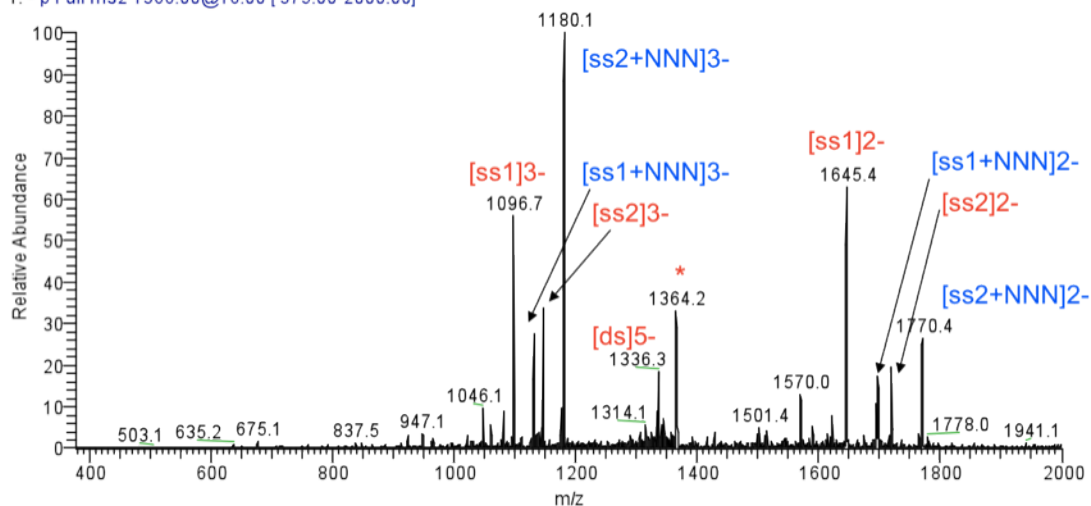


Figure 2.13. CAD experiment on parent ion (\*) from Figure 2.12.

In order to elucidate the sequence preference (if any) of the NNN-5'-OAc with this short oligomer, infrared multiphoton dissociation (IRMPD) experiments were performed by our collaborator, Ms. Smith. CAD and IRMPD on an ion corresponding to a 1:1 complex of the DNA oligomer and NNN at the (-5) charge state results in dissociation of the duplex-NNN ions into single strands. Both the upper and lower strands appear to be modified by NNN at the (-2) and (-3) charge states. Trapping and further fragmentation ( $MS^3$ ) of these ions results in the sequence information shown in Figure 2.14. The fragmentation pattern shows that adduction occurs preferentially at guanosine, specifically the guanosines at the end of the oligomer. This might be due to poorly annealed ends of the duplex (“end effects”). A typical helical turn is comprised of 10 bases, and proper annealing relies on hydrophobic stacking of the bases. An 11-mer lacks the length to have hydrophobic interactions reinforcing duplex formation, leading to slight fraying of the duplex structure. Single-stranded DNA is less sterically hindered than duplex DNA, which means that it is more susceptible to alkylation.

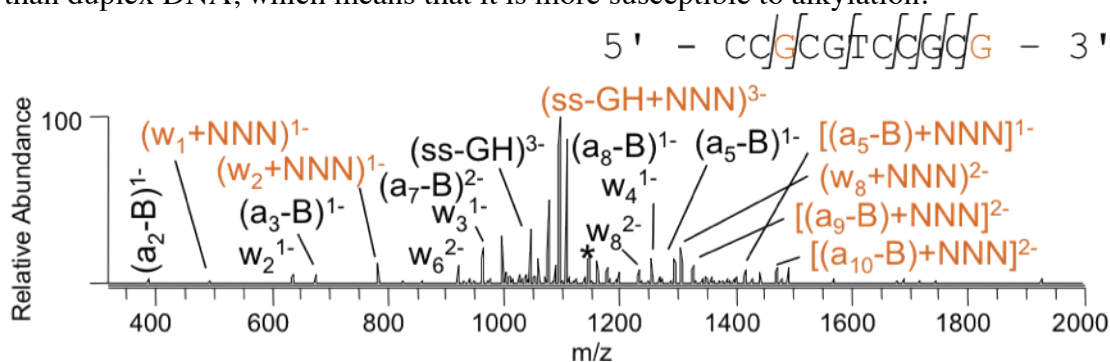


Figure 2.14. Sequence information about the "upper" strand in the 11-mer duplex

Table 2.3 shows a summary of the fragments containing the mass of the proposed organic NNN fragment. The notation on Figure 2.14 is as follows: “a<sub>#</sub>” signifies fragments that begin at the 5'-position and include the specified number of bases. “w<sub>#</sub>” represents fragments that include the specified number of bases from the 3' end of the

sequence. Fragments labeled “+NNN” include the proposed mass of the NNN addition. “-B” indicates loss of the base but not the 2'-deoxyribose. Not every possible fragmentation is observed. The “a” fragments are consistent with modification at the 3'-terminal guanine position. The “w” fragments are consistent with modification at G or C within the 5'-CCGCG- portion of the sequence. Fragment 5 suggests that if modification is, in fact, occurring selectively at G, that the modification is occurring at the first 5' G, because the “-B” indicates loss of the guanine at the 3' end of that fragment, but the mass corresponding to NNN is retained.

Table 2.3. Summary of ions containing proposed mass of NNN adduct

Fragment	Assignment
1	-G-3'+NNN
2	-CG-3'+NNN
3	-CGTCCGCG-3'+NNN
4	5'-CCGCGTCCGCG-3'+NNN-B
5	5'-CCGCG-+NNN-B
6	5'-CCGCGTCCG-+NNN-B
7	5'-CCGCGTCCGC+NNN-B



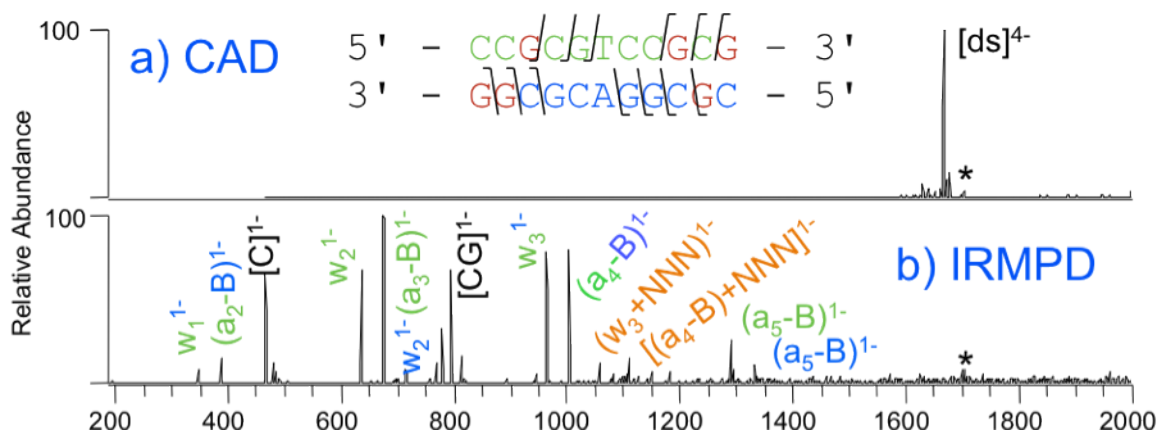


Figure 2.15. CAD and IRMPD spectra of the (-4) charge state of DNA singly adducted with NNN.

Figure 2.15 shows the mass spectra of a singly modified oligomer and the NNN-5'-OAc for the (-4) charge state.<sup>67</sup> Again, the CAD spectrum (a) shows dissociation of the complex by loss of the NNN adduct, leaving the intact duplex. The IRMPD spectrum (b) of the same parent ion shows a variety of sequence ions, with two fragments retaining the adduct. Unfortunately, this fragmentation is insufficient to determine the position of adduction.

With these encouraging ESI-MS results, we were interested in quantifying DNA adduction. In order to view adducts by the complementary technique, polyacrylamide gel electrophoreses (PAGE), a mobility shift assay was performed. This assay uses short 5'-radiolabeled DNA to analyze whether adduct formation is occurring as evidenced by a decrease in electrophoretic mobility due to increased mass and/or charge of the modified DNA. A single-stranded 11-mer, 5'-CCGCGTCCGCG-3' (one of the strands comprising the duplex used for the ESI-MS analysis), showed no change in mobility after a 16 h incubation with NNN-5'-OAc in the presence of pig liver esterase, indicating that either no covalent modification was occurring or that the modification does not cause a change

in mobility. This was disappointing but not unexpected, as the reported adduct on guanosine was neutral, not charged.<sup>21</sup>

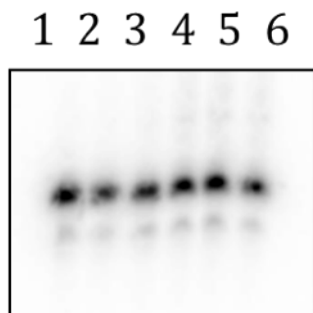


Figure 2.16. EMSA on incubations of NNN-5'-OAc in presence of 11-mer and PLE.

Lane 1: ds-DNA; Lane 2: 10 mM NNN-OAc in presence of PLE; Lane 3: 100 mM NNN-OAc in presence of PLE; Lane 4: 500 mM NNN-OAc in presence of PLE; Lane 5: 500 mM NNN-OAc without PLE; Lane 6: 500 mM NNN-OAc in presence of PLE with ss-DNA.

The DNA was also assayed for cleavage following piperidine-heat treatment. In this experiment, a longer 5'-radiolabeled oligomer (227 bp, derived from PCR on a pUC19 plasmid) was incubated with the NNN-5'-OAc in presence of PLE, purified through ethanol precipitation to remove excess small molecule, and subjected to piperidine-heat treatment to cause cleavage. The lanes with NNN-OAc (Figure 2.17, left) do not show increased cleavage above background (Figure 2.17, right), whereas acrolein (Figure 2.17, middle), the positive control,<sup>68</sup> shows G-selective cleavage above background.

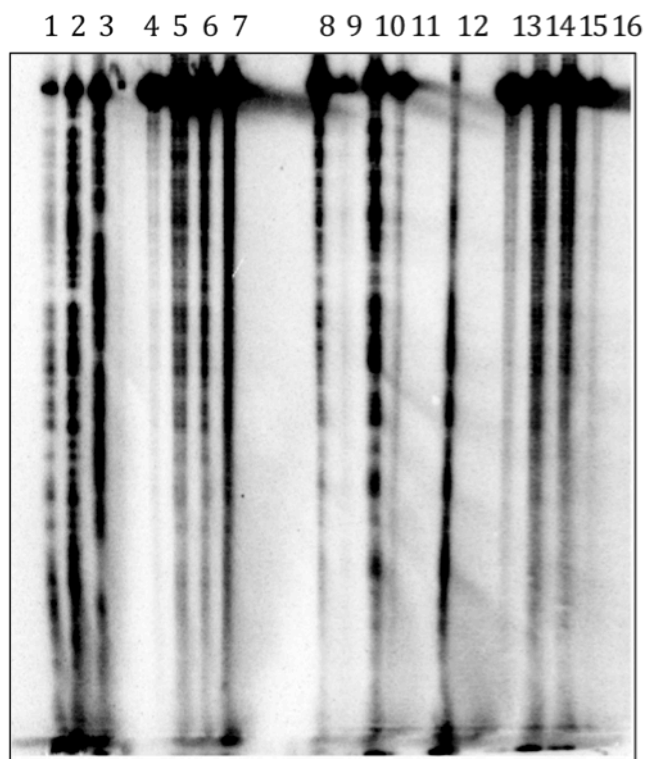
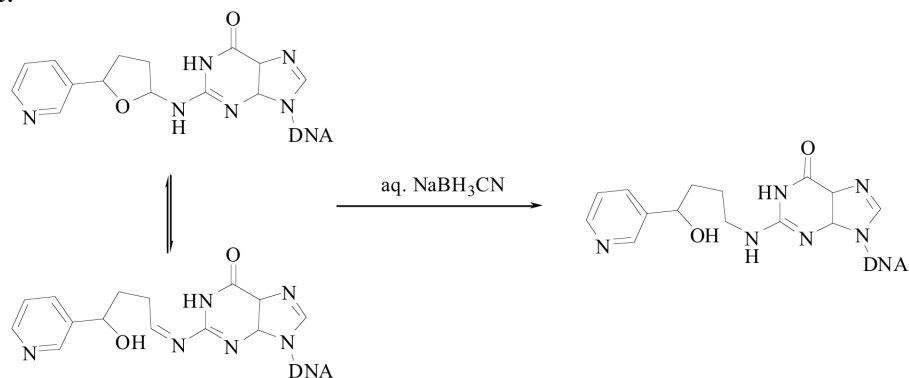


Figure 2.17. PAGE analysis of incubations of 227 bp DNA with acrolein or NNN-5'-OAc in presence of PLE.

Lane 1: Maxam-Gilbert G; Lane 2: Maxam-Gilbert G+A; Lane 3: Maxam-Gilbert T+C; Lane 4: 100 mM NNN-OAc with PLE, no cleavage treatment; Lane 5: 100 mM NNN-OAc with PLE, then 10% aq. piperidine, 90 °C, 30 min.; Lane 6: 100 mM NNN-OAc with PLE, then 20% aq. piperidine, 90 °C, 30 min.; Lane 7: 100 mM NNN-OAc with PLE, then 10% aq. piperidine, 90 °C, 3 h; Lane 8: 100 mM acrolein, no cleavage treatment; Lane 9: 100 mM acrolein, then 10% aq. piperidine, 90 °C, 30 min.; Lane 10: 100 mM acrolein, then 20% aq. piperidine, 90 °C, 30 min.; Lane 11: 100 mM acrolein, then 10% aq. piperidine, 90 °C, 3 h; Lane 12: 100 mM acrolein with PLE, then 10% aq. piperidine, 90 °C, 30 min.; Lane 13: No drug, no cleavage treatment; Lane 14: No drug,

then 10% aq. piperidine, 90 °C, 30 min.; Lane 15: No drug, then 20% aq. piperidine, 90 °C, 30 min.; Lane 16: No drug, then 10% aq. piperidine, 90 °C, 3 h.

The proposed adduct might not be observed by gel electrophoresis for several reasons. First, N2 modification of guanosines does not usually lead to increased cleavage when the DNA is subjected to piperidine-heat treatment.<sup>69</sup> This means that although the DNA is being adducted, no increased cleavage is observed by PAGE analysis. Second, the proposed adducts might be forming reversibly, so exposure to the piperidine-heat treatment or subsequent denaturing gel could cause reversion to unmodified DNA. Third, no adducts might be forming (which is unlikely, given the ESI-MS results). The first possibility is the most likely of the three, as the reported adduct is an N2-guanosine adduct, which is not usually susceptible to cleavage when subjected to piperidine/heat treatment.



Scheme 2.39. Reversibility of NNN-5'-OAc adduct formation with guanosine

In order to test the second possibility (adducts forming reversibly), we treated reaction mixtures with NaBH<sub>3</sub>CN to reduce the adducts, which has been shown to “fix” the reversible modification into an irreversible modification in the case of the known guanosine adducts.<sup>21</sup> Unfortunately, the resulting mobility shift assay did not show adduct formation.

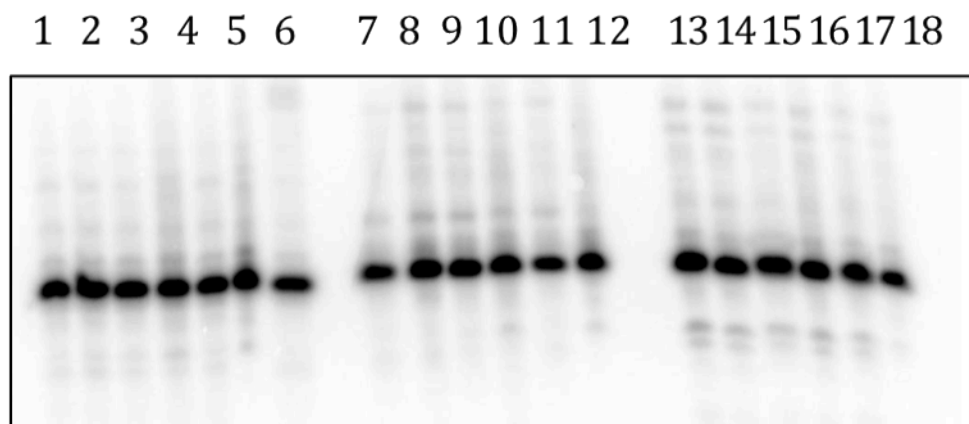


Figure 2.18. EMSA on 11-mer with NNN-5'-OAc in presence of PLE using various post-incubation techniques to try to visualize adduct formation.

Lane 1: 0 mM NNN-OAc with PLE; Lane 2: 10 mM NNN-OAc, 100 mM NNN-OAc with PLE; Lane 4: 500 mM NNN-OAc with PLE; Lane 5: 500 mM NNN-OAc without PLE; Lane 6: 500 mM NNN-OAc with PLE and ss-DNA; Lane 7: 0 mM NNN-OAc with PLE; Lane 8: 10 mM NNN-OAc, 100 mM NNN-OAc with PLE; Lane 9: 500 mM NNN-OAc with PLE; Lane 10: 500 mM NNN-OAc without PLE; Lane 11: 500 mM NNN-OAc with PLE and ss-DNA; Lane 12: 500 mM NNN-OAc with PLE; Lane 13: 0 mM NNN-OAc with PLE; Lane 14: 10 mM NNN-OAc, 100 mM NNN-OAc with PLE; Lane 15: 500 mM NNN-OAc with PLE; Lane 16: 500 mM NNN-OAc without PLE; Lane 17: 500 mM NNN-OAc with PLE and ss-DNA; Lane 18: 500 mM NNN-OAc with PLE. Lanes 1-6: EtOH precipitation. Lanes 7-12: EtOH precipitation, NaCH<sub>3</sub>CN treatment, then EtOH precipitation. Lanes 13-18: EtOH precipitation, then piperidine/heat treatment.

## **2.5. CONCLUSIONS**

In conclusion, a new method to synthesize NNN-OAc in a concise manner was developed. This method could be modified to enable asymmetric synthesis of NNN-OAc. Covalent modification of DNA by NNN-OAc was analyzed by ESI-MS, leading to the suggestion of previously unreported adenosine and cytidine adducts. Unfortunately, the preliminary PAGE analysis did not show any evidence of adduct formation. More complex techniques of analysis such as assays using repair enzymes or interrupted PCR might allow for improved quantitative analysis of the position and frequency of adduct formation.

## EXPERIMENTAL SECTION

### General Notes

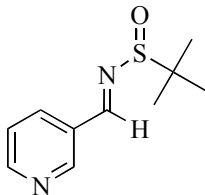
THF was distilled over sodium/benzophenone, and CH<sub>2</sub>Cl<sub>2</sub> and toluene were distilled from CaH<sub>2</sub> immediately prior to use. All reactions were run in oven-dried, argon-flushed round bottom flasks under an argon atmosphere. Solvent ratios are expressed as % by volume. Flash chromatography (FCC) was performed according to the method of Still.<sup>70</sup> NMR was performed using a VARIAN Mercury spectrometer. <sup>1</sup>H NMR was run at 400 MHz; <sup>13</sup>C NMR was run at 100 MHz with broadband proton decoupling unless otherwise specified. Solvent chemical shifts are reported in ppm (δ) and referenced to solvent.<sup>71</sup> IR was obtained on a Nicolet IR100 FT-IR spectrometer. Melting points were obtained in open capillary tubes on a Büchi Melting Pont B-540 and are uncorrected.

**MIS089.** Nicotinaldehyde (Pyridine-3-carboxaldehyde) (515 mg, 4.8 mmol, 1 eq) was combined with cyclopropylamine (1 mL, 14.4 mmol, 3 eq) in dry toluene (0.5 M) and stirred at 80 °C in the presence of 4 Å molecular sieves for 48 h. The reaction was filtered and concentrated to give a pale yellow oil (550 mg, 2.6 mmol, 55%). <sup>1</sup>H NMR (CDCl<sub>3</sub>): δ 8.80 (1H, d, *J* = 1.4); 8.60 (1H, dd, *J* = 4.8, 1.7); 8.46 (1H, s); 8.04 (1H, dt, *J* = 7.9, 1.0); 7.31 (1H, dd, *J* = 7.8, 4.8); 3.06 (1H, septet, *J* = 0.4); 1.02-0.96 (4H, m). <sup>13</sup>C NMR (CDCl<sub>3</sub>): δ 155.2, 150.9, 149.6, 133.9, 132.0, 123.5, 42.2, 9.1. LRMS (CI<sup>+</sup>): 147 (M<sup>+</sup>+1). IR (thin film, CDCl<sub>3</sub>): 3442, 3012, 2965, 1634, 1421, 1387, 1320, 1024, 954, 888, 809, 708 cm<sup>-1</sup>.<sup>27</sup>

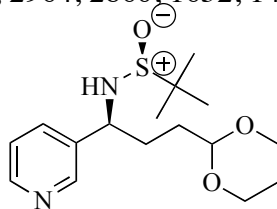
**MIS090** was prepared in accordance with literature procedure (in the same manner as **MIS089**). Spectral data were consistent with the structure assigned.<sup>29</sup>

### (±)-*tert*-Butylsulfonamide<sup>9</sup>

A variation on the published route to the racemic sulfinamide was followed: oxidation of di-*tert*-butyldisulfide by hydrogen peroxide in AcOH<sup>10</sup> afforded the *tert*-butylthiosulfinate, which was then transformed to the *tert*-butyl sulfinyl chloride with SO<sub>2</sub>Cl<sub>2</sub>. Subsequent reaction with NH<sub>4</sub>OH as reported<sup>9</sup> gave the desired product. <sup>1</sup>H, <sup>13</sup>C, and IR were consistent with previously reported data.<sup>32</sup>

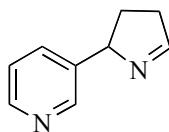


***N*-(3-Pyridinemethylidene)-2-methylpropanesulfinamide (MIS086).**<sup>11</sup> ( $\pm$ )-*tert*-Butyl sulfinamide (400 mg, 3.3 mmol, 1 eq) was dissolved in dry CH<sub>2</sub>Cl<sub>2</sub> (6.6 mL) in a 10 mL round bottom flask. MgSO<sub>4</sub> (2.0 mg, 16.5 mmol, 5 eq) was added, followed by pyridinium *p*-toluenesulfonate (42 mg, 0.17 mmol, 0.05 eq). 3-Nicotinaldehyde (354 mg, 3.3 mmol, 1 eq) was added neat. This cloudy colorless solution was stirred at room temperature for 16 h. The reaction mixture was filtered through Celite, washed with CH<sub>2</sub>Cl<sub>2</sub>, and concentrated to yield a yellow oil that was purified by flash chromatography (SiO<sub>2</sub>, 10–50% EtOAc/Hex) to yield the sulfinimine **MIS086** as a yellow oil (680 mg, 3.2 mmol, 98%). <sup>1</sup>H NMR (400 MHz, CDCl<sub>3</sub>)  $\delta$  8.96 (1H, br s); 8.69 (1H, d, *J* = 4.8 Hz); 8.59 (1H, s); 8.11 (1H, d, *J* = 8.2 Hz); 7.37 (1H, dd, *J* = 7.9, 5.2 Hz); 1.19 (9H, s). <sup>13</sup>C NMR (75 MHz, CDCl<sub>3</sub>)  $\delta$  160.32, 152.79, 150.86, 135.60, 129.54, 123.83, 57.99, 22.48. LRMS (CI<sup>+</sup>): 211 (M<sup>+</sup>+1), 155 (M<sup>-</sup>Bu). HRMS (CI<sup>+</sup>) calc. for C<sub>10</sub>H<sub>15</sub>N<sub>2</sub>OS 211.0905, found 211.0903; IR (thin film): 3411, 2964, 2860, 1652, 1429, 1380 cm<sup>-1</sup>.

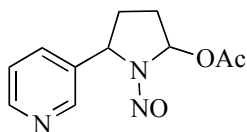




**(±)-N-(3-[1,3]dioxan-2-yl-1-pyridin-3-yl-propyl)-2-methylpropanesulfonamide (MIS087)**. Freshly ground magnesium turnings (1.56 g, 64.2 mmol, 15 eq) were placed in a 50 mL round bottom flask. THF (7.1 mL, 3 M) was added. A solution of 2-(2'-bromoethyl)-1,3-dioxane (1.62 mL, 21.4 mmol, 5 eq) in THF (21.4 mL, 3 M) was added dropwise. With intermittent heating and catalytic iodine (1 small crystal) to initiate the reaction, the mixture was stirred at room temperature for 1h. The Grignard reagent was then transferred via syringe to a clean oven-dried, Ar-flushed 100 mL round bottom flask to remove the excess Mg metal. This solution was cooled to -48 °C. The sulfinimine **MIS086** (900 mg, 4.3 mmol, 1 eq) was added as a solution in THF (4.3 mL, 1 M) at -48 °C. This mixture was stirred at this temperature overnight. After 16 h, the reaction was warmed to room temperature and quenched with satd NH<sub>4</sub>Cl. The reaction mixture was partitioned between satd NH<sub>4</sub>Cl and EtOAc. The aq. layer was extracted (2 x EtOAc), and the combined organic layers were washed with satd NaCl, and dried (Na<sub>2</sub>SO<sub>4</sub>). After evaporation of the solvent, the product was purified by flash chromatography (SiO<sub>2</sub>, 10% MeOH in CH<sub>2</sub>Cl<sub>2</sub>) to yield **MIS087** as a yellow oil (930 mg, 3.6 mmol, 85%). Crystallization from EtOAc/Hex yielded an analytical sample as a white crystalline solid. <sup>1</sup>H NMR (400 MHz, CDCl<sub>3</sub>): δ 8.55 (1H, br s); 8.51 (1H, d, *J* = 4.5 Hz), 7.65 (1H, d, *J* = 7.9 Hz); 7.26 (1H, dd, *J* = 7.7, 5.5 Hz); 4.48 (1H, t, *J* = 5.0 Hz); 4.38 (1H, q, *J* = 6.8 Hz); 4.04 (2H, dd, *J* = 11.7, 4.8 Hz); 3.70 (2H, t, *J* = 11.7 Hz); 3.57 (1H, d, *J* = 4.8 Hz), 2.05-2.15 (2H, m); 1.95-2.05 (1H, m); 1.81-1.92 (1H, m); 1.53-1.63 (1H, m); 1.31 (1H, d of m, *J* = 13.3 Hz), 1.20 (9H, s). <sup>13</sup>C NMR (75 MHz, CDCl<sub>3</sub>): δ 149.1, 148.7, 137.8, 134.8, 123.6, 101.4, 66.8, 57.1, 56.0, 31.2, 30.9, 30.7, 25.6, 22.5. LRMS (CI<sup>+</sup>): 327 (M<sup>+</sup>+1), 231 (M<sup>+</sup>-pyr). HRMS (CI<sup>+</sup>) calc. for C<sub>16</sub>H<sub>27</sub>N<sub>2</sub>O<sub>3</sub>S: 327.1742, found: 327.1746. IR (thin film; CDCl<sub>3</sub>): 3414, 3225, 3051, 2964, 2858, 1710, 1644, 1592, 1578 cm<sup>-1</sup>. mp 99.0-99.5 °C.



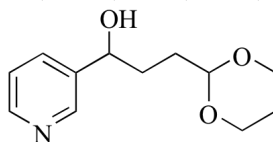
**(±)-5-(3-Pyridyl)-1-pyrroline ((±)-Isomyosmine)<sup>10</sup>**. The sulfinamide **MIS087** (4.34 g, 13.3 mmol, 1 eq) was dissolved in 95% aq. TFA (67 mL, 0.2 M) and stirred at room temperature for 1 h. The reaction was quenched by pouring over saturated NaHCO<sub>3</sub> then extracted (4 x CHCl<sub>3</sub>). The organic layers were combined, dried over Na<sub>2</sub>SO<sub>4</sub>, and concentrated by rotary evaporation. Chromatography on basic alumina (100% EtOAc) or Fluorisil (5% MeOH/CHCl<sub>3</sub>) yielded a brown oil (1.87 g, 13.9 mmol, quant.) whose <sup>1</sup>H NMR spectral data were in accordance with literature values.<sup>12</sup> <sup>13</sup>C NMR (CDCl<sub>3</sub>): δ 168.3, 148.2, 139.3, 133.9, 123.4, 73.5, 61.5, 37.5, 30.1. LRMS (CI<sup>+</sup>) 147 (M<sup>+</sup>+1). HRMS (CI<sup>+</sup>) calc. for C<sub>9</sub>H<sub>11</sub>N<sub>2</sub>: 147.0922, found: 147.0923. IR (thin film): 3019, 2968, 2400 (w), 2253 (w), 1215 cm<sup>-1</sup>.



**(±)-N'-Nitrosonornicotine-5'-acetate.<sup>6</sup>**

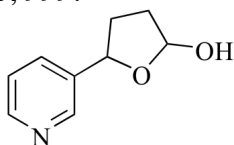
Isomyosmine (87 mg, 0.60 mmol, 1 eq) was dissolved in glacial acetic acid (1 mL, 0.6 M) and cooled to 5 °C. NaNO<sub>2</sub> (53 mg, 0.77 mmol, 1.3 eq) was added, and reaction mixture was allowed to warm to room temperature for 1 h (until complete as judged by TLC). The reaction was quenched by pouring over saturated NaHCO<sub>3</sub> then extracted (3 x CHCl<sub>3</sub>), dried (Na<sub>2</sub>SO<sub>4</sub>), and conc. The resulting brown oil was passed immediately through a Fluorisil column using EtOAc as the eluent. The resultant yellow oil was purified by flash chromatography (SiO<sub>2</sub>, 50–75% EtOAc/Hex) to yield a light yellow oil (48.2 mg, 0.22 mmol, 37%) whose <sup>1</sup>H NMR, IR, and MS spectral data were in accordance with the literature values.<sup>5</sup> Subsequent chromatography (SiO<sub>2</sub>, 75%

EtOAc/Hex) yielded an inseparable mixture of four diastereomers as a pale yellow solid,  $^{13}\text{C}$  NMR ( $\text{CDCl}_3$ ):  $\delta$  169.5, 169.4, 148.8, 148.7, 147.8, 147.1, 135.0, 133.9, 133.5, 132.7, 123.5, 123.4, 85.0, 83.8, 59.3, 58.5, 31.1, 30.5, 29.6, 29.5, 21.1, 21.0. mp 57.4-64.1 °C.



**3-[1,3]-dioxan-2-yl-1-pyridin-3-ylpropan-2-ol. MIS096.** Freshly ground magnesium turnings (1.36 g, 56.0 mmol, 15 eq) were placed in a 100 mL oven-dried, Ar-flushed round bottom flask. THF (18.7 mL, 3 M) was added. A solution of 2-(2'-bromoethyl)-1,3-dioxane (3.03 mL, 22.4 mmol, 1.2 eq) in THF (7.5 mL, 3 M) was added dropwise. With intermittent heating and catalytic iodine (1 small crystal) to initiate the reaction, the mixture was stirred at room temperature for 1 h. The Grignard reagent was then transferred via syringe to a clean oven-dried, Ar-flushed 100 mL round bottom flask to remove the excess Mg metal. This solution was cooled to -78 °C. The pyridine-3-carboxaldehyde (2 g, 18.7 mmol, 1 eq) was added as a solution in THF (18.7 mL, 1 M) at -78 °C. This mixture was warmed to room temperature over 3 h then quenched with satd  $\text{NH}_4\text{Cl}$ . The reaction mixture was partitioned between satd  $\text{NH}_4\text{Cl}$  and EtOAc. The aq. layer was extracted (2 x EtOAc), and the combined organic layers were washed with satd NaCl, and dried ( $\text{Na}_2\text{SO}_4$ ). After evaporation of the solvent, the product was purified by flash chromatography ( $\text{SiO}_2$ , 10% MeOH in  $\text{CH}_2\text{Cl}_2$ ) to yield the product as a yellow oil (3.62 g, 16.2 mmol, 87%).  $^1\text{H}$  NMR ( $\text{CDCl}_3$ ):  $\delta$  8.52 (1H, s); 8.44 (1H, s); 7.70 (1H, d,  $J = 8.0$  Hz); 7.24 (1H, dd,  $J = 7.5, 4.9$  Hz); 4.75 (1H, dd,  $J = 7.0, 5.7$  Hz); 4.58 (1H, t,  $J = 4.7$  Hz); 4.10 (2H, ddd,  $J = 11.3, 3.5, 1.5$  Hz); 3.76 (2H, tt,  $J = 12.1, 2.3$  Hz); 2.06 (1H, m); 1.87 (2H, m); 1.75 (2H, m); 1.34 (1H, d of quint,  $J = 13.5, 1.4$  Hz).  $^{13}\text{C}$  NMR ( $\text{CDCl}_3$ ):  $\delta$  148.4, 147.7, 133.6, 124.0, 123.8, 101.7, 71.6, 66.9, 33.32, 31.3, 25.7. LRMS ( $\text{Cl}^+$ ): 224

( $M^+ + 1$ ), 206 ( $M^+ - H_2O$ ). HRMS ( $CI^+$ ): calcd. for  $C_{12}H_{17}NO_3$ : 224.1827, found 224.1827. IR (thin film from DCM): 3342 (br s), 2958, 2852, 2733 (m), 1655 (m), 1594, 1580, 1471, 1428, 1379, 1287, 1143, 1088, 999.



**5-Pyridin-3-yltetrahydrofuran-2-ol.**<sup>72</sup> **MIS 097**. Acetal **MIS 096** (110 mg, 0.49 mmol, 1 eq) was stirred in 1 M  $H_2SO_4$  (0.1 M with respect to acetal) overnight at room temperature. The reaction was neutralized to pH 7-8 using satd  $NaHCO_3$  (15 mL), then extracted with DCM (3x10 mL). The combined organic layers were dried ( $Na_2SO_4$ ) and concentrated. FCC yielded the desired product as a yellow oil comprised of a 1:1 mixture of diastereomers (58 mg, 0.35 mmol, 71%)  $^1H$  NMR ( $CDCl_3$ ):  $\delta$  8.67 (1H, d,  $J = 2.0$  Hz); 8.59 (1H, d,  $J = 2.3$  Hz); 8.51 (2H, dt,  $J = 4.7, 1.8$  Hz); 7.79 (1H, dt,  $J = 7.8, 1.7$  Hz); 7.64 (1H, dtd,  $J = 7.8, 2.1, 0.6$  Hz); 7.27 (2H, m); 5.79 (1H, dd,  $J = 5.1, 2.2$  Hz); 5.67 (1H, dd,  $J = 4.1, 1.0$  Hz); 5.27 (1H, t,  $J = 7.0$  Hz); 5.03 (1H, m); 2.53 (1H, ddt,  $J = 12.3, 8.2, 6.9$  Hz); 2.35 (1H, m); 2.19 (1H, m); 2.09 (1H, m); 2.05 (1H, m); 1.78 (1H, m).  $^{13}C$  NMR ( $CDCl_3$ ):  $\delta$  148.7, 148.6, 148.0, 147.6, 138.7, 138.0, 134.2, 133.4, 123.42, 123.35, 99.0, 98.7, 80.3, 34.5, 33.1, 32.7, 32.6. LRMS ( $CI^+$ ): 166 ( $M^+ + 1$ ), 148 ( $M^+ - H_2O$ ) HRMS ( $CI^+$ ): calcd. for  $C_9H_{11}NO_2$ : 166.0868, found 166.0869. IR (thin film from DCM): 3269 (br s), 2951, 1686 (m), 1583 (m), 1430 (m), 1352 (m), 1042 (m), 982 (m).

### 2.5.1. Chemical DNA Synthesis

Synthesis was performed on an Expedite 8909 DNA synthesizer from PerSeptive Biosystems. Phosphoramidites, columns, and other related reagents were purchased from Glen Research. Syntheses were performed on a 1  $\mu M$  scale using the "trityl on" method followed by purification on Poly-Pak II columns using the standard protocol.

DNA synthesized:

5'-CCG-CGT-CCG-CG-3'

5'-CCG-MeCGT-CCG-CG-3'

5'-CCG-CGT-MeCCG-CG-3'

5'-CGC-GGA-CGC-GG-3'

5'-CG<sup>Me</sup>C-GGA-CGC-GG-3'

5'-CGC-GGA-MeCGC-GG-3'

5'-CGC-GGA-CG<sup>Me</sup>C-GG-3'

### 2.5.2. Preparation of Duplex DNA for ESI-MS

Duplex DNA was formed by heating equimolar amounts (typically ~200 nmol scale) of the ss-DNA to 90 °C in 0.1 M sodium phosphate buffer (pH 7) for 5 min, then cooling slowly (over ~8 h) to 4 °C and held for at least 10 h at 4 °C.

Duplexes were analyzed for purity by ESI-MS (Brodbeck group) and found to be sufficiently pure for further use.

### 2.5.3. DNA synthesis by PCR

T4 polynucleotide kinase was obtained from New England Biolabs. Taq polymerase and the nucleotide mix were purchased from Roche. [<sup>32</sup>P]-γ-ATP was purchased from GE Healthcare. Primers were synthesized (as above) and purified by native polyacrylamide gel (20%) using UV shadowing to visualize the DNA and 1X TE buffer to elute the DNA. P-6 spin columns were purchased from Bio-Rad.

Primer L151 was radiolabelled by combining L151 stock solution (1  $\mu$ L , 40  $\mu$ M in TE buffer) with PNK buffer (3  $\mu$ L), sterile H<sub>2</sub>O (19  $\mu$ L), [<sup>32</sup>P]-  $\gamma$ -ATP (6  $\mu$ L), and T4 kinase (1  $\mu$ L). This mixture was incubated at 37 °C for 1 h, at which time an additional T4 kinase (1  $\mu$ L) was added and the reaction was incubated an additional 1 h at 37 °C. After incubation, the enzyme was inactivated by heating the reaction mixture to 65 °C for 10 min. The DNA was isolated using P-6 spin columns according to the enclosed protocol.

The volume of eluent was measured, and the radiolabelled primer was combined with R378 primer (1  $\mu$ L, 40  $\mu$ M), dNTP mix (1  $\mu$ L), pUC 19 template (1  $\mu$ L, 10  $\mu$ g/ $\mu$ L), PCR buffer (5  $\mu$ L), water (to 50  $\mu$ L total reaction volume), and 0.5  $\mu$ L Taq polymerase. This mixture was subjected to PCR (13 cycles) followed by purification using a 6% native polyacrylamide gel. DNA was visualized using film, and desired bands were eluted using 1X TE buffer.

DNA was sequenced according to standard protocols.<sup>73</sup>

#### **2.5.4. DNA-Drug Incubations for ESI-MS**

DNA was synthesized and annealed as described above. Pig liver esterase was purchased from Biocatalytics Inc. as a solution in 1 M ammonium sulfate and used without further alteration.

Duplex DNA in 0.1 M sodium phosphate was combined with sterile water and sodium phosphate (0.5 M, pH 7), then treated with the desired drug (*vide supra*) and (when required) pig liver esterase (stock solutions were prepared by dilution with 0.1 M sodium phosphate). NNN-OAc stock solution was prepared by dilution of a 5 M stock in

DMSO with 0.1 M sodium phosphate pH 7. Acrolein stock solutions were prepared by dissolving the acrolein in 0.1 M sodium phosphate. For incubations less than 50  $\mu$ M total volume, 100  $\mu$ L PCR tubes were used for the incubations. Samples were incubated 12-16 h at 37 °C, then given to the Brodbelt group for analysis.

#### **2.5.5. DNA-Drug Incubations with Radiolabelled DNA**

DNA was prepared as described above. DNA (150,000 cpm per sample) was diluted with water and 0.5 M sodium phosphate (pH 7), then treated with the desired drug (*vide supra*) and pig liver esterase (where required; stock solutions were prepared by dilution with 0.1 M sodium phosphate). NNN-OAc stock solutions was prepared by dilution of a 5 M stock in DMSO with 0.1 M sodium phosphate. Acrolein stock solutions were prepared by dissolving the acrolein in 0.1 M sodium phosphate. Samples were incubated for 16 h at 37 °C in 1.5 mL Eppendorf tubes.

Following incubation, samples were extracted 2x using  $\text{CHCl}_3$ . The DNA was then precipitated by adding cold (-20 °C) EtOH (700  $\mu$ L) to the aqueous phase. Samples were cooled at -20 °C for approx. 60 min. Samples were centrifuged at 15,000 x g for 5 min. in the microcentrifuge. The supernatant was removed, and samples were rinsed twice with cold EtOH (200  $\mu$ L). Samples were then redissolved in water (200  $\mu$ L) with 3 M sodium acetate (pH 5, 20  $\mu$ L). Cold (-20 °C) EtOH (500  $\mu$ L) was added, and the DNA was cooled to -20 °C for approx. 60 min. Samples were centrifuged at 15,000 x g for 5 min. in the microcentrifuge. The supernatant was removed, and samples were rinsed twice with cold 70% aqueous EtOH (200  $\mu$ L). Samples were then redissolved in water (200  $\mu$ L) with 3 M sodium acetate (pH 5, 20  $\mu$ L). Cold (-20 °C) EtOH (500  $\mu$ L) was added, and the DNA was cooled to -20 °C for approx. 60 min. Samples were centrifuged

at 15,000 x *g* for 5 min. in the microcentrifuge. The supernatant was removed, and samples were rinsed twice with cold 70% aqueous EtOH (200  $\mu$ L).

The DNA samples were then subjected to piperidine/heat treatment. Each sample was dissolved in 10% aq. piperidine (10  $\mu$ L) and heated to 90 °C for 30 min. Samples were concentrated by centrifuging *in vacuo*. To remove residual piperidine, samples were redissolved in water (30  $\mu$ L), transferred to clean tubes, and concentrated by centrifuging *in vacuo*. Samples were again redissolved in water (20  $\mu$ L) and concentrated. Cleavage was assayed by running 7% denaturing acrylamide gels using formamide loading buffer.

#### **2.5.6. Mobility Shift Assays**

Single-stranded DNA (synthesized as described above) was radiolabeled using T4 polynucleotide kinase following the protocol described above. Following isolation using P6 spin columns, the DNA was concentrated by centrifuging *in vacuo*, then redissolved in 10% aq. piperidine. Samples were heated to 90 °C for 30 min, then concentrated on the Speedvac. Samples were transferred to clean tubes by washing twice with water (20  $\mu$ L, then 10  $\mu$ L) and were concentrated by centrifuging *in vacuo*. DNA was purified using a 20% denaturing acrylamide gel. Film was used to visualize the DNA, and the desired band was eluted with 1X TE buffer. The DNA was then concentrated to a volume of ~100  $\mu$ L, treated with EtOH and cooled to -80 °C. Samples were centrifuged at 15,000 x *g* for 5 min, and the supernatant was removed. Samples were dissolved in 0.1 M sodium phosphate (pH 7) and an excess (2-3 fold) of the complementary strand was added. These samples were heated to 90 °C for 5 min, then cooled slowly to 4 °C and held at 4 °C for ~12 h.



For experiments using long, double-stranded DNA, a 227 bp DNA duplex was obtained by PCR on a pUC19 plasmid using <sup>32</sup>P-labelled 5' primer according to a previously reported procedure.<sup>74</sup>

Incubations were performed in 0.1 M sodium phosphate at pH 7 using 50,000 cpm per sample. NNN-OAc with PLE and acrolein were used in varying concentrations. Samples were incubated at 37 °C for 16 h. Samples were extracted with CHCl<sub>3</sub> (50 µL), then precipitated twice with cold EtOH (as previously described). Samples were analyzed using a 20% denaturing gel and visualized using the phosphorimager.

Acrolein shows cleavage at 100 mM concentration when 16 h incubation is followed by isolation of the DNA by ethanol precipitation and treatment with aqueous piperidine at 90 °C. In the literature, *in vivo* cell experiments were performed using 30 µM acrolein to induce DNA damage.<sup>68</sup>

## 2.6. REFERENCES

- (1) ; National Cancer Institute website: 2004, National Cancer Institute Cancer Fact Sheet.
- (2) Pfeifer, G. P.; Denissenko, M. F.; Olivier, M.; Tretyakova, N.; Hecht, S. S.; Hainaut, P. *Oncogene* **2002**, *21*, 7435-7451.
- (3) Torre, G. L.; de Waure, C.; Specchia, M. L.; Nicolotti, N.; Capizzi, S.; Bilotta, A.; Clemente, G.; Ricciardi, W. *Pancreas* **2009**, *38*, 241-247.
- (4) Catassi, A.; Servent, D.; Paleari, L.; Cesario, A.; Russo, P. *Mutat. Res.* **2008**, *659*, 221-231.
- (5) Egleton, R. D.; Brown, K. C.; Dasgupta, P. *Pharmacol. Ther.* **2009**, *121*, 205-223.
- (6) Service, U. P. H. *Smoking and Health. Report of the Advisory Committee to the Surgeon General of the Public Health Service*, US Department of Health Education and Welfare, 1957.
- (7) Greenblatt, M. S.; Bennett, W. P.; Hollstein, M.; Harris, C. C. *Cancer Res.* **1994**, *69*, 409-416.
- (8) Hainaut, P.; Pfeifer, G. P. *Carcinogenesis* **2001**, *22*, 367-374.
- (9) Danissenko, M. S.; Pao, A.; Tang, M.-s.; Pfeifer, G. P. *Science* **1996**, *274*, 430-432.
- (10) Weaver, R. F. *Molecular Biology*; The McGraw-Hill Companies: St. Louis, 2005.
- (11) Rechkoblit, O.; Zhang, Y.; Guo, D.; Wang, Z.; Amin, S.; Jacek, K.; Louneva, N.; Geacintov, N. E. *J. Biol. Chem.* **2002**, *277*, 30488-30494.
- (12) Ding, J.; Vouros, P. *J. Chromat. A* **2000**, *887*, 103-113.

- (13) Hecht, S. S. *Drug Metab. Rev.* **1994**, *26*, 373-390.
- (14) Julio, E.; Laporte, F.; Reis, S.; Rothan, C.; Dorlac de Borne, F. *Mol. Breed.* **2008**, *21*, 369-381.
- (15) Xu, D.; Shen, Y.; Chappell, J.; Cui, M.; Nielsen, M. *Physiol. Plant.* **2007**, *129*, 307-319.
- (16) Hashimoto, T.; Yamada, Y. *Ann. Rev. Plant Physiol. Plant Mol. Biol.* **1994**, *45*, 257-285.
- (17) Bush, L. P.; Cui, M.; Shi, H.; *et al.* *Recent Advances in Tobacco Science* **2001**, *27*, 23-46.
- (18) Jalas, J. R.; Hecht, S. S.; Murphy, S. E. *Chem. Res. Toxicol.* **2005**, *18*, 95-110.
- (19) Upadhyaya, P.; Sturla, S. J.; Tretyakova, N.; Ziegel, R.; Villalta, P. W.; Wang, M.; Hecht, S. S. *Chem. Res. Toxicol.* **2003**, *16*, 180-190.
- (20) Hecht, S. S.; Villalta, P. W.; Sturla, S. J.; Cheng, G.; Yu, N.; Upadhyaya, P.; Wang, M. *Chem. Res. Toxicol.* **2004**, *17*, 588-597.
- (21) Upadhyaya, P.; McIntee, E. J.; Villalta, P. W.; Hecht, S. S. *Chem. Res. Toxicol.* **2006**, *19*, 426-435.
- (22) Hu, M. W.; Bondinell, W. E.; Hoffman, D. *J. Labelled Compd. Radiopharm.* **1974**, *10*, 79-48.
- (23) Seeman, J. I.; Chavdarian, C. G.; Secor, H. V. *J. Org. Chem.* **1985**, *50*, 5419-5421.
- (24) Hecht, S. S.; Chen, C. B. *J. Org. Chem.* **1979**, *44*, 1563-1566.
- (25) Carmella, S. G.; McIntee, E. J.; Chen, M.; Hecht, S. S. *Carcinogenesis* **2000**, *21*, 839-843.

- (26) Nakane, M.; Hutchinson, C. R. *J. Org. Chem.* **1978**, *43*, 3922-3931.
- (27) Campos, P. J.; Soldevilla, A.; Sampedro, D.; Rodriguez, M. A. *Tetrahedron Lett.* **2002**, *43*, 8811-8813.
- (28) Jarboe, C. H.; Rosene, C. J. *J. Chem. Soc.* **1961**, 2455-2458.
- (29) Campos, P. J.; Soldevilla, A.; Sampedro, D.; Rodriguez, M. A. *Org. Lett.* **2001**, *3*, 4087-4089.
- (30) Sampedro, D.; Soldevilla, A.; Modriguez, M. A.; Campos, P. J.; Olivucci, M. J. *Am. Chem. Soc.* **2005**, *127*, 441-448.
- (31) Soldevilla, A.; Sampedro, D.; Campos, P. J.; Rodriguez, M. A. *J. Org. Chem.* **2005**, *70*, 6976-6979.
- (32) Brinner, K. M.; Ellman, J. A. *Org. Biomol. Chem.* **2005**, *3*, 2109-2113.
- (33) Cogan, D. A.; Liu, G.; Kim, K.; Backes, B. J.; Ellman, J. A. *J. Am. Chem. Soc.* **1998**, *120*, 8011-8019.
- (34) Weix, D. J.; Ellman, J. A. *Org. Synth.* **2005**, *82*, 157-162.
- (35) Liu, G.; Cogan, D. A.; Ellman, J. A. *J. Am. Chem. Soc.* **1997**, *119*, 9913-9914.
- (36) Liu, G.; Cogan, D. A.; Owens, T. D.; Tang, T. P.; Ellman, J. A. *J. Org. Chem.* **1999**, *64*, 1278-1284.
- (37) Brak, K.; Barrett, K. T.; Ellman, J. A. *J. Org. Chem.* **2009**, *74*, 3606-3608.
- (38) Wakayama, M.; Ellman, J. A. *J. Org. Chem.* **2009**, *74*, 2646-2650.
- (39) Moreau, P.; Essiz, M.; Merour, J.-Y.; Bouard, D. *Tetrahedron: Asymmetry* **1997**, *8*, 591-598.
- (40) Yang, T.-K.; Chen, R.-Y.; Lee, D.-S.; Peng, W.-S.; Jiang, Y.-Z.; Mi, A.-Q.; Jong, T.-T. *J. Org. Chem.* **1994**, *59*, 914-921.

- (41) Annunziata, R.; Cinquini, M.; Cozzi, F. *J. Chem. Soc., Perkin Trans. 1* **1982**, 339-343.
- (42) Cogan, D. A.; Ellman, J. A. *J. Am. Chem. Soc.* **1999**, *121*, 268-269.
- (43) Mikolajczyk, M.; Lyzwa, P.; Drabowicz, J.; Wieczorek *Chem. Commun.* **1996**, 1503-1504.
- (44) Lefebvre, I. M.; Evans Jr., S. A. *J. Org. Chem.* **1994**, *62*, 7532-7533.
- (45) Weix, D. J.; Shi, Y.; Ellman, J. A. *J. Am. Chem. Soc.* **2005**, *127*, 1092-1093.
- (46) Cooper, I. R.; Grigg, R.; MacLachlan, W. S.; Thornton-Pett, M.; Sridharan, V. *Chem. Commun.* **2002**, 1372-1373.
- (47) Tang, T. P.; Ellman, J. A. *J. Org. Chem.* **2002**, *67*, 7819-7832.
- (48) Fujisawa, T.; Kooriyama, Y.; Shimizu, M. *Tetrahedron Lett.* **1996**, *37*, 3881-3884.
- (49) Jacobsen, M. F.; Skrydstrup, T. *J. Org. Chem.* **2003**, *68*, 7112-7114.
- (50) Davis, F. A.; Zhou, P. *Tetrahedron Lett.* **1994**, *35*, 7525-7528.
- (51) Ruano, J. L. G.; Fernandez, I.; Cataline, M. d. P.; Cruz, A. A. *Tetrahedron: Asymmetry* **1996**, *7*, 3407-3414.
- (52) Davis, F. A.; Zhou, P.; Reddy, G. V. *J. Org. Chem.* **1994**, *59*, 3242-3245.
- (53) Gonzalez-Gomez, J. C.; Foubelo, F.; Yus, M. *Tetrahedron Lett.* **2008**, *49*, 2343-2347.
- (54) Kong, J.-R.; Cho, C.-W.; Krische, M. J. *J. Am. Chem. Soc.* **2005**, *127*, 11269-11276.
- (55) Lin, X.; Bentley, P. A.; Xie, H. *Tetrahedron Lett.* **2005**, *46*, 7849-7852.
- (56) Feng, L.; Zhang, A.; Kerwin, S. M. *Org. Lett.* **2006**, *8*, 1983-1986.

- (57) Prakash, G. K. S.; Mandal, M.; Olah, G. A. *Angew. Chem., Int. Ed. Engl.* **2001**, *40*, 589-590.
- (58) Zhang, W.-X.; Ding, C.-H.; Luo, Z.-B.; Hou, X.-L.; Dai, L.-X. *Tetrahedron Lett.* **2006**, *47*, 8391-8393.
- (59) Brak, K.; Ellman, J. A. *J. Am. Chem. Soc.* **2009**, *131*, 3850-3851.
- (60) Vedejs, E.; Chapman, R. W.; Fields, S. C.; Lin, S.; Schrimpf, M. R. *J. Org. Chem.* **1995**, *60*, 3020-3027.
- (61) Vedejs, E.; Fields, S. C.; Lin, S.; Schrimpf, M. R. *J. Org. Chem.* **1995**, *60*, 3028-3034.
- (62) Molander, G. A. *J. Org. Chem.* **2009**, *74*, 973-980.
- (63) Soldevilla, A. *e-mail communication*, **2004**.
- (64) Marriner, G. A.; Kerwin, S. M. *J. Org. Chem.* **2009**, *74*, 2891-2892.
- (65) Soldevilla, A. *e-mail communication*, **2008**.
- (66) Upadhyaya, P.; Hecht, S. S. *Chem. Res. Toxicol.* **2008**, *21*, 2164-2171.
- (67) Smith, S.; Marriner, G. A.; Kerwin, S.; Brodbelt, J. S. In *American Society of Mass Spectrometry Conference, poster presentation*; The University of Texas at Austin: Austin, 2007.
- (68) Feng, Z.; Hu, Y.; Tang, M.-s. *Proc. Natl. Acad. Sci. U.S.A.* **2006**, *43*, 15404-15409.
- (69) Lawley, P. D.; Brookes, P. *Biochem. J.* **1963**, *89*, 127-138.
- (70) Still, W. C.; Kahn, M.; Mitra, A. *J. Org. Chem.* **1978**, *43*, 2923-2924.
- (71) Gottlieb, H. E.; Kotlyar, V.; Nudelman, A. *J. Org. Chem.* **1997**, *62*, 7512-7515.

- (72) Loozen, H. J.; Godefroi, E. F.; Besters, J. S. M. M. *J. Org. Chem.* **1975**, *40*, 892-894.
- (73) Slatko, B. E.; Albright, L. M. *DNA Sequencing by the Chemical Method*; John Wiley and Sons: New York, 1999; Vol. 1.
- (74) Tuesuwan, B. Dissertation, The University of Texas at Austin, 2007.

### **3. Structure-Activity Relationships of a Series of Propargylic Alkynylbenzimidazolium Salts on Cytosine and 5-Methylcytosine**

#### **3.1. BACKGROUND**

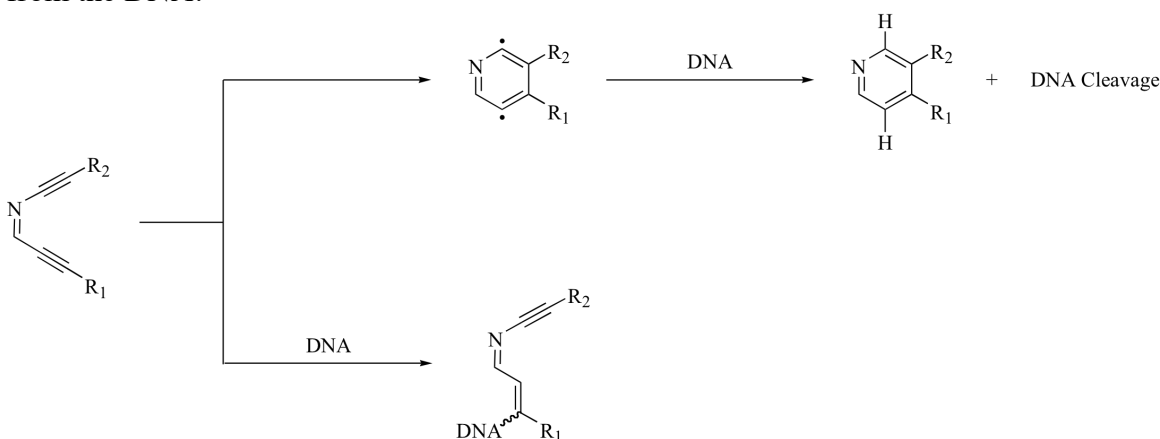
##### **3.1.1. Aza-Enediynes**

Much effort has been spent to improve upon the promising anticancer activity of enediyne natural products (see Section 1.4.3.1)<sup>1</sup>. One approach to improving the cytotoxicity and selectivity of aza-enediynes is to explore alternative diradical-generating cyclizations that may be triggered more selectively or give rise to diradical intermediates which are more selective in their interactions with DNA than the enediynes natural products. In the Kerwin group, the general approach to improved drug-like enediyne compounds has been to synthesize analogs in which a nitrogen atom replaces one of the  $sp^2$ -hybridized carbons (aza-enediynes). In this chapter, a brief background of the previously reported chemistry and biology of aza-enediynes and related systems will be presented. This will be followed by a discussion of DNA methylation and the possible significance of DNA methylation status in the biological effects of a specific class of aza-enediynes. After this introduction, studies of the interaction of a variety of DNA-interactive agents with DNA, including aza-enediynes, will be described. The preparation and evaluation of a small library of benzimidazole-based “skipped” aza-enediynes will be provided. A final conclusion section will describe the significance of the DNA selectivity and structure-activity studies of benzimidazole “skipped” aza-enediynes presented here



### 3.1.2. Diradical-generating cyclizations

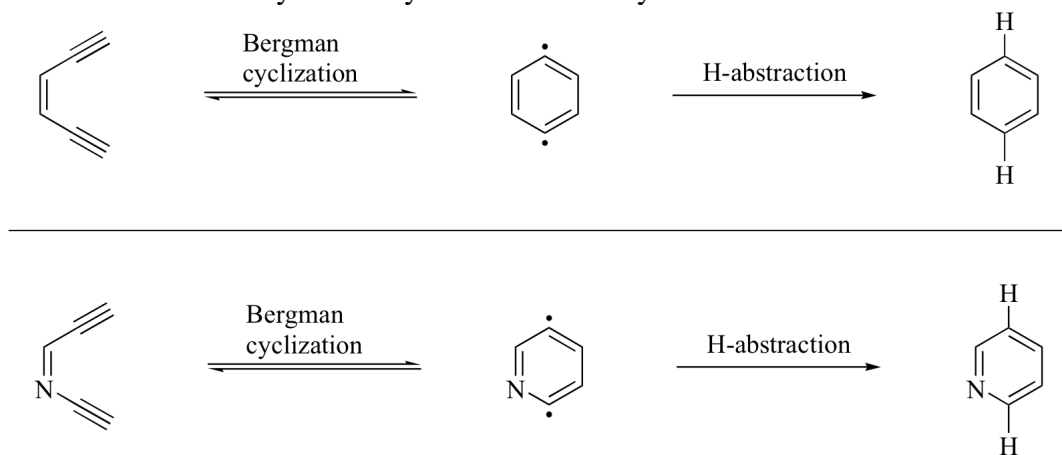
There are several possible mechanisms for modification of DNA by the azaenediyne (Scheme 3.1). The first possibility is simple electrophilic modification. The ynamine portion of the molecule can serve as an electrophile and undergo 1,4 conjugate addition by a nucleoside base. The second possibility is that the azaenediyne can undergo a diradical-generating cyclization and subsequently perform a hydrogen atom abstraction from the DNA.



Scheme 3.1. Possible mechanisms for DNA modification by aza-enediyne

Several diradical cyclizations are possible in azaenediyne and skipped azaenediyne systems. One potential cyclization motif for the azaenediynes is an aza-Bergman cyclization (Scheme 3.2). The Bergman cyclization is a thermal rearrangement of a 1,2-dialkynyl olefin to a diradical *p*-benzyne, which can then be trapped with a H-atom donor (Scheme 3.2).<sup>2</sup> Extensive studies have been performed regarding synthetic enediynes and their requirements for Bergman cyclization.<sup>1</sup> Computational analysis has also been used model of the energetics of the reaction. The initial estimated  $\Delta H^\ddagger$  for the transformation is 32 kcal/mol<sup>2</sup>, with later calculations suggesting that it was near 28 kcal/mol.<sup>3,4</sup> In 1998, calculations comparing the Bergman cyclization to the aza-Bergman

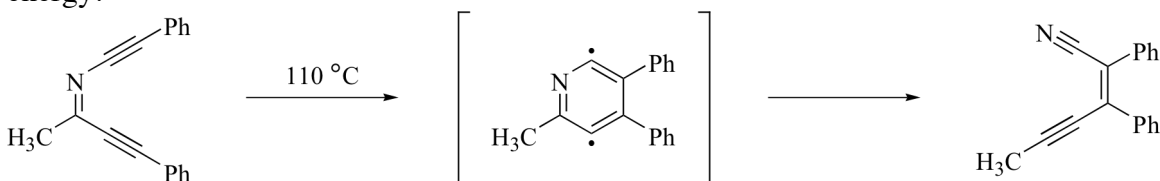
(and aza-Bergman with protonated imine nitrogen) found the results summarized in Table 3.1.<sup>3,4</sup> The authors note that the CASMP calculation places the diradical intermediate too low in energy, whereas the CASSF does better at estimating the energy of the diradical but overestimates the activation energy by approximately 10 kcal/mol.<sup>4</sup> Both computational models suggest that protonation of the aza-enediyne raises the activation energy for the retro-aza-Bergman and, for the CASMP model, lowers the energy of the diradical intermediate significantly. More recently, in 2008, Shields *et al.* performed extensive computational analysis of the activation energy for Bergman and aza-Bergman cyclizations on a wide variety of enediynes and azaenediynes.<sup>5</sup>



Scheme 3.2. Bergman and aza-Bergman cyclization

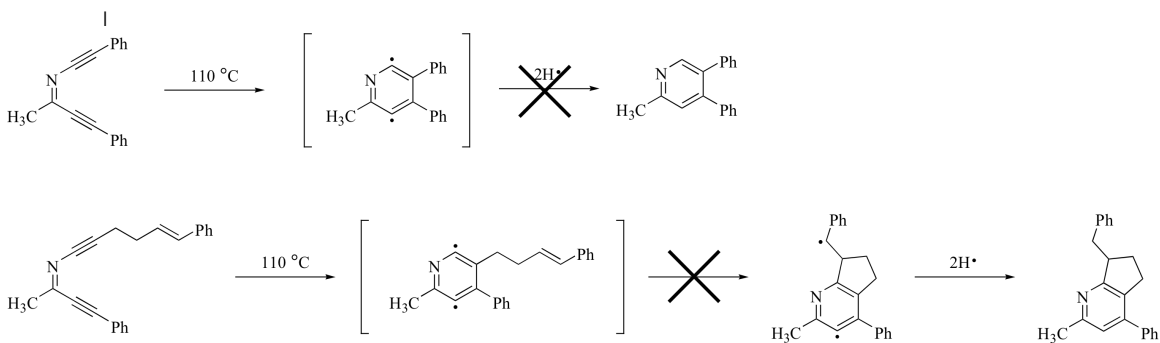
In 1997, Kerwin *et al.* published a study on the aza-Bergman cyclization of an aza-enediyne.<sup>6</sup> Instead of forming the substituted pyridine ring, the aza-enediyne at elevated temperatures (benzene at reflux) yielded a  $\beta$ -alkynyl-acrylonitrile (Scheme 3.3) in 88% isolated yield.<sup>6</sup> The authors propose that the cyclized diradical intermediate rapidly undergoes an intramolecular cycloreversion to form the rearranged product.<sup>6</sup> The first-order rate constant of this transformation at 100 °C in acetonitrile was  $2.43 \times 10^{-4}$ , a  $t_{1/2}$  of 47 min. a more rapid reaction than the Bergman cyclization, which has a half-life of

71 min at 280 °C in acetonitrile, indicating that the aza-enediyne has a lower activation energy.



Scheme 3.3. Aza-Bergman followed by retro-aza-Bergman<sup>6</sup>

In an attempt to trap the proposed diradical, a hydrogen atom donor, cyclohexadiene, was added to the reaction mixture (Scheme 3.4).<sup>6</sup> No trapped product is observed, indicating that the expected trapping is approximately 1000x slower than the cycloreversion.<sup>6</sup> In an attempt to use an intramolecular trap for the predicted diradical, an appendant styrene was added. The exclusive product was the rearranged product rather than the cyclized ring system.<sup>6</sup> This study supports the idea that adding a heteroatom to an enediyne system could lower the activation energy of the cyclization reaction, but the retro-Bergman might proceed too rapidly for trapping reactions. Other substitution patterns on these dialkynylimine systems led to more complex mixtures thought to arise from bimolecular rearrangements.<sup>7</sup>



Scheme 3.4. Unsuccessful attempts to trap proposed 2,5-dihydropyridine intermediate of aza-Bergman cyclization<sup>6</sup>

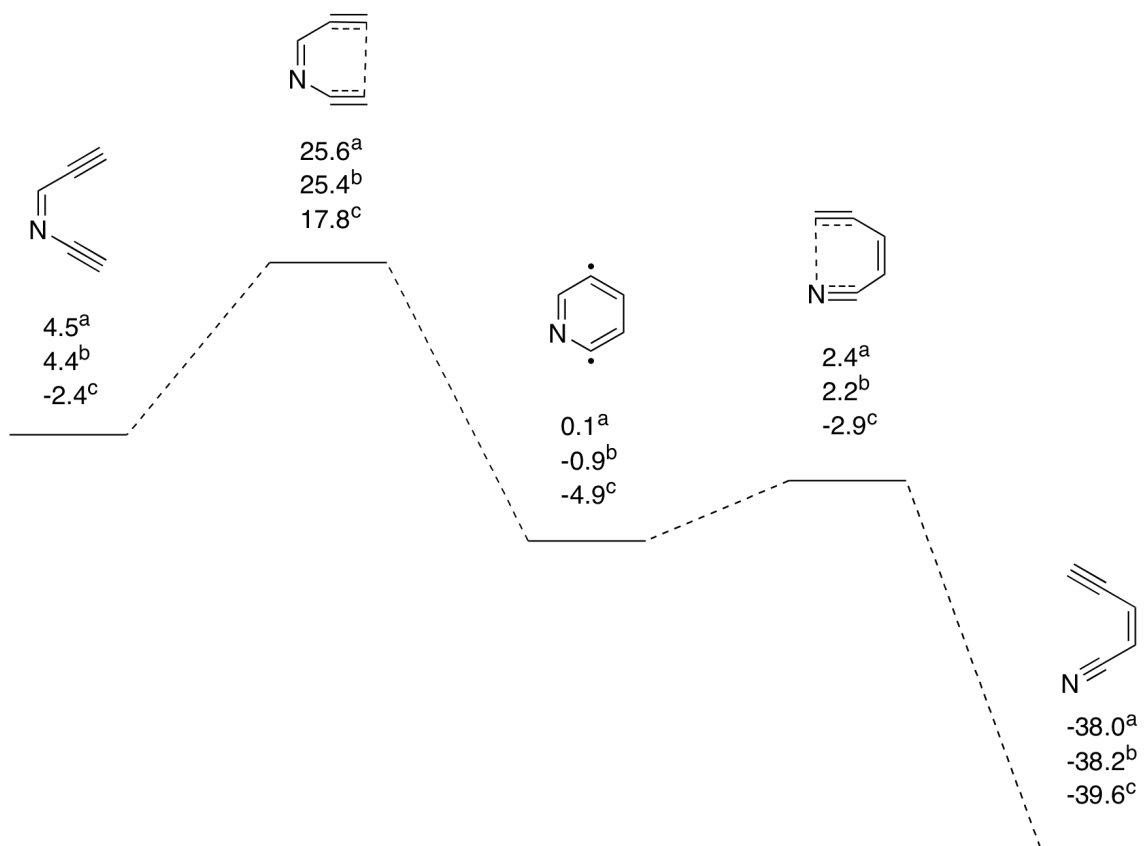


Figure 3.1. Calculated energy for aza-Bergman and retro-aza-Bergman<sup>a</sup> BCCD(T)/cc-pVTZ/(U)BLYP/cc-pVTZ level of theory <sup>b</sup>CCSD(T)/cc-pVTZ/(U)BLYP/cc-pVTZ level of theory <sup>c</sup>(U)BLYP/cc-pVTZ)T level of theory<sup>8</sup>

Table 3.1. Computational estimates for energies of Bergman cyclization<sup>3</sup>

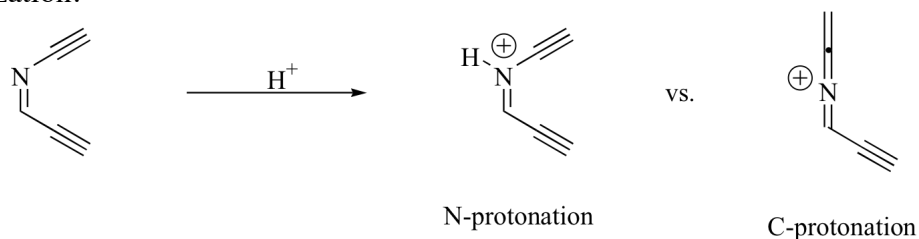
Reaction	Level of Theory	$\Delta H^\ddagger$	Intermediate Diradical	$\Delta H^\ddagger$ for retro-Bergman	$\Delta H$ for retro-Bergman
Bergman	CASSCF(6x6)/6-31G*	39.8	10.0	39.8	-
	CASMP2(6x6)/6-31G*	34.8	-0.7	34.8	-

Aza-	CASSCF(6x6) /6-31G*	33.2	0.5	7.3	-49.0
Bergman	CASMP2(6x6)/6-31G*	27.7	12.1	10.7	-32.6
Protonated	CASSCF(6x6) /6-31G*	32.5	2.1	22.5	-28.3
Aza-	CASMP2(6x6)/6-31G*	29.1	-11.8	28.6	-16.9
Bergman					

Interestingly, calculations suggest that an aza-Bergman cyclization where the nitrogen of the ene-diyne is protonated would have a similar activation barrier to form the diradical but a much higher activation barrier for the retro-Bergman (Table 3.1). In the case of the Bergman cyclization, the cyclization and retro-cyclization are degenerate cases, so the overall  $\Delta H$  and activation barriers are equal. In the case of the aza-Bergman cyclizations, the  $\beta$ -alkynylacrylonitrile is significantly lower in energy, so raising the activation energy for the cyclization should slow the reaction, possibly allowing trapping of the diradical intermediate.

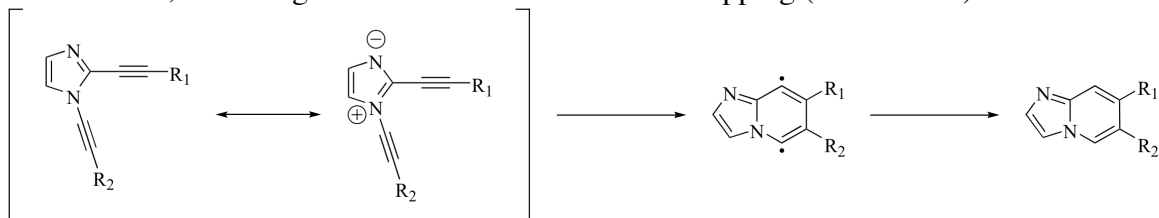
There are two possible sites of protonation on an aza-enediyne. The computations shown in Table 3.1 place the position of protonation of the enediyne at the nitrogen, not at the ynamine carbon, which is the more thermodynamically favored position (Scheme 3.5). The energy required for protonation is determined computationally to be +2.5 kcal/mol as compared to the neutral imine of formaldehyde as a reference molecule.<sup>9</sup> Also, protonation at N is predicted to perturb bond lengths, shortening the N-C single bond by 0.036 Å and lengthening the C-C triple bond  $\alpha,\beta$  to the imine by 0.021 Å.<sup>9</sup> This perturbation of bond lengths implies that conjugation of the system increases upon protonation at N.<sup>9</sup> Cremer *et al.* also note that the positive charge on N resulting from

protonation can be localized through the conjugated  $\pi$  system, which contributes to its stabilization.<sup>9,10</sup>



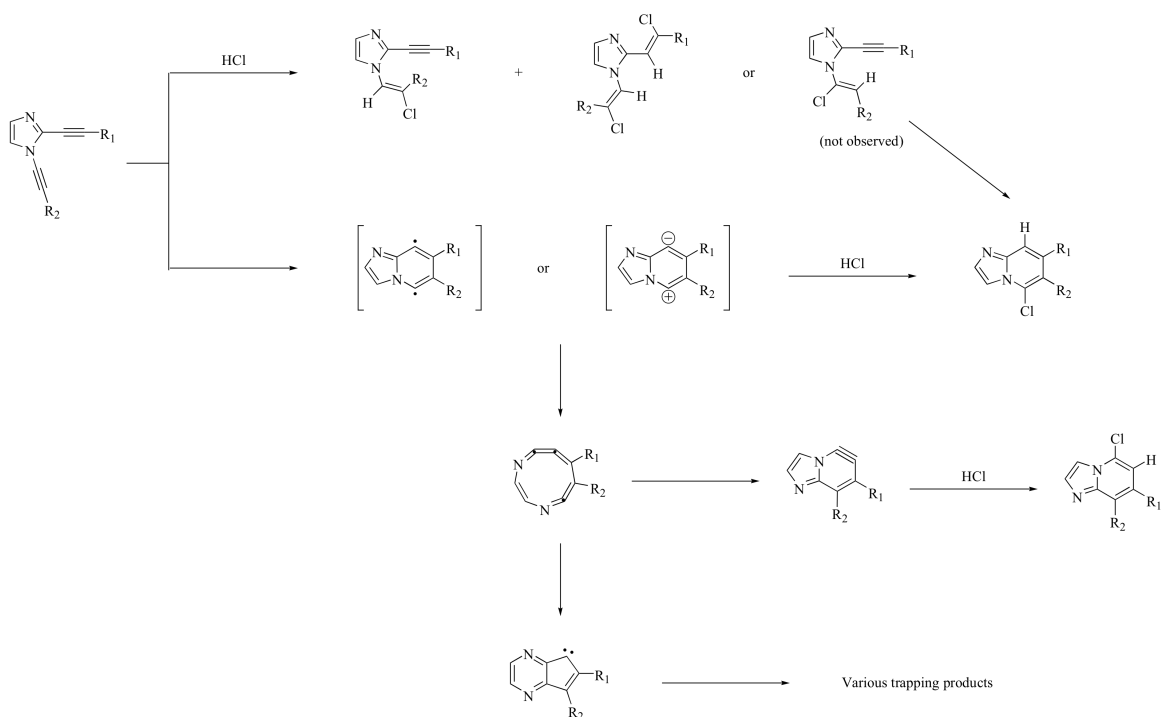
Scheme 3.5. Position of protonation of aza-enediyne

Kerwin *et al.* subsequently reported attempts to perform an aza-Bergman cyclization of a dialkynylimidazole.<sup>11</sup> This system had two advantages compared to the original acyclic system. First, the imidazole ring should prevent the retro-aza-Bergman cyclization, because the  $\beta$ -alkynyl acrylonitrile cannot form. Second, this system might act as a protonated aza-enediyne, which would lower the energy of the proposed diradical intermediate, extending its lifetime to allow efficient trapping (Scheme 3.6).



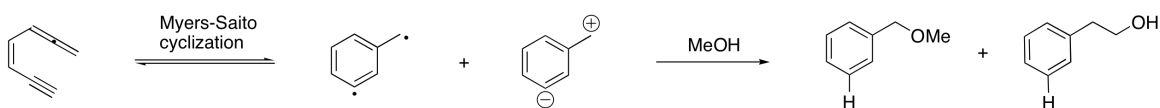
Scheme 3.6. Attempt to mimic a protonated aza-Bergman cyclization.

Unfortunately, this system led to many isolated products under differing reaction conditions.<sup>12,13</sup> It is possible that the aza-Bergman cyclization does occur, but the mechanism for formation of the observed products could not be unambiguously determined. The authors propose the pathways outlined in Scheme 3.7 as possible routes to the observed products.<sup>12</sup>



Scheme 3.7. Proposed mechanistic pathway for products observed in thermolysis of dialkynylimidazoles.<sup>12</sup>

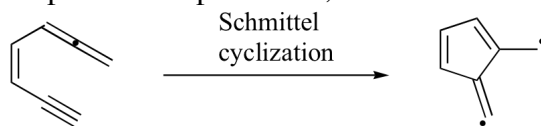
Kerwin and coworkers also explored an alternative diradical-generating cyclization by which “skipped” azaenediynes might modify DNA. Myers and Saito contemporaneously reported a cyclization of enyne-allenes to generate  $\alpha,3$ -dehydrotoluene (Scheme 3.8).<sup>14,15</sup> The trapping of the purported intermediate has been interpreted to imply presence of either a diradical or zwitterionic intermediate.<sup>16,17</sup> In a similar manner to the aza-enediyne cyclizations, Kerwin *et al.* used a propargylic imine (termed a “skipped aza-enydiyne” because of the methylene that disrupts conjugation),<sup>18</sup> which they theorized could generate an enyne-allene under appropriate reaction conditions. They hoped that this aza-enyne-allene could undergo an aza-Myers-Saito cyclization to generate a  $\alpha,3$ -diradical dehydrotoluene.



Scheme 3.8. Myers-Saito cyclization

Experimental data show that the activation energy from the reactive conformer to the  $\alpha,3$ -dehydrotoluene diradical is  $21.8 \pm 0.5$  kcal/mol.<sup>19</sup> The overall  $\Delta G$  for the transformation from the reactive conformer is -19 kcal/mol. Computations at varying levels of theory show activation energies ( $\Delta G^\ddagger$ ) ranging from 20-29 kcal/mol and the overall  $\Delta G$  from 4 to -60 kcal/mol, with most results falling between -8 to -15.<sup>19</sup>

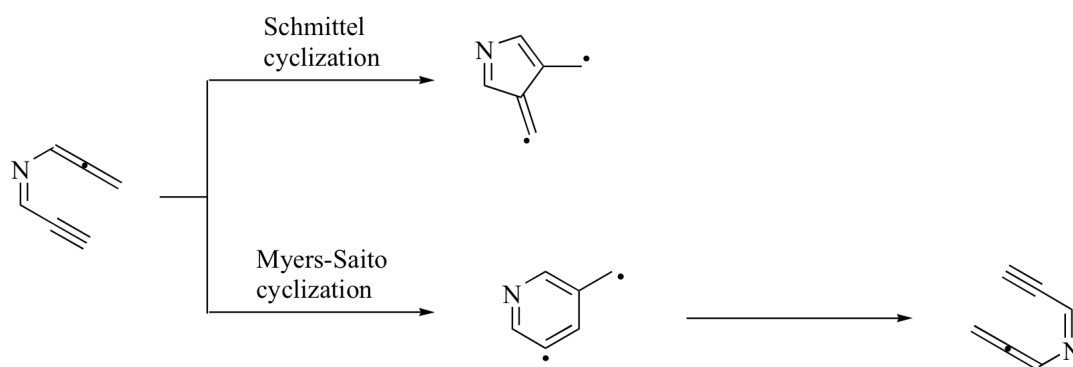
Schmittel *et al.* report a variation on the Myers-Saito cyclization where a fulvene diradical is formed from the enyne-allene in a 2,6-diradical cyclization (Scheme 3.9).<sup>20</sup> Evidence for diradical generation has been observed in studies on electronic effects of substituents,<sup>20</sup> kinetic isotope effect experiments,<sup>21</sup> and use of radical clocks.<sup>22</sup>



Scheme 3.9. Schmittel cyclization

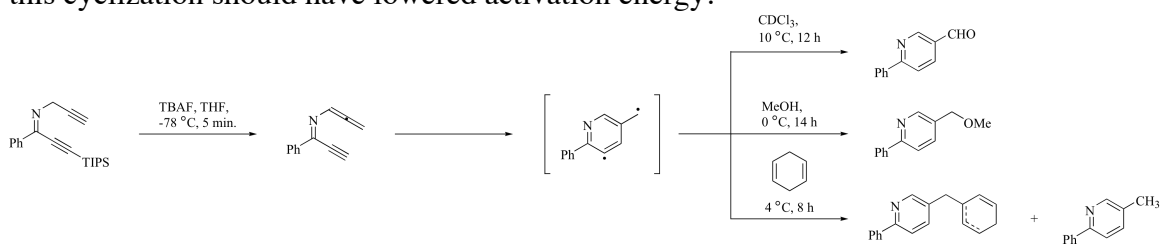
Computations at the (U)B3LYP/6-31G\* level of theory suggest that the aza-Myers cyclization has a lower activation energy and is slightly more exothermic than the corresponding Schmittel cyclization (Scheme 3.10).<sup>18</sup> Kerwin *et al.* synthesized a skipped aza-enediyne that they envisioned isomerizing to the aza-enyneallene and undergoing either an aza-Schmittel or an aza-Myers Saito cyclization.<sup>18</sup> Experimentally, the synthetic skipped aza-enediyne generate products that likely derive from trapping of a 2,6-didehydropicoline diradical (Scheme 3.11).<sup>18</sup>





Scheme 3.10. Aza-Schmittel and Aza-Myers-Saito

The resonances for the proposed allene intermediate were observed by  $^1\text{H}$  and  $^{13}\text{C}$  NMR.<sup>18</sup> Products of trapping were observed at low temperatures. The half-life for a traditional Myers-Saito cyclization is 20.5 h at 39 °C,<sup>14</sup> whereas the aza-variant readily proceeds at low temperatures, which correlates with the computed values suggesting that this cyclization should have lowered activation energy.<sup>18</sup>



Scheme 3.11. Trapping products of an aza-Myers-Saito cyclization<sup>18</sup>

### 3.1.3. Biological Activity of Azaenediynes

Research in the Kerwin group has focused on synthesizing and evaluating compounds designed to undergo aza-variants of these diradical-generating reactions using both acyclic<sup>6,7,18</sup> and cyclic<sup>11,23,24</sup> backbones to induce DNA damage.<sup>24-26</sup> Possible mechanisms for DNA damage (Scheme 3.12) include isomerization of a propargylic benzimidazole to the imine-allene followed by aza-Bergman or aza-Schmittel cyclization to generate the diradical. Alternatively, it is possible that simple electrophilic covalent

adduction might occur. One series that showed promise for its ability to induce DNA damage consistent with a radical process is a series of skipped dialkynyl pyridinium compounds (Figure 3.2).<sup>23</sup>The effective concentrations (Table 3.2) were determined by the nicking assay described in Section 1.3.4.1.

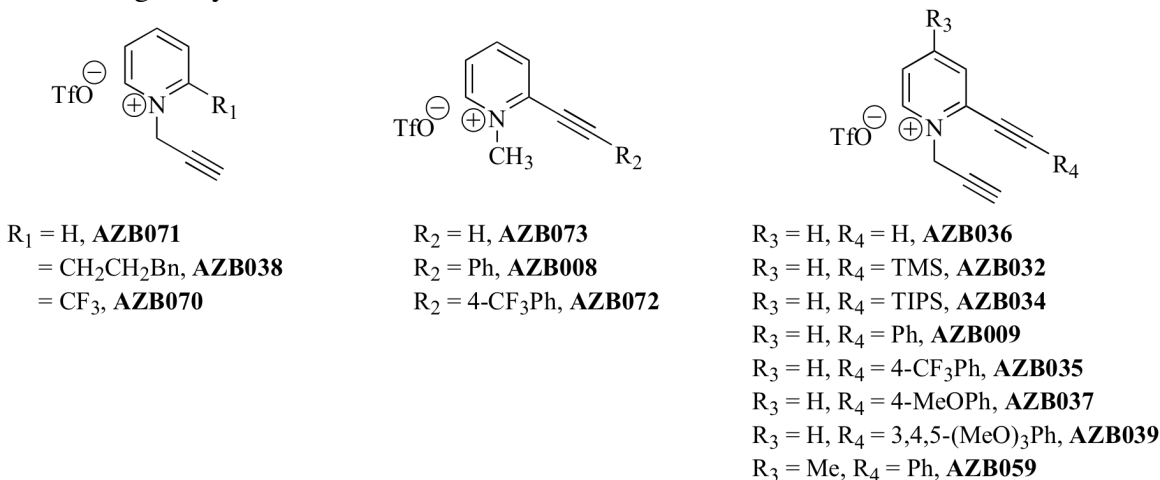


Figure 3.2. Pyridinium skipped aza-enediyne library<sup>27</sup>

Table 3.2.  $\text{EC}_{25}$  for pyridinium skipped aza-enediyne<sup>27</sup>

Compound Number	$\text{EC}_{25}$ ( $\mu\text{M}$ ) at pH 7	$\text{EC}_{25}$ ( $\mu\text{M}$ ) at pH 8
<b>AZB032</b>	4.6±1.5	9.8±2.3
<b>AZB034</b>	23.0±5.2	23.5±6.5
<b>AZB009</b>	15.5±1.5	10.5±1.5
<b>AZB035</b>	21.5±8.5	11.5±1.5
<b>AZB037</b>	6.8±1.7	1.8±1.0
<b>AZB039</b>	28.0±3.0	16.1±1.2
<b>AZB059</b>	16.5±0.5	6.5±0.2
<b>AZB073</b>	37.8±5.2	39.0±3.0
<b>AZB008</b>	>100	>100

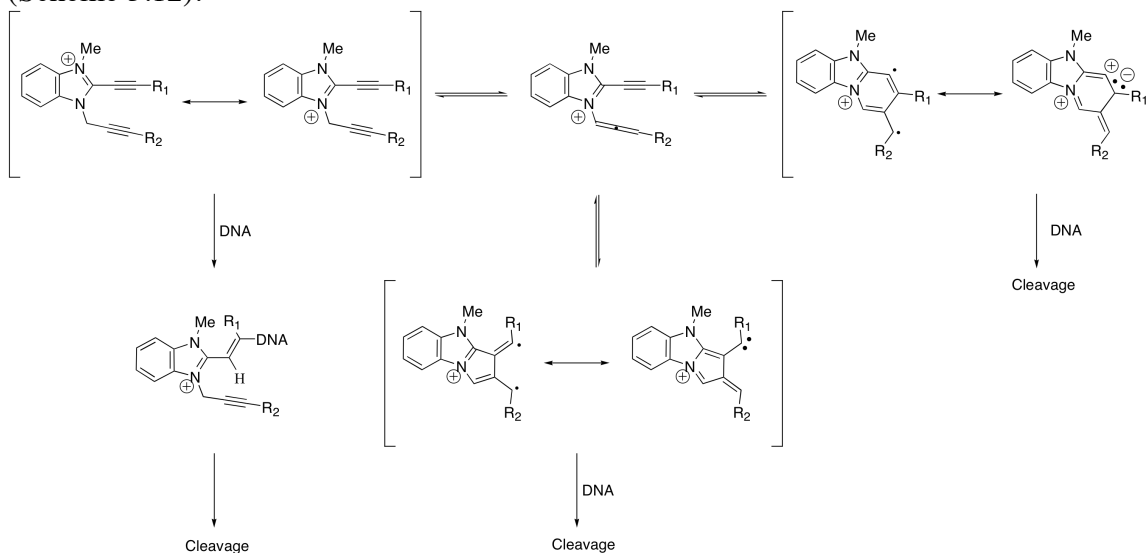
<b>AZB072</b>	>100	>100
<b>AZB071</b>	nd <sup>a</sup>	>100
<b>AZB070</b>	39.5±3.5	44.3±7.3
<b>AZB038</b>	>100	>100
<b>AZB059</b>	39.5±3.5	44.3±7.3

<sup>a</sup> nd = not determined

Comparison of **AZB009**, **035**, and **037** shows a small electronic effect on nicking (Table 3.2), but the effect is not continued through compound **AZB039**, which has 3,4,5-trimethoxy substitution.<sup>23</sup> The most electron-poor pyridinium (**AZB035**) appears to display the least DNA nicking ability. Compounds with both alkyne arms perform better at nicking than compounds where one arm is missing, although the N-propargyl appears to be more important for activity than the 2-alkynyl substituent. Adding a reductant, dithiothreitol, to the nicking reactions, inhibited DNA nicking by **AZB037**.<sup>23</sup> This dialkynyl pyridinium also showed pH dependence, with cleavage increasing as pH increased.<sup>23</sup> Changing the reaction pH from 7 to 8 (in 10 mM Tris buffer) caused a 3.8-fold increase in nicking. The authors propose that the reactive species involves isomerization to the aza-enyneallene, which can be facilitated by base.<sup>23</sup> More detailed studies showed that **AZB037** causes DNA damage by two modes of reactivity.<sup>23</sup> First, the dialkynylpyridinium was oxidizing guanosines to cause base-selective cleavage.<sup>23</sup> Second, **AZB037** was causing frank strand breaks by abstraction of hydrogen atoms from the ribose units at either C4' or C5'.

Another system of skipped aza-enediynes reported by Kerwin *et al.* that showed promising biological activity is a series of benzimidazolium and benzothiazolium compounds. These compounds might cause damage *via* generation of a reactive diradical

species, but they could also simply serve as an electrophilic trap for a nucleotide base (Scheme 3.12).



Scheme 3.12. Possible modes of DNA modification by propargyl alkynebenzimidazolium **AZB017**

The DNA cleavage ability of the propargyl alkynebenzothiazolium triflate and tetrafluoroborate compounds (Figure 3.3) was evaluated in a nicking assay on supercoiled DNA,  $\phi$ X174. The supercoiled DNA showed varying degrees of cleavage to the relaxed form (Form II) at 100  $\mu$ M concentrations of the compounds.<sup>24</sup>

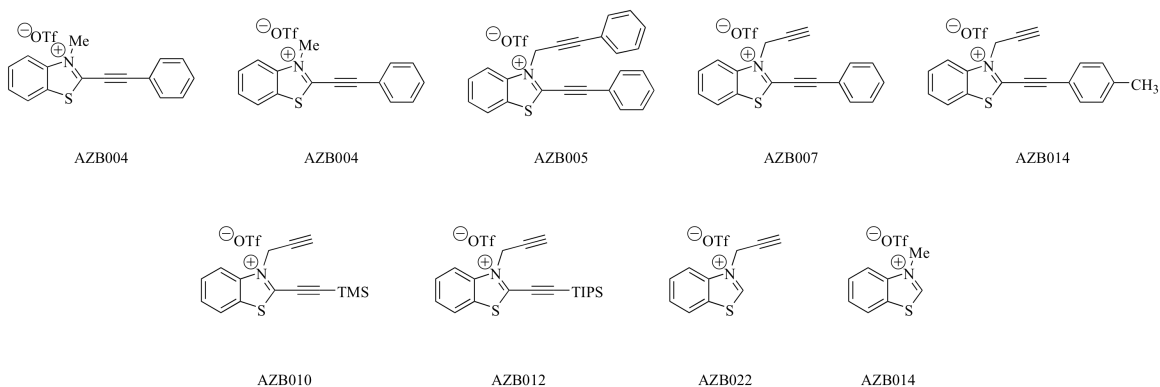


Figure 3.3. Propargyl alkynebenzothiazolium salts and relevant control compounds

Table 3.3. Nicking ability of benzothiazolium salts at 100  $\mu\text{M}$ <sup>24</sup>

Compound	% nicking at pH 8	% nicking at pH 9
<b>AZB007</b>	30 $\pm$ 19	40 $\pm$ 13
<b>AZB014</b>	33 $\pm$ 18	42 $\pm$ 1
<b>AZB010</b>	20 $\pm$ 4	33 $\pm$ 5
<b>AZB012</b>	7 $\pm$ 4	7 $\pm$ 1
<b>AZB004</b>	39 $\pm$ 15	48 $\pm$ 15
<b>AZB014</b>	2.7 $\pm$ 0.7	Not determined
<b>AZB022</b>	16 $\pm$ 0.2	Not determined

Neutral benzimidazole **AZB001** did not show DNA cleavage, nor did **AZB006**, which contains only one alkyne; however, **AZB002** showed complete DNA nicking (exclusively Form I) at 1 mM (Table 3.3).<sup>26</sup> The benzimidazolium triflate and tetrafluoroborate compounds showed similar DNA nicking ability (Table 3.4), implying that changing the noncoordinating counterion does not change the activity of the compound.

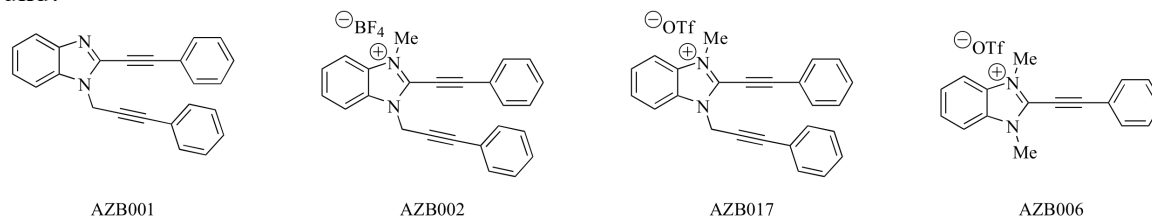


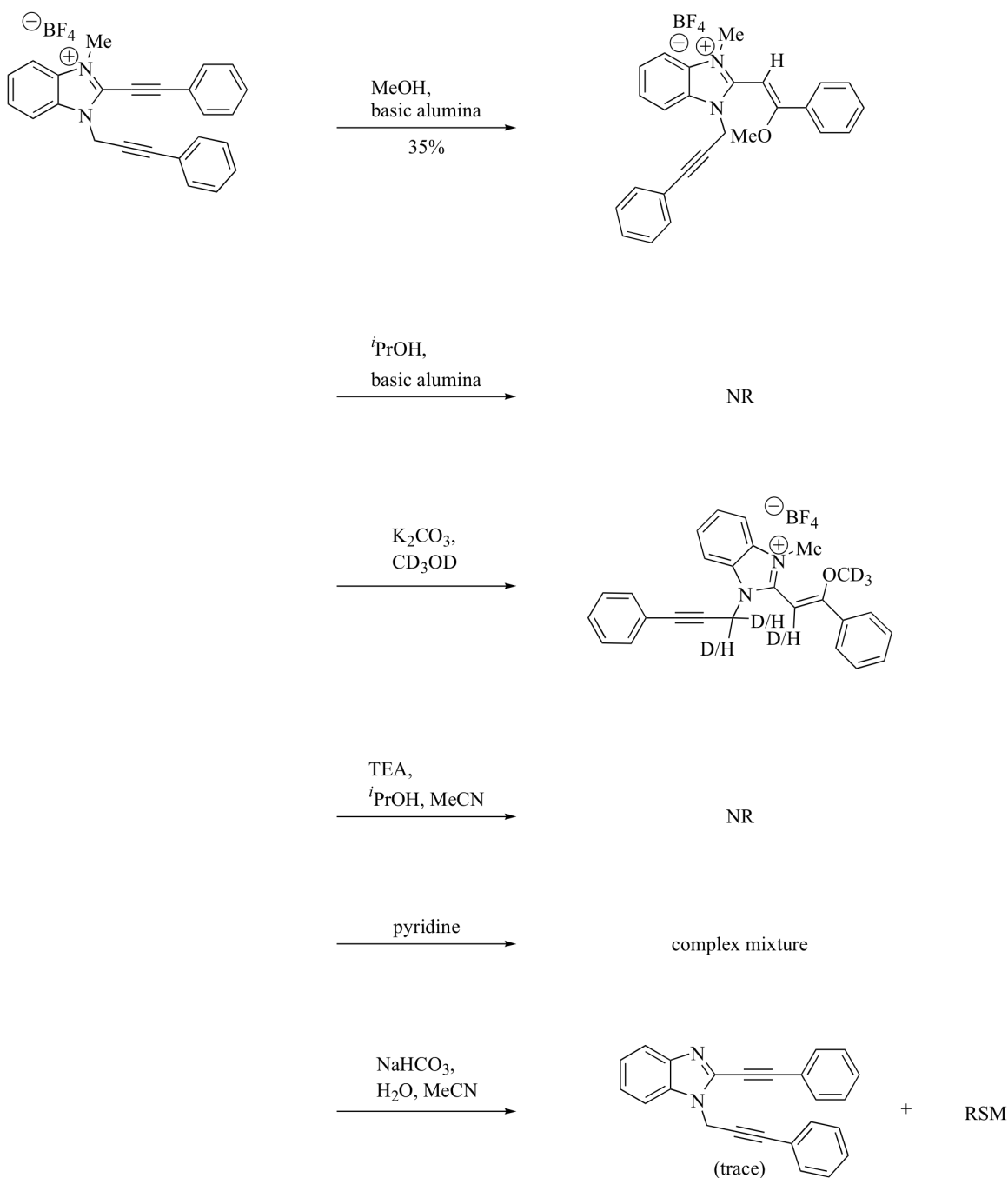
Figure 3.4. Benzimidazole compounds used in nicking assay

Table 3.4. Nicking ability of benzimidazolium salts

Compound	% Nicking at 100 $\mu\text{M}$	% Nicking at 1 mM
<b>AZB001</b>	0	0

<b>AZB002</b>	30	96
<b>AZB017</b>	33	100
<b>AZB006</b>	0	4.5

In order to determine what sort of DNA modification might be occurring (a radical process leading to H-atom abstraction, or simple electrophilic trapping), **AZB017** was combined with various nucleophiles (Scheme 3.13).<sup>26,28</sup> A deuterium-exchange reaction shows that to deprotonate the propargylic position and facilitate isomerization to the aza-enyneallene, stronger bases (i.e.  $K_2CO_3$ ) are required, whereas  $NaHCO_3$  in MeOH shows no nucleophilic addition and only trace conversion to the neutral benzimidazole.<sup>26</sup> Methanol over basic alumina was the only nucleophile that showed nucleophilic trapping.<sup>26</sup> The fact that higher pH is required for deuterium-exchange to form the proposed allene and that simple 1,4-addition does not require high pH is consistent with both proposed mechanisms for DNA adduction.



Scheme 3.13. Possible outcomes of benzimidazolium with various nucleophiles

Kerwin and Brodbelt *et al.* performed ESI-MS analysis on incubations of **AZB017** with short oligomers.<sup>29</sup> They report that **AZB017** covalently modifies cytosines,

as evidenced by observation of a DNA+**AZB017** peak for the oligomer dCT<sub>5</sub> at pH 6 or 8.<sup>29</sup> It appeared that C-adduction occurs more readily at pH 6 than at pH 8. When an oligomer without cytosine (dT<sub>6</sub>) was used, loss of mass corresponding to **AZB017** was observed when the oligomer was subjected to CAD (collision-activated dissociation), implying that there was no covalent interaction, merely an association.<sup>29</sup> This interaction might be due to electrostatic attraction between the anionic phosphate backbone and the cationic benzimidazolium ring.

These skipped dialkynyl heteroaryl compounds have shown an interesting ability to modify DNA in a range of mechanisms with varying sequence selectivity. We hoped to harness this novel reactivity to target a post-transcriptional DNA modification, methylated cytosines.

### **3.1.4. DNA Methylation**

#### ***3.1.4.1. Occurrence of Cytosine Methylation in Biological Systems***

More than 50 years after the elucidation of the structure of DNA, the epigenome is becoming a focus of research. The epigenome consists of chromatin and its modifications, both to its associated proteins and the DNA bases themselves.<sup>30,31</sup> The epigenome is responsible for regulation of the genome and has been found to be variable in an organism both throughout cell types and over time.<sup>32</sup> While chromatin protein modifications are common, modifications to DNA bases are relatively rare. One such modification of the bases of DNA, found in vertebrates,<sup>33</sup> is the covalent modification of cytosine by addition of a methyl group at the 5 position of cytosines at CpG intervals.<sup>34</sup> In mammalian cells, 3% to 5% of cytosines are methylated, depending on the cell type and growth stage.<sup>35</sup>



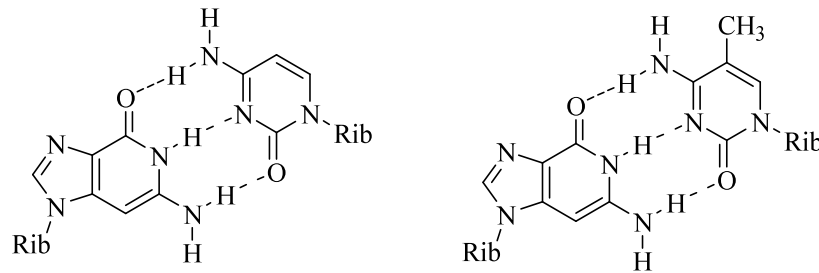


Figure 3.5. G-C base pair with unmodified cytosine (left) and 5-methylcytosine

Until the recent discovery of a DNA demethylase,<sup>36</sup> DNA methylation had been considered to be an irreversible process, whereby DNA is methylated according to a pattern predetermined during development and maintained through life. Newer research suggests that DNA methylation is dynamic, with DNA methyl transferase enzymes catalyzing transfer of a methyl group from a methyl donor, S-adenosyl methionine, to the 5-position of cytosine<sup>35,37,38</sup> and demethylases catalyzing removal of methyl groups from cytosine residues.<sup>36</sup> While primary DNA sequence fidelity in mammals is over 99.999%, methylation patterns are reproduced with only 96-99% fidelity.<sup>39</sup> DNA methylation occurs following transcription at CpG sites. In addition to being likely promoters of mutagenesis, methylated bases can also influence adduct formation by exogenous carcinogens.<sup>40</sup> Mutations, permanent changes in the nucleotide sequence of DNA, lead to lowered fidelity in DNA replication and can be classified as either silent (having little or no observed effect on gene function), advantageous (which is rare), or deleterious.<sup>41</sup>

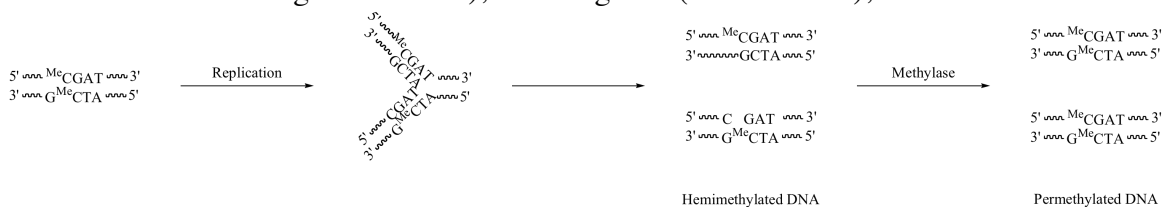


Figure 3.6. DNA methylation following replication<sup>41</sup>

DNA methylation patterns are linked to cancer in two ways: hypermethylation of tumor suppressor genes and global hypomethylation of cancer cells.<sup>42,43</sup> DNA hypermethylation at tumor suppressor genes silences genes in the same way as deletions or mutations, changing their expression or function.<sup>44</sup> CpG methylation profiles are correlated not only with different types of cancer<sup>45-47</sup> but also with staging of cancers and response to chemotherapy.<sup>42,45,48-50</sup>

#### ***3.1.4.2. Effects of 5-Methylcytosine on Adduct Formation***

It is well-established that cytosine methylation affects position and frequency of adduct formation (mutations).<sup>51</sup> This effect appears to depend on the size of the carcinogen and mechanism of adduction. Studies by Waring *et al.* show that methylation has a dramatic effect on DNA binding by intercalators.<sup>52</sup> DNase footprints of daunomycin and other known intercalators were compared using DNA containing methylated cytosines to DNA containing unmodified cytosines, uracils, or methylated uracils were compared. The methylated cytosines and uracils showed a previously unobserved footprint, or region of decreased cleavage, indicating that a new binding site was created (See Section 1.3.3).<sup>52</sup> They propose that the change can be explained by changes in local structure, possibly a narrowing of the minor groove or a change in curvature. It has been shown by X-ray crystallography that the minor groove of DNA rich in 5-methyl cytosine has geometry resembling AT-rich DNA, not GC-rich.<sup>53</sup> Additionally, Waring *et al.* note that the methylation at cytosine should reduce the dipole moment of the GC base pair.<sup>52</sup>

Effects of cytosine methylation have been studied on covalent DNA-drug interactions as well. Flanking methyl cytosines (MeCs) at CpG mutational hotspots on tumor suppressor gene p53 enhance the reactivity of guanine with benzo[ $\alpha$ ]pyrenediol

epoxides (BDPEs).<sup>54</sup> In unmethylated regions of p53, the BDPE acts as a minor groove binder, whereas in methylated systems, the conformational changes caused by the additional methyl group cause BDPE to act as an intercalator, affecting covalent modification of the DNA. It has been shown that BDPEs preferentially form covalent adducts at methylated CpG sites corresponding to mutational hotspots on p53.<sup>55</sup> In smoking-related lung cancers, p53 mutations are concentrated at methylated CpG sites, including codons 157, 158, 175, 245, 248, 273, and 282.<sup>56</sup> Lung cancer shows a characteristic and unusual mutation where 40% of the total mutations are G→T transversions (commonly found at codon 157).<sup>40</sup> Such a mutation is unusual because unlike G→A mutations (transitions), transversions involve replacement of a purine base with a pyrimidine base, but only 9% of mutations in lung cancer involve a transition.<sup>40</sup> *N*-Hydroxyl-4-aminobiphenyl has been shown to preferentially bind two hotspots on p53 at codons 175 and 248 only after the CpG sites are methylated.<sup>57</sup> Additionally, acrolein exhibits enhanced adduct formation at guanines complementary to methylated sites on exons 5 and 7 of p53 in a way that mimics mutational hotspots.<sup>51</sup> In a similar study, Shank and coworkers used aflatoxin B<sub>1</sub>-8,9-epoxide as a probe to analyze effects of cytosine methylation on adduct formation.<sup>58</sup> They did not observe increased adduct formation at guanines next to a MeC (either 5' or 3') in either a short 11-mer which contained one MeC site or a longer oligomer (a restriction fragment of the regulatory *HRPT* gene).<sup>58</sup>

In non-small cell lung carcinoma, an unusually high number of non-CpG residues in GC rich regions are methylated.<sup>59</sup> However, a report from Tretyakova *et al.* shows that methylation at cytosine has a protective effect on adduct formation at both the N7 or O<sup>6</sup> position of neighboring guanines, showing a 17-27% reduction on N7 adducts and a 65-75% reduction on O<sup>6</sup> adducts.<sup>60</sup> The overall effects of methylation on DNA damage

remain unclear; some carcinogens form adducts with greater facility adjacent to methylated cytosines and some do not.

In summary, the overall effects of methylation on adduct formation are unclear. Research involving adduct formation at these sites might be able to resolve issues involving carcinogenesis (e.g. genetic predisposition) and develop new therapeutic regimens which target these genes with unusual methylation status.

### **3.2. PROPOSED RESEARCH: SELECTIVE TARGETING OF UNMETHYLATED CYTOSINES IN PRESENCE OF METHYLATED CYTOSINES**

Selectively targeting cytosines in presence of methylated cytosines might provide a more selective class of antineoplastic agents, given the hypomethylation found in cancer cells. We hoped to design compounds that would selectively modify unmethylated cytosines in presence of methylated cytosines. We planned to screen compounds that might exploit this difference by assaying their adduction to synthetic DNA, which allows incorporation of a methylated cytosine consistently at each CpG position. If any compounds showed promising selectivity, we planned to synthesize a small library to try to improve selectivity and activity.

#### **3.2.1. Kinetics**

Reaction of the radiolabeled DNA with the substituted electrophile should follow pseudo-first order kinetics. The concentration of labeled DNA will be very low (mid nM range) compared to the electrophile (mM range). Bimolecular ( $S_N2$ ) reactions proceed with second order kinetics, with the following rate equation:<sup>61</sup>

$$K = k[Nucleophile][Electrophile] = \frac{d[Nucleophile]}{dt} = -\frac{d[Electrophile]}{dt}$$

For this work, the DNA serves as the nucleophile, and a small molecule (“Drug”) will be the electrophile, so

$$K=k[\text{DNA}][\text{Drug}]$$

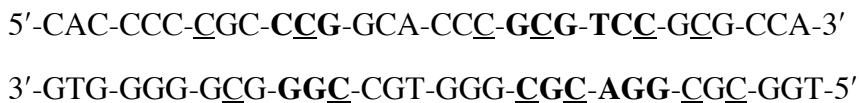
But if the relative concentration of drug is unchanging with respect to DNA concentration, the rate law can be simplified to<sup>62</sup>

$$K=k_{\text{obs}}[\text{DNA}]$$

Also, for this experiment, “single-hit kinetics” is required. Because adduct formation is being analyzed using cleavage of radiolabeled DNA, multiple adductions will not be observed; only cleavage caused by adducts formed nearest to the 5' <sup>32</sup>P label can be observed and quantified.

### 3.2.2. DNA Sequence Selection

The DNA sequence we wanted to examine was a part of exon5 (codons 150-160) of the p53 tumor suppressor gene. Damage at codons 154, 157, and 158 (bold) are correlated with lung cancer.<sup>56,63</sup> The sequence is as follows (underlined Cs are methylation sites):



#### 3.2.2.1. 11-mer Sequence

We planned to generate the desired sequence, with appropriate methylation status, using an automated DNA synthesizer. In designing an oligomer to use as a model system,

a segment of exon 5 of the p53 gene was used. The first oligomers synthesized were a G-C rich 11 base oligomer and its complement.

5'-CCGCGTCCGCG-3'

3'-GGCGCAGGCGC-5'

This oligomer contains 8 CpG intervals (underlined), each of which would be methylated *in vivo*. For ease of ESI-MS analysis, multiple oligomers were synthesized, each with a single methyl cytosine (<sup>Me</sup>C) at a different CpG step. The cytosines close to the end of each strand were not modified because of concerns about “end effects,” in which the ends of each strand are not properly annealed. Each helical turn contains about 10 bases, so the ends of such a short oligomer might show significant denaturation (fraying).

The radiolabelled DNA and its unlabelled complement were annealed in 0.1 M sodium phosphate and analyzed by ESI-MS and non-denaturing gel. ESI-MS showed fully annealed duplex, but the gel showed no annealed DNA. The working concentrations (5 mM for ESI-MS, low nM for radiolabelling work) are very different, which may explain the problems annealing. Figure 3.7 shows a non-denaturing gel that shows no difference between single-stranded labeled DNA and DNA that had been heated and cooled with its complement. The predicted melting temperature of this oligomer was 91.1 °C at 5 mM (in presence of 0.5 M Na<sup>+</sup>) and 50.5 °C at 1 nM (with 0.5 M Na<sup>+</sup>). Under conditions similar to the DNA-drug incubations, 1 nM DNA and 10 mM Na<sup>+</sup>, the predicted T<sub>m</sub> is 31.1 °C. For incubations at 37 °C, the DNA would not be properly annealed.<sup>2</sup> Because the initial ESI-MS work showed complete duplex formation, the annealing was analyzed by gel electrophoresis using non-denaturing PAGE (Figure 3.7).

---

<sup>2</sup> T<sub>m</sub> estimated using OligoAnalyzer 3.1 from IDT (Integrated DNA Technologies), available online at [www.idtdna.com](http://www.idtdna.com). Error is ±1.4 °C.

Unfortunately, complete annealing was not observed under any conditions, and the duration of the electrophoresis did not appear to affect the outcome (Figure 3.7).

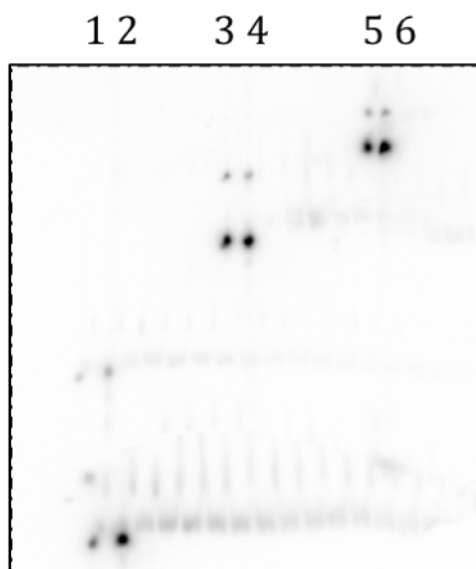


Figure 3.7. Non-denaturing PAGE analysis of annealing of 12-mer.

Lane 1: ss-oligomer, run 6 h; Lane 2: Attempt at annealing, run 6 h; Lane 3: ss-oligomer, run 3 h; Lane 4: Attempt at annealing, run 3 h; Lane 5: ss-oligomer, run 1.5 h; Lane 6: Attempt at annealing, run 1.5 h.

#### **3.2.2.2. *Second DNA Sequence***

To improve annealing by raising temperature at which the oligomer denatures ( $T_m$ ), a 22-mer was synthesized. It includes a repeat of the original 11-mer sequence. Two upper strands were synthesized, one that was unmethylated at both the 5' repeat and the 3' repeat, and one where the 5' repeat was methylated at all CpG steps. The complement was unmethylated at the 5' end and permethylated at the 3' end (at CpG steps as read 5' to 3'). An advantage to this system is that it is possible to have both an internal control (the

unmethylated half of the sequence) and both hemimethylated and bismethylated duplexes at the 5' end of the sequence (with respect to the upper strand).

**Unmethylated upper sequence**

5'-CCGCGTCCGCGCCGCGTCCGCG-3'

3'-GGC<sup>Me</sup>G<sup>Me</sup>CAGG<sup>Me</sup>CG<sup>Me</sup>C GGC GCAGGCGC-5'

**Methylated upper sequence**

5'-C<sup>Me</sup>CG<sup>Me</sup>CGTC<sup>Me</sup>CG<sup>Me</sup>CGCCGCGTCCGCG-3'

3'-GGC<sup>Me</sup>G<sup>Me</sup>CAGG<sup>Me</sup>CG<sup>Me</sup>CGGC GCAGGCGC-5'

The predicted  $T_m$  of this duplex is 73.6 °C at 1 nM DNA in the presence of 0.1 mM Na<sup>+</sup>, and it increases to 79.9 °C in the presence of 1 M Na<sup>+</sup>.<sup>3</sup> This DNA, which contains 90.9% by mass GC content, annealed fully using 1X TE (10 mM Tris, 1 mM EDTA) with 0.5 M NaCl (Figure 3.8).

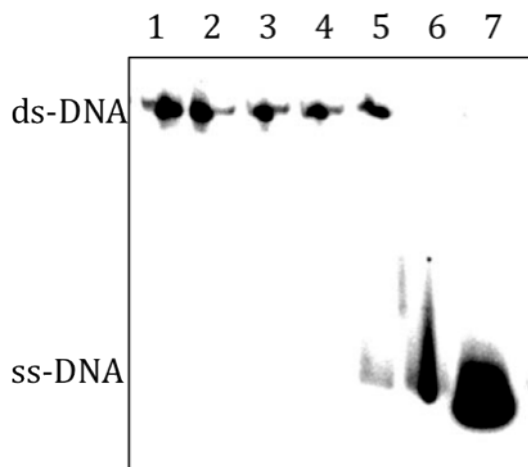


Figure 3.8. Annealing of 22-mer.

<sup>3</sup>  $T_m$  estimated using OligoAnalyzer 3.1 from IDT (Integrated DNA Technologies), available online at [www.idtdna.com](http://www.idtdna.com). Error is  $\pm 1.4$  °C.



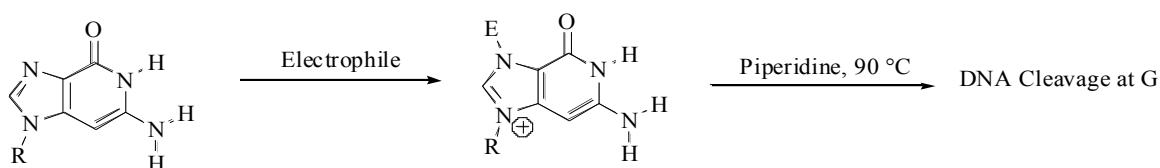
Lane 1: Annealed methylated 22-mer using 1X TE, 0.5 M NaCl; Lane 2: Annealed 22-mer using 1X TE; 0.5 M NaCl; Lane 3: Annealed methylated 22-mer using 1X TE; Lane 4: Partially annealed unmethylated 22-mer using 1X TE; Lane 5: Single-stranded methylated 22-mer; Lane 6: single-stranded unmethylated 22-mer.

### **3.2.3. Small Molecule-DNA Interactions**

With a suitable duplex in hand, we began to screen small molecules for their potential to modify methylated DNA differently than unmethylated DNA. The DNA was labeled at the 5' end by polynucleotide kinase, which removes the labeled phosphate from [ $\gamma$ - $^{32}\text{P}$ ]-ATP (adenosine triphosphate) and adds it to the 5'-hydroxyl group of the synthetic oligomer.<sup>64</sup> This labeled oligomer was then PAGE-purified to remove excess  $^{32}\text{P}$ -ATP and short, labeled oligomers (fail sequences from DNA synthesis). The purified oligomer was then annealed to its complement and incubated with an electrophile. There are several ways to analyze the position of adduct formation (See Section 1.3), but piperidine/heat treatment was chosen because it is operationally the most simple. It cleaves the phosphate backbone of the DNA, allowing mapping of modification based on the fragmentation pattern. The pattern of fragmentation can then be compared to results from Maxam-Gilbert sequencing, a series of base-specific reactions (Section 1.2).<sup>65</sup> Radiolabeling uses very small quantities of DNA (pmols) and affords excellent sensitivity.

#### **3.2.3.1. Guanosine-Selective Alkylating Agents**

N7 modifications on guanosines lead to enhanced cleavage under piperidine-heat treatment (Scheme 3.14, also Section 1.3.1). Other modifications may or may not lead to cleavage of the phosphate backbone.



Scheme 3.14. Modification of guanosine N7, followed by piperidine/heat treatment

After optimizing a model oligomer system, we began our search for compounds that would differentially modify DNA containing methylated and unmethylated cytosines using compounds that could easily be modified electronically. Styrene oxide is known to modify guanosines at N7 (as well as other positions depending on conditions and substituents on the aromatic ring).<sup>66,67</sup> Benzyl bromide is an effective alkylating agent, with many analogs commercially available. Acrolein was used as a positive control, because it has recently been reported not only to modify guanosines, but to show a 2-4-fold increase in adduct formation at guanosines complementary to <sup>Me</sup>C.<sup>51</sup> Cleavage was normalized according to Equation 3.1.

Equation 3.1. Normalization of % cleavage

$$\% \text{ cleavage at a given site} = 100 \times \frac{\text{Density}_{\text{drug}} - \text{Density}_{\text{control}}}{\text{Density}_{\text{uncleaved}}}$$

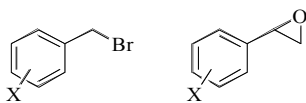


Figure 3.9. Benzyl bromide and styrene oxide

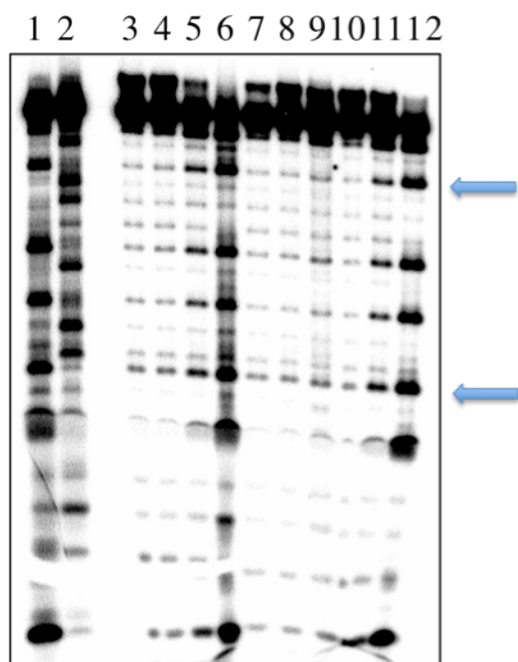


Figure 3.10. Incubation of acrolein, styrene oxide, and benzyl bromide with 22-mer in 50 mM sodium phosphate, pH 6.

Lane 1: Maxam-Gilbert G; Lane 2: Maxam-Gilbert C; Lane 3: no drug; Lane 4: 1 mM acrolein; Lane 5: 10 mM acrolein; Lane 6: 100 mM acrolein; Lane 7: 1 mM styrene oxide; Lane 8: 10 mM styrene oxide; Lane 9: 100 mM styrene oxide; Lane 10: 1 mM benzyl bromide; Lane 11: 10 mM benzyl bromide; Lane 12: 100 mM styrene oxide. Lower arrow denotes modification across from and adjacent to MeC; Upper arrow is same local sequence with no methylation

Table 3.5. Quantitation of DNA cleavage following incubation and piperidine/heat treatment with various alkylating agents.

DNA	100 mM acrolein	1 mM acrolein	100 mM benzyl bromide	1 mM benzyl bromide
-----	-----------------	---------------	-----------------------	---------------------

Unmethylated	2.5	19.5	2.1	12.6
Methylated	1.9	31.4	2.2	18.0

Unfortunately, little difference was observed in adduct formation at guanosines complementary to <sup>Me</sup>Cs when compared to Cs (Figure 3.10) for benzyl bromide. The blue arrows show two sites with the same surrounding sequence in each repeat unit. At high concentrations, adduct formation occurs at multiple sites, leading to higher concentrations of small fragments. Acrolein has been reported to form adducts 2-4 times more frequently at methylated positions.<sup>18</sup> A similar phenomenon is observed here, but the structure of acrolein is not easily modified to allow a systematic study. In order to find a suitable probe, several compounds previously synthesized by the Kerwin group were analyzed, including **CRW054** and **AZB004** (Figure 3.13). **AZB004** had been shown to be active in the nicking assay, and while it did show modification at guanosines, there was only a small appreciable difference in modification of guanosines on the methylated half of the oligomer vs. the unmethylated portion. However, a larger difference in cleavage at methylated cytosines (nearly two-fold) was observed than at guanosines.

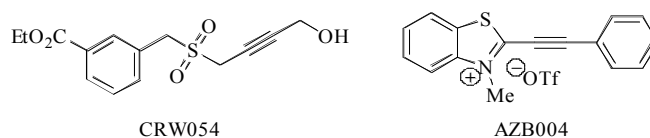


Figure 3.11. Structures of CRW054 and AZB004

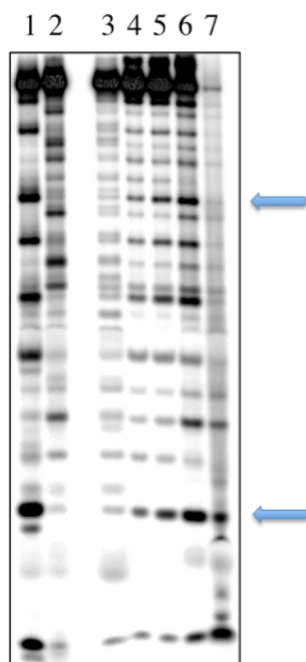


Figure 3.12. AZB004 with 22-mer DNA in 50 mM sodium phosphate, pH 6.

Lane 1: Maxam-Gilbert G; Lane 2: Maxam-Gilbert C; Lane 3: No drug; Lane 4: 10  $\mu$ M drug; Lane 5: 100  $\mu$ M AZB004; Lane 6: 1 mM AZB004; Lane 7: 10 mM AZB004. Lower arrow denotes modification across from and adjacent to MeC; Upper arrow is same local sequence with no methylation

Table 3.6. Quantitation of cleavage induced by piperidine/heat treatment of DNA incubated with **AZB004**

Position Modified	100 $\mu$ M	1 mM
G on unmethylated portion of DNA	12	21
C on unmethylated portion of DNA	6	14
G on methylated portion of DNA	14	30
C on unmethylated portion of DNA	4	8

The apparent difference in adduct formation for **CRW054** can be attributed to the unusually high level of cleavage at G3, which raises the average cleavage from 14% to 21%.

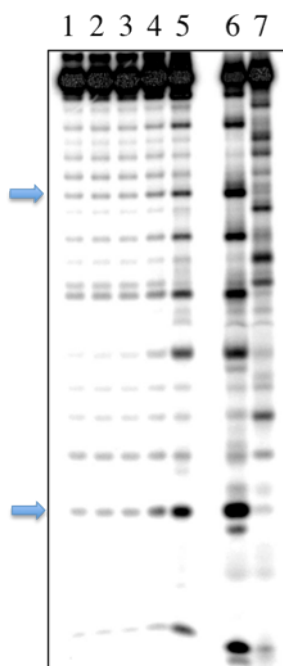


Figure 3.13. **CRW054** incubated with 22-mer in 50 mM sodium phosphate at pH 8.

Lane 1: No drug; Lane 2: 10  $\mu$ M CRW054; Lane 3: 100  $\mu$ M CRW054; Lane 4: 1 mM CRW054; Lane 5: 10 mM CRW054; Lane 6 Maxam-Gilbert G; Lane 7 Maxam-Gilbert C. Lower arrow denotes modification across from and adjacent to MeC; Upper arrow is same local sequence with no methylation

Table 3.7. Quantitation of DNA cleavage induced by piperidine/heat treatment following incubation of DNA with **CRW054**

Position Modified	pH 8, 100 $\mu$ M	pH 8, 1 mM
G on unmethylated DNA	1	11
G on methylated DNA	0	21

While these results were encouraging, the differences in methylated and unmethylated DNA were less pronounced than we hoped. We theorized that effects at complementary and adjacent guanosines were smaller than if DNA modification were occurring at cytosine itself.

### 3.2.3.2. Cytosine-Selective DNA Modification

**AZB017** (Figure 3.14) was previously reported to modify DNA at Cs, so this compound appeared a likely candidate for showing a difference in adduct formation with varying methylation status.<sup>68</sup> DNA modification occurs on G at pH 8, and C (with some G) and pH 6 (Figure 3.15).

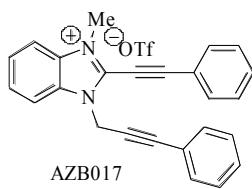


Figure 3.14. **AZB017**

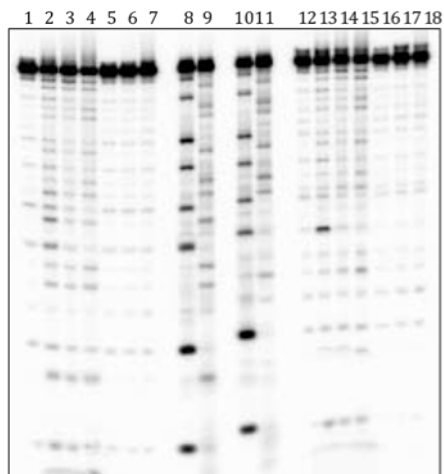


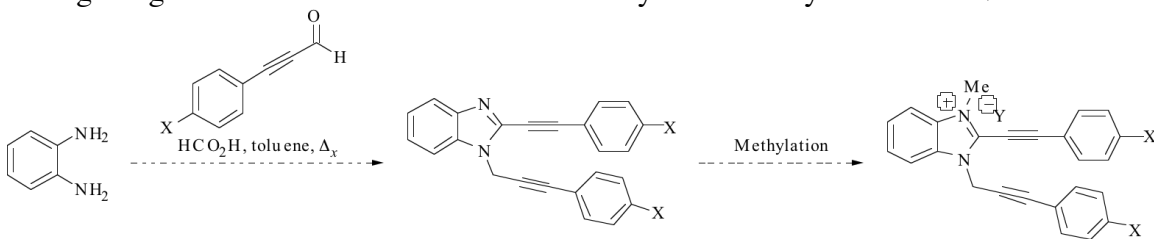
Figure 3.15. Incubations of **AZB017** with unmethylated or methylated DNA in 50 mM sodium phosphate at pH 6 or pH 8.

Lanes 1-7, unmethylated DNA. Lanes 12-18, methylated DNA. Lane 1: no drug, pH 6; Lane 2: 10  $\mu\text{M}$  AZB017 pH 6; Lane 3: 100  $\mu\text{M}$  AZB017 pH 6; Lane 4: 1 mM AZB017 pH 6; Lane 5: 10  $\mu\text{M}$  AZB017 pH 8; Lane 6: 100  $\mu\text{M}$  AZB017 pH 8; Lane 7: 1 mM AZB017, pH 8; Lane 12: no drug, pH 6; Lane 13: 10  $\mu\text{M}$  AZB017 pH 6; Lane 14: 100  $\mu\text{M}$  AZB017 pH 6; Lane 15: 1 mM AZB017 pH 6; Lane 16: 10  $\mu\text{M}$  AZB017 pH 8; Lane 17: 100  $\mu\text{M}$  AZB017 pH 8; Lane 18: 1 mM AZB017, pH 8.

Encouragingly, **AZB017** does show a marked difference in adduct formation at  $\text{Me}^e\text{Cs}$  compared to Cs (Figure 3.15). The extent of guanosine modification shows no appreciable difference. At the highest concentration shown, 1 mM **AZB017** at pH 6, we observe a 10-fold increase in the level of DNA cleavage at methylated cytosines compared to unmethylated cytosines. At lower concentrations, this difference was less pronounced.

### 3.3. SYNTHESIS<sup>68,69</sup>

Synthesis of several **AZB017** analogs would allow us to explore structure-activity relationships of cytosine adduction. This will allow a second generation of compounds that could effectively target unmethylated cytosines preferentially. Also, this set of analogs might show some electronic effects of cytosine methylation on DNA adduction.

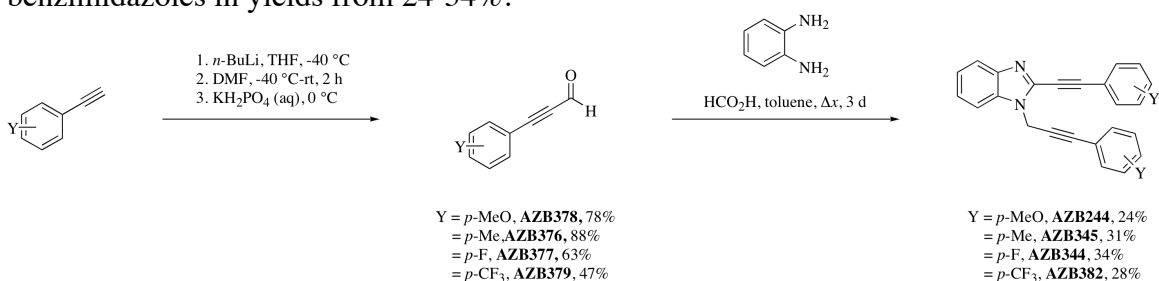


Scheme 3.15. Proposed **AZB017** analog synthesis



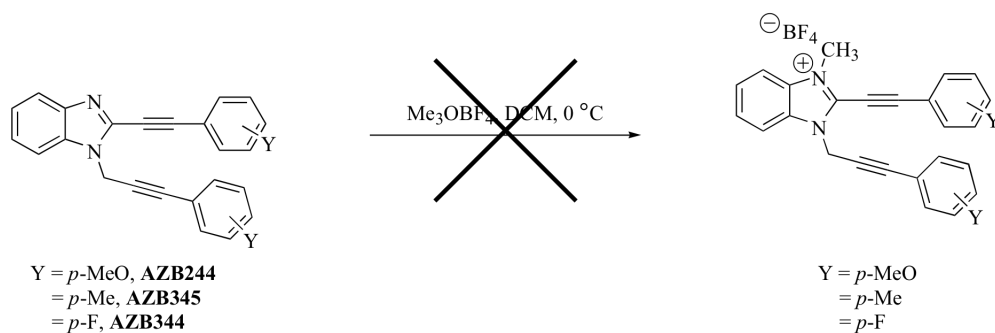
Substituents 4-OMe, 4-Me, 4-F, and 4-CF<sub>3</sub> were chosen for their range of electronic properties. Although this route (Scheme 3.15) is limited to benzimidazoles with identical alkynyl substituents, it allows rapid synthesis of the compounds of interest.

The propargyl aldehydes were synthesized according to literature procedure (Scheme 3.16),<sup>70</sup> using deprotonation of the appropriate terminal acetylene with *n*-BuLi at -40 °C, followed by immediate addition of N,N-dimethylformamide (DMF) at -40 °C. The resultant mixture was then warmed to room temperature and quenched by pouring the reaction over aqueous monobasic potassium phosphate at 0 °C. This method worked best for electron-rich phenylacetylenes but gave only moderate yields for the electron-poor substrates (yields are an average of two trials). These propargyl aldehydes were then condensed onto 1,2-phenylenediamine with formic acid in toluene at reflux for 3 days (Scheme 3.16).<sup>28</sup> This transformation proceeded in modest yield, giving the desired benzimidazoles in yields from 24-34%.



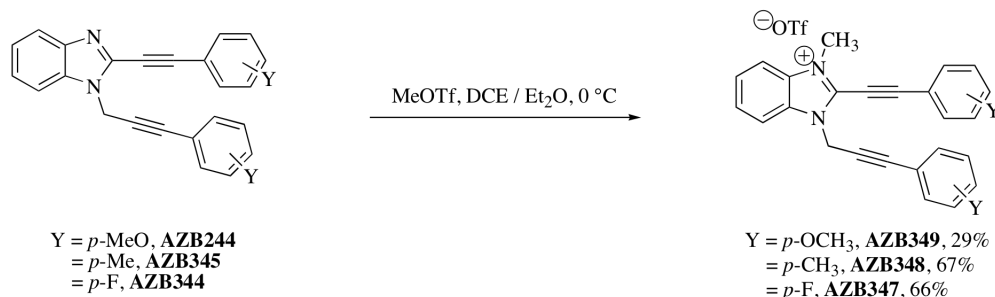
Scheme 3.16. Synthesis of benzimidazoles

Previous work in the Kerwin lab suggested that using methyl triflate might be incompatible with the *p*-MeO skipped dialkynyl benzimidazole;<sup>28</sup> so, methylation was attempted using trimethyloxonium tetrafluoroborate (Scheme 3.17). These transformations appeared to generate the desired product (as determined based on TLC and <sup>1</sup>H NMR), but methylation of **AZB244**, **AZB344** or **AZB345** proved difficult to purify by either recrystallization or chromatography.



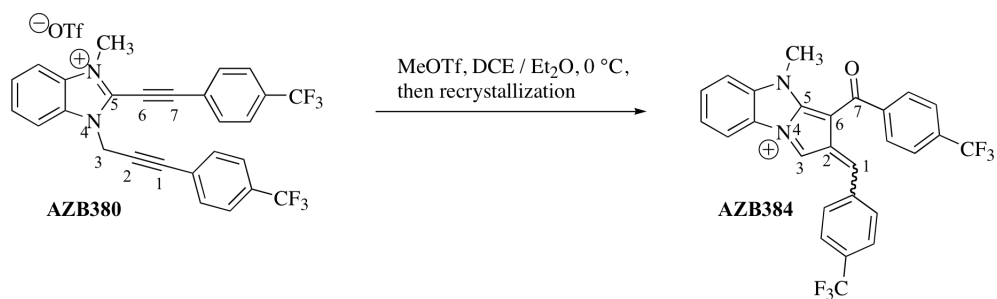
Scheme 3.17. Initial methylation strategy

Methylation of the dialkynylbenzimidazoles using methyl triflate proceeded smoothly in all cases, albeit with diminished yield for the *p*-MeO substrate (Scheme 3.18).<sup>28</sup> The products were isolated by filtration from the reaction mixture and were purified by recrystallization from 1,2-dichloroethane (DCE) and diethyl ether, followed by recrystallization (with hot filtration) from DCM and hexanes to give analytically pure compounds. Compound **AZB349** proved to be somewhat unstable in solution unless oxygen was rigorously excluded, so solvents were deoxygenated by sparging with argon prior to use.



Scheme 3.18. Synthesis of methylated benzimidazolium salts

Interestingly, compound **AZB380** underwent spontaneous cyclization during either methylation or recrystallization. NMR, MS, and IR were consistent with the structure shown in Scheme 3.19.



Scheme 3.19. Cyclization of **AZB380**.

### 3.4. BIOLOGICAL EVALUATION OF AZB LIBRARY

We had originally hoped to use ESI-MS to sequence the position and frequency of adduct formation by the benzimidazolium “skipped” aza-enediynes.

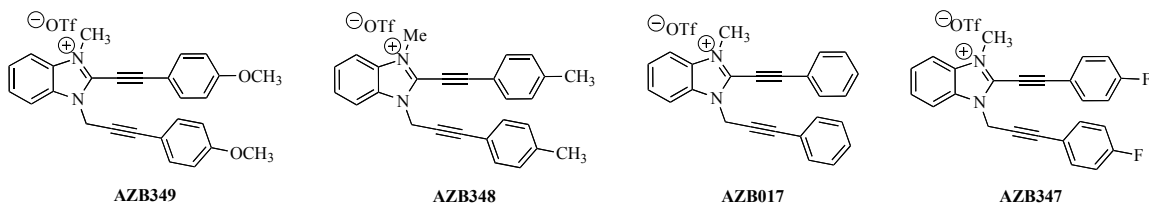


Figure 3.16. Benzimidazolium library

Nicking assays were performed to ascertain the extent of DNA damage by the skipped azaenediyne benzimidazolium salts. Each compound was incubated with supercoiled plasmid  $\phi$ X174 DNA (50  $\mu$ M bp) in 50 mM Tris (pH 8) with the compound added as 10X solution in DMSO. The control reaction included DMSO in the same proportion, 10% by volume, as the other incubations. The final incubation volume as 30  $\mu$ L, as that volume was shown to be the minimum required volume to have consistent results despite water evaporation over the time of the incubation.<sup>28</sup> Cleavage was calculated according to Equation 3.2.

Equation 3.2. Determination of % Nicking

$$\%Nicking = 100 \times \frac{2(FormIII) + FormII}{2(FormIII) + FormII + FormI}$$

In order to account for nicking not caused by the compounds of interest, normalized percent nicking was determined according to Equation 3.3.

Equation 3.3. Normalization of % Nicking

$$Normalized \% Nicking = 100 \times \frac{\% cleavage_{drug} - \% cleavage_{control}}{100 - \% cleavage_{control}}$$

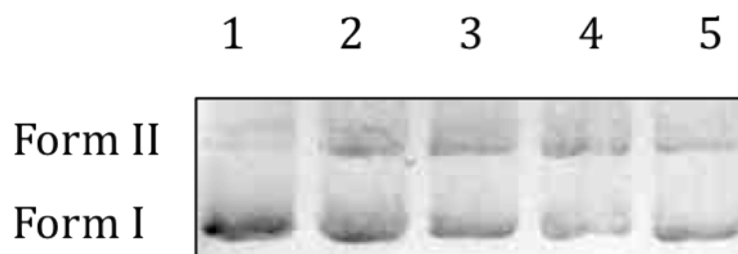


Figure 3.17. Nicking assay on  $\phi$ X174 using skipped benzimidazolium triflates at 0.1 mM in 50 mM Tris, pH 8.

Lane 1: No drug, Lane 2: **AZB349**; Lane 3: **AZB348**; Lane 4: **AZB017**; Lane 5: **AZB347**.

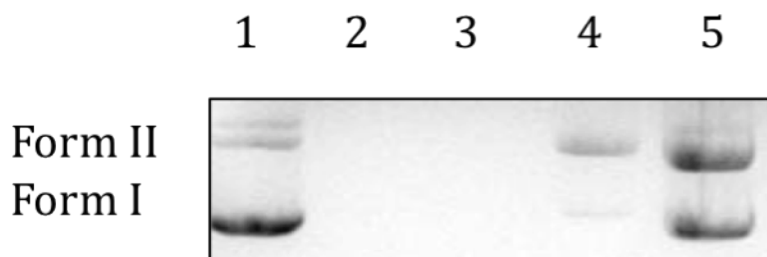


Figure 3.18. Nicking assay on  $\phi$ X174 using skipped benzimidazolium triflates at 1.0 mM in 50 mM Tris, pH 8.

Lane 1: No drug, Lane 2: AZB349; Lane 3: AZB348; Lane 4: AZB017; Lane 5: AZB347.

Results are summarized in Table 3.8. At 1 mM, in presence of the electron-rich compounds **AZB349** and **AZB348**, no DNA could be observed using ethidium bromide stain. The compounds themselves appeared to migrate towards the anode of the gel and could be seen fluorescing above the well. The results for **AZB017** are consistent with the previous report.<sup>26</sup> At 0.1 mM of each compound, nicking could be observed. There does appear to be a trend in electronics that correlated to nicking ability. The benzimidazolium compounds containing electron-rich substituents are generally more able to cleave supercoiled DNA than electron-poor substituents. Compounds **AZB017**, **AZB348**, and **AZB349** cause 11-24% normalized cleavage. The poor nicking ability of **AZB349** might be attributable to its poor stability in DMSO. Upon dissolution, a color change is observed immediately from a pale orange solid to a neon-yellow solution. After 1 h at room temperature, the solution has degraded significantly, as judged by both <sup>1</sup>H NMR and TLC (the product becomes at least three spots, which are poorly resolved). Deoxygenating the DMSO appears to slow decomposition, but not significantly. The error presented is the standard deviation calculated from three “no drug” control reactions.

Table 3.8. Nicking assay to determine extent of DNA cleavage

Compound	Normalized% Nicking at 0.1 mM drug	Normalized% Nicking at 1 mM
<b>AZB349</b>	11	NA <sup>a</sup>
<b>AZB348</b>	19±5	NA <sup>a</sup>
<b>AZB017</b>	24±5	71±5
<b>AZB347</b>	4±5	42±5

<sup>a</sup>NA = not applicable, i.e. the DNA could not be analyzed in this lane. <sup>b</sup>Average of two trials

We were interested to see whether the library had a similar trend in cytotoxicity as it did for DNA damage. The compounds (Figure 3.16) were analyzed for their cytotoxicity, which ranged from high nanomolar to low micromolar (Table 3.9). Ms. Jing Li in the Kerwin group performed cytotoxicity assays using A549 non-small cell carcinoma cells. Interestingly, the results are similar to the nicking assay in terms of the electron-poor **AZB347**. Interestingly, the electron-rich compounds (**AZB349**, **AZB348**) in this case show somewhat improved cytotoxicity compared to **AZB017**.

Table 3.9. Cytotoxicity data on electronically varied benzimidazolium library

Compound	IC <sub>50</sub> (μM)	Std. Dev.
MCC (Control 1)	0.05	±0.02
MCC (Control 2)	0.05	±0.01
MCC (Control 3)	0.05	±0.02
<b>AZB348</b>	1.0	±0.1

<b>AZB349</b>	0.9	±0.4
<b>AZB017</b>	2.3	±0.9
<b>AZB347</b>	5.0	±1.0
<b>AZB384</b>	2.6	±0.9
<b>AZB383</b>	3.2	±0.9

---

### **3.5. CONCLUSIONS**

A small library of dialkynyl benzimidazolium salts was synthesized and evaluated for biological activity. It appears that electronics to play a role in determining DNA nicking ability, as well as cytotoxicity. DNA nicking ability appears to be the highest for **AZB017**. It is difficult to draw any conclusions about the mechanism by which these compounds cause nicking from these data. The slightly improved cytotoxicity could be the result of a number of factors; however, not enough is known about the mechanism by which these compounds cause cell death to draw parallels between cytotoxicity and DNA damage.

### **3.6. FUTURE DIRECTIONS**

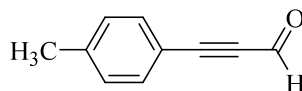
Much work remains in the area of developing compounds that can selectively target unmethylated cytosines. We hope in the future to use the synthetic methylated oligomers to gain information at the level of single bases about electronic effects of the skipped aza-enediynes on adduct formation. Also, the mechanism of cytotoxicity should be explored in order to improve design of these compounds. ESI-MS with an appropriate small DNA oligomer might be of use in rapidly determining sequence selectivity and the structure of the adducts being formed.

### 3.7. EXPERIMENTAL SECTION

#### 3.7.1. Chemistry

##### General Notes

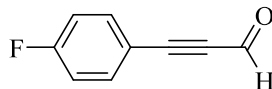
THF was distilled over sodium/benzophenone, and DCE, CH<sub>2</sub>Cl<sub>2</sub>, and toluene were distilled from CaH<sub>2</sub> immediately prior to use. DMF was purchased from Aldrich as “anhydrous” and used without further drying. All reactions were run in oven-dried, argon-flushed round bottom flasks under an argon atmosphere. Solvent ratios are expressed as % by volume. Flash chromatography (FCC) was performed according to the method of Still.<sup>71</sup> NMR was performed using a VARIAN Mercury spectrometer. <sup>1</sup>H NMR was run at 400 MHz; <sup>13</sup>C NMR was run at 100 MHz with broadband proton decoupling unless otherwise specified. Solvent chemical shifts are reported in ppm (δ) and referenced to solvent.<sup>72</sup> IR was obtained on a Nicolet IR100 FT-IR spectrometer. Melting points were obtained in open capillary tubes on a Büchi Melting Pont B-540 and are uncorrected.



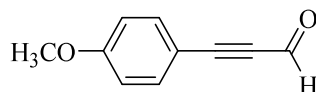
**AZB376. *p*-Tolylpropynal.** *p*-ethynyltoluene (2.0 mL, 15.8 mmol, 1 eq) was dissolved in THF (40 mL, 0.4 M). The solution was cooled to -40 °C, and *n*-BuLi (6.9 mL, 15.8 mmol, 1 eq) was added slowly. Upon completion of the addition, DMF (2.44 mL, 31.5 mmol, 2 eq) was added, and the reaction was allowed to warm to room temperature over 2 h. The reaction mixture was then slowly poured onto a solution (86 mL) of 10% w/v aqueous KH<sub>2</sub>PO<sub>4</sub> (8.59 g, 63.1 mmol, 4 eq KH<sub>2</sub>PO<sub>4</sub>). This solution was extracted 3x with MTBE (40 mL). Combined organic layers were washed with brine (75 mL), dried (Na<sub>2</sub>SO<sub>4</sub>), and conc. The resultant dark yellow oil was purified by FCC (SiO<sub>2</sub>)



using a gradient of Hex-10% EtOAc/Hex as eluant to give the product as a pale yellow oil (2.01 g, 13.9 mmol, 89% yield).  $^1\text{H}$ ,  $^{13}\text{C}$  NMR, and LRMS were in accordance with literature data.<sup>73</sup>

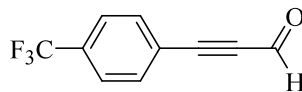


**AZB377. (4-Fluorophenyl)-propynal.** 1-ethynyl-4-fluorobenzene (0.50 g, 477  $\mu\text{L}$ , 4.2 mmol, 1 eq) was dissolved in THF (10.4 mL, 0.4 M). The solution was cooled to  $-40\text{ }^\circ\text{C}$ , and *n*-BuLi (1.66 mL, 4.16 mmol, 1 eq) was added slowly. Upon completion of the addition, DMF (644  $\mu\text{L}$ , 8.33 mmol, 2 eq) was added, and the reaction was allowed to warm to room temperature over 2 h. The reaction mixture was then slowly poured onto a solution (23 mL) of 10% w/v aqueous  $\text{KH}_2\text{PO}_4$  (2.27 g, 16.7 mmol, 4 eq  $\text{KH}_2\text{PO}_4$ ). This solution was extracted 3x with MTBE (25 mL). Combined organic layers were washed with brine (50 mL), dried ( $\text{Na}_2\text{SO}_4$ ), and conc. The resultant dark yellow oil was purified by FCC ( $\text{SiO}_2$ ) using a gradient of Hex-10% EtOAc/Hex as eluant to give the product as a pale yellow oil (485 mg, 3.27 mmol, 78% yield).  $^1\text{H}$ ,  $^{13}\text{C}$  NMR and LRMS were in accordance with literature data.<sup>74</sup>

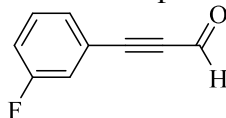


**AZB 378. (4-Methoxyphenyl)-propynal.** *p*-ethynylanisole (1.23 g, 9.3 mmol, 1 eq) was dissolved in THF (23 mL, 0.4M). The solution was cooled to  $-40\text{ }^\circ\text{C}$ , and *n*-BuLi (4.53 mL, 9.3 mmol, 1 eq) was added slowly. Upon completion of the addition, DMF (1.44 mL, 18.6 mmol, 2 eq) was added, and the reaction was allowed to warm to room temperature over 2 h. The reaction mixture was then slowly poured onto a solution (51 mL) of 10% w/v aqueous  $\text{KH}_2\text{PO}_4$  (5.07 g, 37.2 mmol, 4 eq  $\text{KH}_2\text{PO}_4$ ). This solution was extracted 3x with MTBE (25 mL). Combined organic layers were washed with brine (50 mL), dried ( $\text{Na}_2\text{SO}_4$ ), and concentrated *in vacuo*. The resultant dark yellow oil was

purified by FCC (SiO<sub>2</sub>) using a gradient of Hex-10% EtOAc/Hex as eluant to give the product as a pale yellow solid (1.17g, 7.3 mmol, 78% yield). Characterization (<sup>1</sup>H, <sup>13</sup>C NMR, LRMS) was in accordance with literature data<sup>28,74</sup>

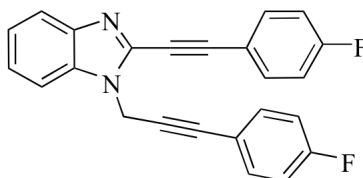


**AZB 379. (4-Trifluoromethylphenyl)-propynal.** 1-ethynyl- $\alpha,\alpha,\alpha$ -trifluorotoluene (2 g, 1.92 mL, 11.8 mmol, 1 eq) was dissolved in THF (0.4 M, 29.5 mL) and cooled to -78 °C. *n*-BuLi (5.7 mL, 11.8 mmol, 1 eq) was added slowly over 30 min. DMF (1.82 mL, 23.5 mmol, 1 eq) was added immediately at -78 °C to the dark red-orange solution, and the reaction was warmed to room temperature, after which time it was a dark yellow solution. The reaction mixture was quenched by pouring it over a 10% aqueous solution of KH<sub>2</sub>PO<sub>4</sub> (64 mL, 47.0 mmol, 4 eq) at 5 °C with stirring. The aqueous mixture was extracted 3x with 40 mL MTBE. The organic extracts were washed with satd NaCl, dried over Na<sub>2</sub>SO<sub>4</sub>, and concentrated *in vacuo*. The compound was isolated by FCC in Hexanes-5% EtOAc/Hexanes to give an off-white solid (1.09 g, 5.5 mmol, 47%). <sup>1</sup>H NMR (CDCl<sub>3</sub>):  $\delta$  9.44 (1H, s); 7.70 (4H, AA'BB',  $J = 18.6, 9.2$  Hz). <sup>13</sup>C NMR (CDCl<sub>3</sub>):  $\delta$  176.4, 133.4, 132.6 (d,  $J_{C-F} = 23$  Hz), 125.7 (d,  $J_{C-F} = 3.0$  Hz), 123.4 (d,  $J_{C-F} = 272$  Hz), 123.2, 92.2, 89.2. LRMS(CI<sup>+</sup>): 149 (M<sup>+</sup>+1) HRMS calcd for C<sub>9</sub>H<sub>5</sub>FO 149.0402, found 149.0403. IR (thin film from CDCl<sub>3</sub>): 3075, 2962, 2204, 1664, 1580, 1485, 1431, 1286, 1173, 1153, 1008, 884, 789, 719, 679 cm<sup>-1</sup>. mp 30.2-31.8 °C.



**AZB 380. (3-Fluorophenyl)-propynal.** 1-Ethynyl-3-fluorobenzene (2 g, 1.92 mL, 16.6 mmol, 1 eq) was dissolved in THF (0.4 M with respect to alkyne) and cooled to -40 °C (MeCN/CO<sub>2</sub> bath). *n*-BuLi (8.1 mL, 16.6 mmol, 1 eq) was added slowly over

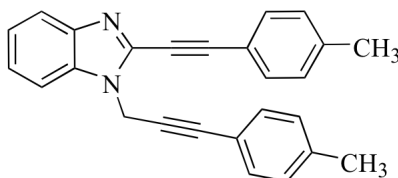
approx. 30 min. Upon completion of this addition, DMF (2.58 mL, 33.3 mmol, 2 eq) was added to the dark orange solution to give a pale yellow solution. The reaction was warmed to room temperature, then poured onto a solution of 10% w/v aqueous  $\text{KH}_2\text{PO}_4$  (91 mL, 66.6 mmol, 4 eq.) at 5 °C with stirring. The solution was extracted 3x with MTBE (40 mL), and the combined organic extracts were washed with brine (60 mL), dried ( $\text{Na}_2\text{SO}_4$ ) and concentrated *in vacuo*. The residue was purified by FCC in Hexanes-5% EtOAc/Hex to give the product as a pale yellow oil (1.06 g, 7.16 mmol, 43%).  $^1\text{H}$  NMR ( $\text{CDCl}_3$ ):  $\delta$  9.33 (1H, s), 7.30-7.28 (2H, m); 7.21-7.18 (1H, m); 7.13-7.08 (1H, m).  $^{13}\text{C}$  NMR ( $\text{CDCl}_3$ ):  $\delta$  176.5, 162.2 ( $J_{\text{C-F}} = 298$  Hz), 129.8 (d,  $J_{\text{C-F}} = 44$  Hz), 129.7 (d,  $J_{\text{C-F}} = 26$  Hz), 121.1 (d,  $J_{\text{C-F}} = 9$  Hz), 119.7 (d,  $J_{\text{C-F}} = 13$  Hz), 118.7 (d,  $J_{\text{C-F}} = 21$  Hz), 92.8 (d,  $J_{\text{C-F}} = 3$  Hz), 88.4. LRMS( $\text{Cl}^+$ ): 199 ( $\text{M}^+ + 1$ ), 179 ( $\text{M}^+ - \text{F}$ ). HRMS calcd for  $\text{C}_9\text{H}_6\text{FO}$ : 149.0403, found: 149.0402. IR (thin film from  $\text{CDCl}_3$ ): 2193, 1664, 1614, 1404, 1332, 1129, 1066, 1015, 842, 732  $\text{cm}^{-1}$ .



**AZB344. 2-(4-Fluorophenylethynyl)-1-[3-(4-fluorophenyl)-prop-2-ynyl]-1H-**

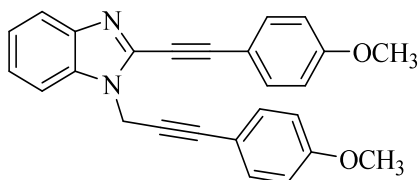
**benzimidazole.** (4-Fluorophenyl)-propynal (800 mg, 5.4 mmol, 2 eq) was dissolved into toluene (14 mL, 0.2 M). 1,2-phenylenediamine (292 mg, 2.7 mmol, 1 eq) was added, and the solution was deoxygenated by bubbling with Ar. Formic acid was added (95  $\mu\text{L}$ , 2.5 mmol, 0.93 eq), and the resulting dark red mixture was refluxed for 3 d. After 3 d, the reaction mixture was cooled to room temperature and absorbed directly to silica gel. The product was isolated by FCC (first column, 1% TEA/Hexanes to 1% TEA in 25% EtOAc/Hexanes; second column 10-25% EtOAc/Hex) followed by crystallization to

yield a white cottony solid (335 mg, 0.91 mmol, 34%). <sup>1</sup>H NMR (CD<sub>2</sub>Cl<sub>2</sub>): 7.76 (1H, d, *J* = 7.8 Hz); 7.70 (2H, dd, *J* = 8.1, 5.3 Hz); 7.62 (1H, d, *J* = 8.2 Hz); 7.40 (3H, dd, *J* = 8.1, 6.8 Hz); 7.34 (1H, t, *J* = 8.1 Hz); 7.15 (2H, t, *J* = 8.8); 7.00 (2H, t, *J* = 8.8); 5.35 (s, 2H). <sup>13</sup>C NMR (CD<sub>2</sub>Cl<sub>2</sub>): 165.1, 164.4, 162.6, 161.9, 143.4, 136.8, 134.7, 134.6, 134.2, 134.1, 124.6, 123.5, 120.5, 118.4, 117.5, 116.5, 116.3, 116.1, 115.9, 94.7, 84.4, 82.0, 78.5, 35.4. <sup>1</sup>H NMR (CDCl<sub>3</sub>): 7.81 (1H, d, *J* = 7.8 Hz); 7.65 (2H, dd, *J* = 8.5, 5.3 Hz); 7.58 (1H, d, *J* = 7.6 Hz); 7.40-7.33 (4H, m); 7.11 (2H, t, *J* = 8.6 Hz); 6.98 (2H, t, *J* = 8.7 Hz); 5.32 (2H, s). <sup>13</sup>C NMR (CDCl<sub>3</sub>): 164.6, 164.0, 162.1, 161.5, 143.0, 136.6, 134.3, 134.2, 133.75, 133.67, 124.28, 123.3, 120.4, 117.9, 117.1, 116.2, 116.0, 115.8, 115.5, 110.1, 94.6, 84.4, 81.4, 78.1, 35.0. LRMS: (CI<sup>+</sup>): 369 (M<sup>+</sup>+1). HRMS (CI<sup>+</sup>): calcd. 368.1125; found 368.1123. IR (KBr pellet): 3059, 2942, 2217, 1600, 1518, 1508, 1490, 1449, 1432, 1391, 1349, 1336, 1235, 1157, 837, 740, 530. EA: calcd: 78.25%C, 3.83 %H, 7.60 %N; found: 78.00 %C, 3.74% H, 7.50% N.

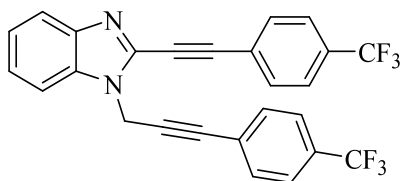


**AZB 345. 2-*p*-Tolylethynyl-1-(3-*p*-tolylprop-2-ynyl)-1*H*-benzimidazole.** *p*-Tolylpropynal (1.09g, 7.6 mmol, 2 eq) was dissolved into toluene (19 mL, 0.2 M). 1,2-phenylenediamine (409 mg, 3.8 mmol, 1 eq) was added, and the solution was deoxygenated by bubbling with Ar. Formic acid was added (133 μL, 3.5 mmol, 0.93 eq), and the resulting dark orange mixture was refluxed for 3 d. After 3 d, the reaction mixture was cooled to room temperature and absorbed directly to silica gel. The product was isolated by FCC (first column, 1% TEA in Hexanes to 1% TEA in 25% EtOAc/Hexanes; second column 10-25% EtOAc/Hex) to give a white solid that was recrystallized from EtOAc/Hex to give a white cottony solid (327 mg, 0.91 mmol, 24%). <sup>1</sup>H NMR (CDCl<sub>3</sub>):

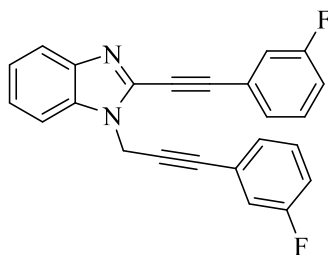
$\delta$  7.80 (1H, dd,  $J = 7.2, 1.3$  Hz); 7.61 (1H, dd,  $J = 7.1, 1.3$  Hz); 7.56 (2H, d,  $J = 8.0$  Hz); 7.35 (2H, dqd,  $J = 7.4, 7.2, 1.3$  Hz); 7.29 (2H, d,  $J = 8.2$  Hz); 7.22 (2H, dd,  $J = 7.8, 0.6$  Hz); 7.09 (2H, dd,  $J = 7.8, 0.6$  Hz); 5.33 (2H, s); 2.40 (3H, s); 2.32 (3H, s).  $^{13}\text{C}$  NMR ( $\text{CDCl}_3$ ):  $\delta$  143.0, 140.3, 139.0, 137.0, 133.8, 132.1, 131.7, 129.4, 129.1, 124.1, 123.2, 120.2, 118.8, 118.0, 110.3, 96.1, 85.6, 81.0, 77.8, 35.1, 21.7, 21.5. LRMS: ( $\text{CI}^+$ ): 361 ( $\text{M}^++1$ ). HRMS ( $\text{CI}^+$ ): calcd. 360.1626; found 360.1623. IR (KBr pellet): 3025, 2943, 2917, 2216, 1561, 1523, 1509, 1489, 1449, 1434, 1392, 1359, 1337, 814, 761, 742, 527  $\text{cm}^{-1}$ .



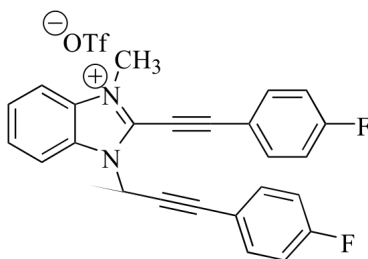
**AZB 244. 2-(4-Methoxyphenylethynyl)-1-[3-(4-methoxyphenyl)-prop-2-ynyl]-1H-benzimidazole.** (4-Methoxy-phenyl)propynal (960 mg, 6.0 mmol, 2 eq) was dissolved into toluene (15 mL, 0.2 M). 1,2-phenylenediamine (324 mg, 3.0 mmol, 1 eq) was added, and the solution was deoxygenated by bubbling with Ar. Formic acid was added (120  $\mu\text{L}$ , 2.8 mmol, 0.93 eq), and the resulting dark red mixture was refluxed for 3 d. After 3 d, the reaction mixture was cooled to room temperature and absorbed directly to silica gel. The product was isolated by FCC (first column, 1% TEA in Hexanes to 1% TEA in 25% EtOAc/Hexanes; second column 10-25% EtOAc/Hex) to give an orange oil (282 mg, 0.72 mmol, 24%) that formed a glassy solid upon standing. An analytical sample was crystallized from EtOAc/Hex to give a pale orange crystalline solid. Characterization data ( $^1\text{H}$  NMR,  $^{13}\text{C}$  NMR, LRMS, HRMS, IR) were in accordance with previously reported data.<sup>28</sup>



**AZB 381. 2-(4-Trifluoromethylphenylethynyl)-1-[3-(4-trifluoromethylphenyl)-prop-2-ynyl]-1H-benzimidazole.** (4-Trifluoromethylphenyl)-propynal (0.811 g, 4.09 mmol, 2 eq) was combined with 1,2-phenylenediamine (221 mg, 2.05 mmol, 1 eq) in toluene (10.2 mL, 0.2 M with respect to 1,2-phenylenediamine). The resultant yellow solution was deoxygenated by bubbling with Ar, then formic acid (72  $\mu$ L, 1.90 mmol, 0.93 eq) and heated to reflux for 3 days. The mixture was adsorbed directly onto SiO<sub>2</sub> and purified by flash column chromatography (1% TEA/Hexanes to 1% TEA in 25% EtOAc/Hex) followed by crystallization from EtOAc/Hex to give a pale yellow needle-like solid (263 mg, 0.56 mmol, 28%). An additional amount of product was isolated from the mother liquor by column chromatography using the same eluent system as previously described (66 mg, 0.14 mmol, 6.9%). <sup>1</sup>H NMR (CDCl<sub>3</sub>): 8.04 (2H, d, *J* = 8.2 Hz); 7.68 (2H, d, *J* = 8.2 Hz); 7.55-7.48 (5H, m); 7.41 (1H, dd, *J* = 3.0 Hz); 7.29 (2H, dd, *J* = 3.0 Hz). <sup>13</sup>C NMR (CDCl<sub>3</sub>):  $\delta$  173.4, 154.4, 141.4, 134.9, 132.1, 131.9, 126.5, 125.3 (d, *J*<sub>C-F</sub> = 3), 123.4, 122.9, 114.4, 108.79, 84.2, 83.6, 78.1, 77.0, 33.2. LRMS (CI<sup>+</sup>): 487 (M<sup>+</sup>+H<sub>2</sub>O), 467 (M<sup>+</sup>-1). HRMS calcd for C<sub>26</sub>H<sub>15</sub>N<sub>2</sub>F<sub>6</sub>: 469.1139, found 469.1136. IR (KBr): 1616, 1578, 1509, 1324, 1162, 1121, 1066, 1014, 843, 770, 742 cm<sup>-1</sup>. mp 159.4-160.0

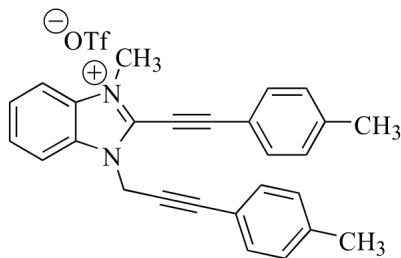


**AZB 382. 2-(3-Fluorophenylethynyl)-1-[3-(3-fluorophenyl)-prop-2-ynyl]-1*H*-benzimidazole.** (3-Fluorophenyl)-propynal (0.531 g, 3.58 mmol, 2 eq) was combined with 1,2-phenylenediamine (193 mg, 1.79 mmol, 1 eq) in toluene (9 mL, 0.2 M with respect to 1,2-phenylenediamine). The resultant yellow solution was deoxygenated by bubbling with Ar, then formic acid (68  $\mu$ L, 0.90 mmol, 0.93 eq) and heated to reflux for 3 days. The mixture was adsorbed directly onto SiO<sub>2</sub> and purified by flash column chromatography (1% TEA/Hexanes to 1% TEA in 25% EtOAc/Hex) followed by crystallization from EtOAc/Hex to give a pale yellow needle-like solid (181 mg, 0.49 mmol, 27%). <sup>1</sup>H NMR (CDCl<sub>3</sub>): 7.83-7.80 (1H, m); 7.60-7.57 (1H, m); 7.47-7.34 (m, 6H); 7.28-7.22 (1H, m); 7.19-7.15 (m, 2H); 7.13-7.08 (1H, m); 7.03 (1H, tdd, *J* = 8.4, 2.5, 1.2) <sup>13</sup>C NMR (CDCl<sub>3</sub>):  $\delta$  162.7 (d, *J*<sub>C-F</sub> = 248 Hz), 143.1, 136.3, 133.7, 130.4, 130.3, 130.0, 129.9, 128.0, 127.6, 124.5, 123.4, 122.7, 120.5, 119.0, 118.7, 118.5, 117.4, 1117.2, 116.4, 116.2, 110.1, 105.0, 94.1, 84.3, 82.5, 79.0, 34.9. LRMS (CI<sup>+</sup>): 369 (M<sup>+</sup>+1). HRMS (CI<sup>+</sup>) calcd for C<sub>24</sub>H<sub>14</sub>F<sub>2</sub>N<sub>2</sub>: 369.1203, found: 369.1204. IR (KBr): 3448, 3066, 2935, 1608, 1579, 1509, 1486, 1439, 1426, 1395, 1285, 1175, 1151, 782, 741, 677 cm<sup>-1</sup>.



**AZB 347. Trifluoromethanesulfonate-2-(4-fluorophenylethynyl)-3-[3-(4-fluorophenyl)-prop-2-ynyl]-1-methyl-3*H*-benzimidazol-1-ium.** The neutral benzimidazole (25 mg, 0.068 mmol, 1 eq) was dissolved in Et<sub>2</sub>O (450  $\mu$ L) and DCE (680  $\mu$ L) (0.06 M final concentration, 3:2 DCE:Et<sub>2</sub>O). A solution of methyl triflate (12.3  $\mu$ L, 0.11 mmol, 1.6 eq) in Et<sub>2</sub>O (440  $\mu$ L) was added dropwise, and the solution was warmed

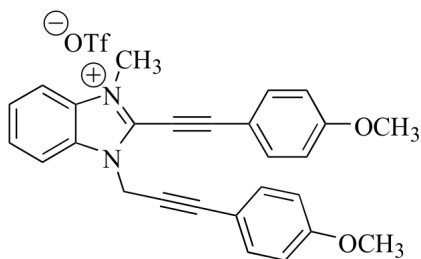
to room temperature. The product formed as a pale yellow solid precipitate which was isolated by vacuum filtration, then recrystallized from DCE/Et<sub>2</sub>O to give a pale yellow, flaky solid (24.0 mg, 0.045 mmol, 66%). On larger scale, an analytical sample was obtained by performing a second recrystallization from DCE/Et<sub>2</sub>O then dissolving the product in DCM, performing a filtration using a syringe-tip 0.2 μM filter, and adding hexanes to precipitate the product in the -20 °C freezer. <sup>1</sup>H NMR (CD<sub>3</sub>CN): δ 8.08-8.06 (1H, m); 7.98 (2H, dd, *J* = 8.9, 5.5 Hz); 7.92-7.90 (1H, m); 7.84-7.80 (2H, m); 7.48 (2H, dd, *J* = 8.9, 5.4 Hz); 7.36 (2H, t, *J* = 8.9 Hz); 7.12 (2H, t, *J* = 8.9 Hz); 5.66 (2H, s); 4.18 (s, 3H). LRMS (CI<sup>+</sup>): 383 (M<sup>+</sup>-OTf); 165. HRMS (CI<sup>+</sup>): calcd. 383.1360, found 383.1351. IR (KBr): 2218, 1600, 1548, 1509, 1484, 1265, 1224, 1155, 1031, 843, 637 cm<sup>-1</sup>. mp 148.4-149.0 (decomp).



**AZB 348. Trifluoromethanesulfonate-1-methyl-2-*p*-tolylethynyl)-3-[3-*p*-tolyl]-prop-2-ynyl]-3*H*-benzimidazol-1-ium.** The neutral benzimidazole (25 mg, 0.069 mmol, 1 eq) was dissolved in Et<sub>2</sub>O (460 μL) and DCE (684 μL) (0.06 M final concentration, 3:2 DCE:Et<sub>2</sub>O). A solution of methyl triflate (12.6 μL, 0.11 mmol, 1.6 eq) in Et<sub>2</sub>O (440 μL) was added dropwise, and the solution was warmed to room temperature. The product formed as a white solid precipitate which was isolated by vacuum filtration, then recrystallized from DCE/Et<sub>2</sub>O to give a white, flaky solid (24 mg, 0.046 mmol, 67%). On larger scale, an analytical sample was obtained by performing a second recrystallization from DCE/Et<sub>2</sub>O then dissolving the product in DCM, performing a filtration using a syringe-tip 0.2 μM filter, and adding hexanes to precipitate the product in the -20 °C

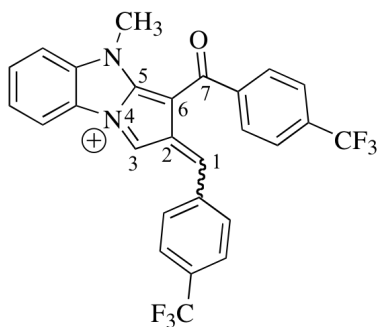


freezer  $^1\text{H}$  NMR ( $\text{CD}_3\text{CN}$ ):  $\delta$  7.86-7.84 (1H, m); 7.69-7.67 (1H, m); 7.61-7.57 (4H, m); 7.22 (2H, d,  $J = 7.9$  Hz); 7.12 (2H, d,  $J = 7.9$  Hz); 6.98 (2H, d,  $J = 7.9$  Hz); 5.43 (2H, s); 3.95 (3H, s); 2.26 (3H, s); 2.12 (3H, s). LRMS ( $\text{CI}^+$ ): 375 ( $\text{M}^+ - \text{OTf}$ ). HRMS ( $\text{CI}^+$ ): calcd: 375.1861. found: 375.1859. IR (KBr): 3031, 2972, 2947, 2214, 1602, 1554, 1511, 1483, 1466, 1435, 1350, 1274, 1223, 1164, 1030, 827, 757, 536, 517  $\text{cm}^{-1}$ . mp (decomp) 151.2-152.3  $^\circ\text{C}$ .



**AZB349. Trifluoromethanesulfonate-2-(4-methoxyphenylethynyl)-3-[3-(4-methoxyphenyl)-prop-2-ynyl]-1-methyl-3*H*-benzimidazol-1-ium.** The neutral benzimidazole (25 mg, 0.064 mmol, 1 eq) was dissolved in  $\text{Et}_2\text{O}$  (430  $\mu\text{L}$ ) and DCE (640  $\mu\text{L}$ ) (0.06 M final concentration, 3:2 DCE: $\text{Et}_2\text{O}$ ). A solution of methyl triflate (11.5  $\mu\text{L}$ , 0.10 mmol, 1.6 eq) in  $\text{Et}_2\text{O}$  (410  $\mu\text{L}$ ) was added dropwise, and the solution was warmed to room temperature. The product formed as an orange solid precipitate which was isolated by vacuum filtration, then recrystallized from DCE/ $\text{Et}_2\text{O}$  to give a pale orange solid (10 mg, 0.019 mmol, 29%). An analytical sample was obtained by performing a second recrystallization from DCE/ $\text{Et}_2\text{O}$  then dissolving the product in DCM, performing a filtration using a syringe-tip 0.2  $\mu\text{M}$  filter, and adding hexanes to precipitate the product in the  $-20$   $^\circ\text{C}$  freezer  $^1\text{H}$  NMR ( $\text{CD}_3\text{CN}$ ):  $\delta$  8.07-8.04 (1H, m); 7.88 (2H, d,  $J = 9.2$  Hz); 7.79-7.77 (1H, m); 7.38 (2H, d,  $J = 8.9$  Hz); 7.13 (2H, d,  $J = 8.9$ ); 6.90 (2H, d,  $J = 8.9$  Hz); 5.62 (2H, s); 4.15 (3H, s); 3.92 (3H, s); 3.79 (3H, s).  $^{13}\text{C}$  NMR could not be obtained, as rate of decomposition occurred on NMR timescale. LRMS ( $\text{CI}^+$ ): 407 ( $\text{M}^+$

OTf). HRMS (CI<sup>+</sup>): calcd: 407.1760, found: 407.1750. IR (KBr): 2968, 2212, 1603, 1552, 1510, 1483, 1466, 1256, 1157, 1030, 841, 756, 637 cm<sup>-1</sup>. mp 140.8-141.9 °C (decomp).



**AZB 384. Trifluoromethanesulfonate-1-methyl-2-(4-trifluoromethylphenylethynyl)-3-[3-(4-trifluoromethylphenyl)-prop-2-ynyl]-3H-benzimidazol-1-ium.** The neutral benzimidazole (150 mg, 0.32 mmol, 1 eq) was dissolved in Et<sub>2</sub>O (2.1 mL) and DCE (3.2 mL) (0.06 M final concentration, 3:2 DCE:Et<sub>2</sub>O). A solution of methyl triflate (58 μL, 0.51 mmol, 1.6 eq) in Et<sub>2</sub>O (2.0 mL) was added dropwise, and the solution was warmed to room temperature. The product formed as an orange solid precipitate which was isolated by vacuum filtration, then recrystallized from DCE/Et<sub>2</sub>O to give a pale yellow solid (126.3 mg, 0.20 mmol, 62%). An analytical sample was obtained by performing a second recrystallization from DCE/Et<sub>2</sub>O then dissolving the product in DCM, performing a filtration using a syringe-tip 0.2 μM filter, and adding hexanes to precipitate the product in the -20 °C freezer (60 mg, 0.094 mmol, 29%). <sup>1</sup>H NMR (MeCN): δ 8.11 (2H, d, *J* = 8.0 Hz); 8.04-8.01 (1H, m); 7.96-7.93 (1H, m); 7.83 (2H, d, *J* = 8.2 Hz); 7.80-7.77 (2H, m); 7.56 (2H, d, *J* = 8.0 Hz); 7.34 (2H, d, *J* = 8.0 Hz); 5.54 (2H, s); 4.02 (3H, s). <sup>13</sup>C NMR could not be obtained, as rate of decomposition occurred on NMR timescale. LRMS (CI<sup>+</sup>): 481 (M<sup>+</sup>-OTf-H<sub>2</sub>). HRMS calcd for C<sub>27</sub>H<sub>17</sub>F<sub>6</sub>N<sub>2</sub><sup>+</sup> 483.1290, found 481.1342. IR (KBr): 3421, 2921, 1655, 1618, 1581, 1545, 1510, 1480, 1460, 1438, 1262, 1224, 1152, 1032, 799, 638 cm<sup>-1</sup>. Mp (decomp): 248.3-250.3 °C.

## **3.7.2. Biology**

### **3.7.2.1. General**

<sup>32</sup>P-γ-ATP (Ultratide Isoblu) was purchased from MP Biomedicals. T4 polynucleotide kinase was purchased from either Invitrogen or New England Biolabs. Pre-mixed 5x polynucleotide kinase buffer from Invitrogen was used with both enzymes. Formamide loading buffer was a mixture of formamide (Aldrich) with 0.05 M EDTA (pH 8 before mixing). For preparative gels, no dyes were added. For analytical gels, 0.25% by weight each bromophenol blue and xylene cyanol were added. φx174RF plasmids were obtained from Fermentas.

### **3.7.2.2. General protocol for radiolabeling DNA**

In an 1.5 mL sterile Eppendorf tube, 1 μL DNA (40 μM in 1X TE buffer, 1 pmol) was combined with 6 μL 5x PNK buffer, 16 μL sterile H<sub>2</sub>O. To this mixture was added 6 μL <sup>32</sup>P-ATP and 1 unit (1 μL) T4-polynucleotide kinase. Samples were mixed gently, then incubated in a 37 °C water bath for 1 h. After 1 h, an additional 1 unit (1 μL) T4-PNK was added, and the labeling reaction was incubated for 1 h further. After 2 h total incubation, the enzyme was inactivated by heating to 65 °C for 10 min, after which excess <sup>32</sup>P-ATP was removed by purification via Bio-Rad P-6 micro bio-spin column (according to manufacturer insert).

### **3.7.2.3. General protocol for DNA Purification**

DNA was concentrated to dryness under vacuum centrifugation then treated with 70 μL 10% aqueous piperidine at 90 °C for 30 min. After piperidine/heat treatment, samples were again concentrated by vacuum centrifugation. Samples were diluted to 55 μL using formamide loading buffer, then purified on a 20% denaturing acrylamide gel

(75 mm spacer thickness, 14 x17 inches). Electrophoresis was run at 1100-1200 V (to maintain a temperature of approx. 60 °C) in 1X TBE buffer for times varying with the size of the DNA. The 22-mer required 2.5 h to obtain good separation. Bands were visualized using X-ray film, cut out, and extracted with water overnight. The water containing the eluted DNA was concentrated by vacuum centrifugation to 100 µL, and 20 µL 3M NaOAc (pH 5) was added, then 500 µL cold (-20 °C) EtOH was added. Samples were cooled to -20 °C for approx. 1 h, then pelleted by centrifuging at 15,000xg for 6 min. The supernatant was removed by pipet, and the pelleted DNA was washed twice with 200 µL cold EtOH. The pellet was redissolved in 100 µL H<sub>2</sub>O and 20 µL 3M NaOAc (pH 5), then treated with 500 µL cold EtOH. The sample was cooled to -20 °C, for approx. 1 h, then the same procedure was followed to pellet the DNA. The pellet was rinsed with cold (-20 °C) 70% aqueous EtOH (2x 200 µL). The resuspension and pelleting process was repeated once more to ensure full removal of urea and salts.

#### ***3.7.2.4. General protocol for DNA Annealing***

Radiolabeled DNA (combined from 4 labeling reactions) was diluted with water buffer to a volume of 38 µL in a 250 µL PCR tube. To this was added 5 µL 10X TE buffer (to make 1X final concentration), 5 µL 5 M NaCl (to make 0.5 M final concentration), and 2 µL of the complementary sequence (40 µM, 40 pmol). The oligomer was annealed according to the following temperature regime: Heated to 90 °C for 5 min, then cooled at a rate of 10 °C every 10 min, pausing at T<sub>m</sub>. Annealing was analyzed by running a non-denaturing analytical gel, 20% acrylamide at 1200 V at 4 °C, exposing the gel to a phosphor screen, and using a phosphorimager to visualize the results.

Maxam-Gilbert sequencing was performed according to literature.<sup>64</sup>

### **3.7.2.5. General protocol for DNA/drug incubations**

In a 1.5 mL Eppendorf tube was combined H<sub>2</sub>O, sodium phosphate buffer, DNA (50,000 cpm), and the AZB derivative in DMSO. Samples were incubated at 37 °C for 2 h. Following incubation, the reaction mixture was extracted with 50 µL CHCl<sub>3</sub>, then 20 µL 3M NaOAc (pH 5) and 500 µL cold EtOH (-20 °C) was added. Samples were cooled to -20 °C for approx. 1h, then pelleted by centrifuging at 15,000xg for 6 min. The pellet was rinsed with cold (-20 °C) 70% aqueous EtOH (2x 200 µL). Samples were then diluted with formamide loading buffer (formamide with 0.05 M EDTA, pH 8, 0.25% w/v xylene cyanol and 0.25% w/v bromophenol blue) and run on a 20% denaturing analytical acrylamide gel (20 mm spacer thickness, 14"x17") at 2000 V for approx. 2.5 h. The gel was then dried for 60 min. *in vacuo* with heating to 90 °C. Following overnight exposure to a phosphor screen, the gel was imaged using a Typhoon Trio phosphorimager (GE Healthcare). Quantitation was performed using ImageQuant TL 2005 from Amersham Biosciences. Lanes and bands were automatically detected, then manually resized. Background subtraction was "rolling ball" type, typically set to a radius size of 12. Images were manipulated using Adobe Photoshop Elements 6.0 to crop, adjust contrast, and sharpen blurring. No processing was performed which would change the relative intensity of the bands, and processing was done following quantitation.

Nicking assays were analyzed using 0.8% TAE-Agarose gel electrophoresis with 5 µg/mL ethidium bromide (gel volume approx. 50 mL). Plasmids were diluted with 1/6 volume of 6X DNA loading dye and the samples were electrophoresed for 30 minutes at 100 V, at 300 mA. After electrophoresis, DNA was visualized using a UV illumination source. Quantitation was performed using ImageQuant TL 2005 from Amersham Biosciences. Lanes and bands were automatically detected, then manually resized. Background subtraction was "rolling ball" type, typically set to a radius size of 12.

Images were manipulated using Adobe Photoshop Elements 6.0 to crop, adjust contrast, and sharpen blurring. No processing was performed which would change the relative intensity of the bands, and processing was done following quantitation.

### 3.8. REFERENCES

- (1) Nicolaou, K. C.; Smith, A. L. *Acc. Chem. Res.* **1992**, *25*, 497-503.
- (2) Jones, R. R.; Bergman, R. G. *J. Am. Chem. Soc.* **1972**, *94*, 660-661.
- (3) Cramer, C. J. *J. Am. Chem. Soc.* **1998**, *120*, 6261-6269.
- (4) Hoffner, J.; Schottelius, M. J.; Feichtinger, D.; Chen, P. *J. Am. Chem. Soc.* **1998**, *120*, 376-385.
- (5) Sherer, E. C.; Kirschner, K. N.; Pickard IV, F. C.; Rein, C.; Felgus, S.; Shields, G. *C. J. Phys. Chem. B* **2008**, *112*, 16917-16934.
- (6) David, W. M.; Kerwin, S. M. *J. Am. Chem. Soc.* **1997**, *119*, 1464-1465.
- (7) Feng, L.; Zhang, A.; Kerwin, S. M. *Org. Lett.* **2006**, *8*, 1983-1986.
- (8) Winkler, M.; Cakir, B.; Sander, W. *J. Am. Chem. Soc.* **2004**, *126*, 6135-6149.
- (9) Kraka, E.; Cremer, D. *J. Mol. Struct.* **2000**, *506*, 191-211.
- (10) Kraka, E.; Cremer, D. *J. Comput. Chem.* **2001**, *22*, 216-229.
- (11) Kerwin, S. M.; Nadipuram, A. *Synlett* **2004**, *8*, 1404-1408.
- (12) Nadipuram, A. K.; Kerwin, S. M. *Tetrahedron* **2006**, *62*, 3798-3808.
- (13) Nadipuram, A. K.; Kerwin, S. M. *Tetrahedron Lett.* **2006**, *47*, 353-356.
- (14) Myers, A. G.; Kuo, E. Y.; Finney, N. S. *J. Am. Chem. Soc.* **1989**, *111*, 8057-8059.
- (15) Nagata, R.; Yamanaka, H.; Okazaki, E.; Saito, I. *Tetrahedron Lett.* **1989**, *30*, 4995-4998.
- (16) Myers, A. G.; Dragovich, P. S.; Kuo, E. Y. *J. Am. Chem. Soc.* **1992**, *114*, 9369-9386.

- (17) Cremeens, M. E.; Hughes, T. S.; Carpenter, B. K. *J. Am. Chem. Soc.* **2005**, *127*, 6652-6651.
- (18) Feng, L.; Kumar, D.; Birney, D. M.; Kerwin, S. M. *Org. Lett.* **2004**, *6*, 2059-2062.
- (19) Schreiner, P. R.; Navarro-Vasquez, A.; Prall, M. *Acc. Chem. Res.* **2005**, *38*, 29-37.
- (20) Schmittel, M.; Strittmatter, M.; Kiau, S. *Tetrahedron Lett.* **1995**, *36*, 4975-4978.
- (21) Schmittel, M.; Vavilala, C. *J. Org. Chem.* **2005**, *70*, 4865-4868.
- (22) Schmittel, M.; Mahajan, A. A.; Bucher, G.; Bats, J. W. *J. Org. Chem.* **2007**, *72*, 2166-2173.
- (23) Tuesuwan, B. Dissertation, The University of Texas at Austin, 2007.
- (24) Kumar, D. *Bioorg. Med. Chem. Lett.* **2001**, *11*, 2971-2974.
- (25) Tuntiwechapikul, W.; David, W. M.; Kumar, D.; Salazar, M.; Kerwin, S. M. *Biochemistry* **2002**, *41*, 5283-5290.
- (26) David, W. M.; Kumar, D.; Kerwin, S. M. *Bioorg. Med. Chem. Lett.* **2000**, *10*, 2509-2512.
- (27) Tuesuwan, B.; Kerwin, S. M. *Biochemistry* **2006**, *45*, 7265-7276.
- (28) David, W. M. Dissertation, The University of Texas at Austin, 2000.
- (29) Sherman, C. L.; Pierce, S. E.; Brodbelt, J. S.; Tuesuwan, B.; Kerwin, S. M. *J. Am. Soc. Mass Spectrom.* **2006**, *17*, 1342-1352.
- (30) Strahl, B. D.; Allis, C. D. *Nature* **2000**, *403*, 41-45.
- (31) Jenuwein, T.; Allis, C. D. *Science* **2001**, *293*, 1074-1180.
- (32) Szyf, M. *Biochemistry (Moscow)* **2005**, *70*, 533-549.
- (33) Razin, A.; Riggs, A. D. *Science* **1980**, *210*, 604-610.



- (34) Razin, A.; Szyf, M. *Biochim. Biophys. Acta* **1984**, *782*, 29-36.
- (35) Momparler, R. L.; Bovenzi, V. *J. Cell. Physiol.* **2000**, *183*, 145-154.
- (36) Ramchandani, S.; Bhattacharya, S. K.; Cervoni, N.; Szyf, M. *Proc. Natl. Acad. Sci. U. S. A.* **1999**, *96*, 6107-6112.
- (37) Turnbull, J. F.; Adams, R. L. *Nucleic Acids Res.* **1976**, *3*, 677-695.
- (38) Pradhan, S.; Esteve, P. O. *Clin. Immunol. Immunopathol.* **2003**, *109*, 6-16.
- (39) Ordway, J. M.; Bedell, J. A.; Citek, R. W.; Nunberg, A.; Garrido, A.; Kendall, R.; Stevens, J. R.; Cao, D.; Doerge, R. W.; Korshunova, Y.; Holemon, H.; McPherson, J. D.; Lakey, N.; Leon, J.; Martienssen, R. A.; Jeddloh, J. A. *Carcinogenesis* **2006**, *27*, 2409-2423.
- (40) Denissenko, M. F.; Chem, J. X.; Tang, M.-s.; Pfeifer, G. P. *Proc. Natl. Acad. Sci. U. S. A.* **1997**, *94*, 3893-3898.
- (41) Nelson, D. L.; Cox, M. M. *Lehninger Principles of Biochemistry*; Third ed.; Worth Publishers: New York, 2000.
- (42) Bae, J.-B.; Kim, Y.-J. *Animal and Cell Systems* **2008**, *12*, 117-135.
- (43) Baylin, S. B.; Makos, M.; Wu, J.; Yen, R.-W. C.; deBustrs, A.; Vertino, P.; Nelkin, B. D. *Cancer Cells* **1991**, *3*, 383-390.
- (44) Esteller, M.; Fraga, M. F.; Guo, M.; Garcia-Foncillas, J.; Hedenfalk, I.; Godwin, W. K.; Trojan, J.; Vaurs-Barriere, C.; Bignon, Y. J.; Ramus, S.; Benitez, J.; Caldes, T.; Akiyama, Y.; Yuasa, Y.; Launonen, V.; Canal, M. J.; Rodriguez, R.; Capella, G.; Peinado, M. A.; Borg, A.; Aaltonen, L. A.; Ponder, B. A.; Baylin, S. B.; Herman, J. G. *Hum. Mol. Genet.* **2001**, *10*, 3001-3007.

- (45) Shi, H.; Maier, S.; Nimmrich, I.; Yan, P. S.; Caldwell, C. W.; Olek, A.; Huang, T. *H. J. Cell. Biochem.* **2003**, *88*, 138-143.
- (46) Paz, M. F.; Fraga, M. F.; Avila, S.; Guo, M.; Pollan, M.; Herman, J. G.; Esteller, M. *Cancer Res.* **2003**, *63*, 1114-1121.
- (47) Uhlmann, K.; Rohde, K.; Zeller, C.; Szymas, J.; Vogel, S.; Marczinek, K.; Thiel, G.; Nurnberg, P.; Laird, P. W. *Int. J. Cancer* **2003**, *106*, 52-59.
- (48) Adorjan, P.; Distler, J.; Lipscher, E.; Model, F.; Muller, J.; Pelet, C.; Baun, A.; Florl, A. R.; Gutig, D.; Grabs, G.; Howe, A.; Kursar, M.; Lesche, R.; Leu, E.; Lewin, A.; Maier, S.; Muller, V.; Otto, T.; Scholz, C.; Shulz, W. A.; Seifert, H. H.; Schwoppe, I.; Ziebarth, H.; Berlin, K.; Piepenbrock, C.; Olek, A. *Nucleic Acids Res.* **2002**, *20*, 21.
- (49) Chen, C. M.; Chen, H. L.; Hsiau, A. H.; Shi, H.; Brock, G. J.; Wei, S. H.; Caldwell, C. W.; Yan, P. S.; Huang, T. H. *Am. J. Pathol.* **2003**, *163*, 37-45.
- (50) Vanyushin, B. F. *Biochemistry (Moscow)* **2005**, *70*, 598-611.
- (51) Feng, Z.; Hu, Y.; Tang, M.-s. *Proc. Natl. Acad. Sci. U. S. A.* **2006**, *43*, 15404-15409.
- (52) Minnock, A.; Crow, S.; Bailly, C.; Waring, M. J. *Biochem. Biophys. Acta* **1999**, *1489*, 233-248.
- (53) Heinemann, U.; Alings, C.; Hahn, M. *Biophys. Chem.* **1994**, *50*, 157-167.
- (54) Zhang, N.; Lin, C.; Huang, X.; Kolbanovskiy, A.; Hingerty, B. E.; Amin, S.; Broyde, S.; Geacintov, N. E.; Patel, D. J. *J. Mol. Biol.* **2005**, *246*, 951-965.
- (55) Smith, L. E.; Denissenko, M. F.; Bennett, W. P.; Li, H.; Amin, S.; Tang, M.-s.; Pfeifer, G. P. *J. Natl. Cancer Inst.* **2000**, *92*, 803-811.

- (56) Greenblatt, M. S.; Bennett, W. P.; Hollstein, M.; Harris, C. C. *Cancer Res.* **1994**, *54*, 4855-4878
- (57) Feng, Z.; Hu, W.; Rom., W. N.; Beland, F. A.; Tang, M.-s. *Biochemistry* **2002**, *41*, 6414-6421.
- (58) Ross, M. K.; Mathison, B. H.; Said, B.; Shank, R. C. *Biochem. Biophys. Res. Commun.* **1999**, *254*, 114-119.
- (59) Kouidou, S.; Agidou, T.; Kyrkou, A.; Andreou, A.; Katopodi, T.; Georgiou, E.; Krikelis, D.; Dimitriadou, A.; Spanos, P.; Tsilikas, C.; Destouni, H.; Tzimagiorgis, G. *Lung Cancer* **2005**, *50*, 299-307.
- (60) Ziegel, R.; Shallop, A.; Upadhyaya, P.; Jones, R.; Tretyakova, N. *Biochemistry* **2004**, *43*, 540-549.
- (61) Carey, F. A.; Sundberg, R. J. *Advanced Organic Chemistry, Part A: Structure and Mechanisms*; 4 ed.; Kluwer Academic / Plenum Publishers: New York, 2000.
- (62) Lowry, T. H.; Richardson, K. S. *Mechanism and Theory in Organic Chemistry*; 3 ed.; HarperCollinsPublishers, Inc.: New York, 1987.
- (63) Patrinos, G. P.; Garinic, G.; Kounelis, S.; Kouri, E.; Menounos, P. *J. Mol. Med.* **1999**, *77*, 686-689.
- (64) Sambrook, J.; Russell, D. W. *Molecular Cloning: A Laboratory Manual*; Cold Spring Harbor Laboratory Press: Cold Spring Harbor, 2001.
- (65) Slatko, B. E.; Albright, L. M. In *Current Protocols in Molecular Biology*; John Wiley and Sons: New York; Vol. 1, p 7.5.1-7.6.13.
- (66) Barlow, T.; Dipple, A. *Chem. Res. Toxicol.* **1998**, *11*, 44-53.

- (67) Latif, F.; Moschel, R. C.; Hemminki, K.; Dipple, A. *Chem. Res. Toxicol.* **1988**, *1*, 364-369.
- (68) Tuntiwechapikul, W.; David, W. M.; Kumar, D.; Salazar, M.; Kerwin, S. M. *Biochemistry* **2002**, *41*, 5283-5290.
- (69) Müller, E.; Zountas, G. *Chem. Ber.* **1972**, *105*, 2529-2533.
- (70) Journet, M.; Cai, D.; DiMichele, L. M.; Larsen, R. D. *Tetrahedron Lett.* **1998**, *39*, 6427-6428.
- (71) Still, W. C.; Kahn, M.; Mitra, A. *J. Org. Chem.* **1978**, *43*, 2923-2924.
- (72) Gottlieb, H. E.; Kotlyar, V.; Nudelman, A. *J. Org. Chem.* **1997**, *62*, 7512-7515.
- (73) Lee, K. Y.; Lee, M. J.; GowriSankar, S.; Kim, J. N. *Tetrahedron Lett.* **2004**, *45*, 5043-5046.
- (74) Wadsworth, D. H.; Geer, S. M.; Detty, M. R. *J. Org. Chem.* **1987**, *52*, 3662-3668.

## 4. UK-1 Analog Synthesis

### 4.1. BACKGROUND

Benzoxazole natural products have been shown to have promising biological activity.<sup>1-7</sup> This chapter will describe efforts towards synthesizing analogs of UK-1 using a palladium-catalyzed biaryl coupling. First, background will be provided on the biological activity of some known anticancer benzoxazole natural products. Then, current methods to synthesize 2-arylbenzoxazoles will be reviewed. The route to UK-1 analogs and its optimization will then be presented, and future structure-activity relationship studies will be described.

#### 4.1.1. Benzoxazole Natural Products

Benzoxazole natural products are relatively uncommon and show novel biological properties, including potent cytotoxicity.

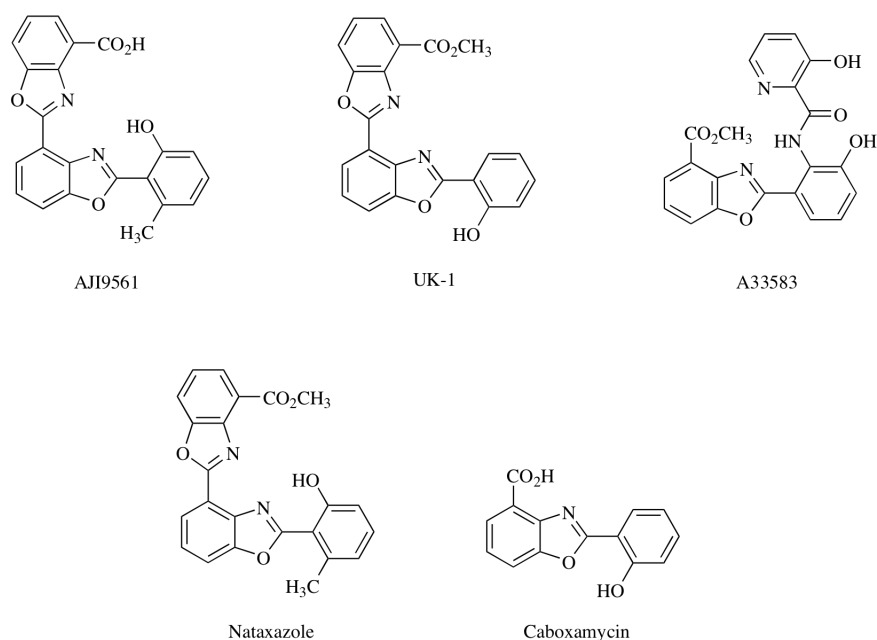


Figure 4.1. Benzoxazole-containing natural products.

Many of these benzoxazole natural products (Figure 4.1) have been isolated as part of a natural product isolation program focused on small molecule organic compounds produced in the

fermentation broth of *streptomyces* samples from diverse locations. All of the isolated bis(benzoxazoles) are connected from C4 of one ring to C2 of the second heterocycle. Bis(benzoxazole) AJI9561, isolated from fermentation of soil samples collected at Chibra, Japan, displays activity against Jurkat and P388 cells (0.88 and 1.63  $\mu\text{M}$ , respectively).<sup>5</sup> A33583 was isolated from a fermentation broth of *streptomyces* strain NRRL 12068. It was originally characterized as having antibiotic activity, but more recently, it was reported to have good antileishmanial (antiparasitic) activity.  $\text{IC}_{50}$  values against *L. donovani*, a common vector for antileishmaniasis, a parasitic infection, were 50 nM.<sup>7</sup> The compound's activity is not attributable to general cytotoxicity, because it has a much higher an  $\text{IC}_{50}$  against L6 cells (14  $\mu\text{M}$ ) than its antileishmanial effective dose.<sup>7</sup>

Nataxazole, isolated in 2008, is isolated from *streptomyces* strain Tü 6176, a sample collected at Mata de Estrela, RN, Brazil.<sup>6</sup> Its  $\text{ED}_{50}$  was measured in MCF7 (breast adenocarcinoma, 0.68  $\mu\text{g/mL}$ ), HepG2 (hepatocellular carcinoma, 0.068  $\mu\text{g/mL}$ ), and AGS (gastric adenocarcinoma, 0.4  $\mu\text{g/mL}$ ) cells.<sup>6</sup> A cell cycle study showed accumulation of cells at S phase and reduced numbers at G2/M phase. UK-1 (*vide supra*) shows a similar pattern, implying that they operate by the same mechanism, and also that they are both topoisomerase II inhibitors.<sup>6</sup>

Caboxamycin is a monobenzoxazole isolated from a marine strain of *streptomyces* collected in the Canary Basin (located near Morocco in the Atlantic Ocean) strain NTK 937.<sup>4</sup> Unlike many of the other *streptomyces*-produced benzoxazoles, Caboxamycin shows antibiotic activity against many strains of bacteria and yeast, summarized in Table 4.1.<sup>4</sup> Cytotoxicity was measured for cell types AGS (7.5  $\mu\text{g/mL}$ ), Hep G2 (7.4  $\mu\text{g/mL}$ ), and MCF7 (7.3  $\mu\text{g/mL}$ ).<sup>4</sup>

Table 4.1. Activity of Caboxamycin against various bacteria and yeasts

Biological	Caboxamycin $\text{EC}_{50}$ ( $\mu\text{M}$ )	Positive control ( $\mu\text{M}$ ) <sup>1</sup>
<i>Bacillus subtilis</i>	8	9
<i>Staphylococcus lentus</i>	20	14

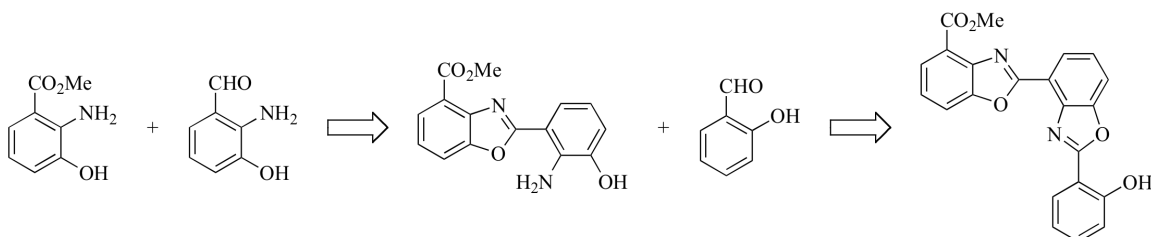
<i>Candida glabrata</i>	117	4
<i>Xanthomonas campestris</i>	43	6
<i>Ralstonia solanacearum</i>	176	75
<i>Staphylococcus epidermis</i>	43	7

<sup>1</sup>Positive Control for prokaryotes is chloramphenicol, for eukaryotes is cycloheximide

UK-1 is a *bis*(benzoxazole) with anticancer activity but no antifungal or antibacterial activity.<sup>1-3,8</sup> UK-1 was first isolated in 1993 from the mycelial cake of acetoniycete strain 517-02.<sup>8</sup> The acetoniycete strain was found in soil collected from the Sugimoto campus Osaka City University.<sup>8</sup> The stock organism was fermented with a seed medium (100 mL) consisting of 1% glucose, 1% soluble starch, 0.6% wheat germ, 0.5% peptone, 0.3% yeast extract, 0.2% soybean meal, and 0.2% CaCO<sub>3</sub> (pH 7.0 before stabilization).<sup>8</sup> This mixture was incubated on a rotary shaker (220 rpm) at 30 °C for 48 h, after which a small amount (30 mL) of this fermentation was transferred into another 3 L of seed medium.<sup>8</sup> After an additional 48 h of incubation at 30 °C with aeration at 3 L/min and agitation of 500 rpm, the mixture was added to 300 L of production medium consisting of 3% glucose, 0.5% malt extract, 0.5% yeast extract, and 0.2% CaCO<sub>3</sub> and fermented for a final 48 h at 30 °C with agitation at 250 rpm.<sup>8</sup>

Following incubation, the fermentation was filtered, and the solid, the mycelial cake, was extracted with acetone, which was subsequently concentrated and extracted with chloroform.<sup>8</sup> The resultant organic layer was concentrated, then the crude material was purified with silica gel chromatography (eluting with chloroform) and recrystallization from methanol to yield 550 mg pure UK-1.<sup>8</sup> The structure was elucidated through a combination of 2-D NMR spectroscopy and independent fragment synthesis.<sup>2</sup> Ueki and coworkers proposed a biosynthetic pathway that proceeds via condensation of 3-hydroxyanthranilic acid methyl ester onto 2-amino-3-hydroxybenzaldehyde. The subsequent benzoxazole then undergoes a second condensation with salicylaldehyde to form UK-1 (Scheme 4.1).

At concentrations up to 100  $\mu\text{g/mL}$ , UK-1 did not show any inhibitory activity against yeast, fungi, or bacteria (Gram-negative or Gram-positive).<sup>1-3,8</sup> Interestingly, UK-1 did show cytotoxic activity.<sup>8</sup> The effective dose to inhibit growth by 50% ( $\text{ED}_{50}$ ) was 1.17 for B16 cells, 1.22 for HeLa cells, and 0.11  $\mu\text{g/mL}$  for P388 cells (mouse leukemia).<sup>8</sup> In a later report, UK-1 showed an  $\text{ED}_{50}$  of 1.9  $\mu\text{g/mL}$  against AGF cells, 0.65 against MCF7 cells, 0.085 against HepG2 cells.<sup>6</sup>



Scheme 4.1. Proposed Biosynthesis of UK-1<sup>2</sup>

#### 4.1.2. Mode of Action

Although, its mechanism of action is unknown, UK-1 is thought to inhibit topoisomerase II (TopoII).<sup>9</sup> Topoisomerases regulate structure (topology) of DNA via series of cleavages and religations.<sup>9</sup> TopoII, a member of the family of topoisomerases, causes double-stranded breaks in DNA.<sup>9</sup> Compounds that interfere with topoisomerase activity typically cause cell death. Additionally, UK-1 is thought to chelate  $\text{M}^{2+}$  ions (Figure 4.2). UK-1 has a unique biological reactivity profile but suffers from poor solubility in aqueous media, which limits possibilities for drug development. The Kerwin group reported a minimum pharmacophore that is synthetically more accessible but retains similar cytotoxicity.<sup>10</sup>

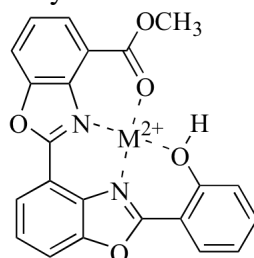


Figure 4.2. UK-1-metal ion complex



### 4.1.3. Previous Total Synthesis of UK-1 and Biaryl Analogs

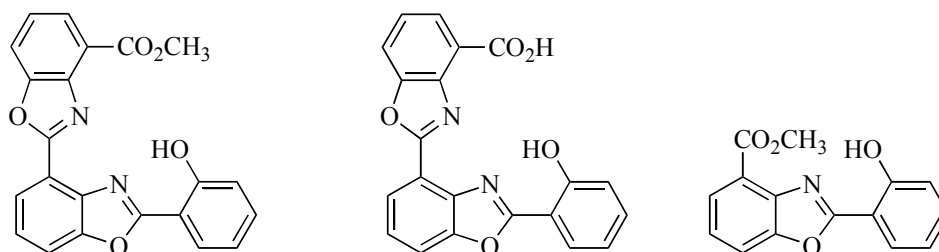
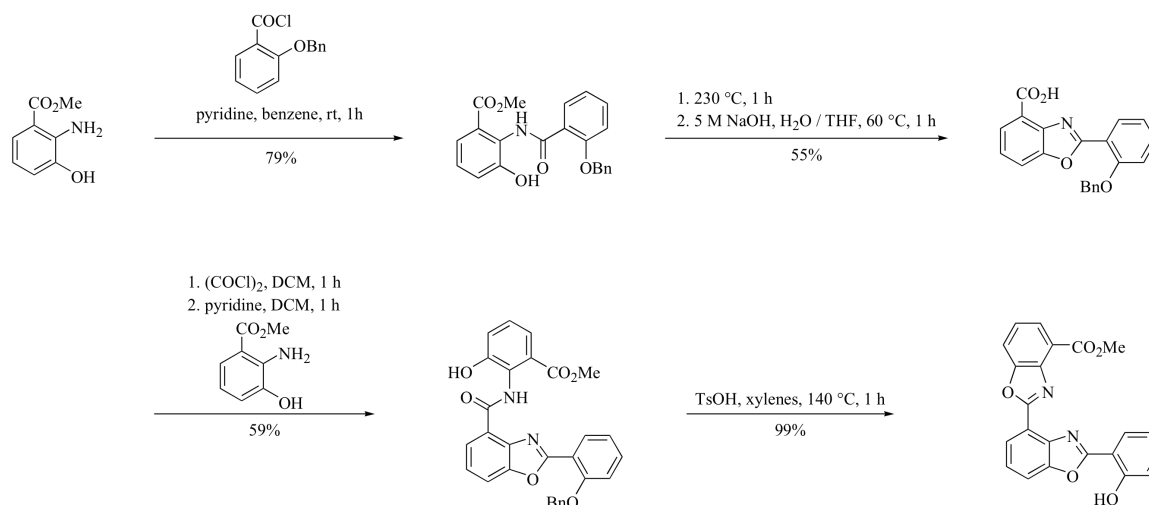


Figure 4.3. UK-1 (l), Demethyl UK-1 (center), and minimum pharmacophore (r).

The Kerwin group became interested in UK-1 for its highly selective cytotoxicity. It is unusual for a compound that is cytotoxic to show little antibiotic or antifungal activity. They reported a total synthesis of UK-1 in 1997 (Scheme 4.2).<sup>11</sup> This total synthesis begins with the methyl ester of 3-hydroxyanthranilic acid. This compound is acylated to form the corresponding amide with the acid chloride of 2-benzyloxybenzoic acid in good yield. The resulting amide is then subjected to neat thermolysis to form the benzoxazole ring *via* condensation, then base is used to saponify the methyl ester. The combined yield for these steps is moderate. The free acid can then be converted to the acid chloride and used to acylate a second 3-hydroxyanthranilic acid methyl ester, which proceeds in moderate yield. The second benzoxazole ring is then closed *via* an acid-catalyzed ring-closing in refluxing xylenes in quantitative yield. Overall, the synthesis requires four steps and generates UK-1 in 25% yield.



Scheme 4.2. Total Synthesis of UK-1<sup>11</sup>

Although the total synthesis of UK-1 (Scheme 4.2) is short and takes advantage of the pseudosymmetry of the *bis*(benzoxazole) system, a new route which allows for higher functional group tolerance and later divergence is needed for an effective analog synthesis. In the case of the minimum pharmacophore, the benzoxazole ring is closed *via* a thermolysis requiring very high temperatures and has proved to be incompatible with several functional groups.<sup>10</sup> Other groups have reported similar approaches to synthesis of analogous benzoxazole systems. Smith *et al.* reported a series of analogs lacking the methyl ester moiety to determine which functional groups were required for TopoII inhibition.<sup>9</sup> They used traditional coupling chemistry to form the same amide from 3-hydroxyanthranilic acid methyl ester and 2-benzyloxybenzoic acid that Kerwin *et al.* used, followed by the same thermolysis.<sup>11</sup> Following deprotection, a second amide coupling generates the open *bis*(benzoxazole) precursor, which is closed using catalytic toluenesulfonic acid in refluxing toluene.<sup>9</sup>

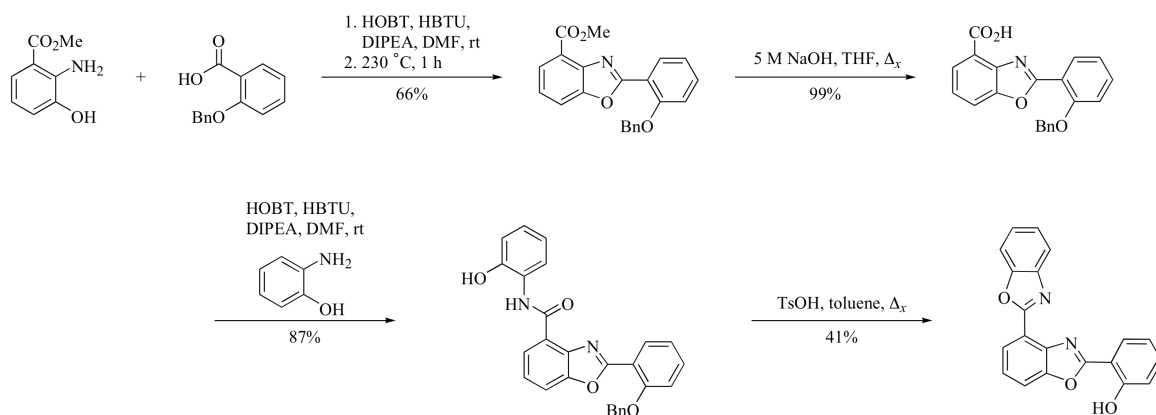


Figure 4.4. Synthesis by Smith *et al.* of analogs of UK-1 lacking C4-methyl ester<sup>12</sup>

Smith *et al.* also produced analogs lacking the 2'-hydroxyl group on the C2-position of the benzoxazole with or without the methyl ester.<sup>9</sup> Using a similar route, involving ring-closing of amides onto phenols, they generated the desired *bis*(benzoxazoles).<sup>9</sup>

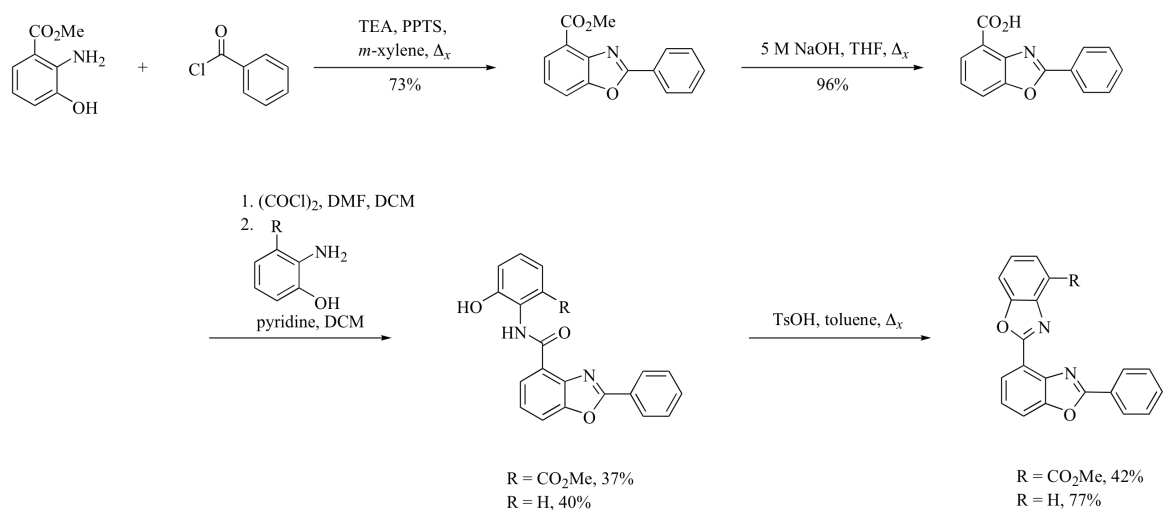


Figure 4.5. Synthesis by Smith *et al.* of UK-1 analogs lacking 2'-hydroxyl group<sup>12</sup>

Activity of the *bis*(benzoxazole) analogs at inhibiting human topoisomerase II was compared to UK-1. Deletion of either the *o*-hydroxyl or the methyl ester does not show a significant effect on topoII inhibition, but deletion of both groups leads to no inhibition at the highest concentrations assayed (80  $\mu$ M). UK-1 shows an IC<sub>50</sub> of 32  $\mu$ M; deletion of the methyl ester leads to an IC<sub>50</sub> of 20  $\mu$ M, and deletion of the *o*-hydroxyl group gives an IC<sub>50</sub> of 38  $\mu$ M.<sup>9</sup>

Smith *et al.* propose that distance between the Lewis basic sites on the system is critical for activity.<sup>9</sup> Computational studies on these analogs found that there appears to be a required geometry of Lewis basic sites for good activity against TopoII. The Lewis basic sites should form a triangle with sides equal to 2.875-3.045 Å on two sides and 4.524-4.727 Å on the third (Figure 4.6).<sup>9</sup> This arrangement likely is required for effective metal ion binding.

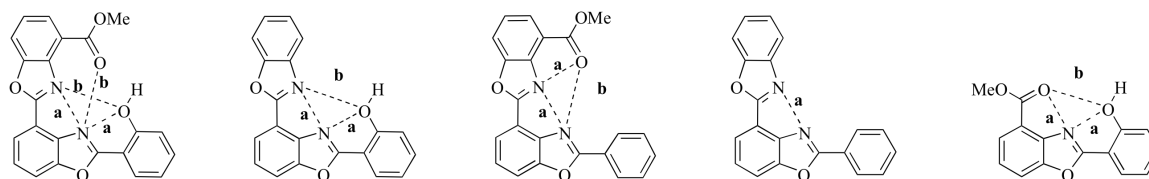


Figure 4.6. Model of Lewis basic sites on topoisomerase II inhibitors.

The modeled distance range for *a* is 2.875-3.045 Å and *b* is 4.524-4.727 Å.<sup>12</sup>

The heteroaromatic ring is not required to be a *bis*(benzoxazole). A *bis*(benzimidazole) analog synthesized by Kerwin *et al.* (Figure 4.7) showed 22.2 μM IC<sub>50</sub> for A549 cells, similar to UK-1 (5.1 μM), and showed low μM activity for a range of cell lines.<sup>12</sup> This structure also can form the requisite arrangement of Lewis basic sites.

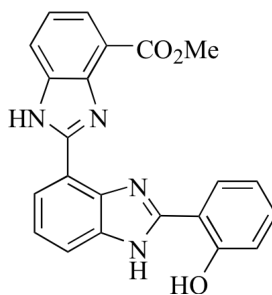
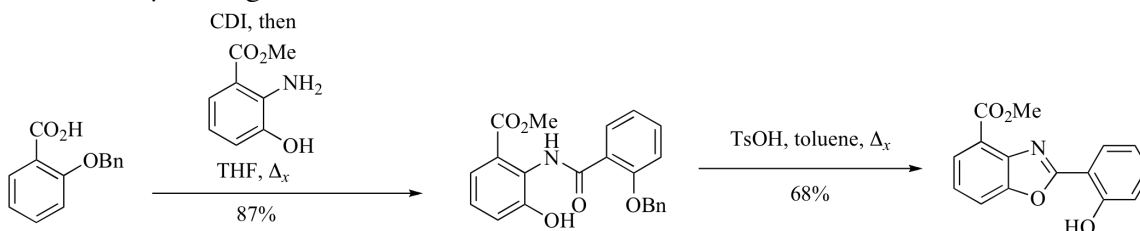


Figure 4.7. *Bis*(benzimidazole) UK1 analog reported by Kerwin *et al.*<sup>9</sup>

#### 4.1.4. Mono-Benzoxazole or -Benzimidazole UK-1 Analogs

The Kerwin group, along with others,<sup>9,12</sup> has been evaluating structure-activity relationships for UK-1 analogs. Because the *bis*(benzoxazole) scaffold is difficult to construct, a scaffold using single benzoxazole, benzimidazole, or benzothiazole was used. In 2001, the

Kerwin lab reported a minimum pharmacophore for UK-1 that retained the unusual selectivity of the parent compound. The compound reported was a mono-benzoxazole with a methyl ester at C4 and a 2-hydroxyphenyl at C2. The activity of this compound, **TOP027**, shown in Table 4.3, was in the low  $\mu\text{M}$  range.



Scheme 4.3. Route to benzoxazole UK-1 analog **TOP027** reported by Kerwin *et al.*<sup>10</sup>

In a series of possible analogs, the analog **TOP027** was shown to be the most cytotoxic without showing significant antibiotic activity. As expected, 2-(2-hydroxyphenyl)benzoxazole was inactive in all assays. Other compounds which did not offer three Lewis basic sites which could readily coordinate metal ions did not show efficacy at concentrations below 100  $\mu\text{M}$ . For example, **TOP003**, **TOP004**, and **TOP029** incorporate a benzyl group capping the phenol and do not show significant cytotoxicity (Table 4.3).

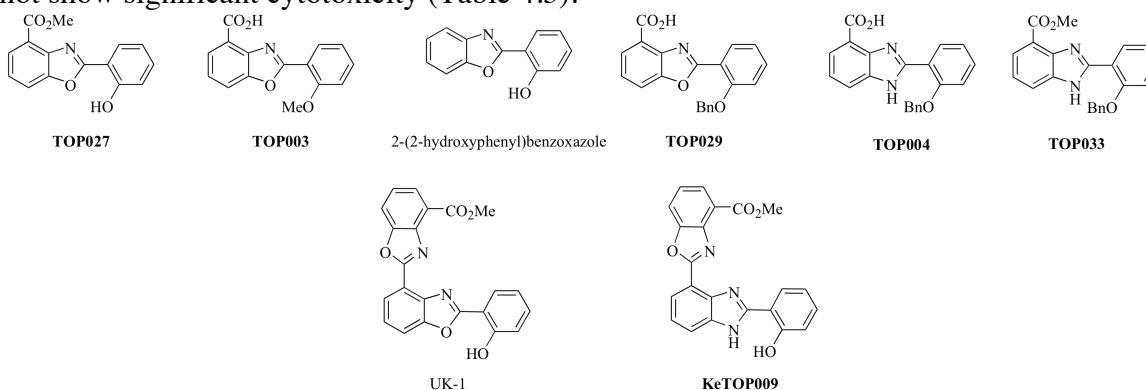


Figure 4.8. Structures assayed to find a minimum pharmacophore

Table 4.2. Cytotoxicity vs. antibacterial activity of minimum pharmacophores reported by Kerwin *et al.*<sup>10</sup>

Analog	<i>S. Aureus</i> IC <sub>50</sub>	<i>S. Aureus</i> (Meth-resistant)	Cytotoxicity <sup>1</sup>
--------	-----------------------------------	-----------------------------------	---------------------------

	$\mu\text{M}$	$\text{IC}_{50}, \mu\text{M}$	$\text{IC}_{50}, \mu\text{M}$
<b>TOP027</b>	NA	NA	0.88-9.1
<b>TOP003</b>	NA	NA	>100
2-(2-hydroxyphenyl) benoxazole	NA	NA	>100
<b>TOP033</b>	NA	NA	>100
<b>TOP009</b>	43	29	>100
UK-1	NA	NA	0.32-65
<b>TOP004</b>	102	102	>100

<sup>1</sup> Range is an average from the following cell lines: MCF7, HL60, HT29, PC-3 after 72h. <sup>2</sup> NA = no activity

In 2006, Chen and coworkers reported a series of benzoxazoles, benzimidazoles, and benzothiazoles (Figure 4.9).<sup>12</sup> They investigated cytotoxicity of benzoxazoles where the carbomethoxy group was located at C7 instead of C4, effectively reversing the nitrogen and oxygen on the benzoxazole ring relative to the ester and phenol.<sup>12</sup> This change proved to dramatically reduce the cytotoxicity of the compounds. Changing the heteroaromatic core but maintaining nitrogen at the 1-position did not cause significant differences in cytotoxicity of the compounds, although the benzothiazole was somewhat less cytotoxic than the benzimidazole or benzoxazoles. Again, maintaining the geometrical relationship between the three Lewis basic sites, the carbonyl at C4, the nitrogen of the benzoxazole or benzimidazole, and the free phenol, appears to provide the lowest  $\text{IC}_{50}$  values.

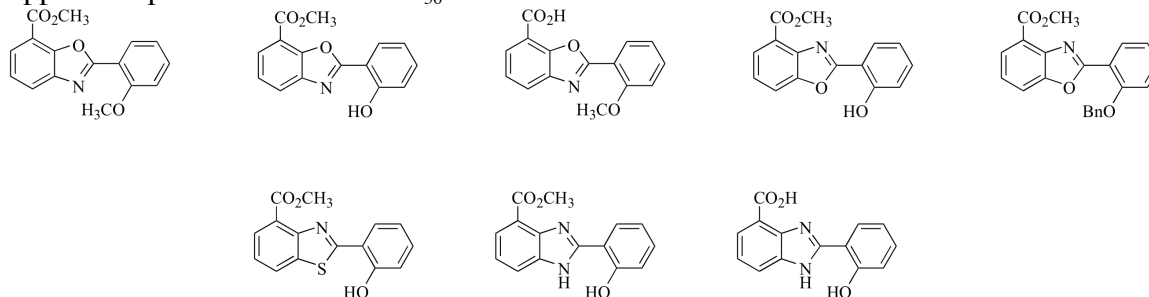


Figure 4.9. Benzimidazole and benzothiazole analogs of UK-1 reported by Chen *et al.*<sup>12</sup>

Table 4.3. Cytotoxicity studies on analogs varying the heteroaromatic ring<sup>12</sup>

Compound	IC <sub>50</sub> against cell line <sup>a</sup>				
	A549 <sup>b</sup>	BFTC-905 <sup>c</sup>	RD <sup>d</sup>	MES-SA <sup>e</sup>	HeLa <sup>f</sup>
N,O bis Me	>100	>100	>100	>100	52.6
N,O Me ester	>100	54.7	>100	89.4	67.6
N,O Me phenol	>100	>100	>100	>100	>100
<b>TOP027</b>	>100	49.6	58.5	>100	75.8
OMe/OBn	>100	89.2	Nd <sup>f</sup>	91.3	82.1
Thiazole	>100	87.3	39.1	76.7	81.6
Benzimid/ Me ester	74.1	37.9	35.9	33.2	31.5
Benzimid bis-OH	38.2	9.6	17.6	52.7	52.5

<sup>a</sup>IC<sub>50</sub> determined after 72 h. <sup>b</sup>Human lung carcinoma cell line <sup>c</sup> Human bladder carcinoma transitional cell line <sup>d</sup> Human rhabdomyosarcoma cell line <sup>e</sup> Human uterine sarcoma line <sup>f</sup> Human epithelial carcinoma cell line <sup>f</sup> Not determined

#### 4.1.5. C4 Benzoxazole Polar Analogs

In order to generate a library of compounds varied enough to acquire useful structure-activity relationship (SAR) data, varying substituents at both C2 (Figure 4.10, R<sub>2</sub>, blue) and C4 (Figure 4.10, R<sub>1</sub>, red) would provide the best possible combination. Previously, the Kerwin lab reported a series of C4 polar analogs and their biological information.<sup>13</sup>

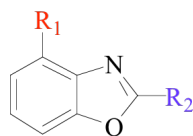
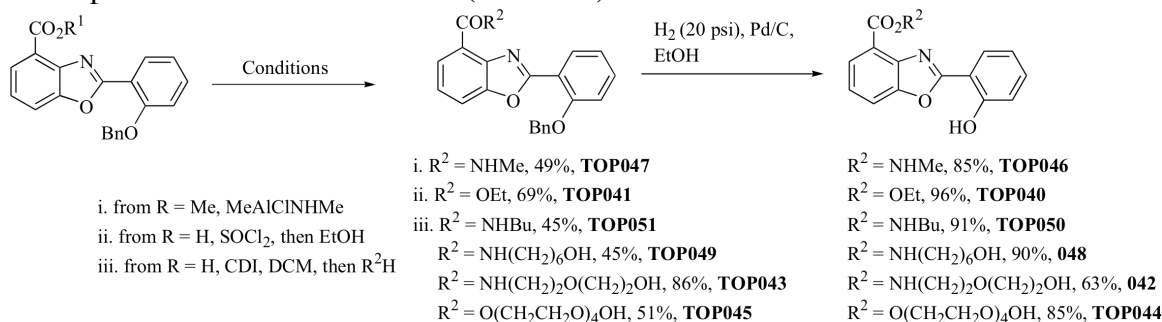


Figure 4.10. Positions to vary for SAR study

Beginning with the free carboxylic acid at C4, a library of amides and esters were synthesized (Scheme 4.4). Deprotection of the benzyl group on the phenol provided the small library of polar analogs. Esters (**TOP040** and **TOP044**) appeared to have low effective concentrations, regardless of size. **TOP046**, with a methyl amide showed comparable

cytotoxicity, but increasing the size of the amide appeared to raise  $IC_{50}$  values, meaning that these compounds were less efficacious (Table 4.4).



Scheme 4.4. C4 analogs of minimum pharmacophore<sup>13</sup>

Table 4.4. Cytotoxicity data for C4 UK-1 minimum pharmacophore analogs.<sup>13</sup>

Entry	Compound Number	IC <sub>50</sub> against	IC <sub>50</sub> against
		A549 (μM)	MCF7 (μM)
1	<b>TOP046</b> (R = NHMe)	10±8	11±1
2	<b>TOP040</b> (R = OEt)	15±5	40±10
3	<b>TOP050</b> (R = NHBu)	30±10	14±4
4	<b>TOP048</b> (R = NH(CH <sub>2</sub> ) <sub>6</sub> OH)	31±7	39±17
5	<b>TOP043</b> (R = NH(CH <sub>2</sub> ) <sub>2</sub> O(CH <sub>2</sub> ) <sub>2</sub> OH)	>50	41±17
6	<b>TOP044</b> (R = O(CH <sub>2</sub> CH <sub>2</sub> O) <sub>4</sub> OH)	13±2	11±1
7	UK-1	1.4±0.9	2.0±0.5

Metal binding of the C4 polar analogs was also assayed. There appeared to be a loose correlation between metal binding affinity; however, certain analogs did not follow the trend. The large ester (**TOP044**) and amide (**TOP043**) showed very tight metal binding, but relatively poor cytotoxicity compared to the other analogs (Table 4.5).

Table 4.5. Metal binding of C4 polar analogs



Entry	R	Mg <sup>2+</sup> (M <sup>-1</sup> )	Cu <sup>2+</sup> (M <sup>-1</sup> )
1	<b>TOP027</b> (R = OMe) <sup>10</sup>	3.2 x 10 <sup>5</sup>	ND
2	<b>TOP046</b> (R = NHMe)	6±2 x 10 <sup>5</sup>	>3 x 10 <sup>7</sup>
3	<b>TOP040</b> (R = OEt)	1.5±0.4 x 10 <sup>5</sup>	>3 x 10 <sup>7</sup>
4	<b>TOP050</b> (R = NHBu)	1.1±0.2 x 10 <sup>4</sup>	>6 x 10 <sup>7</sup>
5	<b>TOP048</b> (R = NH(CH <sub>2</sub> ) <sub>6</sub> OH)	2.4±0.4 x 10 <sup>4</sup>	>2 x 10 <sup>7</sup>
6	<b>TOP043</b> (R = NH(CH <sub>2</sub> ) <sub>2</sub> O(CH <sub>2</sub> ) <sub>2</sub> OH)	3±1 x 10 <sup>5</sup>	>7 x 10 <sup>7</sup>
7	<b>TOP044</b> (R = O(CH <sub>2</sub> CH <sub>2</sub> O) <sub>4</sub> OH)	8±3 x 10 <sup>5</sup>	>7 x 10 <sup>7</sup>
8	<b>TOP009</b> <sup>10</sup>	4.0 x 10 <sup>4</sup>	ND
9	UK-1	5±1 x 10 <sup>5</sup>	>5 x 10 <sup>7</sup>

<sup>1</sup> ND = Not determined

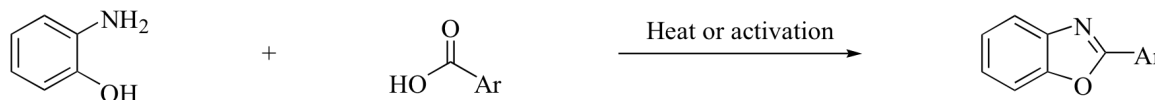
#### 4.1.6. Methods of 2-Arylbenzoxazole Synthesis

To complete a SAR study on the minimum pharmacophore and potentially improve the druglike properties of **TOP027**, a library of C2 aryl analogs was needed. A review of the literature shows some common trends. Sections are divided as follows: condensation reactions, oxidative couplings, closure onto aryl halides, multicomponent couplings, and biaryl couplings at C2.

##### 4.1.6.1. Condensation of aminoalcohols with carboxylic acid or carboxylic acid equivalents

Condensation of an *o*-aminophenol with an aryl carboxylic acid is a classical route to benzoxazoles (Scheme 4.5). These reactions typically require high heat and catalytic acid to promote cyclization and dehydration. Although many varied conditions have been reported, TsOH is a commonly used acid.<sup>14</sup> Other acid catalysis conditions include: boric acid (stoichiometric amounts used in conjunction with a Dean-Stark trap),<sup>15</sup> polyphosphoric acid,<sup>16</sup> polyphosphate ester,<sup>17</sup> acetic anhydride,<sup>18</sup> and others. Milder reaction conditions can provide the product if the carboxylic acid is activated towards amide formation using reagents such as CDI,<sup>14</sup>

*N,N*-dimethyl chlorosulfitemethaniminium chloride (SOCl<sub>2</sub>/DMF),<sup>19</sup> ionic liquid solvent,<sup>20</sup> microwave irradiation,<sup>21</sup> or zeolite E4.<sup>22</sup> Neat reactions containing Lawesson's reagent have been subjected to microwave irradiation to give a range of 2-arylbenzoxazoles in yields ranging from 71-90%.<sup>23</sup>

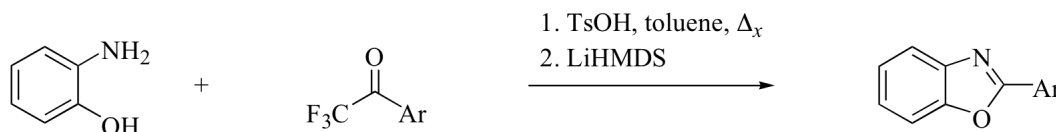


Scheme 4.5. General scheme for C2-aryl benzoxazole from *o*-aminophenol and carboxylic acid.

Another strategy is to use an acid chloride instead of a carboxylic acid (Scheme 4.6). This typically requires a basic additive to promote amide formation followed by a Lewis acidic additive to improve the cyclization and dehydration to the benzoxazole.<sup>14</sup> Recently, there have been several reports of using microwave irradiation as an alternative to the Lewis basic and acidic additives.<sup>24</sup> Reactions run in the microwave using dioxane as solvent and a slight excess of the acid chloride provided the 2-aryl benzoxazoles in good (75-98%) yields after 10 min. at 250 °C.<sup>24</sup>



Scheme 4.6. Combination of acid chloride with *o*-aminophenol.

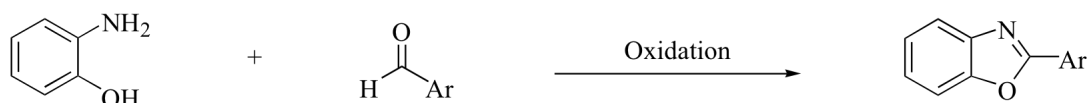


Scheme 4.7. Benzoxazole synthesis from trifluoromethyl ketone and *o*-aminophenol.

Also, instead of a carboxylic acid, a trihalomethylarene can undergo the same conversion when heated with *o*-aminophenol in the presence of catalytic polyphosphoric acid and heat (Scheme 4.7).<sup>25</sup> Yields of this variant, however, are extremely variable, ranging from 35-98% depending on the substrate.<sup>25</sup>

Although trifluoromethylketones are not the same oxidation state as carboxylic acids, they too will form benzoxazoles with *o*-aminophenol.<sup>26</sup> The initial reflux in toluene under acid catalysis yields the trifluoromethyl imine, which, upon treatment with LiHMDS, can undergo nucleophilic attack by the appendant phenolate, which collapses to give the benzoxazole product.<sup>26</sup>

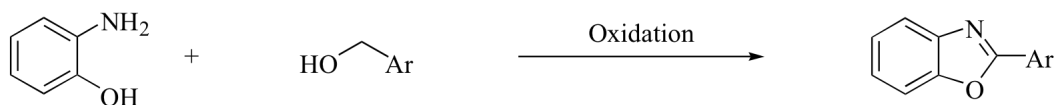
#### 4.1.6.2. Oxidative coupling of aryl aldehydes with aminoalcohols



Scheme 4.8. 2-Aryl benzoxazole formation using *o*-aminophenol and aryl aldehyde

Many mild oxidants can mediate the cyclization between *o*-aminoalcohols and an aromatic aldehyde, including I<sub>2</sub>,<sup>27</sup> PCC (on silica),<sup>28</sup> thianthrene cation radical,<sup>29</sup> DDQ,<sup>30</sup> MnO<sub>2</sub>, Hypervalent iodine reagents can be used as oxidants,<sup>31</sup> including solid-supported hypervalent iodine.<sup>32</sup> One interesting variant is a radical reaction catalyzed by 4-methoxytetramethylpiperidine N-oxide (4-methoxy-TEMPO) using aerobic conditions (so that O<sub>2</sub> is the stoichiometric oxidant).<sup>33</sup> Yields are good for a variety of aromatic aldehydes, with no obvious electronic effects, but the reaction may require refluxing xylenes as the solvent for good yields.

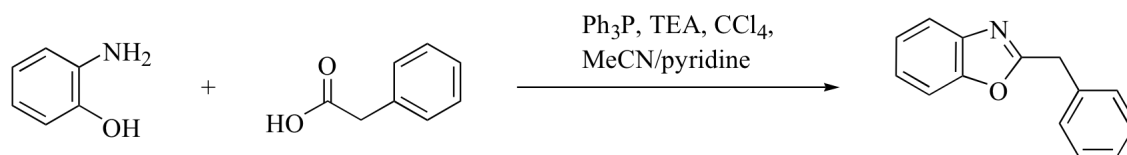
#### 4.1.6.3. Oxidative coupling of benzyl alcohols with aminoalcohols



Scheme 4.9. Synthesis of 2-aryl benzoxazoles using a benzylic alcohol in presence of an oxidant

Using an alcohol instead of an aldehyde has also been reported by Wilfred and Taylor (Scheme 4.9).<sup>34</sup> The authors propose that the oxidant, MnO<sub>2</sub> in this case, oxidizes the alcohol to an aldehyde, which then forms an N,O-acetal.<sup>34</sup> This N,O-acetal can then undergo a second

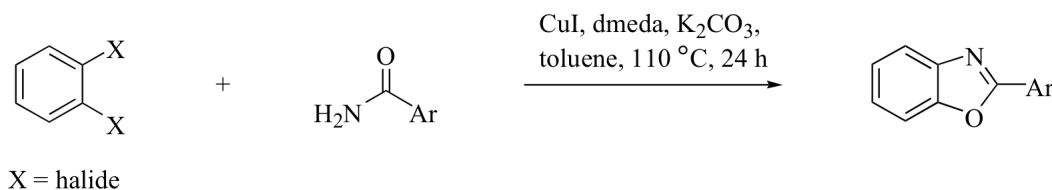
oxidation to the benzoxazole. The reported yield using benzyl alcohol and 2.5 eq. *o*-aminophenol in refluxing toluene with 15 equivalents of activated MnO<sub>2</sub> was 73%.<sup>34</sup>



Scheme 4.10. Triphenylphosphine-carbon tetrachloride mediated coupling of aminoalcohol to carboxylic acid<sup>35</sup>

One method which avoids high temperatures and harsh conditions involved activation of a carboxylic with an aminoalcohol in the presence of triphenylphosphine and carbon tetrachloride (Scheme 4.10).<sup>35</sup> Protection of amines or hydroxyl groups on the aromatic ring of the carboxylic acid was unnecessary when aliphatic aminoalcohols were used.<sup>35</sup> This method has not been reported for coupling of aromatic carboxylic acids with aromatic amino alcohols. Yields ranged from 52-74%, depending on the substituents.<sup>35</sup> A variant of this process is reported with aromatic carboxylic acids involves activation of the carboxylic acid by polymer-supported triphenylphosphine and Cl<sub>3</sub>CCN under microwave irradiation.<sup>36</sup> Microwave heating (to 150 °C) is required to close the intermediate amide into the benzoxazole.<sup>36</sup> Yields for this benzoxazole formation range from 79-97%, with lowered yields observed when an electron-poor group (i.e. carboethoxy ester or nitro) is appended to the benzoxazole ring.<sup>36</sup>

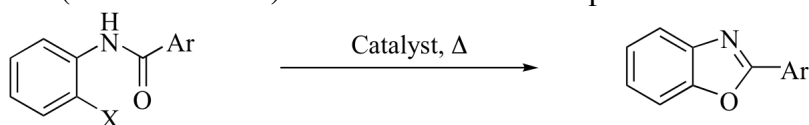
#### 4.1.6.4. Ring-closing onto aryl halides



Scheme 4.11. Benzoxazole formation using copper (I) catalysis to combine 1,2-dihalobenzene and aromatic amide

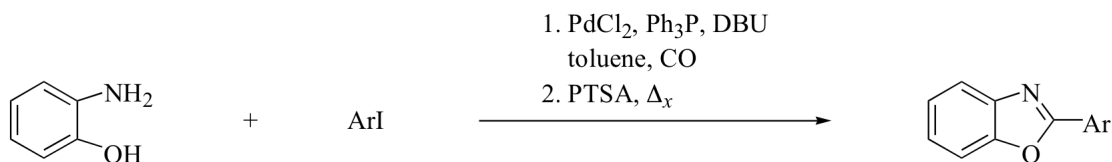
Glorius *et al.* report a benzoxazole synthesis that reverses the sense of electrophilicity and nucleophilicity traditionally used to construct benzoxazoles.<sup>37</sup> In this case, the coupling proceeds

between a 1,2-dihalobenzene and an aromatic amide.<sup>37</sup> Electron-poor amides appear to give slightly higher yields, but all transformations reported proceed in yields ranging from 67-86%. The preformed 2-halo aryl amide will cyclize efficiently under similar conditions (Scheme 4.12).<sup>38,39</sup> One such transformation uses CuI with 1,10-phenanthroline as a ligand in presence of cesium carbonate in refluxing 1,2-dimethoxyethane.<sup>39</sup> Microwave heating speeds conversion.<sup>40</sup> This cyclization of the intermediate 2-halo aryl amide also works in water as a solvent, but the required temperature remains 120 °C, necessitating use of a sealed tube.<sup>41</sup> In addition to Cu(I) catalysts, Fe(III) with a diketone ligand has also been used.<sup>42</sup> This transformation also requires elevated temperature (120 °C in DMF) over extended reaction periods.<sup>42</sup>



Scheme 4.12. O-Arylation to close benzoxazole ring

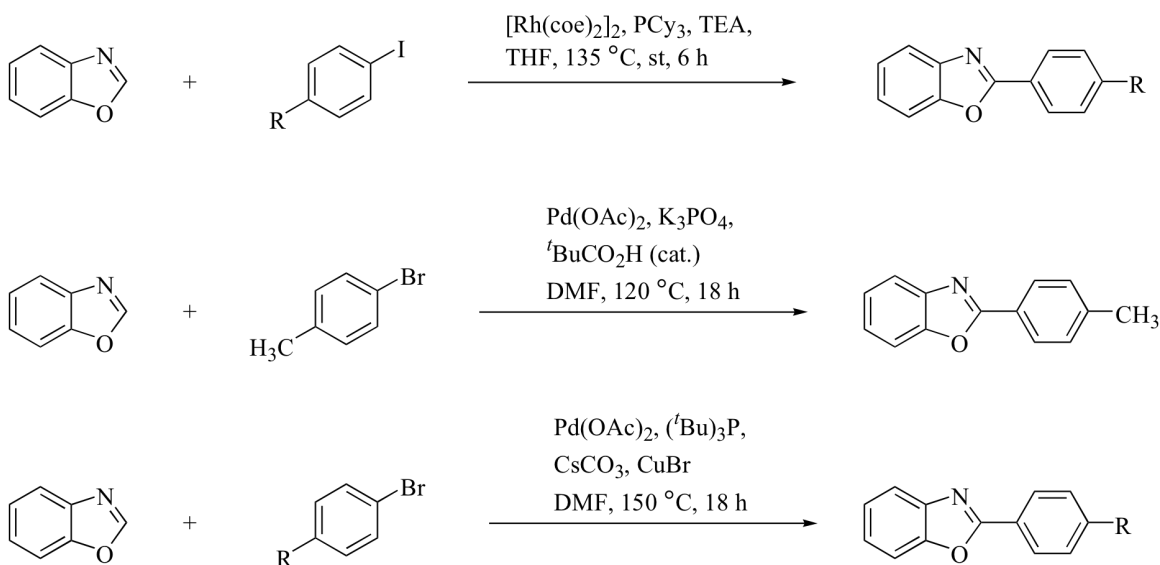
#### 4.1.6.5. Multicomponent Couplings



Scheme 4.13. Pd-catalyzed CO insertion to form benzoxazole ring

*o*-Aminophenol can undergo a multicomponent coupling with CO and an aryl iodide in presence of catalytic palladium to generate the intermediate *o*-amidophenol, which can then be closed under the standard conditions using heat and *p*-toluenesulfonic acid.<sup>43</sup> This transformation provides the final benzoxazoles in 74-97% overall yield.<sup>43</sup> Heteroaromatic aryl iodides participate in this transformation, including 2-iodothiophene and 2-bromopyridine.<sup>43</sup>

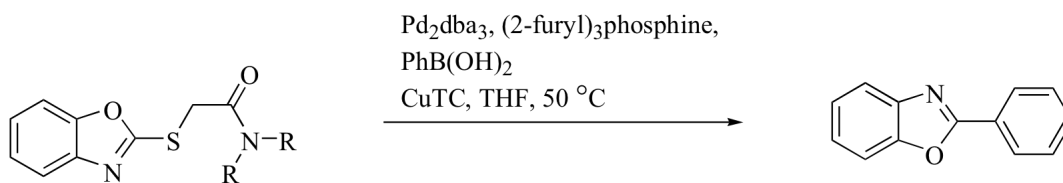
#### 4.1.6.6. Couplings at C2



Scheme 4.14. Coupling at C2 of unsubstituted benzoxazole.<sup>44</sup>

In 2004, Ellman *et al.* reported a coupling on benzoxazoles and benzimidazoles that proceeds via Rh-catalyzed N-heterocyclic carbene formation at the C2 position of the heteroaromatic ring (Scheme 4.14, top).<sup>44</sup> Rhodium (I) in presence of tricyclohexylphosphine and triethylamine generates the N-heterocyclic carbene. The metal center then undergoes oxidative addition by the aryl iodide, followed by reductive elimination to generate the coupled product. Yields were lowest with electron poor aryl halides.<sup>44</sup> When 1-bromo-4-fluorobenzene is used instead of bromobenzene, the yield decreases from 79% to 30%.<sup>44</sup>

Palladium catalysis also allows direct substitution at C2 on the benzoxazole system (Scheme 4.14, bottom). A report in 2009 by You *et al.* does not require CuBr or ligand, using catalytic pivalic acid instead (Scheme 4.14, center).<sup>45</sup> Catalytic palladium and pivalic acid in presence of stoichiometric base (potassium triphosphate) at elevated temperatures in DMF yielded the substituted benzoxazole in 76% yield.<sup>45</sup> No aryl bromides other than *p*-bromotoluene were reported.<sup>45</sup>



Scheme 4.15. Modified Suzuki coupling at C2 of benzoxazole.<sup>46</sup>

Recently, Liebeskind *et al.* reported a modified Suzuki coupling at C2 of benzoxazoles (Scheme 4.15).<sup>46</sup> This coupling is one of the mildest reported to synthesize benzoxazoles.<sup>46</sup> The copper thiophene-2-carboxylate (CuTC) is proposed to both complex the palladium to facilitate oxidative addition and to activate the boronic acid so that it undergoes efficient transmetalation to the palladium.<sup>46</sup> In the original publication, both the free, primary amide and dimethyl amide could undergo coupling with no difference in yield.<sup>46</sup>

#### 4.2. PROPOSED RESEARCH

We wanted to find a route suitable for the rapid assembly of UK-1 analogs, both the *bis*(benzoxazole) and the monobenzoxazole minimum pharmacophore (**TOP027**). Ideally, a wide variety of building blocks would be available to introduce functionality in a systematic manner. We hoped to develop a route that would be very modular, introducing points of difference late in the synthesis using inexpensive starting materials and developing robust, scalable reactions. Also, because we were interested in installing functionalized aryl groups, it was important to try to avoid high temperatures and strong acids. For our initial library, we selected compounds that might distort the arrangement of Lewis basic sites to probe what the requirements are for cytotoxicity. If metal binding is critical, the 2-amino substrate **TOP071** should show good activity. The series of 3- and 4-substituted aromatic rings will show what steric constraints are tolerated, and whether the metal-binding can occur at a slightly longer distance between Lewis bases than previously suggested.<sup>9</sup> **TOP074**, which has a 2-pyridyl substituent, would shorten the geometry, and the bound metal would form a five-membered ring rather than a six-membered ring.

### 4.2.1. Proposed C2 Analog Series

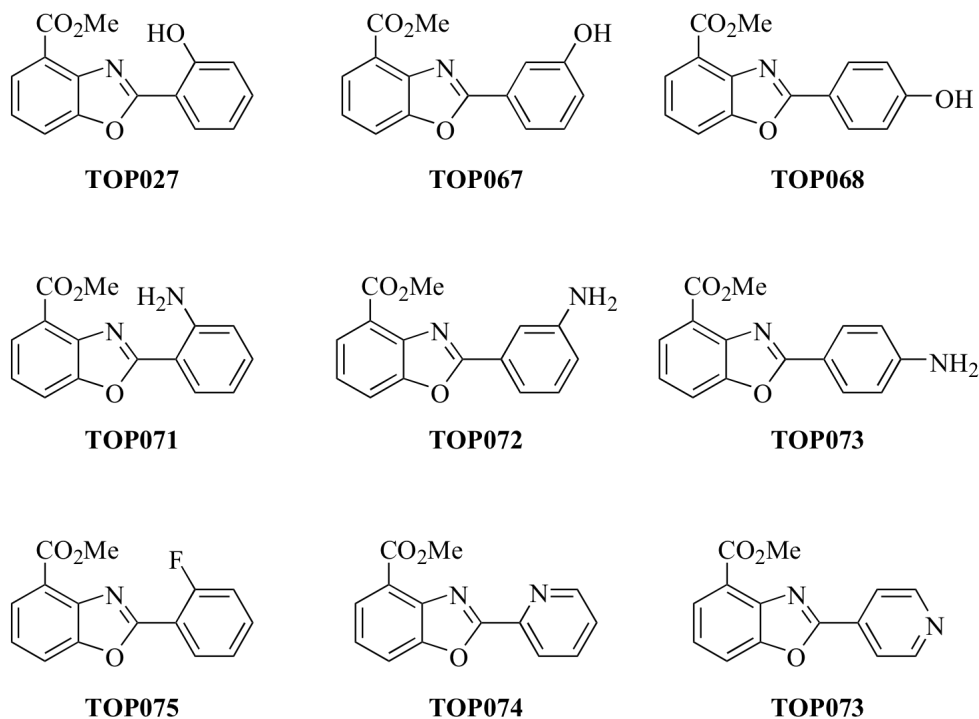
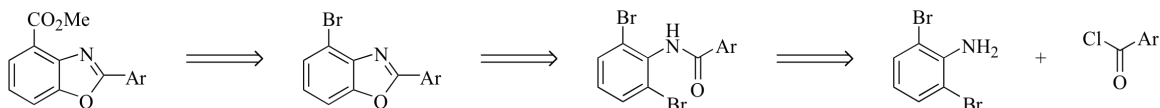


Figure 4.11. Proposed C2 analogs

There are two unique challenges associated with synthesizing these analogs. Although there are many reported methods to generate benzoxazoles, many perform poorly when the *o*-aminophenol includes an electron-withdrawing substituent. The nucleophilicity of the amine is greatly diminished. Additionally, the required intermediate 3-hydroxyanthranilic acid methyl ester is subject to oxidation, and isolation is often difficult. Although it is commercially available, it is expensive. Previous work in the Kerwin lab used the commercially available 3-methoxy-2-nitrobenzoic acid to synthesize the intermediate 2-hydroxyanthranilic acid methyl ester. Our first retrosynthetic analysis took an approach that would allow introduction of differences at both C2 and C7. The route was highly modular and avoided the use of the 3-hydroxyanthranilic acid methyl ester (Scheme 4.16). The carboxymethyl group could be installed by carbonylation of the aryl halide in methanol using palladium catalysis. This would allow installation of a variety of esters or even aryl groups. To assemble the benzoxazole ring, we



chose to use the method reported by Glorius *et al.*<sup>37</sup> to close the amide onto the aryl halide. This method then allows use of a variety of aromatic acid chlorides, which can either be purchased directly or synthesized from the corresponding acid.

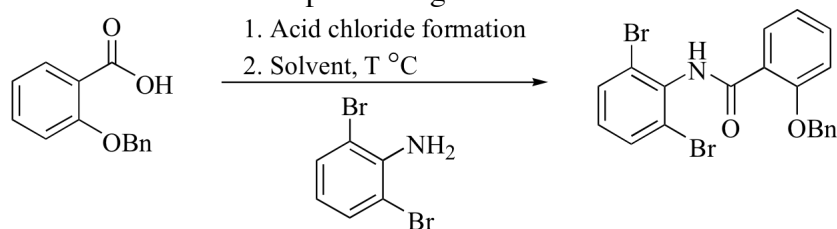


Scheme 4.16. Retrosynthetic analysis of minimum pharmacophore analogs.

### 4.3. SYNTHESIS

#### 4.3.1. Copper (I) Catalyzed Ring Closing

This proposed route would allow improved access to a variety of UK-1 analogs to generate detailed SAR data, which could lead to improved pharmacological properties as an anticancer agent. We began by synthesizing the amide from 2,6-dibromoaniline. Anilines are less nucleophilic than aliphatic amines, and this aniline is extremely hindered because of the flanking bromines, which made this reaction more demanding than a standard amide formation. The reaction was optimized by screening a variety of conditions (Table 4.6). We found that using oxalyl chloride key to obtaining good yields of the amide. The resulting crude product from the optimized conditions (Table 4.6, Entry 11) was clean when analyzed using <sup>1</sup>H NMR and TLC. The procedure was amenable to scale-up to multigram scale.



Scheme 4.17. Amide formation from benzyloxysalicylic acid and 2,6-dibromoaniline

Table 4.6. Amide formation optimization

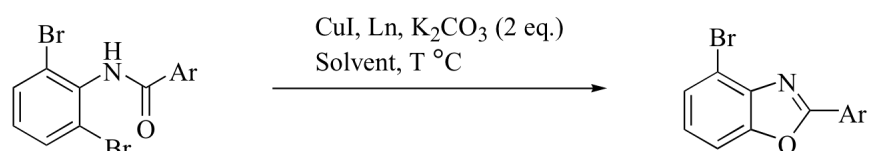
Entry	Formation of	Amide formation	Concentration	Temperature	Percent Yield
-------	--------------	-----------------	---------------	-------------	---------------

	Acid Chloride		(M)	(°C)	
1	SOCl <sub>2</sub>	Pyr (1.2 eq) in DCM	0.2	0→21	0
2	SOCl <sub>2</sub>	Pyr (1.2 eq) in DCM→toluene	0.2	21→110	0
3	SOCl <sub>2</sub>	NaH in THF:DMF	0.2	21	0
4	SOCl <sub>2</sub>	Toluene	0.2	110	22% deprotected <sup>a</sup>
5	SOCl <sub>2</sub>	neat	neat	130	11%; 5 % deprotected
6	SOCl <sub>2</sub>	Neat (2 eq amine)	neat	120; 90 min.	0
7	SOCl <sub>2</sub>	DMF	1M	120	0
8	SOCl <sub>2</sub>	THF	1M	Δ <sub>x</sub>	0
9	(COCl) <sub>2</sub>	DMF (2 eq amine)	10M	130	28%, 13% deprotected
10	(COCl) <sub>2</sub>	DMF	7M	rt	56%, 13% deprotected
11	(COCl) <sub>2</sub>	DMF	7M	50	63%
12	(COCl) <sub>2</sub>	DMF	7M	95	54%, 6% deprotected

<sup>a</sup> Average of two trials

With the amide in hand, we attempted the copper(I)-catalyzed ring closing using conditions similar to those reported by Glorius *et al.*<sup>37</sup> Copper iodide was used as the copper source, with *N,N'*-dimethylethylenediamine (*N,N'*-dmeda) as ligand, two equivalents potassium carbonate, and refluxing toluene. Conditions were optimized by changing the ligand, solvent and temperature (Table 4.7). Elevated temperatures were required. 1,10-phenanthroline was preferred

because doxygenation was easier with a solid than a liquid ligand. Coordinating solvents performed best in this system. We speculate that this is because they compete with product benzoxazole to coordinate the catalyst and improve turnover. Finally, conditions similar to those reported by Batey *et al.*<sup>39</sup> were found to successfully cyclize the amide (Table 4.7, Entry 9). Our cyclization worked nicely even at 5 mol% catalyst loading, giving a crude product that was clean as judged by <sup>1</sup>H NMR and TLC in 82% yield.



Scheme 4.18. Optimization of Cu(I)-catalyzed benzoxazole ring closing.

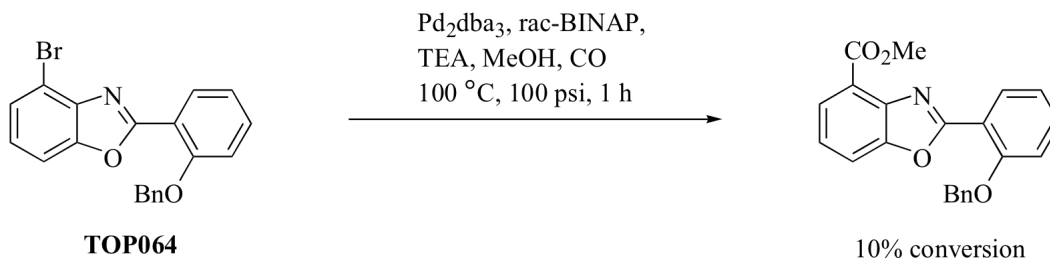
Table 4.7. Optimization of Cu(I)-catalyzed ring-closing

Entry	Catalyst loading (mol%)	Ligand <sup>b</sup>	Solvent	Temp (°C)	Yield
1	5	<i>N,N'</i> -dmeda	toluene	110	RSM <sup>a</sup> only
2	20	<i>N,N'</i> -dmeda	toluene	110	45% <sup>c</sup>
3	30	<i>N,N'</i> -dmeda	toluene	110	26% <sup>c</sup>
4	20	<i>N,N'</i> -dmeda	toluene	130 <sup>d</sup>	44% <sup>c</sup>
5	20	1,2-phenylenediamine	toluene	130	45% <sup>c</sup>
6	20	1,10-phenanthroline	toluene	130	44% <sup>c</sup>
7	20	1,10-phenanthroline	DCE	130	36% <sup>c</sup>
8	20	1,10-phenanthroline	DMSO	130	66%
9	20	1,10-phenanthroline	DME	130	83%
10	5	1,10-phenanthroline	DME	130	82%

<sup>a</sup>RSM = recovered starting material <sup>b</sup> Ligand loading was always 2 eq. with respect to CuI. <sup>c</sup>RSM also isolated.

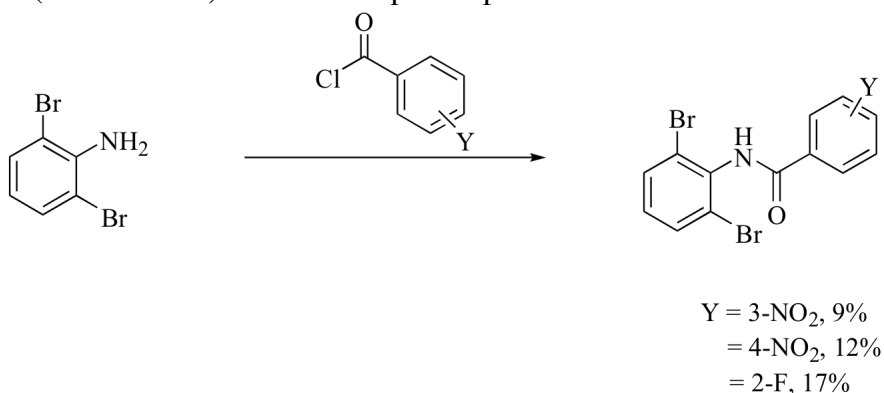
<sup>d</sup>Sealed tube

With optimized conditions in hand, we attempted the carbonyl insertion. A similar process for electronically challenging substrates was recently reported by Albaneze-Walker *et al.*<sup>47</sup> After 1 h, we observed a 10% conversion. We were encouraged to see that the reaction gave 10% conversion to the ester after 1 h. However, the conversion required high temperature and pressure.



Scheme 4.19. CO insertion onto 4-bromobenzoxazole

After establishing that this was a feasible route to C2-aryl analogs, we began to synthesize some related amides using other aryl acid chlorides. To our great disappointment, the conditions optimized for the acid chloride of 2-benzyloxybenzoic acid were not generalizable for other acid chlorides (Scheme 4.20). Initial attempts at optimization were unsuccessful.



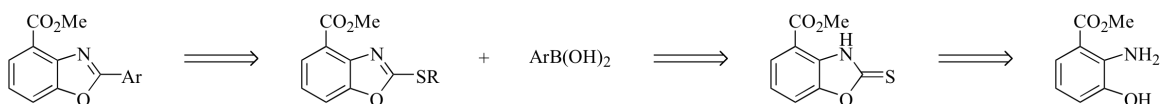
Scheme 4.20. Amide formation with varied acid chlorides.

We realized that this route, which introduced the structural diversity at the first step, might not be the best way to generate our library. If the first step for each partner required optimization, this did not meet the requirement for easy synthesis of many analogs. Also, the forcing conditions (high pressure, high temperature) for both the benzoxazole ring closing and

the carbonylation could become problematic for some library elements with more sensitive functionalities. Finally, the 2,6-dibromoaniline is costly, \$10 per gram. We decided to explore alternative routes to our library that would introduce diversity late in the synthesis, use mild conditions to preserve sensitive functionality, and be cost-effective.

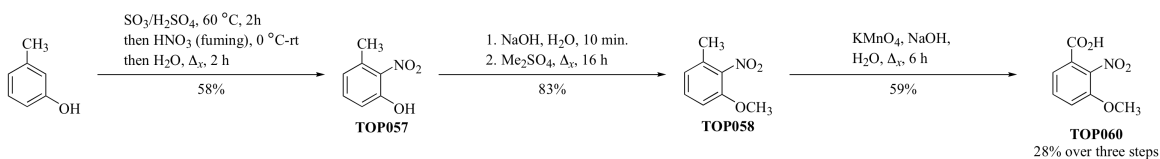
#### 4.3.2. Thiobenzoxazole-Derived Coupling Partner

An alternative to the copper-catalyzed benzoxazole ring formation was a biaryl coupling at C2 of the benzoxazole. These couplings were reported by Liebeskind to proceed under lower temperature than any of the alternative benzoxazole ring closures.<sup>46</sup> We envisioned a route where diversity of the library was introduced at the final step, allowing rapid generation of analogs. Although this route does use the 3-hydroxyanthranilic acid methyl ester, this compound has been used before with success.



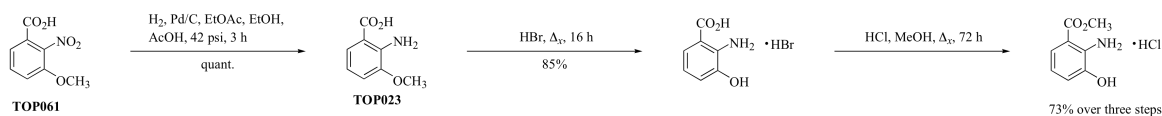
Scheme 4.21. Revised retrosynthetic analysis

Forming the 3-hydroxyanthranilic methyl ester followed previously published procedure and proceeded smoothly (Scheme 4.22).<sup>48</sup> Using the very inexpensive *m*-cresol as the starting material afforded multigram quantities of the desired carboxylic acid. Electrophilic aromatic substitution using sulfonic acid as a blocking group generates **TOP057** in moderate yield. Formation of the sodium phenolate salt under aqueous conditions, followed by concentration to dryness and reflux in dimethylsulfate generates the methyl ether **TOP058** in good yield. Benzylic oxidation using potassium permanganate gives **TOP050**, which is commercially available but somewhat expensive, in moderate yield. These reactions were routinely run using 50 g *m*-cresol.



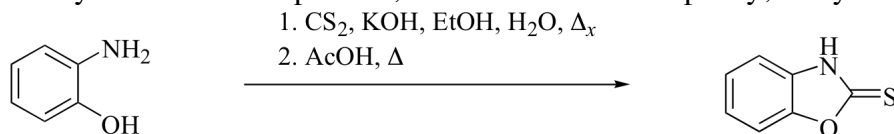
Scheme 4.22. Synthesis of 3-methoxy-2-nitrobenzoic acid.

We then turned our attention to the synthesis of the 3-hydroxyanthranilic acid methyl ester (Scheme 4.23). Hydrogenation proceeded smoothly and in high yield. Conditions previously reported for the deprotection included isolation of the free base using sodium acetate to neutralize the hydrogen bromide salt. We found that the neutralization could be omitted and the salt directly subjected to Fisher esterification without any loss in yield. We hoped to use the hydrochloric acid salt of the anthranilic acid to proceed, as the salt appears to be stable to oxidation at room temperature, whereas the free base is relatively unstable, decomposing even at low temperatures.



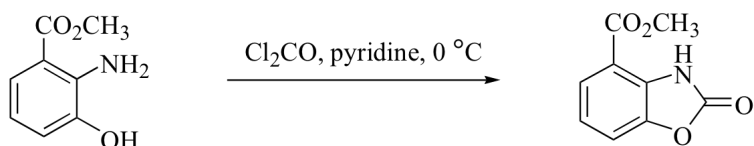
Scheme 4.23. Synthesis of the HCl salt of 3-hydroxyanthranilic acid methyl ester.

The use of carbon disulfide in the presence of aqueous base to generate the thiobenzoxazole was originally reported as an *Organic Syntheses* procedure for forming 2-mercaptobenzimidazole, but the authors note that by replacing the 1,2-phenylene diamine with *o*-aminophenol, they were able to isolate the mercaptobenzoxazole in 80% yield (Scheme 4.24).<sup>49</sup> We were concerned that the aqueous base might also hydrolyze the methyl ester. This transformation did yield the desired product, but it was difficult to purify, and yields were poor.



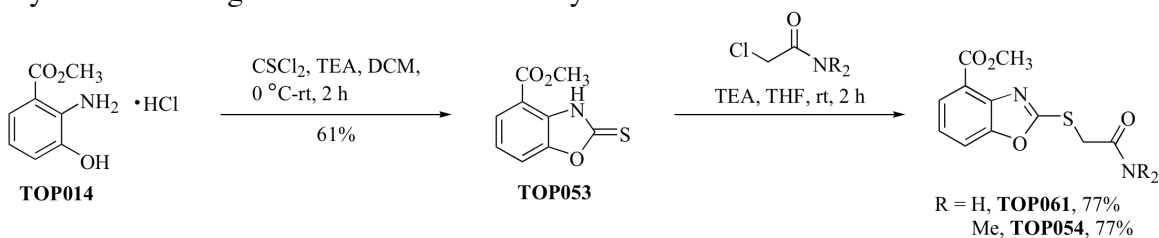
Scheme 4.24. Formation of thiobenzoxazole via aqueous, basic carbon disulfide<sup>49</sup>

An alternative procedure that was likely to be more compatible with the methyl ester was one reported by Fielder and Collins using phosgene to form 7-carbomethoxybenzoxazoline-2-one (Scheme 4.25).<sup>50</sup> It seemed reasonable to try to analogous reaction using thiophosgene. We speculated that we could use the HCl salt of the 3-hydroxyanthranilic acid methyl ester if we used one extra equivalent of base.



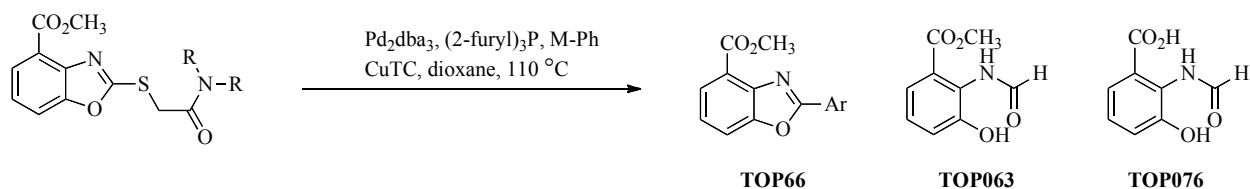
Scheme 4.25. Phosgene addition to 3-hydroxyanthranilic acid methyl ester

Either reaction did produce the desired product; however, the use of thiophosgene gave higher yields, and purification was more facile. Some dimer formation to the thiourea was observed, but it was minimized by using dilute (20 mM) reaction conditions (Scheme 4.26). Additionally, this method proved to be tolerant of deprotonation of the ammonium salt *in situ*, which limited decomposition of the 3-hydroxyanthranilic acid methyl ester. The coupling partner was synthesized using 2-chloroacetamide to alkylate the sulfur.



Scheme 4.26. Synthesis of coupling partner.

The coupling partner, which could generate analogs of the minimum pharmacophore was generated in eight steps with 9% overall yield.<sup>10,48</sup> The coupling reaction was then optimized using phenylboronic acid (Scheme 4.27). Liebeskind *et al.* note that they observed no difference between the primary amide and the dimethyl amide in their couplings.<sup>46</sup> However, in this case, no coupling product could be obtained with the free amide (Table 4.8). The only observed conversion was to a product where both the benzoxazole and the methyl ester were hydrolyzed.



Scheme 4.27. Optimization of Coupling Reaction

Table 4.8. Optimization of Liebeskind coupling for R = H

Entry	Mol % Pd	Ln	Mol% Ln	Conc. (M)	Temp. (°C)	Outcome
1	1	(2-furyl) <sub>3</sub> P	4	0.05	110	4% RSM
2	2	(2-furyl) <sub>3</sub> P	8	0.05	110	38% RSM
3	4	(2-furyl) <sub>3</sub> P	16	0.05	110	49% RSM
4	4	(2-furyl) <sub>3</sub> P	16	0.1	110	65% RSM
5	4	(2-furyl) <sub>3</sub> P	16	0.2	80	39% RSM, trace <b>TOP076</b>
6	4	(Ph) <sub>3</sub> P	16	0.2	80	12% RSM, 16% <b>TOP076</b>
7	4	( <i>o</i> -tolyl) <sub>3</sub> P	16	0.2	80	6% RSM, 11% <b>TOP076</b>
8	4	( <i>o</i> -tolyl) <sub>3</sub> P	16	0.2	110	78% <b>TOP076</b>

We then attempted the same coupling with the dimethylamide **TOP054** (Table 4.9). Luckily, these couplings did give some of the desired coupling product. To determine the origin of the undesired byproduct, control reactions were performed, omitting reagents systematically. It was found that the formation of the byproduct requires both the catalyst/ligand complex and the boronic acid. Thinking that perhaps the boronic acid was responsible for proteolysis, we tried



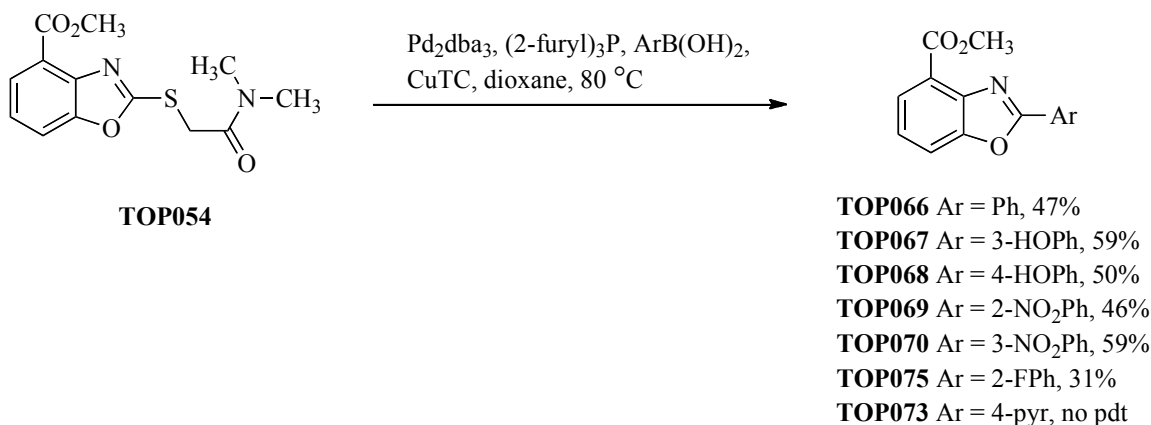
using transmetallating agents that are aprotic, including a borate ester and a potassium trifluoroborate salt (Table 4.9, Entries 6 and 7). None of these cross-couplings were successful. We decided to turn our attention to synthesizing some of our analog library to see whether the yield improved with electronic substituent effects.

Table 4.9. Optimization of Liebeskind coupling for R = Me<sup>a</sup>

Entry	M-Ph (eq)	CuTC eq.	Concentration (M)	Outcome
1	PhB(OH) <sub>2</sub> (1.1)	1.3	0.05	38% <b>TOP066</b> (46% - RSM); 18% RSM, 71% 3 24% <b>TOP066</b> (50% - RSM),
2	PhB(OH) <sub>2</sub> (1.1)	1.3	0.025	38% RSM, 64% <b>TOP076+TOP063</b>
3	PhB(OH) <sub>2</sub> (1.1)	2.2	0.05	22% <b>TOP066</b> , 44% <b>TOP063</b>
4	PhB(OH) <sub>2</sub> (2.2)	1.1	0.05	37% <b>TOP066</b> , 34% <b>TOP063</b>
5	PhB(OH) <sub>2</sub> (2.2)	2.2	0.05	48% <b>TOP066</b> , 19% <b>TOP063</b>
6	PhBF <sub>3</sub> K (1.1)	1.3	0.05	RSM
7	PhBF <sub>3</sub> K (1.1)	0	0.05	RSM
8	PhB(OC(CH <sub>3</sub> ) <sub>2</sub> ) <sub>2</sub> (1.1)	1.3	0.05	RSM, C

<sup>a</sup> Standard conditions: 1 mol% Pd<sub>2</sub>dba<sub>3</sub>, 4 mol% (2-furyl)<sub>3</sub>P, 110 °C, 16 h

The couplings proceeded well (Scheme 4.28). Significant amounts of the byproduct were produced, but in cases where the desired coupling product did not include a phenol, basic extraction efficiently removed the byproduct. In the phenolic cases, the byproduct could be removed during routine chromatography.

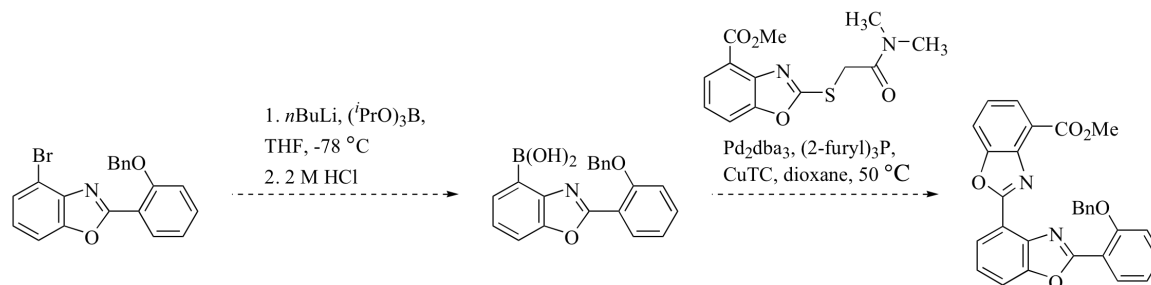


Scheme 4.28. Couplings to assemble library of C2-aryl benzoxazoles

Yields were moderate in most cases. The 2- and 3-nitro compounds serve as precursors to the amines **TOP071** and **TOP072**. Reductions using hydrogenation are currently ongoing. The coupling with 4-pyridylboronic acid was disappointing, giving only the byproduct discussed previously following isolation. There does not appear to be a strong electronic effect of yield of these coupling reactions, as the 3-hydroxyphenylboronic acid and 3-nitrophenylboronic acid give identical yields of their respective products.

#### 4.3.3. Attempted Extension of Thiobenzoxazole Route to Synthesis of UK-1

We realized that the 7-bromobenzoxazole generated from the copper (I) catalyzed ring closing might provide access to UK-1 itself if it would be converted to the corresponding boronic acid.



Scheme 4.29. Proposed route to UK-1.

We realized that it was possible to adapt this route to synthesize UK-1 (Scheme 4.29). With the halide at C7 of the benzoxazole, it might be possible to generate a boronic acid. No benzoxazoles of this structure have been reported in the literature, although C2 boronic acids of benzoxazoles are known. Unfortunately, attempts at metal-halogen exchange were unsuccessful. Initially, the aryl halide was combined with *n*-butyllithium at -78 °C in 0.4 M THF. Unfortunately, using either triisopropylborate or methyl chloroformate to quench the reaction did not generate the desired trapping products. Quenching aliquots with D<sub>2</sub>O showed that while the starting material was consumed after 5 min. at -78 °C, deuterium incorporation at C4 of the benzoxazole ring was not observed. Mass spectrometric analysis of the reaction mixture showed loss of the benzyloxy group. Adding the triisopropylborate as an *in situ* quench did not improve the results. Diluting the reaction mixture for the metal-halogen exchange to 1 mM in THF showed no D-incorporation by mass spectrometry after 30 min., but these reactions also did not show any loss of the benzyl group. Explorations in this area are ongoing.

#### **4.4. CONCLUSIONS**

We have developed a facile route to a library of C2-aryl benzoxazoles. Use of this route to assemble UK-1 or *bis*(benzoxazole) analogs does not appear promising, but optimization is incomplete. The route to the C2-aryl analogs is inexpensive and operationally simple. Also, because it relies on boronic acids, there are many commercially available possibilities for library synthesis. It appears to be highly functional group-tolerant and avoids the harsh conditions (acid and heating) typically required to form benzoxazoles. Synthesis of a full library is ongoing.

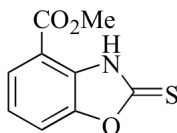
#### **4.5. FUTURE WORK**

These C2-aryl analogs will be assayed for their metal dependent DNA binding properties, as well as their cytotoxicity. It is hoped that this information about the function of the 2-hydroxyphenyl group at C2 will allow synthesis of highly soluble and potent UK-1 analogs that can serve as antineoplastic agents.

## 4.6. EXPERIMENTAL SECTION

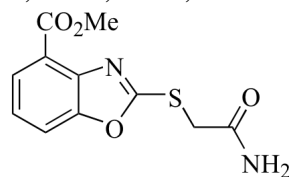
### General Notes

THF, 1,2-dimethoxyethane, and dioxane were distilled over sodium/benzophenone, and  $\text{CH}_2\text{Cl}_2$ , 1,2-dichloroethane, and toluene were distilled from  $\text{CaH}_2$  immediately prior to use. All reactions were run in argon-flushed round bottom flasks that had been dried, either in a 110 °C oven or by flame under vacuum, under an argon atmosphere. Solvent ratios are expressed as % by volume. Flash chromatography (FCC) was performed according to the method of Still.<sup>51</sup> NMR was performed using a VARIAN Mercury spectrometer.  $^1\text{H}$  NMR was run at 400 MHz;  $^{13}\text{C}$  NMR was run at 100 MHz with broadband proton decoupling unless otherwise specified. Solvent chemical shifts are reported in ppm ( $\delta$ ) and referenced to solvent.<sup>52</sup> IR was obtained on a Nicolet IR100 FT-IR spectrometer. Melting points were obtained in open capillary tubes on a Büchi Melting Pont B-540 and are uncorrected.



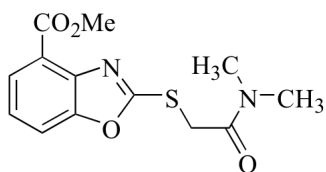
**TOP 053. 2-Thioxo-2,3-dihydrobenzoxazole-4-carboxylic acid methyl ester.** The hydrochloride salt of 3-hydroxyanthranilic acid methyl ester (3.05 g, 15 mmol, 1 eq) was suspended in dry DCM (100 mL) and cooled in an ice-water bath to 0 °C. To this solution was added dry triethylamine (5.23 mL, 37.5 mmol, 2.5 eq). An addition funnel was charged with thiophosgene (1.26 mL, 16.5 mmol, 1.1 eq) in DCM (50 mL), and this solution was added dropwise at 0 °C to the aminoalcohol. The solution was allowed to warm to room temperature overnight. After 16 h, the mixture was poured onto satd  $\text{NH}_4\text{Cl}$  (100 mL). The aqueous layer was extracted with DCM (2x50 mL). The combined organic layers were dried ( $\text{Na}_2\text{SO}_4$ ), and conc. The product was adsorbed to silica and purified via FCC using a gradient of hexanes-50% EtOAc/Hex. The product was isolated as an orange solid (1.90 g, 9 mmol, 61%). This sample was recrystallized to remove any dimeric product (which co-elutes) to give the product as a pale

yellow solid (1.15 g, 34%). <sup>1</sup>H NMR (CDCl<sub>3</sub>): δ 10.42 (1H, br s); 7.82 (1H, dd, *J* = 8.0, 0.9 Hz); 7.49 (1H, d, *J* = 8.2 Hz); 7.28 (1H, t, *J* = 8.2 Hz); 4.01 (3H, s). <sup>13</sup>C NMR (CDCl<sub>3</sub>): δ 180.8, 165.1, 149.1, 131.9, 129.5, 125.7, 123.6, 114.3, 112.6, 52.8. LRMS (CI<sup>+</sup>): 210 (M<sup>+</sup>+1), 178 (M<sup>+</sup>-S). HRMS (CI<sup>+</sup>): calcd. for C<sub>9</sub>H<sub>7</sub>NO<sub>3</sub>S 210.0225, found 210.0221. IR (thin film, DCM): 2919, 1688, 1491, 1421, 1368, 1308, 1259, 1178, 1126, 1012, 929 cm<sup>-1</sup>. mp 197.5-198.3 °C.

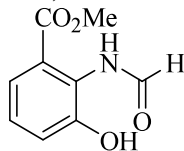


**TOP 061. 2-Carbamoylmethylsulfanylbenzoxazole-4-carboxylic acid methyl ester.**

**TOP053** (830 mg, 4.0 mmol, 1 eq) was dissolved in dry THF (8 mL, 0.5 M) with stirring. To this was added dry triethylamine (1.22 mL, 8.7 mmol, 2.2 eq) followed by 2-chloroacetamide (390 mg, 4.2 mmol, 1.05 eq). The reaction was stirred at room temperature overnight. In the morning, the reaction was partitioned between chloroform (30 mL) and satd NH<sub>4</sub>Cl (30 mL). The aqueous layer was washed with CHCl<sub>3</sub> (3 x 30 mL) until no product remained (as judged by TLC). The combined organic layers were washed with satd NH<sub>4</sub>Cl (30 mL), water (30 mL), and brine (30 mL), dried (Na<sub>2</sub>SO<sub>4</sub>), and concentrated. The product was adsorbed to silica prior to column chromatography. The column was eluted with a gradient system, beginning at 50% EtOAc/Hex (100 mL), increasing to 75% EtOAc/Hex (100 mL), 100% EtOAc (100 mL), 5% MeOH/EtOAc, (100 mL) and 10% MeOH/EtOAc (100 mL). The product was isolated as a light orange solid (771 mg, 2.9 mmol, 77%), which was recrystallized before use in the coupling reactions from EtOAc/Hex. <sup>1</sup>H NMR (CDCl<sub>3</sub>): δ 8.07 (1H, br s); 7.97 (1H, dd, *J* = 7.9, 1.1 Hz); 7.66 (1H, dd, *J* = 8.2, 1.0 Hz); 7.35 (1H, t, *J* = 7.9 Hz); 5.66 (1H, br s); 3.98 (3H, s); 3.92 (2H, s). <sup>1</sup>H NMR (*d*<sub>6</sub>-DMSO): 7.91 (1H, d, *J* = 8.2 Hz); 7.84 (1H, d, *J* = 7.0 Hz), 7.82 (1H, br s); 7.41 (1H, t, *J* = 8.0 Hz); 7.38 (1H, br s); 4.16 (2H, s); 3.32 (3H, s). <sup>13</sup>C NMR (CDCl<sub>3</sub>): δ 170.3, 167.7, 165.1, 152.8, 140.7, 126.8, 123.8, 120.2, 114.5, 52.3, 34.8. LRMS (CI<sup>+</sup>): 267 (M<sup>+</sup>+1). HRMS (CI<sup>+</sup>): calcd. for C<sub>11</sub>H<sub>11</sub>N<sub>2</sub>O<sub>4</sub>S 267.0440, found: 267.0445. IR (KBr pellet): 3388, 3196, 1704, 1661, 1500, 1425, 1301, 1236, 1137, 763 cm<sup>-1</sup>. mp: 163.8-165 °C.



**TOP 054. 2-Dimethylcarbamoylmethylsulfanylbenzoxazole-4-carboxylic acid methyl ester. TOP053** (311 mg, 1.5 mmol, 1 eq) was dissolved in dry THF (3 mL, 0.5 M) with stirring. To this was added dry triethylamine (456  $\mu$ L, 3.3 mmol, 2.2 eq) followed by *N,N*-dimethyl-2-chloroacetamide (161  $\mu$ L, 1.6 mmol, 1.05 eq). The reaction was stirred at room temperature overnight. The reaction was partitioned between chloroform (30 mL) and satd  $\text{NH}_4\text{Cl}$  (30 mL). The aqueous layer was washed with  $\text{CHCl}_3$  (3 x 30 mL) until no product remained (as judged by TLC). The combined organic layers were washed with satd  $\text{NH}_4\text{Cl}$  (30 mL), water (30 mL), and brine (30 mL), dried ( $\text{Na}_2\text{SO}_4$ ), and concentrated. The product was adsorbed to silica prior to column chromatography. The column was eluted with a gradient system, beginning at 50% EtOAc/Hex (100 mL), increasing to 75% EtOAc/Hex (100 mL), 100% EtOAc (100 mL), 5% MeOH/EtOAc, (100 mL) and 10% MeOH/EtOAc (100 mL). The product was isolated as a light orange solid (337 mg, 1.1 mmol, 77%), which was recrystallized before use in the coupling reactions from EtOAc/Hex.  $^1\text{H}$  NMR ( $\text{CDCl}_3$ ):  $\delta$  7.90 (1H, dd,  $J = 7.9, 1.0$ ); 7.59 (1H, d,  $J = 8.2$ ); 7.26 (1H, t,  $J = 8.1$ ); 4.42 (2H, s); 3.96 (3H, s); 3.20 (3H, s); 2.99 (3H, s).  $^{13}\text{C}$  NMR ( $\text{CDCl}_3$ ):  $\delta$  167.1, 166.5, 165.4, 152.5, 141.4, 126.5, 123.2, 120.2, 113.0, 52.2, 37.7, 36.4, 35.9. LRMS ( $\text{CI}^+$ ): 295 ( $\text{M}^+ + 1$ ). HRMS ( $\text{CI}^+$ ): calcd. for  $\text{C}_{13}\text{H}_{14}\text{N}_2\text{O}_4\text{S}$  295.0753, found 295.0753. IR (KBr pellet): 3456, 1721, 1640, 1488, 1423, 1278, 1197, 1123, 750  $\text{cm}^{-1}$ . mp 121.9-123.9  $^\circ\text{C}$ .

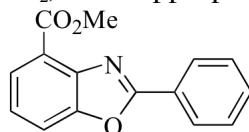


**TOP063. Methyl 2-formamido-3-hydroxybenzoate. TOP054** (50 mg, 0.17 mmol, 1 eq) was combined with phenylboronic acid (45.2 mg, 0.37 mmol, 2.2 eq) in a 7 mL capacity thick-walled tube. The tube was flushed with Ar, and dioxane (2.4 mL) was added.  $\text{Pd}_2\text{dba}_3$ , (0.7 mg, 0.0016 mmol, 1 mol%) and trifurylphosphine (1.4 mg, 0.0014 mmol, 4 mol%) were added as a solution in dioxane (1 mL, final rxn. conc. 0.05 M). The tube was sealed, and the reaction was

heated to 110 °C for 16 h. After 16 h, the reaction was cooled and partitioned between ether (20 mL) and water (15 mL). The aqueous layer was extracted with ether (2x15 mL), and the combined organic layers were washed with satd NaCl (20 mL), dried (MgSO<sub>4</sub>), and conc. The reaction mixture was absorbed to silica and FCC (SiO<sub>2</sub>) in a gradient 10% EtOAc/Hex→25% EtOAc/Hex. Fractions were allowed to evaporate overnight to improve recovery, as the product is not easily seen by TLC. The product was isolated as a white solid (22.7 mg, 0.12 mmol, 71%). An analytical sample was recrystallized from EtOAc/Hex. <sup>1</sup>H NMR (400 MHz, *d*<sub>6</sub>-DMSO): δ 11.80 (1H, br s); 7.63 (1H, d, *J* = 8.2); 7.52 (1H, d, *J* = 8.2); 7.18 (1H, t, *J* = 8.1); 3.87 (3H, s). <sup>13</sup>C (100 MHz, *d*<sub>6</sub>-DMSO): δ 164.4, 154.3, 143.9, 131.2, 124.2, 121.5, 113.9, 113.4, 52.1. LRMS (CI<sup>+</sup>): 194 (100%, M<sup>+</sup>), 162 (M<sup>+</sup>-OCH<sub>3</sub>). mp = 226.8-227.4 °C.

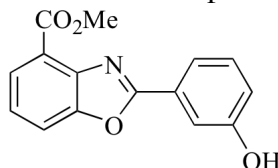
**General procedure for Liebeskind coupling reactions:**

**TOP054** (50 mg, 0.17 mmol, 1 eq) was combined with the appropriate arylboronic acid (0.37 mmol, 2.2 eq) and CuTC (71.2 mg, 0.27 mmol, 2.2 eq) in a 7 mL capacity thick-walled tube. The tub was flushed with Ar, and dioxane (2.4 mL) was added. Pd<sub>2</sub>dba<sub>3</sub>, (0.7 mg, 0.0016 mmol, 1 mol%) and trifurylphosphine (1.4 mg, 0.0014 mmol, 4 mol%) were added as a solution in dioxane (1 mL, final rxn. conc. 0.05 M). The tube was sealed, and the reaction was heated to 110 °C for 16 h. After 16 h, the reaction was cooled and partitioned between ether (20 mL) and satd NaCl (15 mL). The aqueous layer was extracted with ether (2x15 mL), and the combined organic layers were washed twice with 15 mL of 2 M NaOH (except **TOP067** and **TOP068**, for which this step was omitted) with satd NaCl (20 mL), dried (MgSO<sub>4</sub>), and conc. The reaction mixture was absorbed to silica and FCC (SiO<sub>2</sub>) in an appropriate mixture of EtOAc/Hex.

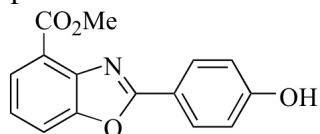


**TOP066. 2-Phenylbenzoxazole-4-carboxylic acid methyl ester.**<sup>53</sup> FCC in 10% EtOAc/Hex. Fractions were allowed to evaporate overnight to improve recovery, as the product is not easily seen by TLC. The product was isolated as a white solid (20.7 mg, 0.08 mmol, 48%). An analytical sample was recrystallized from EtOAc/Hex. <sup>1</sup>H NMR (400 MHz, CDCl<sub>3</sub>): δ 8.33

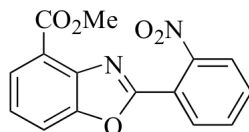
(2H, dd,  $J = 7.7, 1.7$ ); 8.01 (1H, dd,  $J = 7.8, 1.0$ ); 7.75 (1H, dd,  $J = 8.1, 0.9$ ); 7.54-7.48 (3H, m); 7.38 (1H, t,  $J = 8.0$ ) 4.05 (3H, s).  $^{13}\text{C}$  NMR (100 MHz,  $\text{CDCl}_3$ ):  $\delta$  165.7, 164.6, 151.3, 141.6, 132.0, 128.8, 128.1, 126.9, 126.4, 124.3, 121.9, 114.8, 52.4. LRMS ( $\text{CI}^+$ ): 254 ( $\text{M}^++1$ ). HRMS ( $\text{CI}^+$ ): calcd for  $\text{C}_{15}\text{H}_{11}\text{NO}_3$ : 254.0817, found 254.0811. mp 75-80 °C. (lit.<sup>53</sup> 78-81 °C)



**TOP067. 2-(3-Hydroxyphenyl)-benzoxazole-4-carboxylic acid methyl ester.** FCC in Hexanes→25% EtOAc/Hex yielded the product as a white solid (27 mg, 0.10 mmol, 59%).  $^1\text{H}$  NMR ( $\text{CDCl}_3$ ):  $\delta$  8.03 (1H, dd,  $J = 7.8, 1.0$ ); 7.89 (1H, s); 7.84 (1H, d,  $J = 7.8$ ); 7.77 (1H, dd,  $J = 8.0, 1.0$ ); 7.42 (1H, t,  $J = 7.7$ ); 7.37 (1H, t,  $J = 7.9$ ); 7.05 (1H, dd,  $J = 8.0, 1.7$ ); 6.64 (1H, br s); 4.03 (3H, s).  $^{13}\text{C}$  NMR ( $d_6$ -acetone):  $\delta$  166.0, 164.8, 158.8, 152.3, 142.3, 131.2, 128.8, 127.5, 125.5, 123.4, 120.2, 119.9, 115.7, 115.1, 52.3. LRMS ( $\text{CI}^+$ ): 270 ( $\text{M}^++1$ ), 238. HRMS calcd. for  $\text{C}_{15}\text{H}_{11}\text{NO}_4$ , 270.0766 found 270.0762. IR (KBr): 3215, 1781, 1722, 1687, 1635, 1464, 1431, 1320, 1261, 1130, 952, 748, 737  $\text{cm}^{-1}$ . mp 177.8-178.9 °C.

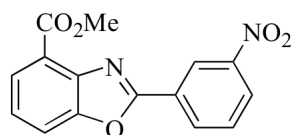


**TOP 068. 2-(4-Hydroxyphenyl)-benzoxazole-4-carboxylic acid methyl ester.** FCC (Hexanes→25% EtOAc/Hex) yielded the product as a white solid (22.7 mg, 0.084 mmol, 50%).  $^1\text{H}$  NMR ( $\text{CDCl}_3$ ):  $\delta$  8.24 (2H, d,  $J = 8.8$ ); 8.01 (1H, dd,  $J = 7.8, 1.0$ ); 7.75 (1H, dd,  $J = 8.0, 1.0$ ); 7.44 (1H, s); 7.38 (1H, t,  $J = 8.0$ ); 7.15 (1H, t,  $J = 8.0$ ); 7.02 (2H, d,  $J = 8.8$ ); 4.05 (3H, s).  $^{13}\text{C}$  NMR( $d_6$ -acetone):  $\delta$  166.2, 165.3, 162.1, 152.3, 142.7, 130.7, 127.3, 124.8, 122.8, 118.9, 116.9, 115.3, 52.2. LRMS ( $\text{CI}^+$ ): 270 ( $\text{M}^++1$ ), 185. HRMS ( $\text{CI}^+$ ): calcd. for  $\text{C}_{15}\text{H}_{11}\text{NO}_4$  270.0766, found 270.0766. IR (KBr): 3352, 1709, 1610, 1597, 1424, 1297, 1269, 1240, 1227, 1197, 1170, 1145, 1053, 848, 757  $\text{cm}^{-1}$ . mp (decomp) 211.7-213.9 °C.

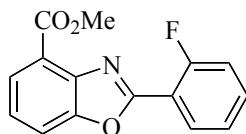




**KeTOP069. 2-(2-Nitrophenyl)-benzoxazole-4-carboxylic acid methyl ester.**<sup>7</sup> FCC (25% EtOAc/Hex) yielded the product as a white solid (23.3 mg, 0.078 mmol, 46%). <sup>1</sup>H NMR (CDCl<sub>3</sub>): δ 9.14 (1H, m), 8.69 (1H, dd, *J* = 7.8, 1.2 Hz); 8.42-8.39 (1H, m); 8.07 (1H, dd, *J* = 7.8, 1.0 Hz); 7.83 (1H, dd, *J* = 8.1, 0.9); 7.74 (1H, t, *J* = 8.0); 4.07 (3H, s). <sup>13</sup>C NMR (CDCl<sub>3</sub>): δ 165.5, 162.1, 151.4, 148.6, 141.2, 133.7, 130.1, 128.3, 127.5, 126.3, 125.4, 122.9, 122.6, 115.2, 52.6. LRMS (CI<sup>+</sup>): 299 (M<sup>+</sup>+1), 269 (M<sup>+</sup>-OCH<sub>3</sub>). HRMS (CI<sup>+</sup>) calcd. for C<sub>15</sub>H<sub>10</sub>N<sub>2</sub>O<sub>5</sub>: 299.0668, found: 299.0666. IR (KBr): 1726, 1532, 1430, 1354, 1289, 1240, 1195, 1146, 1024, 759, 747, 710 cm<sup>-1</sup>. mp 165.3-166.7 °C.

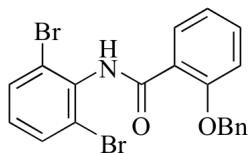


**KeTOP070. 2-(3-Nitrophenyl)-benzoxazole-4-carboxylic acid methyl ester.** FCC (Hexanes-25% EtOAc/Hex) yielded the product as a white solid (29.8 mg, 0.10 mmol, 59%). <sup>1</sup>H NMR (CDCl<sub>3</sub>): δ 9.13 (1H, t, *J* = 1.8); 8.68 (1H, ddd, *J* = 7.8, 1.2, 0.8); 8.40 (1H, ddd, *J* = 8.2, 2.3, 1.2); 8.06 (1H, dd, *J* = 7.8, 1.0); 7.82 (1H, dd, *J* = 8.1, 1.1); 7.74 (1H, t, *J* = 8.0); 7.48 (1H, t, *J* = 7.9); 4.07 (3H, s). <sup>13</sup>C NMR (CDCl<sub>3</sub>): δ 165.4, 162.0, 151.4, 148.6, 141.2, 133.7, 130.1, 128.3, 127.5, 126.3, 125.4, 122.9, 122.6, 115.2, 52.6. LRMS (CI<sup>+</sup>): 299 (M<sup>+</sup>+1). HRMS (CI<sup>+</sup>): calcd for C<sub>15</sub>H<sub>10</sub>N<sub>2</sub>O<sub>5</sub>: 299.0668, found: 299.0670. IR(KBr): 1782, 1735, 1713, 1686, 1655, 1560, 1542, 1509, 1476, 1459, 1421, 1354, 1321, 1299, 1283, 1191, 1064, 794, 748, 710 cm<sup>-1</sup>. mp 157.5-161.4 °C

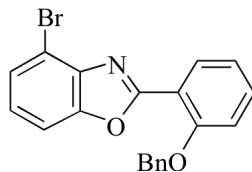


**TOP075. 2-(2-fluorophenyl)-benzoxazole-4-carboxylic acid methyl ester.** FCC (10% EtOAc/Hex) yielded the product as a white solid (14.2 mg, 0.052 mmol, 31%). <sup>1</sup>H NMR (CDCl<sub>3</sub>): δ 8.36 (1H, td, *J* = 7.6, 1.8); 8.06 (1H, d, *J* = 7.8, 1.0); 7.82 (1H, dd, *J* = 8.1, 0.9); 7.55 (1H, dddd, *J* = 12.4, 7.3, 4.9, 0.8); 7.45 (1H, t, *J* = 8.0); 7.32 (1H, td, *J* = 7.8, 1.2); 7.26 (1H, ddd, *J* = 11.0, 8.4, 1.0); 4.07 (3H, s). <sup>13</sup>C NMR (CDCl<sub>3</sub>): δ 165.1, 161.4 (*J* = 4.6), 160.2 (*J*<sub>C-F</sub> = 259.8 Hz); 151.31, 151.29, 141.0, 133.7 (*J*<sub>C-F</sub> = 8.5 Hz); 131.2, 127.2, 124.5 (*J*<sub>C-F</sub> = 3.9 Hz), 122.2,

116.0 ( $J_{C-F} = 21.5$  Hz), 115.1, 115.0 ( $J_{C-F} = 10.8$ ), 52.5. LRMS ( $CI^+$ ): 272 ( $M^+ + 1$ ). HRMS ( $CI^+$ ) calcd for  $C_{15}H_{10}FNO_3$ : 272.0271, found 272.0723. IR (KBr): 2952, 1716, 1655, 1543, 1317, 1294, 1243, 1223, 1174, 1140, 1111, 1073, 1027, 758  $cm^{-1}$ . mp 90.0-90.4 °C.



**TOP 062. 2-Benzyloxy-N-(2,6-dibromophenyl)benzamide.** 2-Benzyloxysalicylic acid (2.90g, 12.7 mmol, 1 eq) was dissolved in DCM (24.4 mL, 0.52 M) and cooled to 0 °C in an ice-water bath. Oxalyl chloride (1.31 mL, 15.3 mmol, 1.2 eq) was added dropwise and the reaction was warmed to room temperature. After gas evolution ceased, 1 drop DMF was added. After 1 h at room temperature, the reaction was concentrated by rotary evaporation to an off-white solid. The solid was dissolved in DMF (1.82 mL, 7 M), and 2,6-dibromoaniline (3.16 g, 12.7 mmol, 1 eq) was added. The mixture was warmed to 50 °C overnight. A white solid formed after approx. 30 min. After 16 h at 50 °C, the reaction was partitioned between  $Et_2O$  (50 mL) and water (50 mL). The aqueous layer was washed 2x with  $Et_2O$  (30 mL), and the combined organic layers were washed with satd NaCl (50 mL) and dried ( $MgSO_4$ ). Concentration *in vacuo* yielded a white crystalline solid that was clean by  $^1H$  NMR and TLC. An analytical sample was crystallized from  $EtOAc/Hex$  to give a white solid (4.18 g, 9.11 mmol, 72%).  $^1H$  NMR ( $CDCl_3$ , 400 MHz):  $\delta$  9.58 (1H, s); 8.34 (1H, dd,  $J = 7.8, 1.1$ ); 7.57 (2H, dd,  $J = 8.1, 0.6$ ); 7.51-7.49 (3H, m); 7.38 (3H, m); 7.14 (2H, q,  $J = 8.0$ ); 7.00 (1H, t,  $J = 8.0$ ) 5.33 (s, 2H).  $^{13}C$  NMR ( $CDCl_3$ , 100 MHz):  $\delta$  163.1, 156.9, 135.4, 135.3, 133.5, 133.0, 132.1, 129.0, 128.9, 128.7, 127.9, 123.6, 121.7, 121.0, 112.9, 71.5. LRMS ( $ESI^+$ ): 483.87. HRMS ( $ESI^+$ ): calcd: 459.9541, found 459.9542. IR (KBr): 3335, 3068 (w), 1670, 1599, 1497, 1480, 1452, 1295, 1223, 754, 724. mp 155.0-156.1 °C.



**TOP064. 2-(2-Benzyloxyphenyl)-4-bromobenzoxazole.** Amide **TOP062** (100 mg, 0.22 mmol, 1 eq) was combined with copper(I) iodide (2 mg, 0.01 mmol, 5 mol%), 1,10-phenanthroline (3.9 mg, 0.02 mmol, 10 mol%), and potassium carbonate (60 mg, 0.44 mmol, 2 eq) were combined in a sealed tube and flushed with Ar. DME was added (670  $\mu$ L, 0.33 M) was added, and the tube was sealed and heated to 130  $^{\circ}$ C overnight. After 16 h, the reaction was cooled to room temperature and partitioned between Et<sub>2</sub>O (10 mL) and water (20 mL). The aqueous layer was washed 2x with Et<sub>2</sub>O (20 mL), and the combined organic extracts were washed with satd NaCl (20 mL), and dried (MgSO<sub>4</sub>). The product was a white crystalline solid (68 mg, 0.18 mmol, 82%) which was clean as judged by TLC and <sup>1</sup>H NMR. An analytical sample was recrystallized from EtOAc/Hex. <sup>1</sup>H NMR (400 MHz, CDCl<sub>3</sub>):  $\delta$  8.26 (1H, d,  $J$  = 7.5); 7.77 (2H, d,  $J$  = 7.2); 7.60-7.52 (3H, m); 7.47 (2H, t,  $J$  = 7.0); 7.37 (1H, t,  $J$  = 7.0); 7.30-7.34 (1H, m); 7.20-7.12 (2H, m); 5.33 (2H, s). <sup>13</sup>C NMR (100 MHz, CDCl<sub>3</sub>):  $\delta$  162.2, 157.6, 150.5, 141.6, 136.6, 133.1, 131.5, 128.5, 127.6, 127.5, 126.7, 125.7, 121.0, 116.1, 113.5, 112.7, 109.5, 70.4. LRMS (CI<sup>+</sup>): 380, 382 (M<sup>+</sup>+1), 290, 292 (M<sup>+</sup>-OBn). HRMS (CI<sup>+</sup>): calcd. for C<sub>20</sub>H<sub>14</sub>BrNO<sub>2</sub> 379.0208, found 379.0204. IR (KBr): 3056, 1612, 1580, 1547, 1497, 1473, 1455, 1444, 1418, 1382, 1293, 1269, 1178, 1167, 1012, 847, 776, 735, 696, 464 cm<sup>-1</sup>. mp 98.4-100.9  $^{\circ}$ C.

- (1) Ueki, M.; Taniguchi, M. *J. of Antibiot.* **1997**, *50*, 788-790.
- (2) Ueki, M.; Ueno, K.; Miyadho, S.; Abe, K.; Shibata, K.; Taniguchi, M.; Oi, S. *J. of Antibiot.* **1993**, *46*, 1089-1094.
- (3) Ueki, M.; Shibata, K.; Taniguchi, M. *J. of Antibiot.* **1998**, *51*, 883-885.
- (4) Hohmann, C.; Schneider, K.; Bruntner, C.; Irran, E.; Nicholson, G.; Bull, A. T.; Jones, A. L.; Brown, R.; Stach, J. E. M.; Goodfellow, M.; Beil, W.; Kramer, M.; Imhoff, J. F.; Sussmuth, R. D.; Fiedler, H.-P. *J. of Antibiot.* **2009**, *62*, 99-104.
- (5) Sato, S.; Kajiura, T.; Noguchi, M.; Takehana, K.; Kobayashi, T.; Tsuji, T. *J. of Antibiot.* **2001**, *54*, 102-104.
- (6) Sommer, P. S. M.; Almeida, R. C.; Schneider, K.; Beil, W.; Sussmuth, R. D.; Fiedler, H.-P. *J. of Antibiot.* **2008**, *61*, 683-686.
- (7) Tipparaju, S. K.; Joyasawal, S.; Pieroni, M.; Kaiser, M.; Brun, R.; Kozikowski, A. P. *J. Med. Chem.* **2008**, *51*, 7344-7347.
- (8) Shibata, K.; Kashiwada, M.; Ueki, M.; Taniguchi, M. *J. of Antibiot.* **1993**, *46*, 1095-1100.
- (9) Wang, B. B.; Maghami, N.; Goodlin, V. L.; Smith, P. J. *Bioorg. Med. Chem. Lett.* **2004**, *14*, 3221-3226.
- (10) Kumar, D.; Jacob, M. R.; Reynolds, M. B.; Kerwin, S. M. *Bioorg. Med. Chem. Lett.* **2002**, *10*, 3997-4004.
- (11) DeLuca, M. R.; Kerwin, S. M. *Tetrahedron Lett.* **1997**, *38*, 199-202.
- (12) Huang, S.-T.; Hseib, I.-J.; Chen, C. *Bioorg. Med. Chem. Lett.* **2006**, *14*, 6106-6119.
- (13) McKee, M. L.; Kerwin, S. M. *Bioorg. Med. Chem. Lett.* **2008**, *16*, 1775-1783.
- (14) Johnson, S. M.; Connelly, S.; Wilson, I. A.; Kelly, J. W. *J. Med. Chem.* **2008**, *51*, 260-270.
- (15) Terashima, M.; Ishii, M. *Synthesis* **1982**, 484-485.
- (16) Hein, D. W.; Alheim, R. J.; Leavitt, J. J. *J. Am. Chem. Soc.* **1957**, *79*, 427-429.
- (17) Kanaoka, Y.; Hamada, T.; Yonemitsu, O. *Chem. Pharm. Bull.* **1970**, *18*, 587-590.
- (18) Sannie, M. C.; Lapin, M. H. *Bulletin de la Societe Chimique de France* **1950**, 322-326.

- (19) Kaul, S.; Kumar, A.; Sain, B.; Bhatnager, A. K. *Synth. Commun.* **2007**, *37*, 2457-2460.
- (20) Nadaf, R. N.; Siddiqui, S. A.; Daniel, T.; Lahoti, R. J.; Srinivasan, K. V. *J. Mol. Catal. A: Chem.* **2002**, *214*, 155-160.
- (21) Kumar, R.; Selvam, C.; Kaur, G.; Chakraborti, A. K. *Synlett* **2005**, *9*, 1401-1404.
- (22) Hegedus, A.; Vigh, I.; Hell, Z. *Heteroatom Chemistry* **2004**, *15*, 428-431.
- (23) Seijas, J. A.; Vazquez-Tato, M. P.; Carballido-Reboredo, M. R.; Cresente-Campo, J.; Tomar-Lopez, L. *Synlett* **2007**, *2*, 0313-0317.
- (24) So, Y.-H.; DeCaire, R. *Synth. Commun.* **1998**, *28*, 4123-4135.
- (25) Pottorf, R. S.; Chadha, N. K.; Katkevics, M.; Ozola, V.; Suna, E.; Ghane, H.; Regberg, T.; Player, M. R. *Tetrahedron Lett.* **2003**, *44*, 175-178.
- (26) Kiselyov, A. *Tetrahedron Lett.* **1999**, *40*, 4119-412.
- (27) Moghaddam, F. M.; Bardajee, R.; Ismaili, H.; Taimoory, S. M. D. *Synth. Commun.* **2006**, *36*, 2543-2548.
- (28) Praveen, C.; Kumar, H.; Miuralidharan, D.; Perumal, P. T. *Tetrahedron* **2008**, *64*, 2369-2374.
- (29) Park, K. H.; Jun, K.; Shin, S. R.; Oh, S. W. *Tetrahedron Lett.* **1996**, *37*, 8869-8870.
- (30) Chang, J.; Zhao, K.; Pan, S. *Tetrahedron Lett.* **2002**, *43*, 951-954.
- (31) Varma, R. S.; Saini, R. K.; Prakash, O. *Tetrahedron Lett.* **1977**, *38*, 2621-2622.
- (32) Kumar, A.; Maurya, R. A.; Ahmad, P. *J. Comb. Chem.* **2009**, *11*, 198-201.
- (33) Chen, Y.-X.; Qian, L.-F.; Zhang, W.; Han, B. *Angew. Chemie, Int. Ed. Engl.* **2008**, *47*, 9330-9333.
- (34) Wilfred, C. D.; Taylor, R. J. K. *Synlett* **2004**, *2004*, 1628-1630.
- (35) Vorbriggen, H.; Krolikiewicz, K. *Tetrahedron Lett.* **1981**, *22*, 4471-4474.
- (36) Wang, Y.; Sarris, K.; Sauer, D. R.; Djuric, S. W. *Tetrahedron Lett.* **2006**, *47*, 4823-4926.
- (37) Altenhoff, G.; Glorius, F. *Adv. Synth. Catal.* **2004**, *346*, 1661-1664.
- (38) Ma, H. C.; Jiang, X. Z. *Synlett* **2008**, *9*, 1335-1340.

- (39) Evindar, G.; Batey, R. A. *J. Org. Chem.* **2006**, *71*, 1802-1808.
- (40) Viirre, R. D.; Evindar, G.; Batey, R. A. *J. Org. Chem.* **2008**, *73*, 3452-3459.
- (41) Barbero, N.; Carril, M.; SanMartin, R.; Dominguez, E. *Tetrahedron* **2007**, *63*, 10425-10432.
- (42) Bonnamour, J.; Bolm, C. *Org. Lett.* **2008**, *10*, 2665-2667.
- (43) Perry, R. J.; Wilson, B. D.; Miller, R. J. *J. Org. Chem.* **1992**, *57*, 2883-2887.
- (44) Lewis, J. C.; Wiedemann, S. H.; Bergman, R. G.; Ellman, J. A. *Org. Lett.* **2004**, *6*, 35-38.
- (45) Zhao, D.; Wang, W.; Lian, S.; Yang, F.; Lan, J.; You, J. *Chem. Eur. J.* **2009**, *15*, 1337-1340.
- (46) Liebeskind, L. S.; Srogl, J. *Org. Lett.* **2002**, *4*, 979-981.
- (47) Albaneze-Walker, J.; Bazaral, C.; Leavey, T.; Dormer, P. G.; Murry, J. A. *Org. Lett.* **2004**, *6*, 2097-2100.
- (48) Warnell, J. L. In *Biochem. Prep.*; Vestling, C. S., Ed.; John Wiley and Sons: New York, 1954, p 20-24.
- (49) VanAllan, J. A.; Deacon, B. D. *Org. Synth.* **1963**, *Coll, Vol. 4*, 569-570.
- (50) Fielder, D. A.; Collins, F. W. *J. Nat. Prod.* **1995**, *58*, 456-458.
- (51) Still, W. C.; Kahn, M.; Mitra, A. *J. Org. Chem.* **1978**, *43*, 2923-2924.
- (52) Gottlieb, H. E.; Kotlyar, V.; Nudelman, A. *J. Org. Chem.* **1997**, *62*, 7512-7515.
- (53) Goldstein, S. W.; Dambek, P. J. *J. Heterocyclic Chem.* **1990**, *27*, 335-336.

## Appendices

### APPENDIX I

#### Scanned $^1\text{H}$ and $^{13}\text{C}$ NMR spectra

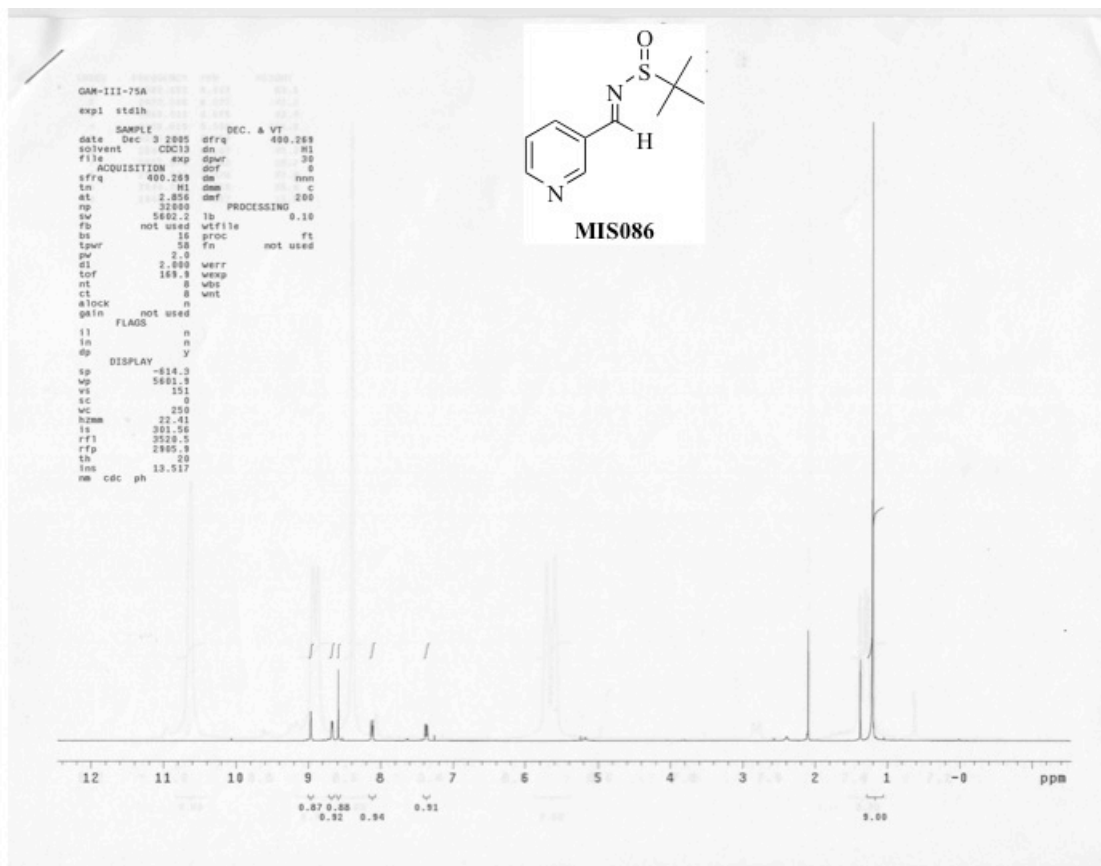


Figure A.1. MIS086  $^1\text{H}$  NMR

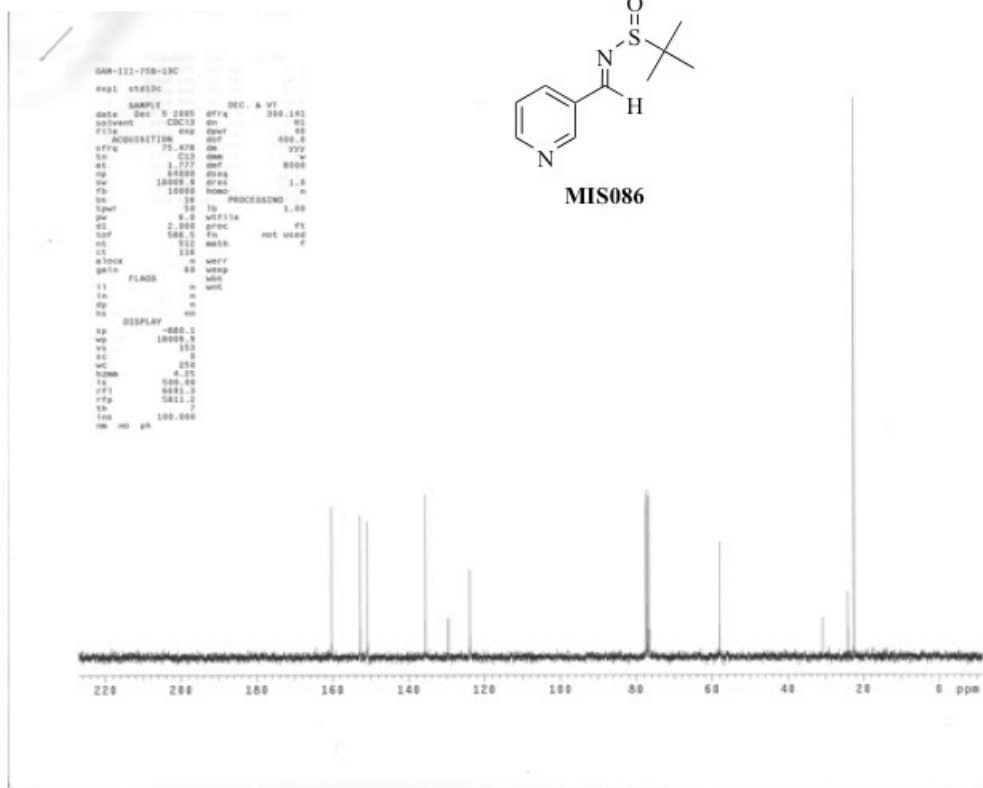


Figure A.2. MIS086 <sup>13</sup>C NMR



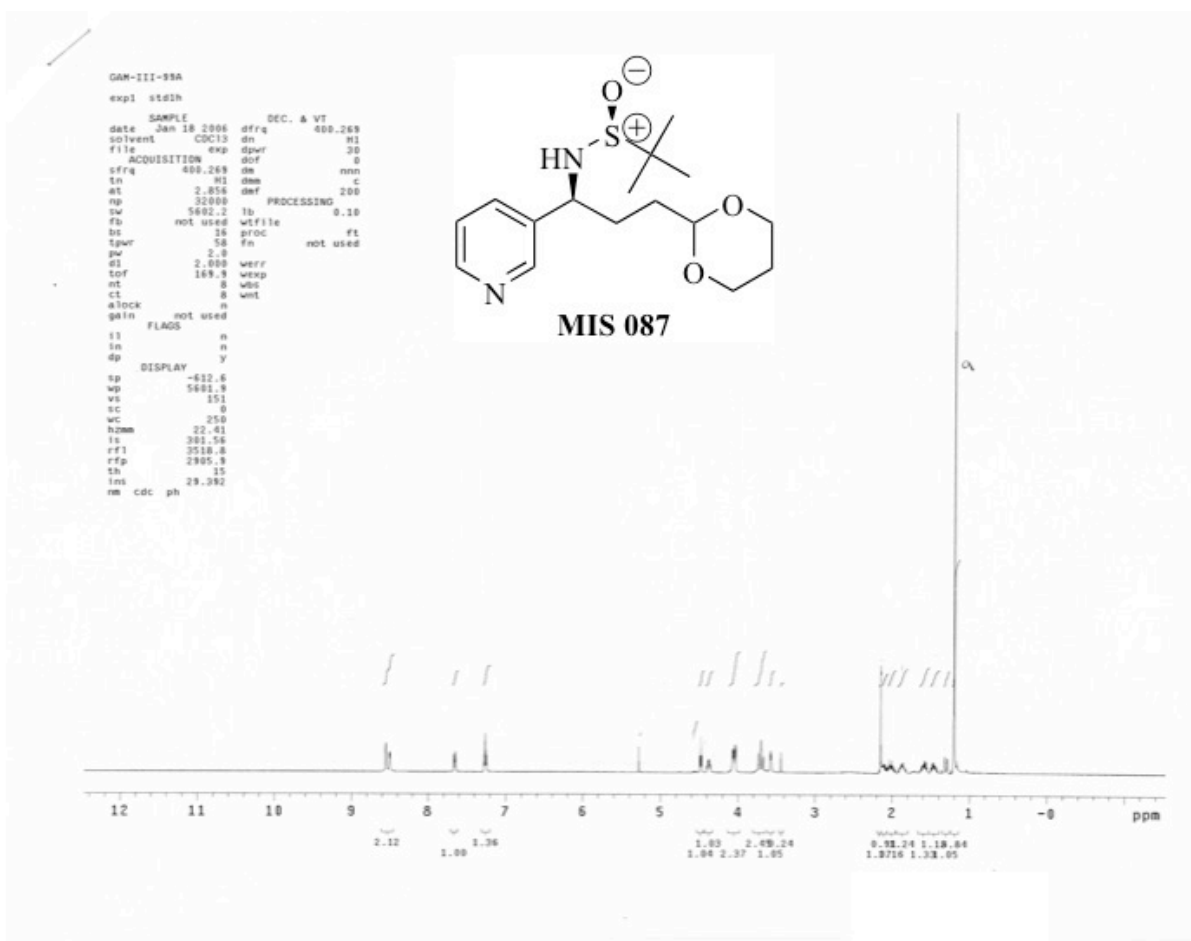


Figure A.3. MIS087 <sup>1</sup>H NMR

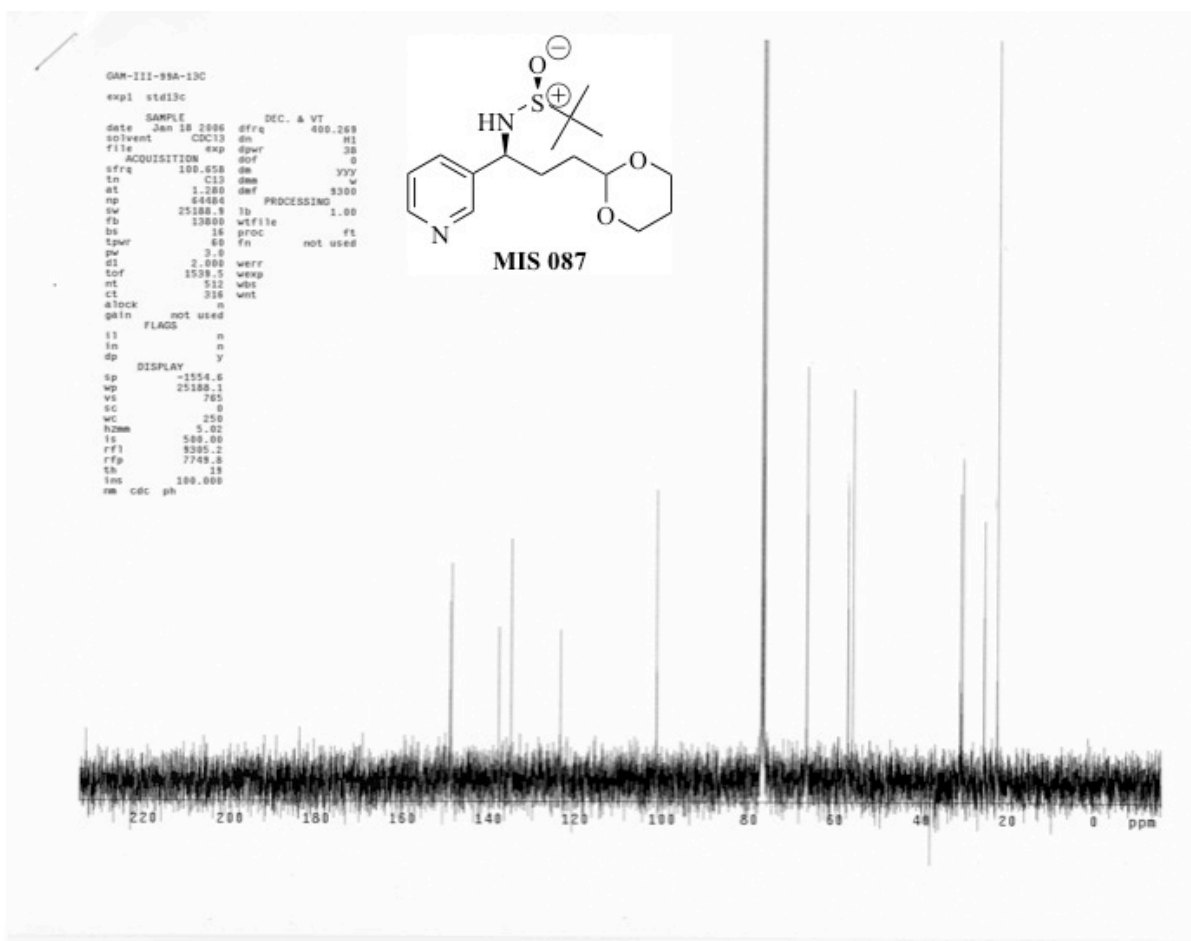


Figure A.4. MIS087 <sup>13</sup>C NMR

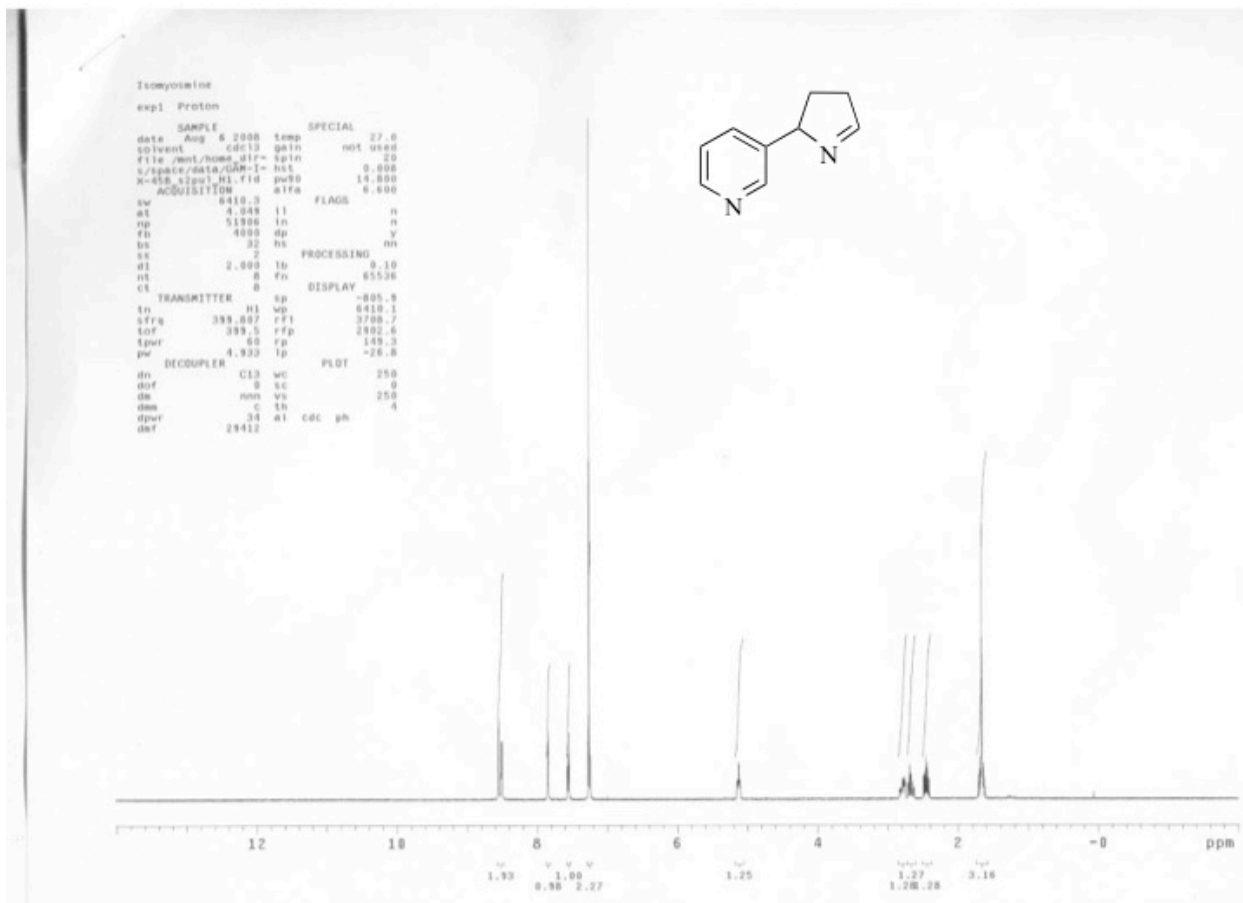


Figure A.5. Isomyosmine  $^1\text{H}$  NMR

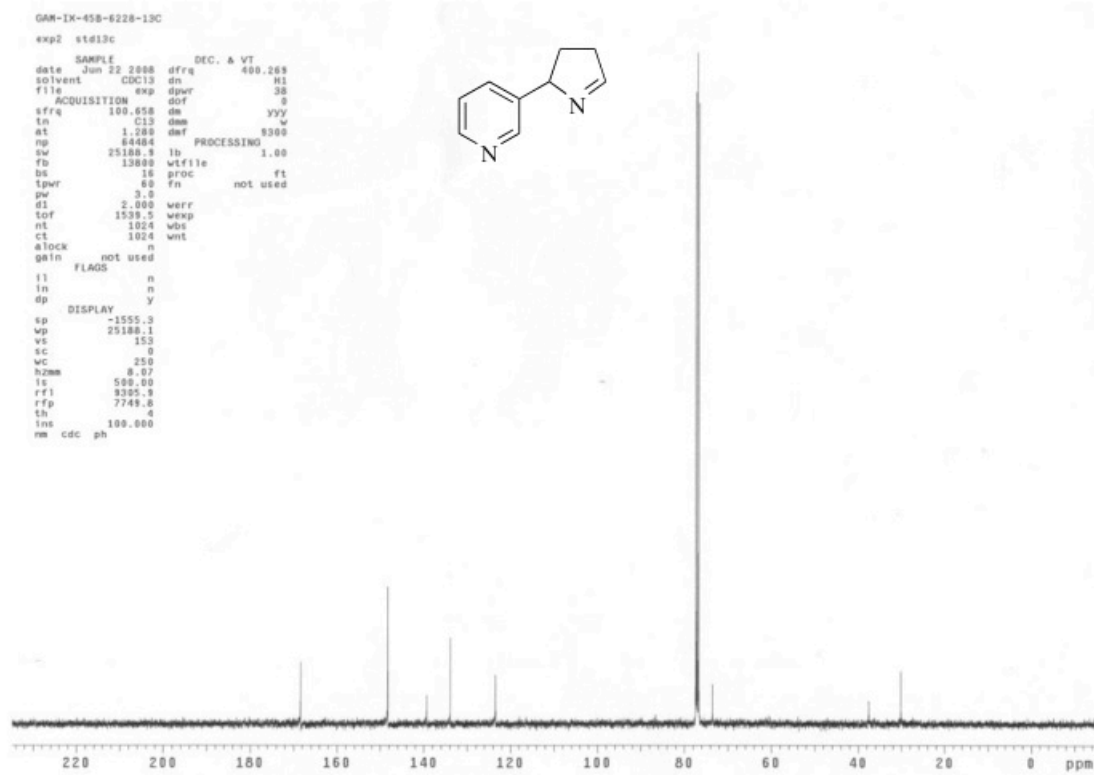


Figure A.6.  $^{13}\text{C}$  NMR of isomyosmine

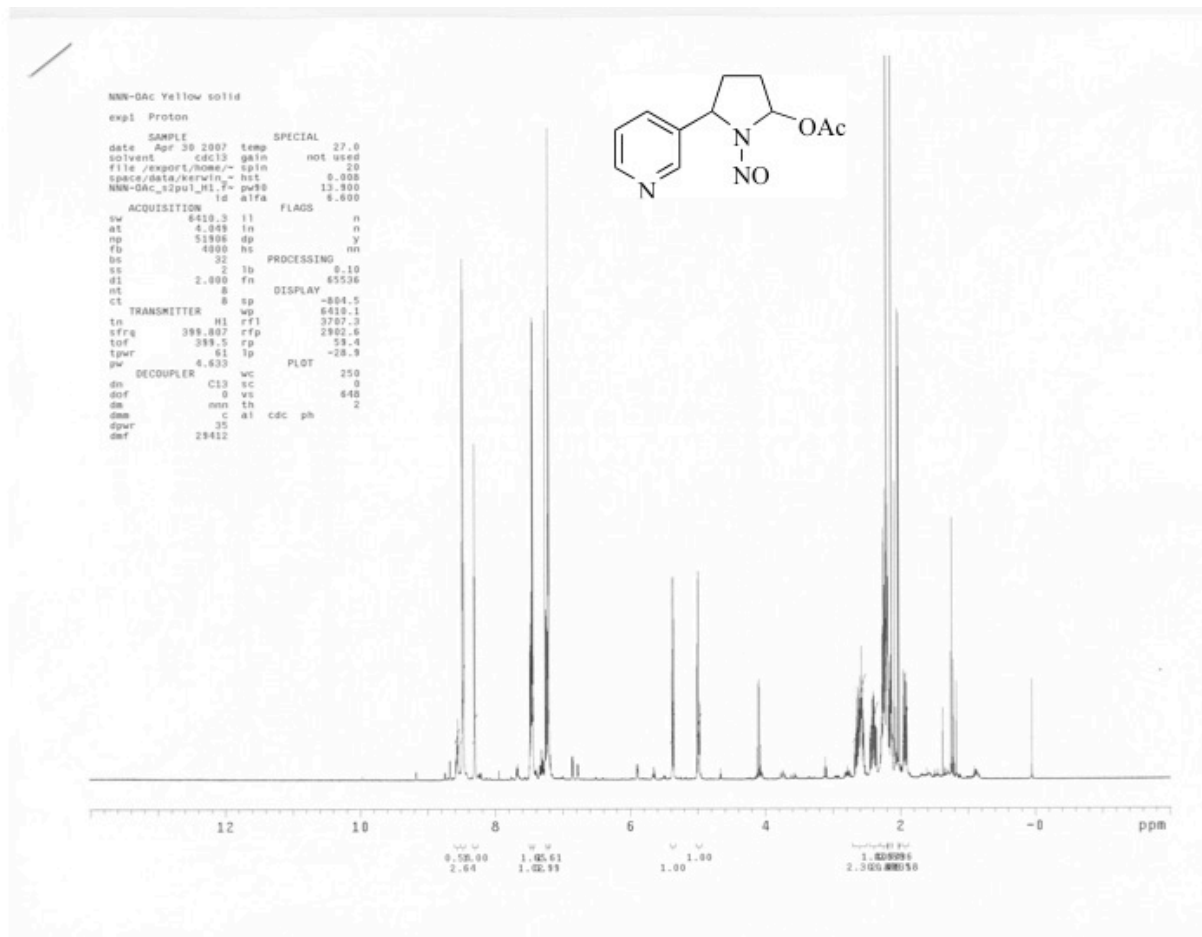


Figure A.7.  $^1\text{H}$  NMR of NNN-5'-OAc

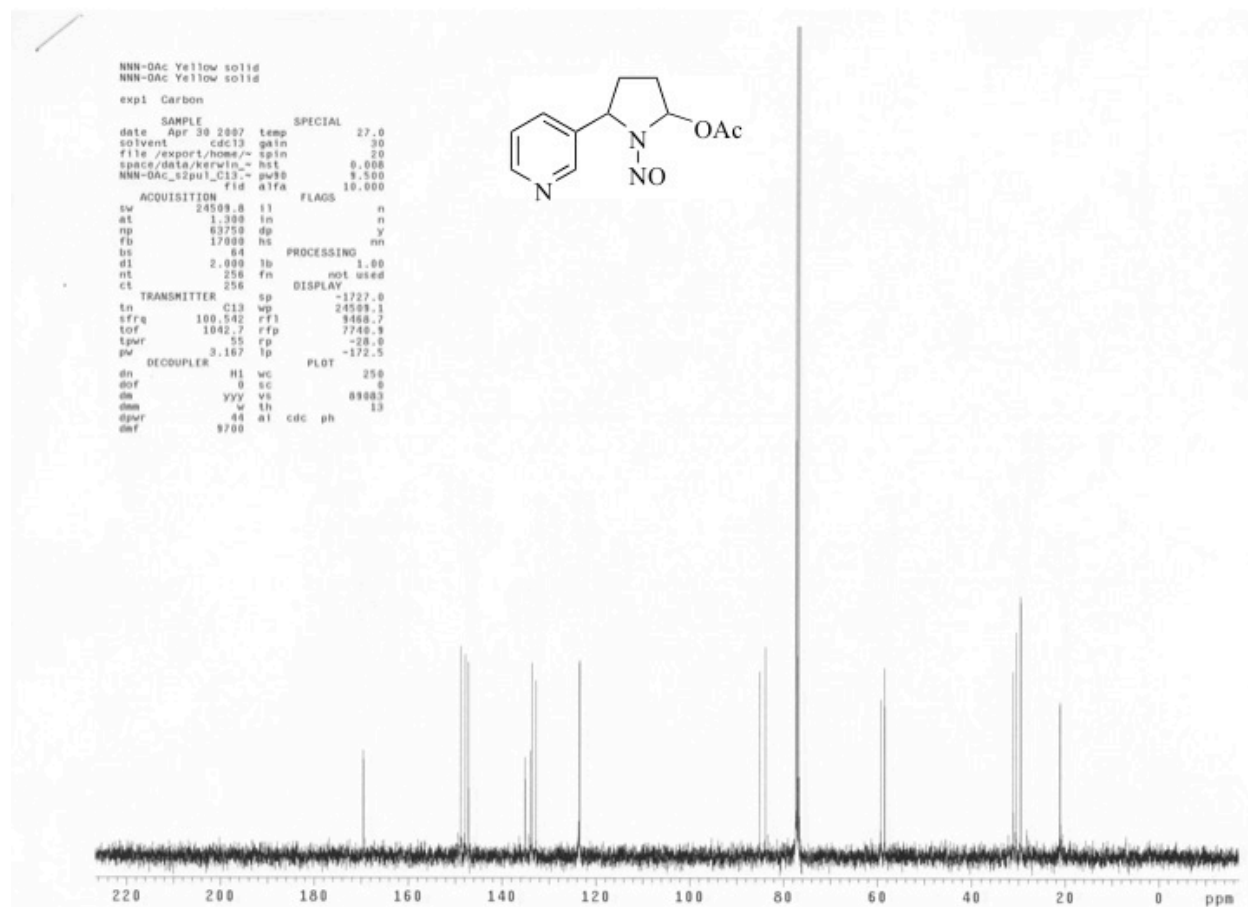


Figure A.8.  $^{13}\text{C}$  NMR of NNN-5'-OAc

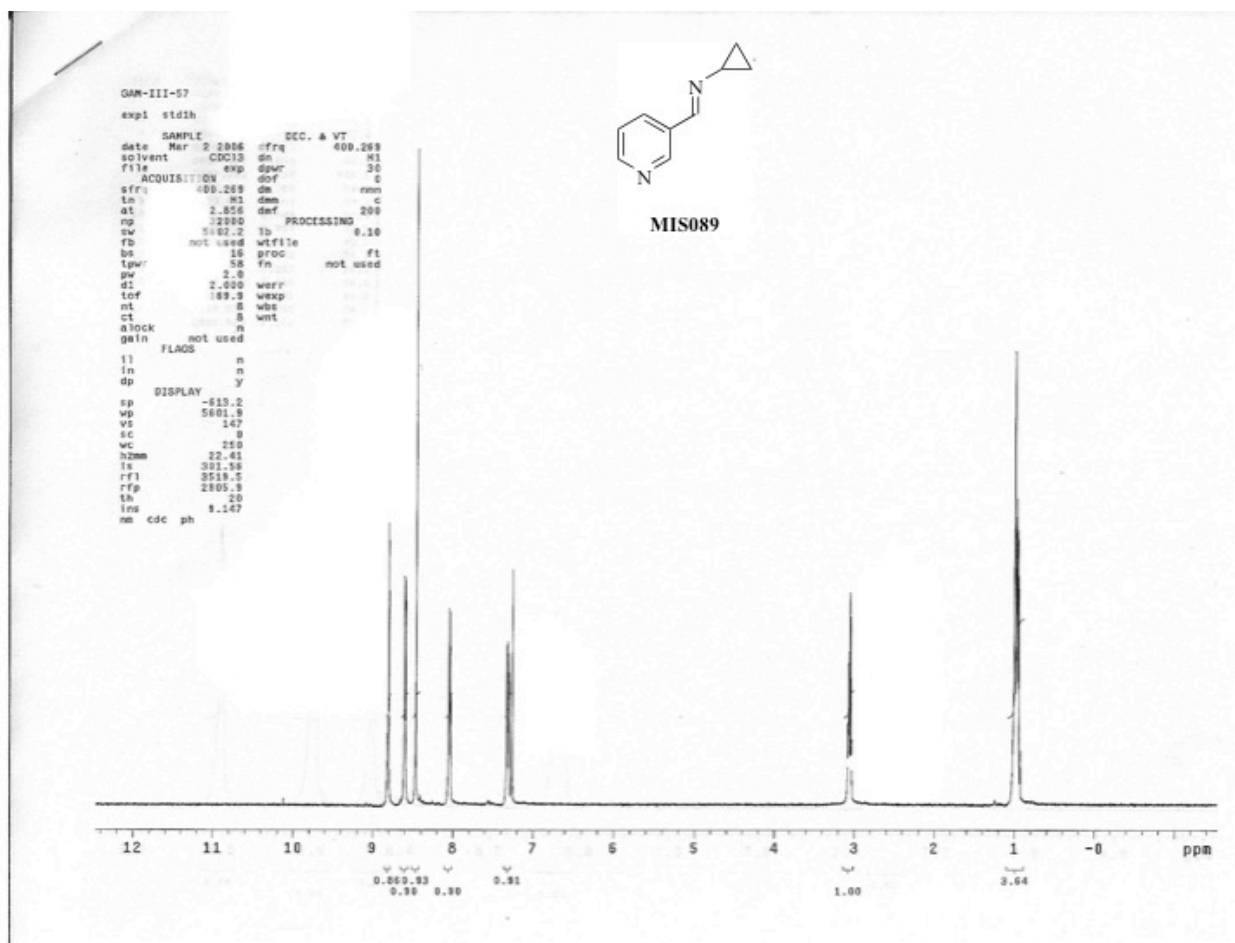


Figure A.9.  $^1\text{H}$  NMR of MIS089.

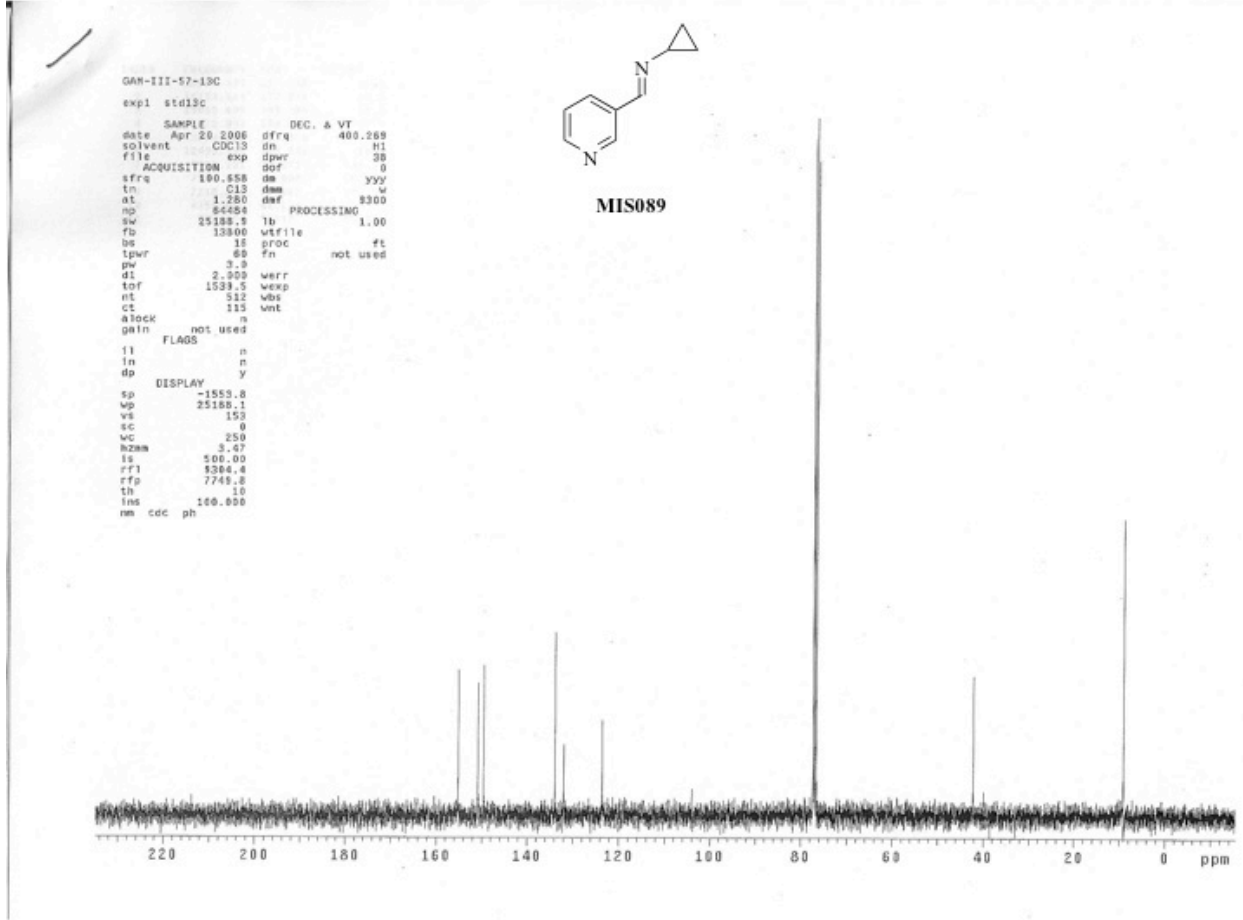


Figure A.10. <sup>13</sup>C NMR of MIS089



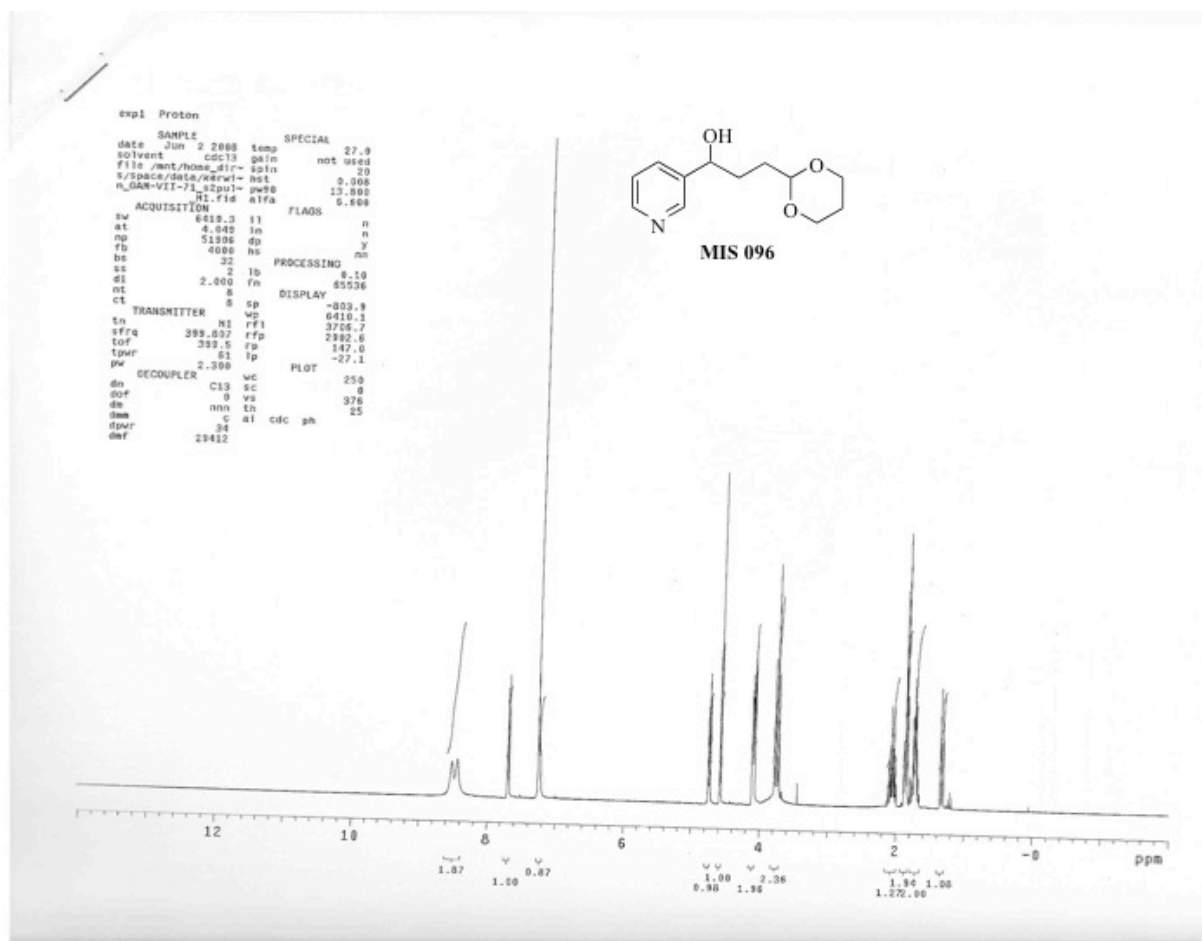


Figure A.11.  $^1\text{H}$  NMR of MIS096

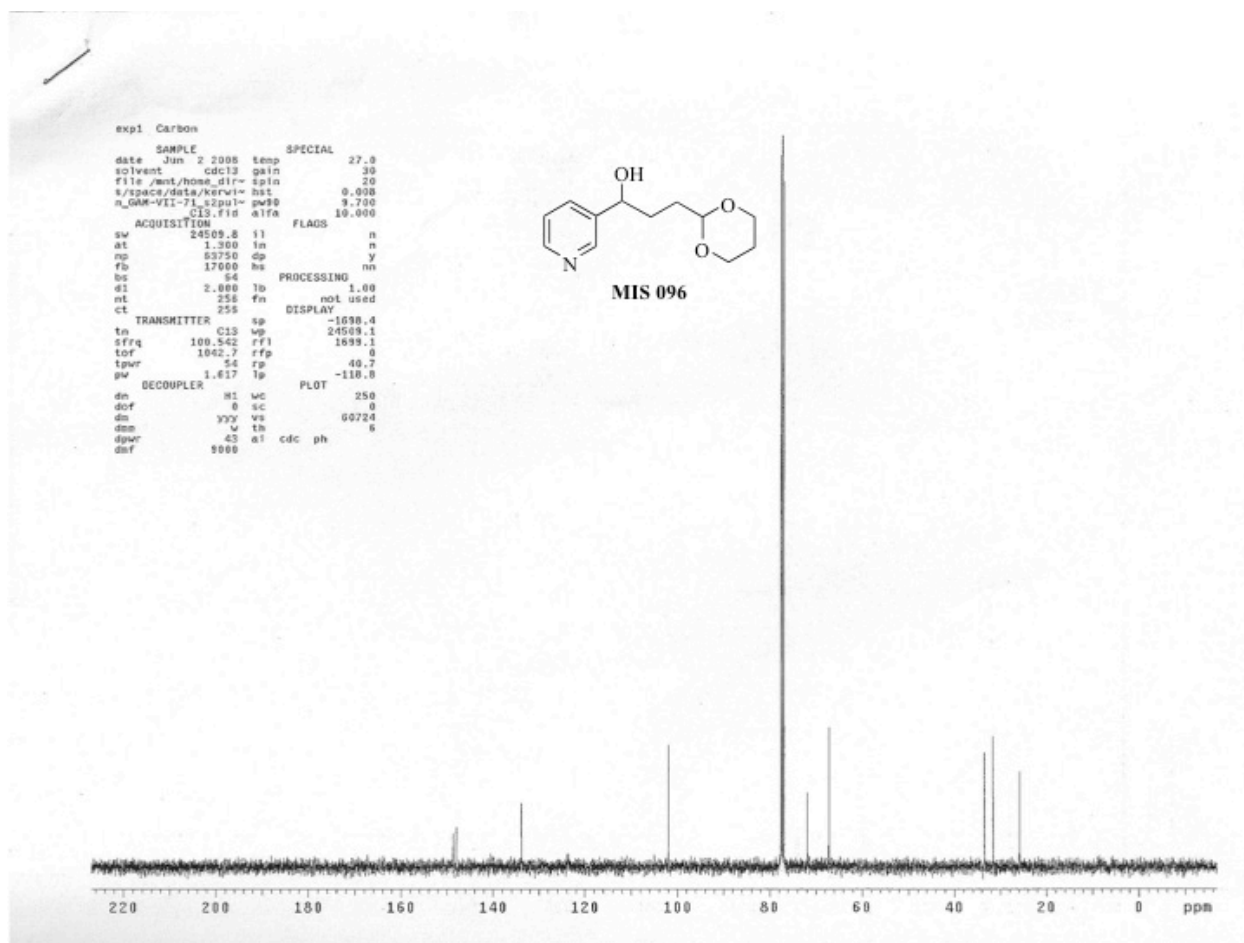


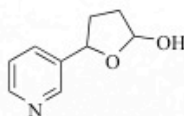
Figure A.12.  $^{13}\text{C}$  NMR of MIS096

2-OH THF FCC again

exp1 Proton

```
SAMPLE          SPECIAL
date Oct 30 2006 temp 27.0
solvent cdcl3 gain not used
file /export/home/~ spin 20
spec/data/kevin_ hst 0.005
QAM-VI-74_2pul_3j= pw90 13.500
l.fid a1fa 0.600

ACQUISITION     FLAGS
sw 640.3 i1 n
at 4.049 in n
ng 51886 dp y
fs 4990 hs
bs 32 PROCESSING
ss 2 lb 0.10
d1 2.000 fm 65536
nt 5 DISPLAY
ct 0 sp -806.1
TRANSMITTER     wp 6410.1
tn H1 rf1 3700.8
efrq 399.807 rfp 2902.8
tof 399.5 rp 63.2
tpr 61 lp -24.7
pw 4.600 PLOT
dn DECOUPLER wc 250
d1 c13 sc 0
dof 0 ve 580
ds nnn th 20
dpc c a1 cdc ph
dnf 29412
```



MIS 097

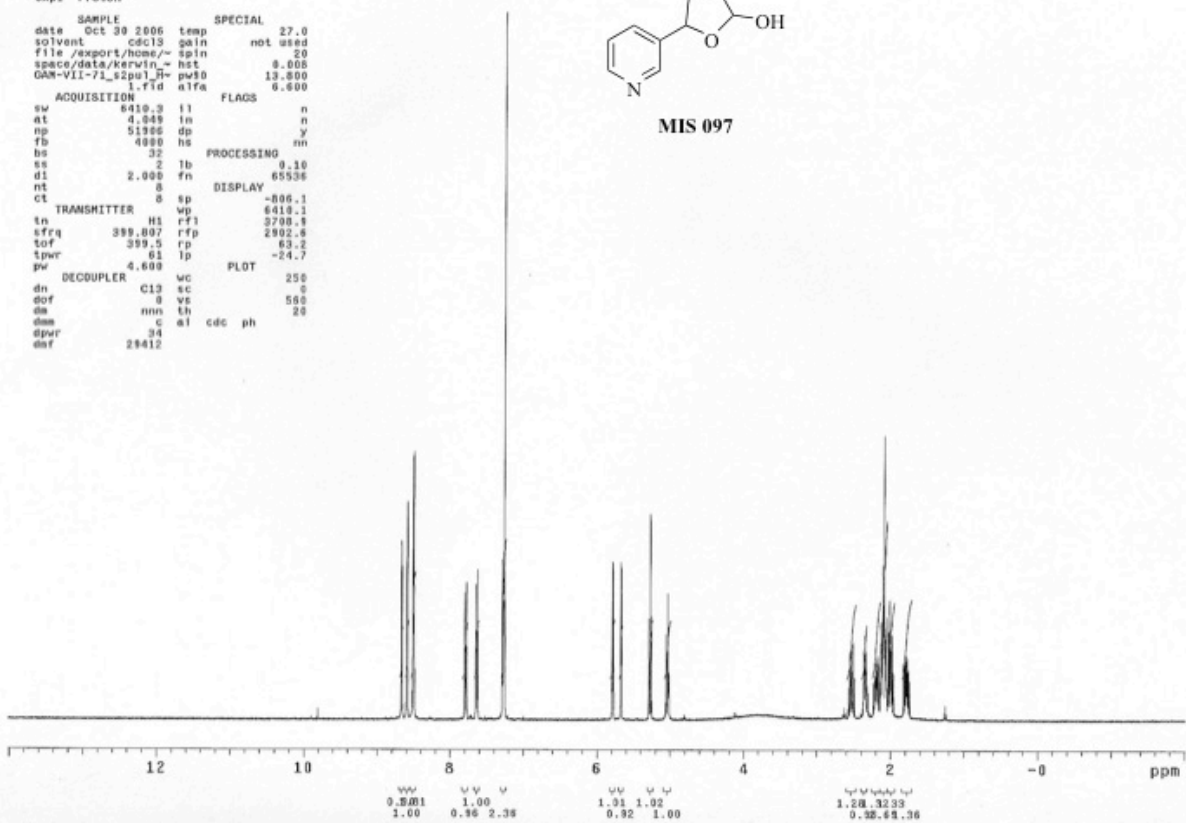


Figure A.13. <sup>1</sup>H NMR of MIS097

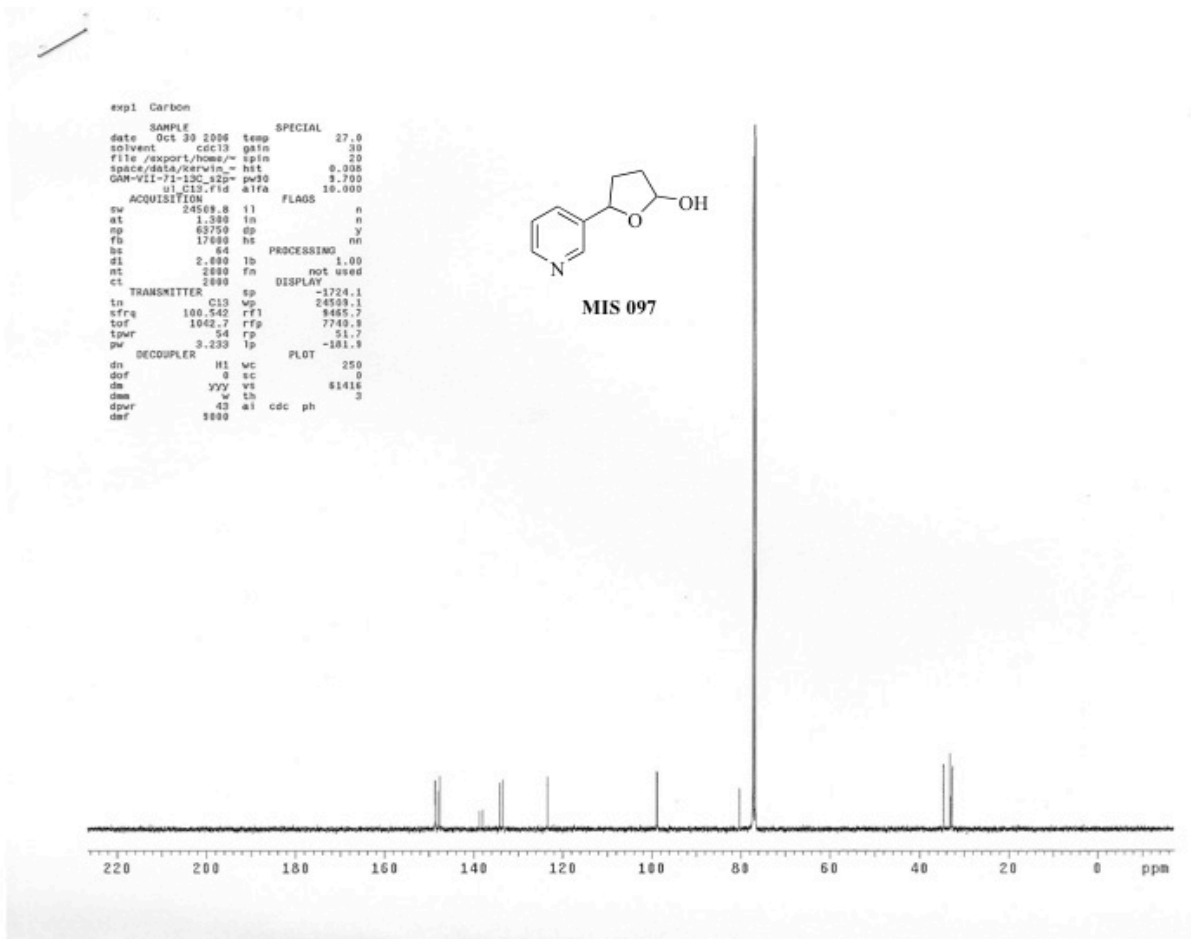


Figure A.14.  $^{13}\text{C}$  NMR of MIS097

### **X-ray Crystallography data**

X-ray Experimental for  $C_{16}H_{26}N_2O_3S$ : Crystals grew as colorless prisms by slow evaporation from DCM. The data crystal was cut from a cluster of crystals and had approximate dimensions; 0.13 x 0.12 x 0.10 mm. The data were collected on a Nonius Kappa CCD diffractometer using a graphite monochromator with  $MoK\alpha$  radiation ( $\lambda = 0.71073\text{\AA}$ ). A total of 323 frames of data were collected using  $\omega$ -scans with a scan range of  $2^\circ$  and a counting time of 134 seconds per frame. The data were collected at 153 K using an Oxford Cryostream low temperature device. Details of crystal data, data collection and structure refinement are listed in Table 1. Data reduction were performed using DENZO-SMN.<sup>1</sup> The structure was solved by direct methods using SIR97<sup>2</sup> and refined by full-matrix least-squares on  $F^2$  with anisotropic displacement parameters for the non-H atoms using SHELXL-97.<sup>3</sup> The hydrogen atoms on carbon were calculated in ideal positions with isotropic displacement parameters set to 1.2xUeq of the attached atom (1.5xUeq for methyl hydrogen atoms). The hydrogen atoms on thioamide nitrogen atoms, N1 and N1a, were observed in a  $\Delta F$  map and refined with isotropic displacement parameters. The function,  $\sum w(|F_o|^2 - |F_c|^2)^2$ , was minimized, where  $w = 1/[(\sigma(F_o))^2 + (0.0498*P)^2 + (0.4537*P)]$  and  $P = (|F_o|^2 + 2|F_c|^2)/3$ .  $R_w(F^2)$  refined to 0.126, with  $R(F)$  equal to 0.0487 and a goodness of fit,  $S$ , = 1.01. Definitions used for calculating  $R(F)$ ,  $R_w(F^2)$  and the goodness of fit,  $S$ , are given below.<sup>4</sup> The data were checked for secondary extinction effects but no correction was necessary. Neutral atom scattering factors and values used to calculate the linear absorption coefficient are from the International Tables for X-ray Crystallography (1992).<sup>5</sup> All figures were generated using SHELXTL/PC.<sup>6</sup> Tables of positional and thermal parameters, bond lengths and angles, torsion angles, and H-bonding interactions are located in tables 1 through 7.

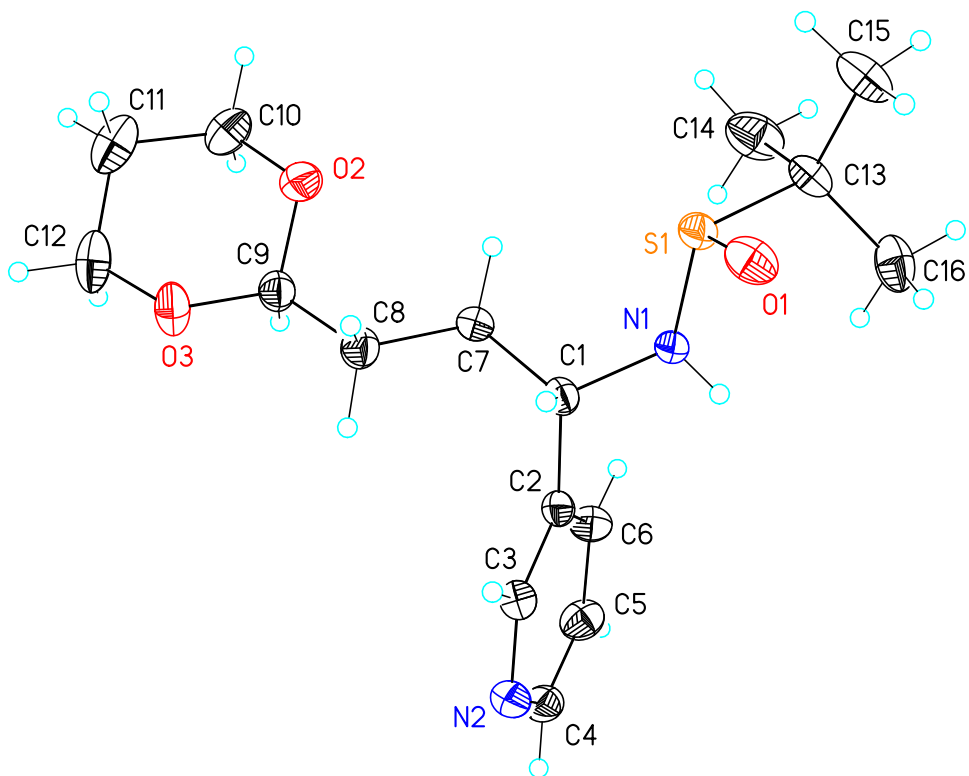


Figure A.15. View of molecule 1 of **MIS087** showing the atom labeling scheme. Displacement ellipsoids are scaled to the 50% probability level.

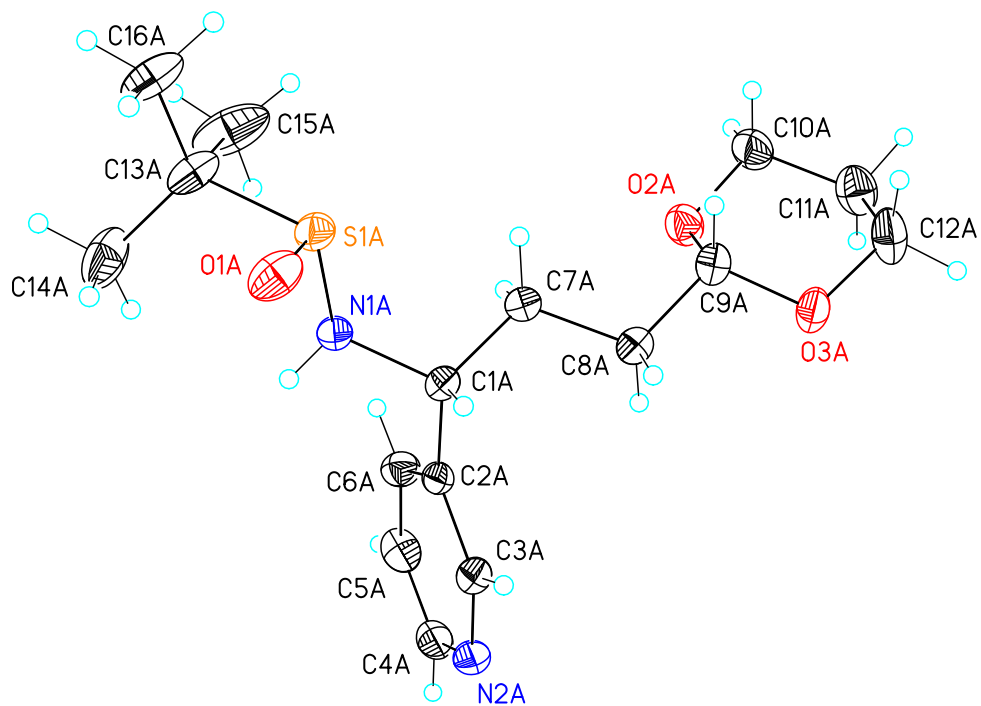


Figure A.16. View of molecule 2 of **MIS087** showing the atom labeling scheme. Displacement ellipsoids are scaled to the 50% probability level.

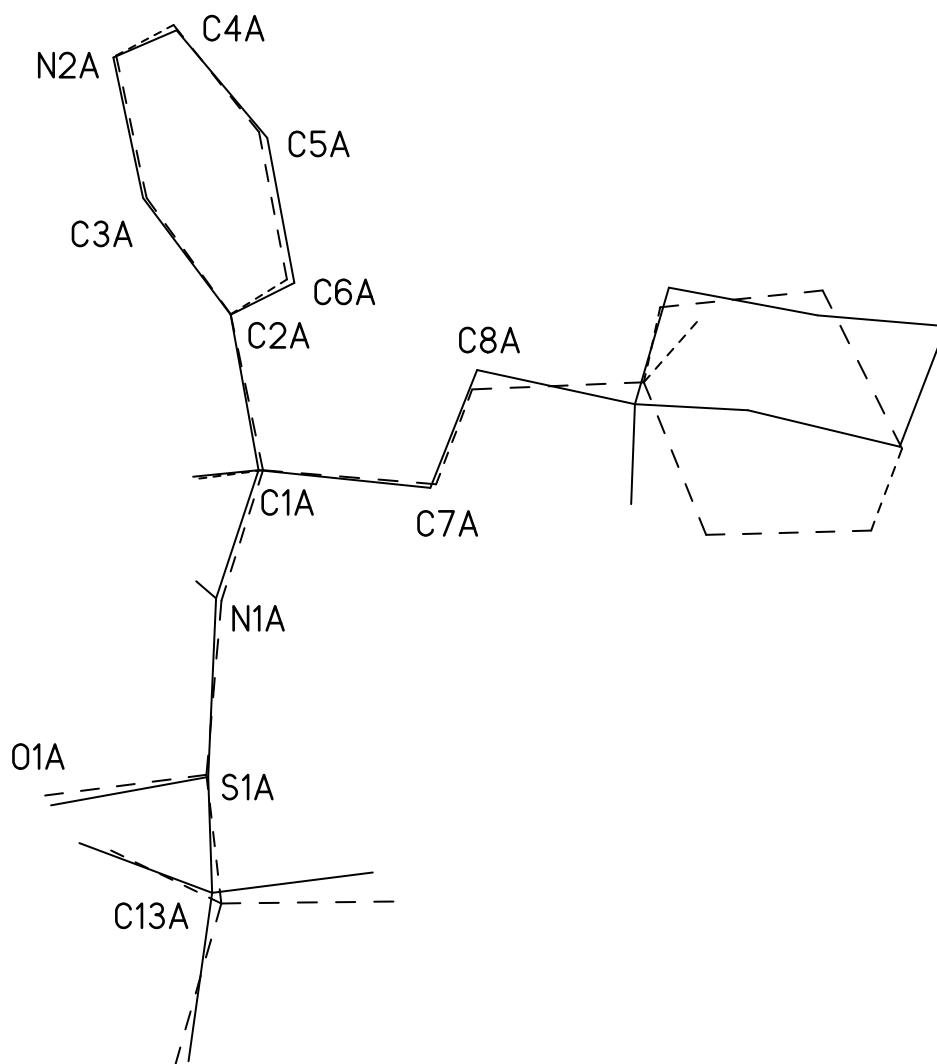


Figure A.17. View of the fit by least-squares of selected atoms of molecule 1 (dashed lines) onto the equivalent atoms of molecule 2 (solid lines). The atoms of molecule 2 used in the fit are labeled.



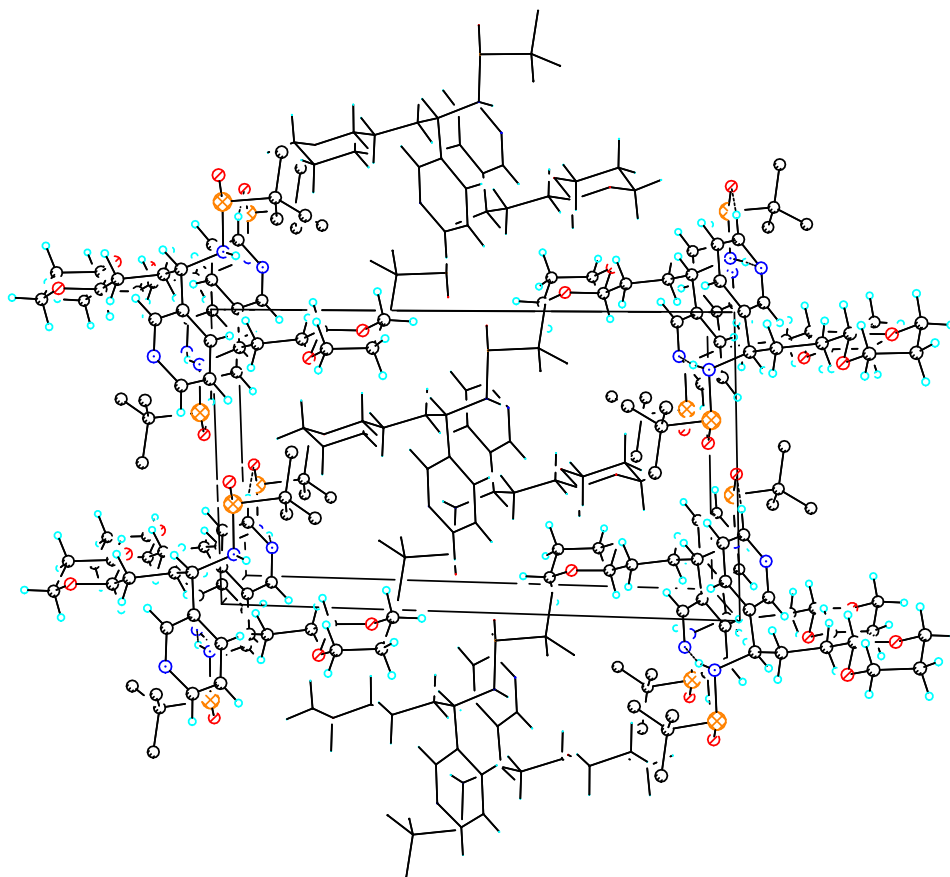


Figure A.18. Unit cell packing figure for **MIS087**. The view is approximately down the **b** axis. Dashed lines are indicative of H-bond interactions (Table 7). Molecules 2 are shown in wireframe form while molecules 1 are in ball-and-stick display format.

Table A.1. Crystal data and structure refinement for 1.

Empirical formula	C <sub>16</sub> H <sub>26</sub> N <sub>2</sub> O <sub>3</sub> S	
Formula weight	326.45	
Temperature	153(2) K	
Wavelength	0.71069 Å	
Crystal system	Triclinic	
Space group	P-1	
Unit cell dimensions	a = 9.9862(5) Å	α = 103.933(2)°.

	$b = 10.0925(5) \text{ \AA}$	$\beta = 91.236(2)^\circ$ .
	$c = 17.6731(10) \text{ \AA}$	$\gamma = 92.306(2)^\circ$ .
Volume	1726.49(16) $\text{\AA}^3$	
Z	4	
Density (calculated)	1.256 $\text{Mg/m}^3$	
Absorption coefficient	0.201 $\text{mm}^{-1}$	
F(000)	704	
Crystal size	0.13 x 0.12 x 0.10 mm	
Theta range for data collection	2.04 to 27.50°.	
Index ranges	-12 ≤ h ≤ 12, -10 ≤ k ≤ 13, -22 ≤ l ≤ 22	
Reflections collected	13579	
Independent reflections	7892 [R(int) = 0.0315]	
Completeness to theta = 27.50°	99.7 %	
Absorption correction	None	
Refinement method	Full-matrix least-squares on F <sup>2</sup>	
Data / restraints / parameters	7892 / 0 / 411	
Goodness-of-fit on F <sup>2</sup>	1.007	
Final R indices [I > 2σ(I)]	R1 = 0.0487, wR2 = 0.1040	
R indices (all data)	R1 = 0.1010, wR2 = 0.1257	
Largest diff. peak and hole	0.673 and -0.326 e.Å <sup>-3</sup>	

Table A.2. Atomic coordinates (  $\times 10^4$ ) and equivalent isotropic displacement parameters ( $\text{\AA}^2 \times 10^3$ ) for 1.

U(eq) is defined as one third of the trace of the orthogonalized  $U^{ij}$  tensor.

	x	y	z	U(eq)
S1A	8659(1)	3405(1)	5400(1)	26(1)
O1A	9508(1)	2218(2)	5383(1)	34(1)
O2A	5440(1)	5279(1)	3186(1)	31(1)
O3A	5688(1)	3574(1)	2048(1)	30(1)
N1A	7030(2)	2919(2)	5347(1)	24(1)
N2A	3530(2)	-208(2)	4172(1)	29(1)
C1A	6468(2)	2380(2)	4539(1)	22(1)

C2A	5085(2)	1737(2)	4587(1)	20(1)
C3A	4732(2)	428(2)	4161(1)	24(1)
C4A	2613(2)	503(2)	4624(1)	30(1)
C5A	2857(2)	1820(2)	5063(1)	32(1)
C6A	4111(2)	2449(2)	5052(1)	27(1)
C7A	6407(2)	3549(2)	4126(1)	26(1)
C8A	5969(2)	3045(2)	3271(1)	26(1)
C9A	6142(2)	4127(2)	2824(1)	27(1)
C10A	5615(2)	6348(2)	2784(1)	34(1)
C11A	5140(2)	5843(2)	1943(1)	38(1)
C12A	5847(2)	4558(2)	1588(1)	39(1)
C13A	8740(2)	4413(2)	6416(1)	33(1)
C14A	8242(2)	3544(3)	6955(1)	47(1)
C15A	7925(3)	5670(3)	6461(2)	62(1)
C16A	10230(2)	4810(2)	6575(1)	43(1)
S1	6459(1)	1475(1)	-384(1)	24(1)
O1	5645(1)	2679(1)	-392(1)	31(1)
O2	8405(1)	-283(1)	1925(1)	31(1)
O3	9320(1)	1438(2)	2951(1)	34(1)
N1	8108(2)	1911(2)	-387(1)	22(1)
N2	11506(2)	5225(2)	819(1)	29(1)
C1	8694(2)	2492(2)	413(1)	21(1)
C2	10033(2)	3215(2)	364(1)	21(1)
C3	10333(2)	4527(2)	814(1)	25(1)
C4	12450(2)	4586(2)	357(1)	30(1)
C5	12256(2)	3279(2)	-113(1)	31(1)
C6	11028(2)	2587(2)	-116(1)	27(1)
C7	8841(2)	1342(2)	838(1)	23(1)
C8	9011(2)	1901(2)	1715(1)	27(1)
C9	9339(2)	833(2)	2146(1)	25(1)
C10	8726(2)	-1335(2)	2309(1)	39(1)
C11	8761(2)	-779(2)	3182(1)	42(1)
C12	9687(2)	483(2)	3395(1)	40(1)
C13	6282(2)	342(2)	-1366(1)	28(1)
C14	6938(2)	-987(2)	-1328(2)	44(1)
C15	4767(2)	98(2)	-1513(1)	39(1)

C16

6904(2)

1011(2)

-1967(1)

36(1)

---

Table A.3. Bond lengths [Å] and angles [°] for **MIS087**.

S1A-O1A	1.4907(15)	C11A-C12A	1.508(3)
S1A-N1A	1.6744(17)	C11A-H11A	0.99
S1A-C13A	1.836(2)	C11A-H11B	0.99
O2A-C9A	1.407(2)	C12A-H12A	0.99
O2A-C10A	1.435(2)	C12A-H12B	0.99
O3A-C9A	1.408(2)	C13A-C14A	1.520(3)
O3A-C12A	1.432(2)	C13A-C15A	1.521(3)
N1A-C1A	1.489(2)	C13A-C16A	1.528(3)
N1A-H1NA	0.81(2)	C14A-H14A	0.98
N2A-C3A	1.342(2)	C14A-H14B	0.98
N2A-C4A	1.342(3)	C14A-H14C	0.98
C1A-C2A	1.515(3)	C15A-H15A	0.98
C1A-C7A	1.532(3)	C15A-H15B	0.98
C1A-H1A	1.00	C15A-H15C	0.98
C2A-C3A	1.381(3)	C16A-H16A	0.98
C2A-C6A	1.394(3)	C16A-H16B	0.98
C3A-H3A	0.95	C16A-H16C	0.98
C4A-C5A	1.377(3)	S1-O1	1.4910(14)
C4A-H4A	0.95	S1-N1	1.6884(16)
C5A-C6A	1.384(3)	S1-C13	1.835(2)
C5A-H5A	0.95	O2-C9	1.406(2)
C6A-H6A	0.95	O2-C10	1.433(2)
C7A-C8A	1.521(3)	O3-C9	1.407(2)
C7A-H7A1	0.99	O3-C12	1.435(2)
C7A-H7A2	0.99	N1-C1	1.492(2)
C8A-C9A	1.502(3)	N1-H1N	0.82(2)
C8A-H8A1	0.99	N2-C3	1.341(2)
C8A-H8A2	0.99	N2-C4	1.341(3)
C9A-H9A	1.00	C1-C2	1.512(3)
C10A-C11A	1.509(3)	C1-C7	1.536(2)
C10A-H10A	0.99	C1-H1	1.00
C10A-H10B	0.99	C2-C3	1.388(3)

C2-C6	1.391(3)	C11-C12	1.510(3)
C3-H3	0.95	C11-H11C	0.99
C4-C5	1.383(3)	C11-H11D	0.99
C4-H4	0.95	C12-H12C	0.99
C5-C6	1.386(3)	C12-H12D	0.99
C5-H5	0.95	C13-C16	1.520(3)
C6-H6	0.95	C13-C15	1.529(3)
C7-C8	1.520(3)	C13-C14	1.531(3)
C7-H7A	0.99	C14-H14D	0.98
C7-H7B	0.99	C14-H14E	0.98
C8-C9	1.504(3)	C14-H14F	0.98
C8-H8A	0.99	C15-H15D	0.98
C8-H8B	0.99	C15-H15E	0.98
C9-H9	1.00	C15-H15F	0.98
C10-C11	1.509(3)	C16-H16D	0.98
C10-H10C	0.99	C16-H16E	0.98
C10-H10D	0.99	C16-H16F	0.98
O1A-S1A-N1A	110.63(9)	N2A-C3A-C2A	124.64(19)
O1A-S1A-C13A	105.77(9)	N2A-C3A-H3A	117.7
N1A-S1A-C13A	98.08(9)	C2A-C3A-H3A	117.7
C9A-O2A-C10A	110.84(15)	N2A-C4A-C5A	123.28(19)
C9A-O3A-C12A	111.05(16)	N2A-C4A-H4A	118.4
C1A-N1A-S1A	114.53(13)	C5A-C4A-H4A	118.4
C1A-N1A-H1NA	109.7(16)	C4A-C5A-C6A	119.1(2)
S1A-N1A-H1NA	112.8(15)	C4A-C5A-H5A	120.4
C3A-N2A-C4A	116.62(18)	C6A-C5A-H5A	120.4
N1A-C1A-C2A	108.31(15)	C5A-C6A-C2A	119.0(2)
N1A-C1A-C7A	109.43(15)	C5A-C6A-H6A	120.5
C2A-C1A-C7A	111.16(15)	C2A-C6A-H6A	120.5
N1A-C1A-H1A	109.3	C8A-C7A-C1A	112.17(16)
C2A-C1A-H1A	109.3	C8A-C7A-H7A1	109.2
C7A-C1A-H1A	109.3	C1A-C7A-H7A1	109.2
C3A-C2A-C6A	117.36(18)	C8A-C7A-H7A2	109.2
C3A-C2A-C1A	121.20(17)	C1A-C7A-H7A2	109.2
C6A-C2A-C1A	121.43(18)	H7A1-C7A-H7A2	107.9

C9A-C8A-C7A	112.79(16)	C13A-C14A-H14A	109.5
C9A-C8A-H8A1	109.0	C13A-C14A-H14B	109.5
C7A-C8A-H8A1	109.0	H14A-C14A-H14B	109.5
C9A-C8A-H8A2	109.0	C13A-C14A-H14C	109.5
C7A-C8A-H8A2	109.0	H14A-C14A-H14C	109.5
H8A1-C8A-H8A2	107.8	H14B-C14A-H14C	109.5
O2A-C9A-O3A	112.18(15)	C13A-C15A-H15A	109.5
O2A-C9A-C8A	109.45(16)	C13A-C15A-H15B	109.5
O3A-C9A-C8A	108.55(16)	H15A-C15A-H15B	109.5
O2A-C9A-H9A	108.9	C13A-C15A-H15C	109.5
O3A-C9A-H9A	108.9	H15A-C15A-H15C	109.5
C8A-C9A-H9A	108.9	H15B-C15A-H15C	109.5
O2A-C10A-C11A	110.09(17)	C13A-C16A-H16A	109.5
O2A-C10A-H10A	109.6	C13A-C16A-H16B	109.5
C11A-C10A-H10A	109.6	H16A-C16A-H16B	109.5
O2A-C10A-H10B	109.6	C13A-C16A-H16C	109.5
C11A-C10A-H10B	109.6	H16A-C16A-H16C	109.5
H10A-C10A-H10B	108.2	H16B-C16A-H16C	109.5
C12A-C11A-C10A	108.51(18)	O1-S1-N1	110.14(8)
C12A-C11A-H11A	110.0	O1-S1-C13	106.52(8)
C10A-C11A-H11A	110.0	N1-S1-C13	98.56(9)
C12A-C11A-H11B	110.0	C9-O2-C10	110.54(15)
C10A-C11A-H11B	110.0	C9-O3-C12	110.72(16)
H11A-C11A-H11B	108.4	C1-N1-S1	112.52(12)
O3A-C12A-C11A	111.04(18)	C1-N1-H1N	109.3(14)
O3A-C12A-H12A	109.4	S1-N1-H1N	111.5(14)
C11A-C12A-H12A	109.4	C3-N2-C4	116.63(18)
O3A-C12A-H12B	109.4	N1-C1-C2	109.76(15)
C11A-C12A-H12B	109.4	N1-C1-C7	109.53(15)
H12A-C12A-H12B	108.0	C2-C1-C7	111.06(15)
C14A-C13A-C15A	112.7(2)	N1-C1-H1	108.8
C14A-C13A-C16A	110.73(19)	C2-C1-H1	108.8
C15A-C13A-C16A	111.02(19)	C7-C1-H1	108.8
C14A-C13A-S1A	110.20(15)	C3-C2-C6	117.19(18)
C15A-C13A-S1A	107.97(16)	C3-C2-C1	121.05(17)
C16A-C13A-S1A	103.81(15)	C6-C2-C1	121.74(18)

N2-C3-C2	124.77(19)	C10-C11-C12	109.23(18)
N2-C3-H3	117.6	C10-C11-H11C	109.8
C2-C3-H3	117.6	C12-C11-H11C	109.8
N2-C4-C5	123.28(19)	C10-C11-H11D	109.8
N2-C4-H4	118.4	C12-C11-H11D	109.8
C5-C4-H4	118.4	H11C-C11-H11D	108.3
C4-C5-C6	119.0(2)	O3-C12-C11	110.19(17)
C4-C5-H5	120.5	O3-C12-H12C	109.6
C6-C5-H5	120.5	C11-C12-H12C	109.6
C5-C6-C2	119.2(2)	O3-C12-H12D	109.6
C5-C6-H6	120.4	C11-C12-H12D	109.6
C2-C6-H6	120.4	H12C-C12-H12D	108.1
C8-C7-C1	111.66(16)	C16-C13-C15	111.03(17)
C8-C7-H7A	109.3	C16-C13-C14	112.61(18)
C1-C7-H7A	109.3	C15-C13-C14	110.71(18)
C8-C7-H7B	109.3	C16-C13-S1	111.09(14)
C1-C7-H7B	109.3	C15-C13-S1	104.37(14)
H7A-C7-H7B	107.9	C14-C13-S1	106.64(14)
C9-C8-C7	113.57(16)	C13-C14-H14D	109.5
C9-C8-H8A	108.9	C13-C14-H14E	109.5
C7-C8-H8A	108.9	H14D-C14-H14E	109.5
C9-C8-H8B	108.9	C13-C14-H14F	109.5
C7-C8-H8B	108.9	H14D-C14-H14F	109.5
H8A-C8-H8B	107.7	H14E-C14-H14F	109.5
O2-C9-O3	111.69(15)	C13-C15-H15D	109.5
O2-C9-C8	109.56(15)	C13-C15-H15E	109.5
O3-C9-C8	108.09(16)	H15D-C15-H15E	109.5
O2-C9-H9	109.2	C13-C15-H15F	109.5
O3-C9-H9	109.2	H15D-C15-H15F	109.5
C8-C9-H9	109.2	H15E-C15-H15F	109.5
O2-C10-C11	110.23(18)	C13-C16-H16D	109.5
O2-C10-H10C	109.6	C13-C16-H16E	109.5
C11-C10-H10C	109.6	H16D-C16-H16E	109.5
O2-C10-H10D	109.6	C13-C16-H16F	109.5
C11-C10-H10D	109.6	H16D-C16-H16F	109.5
H10C-C10-H10D	108.1	H16E-C16-H16F	109.5



---

Table A.4. Anisotropic displacement parameters ( $\text{\AA}^2 \times 10^3$ ) for **MIS087**.

The anisotropic displacement factor exponent takes the form:  $-2\pi^2 [h^2 a^{*2}U^{11} + \dots + 2 h k a^* b^* U^{12}]$

	U <sup>11</sup>	U <sup>22</sup>	U <sup>33</sup>	U <sup>23</sup>	U <sup>13</sup>	U <sup>12</sup>
S1A	21(1)	33(1)	25(1)	7(1)	-1(1)	-7(1)
O1A	23(1)	37(1)	35(1)	-3(1)	0(1)	2(1)
O2A	38(1)	28(1)	27(1)	7(1)	5(1)	3(1)
O3A	41(1)	29(1)	19(1)	4(1)	-3(1)	5(1)
N1A	22(1)	29(1)	22(1)	9(1)	-2(1)	-8(1)
N2A	30(1)	30(1)	27(1)	9(1)	-7(1)	-11(1)
C1A	23(1)	23(1)	20(1)	4(1)	-2(1)	-3(1)
C2A	20(1)	21(1)	20(1)	8(1)	-3(1)	-2(1)
C3A	25(1)	26(1)	21(1)	5(1)	-2(1)	-2(1)
C4A	22(1)	39(1)	32(1)	17(1)	-6(1)	-8(1)
C5A	24(1)	41(1)	36(1)	16(1)	3(1)	4(1)
C6A	28(1)	22(1)	30(1)	5(1)	-1(1)	1(1)
C7A	28(1)	26(1)	23(1)	6(1)	-3(1)	-6(1)
C8A	27(1)	25(1)	23(1)	4(1)	-2(1)	-1(1)
C9A	30(1)	30(1)	21(1)	5(1)	-1(1)	2(1)
C10A	45(1)	26(1)	34(1)	11(1)	2(1)	1(1)
C11A	43(1)	38(1)	35(1)	14(1)	4(1)	12(1)
C12A	53(2)	45(2)	24(1)	13(1)	4(1)	13(1)
C13A	25(1)	32(1)	34(1)	-8(1)	-4(1)	-2(1)
C14A	33(1)	78(2)	24(1)	1(1)	2(1)	-4(1)
C15A	38(2)	37(2)	94(2)	-16(2)	-13(1)	7(1)
C16A	24(1)	43(2)	50(2)	-10(1)	-9(1)	-4(1)
S1	20(1)	30(1)	23(1)	7(1)	-1(1)	-5(1)
O1	24(1)	31(1)	34(1)	0(1)	1(1)	2(1)
O2	31(1)	32(1)	34(1)	14(1)	-3(1)	-4(1)
O3	45(1)	37(1)	20(1)	6(1)	-2(1)	6(1)
N1	20(1)	28(1)	20(1)	8(1)	-2(1)	-7(1)
N2	31(1)	27(1)	29(1)	8(1)	-7(1)	-7(1)

C1	21(1)	23(1)	19(1)	3(1)	0(1)	1(1)
C2	22(1)	21(1)	21(1)	8(1)	-5(1)	-1(1)
C3	27(1)	26(1)	22(1)	7(1)	-2(1)	-2(1)
C4	23(1)	35(1)	36(1)	17(1)	-7(1)	-7(1)
C5	24(1)	33(1)	37(1)	13(1)	5(1)	3(1)
C6	26(1)	22(1)	31(1)	5(1)	1(1)	0(1)
C7	24(1)	21(1)	23(1)	5(1)	-1(1)	-3(1)
C8	33(1)	26(1)	22(1)	5(1)	1(1)	0(1)
C9	25(1)	29(1)	22(1)	6(1)	1(1)	1(1)
C10	46(1)	36(1)	40(1)	20(1)	5(1)	2(1)
C11	46(2)	49(2)	39(1)	24(1)	14(1)	18(1)
C12	48(2)	54(2)	23(1)	14(1)	-1(1)	16(1)
C13	22(1)	27(1)	29(1)	0(1)	-6(1)	-1(1)
C14	37(1)	31(1)	60(2)	3(1)	-6(1)	3(1)
C15	29(1)	39(1)	42(1)	-5(1)	-10(1)	-2(1)
C16	34(1)	50(2)	23(1)	4(1)	-1(1)	9(1)

---

Table A.5. Hydrogen coordinates ( $\times 10^4$ ) and isotropic displacement parameters ( $\text{\AA}^2 \times 10^{-3}$ ) for 1.

	x	y	z	U(eq)
H1A	7060	1668	4246	26
H3A	5388	-57	3837	29
H4A	1752	77	4643	36
H5A	2174	2290	5370	38
H6A	4305	3352	5357	32
H7A1	5770	4219	4394	31
H7A2	7303	4021	4163	31
H8A1	6500	2255	3028	31
H8A2	5014	2726	3237	31
H9A	7117	4399	2827	32
H10A	6574	6650	2808	41
H10B	5099	7141	3040	41
H11A	4158	5649	1913	45
H11B	5344	6549	1654	45
H12A	5478	4161	1054	47
H12B	6814	4786	1552	47
H14A	8688	2674	6837	71
H14B	7271	3369	6876	71
H14C	8448	4029	7498	71
H15A	8052	6286	6981	93
H15B	6973	5391	6364	93
H15C	8226	6144	6067	93
H16A	10540	5336	6207	65
H16B	10739	3982	6510	65
H16C	10367	5368	7110	65
H1	8074	3170	709	25
H3	9657	4963	1142	30
H4	13293	5054	353	36

H5	12954	2862	-430	37
H6	10867	1695	-442	32
H7A	8037	713	722	27
H7B	9630	814	642	27
H8A	9736	2626	1823	33
H8B	8172	2325	1917	33
H9	10258	513	2010	30
H10C	9610	-1689	2142	46
H10D	8046	-2100	2160	46
H11C	9084	-1478	3442	50
H11D	7848	-548	3360	50
H12C	9634	914	3959	48
H12D	10623	226	3288	48
H14D	6483	-1394	-947	66
H14E	7886	-790	-1170	66
H14F	6866	-1626	-1843	66
H15D	4588	-566	-2013	59
H15E	4365	962	-1527	59
H15F	4379	-258	-1093	59
H16D	6678	450	-2492	54
H16E	7880	1093	-1885	54
H16F	6554	1922	-1912	54
H1N	8250(20)	2460(20)	-657(12)	26(6)
H1NA	6860(20)	2380(20)	5608(13)	32(6)

---

Table A.6. Torsion angles [°] for 1.

O1A-S1A-N1A-C1A	-85.56(15)	O1A-S1A-C13A-C15A	178.09(16)
C13A-S1A-N1A-C1A	164.15(14)	N1A-S1A-C13A-C15A	-67.71(17)
S1A-N1A-C1A-C2A	169.27(13)	O1A-S1A-C13A-C16A	60.18(17)
S1A-N1A-C1A-C7A	-69.41(18)	N1A-S1A-C13A-C16A	174.38(15)
N1A-C1A-C2A-C3A	-128.79(18)	O1-S1-N1-C1	86.58(14)
C7A-C1A-C2A-C3A	110.95(19)	C13-S1-N1-C1	-162.23(13)
N1A-C1A-C2A-C6A	52.2(2)	S1-N1-C1-C2	-164.26(13)
C7A-C1A-C2A-C6A	-68.0(2)	S1-N1-C1-C7	73.56(17)
C4A-N2A-C3A-C2A	1.0(3)	N1-C1-C2-C3	130.96(18)
C6A-C2A-C3A-N2A	-0.9(3)	C7-C1-C2-C3	-107.78(19)
C1A-C2A-C3A-N2A	-179.92(17)	N1-C1-C2-C6	-50.7(2)
C3A-N2A-C4A-C5A	0.0(3)	C7-C1-C2-C6	70.6(2)
N2A-C4A-C5A-C6A	-0.9(3)	C4-N2-C3-C2	-0.6(3)
C4A-C5A-C6A-C2A	0.9(3)	C6-C2-C3-N2	-0.2(3)
C3A-C2A-C6A-C5A	-0.1(3)	C1-C2-C3-N2	178.29(17)
C1A-C2A-C6A-C5A	178.91(17)	C3-N2-C4-C5	0.6(3)
N1A-C1A-C7A-C8A	174.43(16)	N2-C4-C5-C6	0.3(3)
C2A-C1A-C7A-C8A	-66.0(2)	C4-C5-C6-C2	-1.1(3)
C1A-C7A-C8A-C9A	-169.58(17)	C3-C2-C6-C5	1.1(3)
C10A-O2A-C9A-O3A	-61.0(2)	C1-C2-C6-C5	-177.38(17)
C10A-O2A-C9A-C8A	178.45(16)	N1-C1-C7-C8	-162.17(15)
C12A-O3A-C9A-O2A	59.8(2)	C2-C1-C7-C8	76.4(2)
C12A-O3A-C9A-C8A	-179.17(16)	C1-C7-C8-C9	-172.42(16)
C7A-C8A-C9A-O2A	-56.1(2)	C10-O2-C9-O3	-62.3(2)
C7A-C8A-C9A-O3A	-178.86(16)	C10-O2-C9-C8	177.99(17)
C9A-O2A-C10A-C11A	58.1(2)	C12-O3-C9-O2	62.1(2)
O2A-C10A-C11A-C12A	-54.0(2)	C12-O3-C9-C8	-177.34(17)
C9A-O3A-C12A-C11A	-56.1(2)	C7-C8-C9-O2	-51.5(2)
C10A-C11A-C12A-O3A	53.3(3)	C7-C8-C9-O3	-173.42(16)
O1A-S1A-C13A-C14A	-58.43(17)	C9-O2-C10-C11	57.6(2)
N1A-S1A-C13A-C14A	55.77(16)	O2-C10-C11-C12	-53.0(2)

C9-O3-C12-C11	-57.1(2)
C10-C11-C12-O3	52.7(2)
O1-S1-C13-C16	65.27(15)
N1-S1-C13-C16	-48.80(15)
O1-S1-C13-C15	-54.45(16)
N1-S1-C13-C15	-168.52(14)
O1-S1-C13-C14	-171.68(14)
N1-S1-C13-C14	74.24(15)

Table A.7. Hydrogen bonds for **MIS087** [ $\text{\AA}$  and  $^\circ$ ].

D-H...A	d(D-H)	d(H...A)	d(D...A)	$\angle(\text{DHA})$
N1-H1N...N2#1	0.82(2)	2.43(2)	3.173(2)	151.4(19)
N1A-H1NA...N2A#2	0.81(2)	2.33(2)	3.088(2)	155(2)

Symmetry transformations used to generate equivalent atoms:

#1  $-x+2, -y+1, -z$  #2  $-x+1, -y, -z+1$



## References

- 1) DENZO-SMN. (1997). Z. Otwinowski and W. Minor, Methods in Enzymology, **276**: Macromolecular Crystallography, part A, 307 – 326, C. W. Carter, Jr. and R. M. Sweets, Editors, Academic Press.
- 2) SIR97. A program for crystal structure solution. Altomare A.; Burla M. C.; Camalli M., Cascarano G. L.; Giacovazzo C. , Guagliardi A.; Moliterni A. G. G.; Polidori G.; Spagna R. *J. Appl. Cryst.* **1999**, 32, 115-119.
- 3) Sheldrick, G. M. (1994). SHELXL97. Program for the Refinement of Crystal Structures. University of Gottingen, Germany.
- 4)  $R_w(F^2) = \{\sum w(|F_o|^2 - |F_c|^2)^2 / \sum w(|F_o|^4)\}^{1/2}$  where w is the weight given each reflection.  
 $R(F) = \sum(|F_o| - |F_c|) / \sum |F_o|$  for reflections with  $F_o > 4(\sigma(F_o))$ .  
 $S = [\sum w(|F_o|^2 - |F_c|^2)^2 / (n - p)]^{1/2}$ , where n is the number of reflections and p is the number of refined parameters.
- 5) International Tables for X-ray Crystallography (1992). Vol. C, Tables 4.2.6.8 and 6.1.1.4, A. J. C. Wilson, editor, Boston: Kluwer Academic Press.
- 6) Sheldrick, G. M. (1994). SHELXTL/PC (Version 5.03). Siemens Analytical X-ray Instruments, Inc., Madison, Wisconsin, USA.

## APPENDIX II

### Scanned $^1\text{H}$ and $^{13}\text{C}$ NMR spectra

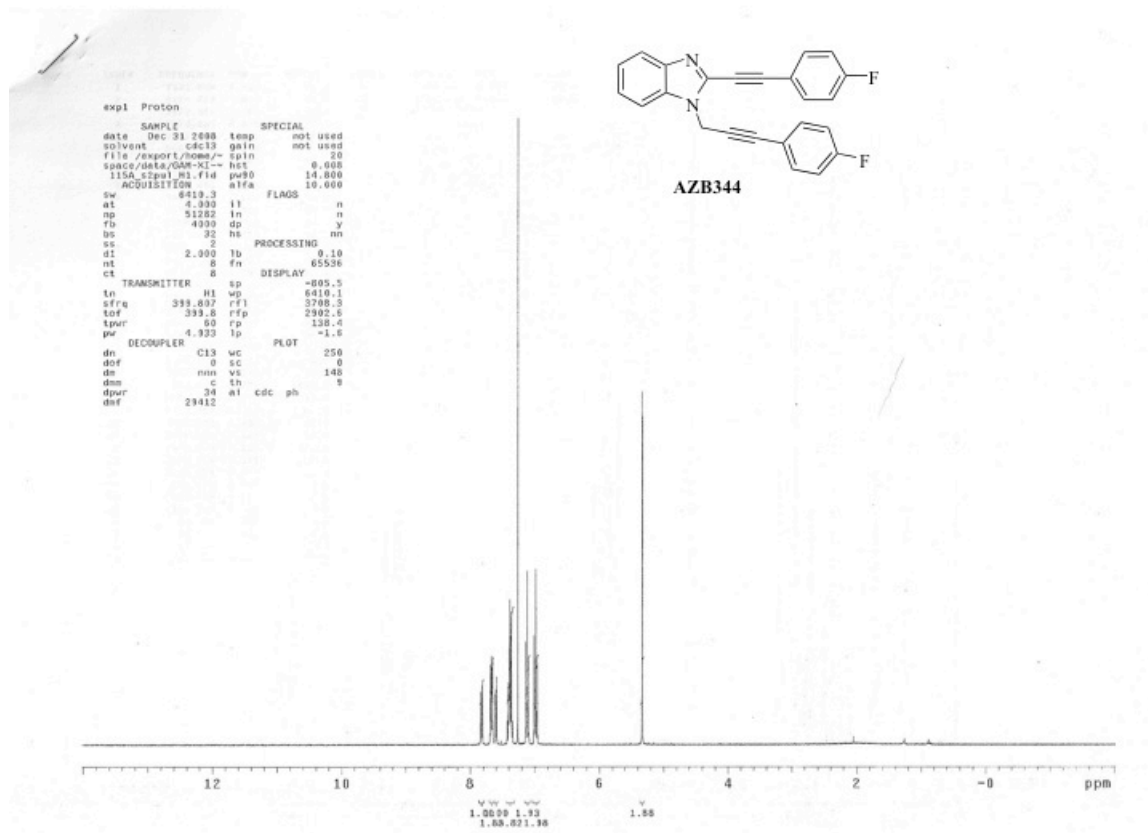


Figure A2.1.  $^1\text{H}$  NMR of AZB344

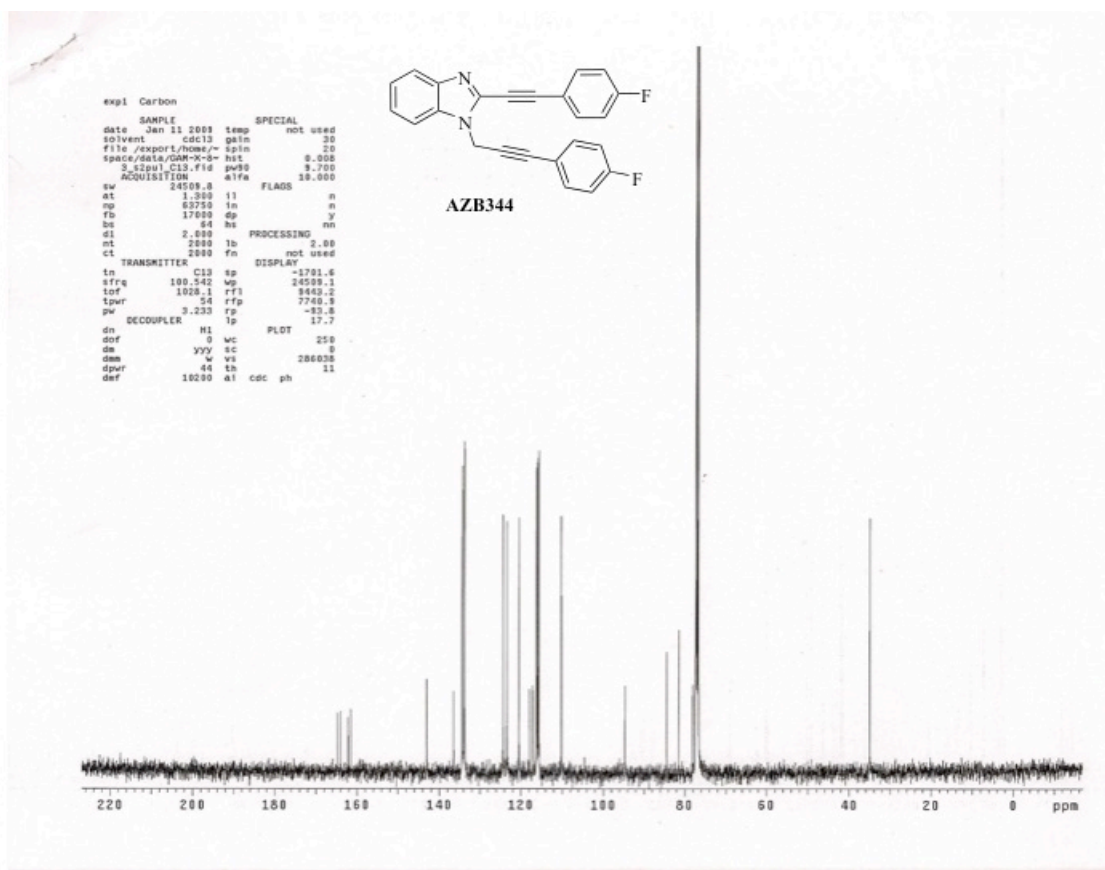


Figure A2.2.  $^{13}\text{C}$  NMR of AZB344

```

Bis-Me Skipped dialkynylbenzimidazole
expl Proton
SAMPLE
date Jan 3 2008 temp NOT used
solvent cdcl3 gain not used
file /export/home/~ spin 25
space/data/GM-XI-- hst 0.830
BIA_s2pul_H1.fid pws9 14.888
ACQUISITION d1fa 10.000
sw 6418.3 FLAGS
st 4.228 11 m
sp 51282 1n m
fb 4000 ep v
ss 32 ht nm
ss 2 PROCESSING
ml 2.000 1b 0.10
nt 5 Fv 65536
ct 8 DISPLAY
TRANSMITTER ep -805.7
M1 wp 8410.1
sfrq 399.807 rfr 3700.5
tof 399.5 rfp 2902.5
tpwr 60 fp 133.1
pw DECOUPLER 1p 12.3
C13 wc 250
dof 9 sc 3
do nms vs 153
dam c th 39
dprc 34 at cdc ph
dof 23412

```

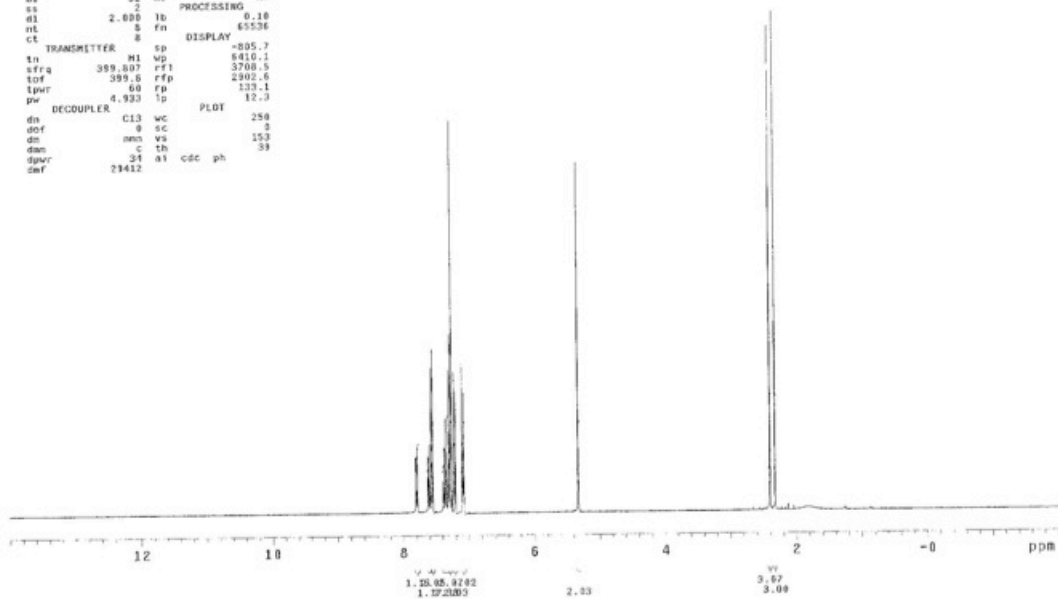
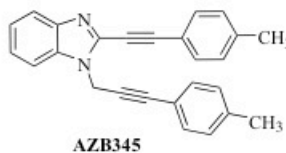


Figure A2.3.  $^1\text{H}$  NMR of AZB345

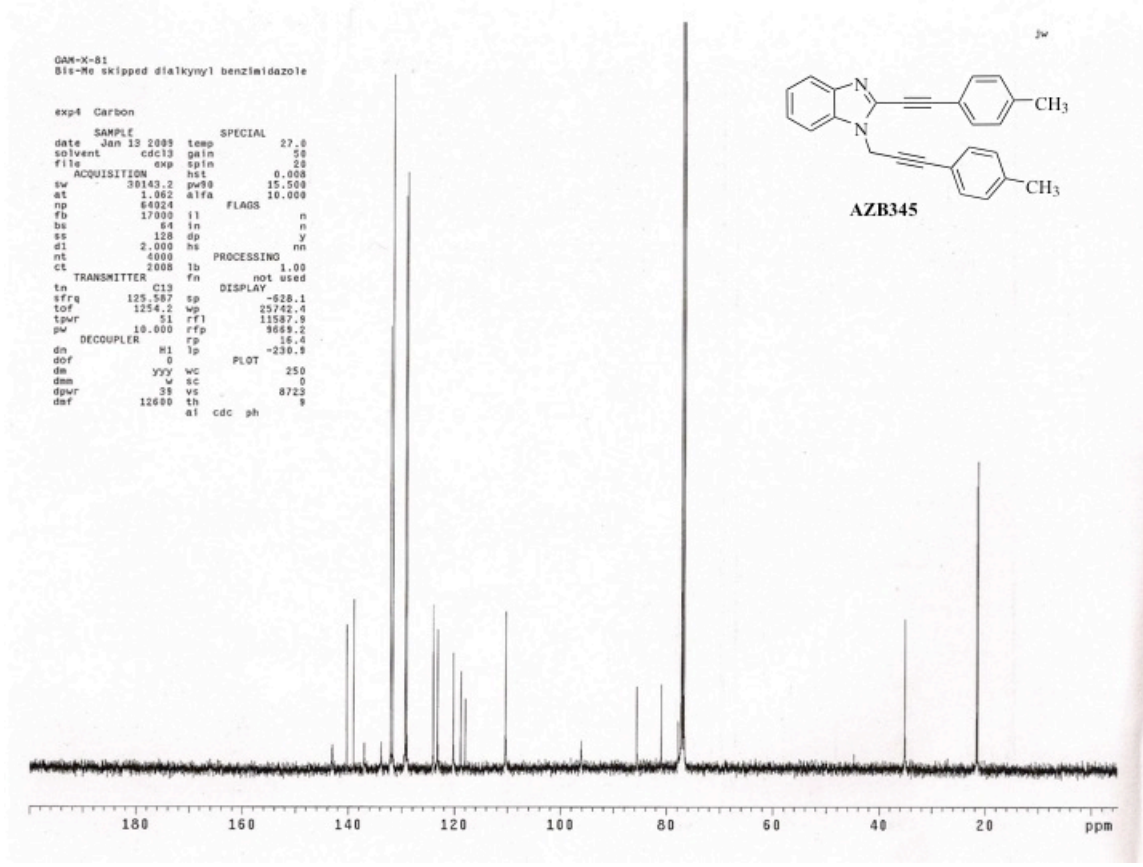


Figure A2.4. <sup>13</sup>C NMR of AZB345

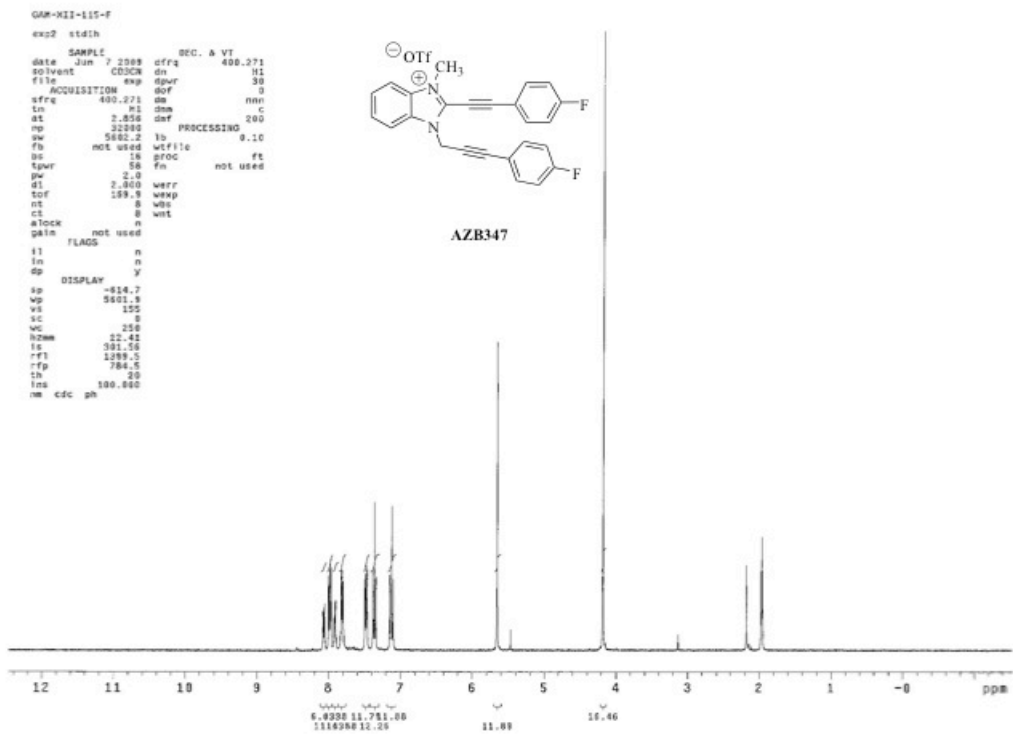


Figure A2.5.  $^1\text{H}$  NMR of AZB347

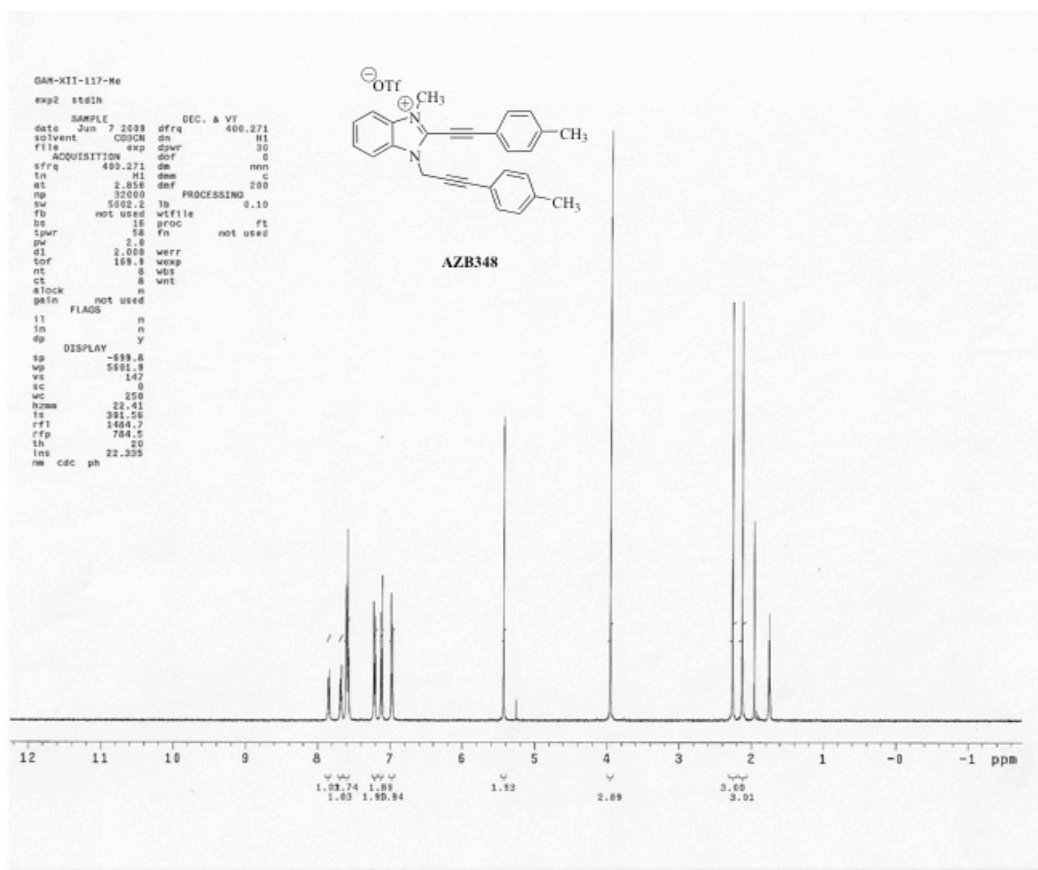


Figure A2.6.  $^1\text{H}$  NMR of AZB348

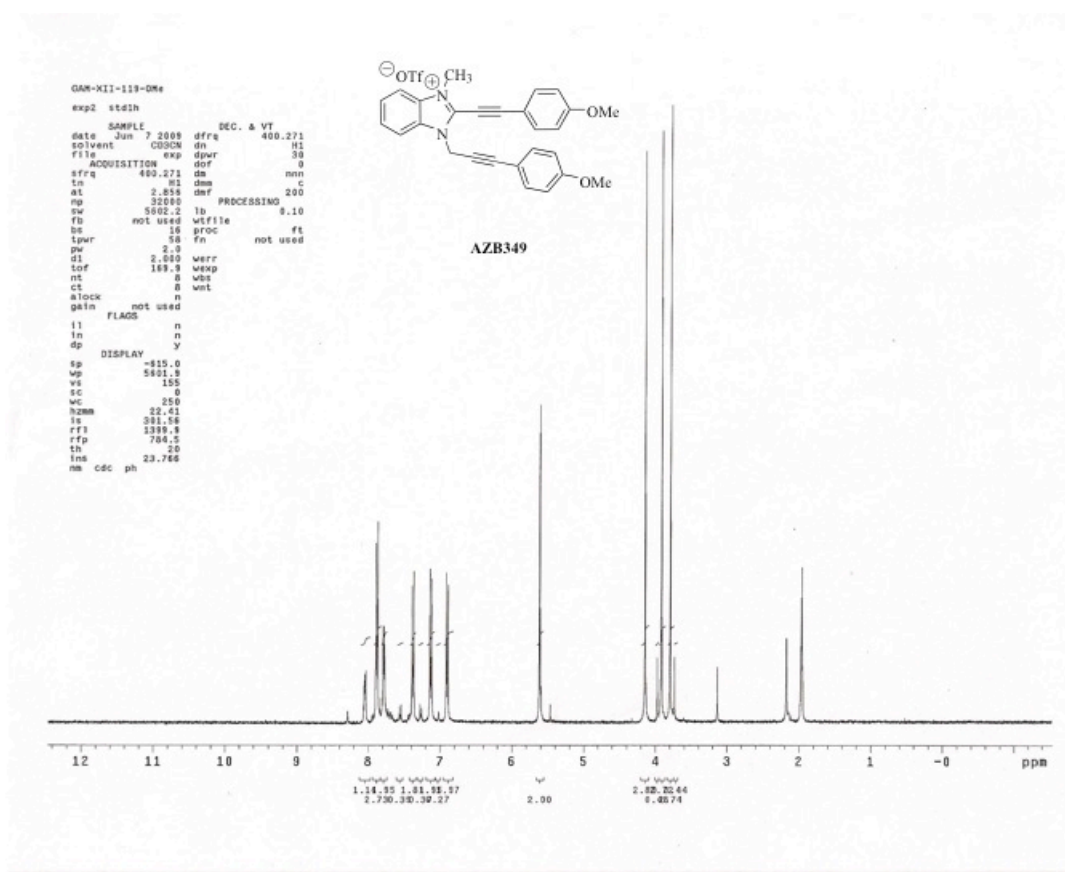


Figure A2.7.  $^1\text{H}$  NMR of AZB349



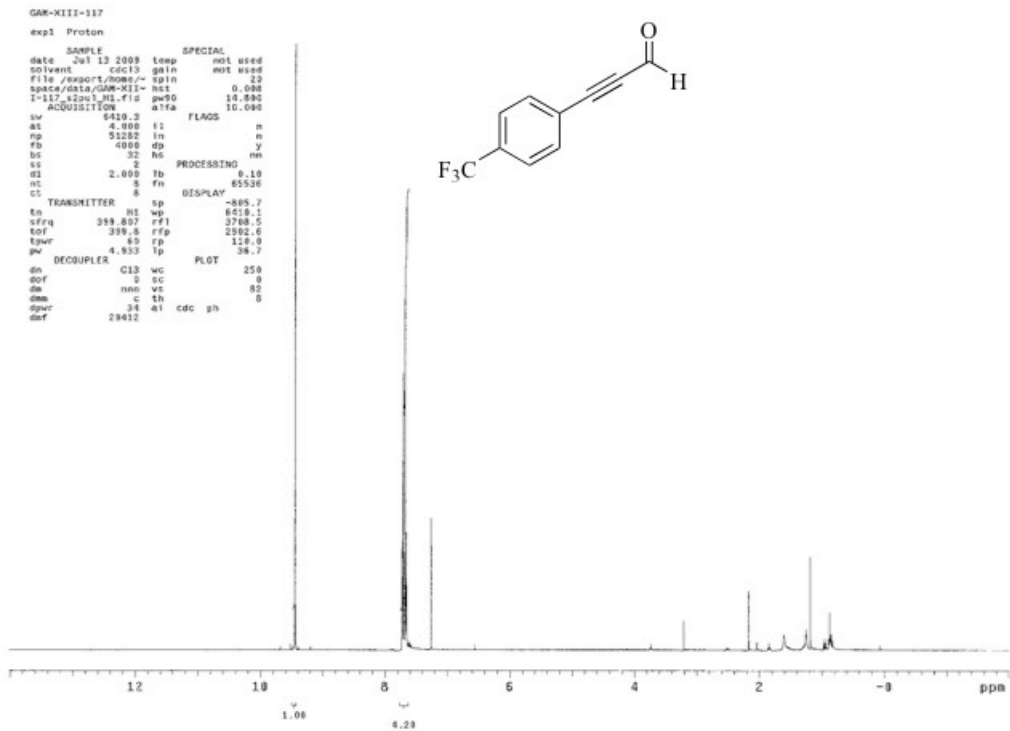


Figure A2.8.  $^1\text{H}$  NMR of AZB379

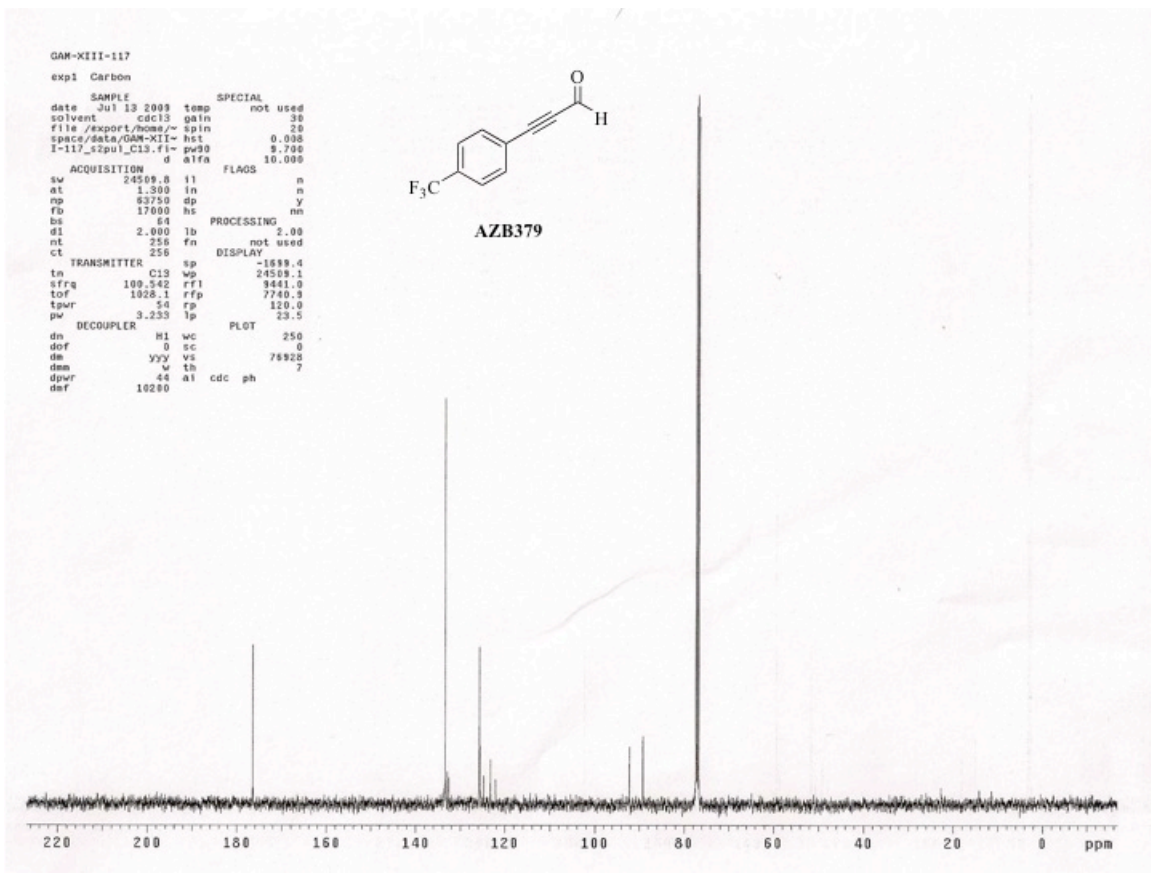


Figure A2.9. <sup>13</sup>C NMR of AZB379

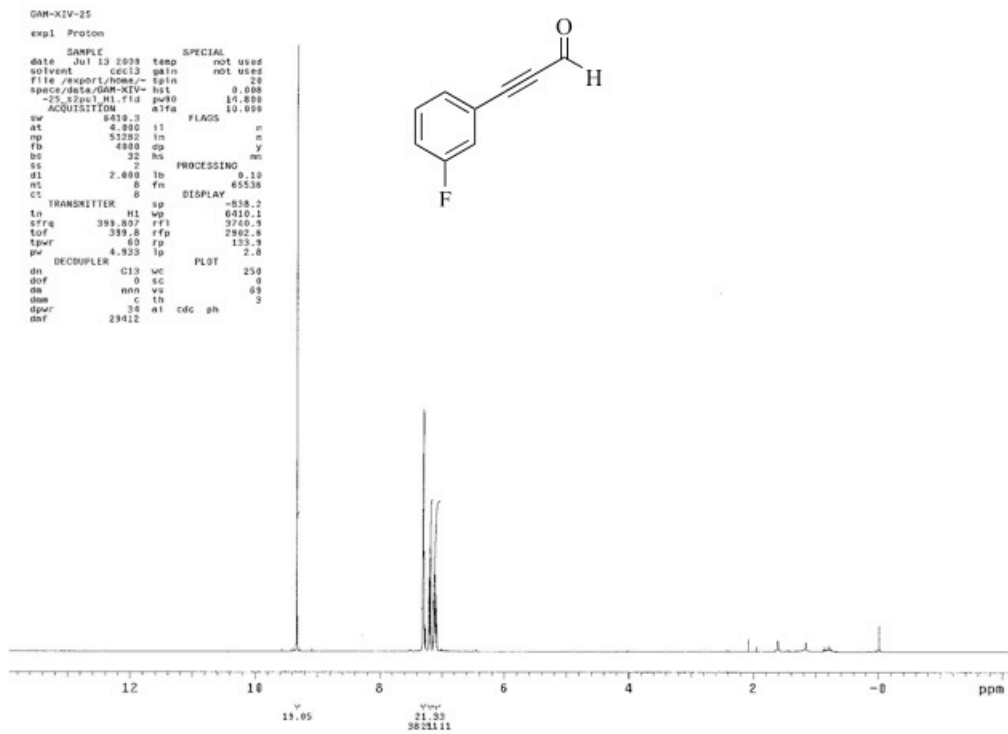


Figure A2.10.  $^1\text{H}$  NMR of AZB380

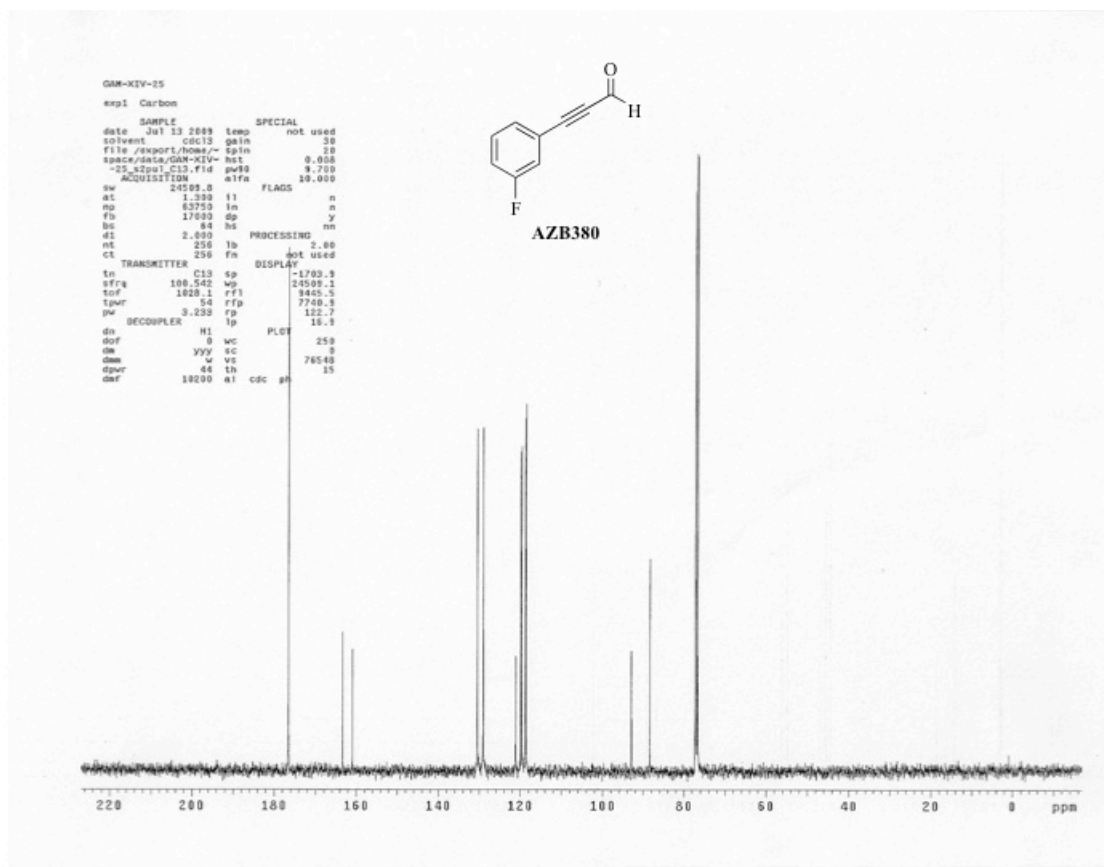


Figure A2.11.  $^{13}\text{C}$  NMR of AZB380

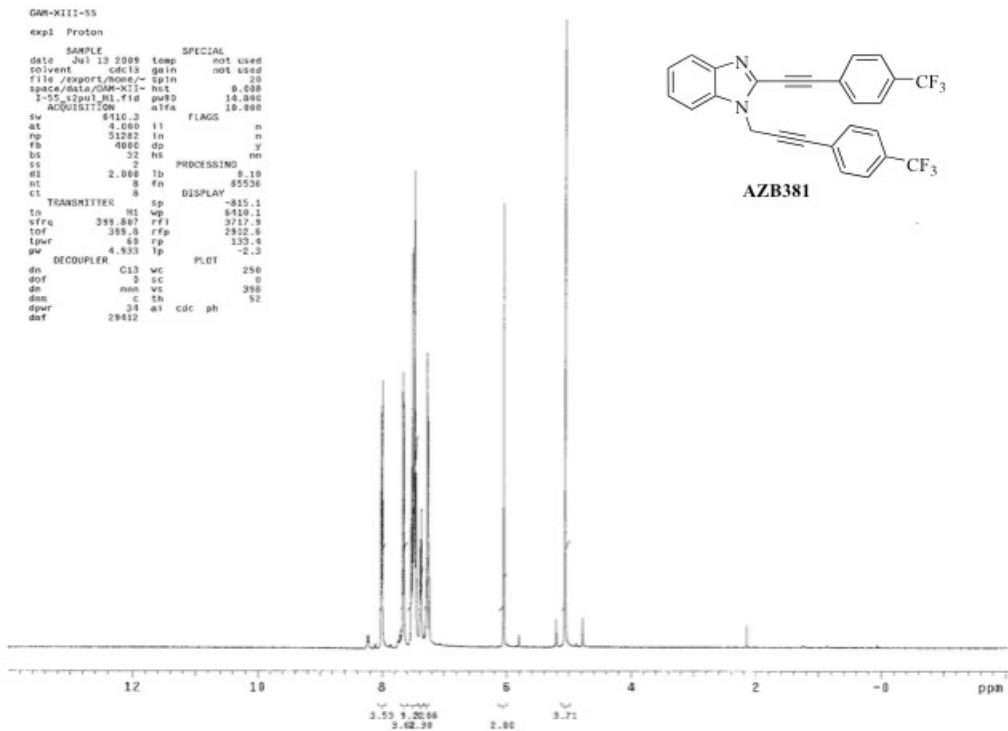


Figure A2.12. <sup>1</sup>H NMR of AZB381

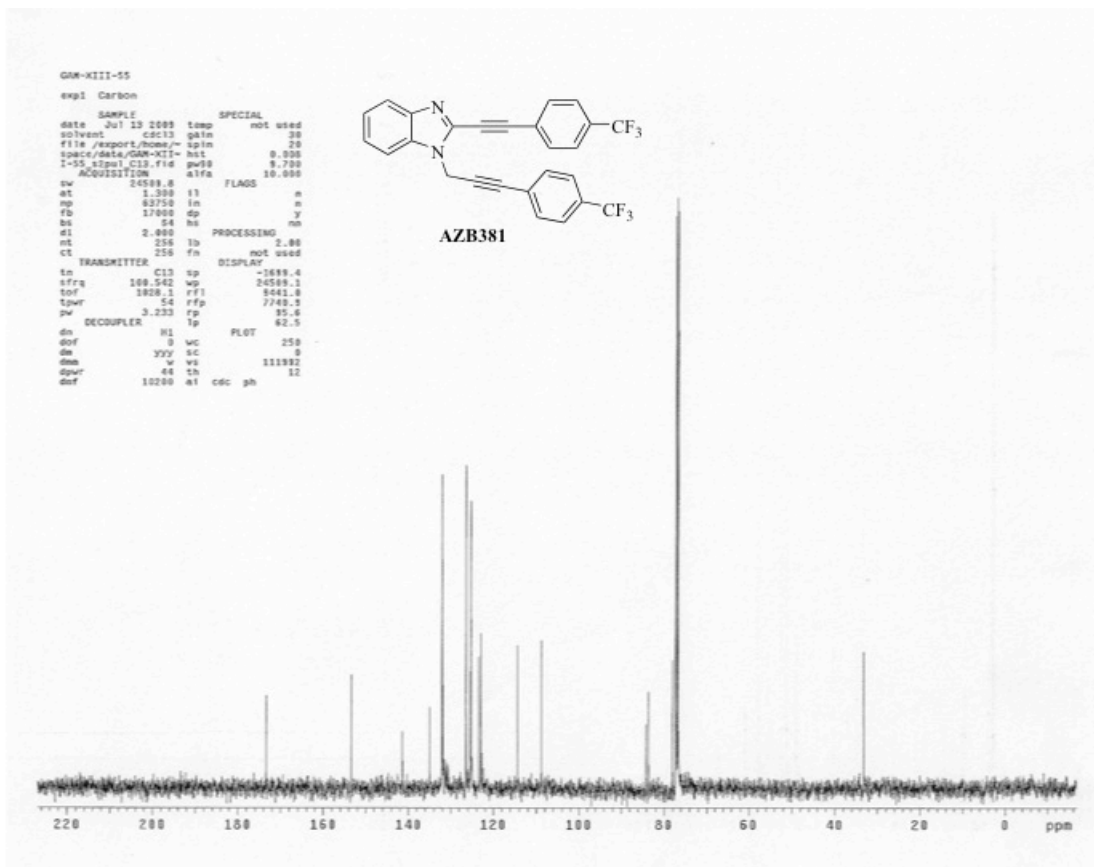


Figure A2.13.  $^{13}\text{C}$  NMR of AZB381

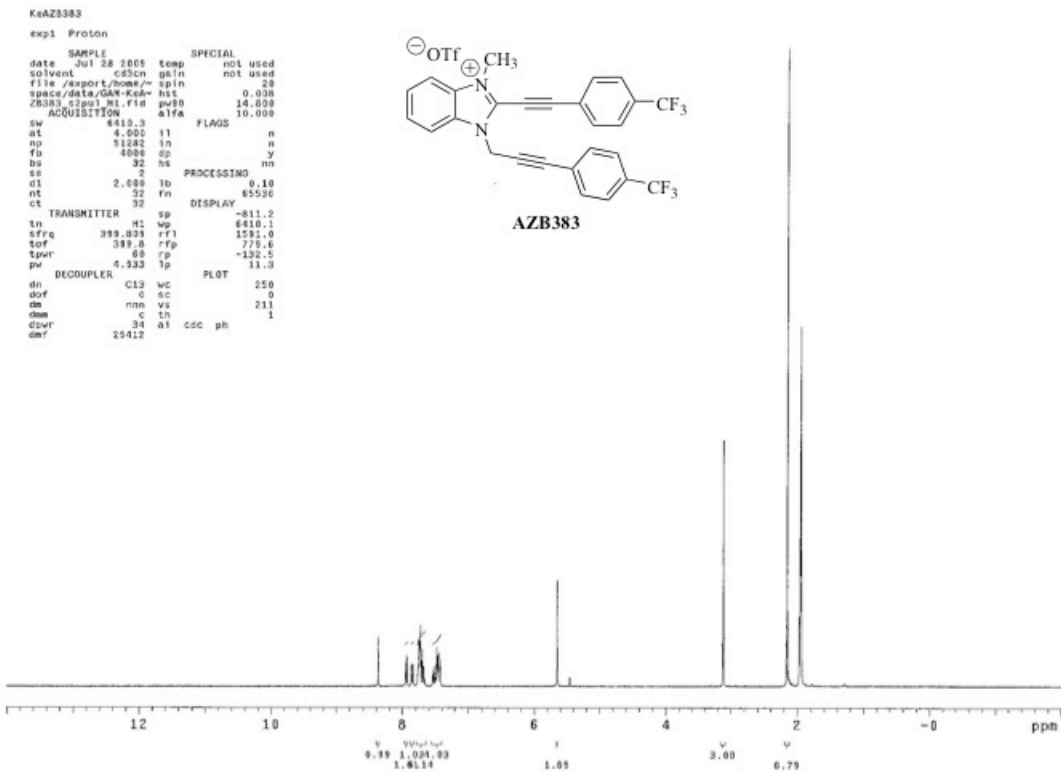


Figure A2.14.  $^1\text{H}$  NMR of AZB384

## APPENDIX III

### Scanned $^1\text{H}$ and $^{13}\text{C}$ NMR spectra

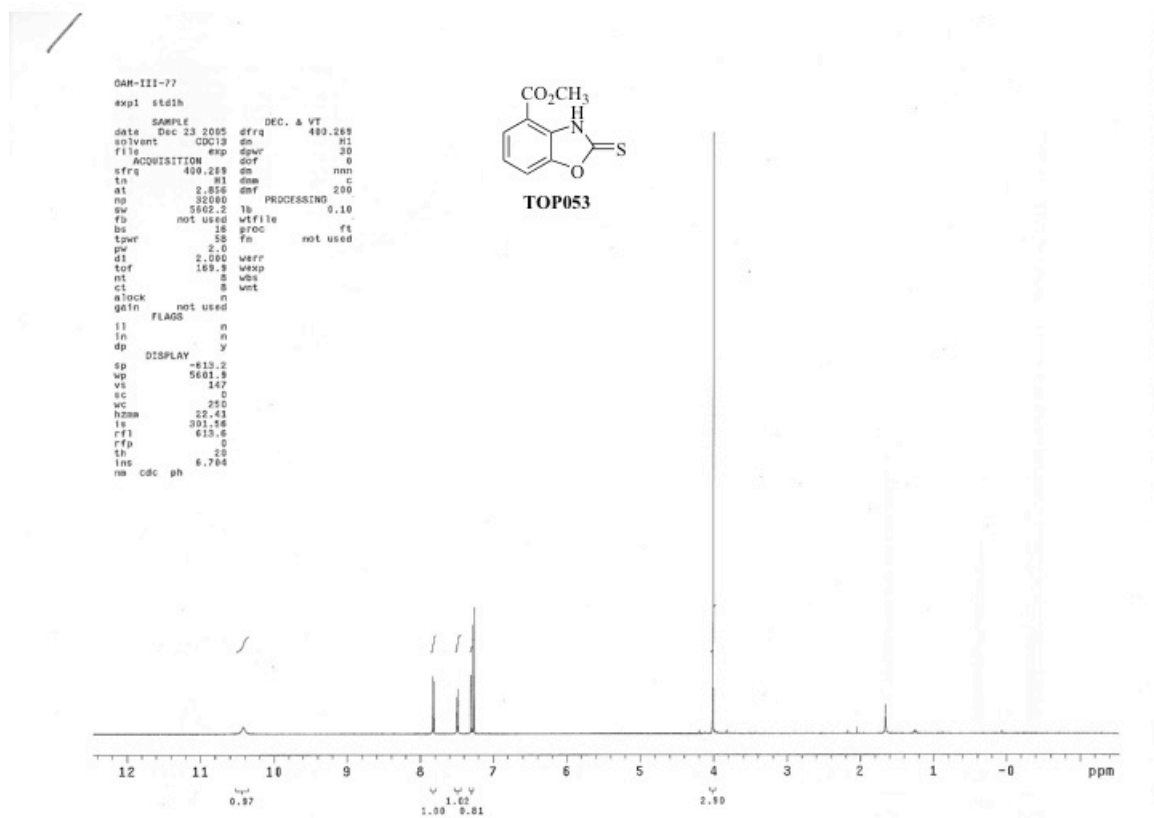


Figure A3.1.  $^1\text{H}$  NMR of TOP053



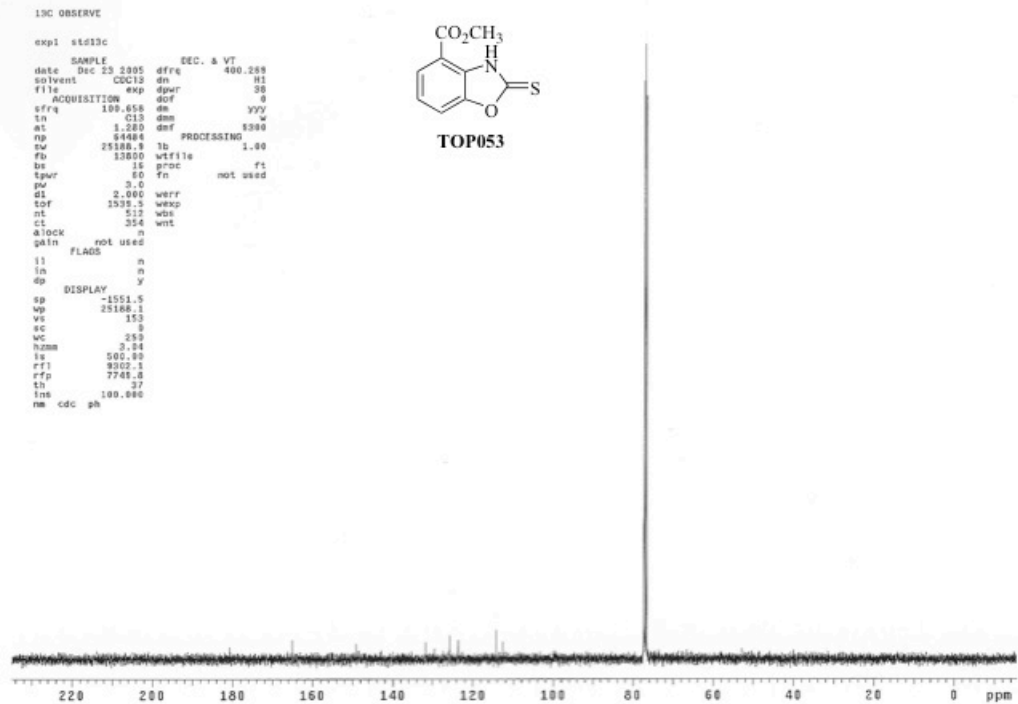


Figure A3.2.  $^{13}\text{C}$  NMR of **TOP053**

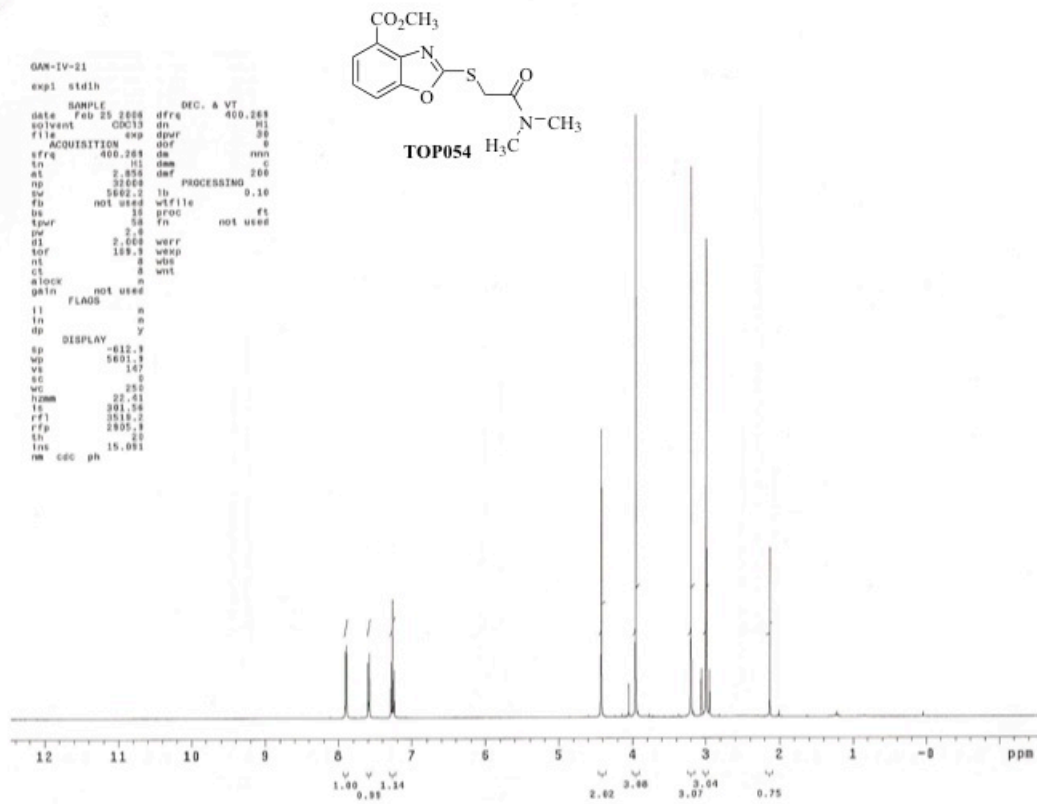


Figure A3.3. <sup>1</sup>H NMR of TOP054

```

13C OBSERVE
exp1 s1013c
SAMPLE
date Feb 25 2006 dfrq 400.265
solvent CDCl3 dn R1
file ACQUISITION exp dpwr 38
          dof 0
sfrq 100.658 dm
ln C13 dm w
nt 1.280 def 3300
np 64484
sw 25180.1 fu PROCESSING 1.00
fb 13080 wf11e
bs 16 proc ft
tpwr 80 fn not used
pr 3.0
d1 2.000 werr
tof 1531.5 wexp
nt 512 wds
ct 335 wnt
nlock n
data not used
ii FLAGS
ln n
ln n
dp DISPLAY Y
sp -1559.9
wp 25180.1
vs 153
sc 0
wc 259
hzam 4.28
ls 500.00
rfi 9310.4
rfp 7749.4
th 7
ins 100.000
mk cdc ph

```

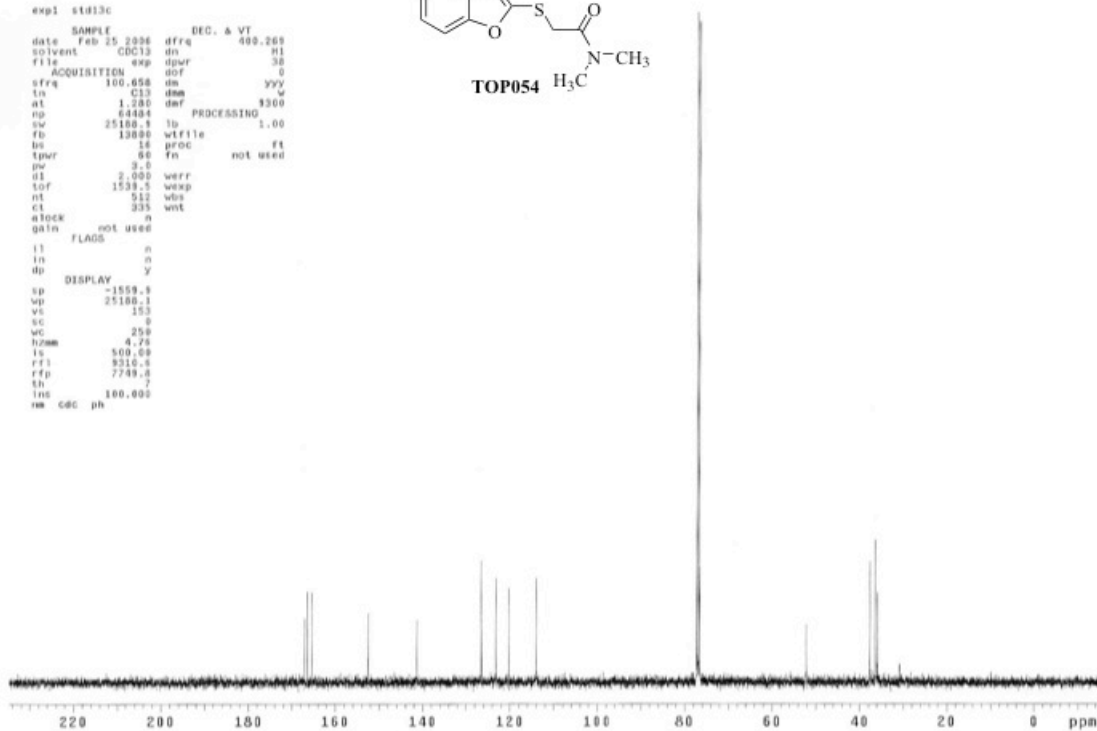
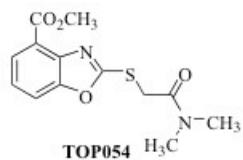


Figure A3.4.  $^{13}\text{C}$  NMR of **TOP054**

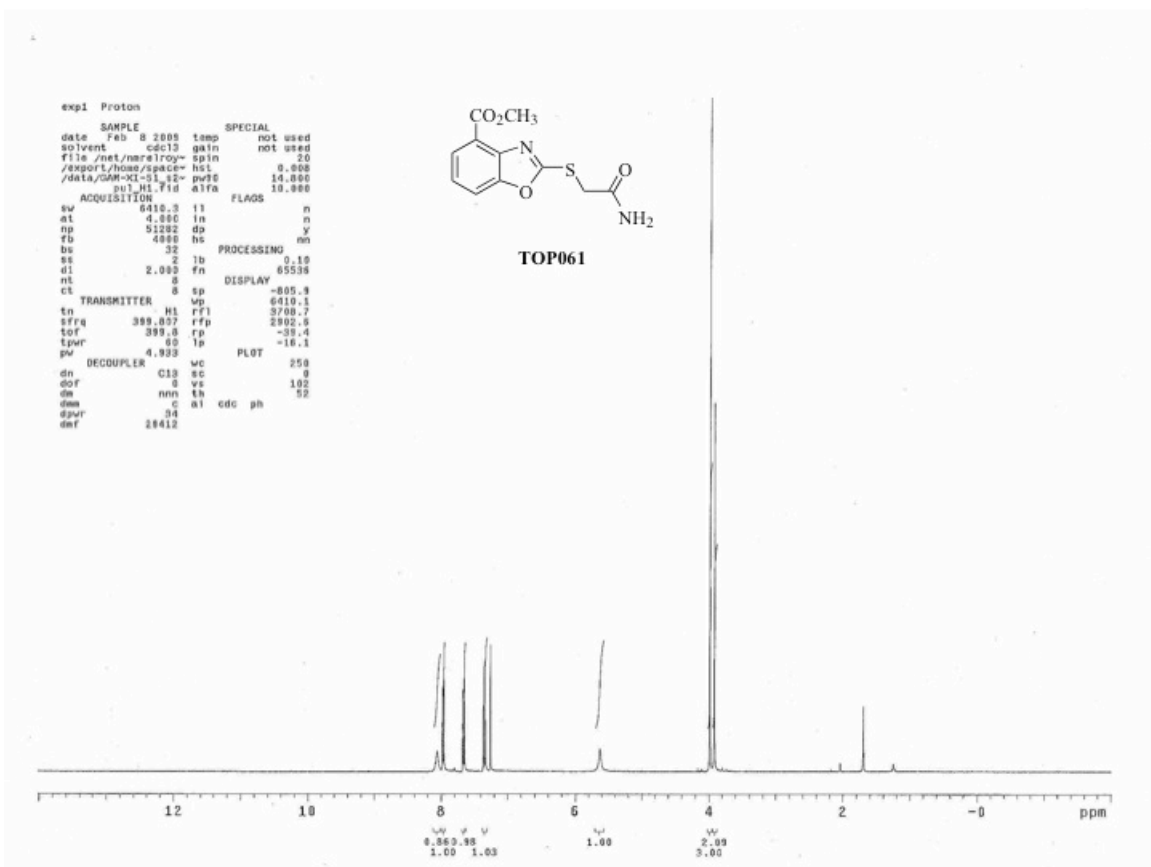


Figure A3.5.  $^1\text{H}$  NMR of TOP061

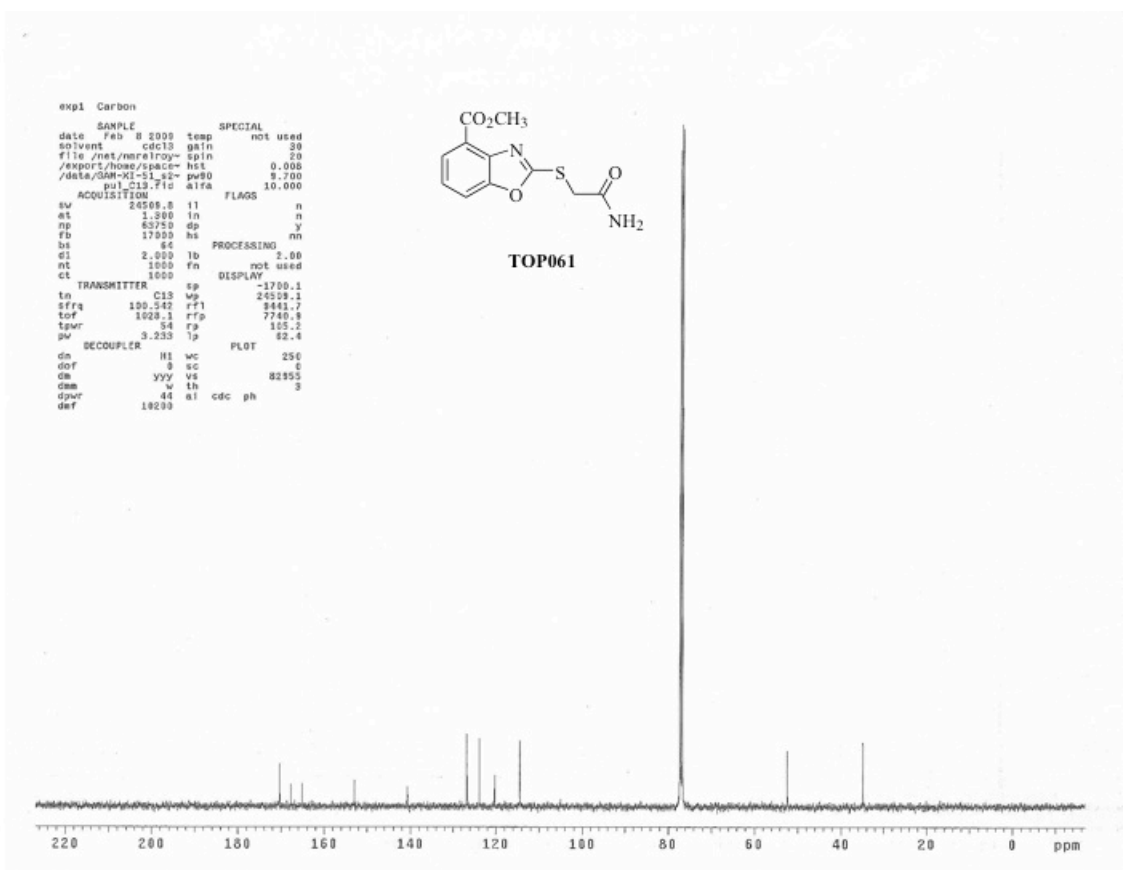


Figure A3.6.  $^{13}\text{C}$  NMR of TOP061

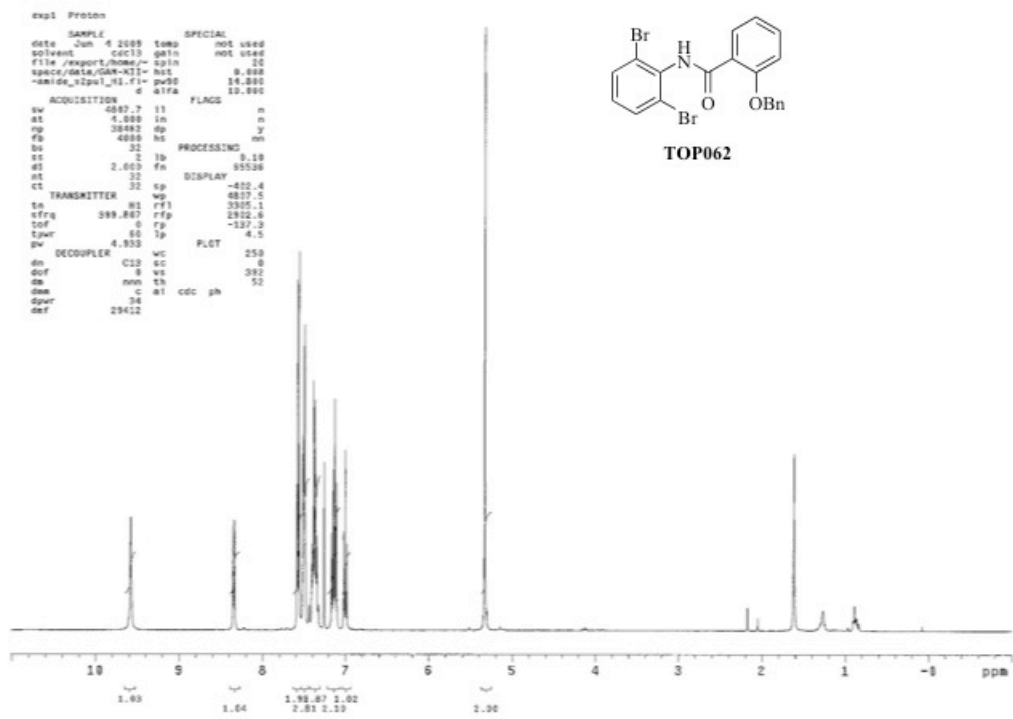


Figure A3.7. <sup>1</sup>H NMR of TOP062

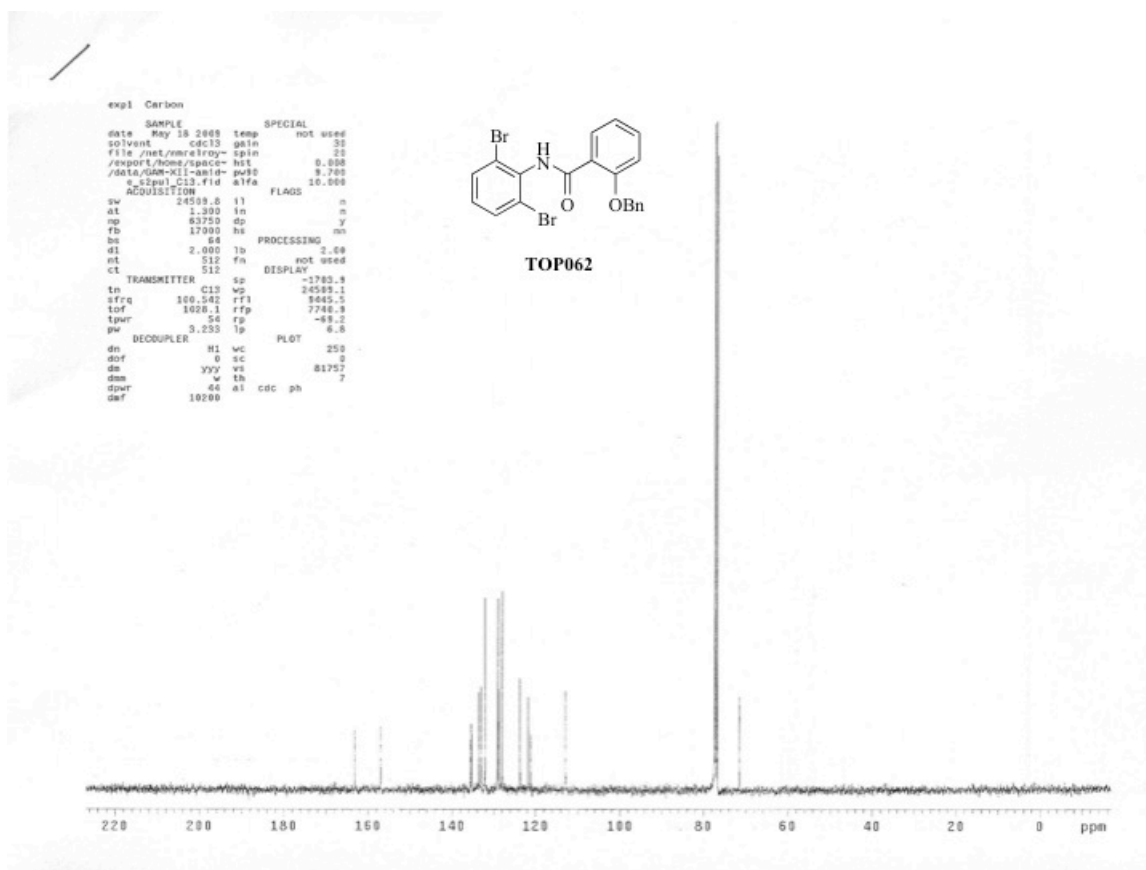


Figure A3.8.  $^{13}\text{C}$  NMR of TOP062

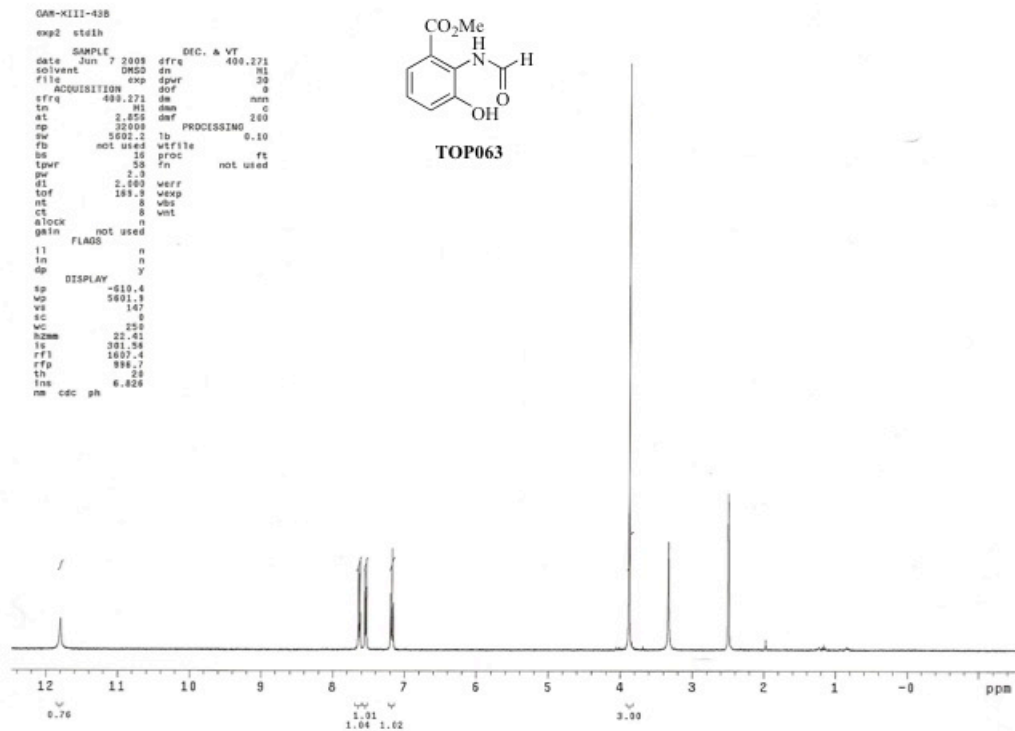


Figure A3.9.  $^1\text{H}$  NMR of TOP063



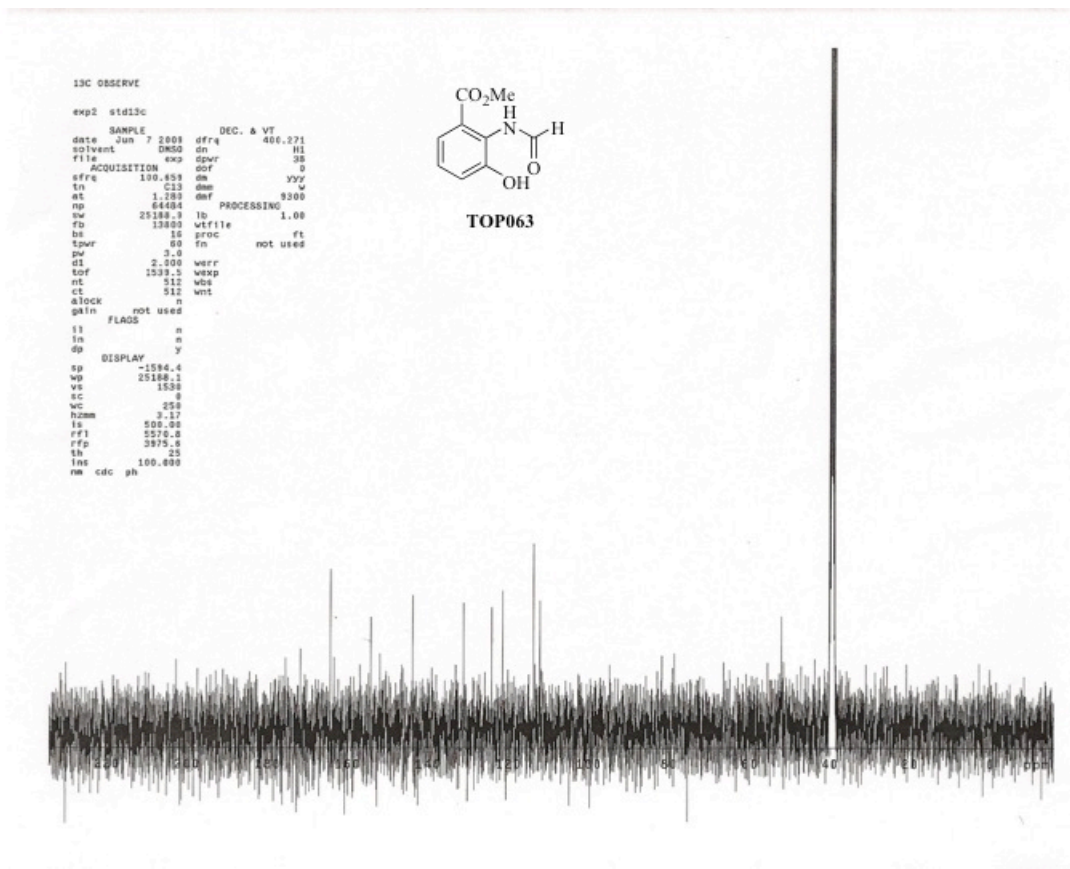


Figure A3.10.  $^{13}\text{C}$  NMR of TOP063

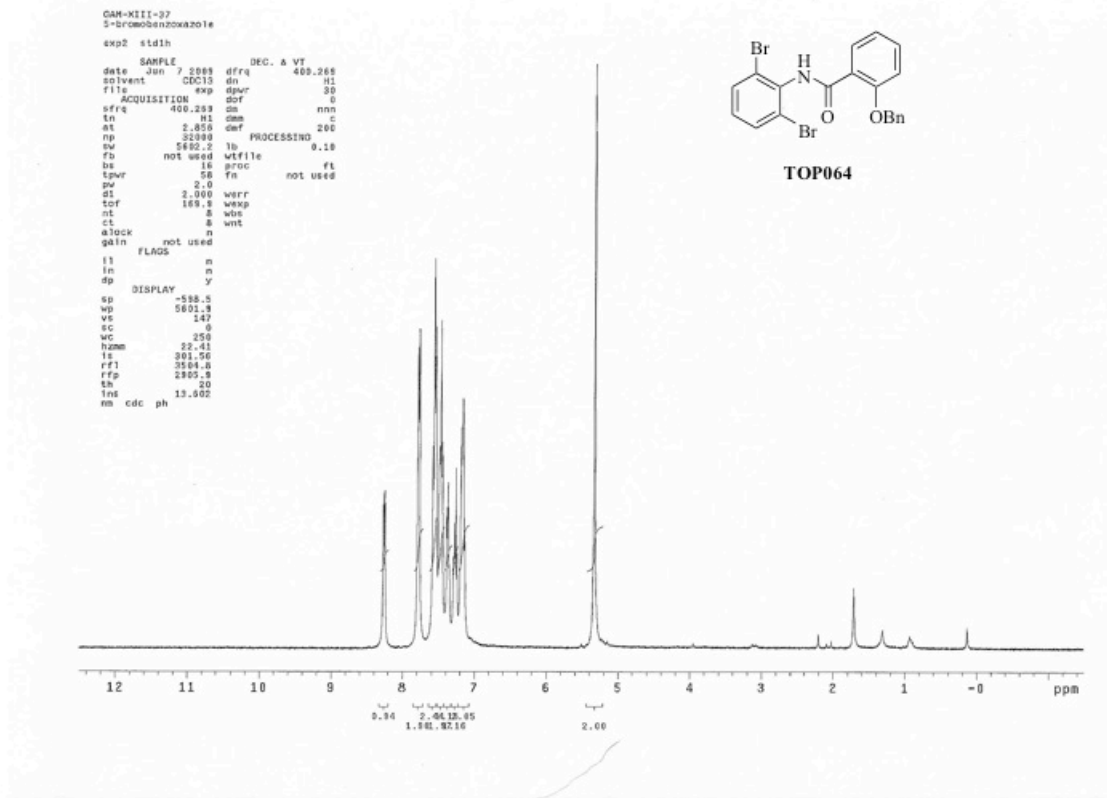
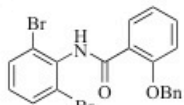


Figure A3.11.  $^1\text{H}$  NMR of TOP064

```

GAM-XIII-37-19C
exp2 std13c
SAMPLE DEC. & VT
date Jun 7 2009 dfrq 400.269
solvent CDCl3 dm H1
file exp dpar 38
ACQUISITION dof 0
sfrq 100.628 dm yyy
tn C13 dm v
at 1.280 def 9390
np 64484 PROCESSING
pv 25188.9 lb 1.00
fb 13800 wffile
bs 16 pfac ft
tpwr 60 fn not used
pv 3.0
d1 2.000 werr
tof 1539.5 wexp
nt 512 wbs
ct 512 wnt
atock n
gain not used
FLAGS
ll n
ln n
dp Y
DISPLAY
sp -1556.9
wp 25188.1
vs 153
sc 0
wc 250
hzmm 3.44
ls 500.00
rf1 8307.5
rfp 7749.6
th 6
ins 100.000
nm cdc ph

```



TOP064

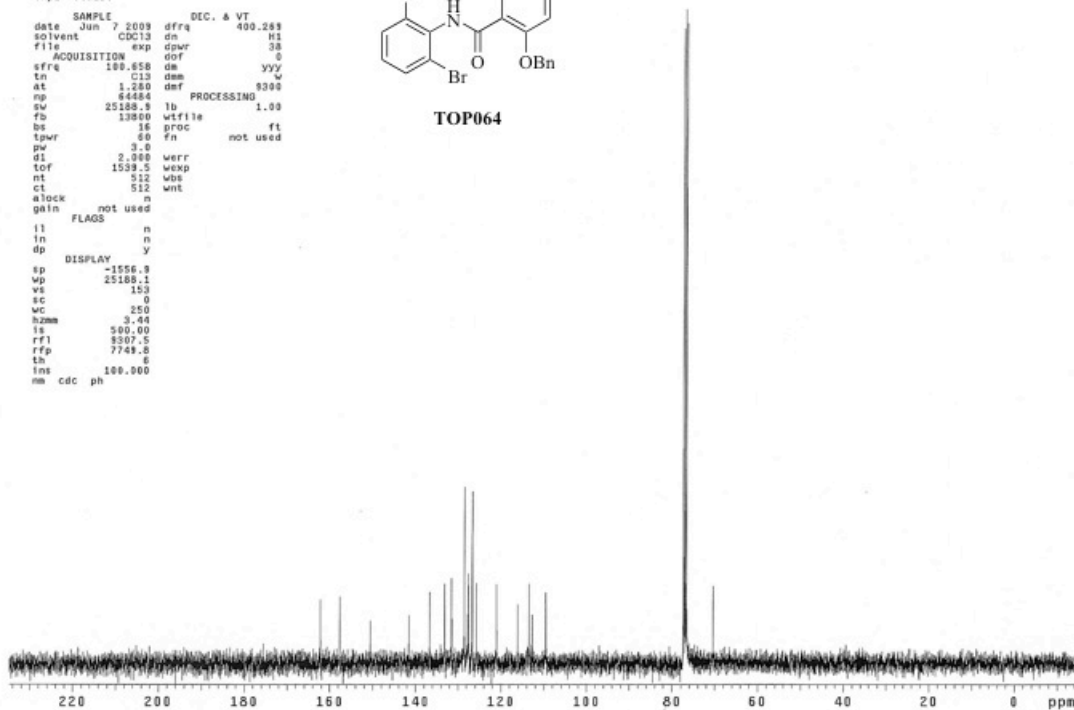


Figure A3.12. <sup>13</sup>C NMR of TOP064

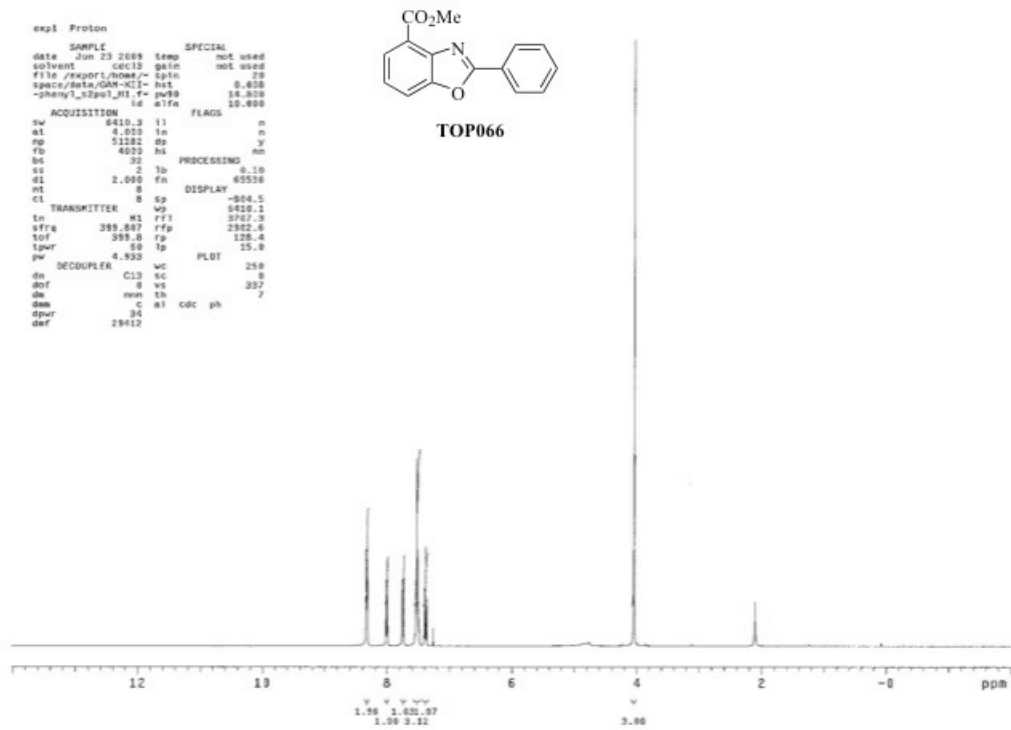


Figure A3.13.  $^1\text{H}$  NMR of **TOP066**

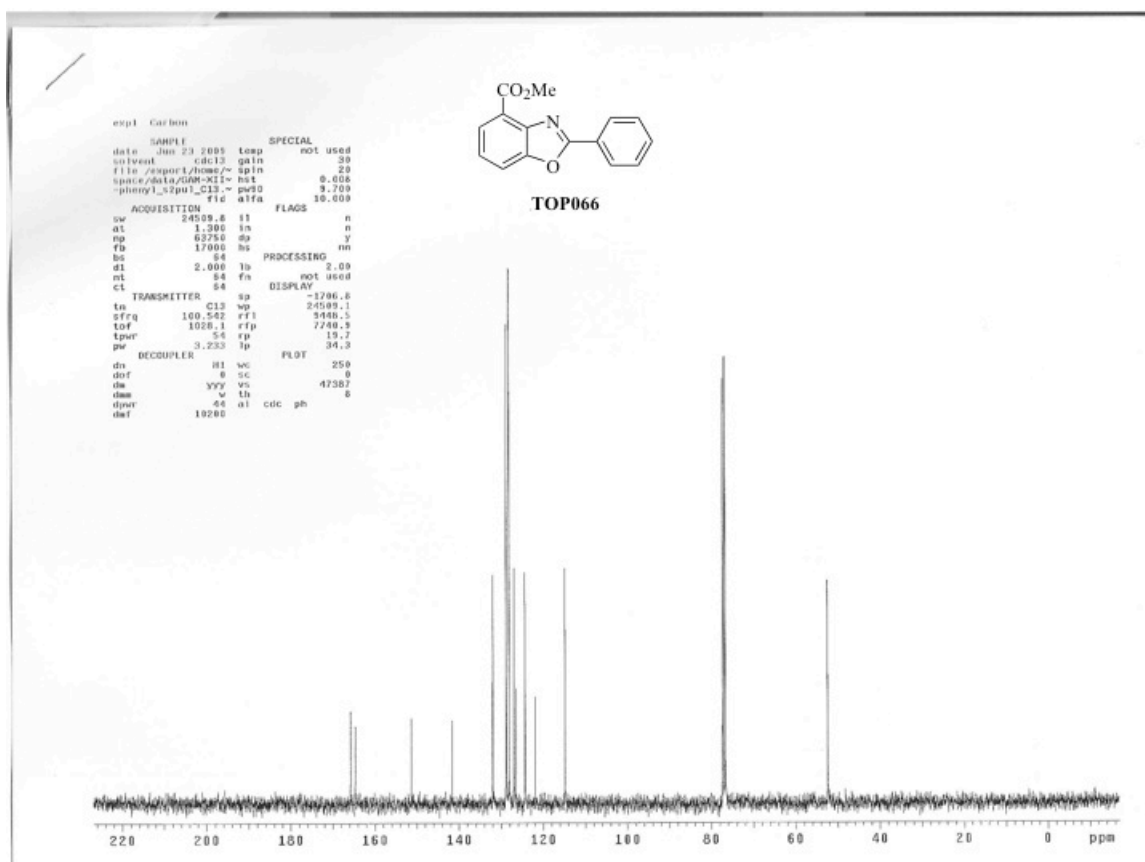


Figure A3.14. <sup>13</sup>C NMR of TOP066

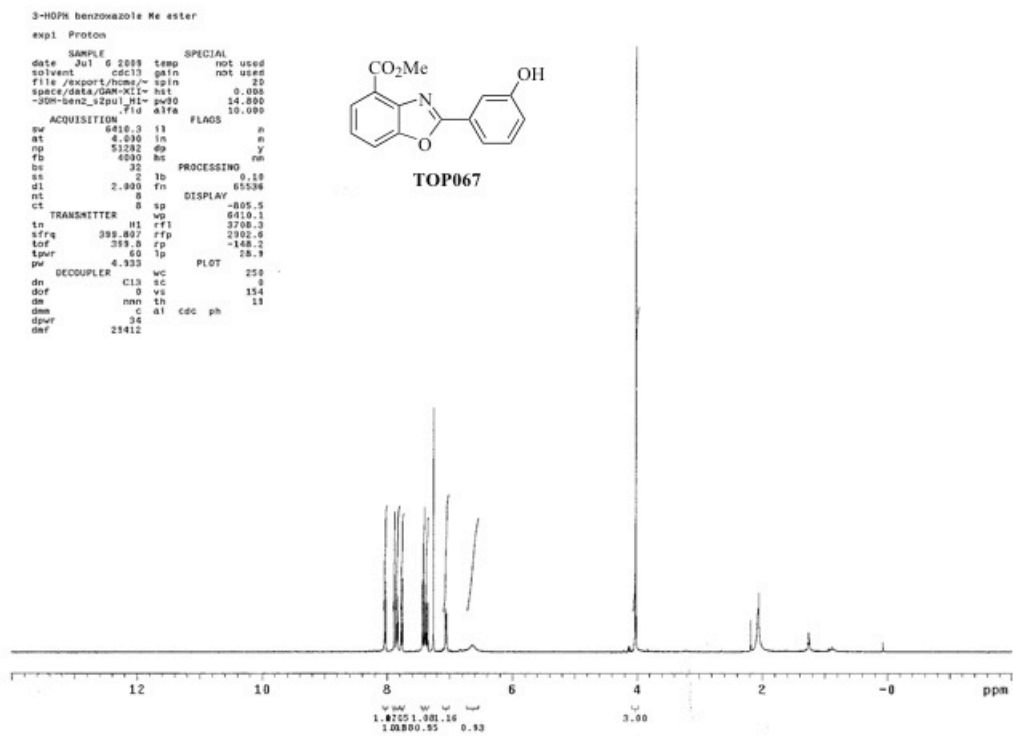


Figure A3.15.  $^1\text{H}$  NMR of TOP067

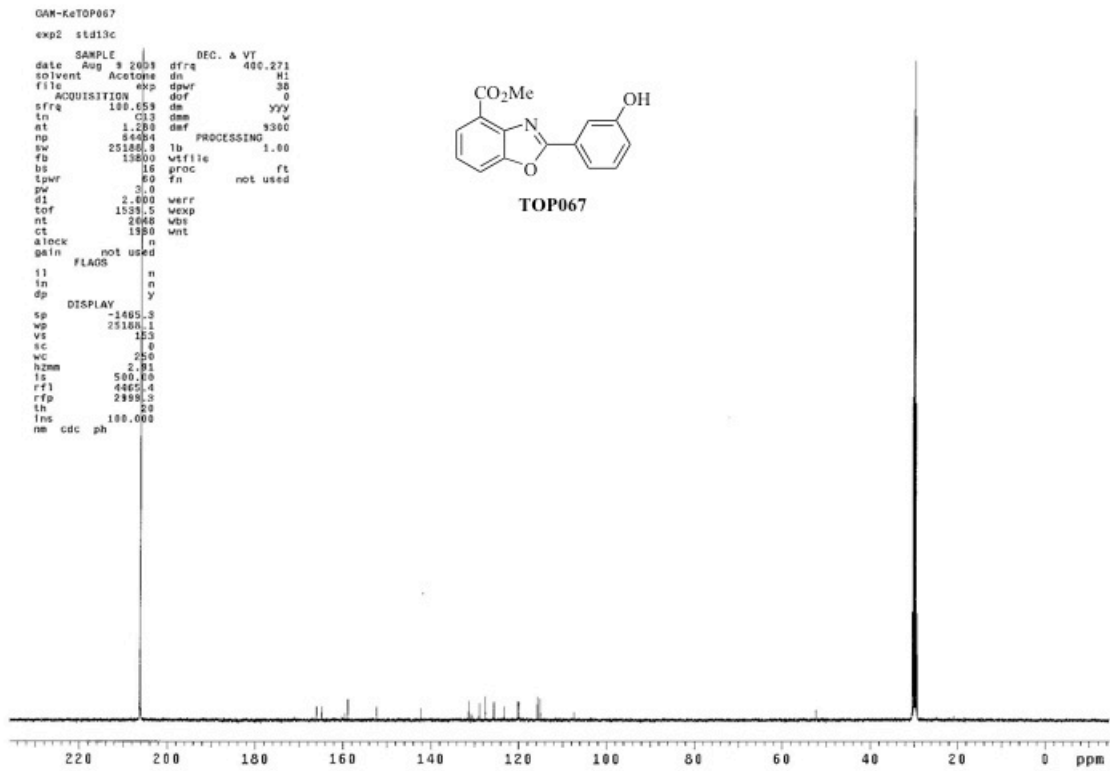


Figure A3.16.  $^{13}\text{C}$  NMR of TOP067

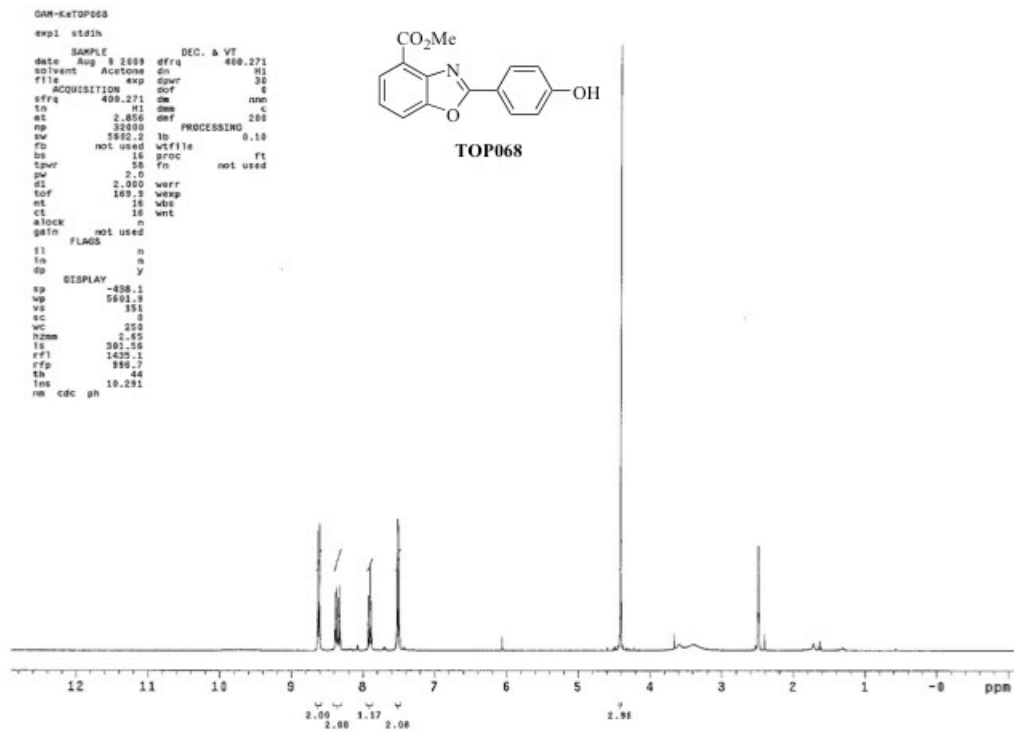


Figure A3.17.  $^1\text{H}$  NMR of **TOP068**



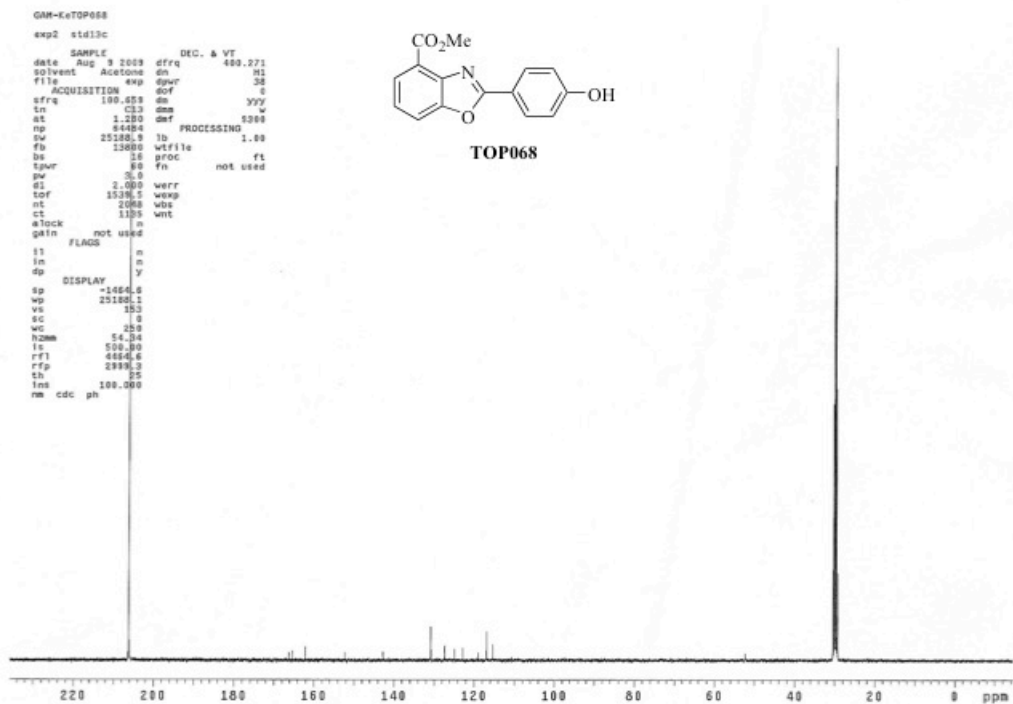


Figure A3.19.  $^{13}\text{C}$  NMR of TOP068

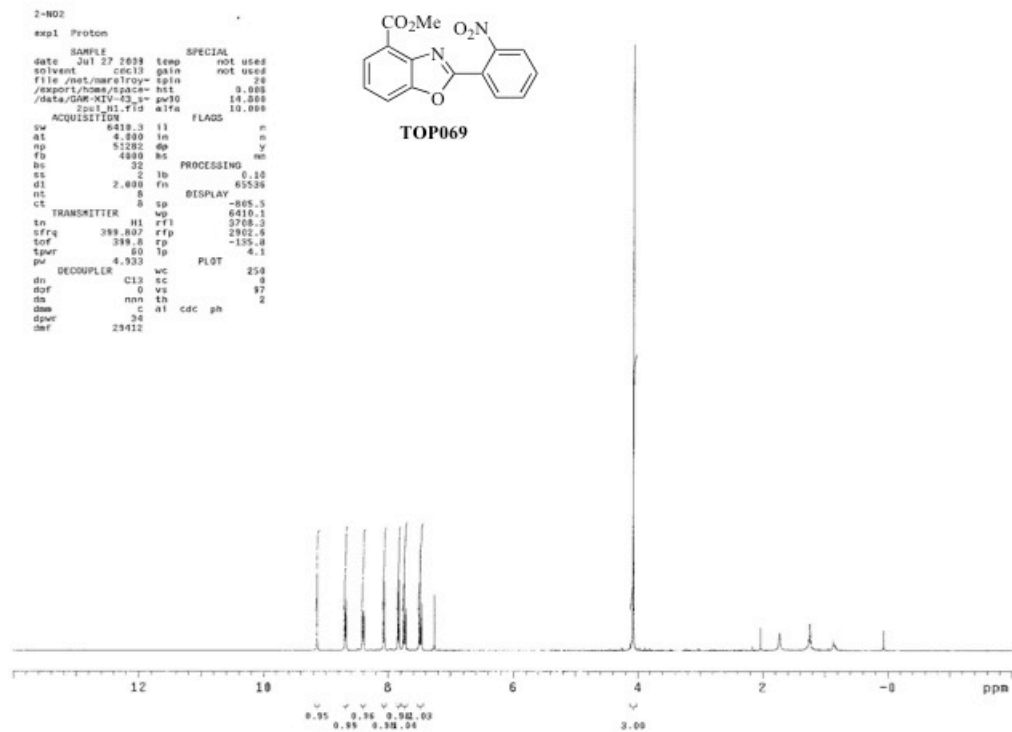


Figure A3.20.  $^1\text{H}$  NMR of **TOP069**

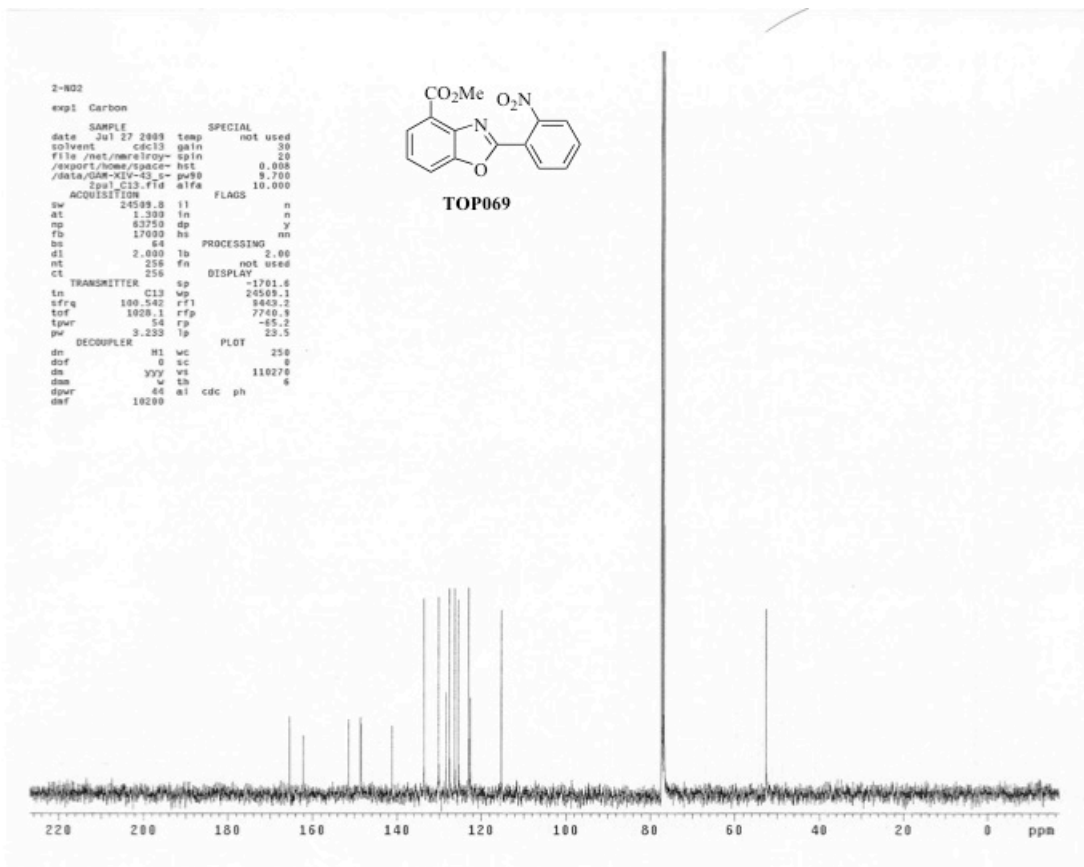


Figure A3.21.  $^{13}\text{C}$  NMR of TOP069

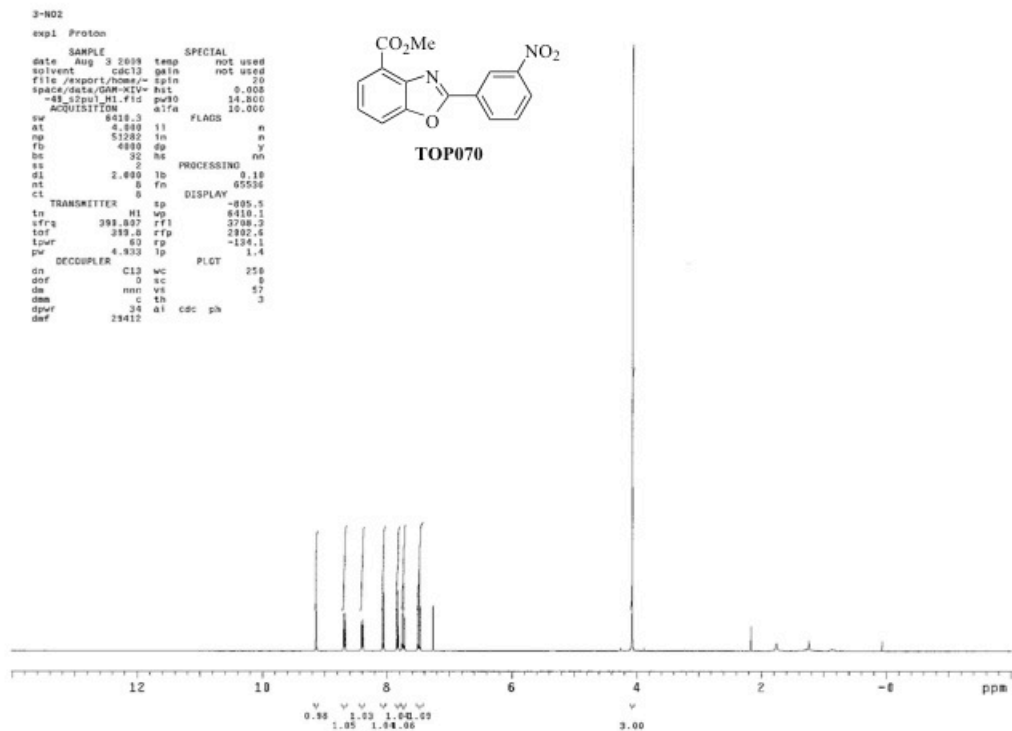


Figure A3.22. <sup>1</sup>H NMR of **TOP070**

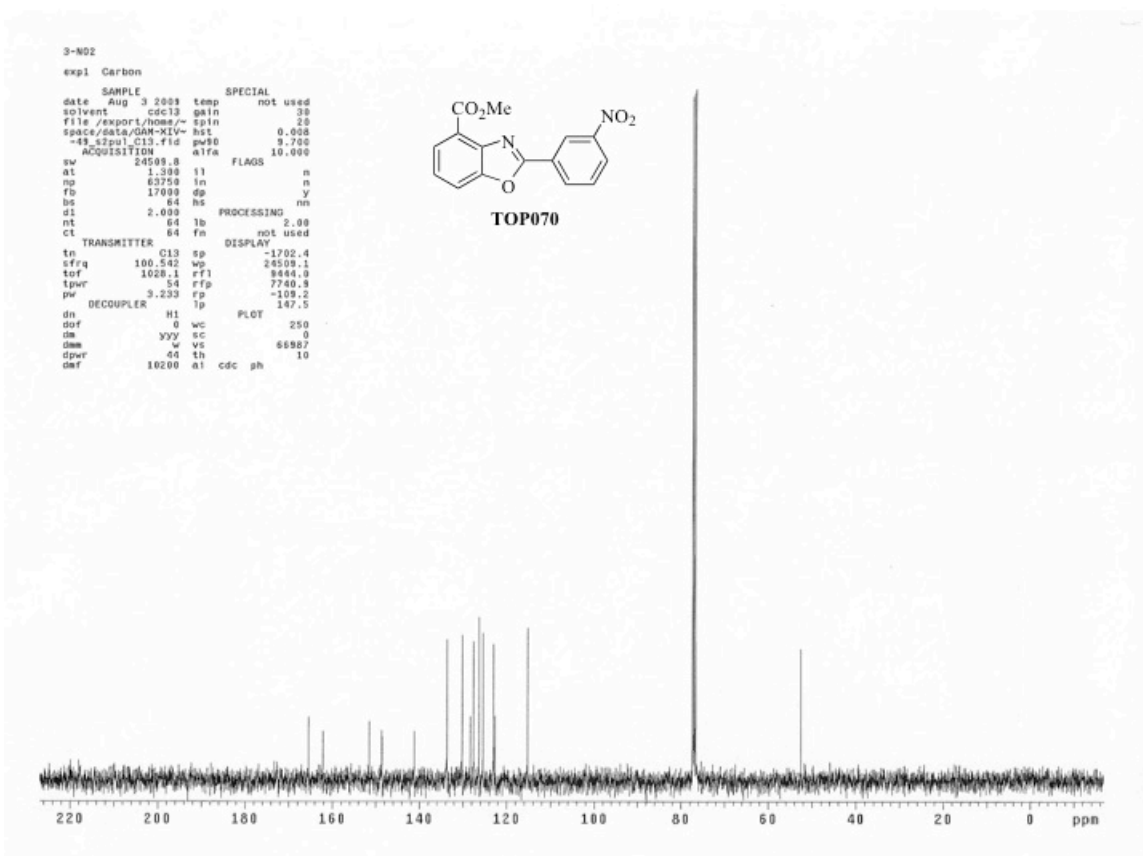


Figure A3.23.  $^{13}\text{C}$  NMR of TOP070

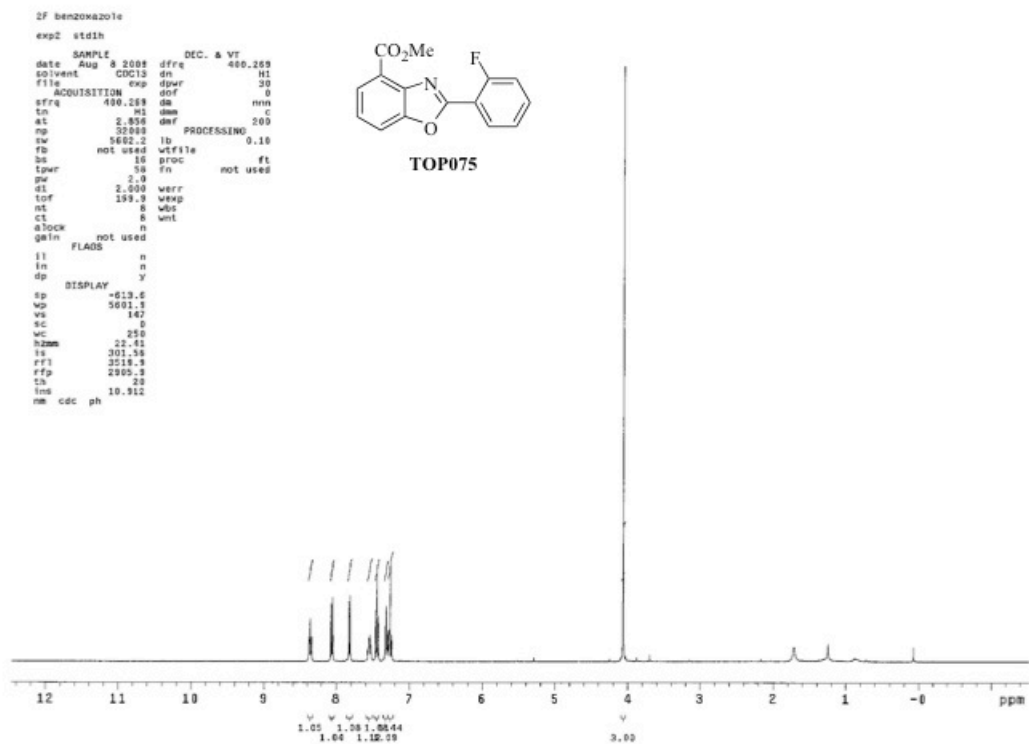


Figure A3.24.  $^1\text{H}$  NMR of **TOP075**

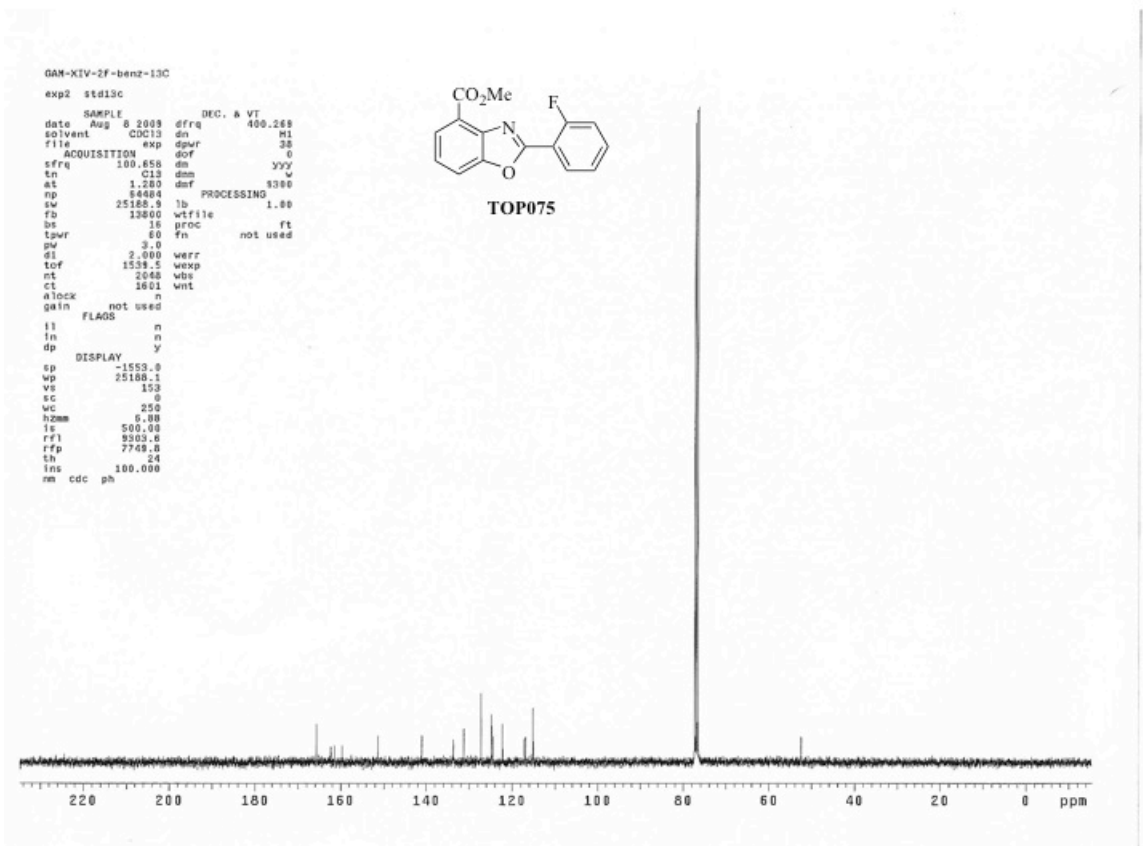


Figure A3.25. <sup>13</sup>C NMR of TOP075

## References

- Adorjan, P.; Distler, J.; Lipscher, E.; Model, F.; Muller, J.; Pelet, C.; Baun, A.; Florl, A. R.; Gutig, D.; Grabs, G.; Howe, A.; Kursar, M.; Lesche, R.; Leu, E.; Lewin, A.; Maier, S.; Muller, V.; Otto, T.; Scholz, C.; Shulz, W. A.; Seifert, H. H.; Schwope, I.; Ziebarth, H.; Berlin, K.; Piepenbrock, C.; Olek, A. *Nucleic Acids Res.* **2002**, *20*, 21.
- Aich, P.; Dasgupta, D. *Biochemistry* **1995**, *34*, 1376-1385.
- Akerman, B. *Biophys. J.* **1998**, *74*, 3140-3151.
- Albaneze-Walker, J.; Bazaral, C.; Leavey, T.; Dormer, P. G.; Murry, J. A. *Org. Lett.* **2004**, *6*, 2097-2100.
- Albaneze-Walker, J.; Bazaral, C.; Leavey, T.; Dormer, P. G.; Murry, J. A. *Org. Lett.* **2004**, *6*, 2097-2100.
- Altenhoff, G.; Glorius, F. *Adv. Synth. Cat.* **2004**, *346*, 1661-1664.
- Altenhoff, G.; Glorius, F. *Adv. Synth. Catal.* **2004**, *346*, 1661-1664.
- Altomare A., Burla M. C.; Camalli M.; Cascarano G. L.; Giacovazzo C.; Guagliardi A.; Moliterni A. G. G.; Polidori G.; Spagna R. *J. Appl. Cryst.* **1999**, *32*, 115-119.
- Annunziata, R.; Cinquini, M.; Cozzi, F. *J. Chem. Soc., Perkin Trans. 1* **1982**, 339-343.
- Bae, J.-B.; Kim, Y.-J. *Animal and Cell Systems* **2008**, *12*, 117-135.
- Banville, D. L.; Keniery, M. A.; Shafer, R. H. *Biochemistry* **1990**, *29*, 9294-9302.
- Barbero, N.; Carril, M.; SanMartin, R.; Dominguez, E. *Tetrahedron* **2007**, *63*, 10425-10432.
- Barbero, N.; Carril, M.; SanMartin, R.; Dominguez, E. *Tetrahedron* **2007**, *63*, 10425-10432.
- Barlow, T.; Dipple, A. *Chem. Res. Toxicol.* **1998**, *11*, 44-53.



- Baruah, H.; Barry, C. G.; Bierback, U. *Curr. Top. Med. Chem.* **2004**, *4*, 1537-1549.
- Baylin, S. B.; Makos, M.; Wu, J.; Yen, R.-W. C.; deBustrs, A.; Vertino, P.; Nelkin, B. D. *Cancer Cells* **1991**, *3*, 383-390.
- Beck, J. L.; Colgrave, M. L.; Ralph, S. F.; Sheil, M. M. *Mass Spectrom. Rev.* **2001**, *20*, 61-87.
- Bellis, G. D.; Salani, G.; Battaglia, C.; Pietta, P.; Rosti, E.; Mauri, P. *Rapid Commun. Mass Spectrom.* **2000**, *14*, 243-249.
- Biggins, J. B.; Prudent, J. R.; Marshall, D. J.; Ruppen, M.; Thorson, J. S. *Proc. Natl. Acad. Sci. U.S.A.* **2000**, *97*, 13537-13542.
- Bingham, J. P.; Hartley, J. A.; Souhami, R. L.; Grimaldi, K. A. *Nucleic Acids Res.* **1996**, *24*, 987-989.
- Bolzan, A. D.; Bianchi, M. S. *Mutat. Res.* **2002**, *512*, 121-134.
- Bonnamour, J.; Bolm, C. *Org. Lett.* **2008**, *10*, 2665-2667.
- Bonnamour, J.; Bolm, C. *Org. Lett.* **2008**, *10*, 2665-2667.
- Brak, K.; Barrett, K. T.; Ellman, J. A. *J. Org. Chem.* **2009**, *74*, 3606-3608.
- Brak, K.; Ellman, J. A. *J. Am. Chem. Soc.* **2009**, *131*, 3850-3851.
- Brinner, K. M.; Ellman, J. A. *Org. Biomol. Chem.* **2005**, *3*, 2109-2113.
- Broggini, M.; Coley, H. M.; Mongelli, N.; Pesenti, E.; Wyatt, M. D.; Hartley, J. A.; D'Incalci, M. *Nucleic Acids Res.* **1995**, *23*, 81-87.
- Bush, L. P.; Cui, M.; Shi, H.; *et al.* *Recent Advances in Tobacco Science* **2001**, *27*, 23-46.
- Cadet, J.; Douki, T.; Frelon, S.; Sauviago, S.; Pouget, J.-P.; Ravanat, J.-L. *Free Radical Biol. Med.* **2002**, *33*, 441-449.
- Campos, P. J.; Soldevilla, A.; Sampedro, D.; Rodriguez, M. A. *Org. Lett.* **2001**, *3*, 4087-4089.

- Campos, P. J.; Soldevilla, A.; Sampedro, D.; Rodriguez, M. A. *Tetrahedron Lett.* **2002**, *43*, 8811-8813.
- Carey, F. A.; Sundberg, R. J. *Advanced Organic Chemistry, Part A: Structure and Mechanisms*; 4 ed.; Kluwer Academic / Plenum Publishers: New York, 2000.
- Carmella, S. G.; McIntee, E. J.; Chen, M.; Hecht, S. S. *Carcinogenesis* **2000**, *21*, 839-843.
- Cashmore, A. R.; Petersen, G. B. *Biochim. Biophys. Acta* **1969**, *174*, 591-603.
- Catassi, A.; Servent, D.; Paleari, L.; Cesario, A.; Russo, P. *Mutat. Res.* **2008**, *659*, 221-231.
- Chaires, J. B.; Herrera, J. E.; Waring, M. J. *Biochemistry* **1990**, *29*, 6145-6153.
- Chaires, J. B.; Priebe, W.; Graves, D. E.; Burke, T. G. *J. Am. Chem. Soc.* **1993**, *115*, 5360-5364.
- Chang, J.; Zhao, K.; Pan, S. *Tetrahedron Lett.* **2002**, *43*, 951-954.
- Chang, J.; Zhao, K.; Pan, S. *Tetrahedron Lett.* **2002**, *43*, 951-954.
- Cheh, A. M.; Yagi, H.; Jerina, D. M. *Chem. Res. Toxicol.* **1990**, *3*, 545-550.
- Chen, C. M.; Chen, H. L.; Hsiau, A. H.; Shi, H.; Brock, G. J.; Wei, S. H.; Caldwell, C. W.; Yan, P. S.; Huang, T. H. *Am. J. Pathol.* **2003**, *163*, 37-45.
- Chen, Y.-X.; Qian, L.-F.; Zhang, W.; Han, B. *Angew. Chem., Int. Ed. Engl.* **2008**, *47*, 9330-9333.
- Chen, Y.-X.; Qian, L.-F.; Zhang, W.; Han, B. *Angew. Chemie, Int. Ed. Engl.* **2008**, *47*, 9330-9333.
- Churchill, M. E. A.; Hayes, J. J.; Tullius, T. D. *Biochemistry* **1990**, *29*, 6043-6050.
- Cogan, D. A.; Ellman, J. A. *J. Am. Chem. Soc.* **1999**, *121*, 268-269.
- Cogan, D. A.; Liu, G.; Kim, K.; Backes, B. J.; Ellman, J. A. *J. Am. Chem. Soc.* **1998**, *120*, 8011-8019.

- Collier, D. A.; Neidle, S.; Brown, J. R. *Biochem. Pharmacol.* **1984**, *33*, 2877-2880.
- Colvin, M.; Hilton, J. *Cancer Treatment Reports* **1981**, *65*, 89-95.
- Cons, B. M. G.; Fox, K. R. *FEBS Lett.* **1990**, *264*, 100-104.
- Cooper, I. R.; Grigg, R.; MacLachlan, W. S.; Thornton-Pett, M.; Sridharan, V. *Chem. Commun.* **2002**, 1372-1373.
- Corbleet, M. A.; Stuart-Harris, R. C.; Smith, I. E.; Coleman, R. E.; Rubens, R. D.; McDonald, M.; Mouridsen, H. T.; Ranier, H.; van Oosterom, A. T.; Smyth, J. F. *European Journal of Cancer and Clinical Oncology* **1984**, *20*, 1141-1146.
- Cramer, C. J. *J. Am. Chem. Soc.* **1998**, *120*, 6261-6269.
- Cremeens, M. E.; Hughes, T. S.; Carpenter, B. K. *J. Am. Chem. Soc.* **2005**, *127*, 6652-6651.
- Cushnir, J. R.; Naylor, S.; Lamb, J. H.; Farmer, P. B.; Brown, N. A.; Mirkes, P. E. *Rapid Commun. Mass Spectrom.* **1990**, *4*, 410-414.
- Cutts, S. M.; Masta, A.; Panousis, C.; Parsons, P. G.; Sturm, R. A.; Phillips, D. R. In *Drug-DNA Interaction Protocols*; Fox, K. R., Ed.; Humana Press: Totowa, New Jersey, 1997; Vol. 90, p 1-22.
- Cutts, S. M.; Panousis, C.; Masta, A.; Phillips, D. R. In *Drug-DNA Interaction Protocols*; Fox, K. R., Ed.; Humana Press: Totowa, New Jersey, 1997; Vol. 90, p 1-22.
- Dackiewicz, P.; Skladanowski, A.; Konopa, J. *Chem.-Biol. Interact.* **1995**, *98*, 153-166.
- Danissenko, M. S.; Pao, A.; Tang, M.-s.; Pfeifer, G. P. *Science* **1996**, *274*, 430-432.
- David, W. M. Dissertation, The University of Texas at Austin, 2000.
- David, W. M.; Kerwin, S. M. *J. Am. Chem. Soc.* **1997**, *119*, 1464-1465.
- David, W. M.; Kumar, D.; Kerwin, S. M. *Bioorg. Med. Chem. Lett.* **2000**, *10*, 2509-2512.
- Davis, F. A.; Zhou, P. *Tetrahedron Lett.* **1994**, *35*, 7525-7528.
- Davis, F. A.; Zhou, P.; Reddy, G. V. *J. Org. Chem.* **1994**, *59*, 3242-3245.

- DeLuca, M. R.; Kerwin, S. M. *Tetrahedron Lett.* **1997**, *38*, 199-202.
- DeLuca, M. R.; Kerwin, S. M. *Tetrahedron Lett.* **1997**, *38*, 199-202.
- Denissenko, M. F.; Chem, J. X.; Tang, M.-s.; Pfeifer, G. P. *Proc. Natl. Acad. Sci. U. S. A.* **1997**, *94*, 3893-3898.
- DENZO-SMN. (1997). Z. Otwinowski and W. Minor, *Methods in Enzymology*, **276**: Macromolecular Crystallography, part A, 307 – 326, C. W. Carter, Jr. and R. M. Sweets, Editors, Academic Press.
- Devi, P. G.; Pal, S.; Banerjee, R.; Dasgupta, D. *J. Inorg. Biochem.* **2007**, *101*, 127-137.
- Dickerson, R. E.; Drew, H.; Conner, B. N.; Wing, R. M.; Fratini, A. V.; Kopka, M. L. *Science* **1982**, *216*, 475-485.
- Ding, J.; Vouros, P. *J. Chromat. A* **2000**, *887*, 103-113.
- Dooley, T. P.; Weiland, K. L. In *Drug-DNA Interaction Protocols*; Fox, K. R., Ed.; Humana Press: Totowa, New Jersey, 1997; Vol. 90, p 1-22.
- Dougherty, G.; Pilbrow, J. R. *Int. J. Biochem.* **1984**, *16*, 1179-1192.
- Dyke, M. W. V.; Dervan, P. B. *Biochemistry* **1983**, *22*, 2373-2377.
- Dyke, M. W. V.; Hertzberg, R. P.; Dervan, P. B. *Proc. Natl. Acad. Sci. U. S. A.* **1982**, *79*, 5470-5474.
- Egleton, R. D.; Brown, K. C.; Dasgupta, P. *Pharmacol. Ther.* **2009**, *121*, 205-223.
- Ehrenfield, G. M.; Shipley, J. B.; Heimbrook, D. C.; Sugiyama, H.; Long, E. E.; van Bloom, J. J.; van der Marel, G. A.; Oppenheimer, N. J.; Hecht, S. M. *Biochemistry* **1987**, *36*, 931-942.
- Eisenbrand, G.; Muller, N.; Denker, E.; Sterzel, W. *Journal of Cancer Research and Clinical Oncology* **1986**, *112*, 196-204.
- Epstein, J. L.; Zhang, X.; Doss, G. A.; Liesch, J. M.; Krishnan, B.; Stubbe, J.; Kozarich, J. W. *J. Am. Chem. Soc.* **1997**, *119*, 6731-6738.

- Esteller, M.; Fraga, M. F.; Guo, M.; Garcia-Foncillas, J.; Hedenfalk, I.; Godwin, W. K.; Trojan, J.; Vaurs-Barriere, C.; Bignon, Y. J.; Ramus, S.; Benitez, J.; Caldes, T.; Akiyama, Y.; Yuasa, Y.; Launonen, V.; Canal, M. J.; Rodriguez, R.; Capella, G.; Peinado, M. A.; Borg, A.; Aaltonen, L. A.; Ponder, B. A.; Baylin, S. B.; Herman, J. G. *Hum. Mol. Genet.* **2001**, *10*, 3001-3007.
- Evindar, G.; Batey, R. A. *J. Org. Chem.* **2006**, *71*, 1802-1808.
- Evindar, G.; Batey, R. A. *J. Org. Chem.* **2006**, *71*, 1802-1808.
- Faulds, D.; Balfour, J. A.; Chrisp, P.; Langtry, H. D. *Drugs* **1991**, *41*, 400-449.
- Feng, L.; Kumar, D.; Birney, D. M.; Kerwin, S. M. *Org. Lett.* **2004**, *6*, 2059-2062.
- Feng, L.; Zhang, A.; Kerwin, S. M. *Org. Lett.* **2006**, *8*, 1983-1986.
- Feng, Z.; Hu, W.; Rom., W. N.; Beland, F. A.; Tang, M.-s. *Biochemistry* **2002**, *41*, 6414-6421.
- Feng, Z.; Hu, Y.; Tang, M.-s. *Proc. Natl. Acad. Sci. U. S. A.* **2006**, *43*, 15404-15409.
- Fielder, D. A.; Collins, F. W. *J. Nat. Prod.* **1995**, *58*, 456-458.
- Fielder, D. A.; Collins, F. W. *J. Nat. Prod.* **1995**, *58*, 456-458.
- Ford, G. P.; Scribner, J. D. *Chem. Res. Toxicol.* **1990**, *3*, 219-230.
- Fox, K. R. In *Methods in Molecular Biology*; Walker, J. M., Ed.; Humana Press: Totowa, 1997; Vol. 90, p 278.
- Fox, K. R.; Howarth, N. R. *Nucleic Acids Res.* **1985**, *13*, 8695-8714.
- Fox, K. R.; Waring, M. J. *Biochemistry* **1986**, *25*, 4349-3456.
- Fox, K. R.; Waring, M. J. *Nucleic Acids Res.* **1984**, *12*, 9271-9285.
- Franca, L. T. C.; Carrilho, E.; Kist, T. B. L. *Q. Rev. Biophys.* **2002**, *35*, 169-200.
- Fritzche, H.; Triebel, H.; Chaires, J. B.; Dattagupta, N.; Crothers, D. M. *Biochemistry* **1982**, *21*, 3940-3946.

- Fritzsche, H.; Wahnert, U.; Chaires, J. B.; Dattagupta, N.; Schlessinger, F. B.; Crothers, D. M. *Biochemistry* **1987**, *26*, 1996-2000.
- Fujisawa, T.; Kooriyama, Y.; Shimizu, M. *Tetrahedron Lett.* **1996**, *37*, 3881-3884.
- Galas, D. J.; Schmitz, A. *Nucleic Acids Res.* **1978**, *5*, 3157-3170.
- Giloni, L.; Takeshita, M.; Johnson, F.; Iden, C.; Grollman, A. P. *The Journal of Biological Chemistry* **1981**, *256*, 8608-8615.
- Gold, B.; Marky, L. M.; Stone, M. P.; Williams, L. D. *Chem. Res. Toxicol.* **2006**, *19*, 1402-1414.
- Goldstein, S. W.; Dambek, P. J. *J. Heterocycl. Chem.* **1990**, *27*, 335-336.
- Goldstein, S. W.; Dambek, P. J. *J. Heterocyclic Chem.* **1990**, *27*, 335-336.
- Gonzalez-Gomez, J. C.; Foubelo, F.; Yus, M. *Tetrahedron Lett.* **2008**, *49*, 2343-2347.
- Gorbacheva, L. B.; Dederer, L. Y. *Pharm. Chem. J.* **2009**, *43*, 73-76.
- Gottlieb, H. E.; Kotlyar, V.; Nudelman, A. *J. Org. Chem.* **1997**, *62*, 7512-7515.
- Gottlieb, H. E.; Kotlyar, V.; Nudelman, A. *J. Org. Chem.* **1997**, *62*, 7512-7515.
- Greenblatt, M. S.; Bennett, W. P.; Hollstein, M.; Harris, C. C. *Cancer Res.* **1994**, *69*, 409-416.
- Greenblatt, M. S.; Bennett, W. P.; Hollstein, M.; Harris, C. C. *Cancer Res.* **1994**, *54*, 4855-4878
- Greer, S.; Zamenhof, S. *J. Mol. Biol.* **1962**, *4*, 123-141.
- Grimaldi, K. A.; Bingham, J. P.; Souhami, R. L.; Hartley, J. A. *Anal. Biochem.* **1994**, *222*, 236-242.
- Grundy, W. E.; Goldstein, A. W.; Rickher, C. J.; Hanes, M. E.; Warren, H. B., Jr.; Sylvester, J. C. *Antibiotic Chemotherapeutics* **1953**, *3*, 1215-1217.
- Guan, L. L.; Kuwahara, J.; Sugiura, Y. *Biochemistry* **1993**, *1993*, 6141-6145.
- Hainaut, P.; Pfeifer, G. P. *Carcinogenesis* **2001**, *22*, 367-374.

- Hanka, L. J.; Dietz, S. A.; Gerpheide, S. A.; Kuentzel, S. L.; Martin, D. G. *J. Antibiot.* **1978**, *XXXI*, 1211-1217.
- Hartley, J. A.; Souhami, R. L.; Berardini, M. D. *J. Chromatogr.* **1993**, *618*, 277-288.
- Hashimoto, T.; Yamada, Y. *Ann. Rev. Plant Physiol. Plant Mol. Biol.* **1994**, *45*, 257-285.
- Hecht, S. S. *Drug Metab. Rev.* **1994**, *26*, 373-390.
- Hecht, S. S.; Chen, C. B. *J. Org. Chem.* **1979**, *44*, 1563-1566.
- Hecht, S. S.; Villalta, P. W.; Sturla, S. J.; Cheng, G.; Yu, N.; Upadhyaya, P.; Wang, M. *Chem. Res. Toxicol.* **2004**, *17*, 588-597.
- Hegedus, A.; Vigh, I.; Hell, Z. *Heteroat. Chem.* **2004**, *15*, 428-431.
- Hegedus, A.; Vigh, I.; Hell, Z. *Heteroatom Chemistry* **2004**, *15*, 428-431.
- Hein, D. W.; Alheim, R. J.; Leavitt, J. J. *J. Am. Chem. Soc.* **1957**, *79*, 427-429.
- Hein, D. W.; Alheim, R. J.; Leavitt, J. J. *J. Am. Chem. Soc.* **1957**, *79*, 427-429.
- Heinemann, U.; Alings, C.; Hahn, M. *Biophys. Chem.* **1994**, *50*, 157-167.
- Hemminki, K.; Ludlum, D. B. *J. Natl. Cancer Inst.* **1984**, *73*, 1021-1028.
- Hertzberg, R. P.; Dervan, P. B. *Biochemistry* **1984**, *23*, 3934-3945.
- Hoffner, J.; Schottelius, M. J.; Feichtinger, D.; Chen, P. *J. Am. Chem. Soc.* **1998**, *120*, 376-385.
- Hohmann, C.; Schneider, K.; Bruntner, C.; Irran, E.; Nicholson, G.; Bull, A. T.; Jones, A. L.; Brown, R.; Stach, J. E. M.; Goodfellow, M.; Beil, W.; Kramer, M.; Imhoff, J. F.; Sussmuth, R. D.; Fiedler, H.-P. *J. Antibiot.* **2009**, *62*, 99-104.
- Hohmann, C.; Schneider, K.; Bruntner, C.; Irran, E.; Nicholson, G.; Bull, A. T.; Jones, A. L.; Brown, R.; Stach, J. E. M.; Goodfellow, M.; Beil, W.; Kramer, M.; Imhoff, J. F.; Sussmuth, R. D.; Fiedler, H.-P. *J. of Antibiot.* **2009**, *62*, 99-104.
- Hopkins, P. B.; Millard, J. T.; Woo, J.; Weidner, M. F.; Kirchner, J. J.; Sigurdsson, S. T.; Raucher, S. *Tetrahedron* **1991**, *47*, 2475-2489.

- Hou, M.-H.; Wang, A. H.-J. *Nucleic Acids Res.* **2005**, *33*, 1352-1361.
- Hu, M. W.; Bondinell, W. E.; Hoffman, D. J. *Labelled Compd. Radiopharm.* **1974**, *10*, 79-48.
- Huang, S.-T.; Hseib, I.-J.; Chen, C. *Bioorg. Med. Chem. Lett.* **2006**, *14*, 6106-6119.
- Huang, S.-T.; Hseib, I.-J.; Chen, C. *Bioorg. Med. Chem. Lett.* **2006**, *14*, 6106-6119.
- Hurley, L. H.; Reck, T.; Thurston, D. E.; Langley, D. R.; Holden, K. G.; Hertzberg, R. P.; Hoover, J. R. E.; Gallagher, G.; Faucette, L. F.; Mong, S.-M.; Johnson, R., K. *Chem. Res. Toxicol.* **1988**, *1*.
- Hurley, L. H.; Reynolds, V. L.; Swenson, D. H.; Petzold, G. L.; Scahill, T. A. *Science* **1984**, *226*, 843-844.
- Hutchison, C. A. *Nucleic Acids Res.* **2007**, *35*, 6227-6237.
- International Tables for X-ray Crystallography (1992). Vol. C, Tables 4.2.6.8 and 6.1.1.4, A. J. C. Wilson, editor, Boston: Kluwer Academic Press.
- Jacobsen, M. F.; Skrydstrup, T. *J. Org. Chem.* **2003**, *68*, 7112-7114.
- Jain, S. C.; Tsai, C.-C.; Sobell, H. M. *J. Mol. Biol.* **1977**, *114*, 317-331.
- Jalas, J. R.; Hecht, S. S.; Murphy, S. E. *Chem. Res. Toxicol.* **2005**, *18*, 95-110.
- Jarboe, C. H.; Rosene, C. J. *J. Chem. Soc.* **1961**, 2455-2458.
- Jenkins, T. C. In *Methods in Molecular Biology*; Walker, J. M., Ed.; Humana Press: Totowa, 1997; Vol. 90, p 278.
- Jenuwein, T.; Allis, C. D. *Science* **2001**, *293*, 1074-1180.
- Johnson, S. M.; Connelly, S.; Wilson, I. A.; Kelly, J. W. *J. Med. Chem.* **2008**, *51*, 260-270.
- Johnson, S. M.; Connelly, S.; Wilson, I. A.; Kelly, J. W. *J. Med. Chem.* **2008**, *51*, 260-270.



- Jolles, B.; Laigle, A.; Priebe, W.; Garnier-Suillerot, A. *Chem.-Biol. Interact.* **1996**, *100*, 165-176.
- Jones, R. R.; Bergman, R. G. *J. Am. Chem. Soc.* **1972**, *94*, 660-661.
- Joshua-Tor, L.; Sussman, J. L. *Curr. Opin. Struct. Bio.* **1993**, *3*, 323-335.
- Journet, M.; Cai, D.; DiMichele, L. M.; Larsen, R. D. *Tetrahedron Lett.* **1998**, *39*, 6427-6428.
- Julio, E.; Laporte, F.; Reis, S.; Rothan, C.; Dorlac de Borne, F. *Mol. Breed.* **2008**, *21*, 369-381.
- Kalben, A.; Pal, S.; Andreotti, A. H.; Walker, S.; Gange, D.; Biswas, K.; Kahne, D. *J. Am. Chem. Soc.* **2000**, *122*, 8403-8412.
- Kanaoka, Y.; Hamada, T.; Yonemitsu, O. *Chem. Pharm. Bull.* **1970**, *18*, 587-590.
- Kanaoka, Y.; Hamada, T.; Yonemitsu, O. *Chem. Pharm. Bull.* **1970**, *18*, 587-590.
- Kappen, L. S.; Goldberg, I. H. *Biochemistry* **1993**, *32*, 13138-13145.
- Kaul, S.; Kumar, A.; Sain, B.; Bhatnager, A. K. *Synth. Commun.* **2007**, *37*, 2457-2460.
- Kaul, S.; Kumar, A.; Sain, B.; Bhatnager, A. K. *Synth. Commun.* **2007**, *37*, 2457-2460.
- Kelly, J. D.; Shah, D.; Chen, F.-X.; Wurdeman, R.; Gold, B. *Chem. Res. Toxicol.* **1998**, *11*, 1481-1486.
- Keniry, M. A.; Shafer, R. H. In *Methods Enzymol.*; Academic Press: New York, 1995; Vol. 261, p 575-604.
- Kerwin, S. M.; Nadipuram, A. *Synlett* **2004**, *8*, 1404-1408.
- Kiselyov, A. *Tetrahedron Lett.* **1999**, *40*, 4119-412.
- Kiselyov, A. *Tetrahedron Lett.* **1999**, *40*, 4119-412.
- Kohn, K. W.; Hartlet, J. A.; Mattes, W. B. *Nucleic Acids Res.* **1987**, *14*, 10531-10549.
- Kong, J.-R.; Cho, C.-W.; Krische, M. J. *J. Am. Chem. Soc.* **2005**, *127*, 11269-11276.

- Kouidou, S.; Agidou, T.; Kyrkou, A.; Andreou, A.; Katopodi, T.; Georgiou, E.; Krikelis, D.; Dimitriadou, A.; Spanos, P.; Tsilikas, C.; Destouni, H.; Tzimagiorgis, G. *Lung Cancer* **2005**, *50*, 299-307.
- Kraka, E.; Cremer, D. *J. Comput. Chem.* **2001**, *22*, 216-229.
- Kraka, E.; Cremer, D. *J. Mol. Struct.* **2000**, *506*, 191-211.
- Kumar, A.; Maurya, R. A.; Ahmad, P. *J. Comb. Chem.* **2009**, *11*, 198-201.
- Kumar, A.; Maurya, R. A.; Ahmad, P. *J. Comb. Chem.* **2009**, *11*, 198-201.
- Kumar, D. *Bioorg. Med. Chem. Lett.* **2001**, *11*, 2971-2974.
- Kumar, D.; Jacob, M. R.; Reynolds, M. B.; Kerwin, S. M. *Bioorg. Med. Chem. Lett.* **2002**, *10*, 3997-4004.
- Kumar, D.; Jacob, M. R.; Reynolds, M. B.; Kerwin, S. M. *Bioorg. Med. Chem. Lett.* **2002**, *10*, 3997-4004.
- Kumar, R.; Selvam, C.; Kaur, G.; Chakraborti, A. K. *Synlett* **2005**, *9*, 1401-1404.
- Kumar, R.; Selvam, C.; Kaur, G.; Chakraborti, A. K. *Synlett* **2005**, *9*, 1401-1404.
- Lane, M. J.; Dabrowiak, J. C.; Vournakis, J. N. *Proc. Natl. Acad. Sci. U.S.A.* **1983**, *80*, 3260-3264.
- Latif, F.; Moschel, R. C.; Hemminki, K.; Dipple, A. *Chem. Res. Toxicol.* **1988**, *1*, 364-369.
- Lawley, P. D.; Brookes, P. *Biochem. J.* **1963**, *89*, 127-138.
- Lawley, P. D.; Orr, D. J. *Chem.-Biol. Interact.* **1970**, *2*, 154-157.
- Lawley, P. D.; Orr, D. J. *Chem.-Biol. Interact.* **1970**, *2*, 61-164.
- Lee, K. Y.; Lee, M. J.; GowriSankar, S.; Kim, J. N. *Tetrahedron Lett.* **2004**, *45*, 5043-5046.
- Lefebvre, I. M.; Evans Jr., S. A. *J. Org. Chem.* **1994**, *62*, 7532-7533.
- LePecq, J.-B.; Paoletti, C. *J. Mol. Biol.* **1967**, *27*, 87-106.

Lewis, J. C.; Wiedemann, S. H.; Bergman, R. G.; Ellman, J. A. *Org. Lett.* **2004**, *6*, 35-38.

Lewis, J. C.; Wiedemann, S. H.; Bergman, R. G.; Ellman, J. A. *Org. Lett.* **2004**, *6*, 35-38.

Lhomme, J.; Constant, J.-F.; Demeunynck, M. *Biopolymers* **1999**, *52*, 65-83.

Liebeskind, L. S.; Srogl, J. *Org. Lett.* **2002**, *4*, 979-981.

Liebeskind, L. S.; Srogl, J. *Org. Lett.* **2002**, *4*, 979-981.

Likussar, W.; Boltz, D. F. *Anal. Chem.* **1971**, *43*, 1265-1272.

Lin, C. H.; Sun, D.; Hurley, L. H. *Chem. Res. Toxicol.* **1991**, *4*, 21-26.

Lin, X.; Bentley, P. A.; Xie, H. *Tetrahedron Lett.* **2005**, *46*, 7849-7852.

Lindh, R.; Ryde, U.; Schutz, M. *Theor. Chem. Acc.* **1997**, *97*, 203-210.

Liu, C.; Chen, F.-M. *Biochemistry* **1994**, *33*, 1419-1424.

Liu, G.; Cogan, D. A.; Ellman, J. A. *J. Am. Chem. Soc.* **1997**, *119*, 9913-9914.

Liu, G.; Cogan, D. A.; Owens, T. D.; Tang, T. P.; Ellman, J. A. *J. Org. Chem.* **1999**, *64*, 1278-1284.

Loozen, H. J.; Godefroi, E. F.; Besters, J. S. M. M. *J. Org. Chem.* **1975**, *40*, 892-894.

Low, C. M. L.; Drew, H. R.; Waring, M. J. *Nucleic Acids Res.* **1984**, *12*, 4865-4879.

Low, C. M. L.; Olsen, R. K.; Waring, M. J. *FEBS Lett.* **1984**, *176*, 414-420.

Lowry, T. H.; Richardson, K. S. *Mechanism and Theory in Organic Chemistry*; 3 ed.; HarperCollinsPublishers, Inc.: New York, 1987.

Ma, H. C.; Jiang, X. Z. *Synlett* **2008**, *9*, 1335-1340.

Ma, H. C.; Jiang, X. Z. *Synlett* **2008**, *9*, 1335-1340.

Maccrubin, A. E.; Caballes, L.; Riordan, J. M.; Huang, D. H.; Gurtoo, H. L. *Cancer Res.* **1991**, *51*, 886-892.

Mah, S. C.; Townsend, C. A.; Tullius, T. D. *Biochemistry* **1994**, *33*, 614-621.

Marriner, G. A.; Kerwin, S. M. *J. Org. Chem.* **2009**, *74*, 2891-2892.

Mattes, W. B.; Hartley, J. A.; Kohn, K. W. *Biochim. Biophys. Acta* **1986**, *868*, 71-76.

- Maxam, A. M.; Gilbert, W. *Proc. Natl. Acad. Sci. U.S.A.* **1977**, *74*, 560-564.
- McKee, M. L.; Kerwin, S. M. *Bioorg. Med. Chem. Lett.* **2008**, *16*, 1775-1783.
- McKee, M. L.; Kerwin, S. M. *Bioorg. Med. Chem. Lett.* **2008**, *16*, 1775-1783.
- Mikolajczyk, M.; Lyzwa, P.; Drabowicz, J.; Wieczorek *Chem. Commun.* **1996**, 1503-1504.
- Millard, J. T.; Raucher, S.; Hopkins, P. B. *J. Am. Chem. Soc.*, *112*, 2459-2460.
- Miller, J. N. *Analyst* **2005**, *130*, 265-270.
- Minnock, A.; Crow, S.; Bailly, C.; Waring, M. J. *Biochem. Biophys. Acta* **1999**, *1489*, 233-248.
- Moghaddam, F. M.; Bardajee, R.; Ismaili, H.; Taimoory, S. M. D. *Synth. Commun.* **2006**, *36*, 2543-2548.
- Moghaddam, F. M.; Bardajee, R.; Ismaili, H.; Taimoory, S. M. D. *Synth. Commun.* **2006**, *36*, 2543-2548.
- Molander, G. A. *J. Org. Chem.* **2009**, *74*, 973-980.
- Mollegaard, N. E.; Nielsen, P. E. In *Drug-DNA Interaction Protocols*; Fox, K. R., Ed.; Humana Press: Totowa, New Jersey, 1997; Vol. 90, p 1-22.
- Momparler, R. L.; Bovenzi, V. *J. Cell. Physiol.* **2000**, *183*, 145-154.
- Moreau, P.; Essiz, M.; Merour, J.-Y.; Bouard, D. *Tetrahedron: Asymmetry* **1997**, *8*, 591-598.
- Morgan, A. R.; Lee, J. S.; Pulleyblank, D. E.; Murray, N. L.; Evans, D. H. *Nucleic Acids Res.* **1979**, *7*, 547-569.
- Moro, S.; Beretta, G. L.; Dal Ben, D.; Nitiss, J.; Palumbo, M.; Capranico, G. *Biochemistry* **2004**, *43*, 7503-7513.
- Müller, E.; Zountas, G. *Chem. Ber.* **1972**, *105*, 2529-2533.
- Murray, K. R. *J. Mass Spectrom.* **1996**, *31*, 1203-1215.

- Myers, A. G.; Dragovich, P. S.; Kuo, E. Y. *J. Am. Chem. Soc.* **1992**, *114*, 9369-9386.
- Myers, A. G.; Kuo, E. Y.; Finney, N. S. *J. Am. Chem. Soc.* **1989**, *111*, 8057-8059.
- Nadaf, R. N.; Siddiqui, S. A.; Daniel, T.; Lahoti, R. J.; Srinivasan, K. V. *J. Mol. Catal. A: Chem.* **2002**, *214*, 155-160.
- Nadaf, R. N.; Siddiqui, S. A.; Daniel, T.; Lahoti, R. J.; Srinivasan, K. V. *J. Mol. Catal. A: Chem.* **2002**, *214*, 155-160.
- Nadipuram, A. K.; Kerwin, S. M. *Tetrahedron* **2006**, *62*, 3798-3808.
- Nadipuram, A. K.; Kerwin, S. M. *Tetrahedron Lett.* **2006**, *47*, 353-356.
- Nagata, R.; Yamanaka, H.; Okazaki, E.; Saito, I. *Tetrahedron Lett.* **1989**, *30*, 4995-4998.
- Nakane, M.; Hutchinson, C. R. *J. Org. Chem.* **1978**, *43*, 3922-3931.
- National Cancer Institute website: 2004, National Cancer Institute Cancer Fact Sheet.
- Needham-VanDevanter, D. R.; Hurley, L. H.; Reynolds, V. L.; Thierault, N. Y.; Krueger, W. C.; Wierenga, W. *Nucleic Acids Res.* **1984**, *12*, 6159-6168.
- Neidle, S. *Nucleic Acid Structure and Recognition*; Oxford University Press: New York, 2002.
- Nelson, D. L.; Cox, M. M. *Lehninger Principles of Biochemistry*; Third ed.; Worth Publishers: New York, 2000.
- Nelson, S. M.; Ferguson, L. R.; Denny, W. A. *Mutat. Res.* **2007**, *623*, 24-40.
- Newkome, G. R.; Kawato, T.; Kohli, D. K.; Puckett, W. E.; Olivier, B. D.; Chiari, G.; Fronczek, F. R.; Deutsch *J. Am. Chem. Soc.* **1981**, *103*, 3423-3429.
- Nicolaou, K. C.; Smith, A. L. *Acc. Chem. Res.* **1992**, *25*, 497-503.
- Nielsen, P. E.; Hiort, C.; Sonnichsen, S. H.; Buchardt, O.; Dahl, O.; Norden, B. *J. Am. Chem. Soc.* **1992**, *114*, 4967-4975.
- Nielsen, P. E.; Jeppesen, C.; Buchardt, O. *FEBS Lett.* **1988**, *235*, 122-124.

- Ordway, J. M.; Bedell, J. A.; Citek, R. W.; Nunberg, A.; Garrido, A.; Kendall, R.; Stevens, J. R.; Cao, D.; Doerge, R. W.; Korshunova, Y.; Holemon, H.; McPherson, J. D.; Lakey, N.; Leon, J.; Martienssen, R. A.; Jeddelloh, J. A. *Carcinogenesis* **2006**, *27*, 2409-2423.
- Park, K. H.; Jun, K.; Shin, S. R.; Oh, S. W. *Tetrahedron Lett.* **1996**, *37*, 8869-8870.
- Park, K. H.; Jun, K.; Shin, S. R.; Oh, S. W. *Tetrahedron Lett.* **1996**, *37*, 8869-8870.
- Patrinou, G. P.; Garinich, G.; Kounelis, S.; Kouri, E.; Menounos, P. *J. Mol. Med.* **1999**, *77*, 686-689.
- Paz, M. F.; Fraga, M. F.; Avila, S.; Guo, M.; Pollan, M.; Herman, J. G.; Esteller, M. *Cancer Res.* **2003**, *63*, 1114-1121.
- Peek, M. E.; Williams, L. D. In *Methods Enzymol.*; Academic Press: New York, 2001; Vol. 340, p 282-290.
- Perry, R. J.; Wilson, B. D.; Miller, R. J. *J. Org. Chem.* **1992**, *57*, 2883-2887.
- Perry, R. J.; Wilson, B. D.; Miller, R. J. *J. Org. Chem.* **1992**, *57*, 2883-2887.
- Pfeifer, G. P.; Denissenko, M. F.; Olivier, M.; Tretyakova, N.; Hecht, S. S.; Hainaut, P. *Oncogene* **2002**, *21*, 7435-7451.
- Pfeifer, G. P.; Denissenko, M. F.; Tang, M.-s. *Toxicol. Lett.* **1998**, *102-103*, 447-451.
- Ponti, M.; Souhami, R. L.; Fox, B. W.; Hartley, J. A. *Br. J. Cancer* **1991**, *63*, 743-747.
- Pottorf, R. S.; Chadha, N. K.; Katkevics, M.; Ozola, V.; Suna, E.; Ghane, H.; Regberg, T.; Player, M. R. *Tetrahedron Lett.* **2003**, *44*, 175-178.
- Pottorf, R. S.; Chadha, N. K.; Katkevics, M.; Ozola, V.; Suna, E.; Ghane, H.; Regberg, T.; Player, M. R. *Tetrahedron Lett.* **2003**, *44*, 175-178.
- Povirk, L. F.; Goldberg, I. H. *Nucleic Acids Res.* **1982**, *10*, 6255-6264.
- Povirk, L.; Shuker, D. E. *Mutat. Res.* **1994**, *318*, 205-226.
- Pradhan, S.; Esteve, P. O. *Clin. Immunol. Immunopathol.* **2003**, *109*, 6-16.

- Prakash, G. K. S.; Mandal, M.; Olah, G. A. *Angew. Chem., Int. Ed. Engl.* **2001**, *40*, 589-590.
- Praveen, C.; Kumar, H.; Miuralidharan, D.; Perumal, P. T. *Tetrahedron* **2008**, *64*, 2369-2374.
- Praveen, C.; Kumar, H.; Miuralidharan, D.; Perumal, P. T. *Tetrahedron* **2008**, *64*, 2369-2374.
- Price, C. C.; Gaucher, G. M.; Koneru, P.; Shibakawa, R.; Sowa, J. R.; Yamaguchi, M. *Biochim. Biophys. Acta* **1968**, *166*, 327-359.
- Price, P. A. *J. Biol. Chem.* **1975**, *250*, 1981-1986.
- Ramchandani, S.; Bhattacharya, S. K.; Cervoni, N.; Szyf, M. *Proc. Natl. Acad. Sci. U. S. A.* **1999**, *96*, 6107-6112.
- Randerath, E.; Agrawal, H. P.; Weaver, J. A.; Bordelon, C. B.; Randerath, K. *Carcinogenesis* **1985**, *6*, 1117-1126.
- Randerath, K.; Randerath, E.; Agrawal, H. P.; Gupta, R. C.; Schurdak, M. E.; Reddy, M. V. *Environ. Health Perspect.* **1985**, *62*, 57-65.
- Randerath, K.; Reddy, M. V.; Gupta, R. C. G. *Proc. Natl. Acad. Sci. U. S. A.* **1981**, *78*, 6126-6129.
- Razin, A.; Riggs, A. D. *Science* **1980**, *210*, 604-610.
- Razin, A.; Szyf, M. *Biochim. Biophys. Acta* **1984**, *782*, 29-36.
- Rechkoblit, O.; Zhang, Y.; Guo, D.; Wang, Z.; Amin, S.; Jacek, K.; Louneva, N.; Geacintov, N. E. *J. Biol. Chem.* **2002**, *277*, 30488-30494.
- Reddy, M. V.; Gupta, R. C.; Randerath, K. *Anal. Biochem.* **1981**, *117*, 271-279.
- Reddy, M. V.; Randerath, K. *Carcinogenesis* **1986**, *7*, 1543-1551.
- Reddy, M. V.; Randerath, K. *Environ. Health Perspect.* **1987**, *76*, 41-47.
- Ren, J.; Chaires, J. B. *Biochemistry* **1999**, *38*, 16067-16075.

- Reynolds, V. L.; Molineux, I. J.; Kaplan, D. J.; Swenson, D. H.; Hurley, L. R. *Biochemistry* **1985**, *24*, 6228-6237.
- Ross, M. K.; Mathison, B. H.; Said, B.; Shank, R. C. *Biochem. Biophys. Res. Commun.* **1999**, *254*, 114-119.
- Ruano, J. L. G.; Fernandez, I.; Cataline, M. d. P.; Cruz, A. A. *Tetrahedron: Asymmetry* **1996**, *7*, 3407-3414.
- Russu, I. M. *Trends Biotechnol.* **1991**, *9*, 96-104.
- Saiki, R. K.; Scharf, S.; Faloona, F.; Mullis, K. B.; Horn, G. T.; Erlich, H. A.; Arnheim, N. *Science* **1985**, *230*, 1350-1354.
- Sambrook, J.; Russell, D. W. *Molecular Cloning: A Laboratory Manual*; Cold Spring Harbor Laboratory Press: Cold Spring Harbor, 2001.
- Sampedro, D.; Soldevilla, A.; Modriguez, M. A.; Campos, P. J.; Olivucci, M. *J. Am. Chem. Soc.* **2005**, *127*, 441-448.
- Sannie, M. C.; Lapin, M. H. *Bull. Soc. Chim. Fr.* **1950**, 322-326.
- Sannie, M. C.; Lapin, M. H. *Bulletin de la Societe Chimique de France* **1950**, 322-326.
- Sato, S.; Kajiura, T.; Noguchi, M.; Takehana, K.; Kobayashi, T.; Tsuji, T. *J. Antibiot.* **2001**, *54*, 102-104.
- Sato, S.; Kajiura, T.; Noguchi, M.; Takehana, K.; Kobayashi, T.; Tsuji, T. *J. of Antibiot.* **2001**, *54*, 102-104.
- Scamrov, A. V.; Beabealashvilli, R. S. *FEBS Lett.* **1983**, *164*, 97-101.
- Schacter, L. P.; Anderson, C.; Canetta, R. M.; Kelley, S.; Nicaise, C.; Onetto, N.; Rozenzweig, M.; Smaldone, L.; Winograd, B. *Seminars in Oncology* **1992**, *19*, 613-621.
- Schmittel, M.; Mahajan, A. A.; Bucher, G.; Bats, J. W. *J. Org. Chem.* **2007**, *72*, 2166-2173.



Schmittel, M.; Strittmatter, M.; Kiau, S. *Tetrahedron Lett.* **1995**, *36*, 4975-4978.

Schmittel, M.; Vavilala, C. *J. Org. Chem.* **2005**, *70*, 4865-4868.

Schreiner, P. R.; Navarro-Vasquez, A.; Prall, M. *Acc. Chem. Res.* **2005**, *38*, 29-37.

Seawell, P. C.; Ganesan, A. K. In *DNA Repair*; Dekker: New York, 1981, p 425-430.

Seeman, J. I.; Chavdarian, C. G.; Secor, H. V. *J. Org. Chem.* **1985**, *50*, 5419-5421.

Seijas, J. A.; Vazquez-Tato, M. P.; Carballido-Reboredo, M. R.; Cresente-Campo, J.; Tomar-Lopez, L. *Synlett* **2007**, *2*, 0313-0317.

Seijas, J. A.; Vazquez-Tato, M. P.; Carballido-Reboredo, M. R.; Cresente-Campo, J.; Tomar-Lopez, L. *Synlett* **2007**, *2*, 0313-0317.

Sheldrick, G. M. (1994). SHELXL97. Program for the Refinement of Crystal Structures. University of Gottingen, Germany.

Sheldrick, G. M. (1994). SHELXTL/PC (Version 5.03). Siemens Analytical X-ray Instruments, Inc., Madison, Wisconsin, USA.

Sherer, E. C.; Kirschner, K. N.; Pickard IV, F. C.; Rein, C.; Felgus, S.; Shields, G. C. *J. Phys. Chem. B* **2008**, *112*, 16917-16934.

Sherman, C. L.; Pierce, S. E.; Brodbelt, J. S.; Tuesuwan, B.; Kerwin, S. M. *J. Am. Soc. Mass Spectrom.* **2006**, *17*, 1342-1352.

Shi, H.; Maier, S.; Nimmrich, I.; Yan, P. S.; Caldwell, C. W.; Olek, A.; Huang, T. H. *J. Cell. Biochem.* **2003**, *88*, 138-143.

Shibata, K.; Kashiwada, M.; Ueki, M.; Taniguchi, M. *J. Antibiot.* **1993**, *46*, 1095-1100.

Shibata, K.; Kashiwada, M.; Ueki, M.; Taniguchi, M. *J. of Antibiot.* **1993**, *46*, 1095-1100.

Sigman, D. S. *Biochemistry* **1990**, *29*, 9097-9105.

Singer, B. *J. Natl. Cancer Inst.* **1979**, *62*, 1329-1339.

Singh, R.; Farmer, P. B. *Carcinogenesis* **2006**, *27*, 178-196.

Skibo, E. B.; Xing, C.; Groy, T. *Bioorg. Med. Chem. Lett.* **2001**, *9*, 244502459.

- Slatko, B. E.; Albright, L. M. *DNA Sequencing by the Chemical Method*; John Wiley and Sons: New York, 1999; Vol. 1.
- Slatko, B. E.; Albright, L. M. In *Current Protocols in Molecular Biology*; John Wiley and Sons: New York; Vol. 1, p 7.5.1-7.6.13.
- Smith, L. E.; Denissenko, M. F.; Bennett, W. P.; Li, H.; Amin, S.; Tang, M.-s.; Pfeifer, G. P. *J. Natl. Cancer Inst.* **2000**, *92*, 803-811.
- Smith, S.; Marriner, G. A.; Kerwin, S.; Brodbelt, J. S. In *American Society of Mass Spectrometry Conference, poster presentation*; The University of Texas at Austin: Austin, 2007.
- So, Y.-H.; DeCaire, R. *Synth. Commun.* **1998**, *28*, 4123-4135.
- So, Y.-H.; DeCaire, R. *Synth. Commun.* **1998**, *28*, 4123-4135.
- Soldevilla, A. *e-mail communication*, **2004**.
- Soldevilla, A. *e-mail communication*, **2008**.
- Soldevilla, A.; Sampedro, D.; Campos, P. J.; Rodriguez, M. A. *J. Org. Chem.* **2005**, *70*, 6976-6979.
- Sommer, P. S. M.; Almeida, R. C.; Schneider, K.; Beil, W.; Sussmuth, R. D.; Fiedler, H.-P. *J. Antibiot.* **2008**, *61*, 683-686.
- Sommer, P. S. M.; Almeida, R. C.; Schneider, K.; Beil, W.; Sussmuth, R. D.; Fiedler, H.-P. *J. of Antibiot.* **2008**, *61*, 683-686.
- Sousa, F.; Tomaz, C. T.; Prazeres, D. M. F.; Queiroz, J. A. *Anal. Biochem.* **2005**, *343*, 183-185.
- Spassky, A.; Sigman, D. S. *Biochemistry* **1985**, *24*, 8050-8056.
- Still, W. C.; Kahn, M.; Mitra, A. *J. Org. Chem.* **1978**, *43*, 2923-2924.
- Still, W. C.; Kahn, M.; Mitra, A. *J. Org. Chem.* **1978**, *43*, 2923-2924.
- Stofer, E.; Chipot, C.; Lavery, R. *J. Am. Chem. Soc.* **1999**, *121*, 9503.

- Strahl, B. D.; Allis, C. D. *Nature* **2000**, *403*, 41-45.
- Stuart, G. R.; Chambers, R. W. *Nucleic Acids Res.* **1987**, *15*, 7451-7562.
- Sturla, S. J. *Current Opinion in Molecular Biology* **2007**, *11*, 293-299.
- Sugiura, Y.; Uesawa, Y.; Takahashi, Y.; Kuwahara, J.; Golik, J.; Doyle, T. W. *Proc. Natl. Acad. Sci. U. S. A.* **1989**, *86*, 7672-7676.
- Sun, D.; Lin, C. H.; Hurley, L. H. *Biochemistry* **1993**, *32*, 4487-4495.
- Szeliga, J.; Lee, H.; Harvey, R. G.; Page, J. E.; Ross, H. L.; Routledge, M. N.; Hilton, B. D.; Dipple, A. *Chem. Res. Toxicol.* **1994**, *7*, 420-427.
- Szyf, M. *Biochemistry (Moscow)* **2005**, *70*, 533-549.
- Tang, M.-s.; Lee, C.-S.; Doisy, R.; Ross, L.; Needham-VanDevanter, D. R.; Hurley, L. H. *Biochemistry* **1988**, *27*, 893-901.
- Tang, T. P.; Ellman, J. A. *J. Org. Chem.* **2002**, *67*, 7819-7832.
- Terashima, M.; Ishii, M. *Synthesis* **1982**, 484-485.
- Terashima, M.; Ishii, M. *Synthesis* **1982**, 484-485.
- Terron, A.; Fiol, J. J.; Garcia-Raso, A.; Barcelo-Oliver, M.; Moreno, V. *Coord. Chem. Rev.* **2007**, *251*, 1973-1986.
- Tipparaju, S. K.; Joyasawal, S.; Pieroni, M.; Kaiser, M.; Brun, R.; Kozikowski, A. P. *J. Med. Chem.* **2008**, *51*, 7344-7347.
- Tipparaju, S. K.; Joyasawal, S.; Pieroni, M.; Kaiser, M.; Brun, R.; Kozikowski, A. P. *J. Med. Chem.* **2008**, *51*, 7344-7347.
- Tong, W. P.; Ludlum, D. B. *Biochim. Biophys. Acta* **1980**, *608*, 174-181.
- Torre, G. L.; de Waure, C.; Specchia, M. L.; Nicolotti, N.; Capizzi, S.; Bilotta, A.; Clemente, G.; Ricciardi, W. *Pancreas* **2009**, *38*, 241-247.
- Tsai, C.-C.; Jain, S.; Sobell, H. M. *J. Mol. Biol.* **1977**, *114*, 301-315.
- Tuesuwan, B. Dissertation, The University of Texas at Austin, 2007.

- Tuesuwan, B.; Kerwin, S. M. *Biochemistry* **2006**, *45*, 7265-7276.
- Tuntiwechapikul, W.; David, W. M.; Kumar, D.; Salazar, M.; Kerwin, S. M. *Biochemistry* **2002**, *41*, 5283-5290.
- Turnbull, J. F.; Adams, R. L. *Nucleic Acids Res.* **1976**, *3*, 677-695.
- Ueki, M.; Shibata, K.; Taniguchi, M. *J. Antibiot.* **1998**, *51*, 883-885.
- Ueki, M.; Shibata, K.; Taniguchi, M. *J. of Antibiot.* **1998**, *51*, 883-885.
- Ueki, M.; Taniguchi, M. *J. Antibiot.* **1997**, *50*, 788-790.
- Ueki, M.; Taniguchi, M. *J. of Antibiot.* **1997**, *50*, 788-790.
- Ueki, M.; Ueno, K.; Miyadho, S.; Abe, K.; Shibata, K.; Taniguchi, M.; Oi, S. *J. Antibiot.* **1993**, *46*, 1089-1094.
- Ueki, M.; Ueno, K.; Miyadho, S.; Abe, K.; Shibata, K.; Taniguchi, M.; Oi, S. *J. of Antibiot.* **1993**, *46*, 1089-1094.
- Uhlmann, K.; Rohde, K.; Zeller, C.; Szymas, J.; Vogel, S.; Marczinek, K.; Thiel, G.; Nurnberg, P.; Laird, P. W. *Int. J. Cancer* **2003**, *106*, 52-59.
- Upadhyaya, P.; Hecht, S. S. *Chem. Res. Toxicol.* **2008**, *21*, 2164-2171.
- Upadhyaya, P.; McIntee, E. J.; Villalta, P. W.; Hecht, S. S. *Chem. Res. Toxicol.* **2006**, *19*, 426-435.
- Upadhyaya, P.; Sturla, S. J.; Tretyakova, N.; Ziegel, R.; Villalta, P. W.; Wang, M.; Hecht, S. S. *Chem. Res. Toxicol.* **2003**, *16*, 180-190.
- US Public Health Servies *Smoking and Health. Report of the Advisory Committee to the Surgeon General of the Public Health Service*, US Department of Health Education and Welfare, 1957.
- VanAllan, J. A.; Deacon, B. D. *Org. Synth.* **1963**, *Coll, Vol. 4*, 569-570.
- VanAllan, J. A.; Deacon, B. D. *Org. Synth.* **1963**, *Coll, Vol. 4*, 569-570.
- Vanyushin, B. F. *Biochemistry (Moscow)* **2005**, *70*, 598-611.

- Varma, R. S.; Saini, R. K.; Prakash, O. *Tetrahedron Lett.* **1977**, 38, 2621-2622.
- Varma, R. S.; Saini, R. K.; Prakash, O. *Tetrahedron Lett.* **1977**, 38, 2621-2622.
- Vedejs, E.; Chapman, R. W.; Fields, S. C.; Lin, S.; Schrimpf, M. R. *J. Org. Chem.* **1995**, 60, 3020-3027.
- Vedejs, E.; Fields, S. C.; Lin, S.; Schrimpf, M. R. *J. Org. Chem.* **1995**, 60, 3028-3034.
- Viirre, R. D.; Evindar, G.; Batey, R. A. *J. Org. Chem.* **2008**, 73, 3452-3459.
- Viirre, R. D.; Evindar, G.; Batey, R. A. *J. Org. Chem.* **2008**, 73, 3452-3459.
- Vorbriggen, H.; Krolikiewicz, K. *Tetrahedron Lett.* **1981**, 22, 4471-4474.
- Vorbriggen, H.; Krolikiewicz, K. *Tetrahedron Lett.* **1981**, 22, 4471-4474.
- Voss, J. J. D.; Hangeland, J. J.; Townsend, C. A. *J. Am. Chem. Soc.* **1990**, 112, 4554-4556.
- Voss, J. J. D.; Townsend, C. A.; Ding, W.-D.; Orton, G. O.; Ellestad, G. A.; Zein, N.; Tabor, A. B.; Schreiber, S. L. *J. Am. Chem. Soc.* **1990**, 112, 9699-9670.
- Wadsworth, D. H.; Geer, S. M.; Detty, M. R. *J. Org. Chem.* **1987**, 52, 3662-3668.
- Wakayama, M.; Ellman, J. A. *J. Org. Chem.* **2009**, 74, 2646-2650.
- Wang, B. B.; Maghami, N.; Goodlin, V. L.; Smith, P. J. *Bioorg. Med. Chem. Lett.* **2004**, 14, 3221-3226.
- Wang, B. B.; Maghami, N.; Goodlin, V. L.; Smith, P. J. *Bioorg. Med. Chem. Lett.* **2004**, 14, 3221-3226.
- Wang, Y.; Sarris, K.; Sauer, D. R.; Djuric, S. W. *Tetrahedron Lett.* **2006**, 47, 4823-4926.
- Wang, Y.; Sarris, K.; Sauer, D. R.; Djuric, S. W. *Tetrahedron Lett.* **2006**, 47, 4823-4926.
- Warnell, J. L. In *Biochem. Prep.*; Vestling, C. S., Ed.; John Wiley and Sons: New York, 1954, p 20-24.
- Warnell, J. L. In *Biochem. Prep.*; Vestling, C. S., Ed.; John Wiley and Sons: New York, 1954, p 20-24.

Warpehoski, M. A.; Hurley, L. H. *Chem. Res. Toxicol.* **1988**, *1*, 315-333.

Weaver, R. F. *Molecular Biology*; The McGraw-Hill Companies: St. Louis, 2005.

Weix, D. J.; Ellman, J. A. *Org. Synth.* **2005**, *82*, 157-162.

Weix, D. J.; Shi, Y.; Ellman, J. A. *J. Am. Chem. Soc.* **2005**, *127*, 1092-1093.

Wilfred, C. D.; Taylor, R. J. K. *Synlett* **2004**, *2004*, 1628-1630.

Wilfred, C. D.; Taylor, R. J. K. *Synlett* **2004**, *2004*, 1628-1630.

Wilson, W. D.; Tanious, F. A.; Fernandez-Saiz, M.; Rigl, C. T. In *Methods in Molecular Biology*; Walker, J. M., Ed.; Humana Press: Totowa, 1997; Vol. 90, p 278.

Winkler, M.; Cakir, B.; Sander, W. *J. Am. Chem. Soc.* **2004**, *126*, 6135-6149.

Wohlert, S. E.; Kunzel, E.; Machinek, R.; Mendez, C.; Salas, J. A.; Rohr, J. *J. Nat. Prod.* **1999**, *62*, 119-121.

Wurdeman, R. L.; Church, K. M.; Gold, B. *J. Am. Chem. Soc.* **1989**, *111*, 6408-6412.

Xu, D.; Shen, Y.; Chappell, J.; Cui, M.; Nielsen, M. *Physiol. Plant.* **2007**, *129*, 307-319.

Xu, Y.-j.; Xi, Z.; Zhen, Y.-s.; Goldberg, I. H. *Biochemistry* **1997**, *36*, 14975-14984.

Yang, T.-K.; Chen, R.-Y.; Lee, D.-S.; Peng, W.-S.; Jiang, Y.-Z.; Mi, A.-Q.; Jong, T.-T. *J. Org. Chem.* **1994**, *59*, 914-921.

Zein, N.; McGahren, W. J.; Morton, G. O.; Ashcroft, J.; Ellestad *J. Am. Chem. Soc.* **1989**, *111*, 6888-6890.

Zhang, N.; Lin, C.; Huang, X.; Kolbanovskiy, A.; Hingerty, B. E.; Amin, S.; Broyde, S.; Geacintov, N. E.; Patel, D. J. *J. Mol. Biol.* **2005**, *246*, 951-965.

Zhang, W.-X.; Ding, C.-H.; Luo, Z.-B.; Hou, X.-L.; Dai, L.-X. *Tetrahedron Lett.* **2006**, *47*, 8391-8393.

Zhao, D.; Wang, W.; Lian, S.; Yang, F.; Lan, J.; You, J. *Chem. Eur. J.* **2009**, *15*, 1337-1340.

Zhao, D.; Wang, W.; Lian, S.; Yang, F.; Lan, J.; You, J. *Chem. Eur. J.* **2009**, *15*, 1337-1340.

Ziegel, R.; Shallop, A.; Upadhyaya, P.; Jones, R.; Tretyakova, N. *Biochemistry* **2004**, *43*, 540-549.

## Vita

Gwendolyn Ann Marriner was born in Aurora, IL to John and Ann Marriner. She attended West Aurora High School, then matriculated to University of Illinois at Urbana-Champaign. While there, she earned a B. S. in Chemistry with distinction and performed chemistry research in the labs of Prof. J. A. Katzenellenbogen. Her publications include:

“Estrogen receptor-beta potency-selective ligands: structure-activity relationship studies of diarylpropionitriles and their acetylene and polar analogues.” Meyers, M. J.; Sun, J.; Carlson, K. E.; **Marriner, G. A.**; Katzenellenbogen, B. S.; Katzenellenbogen, J. *A. J. Med. Chem.*, **2001**, *44*, 4230-4251.

“Metallo-Aldehyde Enolates via Enal Hydrogenation: Catalytic Cross Aldolization with Glyoxal Partners As Applied to the Synthesis of 3,5-Disubstituted Pyridazines.” **Marriner, G. A.**; Garner, S. A.; Jang, H.-Y.; Krische, M. J. *J. Org. Chem.* **2004**, *69*, 1380-1382.

“An Improved Synthesis of *N'*-Nitroso-Nornicotine-5'-Acetate.” **Marriner, G. A.**; Kerwin, S. M. *J. Org. Chem.* **2009**, *74*, 2891-2892.

Permanent address: 7500 Woodmont Dr., Apt. L04 Bethesda, MD 20814

This dissertation was typed by the author.